CHARACTERISATION OF NOVEL FUNCTIONS OF THE ANAPHASE PROMOTING COMPLEX/CYCLOSOME AND ITS REGULATION THROUGH POST-TRANSLATIONAL MODIFICATION

by

PAUL EDWARD MINSHALL

A thesis submitted to
the University of Birmingham
for the degree of
DOCTOR OF PHILOSOPHY

School of Cancer Sciences
College of Medical and Dental Sciences
University of Birmingham
October 2014

ABSTRACT

The Anaphase Promoting Complex/Cyclosome (APC/C) is a multi-subunit E3 ubiquitin ligase that regulates mitotic progression through targeting substrates for degradation by the 26S proteasome. In order to assess APC/C post-translational modification status, and identify novel APC/C substrates and regulators, a comprehensive analysis of the APC/C and APC/C-interacting proteins by mass spectrometry was undertaken.

RNA polymerase I was identified as an APC/C-interacting complex, and the interaction was validated by reciprocal co-immunoprecipitation, GST pull-down and immunofluorescent confocal microscopy. Both RPA194 protein levels and RNA Polymerase I transcription were shown to be dependent upon APC/C activity. Ablation of APC/C function by RNAi increased RPA194 protein levels, and elevated RNA polymerase I activity significantly, as quantified by 5'-Fluorouridine incorporation into nascent pre-rRNA, and the increase in absolute levels of 45S, 28S and 18S rRNA transcripts, relative to non-silencing controls.

A number of other potential APC/C substrates and regulators were identified by mass spectrometry. Many of these interacting proteins contained APC/C consensus degron motifs. The APC/C was also shown to be a major substrate for acetylation; a number of APC/C subunits were identified as being acetylated *in vivo*. In this regard, APC3 was shown to be a substrate for both CBP and p300 acetyltransferases.

ACKNOWLEDGEMENTS

I would like to take this opportunity to thank my supervisors, Andy Turnell and Roger Grand, for all their help over the last few years. I am extremely grateful for all their assistance in the lab and guidance with my research, as well as their advice on the content of this thesis. I would also like to thank all members of our group, past and present, particularly Nat and Rakesh, for teaching me how to do everything and for helping me to settle in. I am also extremely grateful to Cancer Research UK for funding this research.

I would also like to thank Ashley Martin and Neil Shimwell for all things mass spec-related. Without them, a lot of the research within this thesis would not have happened. I am also extremely grateful to Joe Teodoro and the McGill University for hosting me for three months, to Joe's student Thomas Kucharski for his help whilst there, and to the College of Medical and Dental Sciences, University of Birmingham for providing the travel grant that allowed me this opportunity.

Finally I would like to thank Kathryn for all her support and understanding, and for driving over a hundred miles to see me on weekends, only for me to spend most of it in the lab.

LIST OF CONTENTS

LIST OF FIGURES AND TABLES

ABBREVIATIONS

5-FUrd	5-Fluorouridine
ABC	Ammonium Bicarbonate
Ac-CoA	Acetyl-Coenzyme A
AcN	Acetonitrile
Act D	Actinomycin D
APC/C	Anaphase Promoting Complex/Cyclosome
APS	Ammonium Persulphate
ATM	Ataxia Telangiectasia-Mutated
ATR	Ataxia Telangiectasia and Rad53-Related
BER	Base Excision Repair
bHLH	basic Helix-Loop-Helix
BrdU	5-bromo-2'-deoxyuridine
BSA	Bovine Serum Albumin
CAV	Chicken Anaemia Virus
CBP	CREB-binding Protein
Cdc	Cell Division Cycle
Cdk	Cyclin-dependent Kinase
cDNA	Complementary DNA
CKI	Cyclin-dependent Kinase Inhibitor
CMG	Cdc45-MCM-GINS complex
Cryo-EM	Cryo-Electron Microscopy
Cul	Cullin
Da	Dalton
DAPI	4',6-diamidino-2-phenylindole
DDK	Dbf4-dependent Kinase
DDR	DNA Damage Response
DFC	Dense Fibrillar Component
DMEM	Dulbecco's Modified Eagle's Medium
DMSO	Dimethyl sulfoxide
DNA	Deoxyribonucleic Acid
Dox	Doxycycline
DSB	Double-strand breaks
DTT	Dithiothreitol
DUB	Deubiquitinating enzymes
EDTA	Ethylenediaminetetraacetic acid
Emi1	Early Mitotic Inhibitor 1
eNoSC	Energy-dependent Nucleolar Silencing Complex
ETS	External Transcribed Spacer
FA	Formic Acid
FASP	Filter-Aided Sample Preparation

FC	Fibrillar Centre
FCS	Foetal Calf Serum
FDR	False Discovery Rate
FPLC	Fast Protein Liquid Chromatography
FRT	Flp Recombinase Target
GC	Granular Component
gDNA	Genomic DNA
GST	Glutathione-S-Transferase
HA	Haemagglutinin
HAT	Histone Acetyl Transferase
HDAC	Histone Deacetylases
HiDi	Highly Deionised Formamide
HINGS	Heat-Inactivated Normal Goat Serum
HPLC	High-Performance Liquid Chromatography
HR	Homologous Recombination
HRP	Horseradish Peroxidase
IF	Immunofluorescence
IgG	Immunoglobulin G
IGS	Intergenic Spacer
IP	Immunoprecipitation
IPTG	Isopropyl-β-D-thio-galactoside
IR	Ionising Radiation
ITS	Internal Transcribed Spacer
IVT	*In Vitro* Transcribed/Translated
LB	Luria Broth
LC-MS/MS	Liquid Chromatography - Tandem Mass Spectrometry
MCM	Mini Chromosome Maintenance
MMR	Mismatch Repair
mRNA	Messenger RNA
MW	Molecular Weight
NEBD	Nuclear Envelope Breakdown
NER	Nucleotide Excision Repair
NETN	NaCl-EDTA-Tris-NP-40
NHEJ	Non-homologous End Joining
NOR	Nucleolar Organiser Region
NoRC	Nucleolar Remodelling Complex
NP-40	Nonidet P-40
NPC	Nuclear Pore Complex
NuRD	Nucleosome Remodelling and Deacetylation Complex
ORC	Origin of Replication Complex
P/CAF	p300/CREB binding protein Associated Factor
Pa	Pascal
PARP	poly(ADP)ribose polymerase
PBS	Phosphate-Buffered Saline

PC	Proteasome-Cyclosome
PCR	Polymerase Chain Reaction
PFA	Paraformaldehyde
pfu	Plaque Forming Unit
PIC	Pre-Initiation Complex
PLK	Polo-like Kinase
PNB	Prenucleolar Body
Pol I	RNA Polymerase I
Pol II	RNA Polymerase II
pre-RC	Pre-Replication Complex
PTM	Post-Translational Modification
qPCR	quantitative PCR
rDNA	Ribosomal DNA
RFC	Replication Factor C
RING	Really Interesting New Gene
RNA	Ribonucleic Acid
RNP	Ribonucleoprotein
rRNA	Ribosomal RNA
RT-PCR	Reverse Transcription - PCR
S	Svedberg Unit
SAC	Spindle Assembly Checkpoint
SC	Sequence Coverage
SCF	Skp1-Cul1-Fbox-Roc1
SDS-PAGE	Sodium Dodecyl Sulphate - Polyacrylamide Gel Electrophoresis
shRNA	Short Hairpin RNA
siRNA	Small Interfering RNA
Skp	S-phase Kinase-associated Protein
SL1	Selectivity Factor 1
snoRNA	small nucleolar RNA
SUMO	Small Ubiquitin-like Modifier
TAF	TBP-Associated Factor
TBP	TATA-Binding Protein
TBST	Tris-Buffered Saline - Tween 20
TEAB	Tetraethylammonium bromide
TEMED	Tetramethylethylenediamine
TGF-β	Transforming Growth Factor β
TOP	DNA Topoisomerase
TPR	Tetratricopeptide Repeat
USP	Ubiquitin-Specific Protease
UTB	Urea-Tris-β-Mercaptoethanol
UTP	U Three Protein complex
UV	Ultraviolet
β-TrCP	β-Transducin Repeat-Containing Protein

1. INTRODUCTION

1.1. The Anaphase Promoting Complex/Cyclosome

The Anaphase Promoting Complex/Cyclosome (APC/C) is a multi-subunit Cullin-RING E3 ubiquitin ligase which targets substrates for degradation by the 26S proteasome in order to regulate cell cycle progression (Peters 2006, Pines 2011). The APC/C was identified independently by two separate groups: the first group identified a 20S complex in *Xenopus* extract which they termed the "Anaphase Promoting Complex" whilst the second group identified a 1.5MDa complex in clams, which they termed the "Cyclosome"; both complexes were shown to possess E3 ubiquitin ligase activity which could target Cyclin B for degradation (King, Peters et al. 1995, Sudakin, Ganoth et al. 1995). Over the last two decades, further investigation has uncovered additional APC/C subunits (Table 1) and a multitude of substrates (Table 2) (Pines 2011, Primorac and Musacchio 2013). Through its E3 ubiquitin ligase activity, the APC/C has been described as a master regulator of the cell cycle, controlling the onset of anaphase and coordinating mitotic exit, as well as preventing early S phase entry. Further roles for the APC/C have been described in the DNA damage response, as well as cell cycle-independent functions in neuronal development (Sudo, Ota et al. 2001, Bassermann, Frescas et al. 2008, Manchado, Eguren et al. 2010, Cotto-Rios, Jones et al. 2011, Eguren, Manchado et al. 2011). The APC/C has also been implicated in the regulation of transcription, both through epigenetic control of the chromatin state and through direct targeting of transcription factors (Turnell, Stewart et al. 2005, Turner, Malo et al. 2010, Islam, Turner et al. 2011, Nath, Banerjee et al. 2011). The APC/C also has strong links to tumourigenesis, and has been described as possessing, perhaps paradoxically, both oncogenic and tumour suppressive properties, and as such is of interest therapeutically in the

treatment of cancer (Turnell, Stewart et al. 2005, Penas, Ramachandran et al. 2011, Zhang, Wan et al. 2014).

1.2. The Ubiquitin-Proteasome Pathway

Ubiquitin was discovered within the bovine thymus in 1975 by Gideon Goldstein, and was shown to be a highly conserved 76 amino acid protein (Goldstein, Scheid et al. 1975). Nearly three decades later, the 2004 Nobel Prize in Chemistry was awarded to Aaron Ciechanover, Avram Hershko and Irwin Rose for elucidating the role of ubiquitin in the cellular proteasomal degradation of proteins.

The addition of a ubiquitin moiety to a target substrate is a process termed ubiquitylation. This often occurs upon the ε-amino group upon lysine residues, although other sites, such as serines and N-terminal α-amino groups, have also been described. Ubiquitin chains can form through any of its seven lysine residues at positions K6, K11, K27, K33, K48 and K63. Polyubiquitin chains most commonly implicated within the cell cycle are K11, K48 and K63, with K48 chains being the most commonly utilised proteasomal degradation signal. As yet, the APC/C is the only enzyme for which K11 ubiquitylation has been reported (Kerscher, Felberbaum et al. 2006, Xu, Duong et al. 2009, Clague and Urbe 2010).

The ubiquitylation pathway consists of an enzymatic cascade of three ubiquitin-binding complexes (Glickman and Ciechanover 2002). Firstly, an E1 ubiquitin-activating enzyme catalyses ATP-dependent acyl-adenylation of the C-terminus of a ubiquitin moiety. This is then transferred to the catalytic cysteine residue of the E1, forming a high energy thioester bond (Figure Int.1i). This E1-ubiquitin is then recognised by, and interacts with, an E2 ubiquitin-conjugating enzyme, resulting in the transfer of ubiquitin onto the E2 (Figure Int.1ii). This activated E2 then transfers ubiquitin either directly onto a target substrate, or via an E3 ubiquitin ligase (Figure Int.1iii). An E3 enzyme can bind

the activated E2 as well as target substrates, thereby bringing the charged ubiquitin and target substrate together. It remains unclear whether the E3 ligase itself is ubiquitylated during this process, or whether it merely facilitates the transfer of activated ubiquitin from the E2 to the substrate. Should another activated E2 subsequently bind the E3, another ubiquitin molecule will be added to the target substrate, resulting in a polyubiquitin chain in a process which may be enhanced by E4 ubiquitin-elongation enzymes (Figure Int.1iv) (Ciechanover and Schwartz 1998, Koegl, Hoppe et al. 1999, Hochstrasser 2006, Schulman and Harper 2009). Currently, there are three known types of E3 ligases: HECT-domain, U-box and RING-finger-domains. Of the RING-finger E3 ligases, another subcategory consists of those which also contains a Cullin protein, including the Skp1-Cul1-Fbox-Roc1 (SCF) E3 ligases and the APC/C (Bedford, Lowe et al. 2011).

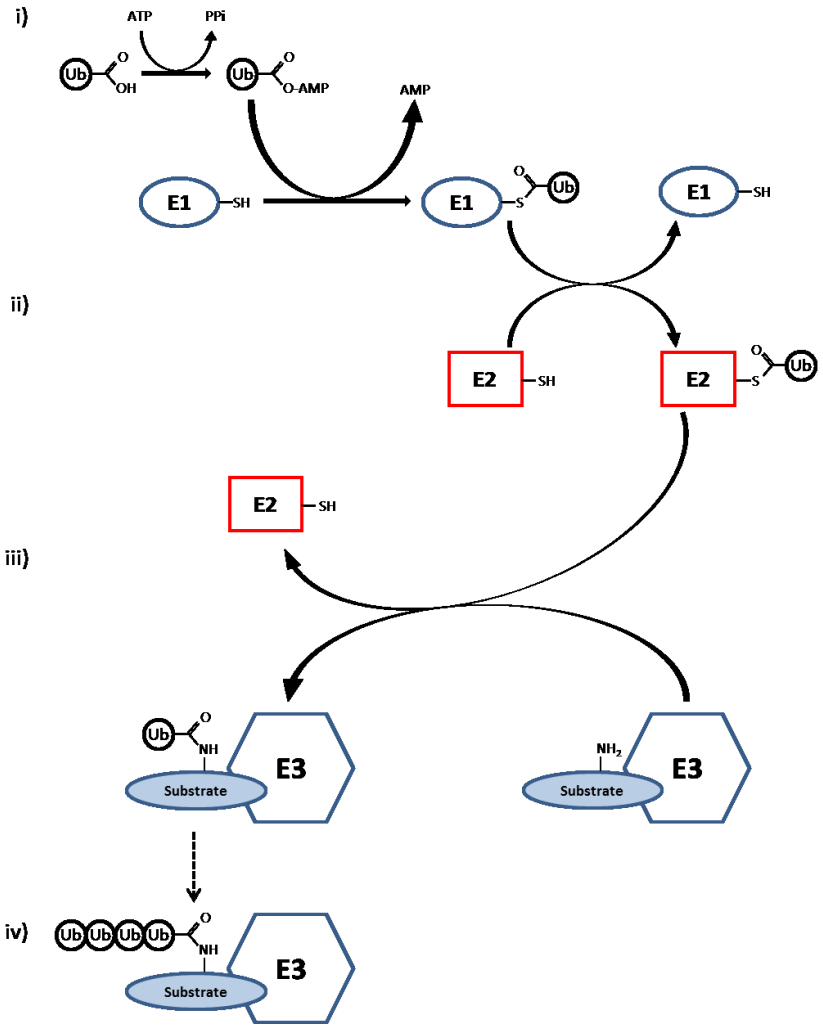

Figure Int.1 – The Ubiquitylation Pathway

i) Ubiquitin (Ub) is activated by E1 and ATP, and forms an E1-Ub intermediate
ii) Ubiquitin is transferred from E1 to E2
iii) E3 mediates the transfer of Ubiquitin from E2 to substrate
iv) Repeated Ubiquitin transfer from E2-Ub onto substrate forms a polyubiquitin chain

One possible consequence of ubiquitylation is the degradation of the target protein. This can occur through proteasomal and lysosomal pathways (Clague and Urbe 2010). Proteins polyubiquitylated with K48 chain linkages are targets for degradation by the 26S proteasome, whereupon they are recognised by 19S polar regulatory particles (Finley 2009). Other "scavenger" proteins are also involved in the recruitment of substrates for proteasomal degradation. These include UBL/UBA proteins, which act as a bridge between the regulatory subunits and ubiquitin, conferred by binding through its UBA (Ubiquitin-associated) and UBL (Ubiquitin-like) domains, respectively (Clague and Urbe 2010).

The roles of the regulatory particles are twofold: to unfold the proteins to permit entry into the 20S core compartment and to remove and recycle ubiquitin. A hexameric ring of ATPases catalyses the ATP-dependent unfolding of the target protein, thereby allowing it to pass into the 20S subunit for degradation. Prior to this, ubiquitin is removed by a series of deubiquitinating enzymes (DUBs) (Lee, Lee et al. 2011). Deubiquitylation recycles ubiquitin, maintaining the cellular pool at a constant level, rather than letting it simply be degraded along with the rest of the protein. Different DUBs have specificity for a certain K-linked ubiquitin (Soboleva and Baker 2004). It is hypothesised that this may act as a proof-reading mechanism, thereby ensuring transition to the proteolytic subunit can only occur if the ubiquitin signal, *i.e.* length and type of chain, is exactly correct for 26S proteasomal degradation (Lam, Xu et al. 1997).

The 20S core particle consists of two copies of each of seven different α- and β-subunits. These are arranged as a stack of four heptameric rings and form a barrel-like structure, into which unfolded proteins may fit (Voges, Zwickl et al. 1999, Verma, Chen et al. 2000). The α-subunits form the two outer rings whilst the catalytic β-subunits lie within the inner two rings of the barrel, which contain the active sites of the proteasome. The β-subunits exhibit trypsin-, chymotrypsin- and caspase-like proteolytic activity (Wilk and Orlowski 1983).

1.3. Form and Function of the APC/C

1.3.1. Structure and Subunits of the APC/C

The human APC/C is currently thought to contain 20 subunits in a 1.2MDa complex (Table 1) (Chang, Zhang et al. 2014). Many of these subunits are conserved across eukaryotes, although some species-specific subunits have been described, such as the budding yeast-specific Apc9, fission yeast-specific Apc14, as well as APC7 and APC16 which are only found in higher eukaryotes (Table 1) (Schreiber, Stengel et al. 2011, Primorac and Musacchio 2013, Zhang, Yang et al. 2013, Chang, Zhang et al. 2014).

The precise structure of the *S. cerevisiae* APC/C was established using recombinant protein expression coupled with electron microscopy, mass spectrometry and X-ray crystallography (Schreiber, Stengel et al. 2011). Recently, the corresponding APC/C structure within *H. sapiens* was elucidated using a recombinant APC/C together with electron microscopy and single-particle analysis, with a further study utilising cryo-electron microscopy (cryo-EM) providing even greater detail (Figure Int.2) (Zhang, Yang et al. 2013, Chang, Zhang et al. 2014).

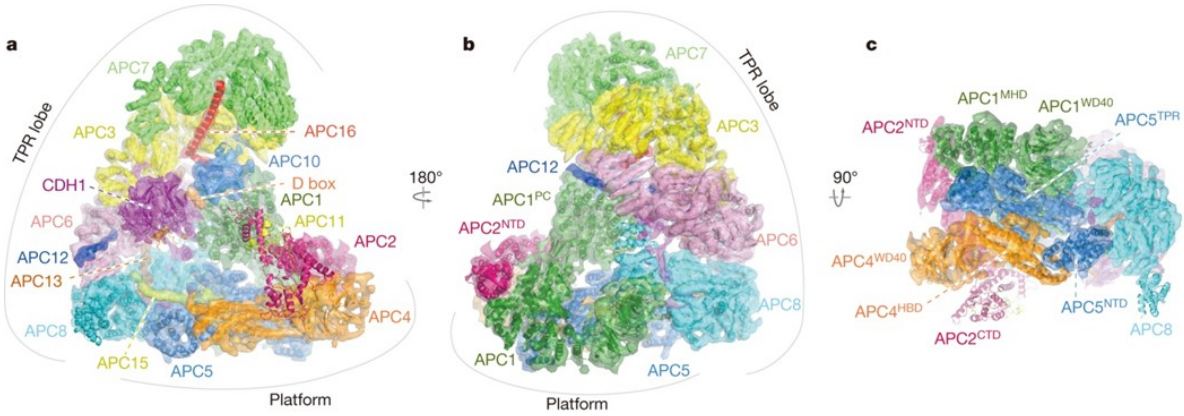

Figure Int.2 – Structure of an APC/C-Cdh1-substrate complex, elucidated by Cryo-EM

Structural determination of each subunit within the human APC/C-Cdh1-substrate complex by Cryo-EM, viewed in three planes (a, b, c). Shown are the TPR lobe (APC3, APC6, APC7, APC8, APC12 APC13, APC16) and the Platform (APC1, APC4, APC5, APC15). Also shown are APC2, APC10, APC11 and Cdh1 within the central cavity. *Taken from (Chang, Zhang et al. 2014).*

The APC/C has been shown to possess three distinct regions, known as the “TPR lobe”, the “platform” and the “central cavity” (Figure Int.2). Within the human APC/C TPR lobe, also called the “arc lamp”, are the four canonical TPR subunits APC3, APC6, APC7 and APC8, which all contain multiple TPR (tetratricopeptide repeats) motifs and exist as homodimers (Dube, Herzog et al. 2005, Pines 2011, Schreiber, Stengel et al. 2011, Zhang, Chang et al. 2013, Chang, Zhang et al. 2014). Also found within this TPR lobe are the accessory subunits APC13 and APC16, as well as an APC12/Cdc26 homodimer (Schreiber, Stengel et al. 2011, Chang, Zhang et al. 2014). APC12 and APC13/Swm1 stabilise this TPR subcomplex, whilst the function of APC16 is currently unknown, although, given its location spanning both APC3 and APC7, it is also thought be to be involved in stabilisation (Schwickart, Havlis et al. 2004, Wang, Dye et al. 2009, Chang, Zhang et al. 2014). Other accessory stabilising proteins have been identified in other organisms, including Apc9 in *S. cerevisiae* and Apc14 in *S. pombe* (Ohi, Feoktistova et al. 2007, Pines 2011, Schreiber, Stengel et al. 2011).

The platform subcomplex of the APC/C contains APC1, APC4 and APC5 (Schreiber, Stengel et al. 2011, Chang, Zhang et al. 2014). These proteins act as scaffolds, binding both the TPR subcomplex and the substrate recognition/E3 ubiquitin ligase components, thereby holding the two subcomplexes together (Vodermaier, Gieffers et al. 2003, Thornton, Ng et al. 2006). APC1 and APC5 both bind to APC8 within the TPR lobe, with the ancillary protein APC15/Mnd2 acting as a bridging factor between APC5 and APC8 (Schreiber, Stengel et al. 2011, Chang, Zhang et al. 2014). Whilst the proteasome-cyclosome (PC) motif within APC1 mediates its interaction with APC8, it is also necessary for the APC1-APC10/Doc1 interface.

The central cavity contains the catalytic core of the APC/C, such that it contains the substrate recognition particle, a heterodimer between APC10/Doc1 and co-activator, as well as the Cullin and RING-finger E3 ligase subunits APC2 and APC11. These reside in a flexible state upon the edge of the platform, such that the C-terminal domain of APC2 and APC11 protrude into the cavity, above which

the processing factor APC10 and one of the co-activators (Cdc20 or Cdh1) are found (Schreiber, Stengel et al. 2011, Chang, Zhang et al. 2014). Together, these recognise target substrates and perform the E3 ubiquitin ligase activity of the APC/C (Peters 2006, Pines 2011, Primorac and Musacchio 2013). Further to its interaction with APC1, APC10 also binds through its isoleucine-arginine (I-R) tail to one monomer of the APC3 heterodimer within the TPR lobe (Wendt, Vodermaier et al. 2001).

Co-activator binding differs slightly between yeast and man. For both organisms, Cdh1 and Cdc20 bind through C-terminal I-R motifs to TPR domains within both APC3 and APC8, albeit the opposite APC3 subunit to which APC10 binds, as well as binding APC2 via a C-box and also contacting APC6 (Schwab, Neutzner et al. 2001, Thornton, Ng et al. 2006, Buschhorn, Petzold et al. 2011, Schreiber, Stengel et al. 2011, Chang, Zhang et al. 2014). However, in humans, APC7 has been shown to interact with the I-R domain of Cdh1 and more weakly with Cdc20 (Vodermaier, Gieffers et al. 2003). As APC7 appears to be a metazoan-specific subunit thought to be formed by duplication of the APC3 gene, the absence of a corresponding interaction in yeast is understandable (Vodermaier, Gieffers et al. 2003). The precise mechanism of co-activator binding also appears to differ between organisms. In yeast, should either the C-box or I-R dipeptide be mutated, the co-activator ceases to bind; in higher eukaryotes mutation of either motif decreases binding, whilst mutation of both causes a greater decrease in binding, signifying a cooperative mechanism for co-activator binding to the APC/C (Vodermaier, Gieffers et al. 2003, Thornton, Ng et al. 2006). Similarly, a vertebrate APC/C complex lacking APC2-APC11 is still capable of binding Cdh1, further showing that APC2 is dispensable for co-activator binding (Vodermaier, Gieffers et al. 2003).

No. in human APC/C	*Human*	*Budding Yeast*	*Fission Yeast*	*Fly*	*Worm*	Structural motifs	Location	Function and properties
1	APC1	Apc1	cut4	Shattered	MAT-2 (POD-3)	PC repeats/ WD40/ mid-helical	Platform	Scaffolding
1	APC2	Apc2	apc2	Morula	K06H7.6	Cullin homology	Catalytic Module	Catalytic
2	APC3	Cdc27	nuc2	CDC27	MAT-1 (POD-5)	TPR motifs	TPR lobe	Binds APC10 and Cdc20/Cdh1 Scaffolding
1	APC4	Apc4	cut20 (lid1)	CG4350	EMB-30	WD40/ four-helix-bundle	Platform	Scaffolding
1	APC5	Apc5	apc5 (spac959)	IDA	M163.4	TPR motifs/ N-terminal helical	Platform	Scaffolding
2	APC6	Cdc16	cut9	CDC16	EMB-27 (POD-6)	TPR motifs	TPR lobe	Binds Cdc20 Scaffolding
2	APC7	-	-	APC7	-	TPR motifs	TPR lobe	Scaffolding
2	APC8	Cdc23	cut23 (cdc23)	CDC23	MAT-3 (POD-4)	TPR motifs	TPR lobe	Binds CDC20 and Cdh1 Scaffolding
-	-	Apc9	-	-	-	-	TPR lobe	Stabilizes CDC27
1	APC10	Doc1	apc10	APC10	F15H10.3	DOC domain/ I-R tail	Substrate recognition module	D/KEN box recognition
1	APC11	Apc11	apc11	Lemming	F35G12.9	RING finger	Catalytic Module	Binds E2 enzyme Catalytic
2	APC12	Cdc26	hcn1	-	-	Extended/α-helix	TPR lobe	APC6 stability
1	APC13	Swm1	apc13	APC13	-	Extended/α-helix	TPR lobe	APC8 stability
-	-	-	apc14	-	-	-	-	-
1	APC15	Mnd2	apc15	-	-	Extended/α-helix	Platform	MCC interaction Inhibits Ama1 (budding yeast)
1	APC16	-	-	-	EMB-1	α-helix	TPR lobe	-
1	Cdc20	Cdc20	slp1	Fizzy	FZY-1	WD40/IR/ C-box/ helical	Substrate recognition module	Mitotic regulator D/KEN box recognition
1	Cdh1	Cdh1 (Hct1)	ste9 (srw1)	FZR	FZR-1	WD40/IR/ C-box/ helical	Substrate recognition module	G1 and endoreplication D/KEN box recognition
-	-	-	-	FZR2	-	WD40	Substrate recognition module?	Meiosis regulator D/KEN box recognition
-	-	-	-	Cortex	-	WD40	Substrate recognition module?	Meiosis regulator D/KEN box recognition
1	AMA1	Ama1	mfr1 (fzr1)	-	-	WD40 and IR	Substrate recognition module?	Meiosis regulator D/KEN box recognition

Table 1 – list of APC/C subunits and co-activators in different species

Subunits, domains, locations and functions which have not been characterised are denoted by "-"
Adapted from (Pines 2011, Primorac and Musacchio 2013, Zhang, Wan et al. 2014)

1.3.2. Substrate Recognition

Substrate specificity for the APC/C is conferred by the binding of a co-activator such as Cdh1 or Cdc20 (Table 1), with over a hundred APC/C substrates currently identified (Table 2) (Pfleger, Lee et al. 2001, Pines 2011, Primorac and Musacchio 2013). Co-activator binding is regulated temporally, such that Cdc20 is only able to form an active complex with the APC/C from the beginning of mitosis, following satisfaction of the Spindle Assembly Checkpoint (SAC) and the onset of anaphase, whilst APC/C-Cdh1 is active during the latter mitotic stages and subsequent G1. This switch in co-activator binding permits a change in the substrates targeted by the APC/C (Peters 2006, Pines 2011).

Co-activators recognise specific motifs within target substrates termed degrons. The canonical degron motifs include the D-box (RxxL) and KEN-box (KEN) (Pines 2011). The D-box was first identified upon comparison of sequence homology between cyclins of different organisms, and was shown to consist of a conserved RxxLxxxxN motif which, when deleted, inhibited proteolysis (Glotzer, Murray et al. 1991). Further variants upon this D-box have also been described, such as RxxLxN/D/E, RxxLxxI/VxN or RxxLxxL/I/V/M (Glotzer, Murray et al. 1991, Peters 2006, Barford 2011, Dinkel, Van Roey et al. 2014). Similarly, an extended KEN-box has also been discovered, consisting of the sequence KENxxxN/D (Pfleger and Kirschner 2000). APC/C activated by Cdc20 (APC/C-Cdc20) tends to recognise D-boxes, whilst APC/C activated by Cdh1 (APC/C-Cdh1) preferentially recognises KEN-boxes, although these are not exclusive (Zur and Brandeis 2002, Passmore and Barford 2005). Initially, most KEN-boxes appeared in proteins alongside D-boxes, although further studies demonstrated more proteins containing either one or the other (Pfleger and Kirschner 2000, Zur and Brandeis 2002). Interestingly, proteins which contain both D- and KEN-boxes can be targeted for ubiquitylation by both APC/C-Cdc20 and APC/C-Cdh1, and often both degrons are required for efficient co-activator binding and ubiquitylation (Burton and Solomon 2001, Passmore, McCormack et al. 2003, Burton and Solomon 2007, Tian, Li et al. 2012).

Cdc20 and Cdh1 contain a WD40 propeller motif, which is able to bind KEN and D-box motifs (Kraft, Vodermaier et al. 2005, He, Chao et al. 2013). Although the co-activator-D-box interaction can occur in the absence of the APC/C, it does so with relaxed specificity and reduced affinity, suggesting that the APC/C facilitates this interaction (Burton and Solomon 2001, Hilioti, Chung et al. 2001, Pfleger, Lee et al. 2001, Schwab, Neutzner et al. 2001). Furthermore, the binding between Cdh1 and substrate appears to strengthen upon simultaneous APC/C-Cdh1 interaction (Vodermaier, Gieffers et al. 2003, Burton, Tsakraklides et al. 2005, Passmore and Barford 2005). Indeed, the binding of D-boxes to the APC/C has been shown to occur cooperatively through both Cdh1 and the APC/C subunit APC10/Doc1, such that Cdh1 and APC10/Doc1 can bind D-boxes independently, yet both are required for sufficient APC/C-substrate binding and ubiquitylation (Carroll, Enquist-Newman et al. 2005, Buschhorn, Petzold et al. 2011, da Fonseca, Kong et al. 2011, Chang, Zhang et al. 2014). Conversely, it has also been demonstrated that the recognition of KEN-boxes is mediated by Cdh1 only, and that other APC/C subunits, such as APC10, are not required (Barford 2011, Chao, Kulkarni et al. 2012).

Although the majority of targets for APC/C-mediated ubiquitylation contain either D-boxes or KEN-boxes, several non-canonical degrons have been described. These include the A-box, a conserved peptide motif within vertebrate Aurora A kinases which, together with a C-terminal D-box, is required for recognition by the APC/C-Cdh1 during mitotic exit (Littlepage and Ruderman 2002). Similarly, an A-box derivative is present within Aurora B which is necessary for its degradation (Nguyen, Chinnappan et al. 2005). Other non-canonical binding motifs include the CRY box in Cdc20 (Reis, Levasseur et al. 2006), the KEN derivative, GxEN, within *Xenopus* XKid (Castro, Vigneron et al. 2003), the O-box within *Drosophila* ORC1 (Araki, Yu et al. 2005) and an LxExxxxN motif within the *S. cerevisiae* meiotic regulator Spo13 (Sullivan and Morgan 2007). Claspin also contains a conserved N-terminal LLK motif which is required for Cdh1-mediated degradation (Gao, Inuzuka et al. 2009).

Some substrates appear to be able to bind the APC/C in the absence of a co-activator. Indeed, this is an integral mechanism for the degradation of substrates during the SAC. Such examples include NEK2A, which, upon the formation of homodimers, can bind to the APC/C through a C-terminal M-R dipeptide similar to the I-R tail upon Cdc20 and Cdh1, although a small proportion of Cdc20, free from SAC-inhibition, is still required for D-box-mediated degradation of NEK2A (Hames, Wattam et al. 2001, Hayes, Kimata et al. 2006, Kimata, Baxter et al. 2008, Sedgwick, Hayward et al. 2013). Similarly, KIF18A contains a C-terminal L-R dipeptide which also binds the APC/C during the SAC, however its degradation is delayed until anaphase, thereby suggesting further as yet unknown regulatory mechanisms (Sedgwick, Hayward et al. 2013).

Substrate	UniProt ID	Gene	Reference
Anillin	Q9NQW6	ANLN	(Zhao and Fang 2005)
Aurora A	O14965	AURKA	(Honda, Mihara et al. 2000, Taguchi, Honda et al. 2002)
Aurora B	Q96GD4	AURKB	(Stewart and Fang 2005, Feine, Zur et al. 2007)
B99	Q9NYZ3	GTSE1	(Pfleger and Kirschner 2000)
BARD1	Q99728	BARD1	(Song and Rape 2010)
BRD7	Q9NPI1	BRD7	(Hu, Liao et al. 2014)
BRSK2	Q8IWQ3	BRSK2	(Li, Wan et al. 2012)
BUB1	O43683	BUB1	(Qi and Yu 2007)
BUBR1	O60566	BUB1B	(Choi, Choe et al. 2009)
CBP	Q92793	CREBBP	(Turnell, Stewart et al. 2005)
Cdc20	Q12834	CDC20	(Pfleger and Kirschner 2000)
Cdc25A	P30304	CDC25A	(Donzelli, Squatrito et al. 2002)
Cdc25B	P30305	CDC25B	(Kieffer, Lorenzo et al. 2007)
Cdc25C	P30307	CDC25C	(Chen, Zhang et al. 2002)
Cdc6	Q99741	CDC6	(Petersen, Wagener et al. 2000)
Cdh1	Q9UM11	FZR	(Listovsky, Oren et al. 2004)
CDR2	Q01850	CDR2	(O'Donovan, Diedler et al. 2010)
Cdt1	Q9H211	CDT1	(Sugimoto, Kitabayashi et al. 2008)
CENPF	P49454	CENPF	(Gurden, Holland et al. 2010)
Centrin	O15182	**C**ETN3	(Lukasiewicz, Greenwood et al. 2011)
CKAP2	Q8WWK9	CKAP2	(Seki and Fang 2007)
Cks1	P61024	CKS1B	(Bashir, Dorrello et al. 2004)
Claspin	Q9HAW4	CLSPN	(Bassermann, Frescas et al. 2008, Gao, Inuzuka et al. 2009)
Cyclin A	P20248	CCNA2	(Sudakin, Ganoth et al. 1995, Geley, Kramer et al. 2001)
Cyclin B1	P14635	CCNB1	(King, Peters et al. 1995, Sudakin, Ganoth et al. 1995)
Cyclin B3	Q8WWL7	CCNB3	(Nguyen, Manova et al. 2002)
Cyclin D1	P24385	CCND1	(Agami and Bernards 2000, Pawar, Sarkar et al. 2010)
Drp1	O00429	DNM1L	(Horn, Thomenius et al. 2011)
DVC1	Q9H040	SPRTN	(Mosbech, Gibbs-Seymour et al. 2012)
DVL1P1	P54792	DVL1P1	(Ganner, Lienkamp et al. 2009)
E2F1	Q01094	E2F1	(Peart, Poyurovsky et al. 2010, Budhavarapu, White et al. 2012)
E2F3	O00716	E2F3	(Ping, Lim et al. 2012)
Ect2	Q9H8V3	ECT2	(Liot, Seguin et al. 2011)
ERBB4	Q15303	ERBB4	(Strunk, Husted et al. 2007)
ETS2	P15036	ETS2	(Li, Shin et al. 2008)
FAN1	Q9Y2M0	FAN1	(Lai, Hu et al. 2012)

FBXW5	Q969U6	FBXW5	(Puklowski, Homsi et al. 2011)
FoxM1	Q08050	FoxM1	(Park, Costa et al. 2008)
G9a	Q96KQ7	EHMT2	(Takahashi, Imai et al. 2012)
Geminin	O75496	GMNN	(McGarry and Kirschner 1998)
GLP	Q96KQ7	EHMT1	(Takahashi, Imai et al. 2012)
Glutamate receptor 1	P42261	GRIA1	(Fu, Hung et al. 2011)
Glutaminase 1	O94925	GLS	(Colombo, Palacios-Callender et al. 2010)
Hec1	O14777	NDC80	(Li, Zhou et al. 2011)
Hmmr	O75330	HMMR	(Song and Rape 2010)
HOXC10	Q9NYD6	HOXC10	(Gabellini, Colaluca et al. 2003)
HSF2	Q03933	HSF2	(Ahlskog, Björk et al. 2010)
HURP	Q15398	DLGAP5	(Song and Rape 2010)
ID1	P41134	ID1	(Kim, Puram et al. 2009)
ID2	Q02363	ID2	(Lasorella, Stegmuller et al. 2006)
JNK1	P45983	MAPK8	(Gutierrez, Tsuji et al. 2010)
JNK2	P45984	MAPK9	(Gutierrez, Tsuji et al. 2010)
KIF11	P52732	KIF11	(Drosopoulos, Tang et al. 2014)
KIF18A	Q8NI77	KIF18A	(Sedgwick, Hayward et al. 2013)
KIF22	Q14807	KIF22	(Feine, Zur et al. 2007)
KIF2C	Q99661	KIF2C	(Singh, Winter et al. 2014)
KIF4A	O95239	KIF4A	(Singh, Winter et al. 2014)
KIFC1	Q9BW19	KIFC1	(Singh, Winter et al. 2014)
MAD2L2	Q9UI95	MAD2L2	(Listovsky and Sale 2013)
Mcl1	Q07820	MCL1	(Harley, Allan et al. 2010)
MCPH1	Q8NEM0	MCPH1	(Arquint and Nigg 2014)
MOAP-1	Q96BY2	MOAP1	(Huang, Zhang et al. 2012)
Mps1	P33981	TTK	(Cui, Cheng et al. 2010)
Myf5	P13349	MYF5	(Lindon, Albagli et al. 2000)
NEK2A	P51955	NEK2	(Hames, Wattam et al. 2001)
NEDL2	Q9P2P5	NEDL2	(Lu, Hu et al. 2013)
NeuroD2	Q15784	NEUROD2	(Yang, Kim et al. 2009)
NIPA	Q86WB0	ZC3HC1	(Klitzing, Huss et al. 2011)
Nlp	Q9Y2I6	NINL	(Wang and Zhan 2007)
NuSAP	Q9BXS6	NUSAP1	(Li, Zhou et al. 2007, Song and Rape 2010)
OCT1	P14859	POU2F1	(Kang, Goodman et al. 2011)
p190RhoGAP	Q9NRY4	ARHGAP35	(Naoe, Araki et al. 2010)
p21	P38936	CDKN1A	(Amador, Ge et al. 2007)
p63	Q9H3D4	TP63	(Hau, Yip et al. 2011)
p300	Q09472	EP300	(Turnell, Stewart et al. 2005)
PAF	Q15004	PAF	(Emanuele, Ciccia et al. 2011, Williamson, Banerjee et al. 2011)

Pfkfb3	Q16875	PFKFB3	(Herrero-Mendez, Almeida et al. 2009)
PIF	Q9H611	PIF1	(Mateyak and Zakian 2006)
Plk1	P53350	PLK1	(Lindon and Pines 2004)
RAC1	P63000	RAC1	(Lanning, Daddona et al. 2004, Pop, Aktories et al. 2004)
RAD17	O75943	RAD17	(Zhou, Jing et al. 2013)
RAP80	Q96RL1	UIMC1	(Cho, Lee et al. 2012)
RASSF1A	Q9NS23	RASSF1A	(Chow, Wong et al. 2012)
Rcs1	Q9BSJ6	FAM64A	(Zhao, Coppinger et al. 2008)
REV1	Q9UBZ9	REV1	(Chun, Kok et al. 2013)
Securin	Q5FBB7	PTTG1	(Zou, McGarry et al. 1999)
Sgo1	Q5FBB7	SGOL1	(Fu, Hua et al. 2007)
Skp2	Q13309	SKP2	(Bashir, Dorrello et al. 2004)
SnoN	P12757	SKIL	(Stroschein, Bonni et al. 2001, Wan, Liu et al. 2001)
Sororin	Q96FF9	CDCA5	(Rankin, Ayad et al. 2005)
Sp100	P23497	SP100	(Wang, Li et al. 2011)
TK1	P04183	TK1	(Ke and Chang 2004)
TMPK	P23919	DTYMP	(Ke and Chang 2004)
Tome-1	Q99618	CDCA3	(Ayad, Rankin et al. 2003)
TOP2A	P11388	TOP2A	(Eguren, Álvarez-Fernández et al. 2014)
TPX2	Q9ULW0	TPX2	(Stewart and Fang 2005)
TRB3	Q96RU7	TRIB3	(Ohoka, Sakai et al. 2010)
UbcH10	O00762	UBE2C	(Rape and Kirschner 2004)
USP1	O94782	USP1	(Cotto-Rios, Jones et al. 2011)
USP37	Q86T82	USP37	(Huang, Summers et al. 2011)
VHL	P40337	VHL	(Liu, Xin et al. 2011)

Table 2 – List of known human APC/C substrates

Adapted from (Meyer and Rape 2011, Liu, Yuan et al. 2012, Min, Mayor et al. 2013).

1.3.3. Mechanism of APC/C E3 ubiquitylation

The catalytic E3 ubiquitin ligase activity of the APC/C is conferred by APC11, containing a RING (Really Interesting New Gene) domain, and the Cullin-containing APC2 (Yu, Peters et al. 1998, Zachariae, Shevchenko et al. 1998, Leverson, Joazeiro et al. 2000). Indeed, under specific conditions, APC2 and APC11, together with E1 and E2 enzymes Ubc4 or UbcH10, are sufficient to reconstitute the ligase activity of the human APC/C *in vitro*, albeit with a lack of substrate specificity (Gmachl, Gieffers et al. 2000, Tang, Li et al. 2001). However, one group has also demonstrated that yeast Apc11 is sufficient to ubiquitylate Clb2p, a B-type Cyclin, *in vitro* independently of Apc2 (Leverson, Joazeiro et al. 2000).

The APC/C uses two types of E2 ubiquitin-conjugating enzymes: a chain-initiating E2, UbcH10 in humans and Ubc4 in yeast, and a chain-elongating E2, such as the human UBE2S and yeast Ubc1 (Rodrigo-Brenni and Morgan 2007, Pines 2011, Primorac and Musacchio 2013, Meyer and Rape 2014). Although UbcH10 is traditionally associated with ubiquitin linkage via the K11 moiety, it has also been suggested to form K48- and K63-linkages (Kirkpatrick, Hathaway et al. 2006, Williamson, Banerjee et al. 2011). Further ubiquitin molecules are then added to form K11-polyubiquitin chains under the influence of UBE2S (Garnett, Mansfeld et al. 2009, Williamson, Wickliffe et al. 2009, Wu, Merbl et al. 2010, Wickliffe, Lorenz et al. 2011). Although these K11-polyubiquitin chains are the traditional degradation signal for APC/C substrates, multiple monoubiquitin tags formed by UbcH10 have also been shown to mediate the degradation of Cyclin B1 (Dimova, Hathaway et al. 2012).

In *S. cerevisiae*, however, K48 chains are predominantly formed through initiation by Ubc4, followed by elongation under Ubc1 (Rodrigo-Brenni and Morgan 2007, Rodrigo-Brenni, Foster et al. 2010). This is a major difference between lower and higher eukaryotic APC/C, and has great implications for further control of substrate stability by DUBs, considering DUBs in yeast and humans must therefore recognise different ubiquitin chains.

Several consensus motifs containing the lysine for the initial ubiquitylation have been described upon the substrate. These are the KEN motif, also utilised for substrate recognition, in particular an SKEN variant, and the linear TEK motif, which has been shown to permit nucleation of ubiquitin chains in Securin (Jin, Williamson et al. 2008, Min, Mayor et al. 2013). Although this TEK motif is conserved in Geminin and Cyclin B1 and has been suggested to be important for APC/C binding and as a ubiquitin acceptor, other authors have suggested, albeit without peer-reviewed publication of data, that it is irrelevant for the APC/C-dependent ubiquitylation and degradation of Cyclin B1 (Pines 2011).

Other ubiquitylation initiation motifs have also been characterised. A series of positively charged amino acids that lie in proximity to the canonical RxxL and KEN motifs have been deemed to be important for the APC/C-dependent ubiquitylation of Geminin and PAF (Williamson, Banerjee et al. 2011). The authors further demonstrate that this initial ubiquitylation acts as the rate-limiting step for the formation of polyubiquitin chains and substrate degradation (Williamson, Banerjee et al. 2011). Interestingly, Jin *et al.* postulated that it is not the linear TEK tripeptide itself which is essential, but the tertiary structure formed by neighbouring charged amino acids (Jin, Williamson et al. 2008).

In addition to their role in substrate recognition, co-activators also appear to be necessary for the stimulation of APC/C activity. The substrate NEK2A, which avoids SAC-inhibition of the APC/C by binding the APC/C directly, does not require Cdc20-mediated recognition, but does require the N-terminal C-box interaction with APC2 (Kimata, Baxter et al. 2008), although Cdc20 needs to be dephosphorylated in order for this activation to occur (Labit, Fujimitsu et al. 2012).

Similarly, the binding of Cdh1 to the APC/C can activate the complex (Pines 2011, Primorac and Musacchio 2013). In humans and *Xenopus*, this is thought to be mediated by a conformational change in the platform subunits of the APC/C, which is proposed to facilitate the transfer of ubiquitin from the E2-conjugating enzyme to the substrate (Dube, Herzog et al. 2005, Herzog, Primorac et al.

2009, Buschhorn, Petzold et al. 2011). Indeed, this was subsequently verified by two separate groups: Chang and colleagues used higher resolution 3D imaging, in which the N-terminal domain of Cdh1 caused a movement within the platform to force the APC2-APC11 catalytic domain upwards, facilitating an interaction with the E2, UbcH10 (Chang, Zhang et al. 2014); Van Voorhis and Morgan, however, adopted a biochemical approach, demonstrating that both E2 sensitivity and catalytic rate increased significantly upon co-activator-APC/C interaction, and was dependent upon substrate degron recognition (Van Voorhis and Morgan 2014). Strikingly, this allosteric transition following Cdh1 binding is not seen by budding yeast APC/C, and thus appears to be a metazoan-specific phenomenon (da Fonseca, Kong et al. 2011).

1.4. The APC/C as a cell cycle regulator

1.4.1. The APC/C is inhibited by the Spindle Assembly Checkpoint

During prophase and prometaphase stages of mitosis, DNA condenses into chromosomes, consisting of sister chromatids joined at the kinetochore and held together by centromeric Cohesin (Nasmyth 2011). During metaphase, these chromosomes align upon the equator of the cell under the influence of microtubules, known as KT fibres, emanating from centrosomes and contacting the kinetochore (Inoue and Sato 1967). These KT fibres can form four types of attachments: amphitelic, monotelic, syntelic and merotelic (Figure Int.3A)(Musacchio and Salmon 2007). In monotelic attachments, only one sister chromatid kinetochore is bound to microtubules (Figure Int.3Ai), whilst in syntelic attachments KT fibres from one centrosome bind kinetochores from both sister chromatids (Figure Int.3Aii). Similarly, merotelic attachments occur when one centrosome binds both kinetochores, whilst the other centrosome only binds one kinetochore (Figure Int.3Aiii)(Musacchio and Salmon 2007). In each of these cases, the Spindle Assembly Checkpoint (SAC) is activated to prevent cell cycle progression, thus preventing inappropriate sister chromatid segregation which would result in aneuploidy. The SAC is exceptionally sensitive, such that one single unattached kinetochore is sufficient to halt cell division (Rieder, Cole et al. 1995, Musacchio and Salmon 2007). Despite this sensitivity, rather than an all-or-nothing response, the SAC has been described as a rheostat, *i.e.* fewer unattached kinetochores results in a lesser inhibitory signal (Collin, Nashchekina et al. 2013).

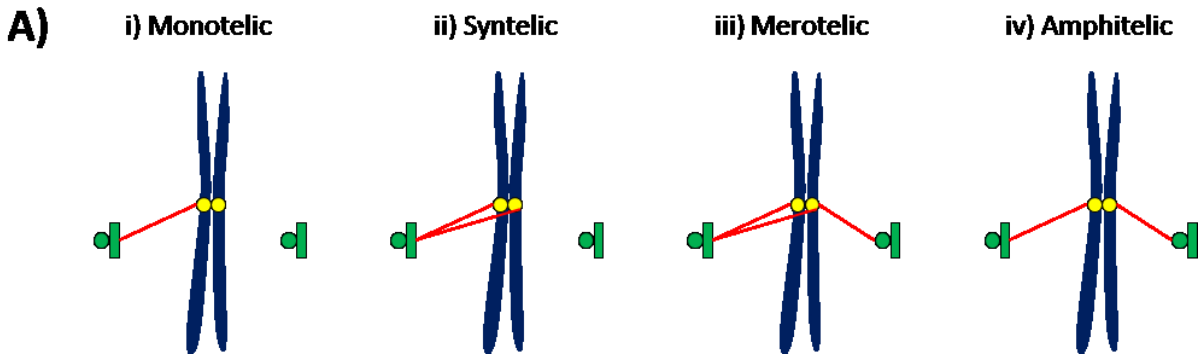

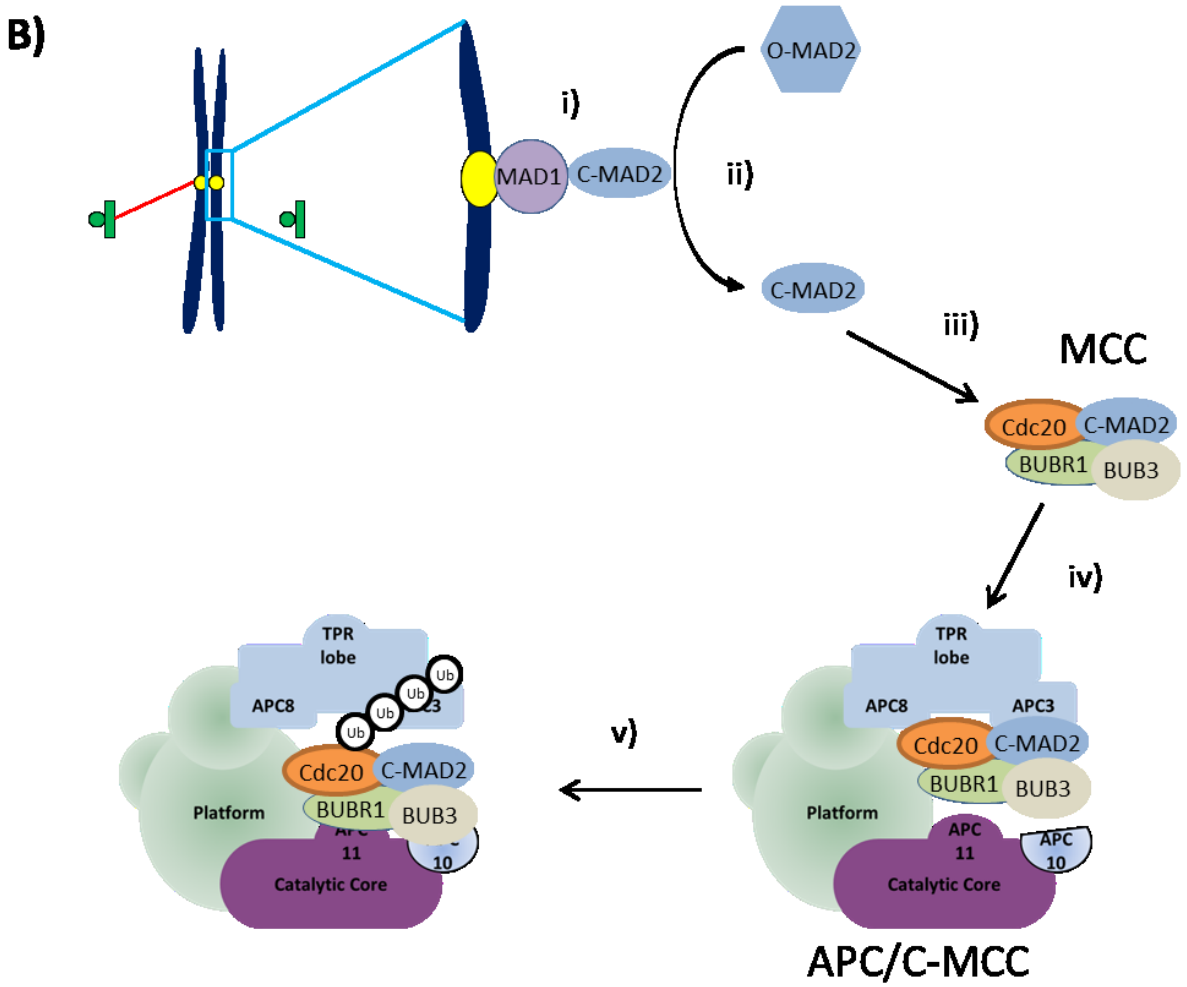

Figure Int.3 –Microtubule attachment to sister chromatid kinetochores and activation of the SAC

A) Types of microtubule attachments. Sister chromatids (blue) are shown with kinetochores (yellow). Centrosomes are shown in green, and microtubules in red (NB – for simplicity, only one microtubule per centrosome/kinetochore is shown).

i) Monotelic: one unattached kinetochore
ii) Syntelic: both kinetochores attached to microtubules from the same centrosome
iii) Merotelic: one kinetochore correctly attached, the other bound to microtubules from both centrosomes
iv) Amphitelic: correct attachment of both kinetochores to microtubules from one centrosome only

B) i) Unattached kinetochores recruit MAD1 (lilac) which recruits MAD2 in a closed conformation (light blue). ii) MAD1/C-MAD2 produces diffusible C-MAD2 which associates into the MCC (iii). iv) MCC binds and inhibits substrate recruitment into the APC/C. v) Cdc20 is ubiquitylated by the APC/C.

The SAC signal is thought to derive from a MAD1-MAD2 dimer which is present upon unattached kinetochores. MAD1 localised to unattached kinetochores binds to MAD2, causing a change in its 3D structure such that it resides in a "closed" conformation (C-MAD2; Figure Int.3Bi) (Luo, Tang et al. 2002, Sironi, Mapelli et al. 2002). MAD1-C-MAD2 dimers interact with another MAD2 protein, inducing a further conformational change in this second MAD2 to form free C-MAD2 (Figure Int.3Bii), which is capable of binding Cdc20 and results in APC/C inhibition (De Antoni, Pearson et al. 2005, Lad, Lichtsteiner et al. 2009).

The main effector mechanism of the SAC is termed the Mitotic Checkpoint Complex (MCC), which in mammals consists of MAD2, BUB3, BUBR1 (Mad3 in budding yeast) and Cdc20 (Figure Int.3Biii), which together inhibit the APC/C (Figure Int.3Biv), thereby preventing Securin degradation and the onset of anaphase (Sudakin, Chan et al. 2001, Tang, Bharadwaj et al. 2001). However, an alternative effector has been described, termed the BBC (BUBR1/BUB3/Cdc20), which requires MAD2 for its formation, but binds and inhibits the APC/C independently of MAD2 (Nilsson, Yekezare et al. 2008, Kulukian, Han et al. 2009, Lara-Gonzalez, Scott et al. 2011). The BBC has been proposed to be formed by the activity of $p31^{Comet}$, which can remove MAD2 from free MCC (Westhorpe, Tighe et al. 2011).

The MCC was originally thought to bind and sequester Cdc20, thus preventing APC/C-Cdc20 complex formation (Musacchio and Salmon 2007). However, further research showed the binding of the MCC/BBC to the APC/C via APC8 resulted in APC/C-mediated ubiquitylation and degradation of Cdc20 (Figure Int.3Bv) (Pan and Chen 2004, Nilsson, Yekezare et al. 2008, Ge, Skaar et al. 2009, Kulukian, Han et al. 2009, Primorac and Musacchio 2013). Interestingly, the APC/C subunit, APC15, is required for this SAC-dependent ubiquitylation of Cdc20, but not for its targeting for degradation by APC/C-Cdh1 during interphase (Mansfeld, Collin et al. 2011, Foster and Morgan 2012, Uzunova, Dye et al. 2012).

The MCC/BBC also inhibits the APC/C by acting as a pseudosubstrate, preventing the recruitment of *bona fide* substrates via the KEN boxes within BUBR1 (Sudakin, Chan et al. 2001, Burton and Solomon 2007, King, van der Sar et al. 2007, Lara-Gonzalez, Scott et al. 2011, Chao, Kulkarni et al. 2012). Structural studies have further shown that binding of the MCC to the APC/C causes conformational changes, such that Cdc20 and APC10 can no longer function cooperatively as the bipartite substrate recognition module, thus preventing substrate binding (Herzog, Primorac et al. 2009, Chao, Kulkarni et al. 2012, Chang, Zhang et al. 2014). Furthermore, alteration of the APC2-APC11 structure by the MCC was suggested to reduce its flexibility and decrease affinity for the E2 enzyme, UbcH10 (Herzog, Primorac et al. 2009, Chang, Zhang et al. 2014).

Another protein related to MAD2, termed MAD2L2, was shown to bind MAD2, but not MAD1, and sequester and inhibit Cdh1 during early mitosis (Listovsky and Sale 2013). Interestingly, MAD2L2 can bind and inhibit Cdh1 *in vitro* and in *Xenopus* extracts, however there is conflicting evidence regarding its ability to bind Cdc20 (Chen and Fang 2001, Pfleger, Salic et al. 2001, Listovsky and Sale 2013).

The role of DNA damage proteins in mitosis is currently under a great deal of investigation, in particular with regard to the inhibition of the DNA damage response on chromosomal arms during mitosis (Cesare 2014, Silva, Stambaugh et al. 2014). However, some DNA damage response proteins have been implicated in containing a damage-independent function during mitosis, particularly ATM. Indeed, recent evidence has suggested that ATM regulates correct spindle assembly and the spindle checkpoint (Eliezer, Argaman et al. 2014, Palazzo, Della Monica et al. 2014, Yang, Hao et al. 2014). ATM-dependent phosphorylation of MAD1 promotes MAD2 binding whilst phosphorylation of γH2AX on kinetochores recruits MDC1 (Eliezer, Argaman et al. 2014, Yang, Hao et al. 2014). MDC1 has previously been demonstrated to be a novel binding partner and regulator of APC/C activity (Coster, Hayouka et al. 2007, Townsend, Mason et al. 2009, Eliezer, Argaman et al. 2014). Interestingly, MDC1

has been shown to bind MAD2, and has been suggested to facilitate the incorporation of Cdc20 into the MCC, thus promoting the SAC (Eliezer, Argaman et al. 2014). Furthermore, ablation of MDC1 accelerates mitotic progression, supposedly due to inappropriate sister chromatid separation and an early anaphase onset (Eliezer, Argaman et al. 2014), although an alternative study has demonstrated that MDC1 knockdown lengthens the mitotic phase through inhibition of APC/C activity (section 1.3.3)(Townsend, Mason et al. 2009).

The APC/C is not completely inhibited during the SAC, however. The substrates NEK2A, HOXC10 and Cyclin A have mechanisms by which they can evade the SAC such that they are still ubiquitylated despite MCC inhibition of the APC/C (den Elzen and Pines 2001, Geley, Kramer et al. 2001, Hames, Wattam et al. 2001, Gabellini, Colaluca et al. 2003, Hayes, Kimata et al. 2006). For Cyclin A, this is mediated by the Cyclin-dependent kinase cofactor Cks; the N-terminal region of Cyclin A dislodges the MCC from Cdc20, and Cks permits Cdc20-Cyclin A binding to the APC/C via an interaction with phosphorylated APC3, resulting in Cyclin A ubiquitylation (Sudakin, Shteinberg et al. 1997, Wolthuis, Clay-Farrace et al. 2008, Di Fiore and Pines 2010). Intriguingly, Cks also permits the binding of Cyclin B1 to the APC/C through APC3. This does not result in its ubiquitylation, although it primes Cyclin B1 for timely degradation upon satisfaction of the SAC (van Zon, Ogink et al. 2010). Another protein, Apollon, has also been shown to interact with the APC/C and promote its ubiquitylation and degradation of Cyclin A during the SAC (Kikuchi, Ohata et al. 2014). Whereas Cks targets Cyclin A/Cdk1 to the APC/C, Apollon binds free Cyclin A, leading the authors to suggest that Cks and Apollon act cooperatively to ensure Cyclin A destruction during the SAC (Kikuchi, Ohata et al. 2014).

NEK2A has evolved a different mechanism for avoiding the SAC. Rather than using accessory binding factors, the C-terminus of NEK2A contains a methionine-arginine (M-R) dipeptide, similar to the I-R motif of Cdc20 and Cdh1, which is necessary for binding to the APC/C independently of Cdc20 (Hayes, Kimata et al. 2006). Although it is not required for binding, Cdc20 does appear to be

necessary for the degradation of NEK2A through its C-box interaction (Kimata, Baxter et al. 2008). Unlike Cyclin A, NEK2A cannot outcompete the MCC in affinity for the APC/C-Cdc20, instead it requires the formation of homodimers, which bind to APC/C uninhibited by the MCC and unbound by co-activator, termed apo-APC/C (Sedgwick, Hayward et al. 2013). Interestingly, an L-R dipeptide motif is present at the C-terminus of the APC/C-Cdc20 substrate, KIF18A, which is necessary for its degradation (Sedgwick, Hayward et al. 2013). Like Cyclin B1, KIF18A associates with the APC/C during the SAC, but is only degraded following the onset of anaphase, suggesting the interaction between APC/C and KIF18A during prometaphase does not result in ubiquitylation, and instead might increase the efficiency of its degradation upon APC/C-Cdc20 activation (Sedgwick, Hayward et al. 2013).

Although the MCC acts as a potent inhibitor of the APC/C, recent evidence has suggested a minor population of the APC/C which is activated by Cdh1 during metaphase (Nagai and Ushimaru 2014). In addition, it was proposed that APC/C-Cdh1 was capable of ubiquitylating Cdc20 during metaphase arrest, and it was suggested that the MCC also inhibits Cdh1 (Nagai and Ushimaru 2014). This would indicate that there is low basal APC/C-Cdh1 activity throughout mitosis, which is capable of degrading APC/C substrates despite SAC activation, opposing all current hypotheses and tenets regarding Cdh1 in mitosis (Pines 2011, Primorac and Musacchio 2013).

A: APC/C Substrates			
Protein	UniProt ID	Gene	Reference
Cdc20	Q12834	CDC20	(Nilsson, Yekezare et al. 2008)
Cyclin A	P20248	CCNA2	(Sudakin, Ganoth et al. 1995, Geley, Kramer et al. 2001)
HOXC10	Q9NYD6	HOXC10	(Gabellini, Colaluca et al. 2003)
NEK2A	P51955	NEK2	(Hames, Wattam et al. 2001)
B: APC/C Inhibitors			
Protein	UniProt ID	Gene	Reference
BUB3	O43684	BUB3	(Sudakin, Chan et al. 2001)
BUBR1	O60566	BUB1B	(Sudakin, Chan et al. 2001)
MAD2	Q13257	MAD2L1	(Sudakin, Chan et al. 2001)
MAD2L2	Q9UI95	MAD2L2	(Chen and Fang 2001, Pfleger, Salic et al. 2001, Listovsky and Sale 2013)
MDC1*	Q14676	MDC1	(Eliezer, Argaman et al. 2014)
C: Other APC/C Interactors			
Protein	UniProt ID	Gene	Reference
Apollon	Q9NR09	BIRC6	(Kikuchi, Ohata et al. 2014)
Cks	P61024	CKS1B	(Wolthuis, Clay-Farrace et al. 2008)
Cyclin B1**	P14635	CCNB1	(van Zon, Ogink et al. 2010)
KIF18A**	Q8NI77	KIF18A	(Sedgwick, Hayward et al. 2013)

Table 3: Substrates (A), inhibitors (B) and other interactors (C) of the human APC/C during the SAC

*MDC1 has been shown to promote the SAC by facilitating the incorporation of Cdc20 into the MCC (Eliezer, Argaman et al. 2014), although it has also been described as an activator of the APC/C (Townsend, Mason et al. 2009).

** Although Cyclin B1 and KIF18A are both APC/C substrates, their association with the APC/C during the SAC does not result in their degradation (van Zon, Ogink et al. 2010, Sedgwick, Hayward et al. 2013)

1.4.2. SAC reactivates the APC/C

Upon correct microtubule attachment at the kinetochores, *i.e.* an amphitelic attachment in which one centrosome contacts one sister chromatid only (Figure Int.3iv), in a bi-orientated manner, the SAC is silenced (Musacchio and Salmon 2007). The amount of MAD2 decreases at attached kinetochores under dynein-mediated relocalisation, thereby preventing nascent MCC formation (Waters, Chen et al. 1998, Musacchio and Salmon 2007, Foley and Kapoor 2013, Jia, Kim et al. 2013). However, if attachment were the only condition to satisfy the SAC, syntelic microtubule arrangements would result in anaphase progression. In these conditions the SAC remains active due to a second checkpoint: the absence of tension between sister chromatids (Musacchio and Salmon 2007). Microtubules are destabilised at kinetochores in both syntelic and merotelic attachments by Aurora B kinase, thus maintaining the SAC (Musacchio and Salmon 2007, Jia, Kim et al. 2013). The SAC is partly switched off by the localised activity of protein phosphatase, PP1, which removes this Aurora B-mediated phosphorylation of the kinetochores, thereby silencing their pro-SAC signalling, as well as counteracting other kinase activity, such as MPS1 (Foley and Kapoor 2013, Jia, Kim et al. 2013).

The production of free C-MAD2 is inhibited at attached kinetochores by the activity of $p31^{Comet}$, which binds and caps the MAD1-C-MAD2 dimer, as well as causing the disassembly of cytosolic, diffusible MCC (Habu, Kim et al. 2002, Reddy, Rape et al. 2007, Yang, Li et al. 2007, Jia, Kim et al. 2013, Primorac and Musacchio 2013). This interaction with the MCC is regulated by the ATPase TRIP13, and is also modulated by phosphorylation, such that phosphorylated $p31^{Comet}$ has decreased affinity for MAD2 in early mitosis (Date, Burrows et al. 2014, Eytan, Wang et al. 2014, Wang, Sturt-Gillespie et al. 2014). Interestingly, another protein, CUEDC2, has also been suggested to be important in the release of Cdc20 from MAD2 (Gao, Li et al. 2011). As discussed earlier, the ubiquitylation of Cdc20 in an APC15-dependent manner causes its release from the MCC, and targets it for degradation as part

of the SAC (Mansfeld, Collin et al. 2011, Foster and Morgan 2012, Uzunova, Dye et al. 2012, Primorac and Musacchio 2013). However, this ubiquitylation is also necessary to reactivate Cdc20 following SAC satisfaction, as it causes disassembly of the MCC concomitant with the prevention of nascent MCC formation, thus preventing further free Cdc20 molecules from becoming inhibited (Reddy, Rape et al. 2007). Furthermore, the ubiquitylation of Cdc20 is counteracted by the DUB USP44, which protects Cdc20 from proteasomal degradation, permitting its reactivation of the APC/C following MCC disassembly (Stegmeier, Rape et al. 2007).

1.4.3. The APC/C promotes sister chromatid separation

Upon silencing of the SAC, APC/C-Cdc20 ubiquitylates Securin and Cyclin B1, resulting in their degradation by the 26S proteasome (Pines 2011, Primorac and Musacchio 2013). The degradation of Securin relieves its inhibition of Separase, which is then free to cleave the Scc1/RAD21 subunit of Cohesin (Ciosk, Zachariae et al. 1998, Jensen, Segal et al. 2001, Stemmann, Zou et al. 2001, Hornig, Knowles et al. 2002, Waizenegger, Gimenez-Abian et al. 2002). This opens the Cohesin ring surrounding the centromere, allowing KT-fibres to pull sister chromatids towards opposite poles, marking the start of anaphase.

Another method of Separase inhibition must exist, however, as cells not expressing Securin still exhibit timely Cohesin degradation and anaphase onset (Jallepalli, Waizenegger et al. 2001, Mei, Huang et al. 2001, Wang, Yu et al. 2001). This is believed to be regulated by Cyclin B1/Cdk1, which inhibits Separase through phosphorylation during early mitosis when Cdk activity is high (Stemmann, Zou et al. 2001, Gorr, Boos et al. 2005). Upon SAC satisfaction, Cyclin B1 is ubiquitylated by APC/C-Cdc20 and is degraded, thereby inactivating Cdk1 (Pines 2011, Primorac and Musacchio 2013). Furthermore, protein phosphatases such as PP1 and Cdc14 counteract Cdk1, removing its inhibitory phosphorylation of Separase and permitting Cohesin cleavage, as well as activating Cdc25 (Skoufias, Indorato et al. 2007, Tumurbaatar, Cizmecioglu et al. 2011).

Another complex has been described which augments APC/C activity to promote the onset of anaphase. The spindle and kinetochore-associated (Ska) complex has been shown to be necessary for accurate mitotic degradation of Cyclin B1 and Securin, perhaps due to Ska complex-mediated localisation of the APC/C to chromosomes, thus enhancing the ubiquitylation of APC/C substrates (Sivakumar, Daum et al. 2014).

Although necessary for APC/C activity, the cellular pool of the E2, UbcH10, becomes depleted during G1 phase due to its ubiquitylation by APC/C-Cdh1 (Rape and Kirschner 2004). However, its transcription is activated by the APC/C-Cdc20 together with CBP/p300, thereby replenishing the cellular supply of UbcH10 such that the APC/C can become fully active upon SAC satisfaction (Nath, Banerjee et al. 2011).

As mentioned in section 1.3.1, MDC1 has been suggested to ensure appropriate SAC signalling through recruitment of Cdc20 in the MCC (Eliezer, Argaman et al. 2014). However a different group have demonstrated that MDC1 interacted with numerous APC/C subunits, and potentiated APC/C activity *in vivo* (Townsend, Mason et al. 2009). Contrary to more recent evidence, this study demonstrated that ablation of MDC1 expression increased the number of cells in mitosis, delayed the metaphase-anaphase transition and decreased the interaction between APC/C and Cdc20 (Townsend, Mason et al. 2009, Eliezer, Argaman et al. 2014). As such, MDC1 was suggested to be a bridging factor for Cdc20 and the APC/C, thereby controlling faithful mitotic progression upon SAC satisfaction (Townsend, Mason et al. 2009).

A: APC/C Substrates			
Protein	UniProt ID	Gene	Reference
Cyclin A	P20248	CCNA2	(Sudakin, Ganoth et al. 1995, Geley, Kramer et al. 2001)
Cyclin B1	P14635	CCNB1	(King, Peters et al. 1995, Sudakin, Ganoth et al. 1995)
Securin	Q5FBB7	PTTG1	(Zou, McGarry et al. 1999)
B: APC/C Activators			
Protein	UniProt ID	Gene	Reference
CBP	Q92793	CREBBP	(Nath, Banerjee et al. 2011)
MDC1	Q14676	MDC1	(Townsend, Mason et al. 2009)
P300	Q09472	EP300	(Nath, Banerjee et al. 2011)
Ska3	Q8IX90	SKA3	(Sivakumar, Daum et al. 2014)

Table 4: Substrates (A) and activators (B) of the human APC/C-Cdc20 during the metaphase-anaphase transition.

1.4.4. The APC/C coordinates mitotic exit

Upon the onset of anaphase, Cdh1 becomes reactivated due to the decrease in Cdk activity promoted by the controlled degradation of Cyclin B1 by APC/C-Cdc20 (Pines 2011). APC/C-Cdc20 also initiates the degradation of the Cdh1-sequestering protein, MAD2L2, during anaphase, thus relieving further inhibition of Cdh1 (Listovsky and Sale 2013). The APC/C then exhibits a co-activator switch from Cdc20 to Cdh1 (Hagting, Den Elzen et al. 2002, Pines 2011). This allows Cdh1-mediated activation of the APC/C, and targets substrates for degradation to promote mitotic exit (Kramer, Scheuringer et al. 2000, Peters 2006, Pines 2011). One of the key targets of APC/C^{Cdh1} is Cdc20, which ensures a rapid transition from Cdc20- to Cdh1-activated APC/C (Shirayama, Zachariae et al. 1998, Robbins and Cross 2010). Interestingly, some APC/C substrates in mitosis are able to be ubiquitylated by either Cdh1 or Cdc20. APC/C-Cdc20 and APC/C-Cdh1 both target the degradation of Cyclins A and B1, ensuring that Cdk activity remains low from anaphase throughout late mitosis and into the next G1 (Peters 2006, van Leuken, Clijsters et al. 2008, Pines 2011). Cdh1-specific substrates are targeted in late mitosis, however, including those whose inactivation is required for mitotic exit, including Aurora A and B kinases, UbcH10 and Plk1 (Lindon and Pines 2004).

The targeting of Aurora kinases by Cdh1 ensures faithful spindle formation and cytokinesis (Floyd, Pines et al. 2008). Despite this, Cdh1 is not essential for cytokinesis, as Cdh1 knockout only produces a mild phenotype resulting from prolonged Aurora A activity (Floyd, Pines et al. 2008). However, problems arise upon entering the next S phase, since Cdh1 plays an important role in replication licensing. The cells also develop chromosomal defects and exhibit aneuploidy, demonstrating that Cdh1 promotes genetic stability (Engelbert, Schnerch et al. 2008, Garcia-Higuera, Manchado et al. 2008).

As previously mentioned, DNA damage proteins have recently been identified as mitotic regulators. Two damage proteins have been described as becoming APC/C targets during mitosis: FAN1 nuclease

and RAP80 (Cho, Lee et al. 2012, Lai, Hu et al. 2012). FAN1 nuclease functions in interstrand crosslink repair, and is targeted by APC/C-Cdh1, whilst RAP80, which localises BRCA1 to damage foci, can be ubiquitylated by either APC/C-Cdc20 or APC/C-Cdh1 (Cho, Lee et al. 2012, Lai, Hu et al. 2012). Although their mitotic function is unknown, overexpression of either FAN1 or RAP80 delays mitotic progression, whilst their knockdown accelerates mitotic exit, suggesting that they act as novel regulators of mitosis (Cho, Lee et al. 2012, Lai, Hu et al. 2012). It is therefore possible that in the future, the mitotic functions of other DNA damage proteins will be elucidated.

APC/C Substrates			
Protein	UniProt ID	Gene	Reference
Aurora A	O14965	AURKA	(Honda, Mihara et al. 2000, Taguchi, Honda et al. 2002)
Aurora B	Q96GD4	AURKB	(Stewart and Fang 2005, Feine, Zur et al. 2007)
Cdc20	Q12834	CDC20	(Robbins and Cross 2010)
Cyclin A	P20248	CCNA2	(Sudakin, Ganoth et al. 1995, Geley, Kramer et al. 2001)
Cyclin B1	P14635	CCNB1	(King, Peters et al. 1995, Sudakin, Ganoth et al. 1995)
FAN1	Q9Y2M0	FAN1	(Lai, Hu et al. 2012)
MAD2L2	Q9UI95	MAD2L2	(Listovsky and Sale 2013)
Plk1	P53350	PLK1	(Lindon and Pines 2004)
RAP80	Q96RL1	UIMC1	(Cho, Lee et al. 2012)
UbcH10	O00762	UBE2C	(Rape and Kirschner 2004)

Table 5: Substrates of the human APC/C during post-anaphase mitosis.

1.4.5. The APC/C prevents early S phase entry

Following cytokinesis, APC/C-Cdh1 remains active to coordinate the subsequent G1 phase of the cell cycle. Under the control of Cdh1, the APC/C mediates the degradation of a number of S-phase-promoting proteins such as Cyclin A, Skp2, Geminin, Ets2 and Tome-1, thereby arresting the cell cycle and preventing S phase entry until the correct signalling mechanisms have been activated (Peters 2006, Li, Shin et al. 2008, van Leuken, Clijsters et al. 2008, Pines 2011). There is also evidence for the APC/C-mediated degradation of Cyclin D1, although this can also be targeted by SCF E3 ubiquitin ligases (Agami and Bernards 2000, Pawar, Sarkar et al. 2010).

It has been suggested that Cdh1 and the Retinoblastoma protein, Rb, function redundantly to control the G1/S transition (Fay, Keenan et al. 2002). Amongst its numerous functions, Rb has been shown to halt S phase progression via the inhibition of two major pro-proliferative proteins, Skp2 and E2F (Dick and Rubin 2013). Hypophosphorylated Rb binds Skp2 and directly inhibits its ubiquitylation of target substrates, resulting in the stabilisation of the Cdk inhibitor (CKI) p27, thereby inhibiting Cdk activity and halting cell cycle progression (Ji, Jiang et al. 2004). However, an alternate mechanism for the inhibition of Skp2 by Rb has been suggested, in which Rb acts as a molecular bridge, presenting Skp2 to the APC/C as a substrate, thereby potentiating APC/C ubiquitylation of Skp2 and stabilising $p27^{Kip1}$ (Binné, Classon et al. 2007). Another Rb family member, p107, has also been shown to downregulate Skp2 protein levels (Rodier, Makris et al. 2005).

Rb also prevents entry into S phase by repressing the activity of E2F transcription factors through binding to their transactivation domains, preventing their transcription of target genes such as Cyclin A, Cyclin E and Emi1 (Chellappan, Hiebert et al. 1991, Hiebert, Chellappan et al. 1992, Dick and Rubin 2013). Furthermore, Rb-E2F complexes are also able to silence DNA through chromatin remodelling by the recruitment of histone deacetylases (HDACs) and SWI/SNF complexes (Brehm, Miska et al. 1998, Luo, Postigo et al. 1998, Magnaghi-Jaulin, Groisman et al. 1998, Zhang and Dean 2001), as well

as binding Polycomb proteins, methyltransferases and co-repressors (Lai, Lee et al. 1999, Meloni, Smith et al. 1999, Dahiya, Wong et al. 2001, Nielsen, Schneider et al. 2001). The Rb family proteins, p107 and p130, are also capable of keeping Cdk2 activity low by binding Cyclin E/Cdk2 and Cyclin A/Cdk2 complexes directly, resulting in their inhibition (Giacinti and Giordano 2006). Interestingly, ablation of APC/C-Cdh1 activity also results in amplification of E2F-mediated transcription of Cyclin E, as well as increased degradation of $p27^{Kip1}$, suggesting that Cdh1 might also influence the inhibition of E2F (Sorensen, Lukas et al. 2000). Further inhibition of the E2F transcription factors, E2F1 and E2F3, have been suggested to be mediated through their ubiquitylation by APC/C-Cdc20 in metaphase followed by APC/C-Cdh1 (Peart, Poyurovsky et al. 2010, Budhavarapu, White et al. 2012, Ping, Lim et al. 2012).

The APC/C also targets Cdc6 and Cdt1 for degradation during early G1 (Petersen, Wagener et al. 2000, Sugimoto, Kitabayashi et al. 2008). These are important in replication licensing (see below), and their degradation prevents the formation of the pre-replication complex upon origins of replication until suitable mitogenic signals stimulate the cell to continue with the cell cycle (Sacco, Hasan et al. 2012).

1.4.6. APC/C-Cdh1 is inhibited to promote S phase progression

The APC/C-Cdh1 holds cells within G1 until suitable mitogenic signals results in its inactivation (Pines 2011). Positive growth signals stimulate pathways such as Ras-MAPK, resulting in downstream kinases such as MEK and ERK becoming activated and phosphorylating downstream targets, including Ets2 (Rivard, Boucher et al. 1999). Mitogenic stimulation induces the transcription and stabilisation of Cyclin D1, which then forms complexes with, and activates, Cdk4 and Cdk6 (Hitomi and Stacey 1999, Anderson, Child et al. 2010). Cyclin D/Cdk4 and Cyclin D/Cdk6 then phosphorylate Rb on a number of

residues, causing a conformational change which releases its repressive binding to E2F and Skp2, thus alleviating its cell cycle inhibition (Dowdy, Hinds et al. 1993, Sherr 1994).

The activation of E2F transcription factors results in the expression of a number of S phase-promoting proteins. One important protein which is expressed in response to E2F is Emi1 (Early Mitotic Inhibitor 1), which inhibits APC/C-Cdh1 (Hsu, Reimann et al. 2002). Emi1 inhibits the APC/C-Cdh1 by acting as a pseudosubstrate, thereby blocking the recognition of *bona fide* substrates (Miller, Summers et al. 2006). More recent studies have suggested molecular mechanisms for the inhibitive features of Emi1; substrate binding is prevented through the interference of the WD40 propeller of Cdh1 (Frye, Brown et al. 2013). Moreover, Emi1 was also shown to inhibit the binding of the E2, Ube2S, through modulation of the APC/C platform, thus preventing polyubiquitin chain formation (Frye, Brown et al. 2013, Wang and Kirschner 2013). Intriguingly, binding of Emi1 to APC/C-Cdh1 causes a similar conformational change to that exhibited by APC/C-Cdh1-substrate and APC/C-MCC complexes, which is necessary for APC/C activation by Cdh1 (Chang, Zhang et al. 2014).

Cyclin E is similarly transcribed under the control of an E2F promoter, whereupon it binds Cdk2 to form an active Cyclin E/Cdk2 complex (Koff, Cross et al. 1991, Dulić, Lees et al. 1992, Koff, Giordano et al. 1992, Duronio and O'Farrell 1995, Ohtani, DeGregori et al. 1995, Rizzardi and Cook 2012). Cyclin E/Cdk2 phosphorylates Rb (Hinds, Mittnacht et al. 1992, Zhang and Kumar 1994, Rizzardi and Cook 2012), providing a greater inhibitive signal than that mediated by D-type Cyclins alone (Lundberg and Weinberg 1998), as well as phosphorylating Skp2 to aid its escape from APC/C-Cdh1-mediated ubiquitylation and degradation (Rodier, Coulombe et al. 2008). Interestingly, Skp2 can also be phosphorylated and protected from degradation by Akt1 upon mitogenic stimulation (Gao, Inuzuka et al. 2009, Gao, Inuzuka et al. 2009). Cyclin E/Cdk2 is also capable of phosphorylating $p21^{Cip1}$ and $p27^{Kip1}$, resulting in their SCF^{Skp2}-mediated proteasomal degradation (Carrano, Eytan et al. 1999, Tsvetkov, Yeh et al. 1999, Rizzardi and Cook 2012). This alleviates their inhibition of Cyclin/Cdk

complexes, thereby permitting increased formation of S-phase promoting complexes of Cyclin E/Cdk2 and Cyclin A/Cdk2 (Rizzardi and Cook 2012).

Another protein under transcriptional control of E2F is Cyclin A (Henglein, Chenivesse et al. 1994). Upon E2F and Skp2 activation, Cyclin A is transcribed and translated, and activates Cdk2 (Pines and Hunter 1990, Tsai, Harlow et al. 1991). Cyclin A/Cdk2 has a number of targets, including Rb, thus further promoting its hyperphosphorylation, and Cdh1. Phosphorylation of Cdh1 causes its dissociation from the APC/C, thus rendering the complex inactive and increasing the pool of "free" unbound Cdh1 (Zachariae, Schwab et al. 1998, Lukas, Sorensen et al. 1999). This free Cdh1 can compete with hypophosphorylated E2F for binding sites upon Rb, thereby increasing the proportion of uninhibited E2F, promoting further transcription of target genes such as Cyclin A and Emi1 (Gao, Inuzuka et al. 2009). There is also evidence that phosphorylated Cdh1 is exported from the nucleus, minimising the possibility of APC/C-Cdh1 contacting its nuclear targets (Jaquenoud, van Drogen et al. 2002, Zhou, Ching et al. 2003).

E2F also promotes the transcription of the DUB, USP37 (Huang, Summers et al. 2011). USP37 binds to Cdh1 and removes APC/C-Cdh1-mediated ubiquitylation of Cyclin A in a Cdk2-dependent manner, thus promoting greater Cyclin A/Cdk2 formation and promoting entry into S phase (Huang, Summers et al. 2011). Interestingly, USP37 itself is also a substrate for the APC/C during Cdk2 inactivity, and becomes degraded upon APC/C-Cdh1 reactivation during the latter stages of mitosis (Huang, Summers et al. 2011).

Although the APC/C is actively inhibited by cellular factors, there is also evidence that it is self-limiting over time (Rape and Kirschner 2004, Pines 2011). The monoubiquitylating E2, UbcH10, is targeted for degradation by APC/C-Cdh1, and becomes progressively depleted as G1 progresses (Rape and Kirschner 2004). Furthermore, there is evidence to suggest that Cdh1 can also mediate its

own degradation (Listovsky, Oren et al. 2004), as well as being targeted by $SCF^{\beta\text{-}TrCP}$ (Fukushima, Ogura et al. 2013).

Together, these pathways represent an irreversible positive feedback loop such that phosphorylation of Rb following mitogenic stimulation triggers the expression of a series of E2F-controlled genes, including Emi1, USP37 and Cyclin A. These further phosphorylate and/or inhibit Rb and Cdh1, accelerating E2F transcription and Skp2 activation until the cell can pass the restriction point and enter S phase.

1.4.7. The APC/C and replication licencing

In most eukaryotic cells, DNA is replicated once per cell division, although exceptions occur following prolonged APC/C-Cdh1 activity in multi-nucleate bodies such as those found in early *Drosophila* embryos and in placentae (Pines 2011). In order to prevent re-replicative events, replication licensing ensures each origin of replication is only fired once per cell cycle (Arias and Walter 2007, Truong and Wu 2011, Sacco, Hasan et al. 2012). This relies upon the temporal regulation of APC/C-Cdh1 and SCF E3 ubiquitin ligases, and their mutual inhibition (Rizzardi and Cook 2012).

The pre-replication complex (pre-RC) forms upon DNA origins of replication, concomitant with sister chromatid separation in mitosis (Arias and Walter 2007, Boos, Frigola et al. 2012, Sacco, Hasan et al. 2012). The pre-RC consists of the Origin of Replication Complex (ORC), the Mini Chromosome Maintenance (MCM) hexamer MCM2-7, Cdt1 and Cdc6 (Arias and Walter 2007, Boos, Frigola et al. 2012, Sacco, Hasan et al. 2012). Firstly, the ORC is recruited to the origin, to which Cdc6 and Cdt1 bind, together with a dimeric MCM2-7 hexamer (Arias and Walter 2007, Boos, Frigola et al. 2012, Sacco, Hasan et al. 2012, Yardimci and Walter 2014). In mammalian cells, further factors are also recruited, including HMGA1, MCM8, MCM9 and HOXD13 (Sacco, Hasan et al. 2012). During G1, Cdt1

and Cdc6 render this pre-RC inactive until S-phase entry (Boos, Frigola et al. 2012, Sacco, Hasan et al. 2012).

Following hyperphosphorylation of Rb and APC/C-Cdh1 inactivation, Cdk activity, Skp2 and Geminin are stabilised, pushing cells toward S phase (Peters 2006, van Leuken, Clijsters et al. 2008, Pines 2011). Subsequently, Cdk and Ddk (Dbf4-dependent kinase) phosphorylate MCM2-7 and promote the recruitment of replication factors to DNA, including Cdc45 and GINS to form the active CMG (Cdc45-MCM-GINS) helicase, as well as MCM10 and DNA polymerase to permit replication fork progression and DNA replication (Arias and Walter 2007, Boos, Frigola et al. 2012, Sacco, Hasan et al. 2012). In vertebrates, further factors are also required for faithful initiation of DNA replication, such as Treslin, DUE-B and GEMC1, which are important for Cdc45 loading, and RecQ4, which regulates GINS recruitment (Sacco, Hasan et al. 2012).

Replication licensing can only occur during G1, and is actively inhibited during S-phase in order to prevent re-replication. During G1, the APC/C-Cdh1 mediates the degradation of Geminin; in S-phase Geminin is no longer ubiquitylated, and is thus free to bind and inhibit Cdt1 recruitment to pre-RCs (Arias and Walter 2007). Cdt1 also becomes phosphorylated by Cyclin A/Cdk2 and Cyclin E/Cdk2, targeting it for proteolysis by SCF^{Skp2}, whilst mammalian Cdt1 is also targeted by PCNA-dependent $Cul4\text{-}DDB1^{Cdt2}$ as well as APC/C-Cdh1 during late mitosis and early G1 (Arias and Walter 2007, Sugimoto, Kitabayashi et al. 2008, Sacco, Hasan et al. 2012).

Interestingly, Geminin binding to Cdt1 during mitosis can also promote pre-RC formation, since it protects Cdt1 from mitotic proteolysis by SCF^{Skp2} (Arias and Walter 2007). Although Geminin-Cdt1 binding does not prevent Cdt1 degradation by $Cul4\text{-}DDB1^{Cdt2}$, this pathway is inactivated during G2, and therefore is not an issue during mitosis (Arias and Walter 2007). Upon APC/C-Cdc20 activation during the metaphase-anaphase transition, Geminin degradation is initiated, and Cdt1 is released, however by this time Cdk activity is diminished by the APC/C and by phosphatases, whilst Skp2 is a

target for the APC/C, culminating in Cdt1 stabilisation (Arias and Walter 2007). Although the APC/C degrades Geminin, this is initially inhibited during early mitosis through its phosphorylation by Aurora A, itself a target for APC/C-mediated ubiquitylation, thus preventing SCF^{Skp2}-mediated degradation of Cdt1 until the APC/C becomes completely active and is able to inhibit Skp2 fully (Tsunematsu, Takihara et al. 2013).

Mammalian ORC also appears to be regulated in order to prevent re-replication, although the evidence for this remains inconclusive. Although the prevalent theory is that Cdk1 inhibits the ORC during mitosis, some studies have suggested that phosphorylation of ORC1 by Cyclin A/Cdk1 is sufficient to prevent its binding to chromatin through nuclear export, and indeed might promote proteolysis during S and G2 phases (Arias and Walter 2007, Sacco, Hasan et al. 2012). Conversely, other groups have shown that inhibition of Cdk activity causes no alteration in ORC1 protein levels or binding to DNA during these phases (Arias and Walter 2007). Interestingly, ORC1 in *Drosophila* is targeted for degradation by the APC/C, although this is not the case in mammals (Araki, Yu et al. 2005).

The regulation of Cdc6 by Cdk activity is also controversial. Phosphorylated Cdc6 is exported from the nucleus during S phase; however, Cdc6 can still be detected upon chromatin during this time (Arias and Walter 2007, Sacco, Hasan et al. 2012). This phosphorylation removes Cdc6 from previously-fired origins until mitosis and early G1, during which time it is targeted for degradation by APC/C-Cdh1, thus preventing another cycle of DNA replication (Petersen, Wagener et al. 2000, Sacco, Hasan et al. 2012).

A: APC/C Substrates			
Protein	UniProt ID	Gene	Reference
Cdc6	Q99741	CDC6	(Petersen, Wagener et al. 2000)
Cdh1	Q9UM11	FZR	(Listovsky, Oren et al. 2004)
Cdt1	Q9H211	CDT1	(Sugimoto, Kitabayashi et al. 2008)
Cyclin A	P20248	CCNA2	(Sudakin, Ganoth et al. 1995, Geley, Kramer et al. 2001)
Cyclin B1	P14635	CCNB1	(King, Peters et al. 1995, Sudakin, Ganoth et al. 1995)
Cyclin D1	P24385	CCND1	(Pawar, Sarkar et al. 2010)
E2F1	Q01094	E2F1	(Peart, Poyurovsky et al. 2010, Budhavarapu, White et al. 2012)
E2F3	O00716	E2F3	(Ping, Lim et al. 2012)
Ets2	P15036	ETS2	(Li, Shin et al. 2008)
Geminin	O75496	GMNN	(McGarry and Kirschner 1998)
Skp2	Q13309	SKP2	(Bashir, Dorrello et al. 2004)
Tome-1	Q99618	CDCA3	(Ayad, Rankin et al. 2003)
UbcH10	O00762	UBE2C	(Rape and Kirschner 2004)
B: APC/C Inhibitors			
Protein	UniProt ID	Gene	Reference
Cdk2	P24941	CDK2	(Lukas, Sorensen et al. 1999)
CUEDC2	Q9H467	CUEDC2	(Zhang, Zhou et al. 2013)
Emi1	Q9UKT4	FBXO5	(Hsu, Reimann et al. 2002)
USP37	Q86T82	USP37	(Huang, Summers et al. 2011)
C: Other APC/C Interactors			
Protein	UniProt ID	Gene	Reference
Rb	P06400	RB1	(Fay, Keenan et al. 2002, Binné, Classon et al. 2007)

Table 6: Substrates (A), inhibitors (B) and activators (C) of the human APC/C during interphase

1.4.8. The role of the APC/C in differentiation and G0

The majority of cells within a metazoan organism exist in a non-replicative state, having exited the cell cycle and entered into quiescence, or G0 (Manchado, Eguren et al. 2010, Eguren, Manchado et al. 2011). Re-entry into G1 is prevented by the maintenance of low levels of Cdk activity and the inhibition of pre-RC formation (Manchado, Eguren et al. 2010, Eguren, Manchado et al. 2011). Cdh1 has been shown to be necessary for exiting the cell cycle and maintaining quiescence, since Cdh1 knockdown prevents mammalian cells from entering quiescence, and APC/C inhibition in quiescent cells causes re-entry into G1 (Wirth, Ricci et al. 2004, Almeida, Bolanos et al. 2005, Garcia-Higuera, Manchado et al. 2008). In yeast the Cdh1 homologue, Hct1, is also important for G1 arrest following treatment with the pheromone, α-factor, through its degradation of Cyclin Clb2, since Hct1 mutant cells are unable to arrest (Schwab, Lutum et al. 1997).

In cycling cells, Cdh1 is inactivated and APC/C activity is repressed during G1 in order to promote the G1/S transition (Pines 2011). If these inhibitory events do not occur, for example due to withdrawal of mitogenic stimuli or the presence of anti-proliferative signals, the cell will enter quiescence (Manchado, Eguren et al. 2010, Eguren, Manchado et al. 2011). This has been shown to rely upon the interaction between Cdh1 and Rb, specifically through the enhancement of Skp2 degradation, as seen during normal G1 phase (Binné, Classon et al. 2007). Indeed, signalling by the mitotic inhibitor TGF-β (Transforming Growth Factor β) results in the APC/C-mediated proteolysis of Skp2 (Liu, Wu et al. 2007). The APC/C also interacts with the TGF-β pathway through its promotion of SnoN degradation in response to SMAD3 activation (Stroschein, Bonni et al. 2001, Wan, Liu et al. 2001).

Differentiation is an important process in development, in which cells become specified, determined and leave the cell cycle to become quiescent. The APC/C has been implicated in the differentiation of a number of cell types, including the lens, muscle tissue and neurons (Manchado, Eguren et al. 2010, Wasch, Robbins et al. 2010). TGF-β signalling within the lens promotes APC/C-Cdh1-mediated

degradation of Skp2 and SnoN, resulting in $p21^{Cip1}$, $p27^{Kip1}$ and p15 activation and cell cycle arrest (Wu, Glickstein et al. 2007), whilst in myogenesis it also induces the degradation of Myf5 and promotes myogenic fusion (Li, Wu et al. 2007).

Cdh1 has also been described as playing a role in neural development and the maintenance of neuronal quiescence. Indeed, Cdh1 has been detected within the nuclei of post-mitotic neurons within both rodent and human brain tissue, and is important in *Drosophila* photoreceptors, in which it maintains cell cycle arrest by ensuring the continuous proteolysis of Cyclin B1 (Gieffers, Peters et al. 1999, Ruggiero, Kale et al. 2012). Furthermore, shRNA knockdown of Cdh1 permits Cyclin B1 re-accumulation, resulting in S phase re-entry and apoptosis (Almeida, Bolanos et al. 2005). Cdh1 has also been shown to control axonal growth and patterning in mammalian brains both *in vivo* and *ex vivo*, and is important in long-term potentiation and memory in the amygdala and hippocampus (Konishi, Stegmuller et al. 2004, Kannan, Lee et al. 2012, Pick, Malumbres et al. 2013, Pick, Wang et al. 2013). These inhibitory mechanisms for Cdh1-mediated neural patterning are exhibited via its aforementioned ability to degrade SnoN in response to TGF-β signalling (Stegmuller, Konishi et al. 2006). Similarly, Cdh1 can also prevent astrocyte proliferation following metabolic stress and hypoxia (Qiu, Zhang et al. 2013).

APC/C-Cdh1 also ubiquitylates ID2, resulting in its degradation and the promotion of neurogenic bHLH transcription factor activity and Nogo receptor accumulation (Lasorella, Stegmuller et al. 2006). Interestingly, ID2 is also a negative regulator of B-cell and erythroid lineage differentiation, thus Cdh1 might hold a role in promoting accurate lymphoid and myeloid development similar to that within the central nervous system (Ji, Li et al. 2008, Wasch, Robbins et al. 2010).

Cdc20 also appears to be important for neural development, since dendritic morphogenesis is reliant upon the stabilisation of polyubiquitylated Cdc20 by centrosomal HDAC6 in order to promote ID1 degradation and cellular differentiation (Kim, Puram et al. 2009). Given that Cdc20 is only active

during a short window during mitosis in cycling cells to promote anaphase, its role in promoting G0 is somewhat surprising, as one would expect Cdh1 to be the major co-activator for the APC/C during these conditions.

A: APC/C Substrates			
Protein	UniProt ID	Gene	Reference
Cyclin B1	P14635	CCNB1	(King, Peters et al. 1995, Sudakin, Ganoth et al. 1995, Almeida, Bolanos et al. 2005)
ID1	P41134	ID1	(Kim, Puram et al. 2009)
ID2	Q02363	ID2	(Lasorella, Stegmuller et al. 2006)
Myf5	P13349	MYF5	(Lindon, Albagli et al. 2000, Li, Wu et al. 2007)
Skp2	Q13309	SKP2	(Binné, Classon et al. 2007, Liu, Wu et al. 2007)
SnoN	P12757	SKIL	(Stroschein, Bonni et al. 2001, Wan, Liu et al. 2001)
B: APC/C Activators			
Protein	UniProt ID	Gene	Reference
HDAC6	Q9UBN7	HDAC6	(Kim, Puram et al. 2009)

Table 7: Substrates (A) and activators (B) of the human APC/C during cell cycle exit and quiescence

1.4.9. The APC/C is reactivated following DNA damage

During their normal life cycle, cells are exposed to many stimuli which can damage DNA, such as Ionising Radiation (IR), UV light or mutagenic chemicals, as well as endogenous sources such as reactive oxygen species (ROS) or incorrect DNA synthesis (Ciccia and Elledge 2010, Iyama and Wilson 2013). Many DNA damage response (DDR) pathways exist in order to repair each specific type of DNA damage, such as single-stranded DNA breaks (SSBs), double-stranded DNA breaks (DSBs), mis-matched DNA bases, modified bases as well as stalled replication forks and transcription machinery (Ciccia and Elledge 2010, Iyama and Wilson 2013).

Ultimately, the aim of the DDR within dividing cells is to halt the cell cycle and inhibit proliferation until the DNA has been repaired, or to promote apoptosis should the damage be irreparable (Ciccia and Elledge 2010). This is achieved through protein kinase cascades, elicited predominantly by ATM and DNA-PK for DSBs and ATR for SSBs, as well as other kinases such as CK2, p38 and MK2. One important outcome of these cascades is the stabilisation of the tumour suppressor p53, which is often mutated or deleted in cancer (Ciccia and Elledge 2010). A plethora of genes are under transcriptional control by p53, including $p21^{Cip1}$, which inhibits Cdk activity in order to prevent cell cycle progression, as well as pro-apoptotic factors such as BAX and PUMA (Riley, Sontag et al. 2008). Continuing cell proliferation in the presence of DNA damage can result in chromosomal aberrations and genetic instability, an important stage in tumourigenesis.

Different repair pathways target different type of breakages. The two main methods of repairing DSBs are Non-Homologous End Joining (NHEJ) and Homologous Recombination (HR) (Ciccia and Elledge 2010, Iyama and Wilson 2013). NHEJ functions during G1, in which the two ends of the DSB are ligated back together, whilst HR occurs during S and G2 following replication of DNA to produce a homologous sister chromatid. In HR, the DSB is resected and associates with the homologous region of DNA, which is then used as a template to synthesise nascent DNA, followed by ligation (Ciccia and

Elledge 2010, Iyama and Wilson 2013). The choice between the two pathways is thought to be a balance between BRCA1 and 53bp1, in that 53bp1 promotes NHEJ, whilst BRCA1 inhibits 53bp1, thereby promoting HR (Ciccia and Elledge 2010, Kakarougkas and Jeggo 2014).

Another DDR pathway is Base Excision Repair (BER), which removes non-bulky adducts caused by deamination, oxidation or alkylation and abasic sites (Ciccia and Elledge 2010, Iyama and Wilson 2013, Caldecott 2014). Here, the damaged base is excised to produce a SSB containing a gap in the DNA sequence, which is synthesised by DNA polymerases and ligated to seal the break. If the gap is a single nucleotide, this occurs by the short-patch pathway, whilst larger DNA gaps between two and twelve nucleotides are repaired by the long-patch pathway (Ciccia and Elledge 2010, Iyama and Wilson 2013, Caldecott 2014).

Similarly, Nucleotide Excision Repair (NER) removes thymidine dimers caused by UV-irradiation and bulky base adducts (Ciccia and Elledge 2010, Iyama and Wilson 2013). Here, the DNA is unwound around the damaged base or stalled Pol II enzyme, followed by excision of the damaged nucleotide. DNA polymerases then synthesise DNA to fill the gap, followed by ligation in a similar mechanism to BER (Ciccia and Elledge 2010, Iyama and Wilson 2013).

Another type of DDR is Mismatch Repair (MMR), in which inappropriately paired bases and insertion-deletion loops are recognised by MutSα (MSH2/MSH6 heterodimer) and MutSβ (MSH2/MSH3 heterodimer), respectively. These recruit a MutLα heterodimer (MLH1/PMS2) which coordinates base excision upon the nascently-synthesised DNA strand, following by DNA resynthesis and ligation (Ciccia and Elledge 2010, Iyama and Wilson 2013).

A back-up mechanism is in place should ligation attempts fail, resulting in deadenylated 5'-AMP modifications upon breaks. These are recognised and removed by Aprataxin, which then permits further ligation attempts (Rass, Ahel et al. 2007, Ciccia and Elledge 2010, Iyama and Wilson 2013, Caldecott 2014).

The APC/C has been shown to be reactivated as part of the DDR. Primarily, this ensures cell cycle arrest through the targeting of pro-proliferative targets for proteasomal degradation, although it is theorised that the APC/C is also reactivated in order to switch off the DDR following successful repair (Turnell AS and Teodoro JS, personal communication).

During G1, APC/C-Cdh1 is active, however during S- and G2-phases Cdh1 is inactivated by Cdk2-mediated phosphorylation (section 1.3.6). Following DNA damage in G2, the phosphatase Cdc14B relocates from the nucleolus to the nucleoplasm whereupon it binds Cdh1 and strips its inhibitory phosphorylation (Bassermann, Frescas et al. 2008). This permits Cdh1 reactivation of the APC/C, allowing it to target substrates for degradation. Furthermore, the yeast Chk2 homologue, Rad53, inactivates the polo kinase Cdc5, thereby preventing further phosphorylation-mediated inhibition of Cdh1 (Zhang, Nirantar et al. 2009).

A number of substrates have been identified for the APC/C following various forms of DNA damage. Although one of its classical mitotic substrates is Cyclin B, the reactivation of Cdh1 by X-irradiation did not cause its degradation, rather it arrested cells in G1 or G2 through the degradation of Cdc20 instead, although this was not seen following UV (Sudo, Ota et al. 2001). Interestingly, Cdc20 transcription is also inhibited by p53 following DNA damage, further preventing mitotic progression (Banerjee, Nath et al. 2009).

Other APC/C mitotic substrates are also degraded as part of the DDR. One such example is Plk1, which is degraded by APC/C-Cdh1 following G2 genotoxic stress (Bassermann, Frescas et al. 2008). Securin is also degraded by the APC/C following UV damage, an interesting result given that Securin also associates with DNA-PK (Romero, Multon et al. 2001, Romero, Gil-Bernabe et al. 2004). Although free Securin is degraded, the total level of Securin-Separase complexes remains constant, thus anaphase is still inhibited. In yeast, an opposite result is seen in which Rad53 activates the Cdk1 homologue, Cdc28, which in turn phosphorylates and stabilises the Securin homologue, Pds1

(Sanchez, Bachant et al. 1999). Other yeast substrates which become degraded include Kip1 and Cin8, thereby preventing the formation of the mitotic spindle and preventing mitotic entry (Zhang, Nirantar et al. 2009).

During G1, Cdh1 is active to prevent early S-phase entry (section 1.3.5). One important consequence of DNA damage in G1 is to ensure the maintained activation of Cdh1. One example of this is its targeting of Cyclin D1 following treatment with IR, thereby releasing $p21^{Cip1}$ from Cdk4 in order to inhibit Cdk2 (Agami and Bernards 2000, Germain, Russell et al. 2000). CUEDC2 is also important in inhibiting Cdh1 at the G1/S transition; however, CUEDC2 undergoes proteolysis following ERK1/2-dependent phosphorylation after treatment with UV (Zhang, Zhou et al. 2013). The APC/C also targets USP1 after UV-irradiation in order to promote PCNA monoubiquitylation and DDR signalling (Cotto-Rios, Jones et al. 2011).

Although Claspin is also a substrate for the APC/C, this is protected from degradation by reactivated APC/C-Cdh1 by the DUB USP28 (Zhang, Zaugg et al. 2006, Bassermann, Frescas et al. 2008). Interestingly, the transcription factor E2F1, a substrate for the APC/C from prometaphase until G1/S transition, was similarly regulated; although E2F1 is ubiquitylated by the APC/C following DNA damage, its proteasomal degradation is inhibited (Peart, Poyurovsky et al. 2010, Budhavarapu, White et al. 2012). Although E2F1-mediated transcription promotes S-phase entry during normal cellular progression, following DNA damage it alters its pattern of activation to induce the expression of a number of pro-apoptotic genes (Blattner, Sparks et al. 1999, Lin, Lin et al. 2001, Pediconi, Ianari et al. 2003).

Other links between the DDR and the APC/C have also been described. The ATR-responsive RAD17 protein has been shown to be under control of the APC/C, whilst its degradation is potentiated by UV-irradiation, although this is perturbed in breast cancer cells (Zhou, Jing et al. 2013). Another example is MAD2L2, also called REV7, which inhibits Cdh1 during early mitosis; however, it has also

been shown to facilitate the APC/C-mediated degradation of REV1, a polymerase important in translesion synthesis at stalled replication forks (Chun, Kok et al. 2013, Listovsky and Sale 2013). Furthermore, the yeast XPC homologue, Rad4, has been suggested to be a novel substrate for the APC/C following UV-irradiation, thus demonstrating a link between the APC/C and NER (Connors, Rochelle et al. 2014).

Similarly, FAN1 nuclease and RAP80 have been shown to be targets for the APC/C-Cdh1, with RAP80 also able to be targeted by Cdc20 (Cho, Lee et al. 2012, Lai, Hu et al. 2012). Given that RAP80 binds BRCA1 and could be important in controlling HR through BRCA1 recruitment to damage foci, it could be possible that its proteolysis by the APC/C during G1 promotes NHEJ in the absence of homologous sister chromatids (Kakarougkas and Jeggo 2014).

The DSB repair protein, MDC1, can potentiate APC/C activity and is important in regulating the SAC and the onset of anaphase (section 1.3.1) (Coster, Hayouka et al. 2007, Townsend, Mason et al. 2009, Eliezer, Argaman et al. 2014). However, the phospho-dependent interaction between MDC1 and APC3 was greater following IR treatment, suggesting it might also have a role in modulating APC/C function as part of the DDR (Coster, Hayouka et al. 2007). Interestingly, another BRCT domain-containing protein, 53bp1, has been shown to interact with APC3 and purported to regulate the APC/C prior to chromosomal condensation (Akhter, Richie et al. 2004).This interaction between APC3 and 53bp1 was also mediated through the BRCT domain of 53bp1, therefore there could be competition between 53bp1 and MDC1 for a binding site upon APC3, which could impact upon APC/C function and the promotion of NHEJ by 53bp1 or HR by MDC1 (Coster and Goldberg 2010, Woods, Mesquita et al. 2012, Panier and Boulton 2014).

A: APC/C Substrates			
Protein	UniProt ID	Gene	Reference
Cdc20	Q12834	CDC20	(Sudo, Ota et al. 2001)
Cyclin A	P20248	CCNA2	(Sudakin, Ganoth et al. 1995, Geley, Kramer et al. 2001)
Cyclin B1	P14635	CCNB1	(King, Peters et al. 1995, Sudakin, Ganoth et al. 1995)
Cyclin D1	P24385	CCND1	(Agami and Bernards 2000)
FAN1	Q9Y2M0	FAN1	(Lai, Hu et al. 2012)
Plk1	P53350	PLK1	(Bassermann, Frescas et al. 2008)
RAD17	O75943	RAD17	(Zhou, Jing et al. 2013)
RAP80	Q96RL1	UIMC1	(Cho, Lee et al. 2012)
REV1	Q9UBZ9	REV1	(Chun, Kok et al. 2013)
Securin	Q5FBB7	PTTG1	(Romero, Gil-Bernabe et al. 2004)
USP1	O94782	USP1	(Cotto-Rios, Jones et al. 2011)
B: APC/C Activators			
Protein	UniProt ID	Gene	Reference
Cdc14B	O60729	CDC14B	(Bassermann, Frescas et al. 2008)
MAD2L2*	Q9UI95	MAD2L2	(Chun, Kok et al. 2013)
MDC1	Q14676	MDC1	(Coster, Hayouka et al. 2007)

Table 8: Substrates (A) and activators (B) of the human APC/C following DNA damage

*Although MAD2L2 inhibits Cdh1 during early mitosis, it promotes APC/C-Cdh1-dependent degradation of REV1 following DNA damage (Pfleger, Salic et al. 2001, Chun, Kok et al. 2013, Listovsky and Sale 2013).

1.5. Regulation of APC/C-mediated ubiquitylation

In order to control the cell cycle effectively, APC/C-mediated degradation must be tightly regulated. This ensures the cell cycle progresses in one direction only, and only upon suitable mitogenic stimulation. Misregulation of the APC/C results in aberrant sister chromatid segregation, genetic instability and cancer susceptibility (Wasch, Robbins et al. 2010, Penas, Ramachandran et al. 2011). Control of the APC/C is exerted in a number of ways, including: post-translational modifications (PTMs); Co-activator binding and activation of the APC/C; affinity for E2s; substrate recognition and binding as well as localisation.

1.5.1. Regulation of co-activators and APC/C subunits

APC/C activity and specificity is regulated predominantly by co-activator binding, which allows for the formation of the substrate recognition particle and, moreover, activation of the APC/C (Pines 2011, Primorac and Musacchio 2013). Although Cdc20 is transcribed from S phase and stabilised by the inactivation of Cdh1, it is prevented from activating the APC/C by Emi1 (section 1.3.6) (Reimann, Freed et al. 2001, Morris, Kaiser et al. 2003, Haugwitz, Tschöp et al. 2004). During S and G2, Emi1 inhibits the APC/C by preventing E2 binding to the catalytic core and by blocking substrate recognition through acting as a pseudosubstrate (Miller, Summers et al. 2006, Frye, Brown et al. 2013, Wang and Kirschner 2013). Emi1 is stable during G2 due to Pin1 preventing its proteolysis (Bernis, Vigneron et al. 2007); however, Plk1 and Cdk1 phosphorylation upon mitotic entry promote its targeting by $SCF^{\beta\text{-}TrCP}$ for proteasomal degradation (Guardavaccaro, Kudo et al. 2003, Margottin-Goguet, Hsu et al. 2003, Moshe, Bar-On et al. 2011). Although the APC/C is no longer inhibited by Emi1, it is still inactive at this point due to the SAC (section 1.3.1).

The interaction between Cdc20 and the APC/C is also regulated by PTMs. Indeed, the APC/C has been shown to be extensively phosphorylated, particularly on the TPR lobe, by Cdk1 and Plk1 during early

mitosis (Kraft, Herzog et al. 2003, Steen, Steen et al. 2008). This phosphorylation is necessary for Cdc20-mediated activation of the APC/C, although Cdc20 has to be dephosphorylated first in order for complete C-box activation (Kramer, Scheuringer et al. 2000, Rudner and Murray 2000, Labit, Fujimitsu et al. 2012).

Similarly, phosphorylation of Cdh1 by Cdk1 inhibits APC/C-Cdh1 binding (Zachariae, Schwab et al. 1998, Kramer, Scheuringer et al. 2000). Mitotic phosphatases, such as Cdc14, then remove this inhibitory phosphorylation of Cdh1, such that it becomes free to activate the APC/C during late mitosis (Jaspersen, Charles et al. 1999, Primorac and Musacchio 2013). Furthermore, Cdh1 is sequestered during early mitosis by MAD2L2, further preventing premature APC/C-Cdh1 activity and ensuring faithful sister chromatid separation (Listovsky and Sale 2013). Cdh1 is again inactivated by Cdk-dependent phosphorylation together with Emi1 inhibition during the G1/S transition (section 1.3.6).

Another important post-translational modification which affects APC/C function is acetylation. Previous work within our group has demonstrated a link between the Histone Acetyl Transferases (HATs) CBP/p300 and the APC/C (Turnell, Stewart et al. 2005). Immunopurified CBP and p300 can promote the polyubiquitylation of Cyclin B1 *in vitro*, and CBP/p300 also potentiates APC/C activity *in vitro*, whilst CBP knockdown delays progression through mitosis and increases the protein levels of known APC/C substrates such as Cyclin B1 (Turnell, Stewart et al. 2005). As such, it is postulated that the HAT activity of CBP/p300 might important in the regulation of APC/C activity. CBP/p300 could also potentiate APC/C activity through their E4 domain, which has been shown to promote the polyubiquitylation of p53 (Grossman, Deato et al. 2003, Shi, Pop et al. 2009). Interestingly, the APC/C subunits APC5 and APC7 have previously been shown to interact with the E4 domain of CBP/p300 (Turnell, Stewart et al. 2005).

There is also evidence to suggest that the co-activators Cdc20 and Cdh1 are acetylated *in* vivo; deacetylation of Cdc20 and Cdh1 by SIRT2 has been show to regulate APC/C activity, and ablation of SIRT2 expression increases the protein levels of known APC/C substrates Aurora A and B (Kim, Vassilopoulos et al. 2011). Furthermore, the fission yeast homologue of APC8, Cut23, has similarly been shown to be acetylated *in vivo* (Kimata, Matsuyama et al. 2008).

Individual subunit protein levels might also be a regulatory mechanism for APC/C activity. Indeed, this phenomenon can be exploited as a tool to investigate APC/C function, as ablation or overexpression of APC/C subunits can, respectively, down- or up-regulate its E3 ubiquitin ligase accordingly. Furthermore, the altered expression of APC/C subunits has been implicated in tumourigenesis (section 1.6). Also, during normal cell cycle, the protein levels of APC5 appear to decrease during mitotic progression (Turnell AS unpublished data; Teodoro JS personal correspondence), and APC3 becomes transcriptionally induced by C/EBPδ to promote APC/C substrate degradation (Pawar, Sarkar et al. 2010). Similarly, Cdc20 transcription is switched on following S phase, which then activates UbcH10 transcription (Morris, Kaiser et al. 2003, Haugwitz, Tschöp et al. 2004, Nath, Banerjee et al. 2011). Both Cdc20 and UbcH10 are also targets for APC/C-mediated ubiquitylation, which, together with the targeting of Cdh1 for degradation by the APC/C and $SCF^{\beta\text{-}TrCP}$, result in the APC/C being self-inhibitory (Shirayama, Zachariae et al. 1998, Listovsky, Oren et al. 2004, Rape and Kirschner 2004, Robbins and Cross 2010, Fukushima, Ogura et al. 2013).

There is also the potential for localisation to be a regulatory mechanism for the APC/C. As discussed in section 1.3.3, the Ska complex is required for appropriate degradation of Securin and Cyclin B1 owing to its ability to ensure the chromosomal localisation of the APC/C, thereby bringing it into close proximity with its target substrates (Sivakumar, Daum et al. 2014). Furthermore, APC5 and APC7 have been described as having important functions in transcriptional regulation by the APC/C (section 1.5) (Turnell, Stewart et al. 2005, Ho, Garg et al. 2013). Evidence for this is provided by the

discovery of APC5 upon actively transcribed regions of the genome, as well as the ability of APC5 and APC7 to localise the APC/C to CBP/p300-responsive gene promoters (Turnell, Stewart et al. 2005), and repress IL-17 promoters through its interaction with A20 (Ho, Garg et al. 2013).

1.5.2. Regulation of APC/C activity by modulation of substrates

Another method by which the activity of the APC/C is regulated is the modulation of its substrates themselves. The major method by which this is achieved is by PTM of substrates, producing a number of consequences such as altered affinity for APC/C-co-activator complexes, relocalisation or modified protein stability.

The PTM most commonly reported upon APC/C substrates which affects its ubiquitylation is phosphorylation, which has important consequences for the cell cycle. Indeed, phosphorylation of Cdc6 by Cyclin E/Cdk2 and Skp2 by Akt and Cdk2 prevent their recognition by the APC/C, thus inhibiting their ubiquitylation and degradation (Mailand and Diffley 2005, Gao, Inuzuka et al. 2009, Gao, Inuzuka et al. 2009). Conversely, Cdc20 requires phosphorylation by Plk1 in its CRY box, and Mcl-1 requires Cyclin B1/Cdk1 phosphorylation for their APC/C-mediated degradation (Harley, Allan et al. 2010, Hyun, Sarantuya et al. 2013). Furthermore, phosphorylation at the serine residue immediately preceding the KEN box (SKEN) in Aurora A potentiates its ubiquitylation, whilst a phosphomimetic mutated SKEN motif, DKEN, in NEK2A exhibited enhanced degradation compared to AKEN, which is unable to be phosphorylated (Littlepage and Ruderman 2002, Min, Mayor et al. 2013). The promotion of ubiquitylation following substrate phosphorylation has been proposed to be due to the negative charge imparted upon the substrate following the addition of the phosphate group, containing a triple-negative charge (Min, Mayor et al. 2013).

Similarly, the acetylation of substrates also appears to be important in their regulation by the APC/C. Cyclin A requires acetylation by P/CAF prior to its mitotic ubiquitylation, whilst, conversely, BUBR1 must exhibit an acetyl-SUMO switch before it can be degraded by the APC/C (Mateo, Vidal-Laliena et al. 2009, Mateo, Vidal-Laliena et al. 2010, Yang, Hu et al. 2012, Yang, Huang et al. 2012). The stability of Skp2 has also been shown to be regulated by acetylation; p300-dependent acetylation of Skp2 protects it from degradation by the APC/C-Cdh1, whilst deacetylation by SIRT3 results in its recognition by Cdh1 (Inuzuka, Gao et al. 2012). Skp2 also exhibits another regulatory mechanism, such that its translocation from the cytoplasm to the nucleus following TGF-β signalling promotes its Cdh1-dependent degradation in order to halt cell cycle progression (Hu, Liu et al. 2011).

Another method by which the activity of the APC/C can be controlled is the removal of ubiquitin from its substrates by a DUB prior to its degradation by the 26S proteasome. USP37, transcribed by E2F transcription factors, removes APC/C-mediated ubiquitin epitopes upon Cyclin A, thus ensuring its stability in order to promote S phase entry (section 1.3.6) (Huang, Summers et al. 2011). Similarly, USP2 has been shown to potentiate Emi-mediated inhibition of the APC/C (Wang and Kirschner 2013). Another example exists in USP44, which strips the APC/C-MCC-induced ubiquitylation of Cdc20 following satisfaction of the SAC, allowing formation of active APC/C-Cdc20 in order to promote anaphase (section 1.3.2) (Stegmeier, Rape et al. 2007). In budding yeast, DUBs such as Ubp15 have been shown to show preference for monoubiquitin rather than polyubiquitin chains upon Pds1, a Securin homologue, and Cyclin B *in vitro* (Schaefer and Morgan 2011). Considering that UBE2S is dispensable for mitotic exit, Emi1 inhibits polyubiquitylation, DUBs preferentially target monoubiquitin, and Cyclin B1 can be degraded following multiple monoubiquitylation, these observations suggest that DUBs form a major regulatory mechanism for UbcH10-mediated ubiquitylation by the APC/C (Garnett, Mansfeld et al. 2009, Schaefer and Morgan 2011, Dimova, Hathaway et al. 2012, Wang and Kirschner 2013). It should, however, be noted the DUB, Cezanne,

can cleave polyubiquitin from K11-chains, indicating there are also regulatory elements for APC/C-mediated polyubiquitin chains as well as monoubiquitin (Bremm, Freund et al. 2010).

1.6. Transcriptional Regulation by the APC/C

Nascent protein synthesis is an essential part of the cell cycle; S phase entry requires transcription of the replicative machinery under control of E2F transcription factors (section 1.3.6), whilst proliferation is inhibited by tumour suppressive transcription factors such as p53 and NF-κB (Giacinti and Giordano 2006).

Other important cellular regulators are CBP and p300 (CBP/p300), which are highly related HATs which possess both distinct and redundant functions (Wang, Marshall et al. 2013). CBP/p300 affect Pol II transcription in a number of ways. Firstly, CBP/p300 can act as an assembly factor to facilitate pre-initiation complex formation through concomitant binding of transcription factors and replication machinery. Secondly, acetylation of histones by CBP/p300 or its binding partners P/CAF and GCN5 remodels chromatin into an active transcribable state, or, thirdly, CBP/p300 can acetylate transcription factors directly (*e.g.* p53), thus affecting their activity (Wang, Marshall et al. 2013). The APC/C has been shown to interact with CBP and p300, with reciprocal regulation such that CBP/p300 potentiates APC/C activity and the APC/C facilitates CBP/p300-dependent acetylation and transcription (Turnell, Stewart et al. 2005). The APC/C-Cdc20 has also been shown to co-operate with CBP/p300 in order to transactivate UbcH10 expression (Nath, Banerjee et al. 2011). Consistent with the studies outlined above, overexpression of the budding yeast orthologue of CBP, Rtt109, can overcome an Apc5 mutant which exhibited aberrant chromatin assembly, whilst deletion of Rtt109's accessory factor, Asf1, augmented the Apc5 mutant phenotype. This suggests that, in yeast, the regulation of chromatin by Apc5 was effected by the CBP orthologue, Rtt109 (Turner, Malo et al. 2010).

One mechanism by which the APC/C is suggested to regulate transcription is by the modulation of histone acetylation by HATs. Indeed, it has been shown that the APC/C controls CBP/p300-dependent acetylation of histone H4 (Turnell, Stewart et al. 2005), whilst in yeast a number of studies have demonstrated the necessity of Apc5 in ensuring faithful chromatin assembly through the regulation of histone acetylation by various HATs, such as Gcn5, Elp3, Rtt109, the HDAC Hda1 and the chromatin assembly factor CAF-1 (Harkness, Davies et al. 2002, Arnason, Pisclevich et al. 2005, Harkness, Arnason et al. 2005, Turner, Malo et al. 2010, Islam, Turner et al. 2011). Interestingly, these studies in yeast from Troy Harkness's group and our laboratory have focused predominantly upon the APC/C subunit APC5, suggesting it has an integral cellular function in localising the APC/C to chromatin in order to regulate transcription. Indeed, APC5, along with other APC/C subunits, is found upon the actively transcribed regions of the genome (Turnell, Stewart et al. 2005).

The APC/C can also promote transcription by targeting repressors for proteasomal degradation. Examples for this have been suggested in yeast, whereby the transcriptional repressors Nrm1 and Yhp1 were shown to be under the proteolytic control of the APC/C (Ostapenko and Solomon 2011). Concomitant with remodelling of chromatin into an active state, this demonstrates a clear pro-transcriptional outcome for the APC/C.

Our laboratory has demonstrated that the APC/C, guided by APC5 and APC7, augments E2F1-dependent transcription in a CBP/p300-dependent manner (Turnell, Stewart et al. 2005). Given that APC/C-Cdh1 can bind Rb and prevent S phase entry by promoting SKP2 degradation, and has also been suggested to mediate the destruction of E2F1 and E2F3, this might seem counterintuitive (Binné, Classon et al. 2007, Peart, Poyurovsky et al. 2010, Pines 2011, Ping, Lim et al. 2012, Dick and Rubin 2013). However, the prevailing hypothesis is that when the APC/C is localised to the promoters by APC5- and APC7-mediated interactions, such as with CBP/p300, it can ubiquitylate transcription

factors, thereby removing them from promoters and permitting another round of transcription (Turnell, Stewart et al. 2005).

Consistent with a role for the APC/C in transcriptional control, several transcription factors have been described as substrates for the APC/C, including the S-phase-promoting Ets2 and FoxM1 (Park, Costa et al. 2008). Furthermore, Tos4 and Pdr3 were identified as putative APC/C substrates in *S. cerevisiae* (Ostapenko, Burton et al. 2012), and both initiate transcription as part of the DNA damage response (Zhu and Xiao 2004, Bastos de Oliveira, Harris et al. 2012). It is therefore possible that their targeting by the APC/C, which is re-activated as part of the DDR (section 1.3.9), is part of the theorised "clean-up" operations of the APC/C in order to switch off the DDR.

APC5 and APC7 have also been shown to associate with the IL-17 receptor, whereupon APC5 acts synergistically with A20 to repress IL-17-induced transcription (Ho, Garg et al. 2013). The mechanism of this inhibition has yet to be elucidated, although A20 has been shown to inhibit IL-17 signalling through its activity as a DUB (Garg, Ahmed et al. 2013, Ho, Garg et al. 2013).

1.7. The APC/C and Cancer

The APC/C has been implicated in tumourigenesis, and appears to be deregulated in a number of different cancers. Indeed, APC/C-Cdh1 has been described as possessing tumour suppressor activity, whilst the APC/C co-activator Cdc20 has been described as an oncogene (Turnell, Stewart et al. 2005, Penas, Ramachandran et al. 2011, Wang, Wan et al. 2013, Zhang, Wan et al. 2014).

The observation that Cdh1 and APC/C subunits are downregulated in a number of human cancers supports the notion that they might possess tumour suppressor activity. Expression of Cdh1 is reduced in a range of tumours, including breast, prostate, ovary, liver, colon and brain (Bassermann, Frescas et al. 2008, Engelbert, Schnerch et al. 2008, Fujita, Liu et al. 2008, Fujita, Liu et al. 2008). Loss

of Cdh1 results in genetic instability which promotes tumourigenesis through increased mis-segregation of chromosomes, aneuploidy, non-disjunction and chromosomal breaks (Ross and Cohen-Fix 2003, Wäsch and Engelbert 2005, Engelbert, Schnerch et al. 2008, Garcia-Higuera, Manchado et al. 2008).

Similarly, APC2 expression is reduced in human cancers. In this regard the APC/C has been purported to promote the ubiquitylation of MDM2; loss of APC2 correlates with overexpression of MDM2 and p53 instability (He, Tollini et al. 2014). APC3 and APC7 are also downregulated in a number of breast cancers (Park, Choi et al. 2005, Pawar, Sarkar et al. 2010). Indeed, this loss of APC3 expression has been correlated with a poor prognosis and survival in breast cancer patients (Talvinen, Karra et al. 2013). Furthermore, APC3, APC4, APC6, APC7 and APC8 were all shown to exist in mutant form in colon cancers (Wang, Moyret-Lalle et al. 2003).

This tumour suppressive function is likely to be exerted by the targeting of APC/C substrates for degradation. Indeed, oncogenic APC/C substrates such as Skp2 have been shown to be overexpressed and relocalised in cancers, coinciding with downregulation of Cdh1 thus preventing its destruction (Gstaiger, Jordan et al. 2001, Signoretti, Di Marcotullio et al. 2002, Fujita, Liu et al. 2008, Gao, Inuzuka et al. 2009, Gao, Inuzuka et al. 2009). Furthermore, experimental knockdown of Cdh1 expression can elicit the same phenotype as seen *in vivo*, whilst knockdown of Skp2 prevents further proliferation (Fujita, Liu et al. 2008). Other APC/C substrates have been shown to be overexpressed in cancer (Lehman, Tibshirani et al. 2007, Penas, Ramachandran et al. 2011), including Securin (Zou, McGarry et al. 1999, Heaney, Singson et al. 2000, Vlotides, Eigler et al. 2007, Smith, Franklyn et al. 2010), Plk1 (Takai, Hamanaka et al. 2005) and Aurora kinase (Giet, Petretti et al. 2005).

The ability of the APC/C to act as a tumour suppressor might also be elicited through its interaction with CBP/p300, through which it can regulate transcription (section 1.5). Deregulation of the tumour suppressive functions of CBP/p300 have previously been implicated in promoting tumourigenesis

(Wang, Marshall et al. 2013). Indeed, it has been established that APC5 and APC7 possess tumour suppressor capabilities through their ability to suppress E1A/activated-Ras transformation of primary rat embryo fibroblasts in a CBP/p300-dependent manner (Turnell, Stewart et al. 2005).

From these data, the APC/C appears to be a good target for cancer therapy, as reactivation ought to ensure the degradation of its oncogenic substrates. However, APC/C subunits have also been described as being overexpressed in other tumours, suggesting it can also function as an oncogene. In particular, Cdc20 is overexpressed in a wide range of cancers and denotes a poor prognosis and survival (Mondal, Sengupta et al. 2007, Marucci, Morandi et al. 2008, Jiang, Jedinak et al. 2011, Rajkumar, Sabitha et al. 2011, Chang, Ma et al. 2012, Kato, Daigo et al. 2012, Choi, Kim et al. 2013, Wu, Hu et al. 2013, Ding, Wu et al. 2014, Karra, Repo et al. 2014, Kim, Choi et al. 2014, Li, Gao et al. 2014, Moura, Delgado et al. 2014). Similarly, the E2, UbcH10, has been shown to be overexpressed in a plethora of cancers and is linked to a poor prognosis, whilst ectopic expression promotes aberrant chromosomes and mitotic slippage (Okamoto, Ozaki et al. 2003, Pallante, Berlingieri et al. 2005, Berlingieri, Pallante et al. 2007, Jiang, Huang et al. 2008, van Ree, Jeganathan et al. 2010, Jiang, Wang et al. 2012, Perrotta, Bruno et al. 2012, Zhao, Jiang et al. 2012, Morikawa, Kawai et al. 2013, Pallante, Malapelle et al. 2013, Zhao, Wu et al. 2013, Matsumoto, Ishibashi et al. 2014, Xie, Powell et al. 2014). The oncogenic properties of Cdc20 and UbcH10 are thought to stem from the early onset of anaphase, thus promoting genetic instability by inaccurate chromosome segregation. Surprisingly, both APC8 and Cdh1 have also been described as being overexpressed (Lehman, Tibshirani et al. 2007, Zhang, Rahbari et al. 2011).

These data clearly show that the APC/C has both tumour suppressive and oncogenic properties, and has subunits which are commonly up- and down-regulated, as well as substrate overexpression, in cancer. As such, it would be appropriate to investigate the role of the APC/C in various cancers further, with an aim to discover novel therapeutic strategies for cancer treatment.

2.1. The nucleolus and RNA Polymerase I

The nucleolus is a distinct region of the nucleus easily visible under a phase contrast microscope. Following its initial documentation in the 19th century, it has since been shown to be highly conserved and function as a "ribosome factory", transcribing ribosomal DNA (rDNA) to produce pre-ribosomal RNA (pre-rRNA), which is subsequently processed to form rRNA and associated with ribosomal proteins to form ribosomes (Hernandez-Verdun, Roussel et al. 2010, Pederson 2011, Grummt 2013).

The nucleolus has also been shown to be a vital component of a number of cellular signalling pathways, including a great number of stress pathways, in which it coordinates the necessary intracellular response and ensures temporal inhibition of ribosomal biogenesis, as well as controlling apoptosis, the cell cycle and telomere formation. Furthermore, it holds novel functions in mRNA processing and formation of the Signal Recognition Particle. The nucleolus has also been implicated in a number of diseases, including ribosomopathies and cancer, in which dysregulation by tumour suppressors and oncogenes affects ribosomal function (Drygin, Rice et al. 2010, Hernandez-Verdun, Roussel et al. 2010, Pederson 2011, Grummt 2013, Quin, Devlin et al. 2014).

2.2. Nucleolar architecture and mitotic regulation

The nucleolus is a membrane-free organelle containing the rDNA genetic loci and a large protein network which forms during the latter stages of mitosis around Nucleolar Organiser Regions (NORs), of which human cells contain ten, upon each of chromosomes 13, 14, 15, 21 and 22. Multiple active NORs often cooperate to form a single nucleolus, such that mammalian cells typically contain between one and four, depending upon the cell type (Raska, Shaw et al. 2006, Hernandez-Verdun, Roussel et al. 2010, Goodfellow and Zomerdijk 2012). Interestingly, one of each NOR allele appears

to be inactivated in a similar manner to X-inactivation in mammalian females (Schlesinger, Selig et al. 2009).

About 400 rDNA repeats are found within the human genome, and are arranged in tandem arrays within each of the NORs. Each rDNA repeat is about 43kb in length, and consists of an intergenic spacer (IGS) region around 30kb long, containing enhancers and both the spacer and 47S pre-rRNA promoter, which is followed by a 5'External transcribed spacer (ETS), the 47S pre-rRNA gene and a 3'ETS (Goodfellow and Zomerdijk 2012).

The nucleolus consists of three morphologically distinct areas: the Fibrillar Centre (FC), the Dense Fibrillar Component (DFC) and the Granular Component (GC) (Figure Int.4). The FC contacts the DFC, around which the GC is formed. Each nucleolar compartment is distinct, containing different DNA and protein elements which relate to its function. As such, the FC contains untranscribed regions of rDNA, RNA Polymerase I (Pol I), Upstream Binding Factor (UBF) and Top1. These promote Pol I transcription either at the FC:DFC interface or in the DFC itself. The DFC contains active rDNA elements (section 2.3.1), and is also important in the early processing of pre-rRNA. Late pre-rRNA processing and ribosomal assembly occurs within the GC prior to nucleolar export (Raska, Shaw et al. 2006, Hernandez-Verdun, Roussel et al. 2010, Goodfellow and Zomerdijk 2012).

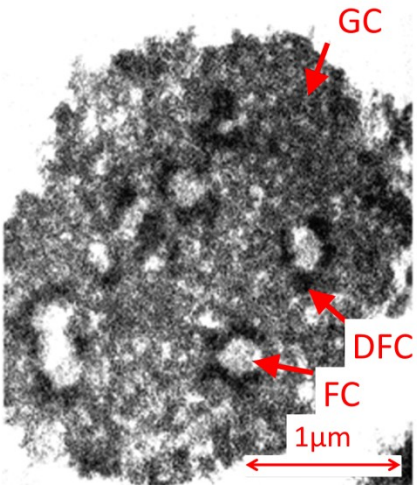

Figure Int.4 – Electron Micrograph of a purified HeLa cell nucleolus.

FC: Fibrillar Centre. DFC: Dense Fibrillar Component. GC: Granular Component.

Taken from (Andersen, Lyon et al. 2002).

During mitotic prophase, nucleoli disassemble prior to nuclear envelope breakdown (NEBD), leaving NORs upon the chromosomes. First rRNA processing then Pol I transcription is inhibited by mitotic kinases such as Cyclin B1/Cdk1, which target Pol I transcription factors, such as SL1, UBF and TTF-I (section 2.3.1). This is followed by the release of nucleolar proteins from the DFC and GC compartments, whilst condensation of chromatin occurs to form a perichromosomal compartment around rDNA, in which pre-rRNA and rRNA processing machinery are located. This perichromosomal complex remains associated with the chromosomes through mitosis, segregating accordingly during anaphase (Hernandez-Verdun 2011).

Nucleolar reassembly commences in late mitosis during telophase, following APC/C-mediated inactivation of Cyclin B1/Cdk1 and reversal of the inhibitory phosphorylation of Pol I-specific transcription factors by PP1 and PP2A. Because Pol I, TTF-I, UBF and SL1 are retained in active NORs during mitosis, release of their inhibition ensures rapid reinitiation of rDNA transcription, since recruitment of the polymerase machinery is not required. In addition, nucleolar reassembly requires the perichromosomal compartments to reorganise with other nucleolar proteins into prenucleolar bodies (PNBs). Over time, proteins relocate from these PNBs into the active NORs, starting with early rRNA processing machinery and DFC reformation, followed by late rRNA processing machinery and reformation of the GC (Hernandez-Verdun 2011).

2.3. RNA Polymerase I

Pol I is a multi-subunit RNA Polymerase which transcribes the rDNA genes to produce the pre-rRNA required for ribosomal assembly. Its subunits are highly conserved throughout eukaryotes, with some shared between Pol I, II and III. The two largest subunits, RPA194 and RPA135, confer the majority of its transcriptional activity, and are unique to Pol I, together with PAF53, RPA43, PAF49

and RPA12. The heterodimer RPA40-RPA19 is shared between Pol I and Pol III, whilst RPB5, RPB6, RPB8, RPB10 and RPB12 are common to all three Pols (Russell and Zomerdijk 2006).

2.4. Ribosomal Assembly

Translation of mRNA to produce nascent polypeptides occurs at the ribosomes. Therefore, the state of the ribosomal pool is integral to controlling *de novo* protein synthesis. As such, the regulation of ribosomal biogenesis is an important control mechanism for cellular homeostasis and the response to cellular stresses and stimuli, with aberrations in this pathway a driving factor for disease (Hernandez-Verdun, Roussel et al. 2010, Pederson 2011, Grummt 2013).

2.4.1. Pol I transcription

The first step in ribosomal biogenesis is the transcription of active rDNA repeats to produce a 47S pre-rRNA transcript. First and foremost, this requires the rDNA locus to be suitably epigenetically regulated such that the chromatin is in an open conformation as euchromatin (Goodfellow and Zomerdijk 2012). A number of nucleolar chromatin regulators have been described, including NoRC (Nucleolar Remodelling Complex) and eNoSC (Energy-dependent Nucleolar Silencing Complex), whilst UBF is also important in regulating chromatin decondensation (Chen, Belmont et al. 2004, Murayama, Ohmori et al. 2008, Goodfellow and Zomerdijk 2012, Guetg and Santoro 2012).

The transcription termination protein TTF-I binds the NoRC subunit, TIP5, which recruits DNA methyltransferases and HDACs to inactive rDNA genes, thereby promoting heterochromatin formation and genetic silencing through promoter CpG methylation and histone modifications (Strohner, Nemeth et al. 2001, Santoro, Li et al. 2002, Zhou, Santoro et al. 2002, Goodfellow and

Zomerdijk 2012). The NoRC complex can also induce rDNA silencing by association with pRNAs produced by Pol I transcription of the IGS, although these pRNAs are also capable of inducing promoter methylation independently of NoRC (Mayer, Schmitz et al. 2006, Mayer, Neubert et al. 2008, Schmitz, Mayer et al. 2010, Goodfellow and Zomerdijk 2012).

Conversely, TTF-I can also maintain active euchromatic rDNA as well as reactivate silenced rDNA through its interaction with CSB and the methyltransferase G9a, whilst reactivation also requires the NuRD (Nucleosome Remodelling and Deacetylation) complex (Längst, Blank et al. 1997, Yuan, Feng et al. 2007, Guetg and Santoro 2012, Xie, Ling et al. 2012). The epigenetic state of active rDNA elements is similarly maintained by a number of mechanisms (Goodfellow and Zomerdijk 2012), including the demethylation of promoters and inhibition of methylases (Brown and Szyf 2007, Zentner, Hurd et al. 2010), removal of methyl-Cytosine bases by the NER pathway (Schmitz, Schmitt et al. 2009) and histone modifications by B-WICH and PHF8 (Feng, Yonezawa et al. 2010, Vintermist, Böhm et al. 2011).

In order to promote rDNA transcription, Pol I associates with a number of ancillary proteins upon the promoter to form a pre-initiation complex (PIC). In addition to the core subunits described in section 2.2, Pol I must also associate with SL1 (selectivity factor 1), consisting of TBP and TAF1A, TAF1B, TAF1C, TAF1D, and TAF12. SL1 has several roles to ensure accurate Pol I transcription, namely by providing promoter selectivity for Pol I by its recruitment to the 47S rDNA promoter along with UBF. SL1 is also important in maintaining hypomethylation of the promoter, and ensuring its correct structural formation (Goodfellow and Zomerdijk 2012).

Other factors to which Pol I has to bind in order to form a PIC and initiate transcription are RRN3, CK2 and UBF. Interestingly, Pol I exists as two different complexes, Pol Iα and Pol Iβ, and it is only Pol Iβ which can form a PIC (Miller, Panov et al. 2001, Goodfellow and Zomerdijk 2012). This is due to the inclusion of RRN3 within Pol Iβ, which binds SL1 and Pol I, promoting their interaction upon rDNA

promoters (Miller, Panov et al. 2001, Goodfellow and Zomerdijk 2012). Furthermore, as a constituent of Pol Iβ, CK2 is capable of phosphorylating TAF1C and UBF to ensure PIC formation and stability, as well as RRN3 to promote transcription elongation (Goodfellow and Zomerdijk 2012).

Another important constituent of the PIC is Top2A, which interacts with RRN3 within the Pol Iβ holoenyzyme. This has been suggested to facilitate the interaction between the holoenzyme and the rDNA promoter by rearranging the torsional state of the rDNA to promote SL1-UBF-Pol Iβ binding (Panova, Panov et al. 2006, Goodfellow and Zomerdijk 2012, Ray, Panova et al. 2013).

The cooperative binding between SL1 and UBF is also important in localising Pol Iβ to rDNA promoters and UBF-mediated transcriptional activation. Furthermore, UBF is also implicated in transcription initiation and promoter escape, whereby Pol I dissociates from its transcriptional activators such as RRN3 and starts transcribing the rDNA genetic element (Panov, Friedrich et al. 2006, Goodfellow and Zomerdijk 2012). As well as UBF-mediated dissociation of RRN3 from Pol I, RRN3 phosphorylation by CK2 has also been shown to be required for promoter escape in mice (Bierhoff, Dundr et al. 2008, Goodfellow and Zomerdijk 2012).

The next step in pre-rRNA synthesis is the elongation of the pre-rRNA transcript. Evidence suggests that SL1 and UBF are also important in this process, in that UBF binds and ensures an active chromatin state throughout the gene, and SL1 recruits factors to promote termination at the end of the elongation step as well as arranging the rDNA and nascent transcripts in a 3D conformation which prevents their entanglement (Stefanovsky, Langlois et al. 2006, Denissov, Lessard et al. 2011, Goodfellow and Zomerdijk 2012). Other nucleolar proteins have also been described as having a function in Pol I transcript elongation, including Nucleolin, the FACT complex and B23, as well as a series of chromatin remodelling enzymes, including histone methylases and HATs (Goodfellow and Zomerdijk 2012). Furthermore, Top2A functions as part of Pol Iβ, which relieves torsional stress exhibited during Pol I transcription (Panova, Panov et al. 2006, Goodfellow and Zomerdijk 2012).

Although it is not part of Pol Iβ, Top1 has also been implicated in transcriptional elongation, potentially functioning with BLM helicase (El Hage, French et al. 2010, Goodfellow and Zomerdijk 2012, Grierson, Acharya et al. 2013). In yeast, Top2A relieves positive torsional stress preceding the Pol I enzyme, whilst Top1 functions after Pol I to remove negative torsion (French, Sikes et al. 2011). There is also evidence for successive Pol I holoenzymes to interact upon rDNA, ensuring a continuous chain of Pol I holoenzymes transcribing the rDNA loci, facilitating pre-rRNA production (Albert, Léger-Silvestre et al. 2011).

The final step in Pol I transcription is termination, which is mediated by TTF-I. TTF-I can bind to the termination domains and force the arrest of the Pol I holoenzyme, which stimulates the PTRF-dependent release of Pol I and pre-rRNA transcript from the rDNA (Jansa and Grummt 1999, Goodfellow and Zomerdijk 2012, Németh, Perez-Fernandez et al. 2013). In yeast, there is evidence that the RPA12 homologue acts as a termination factor, cleaving the 3' end of pre-rRNA (Prescott, Osheim et al. 2004, Kuhn, Geiger et al. 2007, Goodfellow and Zomerdijk 2012). However, in mammals, RPA12 is not involved in termination, and the 3' trimming of pre-rRNA is not mediated by polymerases, nor is it required for termination (Kuhn and Grummt 1989, Németh, Perez-Fernandez et al. 2013).

The presence of multiple independent methods to ensure timely transcription termination would indicate that it is an important cellular process. The reason for such fail-safe mechanisms could be explained by the observation that terminated transcripts promote reinitiation of Pol I transcription, thereby increasing the rate of pre-rRNA synthesis compared to run-off transcripts (Jansa, Burek et al. 2001). Indeed, this phenomenon was only seen upon measuring multiple rounds of transcription, suggesting it made little difference to the efficiency of the first transcript produced (Jansa, Burek et al. 2001).

The reinitiation of Pol I transcription is primarily driven by the creation of loops within rDNA, caused by the binding of TTF-I to multiple binding sites within the rDNA array, including the termination domain downstream of one rDNA genetic element and the two juxtaposed domains in between the spacer and 47S pre-rRNA promoter within the neighbouring rDNA repeat (Németh, Guibert et al. 2008). Reinitiation of transcription also appears to require the termination factor PTRF, the selectivity factor SL1 and c-Myc signalling, as well as the reassociation of RRN3 (Jansa, Burek et al. 2001, Shiue, Berkson et al. 2009, Denissov, Lessard et al. 2011, Goodfellow and Zomerdijk 2012). Indeed, SL1 and UBF remain bound upon the promoter, thus when Pol I finishes one round of transcription, it can reform the Pol Iβ complex with SL1, UBF and RRN3 at neighbouring promoters, but only if FCP1 has removed the CK2-mediated inhibitory phosphorylation of RRN3 (Bierhoff, Dundr et al. 2008, Goodfellow and Zomerdijk 2012).

2.4.2. Pre-rRNA processing and ribosomal assembly

Ribosomal assembly requires four rRNAs: 28S, 18S and 5.8S from Pol I transcripts and 5S from Pol III (Fatica and Tollervey 2002, Mullineux and Lafontaine 2012). As such, the initial 47S pre-rRNA transcript requires processing in order to cleave it into the three mature rRNAs, which requires a multitude of proteins, with a screen identifying 286 in humans, including nucleases and helicases, as well as small nucleolar RNAs (snoRNAs) (Fromont-Racine, Senger et al. 2003, Henras, Soudet et al. 2008, Mullineux and Lafontaine 2012, Tafforeau, Zorbas et al. 2013). Concomitant with rRNA cleavage are maturation events, such as pseudouridylation and methylation, and the association with proteins to form pre-ribosomes (Fatica and Tollervey 2002, Henras, Soudet et al. 2008, Mullineux and Lafontaine 2012).

The first processing event within human cells is the rapid trimming of the 47S pre-rRNA within the 5'-ETS and the 3'-ETS to produce a 45S pre-rRNA. In yeast, but not mammals, the initial pre-rRNA cleavage events occur co-transcriptionally under the control of Rnt1, exonucleases and RNA helicases (Braglia, Heindl et al. 2010, Braglia, Kawauchi et al. 2011, Goodfellow and Zomerdijk 2012).

Two separate pathways can be engaged to generate all three rRNAs, depending upon the order of cleavages. In pathway 1, the 45S pre-rRNA is first trimmed within the 5'- and 3'-ETS regions to produce a 41S rRNA intermediate, following by cleavage within the Internal Transcribed Spacer (ITS), ITS1, between the 18S and 5.8S rRNA genes to produce 32S and 21S rRNA precursors. In pathway 2, the 45S pre-rRNA is first cleaved within ITS1, yielding a 32S and a 30S precursor; the 30S precursor is then cleaved to produce the 21S precursor, realigning the two pathways. The 21S pre-rRNA is subsequently trimmed to produce an 18S-E rRNA, which shuttles into the cytoplasm, whereupon it undergoes final processing to produce the 18S rRNA. The 32S pre-rRNA is similarly cleaved within ITS2 (between the 5.8S and 28S rDNA genes) to produce the 28S rRNA and a 12S pre-rRNA, which relocates to the cytoplasm and is spliced to produce the 5.8S rRNA (Mullineux and Lafontaine 2012).

These events occur within pre-ribosomal structures, containing all the proteins necessary for pre-rRNA processing. As such, the initial splicing occurs as part of a pre-90S ribosome within the DFC. Following production of the 21S precursor, this is then incorporated into the pre-40S ribosome, which shuttles into the cytoplasm for final processing. Similarly, the pre-60S ribosome, after separation of the pre-40S particle from the pre-90S ribosome, undergoes processing starting in the DFC, then the GC and nucleoplasm prior to cytoplasmic relocalisation and final maturation (Fromont-Racine, Senger et al. 2003, Henras, Soudet et al. 2008).

The non-ribosomal proteins incorporated within each pre-ribosome decrease over the maturation pathway, suggesting that as proteins are not needed and the pre-ribosome translocates from the nucleolus into the nucleoplasm and cytoplasm, they become excluded from the pre-ribosomal

complex (Henras, Soudet et al. 2008). Furthermore, human ribosomal proteins have been shown to be associated with pre-ribosomes at different stages; proteins which coordinate early cleavage events associate with early pre-ribosomes, whilst those which mediate later processing events associate with late pre-ribosomes (Robledo, Idol et al. 2008, O'Donohue, Choesmel et al. 2010, Mullineux and Lafontaine 2012). These late ribosomal proteins are also necessary for the migration of pre-ribosomes from the nucleolus into the nucleoplasm, and the subsequent translocation into the cytoplasm prior to final maturation (Rouquette, Choesmel et al. 2005, O'Donohue, Choesmel et al. 2010, Mullineux and Lafontaine 2012).

The cleavage events themselves are mediated by either an endonuclease or exonuclease in cooperation with RNA helicases and sno-RNAs (Fatica and Tollervey 2002, Fromont-Racine, Senger et al. 2003, Henras, Soudet et al. 2008, Sloan, Mattijssen et al. 2013). The precise functions of all the proteins within the pathway have not been identified within mammalian cells; however, they are well documented in yeast (Fatica and Tollervey 2002, Fromont-Racine, Senger et al. 2003, Sloan, Mattijssen et al. 2013). A large number of different endo- and exo-nucleases have been described in yeast, many of which have human homologues, including the Exosome/Rrp6, RNase MRP, Rat1, Xrn1 and the helicase Mtr4 (Fatica and Tollervey 2002, Fromont-Racine, Senger et al. 2003, Henras, Soudet et al. 2008). Given that different nucleases catalyse different cleavage events, this would suggest a highly regulated system, such that rRNA processing can be fine-tuned by modulation of individual cleavages (Fatica and Tollervey 2002, Henras, Soudet et al. 2008).

The snoRNAs are vital for enhancing these cleavage events, in particular the box C/D U3 sno-RNA, which forms an integral part of the U3 snoRNP and is required for early processing and 18S precursor stability in both yeast and humans (Fatica and Tollervey 2002, Fromont-Racine, Senger et al. 2003, Henras, Soudet et al. 2008, Mullineux and Lafontaine 2012). Other protein complexes, such as t-UTP (U Three Protein Complex), UTP-B or UTP-C, also associate with pre-rRNA to form the small subunit

processome, and are important for their cleavage (Fromont-Racine, Senger et al. 2003, Henras, Soudet et al. 2008). The U3 snoRNP complex probably acts as a chaperone, mediating correct folding through complementary base-pair binding, which subsequently permits cleavage in a process requiring supplementary binding- and stability-factors, as well as either an exonuclease or endonuclease and an RNA helicase (Hughes and Ares 1991, Henras, Soudet et al. 2008).

Other snoRNAs are also important in the production of mature rRNAs, including U8 (which is absent in yeast), U22, U14, U17/snR30, U33 and snR10 (absent in mammals), whilst others function only in ensuring accurate rRNA modifications (Henras, Soudet et al. 2008, Watkins and Bohnsack 2012). To form snoRNPs, the box C/D snoRNAs associate with NOP56, NOP58, h15.5K/Snu13 and Fibrillarin/Nop1, whilst H/ACA snoRNAs bind NOP10, NHP2, GAR1 and Dyskerin/Cbf5 (Fromont-Racine, Senger et al. 2003, Watkins and Bohnsack 2012). The pseudouridine and 2'-O-methyl modifications exhibited upon rRNAs are important in regulating their structure, and are formed under the control of snoRNAs. Uridines are converted to pseudouridines by the Dyskerin/Cbf5 component of H/ACA-type snoRNAs, whilst box C/D sno-RNAs promote methylation of the ribose 2'-O through Fibrillarin/Nop1 (Fromont-Racine, Senger et al. 2003, Henras, Soudet et al. 2008, Mullineux and Lafontaine 2012, Watkins and Bohnsack 2012). These modifications persist upon mature rRNAs, and are suggested to play a role in ribosomal function (Henras, Soudet et al. 2008, Mullineux and Lafontaine 2012).

Finally, following pre-60S and pre-40S pre-ribosomal export into the cytoplasm, the pre-ribosomes undergo maturation such that all non-ribosomal proteins are excluded and all ribosomal proteins become incorporated. PTMs which are required for its activation, such as dephosphorylation occur at this time (Fatica and Tollervey 2002, Henras, Soudet et al. 2008). The mature 60S ribosome contains the 28S, 5.8S and 5S rRNAs, whilst the 40S ribosome contains the 18S rRNA. Interestingly, the 5.8S rRNA exists as long and short forms, $5.8S_L$ and $5.8S_S$ (Fromont-Racine, Senger et al. 2003, Heindl and

Martinez 2010, Morello, Hesling et al. 2011, Mullineux and Lafontaine 2012). Given that a 60S ribosome only incorporates one of these forms, it has been suggested that these might hold a preference for different mRNA forms (Mullineux and Lafontaine 2012).

2.5. The nucleolus and stress

The nucleolar proteome is dynamic, such that proteins are constantly shuttling between the cytoplasm, nucleoplasm and nucleolus. They provide surveillance and can relocate in order to signal and respond to endogenous and exogenous stimuli (Andersen, Lam et al. 2005, Mayer and Grummt 2005, Bański, Kodiha et al. 2010, Boisvert and Lamond 2010, Boulon, Westman et al. 2010, Grummt 2013). These proteins can then elicit a response, and promote a downstream signalling cascade causing cell cycle arrest or apoptosis, whilst inducing the shut-off of ribosome production in order to save energy (Mayer and Grummt 2005, Boulon, Westman et al. 2010, Grummt 2013). A plethora of endogenous and exogenous stimuli can induce these nucleolar changes, including nutrient deprivation, hypoxia, and heat shock, as well as genotoxic, metabolic, ribotoxic, transcriptional and osmotic stresses. These all have common effector mechanisms to shut down the production of ribosomes, detailed below (Mayer and Grummt 2005, Boulon, Westman et al. 2010, Grummt 2013).

Inhibition of Pol I transcription through any stress response or nucleolar disassembly activates and sequesters p53 within the nucleolus, promoting cell cycle arrest and apoptosis (Rubbi and Milner 2003, Wsierska-Gadek and Horky 2003, Mayer and Grummt 2005, Boulon, Westman et al. 2010, Grummt 2013). In the absence of *de novo* pre-rRNA production, B23, $p14^{ARF}$ and ribosomal proteins associate with and inhibit HDM2/Mdm2, which reduces its ubiquitylation of p53, causing its stabilisation and accumulation (Zhang, Wolf et al. 2003, Kurki, Peltonen et al. 2004, Yuan, Zhou et al. 2005).

Modulation of ribosomal production occurs at numerous steps, including regulation of Pol I, rDNA transcription, rRNA processing and ribosome assembly. This can be produced by direct modification of proteins, such as those involved in PIC formation, epigenetic regulation of rDNA or even reorganisation of nucleolar structure, thereby affecting the spatial regulation of rRNA processing and transport (Mayer and Grummt 2005, Boulon, Westman et al. 2010, Grummt 2013).

Repression of Pol I transcription can occur in a number of ways, one of which is the inhibition of RRN3/TIF-IA. Stress signalling activates the MAP kinase JNK2, whilst nutritional stress inhibits the mTOR (mammalian target of rapamycin) pathway, which both result in the phosphorylation of RRN3/TIF-IA, albeit on different sites, thus inhibiting its association with Pol I and SL1 as well as forcing its relocalisation into the nucleoplasm, preventing PIC formation (Davis 2000, Mayer, Zhao et al. 2004, Mayer, Bierhoff et al. 2005, Weston and Davis 2007). Similarly, metabolic stress, such as low levels of ATP, stimulate AMPK (AMP-activated protein kinase) which also phosphorylates RRN3/TIF-IA at a different site to JNK2 or mTOR, and prevents association with SL1 but not Pol I (Hoppe, Bierhoff et al. 2009).

Similarly, the acetylation status of the SL1 subunit, TAF_I68/TAF1B is also important in the regulation of Pol I transcription. In interphase, P/CAF acetylates TAF1B to promote its association with the rDNA promoter, whilst its deacetylation by the HDAC SIRT1 in response to oxidative stress and energy levels represses transcription initiation (Muth, Nadaud et al. 2001). Conversely, the HDAC SIRT7 promotes Pol I transcription by deacetylating the Pol I subunit PAF53, thereby enhancing the association of Pol I with rDNA and facilitating elongation (Ford, Voit et al. 2006, Chen, Seiler et al. 2013). Following various stress responses, SIRT7 is excluded from nucleoli, whereupon CBP acetylates PAF53, repressing transcription (Chen, Seiler et al. 2013).

The transcription termination and reinitiation protein, TTF-I, has also been shown to be regulated in response to stress. Its nucleolar localisation is usually controlled by B23, however this interaction is

blocked by $p14^{ARF}$ following nucleolar stress, sequestering TTF-I within the nucleoplasm and therefore inhibiting Pol I transcription (Lessard, Morin et al. 2010). Interestingly, the protein levels of TTF-I have been shown to be tightly regulated, such that both overexpression and underexpression represses ribosome production. This is regulated by the antagonistic relationship between $p14^{ARF}$ and HDM2/Mdm2, such that $p14^{ARF}$ inhibition of HDM2/Mdm2 following stress alleviates its targeting of TTF-I for proteolysis, thus stabilising TTF-I and inhibiting efficient pre-rRNA synthesis (Lessard, Stefanovsky et al. 2012).

Similarly, UBF protein levels have been shown to fluctuate in response to serum starvation in order to control Pol I transcription; however, this was achieved through modulation of *de novo* UBF protein synthesis rather than ubiquitylation-mediated instability (Glibetic, Taylor et al. 1995). However, the ability of UBF to control Pol I transcription and elongation is also impaired as part of a p53-independent stress response through its dephosphorylation downstream of $p14^{ARF}$ (Ayrault, Andrique et al. 2006). A p53-dependent response also exists, whereby p53 binds to SL1 and prevents its interaction with UBF, preventing the formation of the Pol I-SL1-UBF complex and inhibiting transcription initiation (Zhai and Comai 2000).

There is also evidence that the epigenetic state of rDNA can be altered upon cellular stress. In particular, the eNoSC complex, consisting of Nucleomethylin, SIRT1 and the methyltransferase SUV39H1, induces heterochromatin formation upon active rDNA genes in response to glucose starvation and reduced energy levels (Murayama, Ohmori et al. 2008), whilst the TIP5 subunit of NoRC regulates rDNA silencing in response to serum starvation (Zillner, Filarsky et al. 2013). Similarly, the demethylase KDM2A removes the pro-transcriptional methylation of histone H3 on rDNA elements in a response to starvation (Tanaka, Okamoto et al. 2010).

The inhibition of rDNA transcription, whether by stresses, for example DNA damage, or chemical treatments such as Actinomycin D (Act D), promotes a dramatic reorganisation of the nucleolus, such

that the GC and DFC dissociate, with the resulting structure condensing together with nucleoplasmic proteins to form a nucleolar cap (Reynolds, Montgomery et al. 1964, Simard and Bernhard 1966, Shyy, Subjeck et al. 1986, Govoni, Farabegoli et al. 1994, Andersen, Lam et al. 2005, Shav-Tal, Blechman et al. 2005, Grummt 2013). This spatial separation of the FC, DFC and GC inhibits the later stages of the rRNA processing pathway, thus inhibiting ribosomal assembly and nuclear export. Relocalisation of proteins is an important mechanism for the control of ribosomal assembly, and has already been described in the case of SIRT7, TTF-I and RRN3/TIF-IA (Mayer, Zhao et al. 2004, Mayer, Bierhoff et al. 2005, Lessard, Morin et al. 2010, Chen, Seiler et al. 2013).

3. Aims

The APC/C targets substrates for proteasomal degradation in order to coordinate cell cycle progression (Pines 2011, Primorac and Musacchio 2013). As such, the precise regulation of the APC/C is imperative for accurate cell division and the maintenance of genetic stability (Wasch, Robbins et al. 2010, Penas, Ramachandran et al. 2011); this is achieved primarily through the modulation of APC/C activation by Cdc20 and Cdh1, and the affinity of the APC/C holoenzyme for E2's and substrates (Pines 2011, Chao, Kulkarni et al. 2012, Frye, Brown et al. 2013, Primorac and Musacchio 2013, Wang and Kirschner 2013).

The aims of this study were to identify and characterise novel APC/C substrates, regulators and post-translational modifications, and consequently define new functions of the APC/C. The prinicipal experimental objectives were: firstly, to identify novel APC/C-interacting proteins by mass spectrometric analysis of APC/C subunit and co-activator immunoprecipitates and characterise functionally APC/C interactions with new partner proteins, and secondly, to determine the role of acetylation in the regulation of APC/C activity.

4. MATERIALS AND METHODS

4.1. Cell Culture, Drug Treatments and Irradiation

HeLa (human cervical adenocarcinoma) and A549 (human lung carcinoma) cell lines were passaged in growth medium (High Glucose DMEM (Sigma; D5796) supplemented with 8% (v/v) FCS (Sigma)) and cultured in a humidified incubator at 37°C, 5% (v/v) CO_2. HeLa cells are known to contain integrated HPV18 genomes, resulting in the overexpression of C-MYC, as well as a hypertriploid genome (3n+; modal chromosome number=82) and numerous chromosomal rearrangements (Chen 1988, Macville, Schröck et al. 1999). HeLa cells do not contain functional p53 due to the presence of the HPV18 E6 protein (May, Jenkins et al. 1991). A549 cells are hypotriploid (modal chromosome number=66), but have wild-type p53. The growth medium for U2OS-TetR cells (human osteosarcoma; hypertriploid but express wild-type p53; stably transfected with pcDNA6-TR expressing the TetR (Tet Repressor) gene (Life Technologies)) was supplemented with 5µg/ml Puromycin (Life Technologies) and 1.5µg/ml Blasticidin (Source Bioscience) after infection, and HeLa-FRT cells (HeLa cells containing integrated pFRT⁄lacZeo (Life Technologies)) were supplemented with 1.5µg/ml Blasticidin and 500µg/ml Zeocin (Life Technologies) before transfection and 1.5µg/ml Blasticidin together with 200µg/ml Hygromycin B (Life Technologies) after transfection. *Spodoptera frugiperda* (Sf9) cells were grown in TMN-FH medium (Gibco) in a humidified incubator at 26°C, 5% (v/v) CO_2. Cells were trypsinised using TrypLE express (Life Technologies) for 5 min at 37°C, followed by neutralisation in growth medium and centrifugation at 300g for 5 min. Pelleted cells were resuspended in growth medium and, typically, one fifth were reseeded onto a new dish. If a precise number of cells were required, the density of cells was determined using a haemocytometer (Sigma) and an inverted phase-contrast microscope (Nikon eclipse TS100).

Cells were synchronised in mitosis by treatment with 400ng/ml nocodazole (Sigma) for 20h. Mitotic cells were released by mechanical shake-off, washed in Phosphate-Buffered Saline (PBS) and reseeded into fresh medium for the time required.

Pre-rRNA synthesis was inhibited by incubation with Actinomycin D (Fisher Scientific) either at 0, 0.1, 0.5, 1 or 5µg/ml for 2h, or at 0.1µg/ml for 0, ½, 1, 2, 4, 8 or 24h.

Cells were arrested in G1/G0 by glucose and/or serum starvation. HeLa cells were incubated with DMEM powder (Sigma; D5030) dissolved in ddH_2O containing 0.375% (w/v) sodium bicarbonate and 2mM L-Glutamine (Sigma) and passed through a sterile 0.22µm syringe filter. Cells were then incubated with this media, or further supplemented with 4.5g/l Glucose and/or 10% (v/v) FCS for 20h.

DNA damage was induced by irradiating cells with either 25J/m^2 UV-C or 5 Gy of Ionising Radiation (IR) and left to recover in full growth medium for 1, 2, 4, 8 or 24h. Alternatively, cells were treated with Cisplatin (David Bull Laboratories) either at 0, 10, 20, 30, 40 or 50µg/ml for 16h, or at 20µg/ml for 0, 2, 4, 8, 16, 24 or 48h.

4.2. siRNA-mediated knockdown

$3x10^5$ HeLa cells were seeded onto a 6cm dish 18h prior to transfection. 4µl of 40µM siRNA duplexes (Ambion; Table 9) was incubated for 20 min with 1ml OptiMEM and 10µl Lipofectamine RNAiMAX (both Life Technologies), then applied to the cells for 6h, washed and fresh growth medium applied. Cells were harvested 72 h post-knockdown.

Target Protein	5'-3' Sequence
APC3	GGAAAUAGCCGAGAGGUAAdTdT
APC5	AACCTCCGTGTTCAAGATGTTdTdT
APC7	AAGAGCGATCAACACCATCTGdTdT
APC8	GAAAUUAAAUCCUCGGUAUdTdT
Cdc20	CCUUGUGGAUUGGAGUUCUdTdT
Cdh1	CGACUUCUACCUCAAUCUGdTdT
Non-Silencing (LacZ)	CGUACGCGGAAUACUUCGAdTdT
CBP	AATCAACTCCTGTGTCGTCTTdTdT
P300	AAGTTCAAACGCCGAGTCTTCdTdT

Table 9 – sequence of siRNAs used in this study

4.3. Generation of dox-inducible APC3 shRNA cell line

APC3 shRNA sequences were synthesised, with sequences: shRNA1 For – GATCCCCGGAAATAGCCGAGAGGTAATTCAAGAGATTACCTCTCGGCTATTTCCTTTTTA and Rev – AGCTTAAAAAGGAAATAGCCGAGAGGTAATCTCTTGAATTACCTCTCGGCTATTTCCGGG; shRNA2: For – GATCCCCCAAAAGAGCCTTAGTTTAATTCAAGAGATTAAACTAAGGCTCTTTTGTTTTTA and Rev – AGCTTAAAAACAAAAGAGCCTTAGTTTAATCTCTTGAATTAAACTAAGGCTCTTTTGGGG. 3µg of each complementary oligonucleotide strand were annealed in 48µl annealing buffer (100mM NaCl, 50mM HEPES pH7.4) and incubated at 90°C for 4 min, 70°C for 10 min and step-cooled to 37°C for 20 min then step-cooled to room temperature. The annealed oligos were cloned into a pSuperior.Retro.Puro cDNA (Oligoengine) and transfected into 293FT viral packaging cells using Lipofectamine 2000 and OptiMEM (Life Technologies). 48h after transfection, viral progeny were harvested from the medium, passed through a sterile 0.22µm syringe filter and used to infect U2OS-TetR cells (Grant Stewart, University of Birmingham). 24h after infection, U2OS-TetR cells were

selected for positive clones by the addition of 5µg/ml Puromycin and 1.5µg/ml Blasticidin into the growth medium. APC3 shRNA expression was induced by treatment with Doxycycline (Dox; Clontech) at 0, 1, 5, 10 or 50µg/ml for 48h or 72h.

4.4. Targeted recombination of DNA into HeLa-FRT cell lines

Flag-APC3 was mutated to become resistant to siRNA, and was cloned into pcDNA5-FRT (Jakob Nilsson, University of Copenhagen). Flag-APC3-pcDNA5-FRT K336 was mutated to Q or R. An siRNA-resistant 3xFlag-APC8-pcDNA5-FRT (Jakob Nilsson) was used as a template to mutate K359 and K396 to either Q or R. 0.5µg of these pcDNA5-FRT cDNAs were co-transfected with 4.5µg pOG44 (Life Technologies) using the following protocol: HeLa-FRT cells (Stephen Taylor, University of Manchester) were seeded onto a 6cm dish in antibiotic-free growth medium to 80% confluency. DNA was mixed with OptiMEM (Life Technologies) to a total volume of 200µl, and 10µl of Lipofectamine 2000 (Life Technologies) was mixed with 190µl OptiMEM for 5 min. The mixtures were then incubated together for a further 15 min, and then added to HeLa-FRT cells incubated in 1.6ml OptiMEM for a total of 8h. 24h post-transfection, cells were seeded onto a 10cm dish. 48h later, cells were selected with 1.5µg/ml Blasticidin (Source Bioscience) and 200µg/ml Hygromycin B.

4.5. Adenoviral infection

$2x10^6$ HeLa cells were seeded onto 10cm dishes and infected with 20pfu/cell of an adenovirus vector containing either LacZ or HA-Apoptin cDNA (Jose Teodoro, McGill University) in 2ml serum-free DMEM for 2h, followed by further incubation in growth medium for 60h.

4.6. Preparation of Whole-Cell Extracts

Lysates were obtained by washing cells twice in ice-cold saline, and scraping into lysis buffer. For Western blotting, cells were lysed in UTB (9M Urea, 50mM Tris-HCl pH 7.5, 0.15M β-Mercaptoethanol), whilst Immunoprecipitations (IPs) were typically performed in NETN (250mM NaCl, 0.5mM EDTA (Ethylenediaminetetraacetic acid) pH 8, 50mM Tris-HCl pH 7.5, 1% (v/v) Nonidet-

P40 (NP-40)). Cells used for IPs of CBP and p300 for *in vitro* acetyltransferase assays were lysed in 50mM Tris pH 8, 150mM NaCl, 1mM EDTA pH 8, 10mM sodium butyrate, 0.5% (w/v) sodium deoxycholate and 0.5% (v/v) NP-40. For UTB, the sample was sonicated for 10s on ice, whilst samples prepared in NETN were subjected to Dounce homogenisation with a tight pestle for 2x10 strokes. The lysates were then cleared by centrifugation at 16,200g for 30 min at 4°C.

4.7. Protein Concentration Determination

A 1mg/ml solution of Bovine Serum Albumin (BSA; Sigma) was diluted in Bradford reagent (Bio-Rad) to a final concentration of 0, 5, 10, 20, 30µg/ml and the absorbance at 595nm calculated upon a Cecil CE9200 spectrophotometer to give a standard curve. 2µl of protein lysate/GST-protein was added to 1ml Bradford reagent, and the absorbance at 595nm compared to the standard curve to give protein concentration.

4.8. Nuclear Fractionation

A method to perform cellular fractionation into nucleolar and nucleoplasmic fractions was adapted from a published protocol from Angus Lamond's group (Andersen, Lyon et al. 2002). 5x10cm dishes of confluent HeLa cells were obtained by trypsinisation and allowed to swell in 5ml hypotonic buffer (Buffer A; 10mM HEPES pH 7.9, 10mM KCl, 1.5mM $MgCl_2$, 0.5mM DTT) for 5 min. Pure nuclei were obtained by Dounce homogenising with a tight pestle on ice for 20 strokes, left on ice for 10 min, followed by another 20 strokes. The selective permeabilisation of the plasma membrane and the retention of intact nuclei were checked using an inverted phase-contrast microscope (Nikon eclipse TS100) as were all subsequent steps. The nuclei were pelleted by centrifugation at 218g for 5 min at 4°C and purified by resuspension in 3ml Buffer S1 (0.25M Sucrose, 10mM $MgCl_2$) and layering over 3ml Buffer S2 (0.35M Sucrose, 0.5mM $MgCl_2$) followed by centrifugation at 1,430g for 5 min at 4°C. The nuclear pellet was resuspended in 3ml Buffer S2 and sonicated on ice at 35% amplitude for 8x10s, with 10s intervals in between. Further 10s bursts were performed if all nuclei had not lysed.

Sonicated nuclei were then layered over 3ml Buffer S3 (0.88M Sucrose, 0.5mM $MgCl_2$) and centrifuged at 3,000g for 10 min at 4°C. To purify nucleoli, the nucleolar pellet was resuspended in 0.5ml Buffer S2 and centrifuged at 1,430g for 5 min at 4°C. This nucleolar pellet was then resuspended in lysis buffer and sonicated for a further 30s to disrupt the nucleolus completely.

4.9. FPLC (Fast Protein Liquid Chromatography)

Pure nucleoli were solubilised in FPLC Buffer A (20mM Tris pH 7.5, 100mM NaCl, 20mM β-glycerophosphate, 0.2% (v/v) NP-40, 10% (v/v) glycerol, 0.5mM DTT and c*O*mplete, Mini protease inhibitors (Roche)) and passed through a 0.22µm syringe filter. 2.5mg of nucleolar lysate was loaded onto a pre-equilibrated Superose-6 column (GE Healthcare) and run at a flow rate of 0.5ml/min and pressure limit of 1.5MPa. 0.5ml fractions were collected and precipitated using 1ml 100% (v/v) EtOH, followed by centrifugation to pellet the protein. The protein pellet was resolubilised using UTB and sonicated prior to SDS-PAGE and Western blot analysis.

4.10. Immunoprecipitation (IP)

Cells were generally lysed in NETN for IPs, except for *in vitro* enzyme assays (see sections 4.6 and 4.20). Typically, 5µg of antibody was added to lysates, and incubated overnight at 4°C, 15rpm. Negative controls were performed in which the lysates were incubated with non-specific antibodies raised in the same host species as the IP antibody ("normal IgG"). 10µl of packed Protein G-Agarose beads (KPL) were then added, and incubated for an additional 2h at 4°C, 15rpm. The beads were washed 6x by centrifugation at 2,800g, 4°C and resuspended in lysis buffer. For mass spectrometry, 20µg of antibody and 20µl of packed Protein G-agarose beads were used.

4.11. SDS-PAGE

Samples were boiled in sample buffer (6M Urea, 33.3mM Tris pH 7.5, 3.33% (w/v) Sodium Dodecyl Sulphate (SDS), Bromophenol Blue) and separated by SDS-PAGE (SDS-Polyacrylamide Gel Electrophoresis) in running buffer (100mM Tris, 100mM Bicine, 0.1% (w/v) SDS) using a vertical gel

electrophoresis system (Hoefer), typically run overnight at 14mA. Continuous acrylamide gels were cast, containing 100mM Tris, 100mM Bicine, 0.1% (w/v) SDS, 150µl TEMED and 300µl 10% (w/v) APS (all Sigma) made up to 50ml with the desired volume of acrylamide/bis-acrylamide (37.5%) (Severn Biotech) and ddH_2O. For mass spectrometry, samples were boiled in NuPAGE LDS sample buffer (4x) and run on a NuPAGE 4-12% tris/bis-tris gel (both Life Technologies) in MOPS running buffer (50mM MOPS, 50mM Tris, 0.1% (w/v) SDS, 1mM EDTA pH 7.7) at 100V until fully resolved.

4.12. Western Blotting

Proteins were separated by SDS-PAGE, then transferred onto a nitrocellulose membrane (VWR) for 6h at 275mA in transfer buffer (24mM Tris, 193mM Glycine, 20% (v/v) MeOH). Membranes were cut to size, washed in TBST (Tris-buffered Saline – Tween 20; 20mM Tris-HCl pH 7.5, 150mM NaCl, 0.1% (v/v) Tween-20), then blocked in blocking buffer, consisting of 5% (w/v) milk powder in 1x TBST. Antibodies were diluted in blocking buffer at the desired dilution (Table 10) and incubated overnight at 4°C on a rocker. Blots were washed 3x15 min in TBST followed by incubation with secondary antibody conjugated to HRP (Table 10) for 2h at room temperature on a rocker. Blots were washed 3x15 min in 1x TBST and visualised using Immobilon Western Chemiluminescent HRP Substrate (Millipore) and X-ray film (Wolf Laboratories).

Protein	Species	Manufacturer	Catalogue/ Clone No.	IF	IP (WB)	IP (MS)	WB
Ac-K	Rabbit	Upstate	06-933	-	5µg	-	1:500
β-Actin	Mouse	Sigma	A2228	-	-	-	1:10000
APC1	Rabbit	Bethyl	A301-653A	1:50	-	-	-
APC3	Mouse	CRUK/Hiro Yamano	AF3.1	-	5µg/ 200µl	20µg/ 600µl	-
APC3	Mouse	BD Biosciences	610455	-	5µg	-	1:2000
APC5	Mouse	In-house	#4	1:50	5µg	20µg	1:2000
APC5	Mouse	In-house	#24	1:1	-	-	-
APC7	Rabbit	In-house	#197	1:50	5µg	20µg	1:2000
B23	Rabbit	Santa Cruz	sc-6013-R	-	-	-	1:1000
BrdU	Mouse	Sigma	B2531	1:1000	-	-	-
CBP	Rabbit	Santa Cruz	A-22	-	5µg	-	1:200
Cdc20	Mouse	Santa Cruz	sc-13162	-	-	20µg	1:1000
Cdh1	Mouse	Calbiochem	DH01	-	-	20µg	-
Cdh1	Mouse	Santa Cruz	sc-56312	-	-	-	1:1000
Cyclin A	Rabbit	Santa Cruz	sc-751	-	-	-	1:1000
Cyclin B1	Mouse	Santa Cruz	sc-055	-	-	-	1:1000
Cyclin D1	Rabbit	Santa Cruz	sc-754	-	-	-	1:1000
Fibrillarin	Mouse	Abcam	Ab4566	1:1000	-	-	-
Fibrillarin	Rabbit	CST	2639	1:500	-	-	-
HA	Mouse	Covance	MMS-101P	-	-	-	1:1000
normal IgG	Mouse	Sigma	I5381	-	5µg	20µg	-
p300	Rabbit	Santa Cruz	N-15	-	5µg	-	1:200
p53	Mouse	In-house	DO-1	-	-	-	1:10
PARP	Mouse	Santa Cruz	sc-8007	-	-	-	1:1000
RPA135	Goat	Santa Cruz	sc-17914	-	5µg	-	1:500
RPA194	Mouse	Santa Cruz	sc-48385	1:50	5µg	20µg	1:2000
RPA194	Rabbit	Santa Cruz	sc-28714	1:50	-	-	1:1000
RPA40	Mouse	Santa Cruz	sc-374443	-	5µg	-	1:1000
UbcH10	Rabbit	In-house	-	-	-	-	1:1000
α-Goat-Alexa Fluor 488	Donkey	Life Technologies	A11055	1:100	-	-	-
α-Mouse-Alexa Fluor 488	Goat	Life Technologies	A11001	1:100	-	-	-
α-Mouse-Alexa Fluor 594	Donkey	Life Technologies	A21203	1:100	-	-	-
α-Rabbit-Alexa Fluor 488	Donkey	Life Technologies	A21206	1:100	-	-	-
α-Rabbit-Alexa Fluor 594	Donkey	Life Technologies	A21207	1:100	-	-	-
α-Goat-HRP	Rabbit	Dako	P0449	-	-	-	1:3000
α-Mouse-HRP	Goat	Dako	P0447	-	-	-	1:3000
α-Rabbit-HRP	Swine	Dako	P0399	-	-	-	1:4000

Table 10 – Concentration and catalogue numbers of antibodies used for IF, Western blotting (WB), and IPs for Western blotting (IP (WB)) and Mass Spectrometry (IP (MS)).

4.13. Site-directed PCR mutagenesis

DNA mutagenesis was performed using the QuikChange Site-Directed Mutagenesis Kit (Agilent). 50ng cDNA was used as a template together with 125ng forward and reverse primers (Table 11i), 1µl dNTPs, 5µl 10x buffer and 2.5U Pfu Turbo made up to 50µl with nuclease-free H_2O. The PCR conditions used were: 95°C for 30s, followed by 18 cycles of 95°C for 30s, 55°C for 1 min and 68°C for 1 min per kb of cDNA, using a 2720 Thermocycler PCR (Applied Biosystems). Template cDNA was digested by incubation with 10U *Dpn I* for 1h at 37°C. XL-1 blue cells were then transformed with digested DNA, as described below.

i. Mutagenesis Primers

Primer	Sequence/ Catalogue No.	Manufacturer
APC3 siRNA resis For	CACAGAGTGGAAACTCCAGGGAGGTAACTCCAATT	Alta Bioscience
APC3 siRNA resis Rev	AATTGGAGTTACCTCCCTGGAGTTTCCACTCTGTG	Alta Bioscience
APC3 K336Q For	GGCCAAACTGGAACACAGTCTGTCTTCTCACA	Alta Bioscience
APC3 K336Q Rev	TGTGAGAAGACAGACTGTGTTCCAGTTTGGCC	Alta Bioscience
APC3 K336R For	GGCCAAACTGGAACACGGTCTGTCTTCTCACA	Alta Bioscience
APC3 K336R Rev	TGTGAGAAGACAGACCGTGTTCCAGTTTGGCC	Alta Bioscience
APC5 Fr1 For	GTCATGAATTCATGGCCAGCGTCCACGAGAGCCTC	Alta Bioscience
APC5 Fr1 Rev	ATTGCCTCGAGTCTACTGGTCAGTTCCATATCAGC	Alta Bioscience
APC5 Fr2 For	GTCATGAATTCGATGAGGGTGAAAGAAAAATGGAA	Alta Bioscience
APC5 Fr2 Rev	ATTGCCTCGAGCAGAACATAGCTATCGGATCTCTT	Alta Bioscience
APC5 Fr3 For	GTCATGAATTCCTGGAGCATTCTGTGAAGAAGGCA	Alta Bioscience
APC5 Fr3 Rev	ATTGCCTCGAGTGCCTCTGACATTTGGTTCTGAGC	Alta Bioscience
APC5 Fr4 For	GTCATGAATTCCATAAGCTTTTACAAAAATTGTTG	Alta Bioscience
APC5 Fr4 Rev	ATTGCCTCGAGCTAGAGATGGTTTATCAAGGGTAC	Alta Bioscience
APC8 K359Q For	TTCCAGAGAGCCCTGCAACTGAACCCCCGGTATCT	Alta Bioscience
APC8 K359Q Rev	AGATACCGGGGGTTCAGTTGCAGGGCTCTCTGGAA	Alta Bioscience
APC8 K359R For	TTCCAGAGAGCCCTGAGACTGAACCCCCGGTATCT	Alta Bioscience
APC8 K359R Rev	AGATACCGGGGGTTCAGTCTCAGGGCTCTCTGGAA	Alta Bioscience
APC8 K396Q For	GCCATTGAGGTCAACCAACGGGACTACAGAGCTTG	Alta Bioscience
APC8 K396Q Rev	CAAGCTCTGTAGTCCCGTTGGTTGACCTCAATGGC	Alta Bioscience
APC8 K396R For	GCCATTGAGGTCAACAGACGGGACTACAGAGCTTG	Alta Bioscience
APC8 K396R Rev	CAAGCTCTGTAGTCCCGTCTGTTGACCTCAATGGC	Alta Bioscience

ii. Sequencing Primers

Primer	Sequence/ Catalogue No.	Manufacturer
pcDNA3_F	TAATACGACTCACTATAGG	Alta Bioscience
pcDNA3_R	TAGAAGGCACAGTCGAGG	Alta Bioscience
APC3 seq 461	GAATCATTATGTGAAATAGGTGAAAAGCCA	Alta Bioscience
APC3 seq 821	GCAGCTCTTAGTCCATTAACCCCAAGTTTT	Alta Bioscience
APC3 seq 1181	TCCACAACCAAGGAGAATAGCAAAAAATTA	Alta Bioscience
APC3 seq 1531	CCAAATTGGAAGGGCCTATTTTGAACTTTC	Alta Bioscience
APC3 seq 1981	TGCAGAAATGCATTTCCAAAAAGCGCTTGA	Alta Bioscience
APC3 rev seq 253	GCTTGCTGAGATCAACACAAC	Alta Bioscience
APC3 rev seq 830	ATAAGACACTGAGGAATCTGTATT	Alta Bioscience
APC3 rev seq 1130	TGAGAAGACAGACTTTGTTCCAGT	Alta Bioscience
APC3 rev seq 1333	CTGAAATGCTGGAAGAGTCC	Alta Bioscience
APC3 rev seq 1691	TATTCTTTCAGCTTGCATGTA	Alta Bioscience
APC8 seq 421	AAAAATGAGGCGCTTAGAGAAT	Alta Bioscience
APC8 seq 818	TGACAAAGCCCTCTCCATTTTT	Alta Bioscience
APC8 seq 1212	CAGACCTATGAAATCCTTAAGA	Alta Bioscience

iii. qPCR Primer/Probes

Primer	Sequence/ Catalogue No.	Manufacturer
45S pre-rRNA For	TGTCAGGCGTTCTCGTCTC	Alta Bioscience
45S pre-rRNA Rev	AGCACGACGTCACCACATC	Alta Bioscience
Actin For	CAGGAAGGAAGGCTGGAAGA	Alta Bioscience
Actin Rev	GCTGTGCTATCCCTGTACGC	Alta Bioscience
28S rRNA TaqMan Assay - FAM/MGB	Hs03654441_s1	Applied Biosystems
18S rRNA TaqMan Assay - VIC/MGB	4319413E	Applied Biosystems
GAPDH TaqMan Assay - VIC/MGB	Hs03929097_g1	Applied Biosystems
Hprt1 TaqMan Assay - VIC/MGB	Hs03929096_g1	Applied Biosystems
APC3 TaqMan Assay-FAM/MGB	Hs00265810_m1	Applied Biosystems
APC5 TaqMan Assay-FAM/MGB	Hs01102438_m1	Applied Biosystems
Cdc20 TaqMan Assay-FAM/MGB	Hs00426680_mH	Applied Biosystems

Table 11 – list of oligonucleotide primers used in this study

4.14. Purification of DNA by agarose gel electrophoresis and DNA Gel Extraction

Typically, agarose gels were cast at 0.8% (w/v) agarose (AGTC) in 75ml TBE (100mM Tris, 100mM boric acid, 2mM EDTA pH 8.3) containing 3µl SYBR Safe (Life Technologies). DNA was heated at 65°C for 10 min in 6x Gel Juice (30% (v/v) glycerol, 0.25% (w/v) bromophenol blue, 0.25% (w/v) of xylene cyanol FF) and separated by electrophoresis until suitably resolved, as determined by a DNA ladder (DNA Molecular Weight X or XIII; Roche). Gels were visualised under blue light and orange filter (Invitrogen Safe Imager). Bands were excised with a clean scalpel and DNA was extracted using a QIAquick Gel Extraction Kit (Qiagen). Briefly, gels were weighed and solubilised in 3x volume of Buffer QG and heated at 55°C for 10 min, to which 1x volume isopropanol was added. This solution was mixed and centrifuged through a QIAquick column at 16,200g for 1 min. The column was washed by centrifugation with 0.5ml Buffer QG, then 0.75ml Buffer PE. The column was spun again to dry, and moved into a clean collection tube. 50µl nuclease-free H_2O was added, and incubated at room temperature for 1 min prior to centrifugation at 16,200g for 1 min.

4.15. Cloning of DNA

Amplification of DNA sequences typically consisted of a 50µl reaction mixture containing: 100ng DNA, 5pmoles forward and reverse primer, 1µl dNTPs (10mM), 5µl 10x buffer and 1µl Pfu (Promega). The PCR was run in a 2720 Thermocycler PCR (Applied Biosystems) with the following programme: Pre-PCR - 95°C for 5 min, 50°C for 2 min, 72°C for 5 min; 35 cycles of 95°C for 30s, 50°C for 30s, 72°C for 2 min per kb of DNA; Final extension - 72°C for 7 min. PCR products were purified by agarose gel electrophoresis and DNA gel extraction. Alternatively, DNA was subcloned from one vector into another. In both cases, DNA was digested with 1/10x volume restriction endonucleases (NEB, Roche), typically for 2h at 37°C in the correct 10x Buffer, according to Roche and NEB double-digest tables. The vector (listed in Table 13) into which the insert was to be ligated was also digested with the same endonucleases. Digest mixtures were heat-inactivated at 65°C for 10 min and digested DNA was purified by agarose gel electrophoresis. Ligation mixtures were made, initially starting with 1:10

vector:insert volume ratio together with 2µl 10x ligation buffer and 1µl T4 DNA Polymerase (NEB) in 20µl total volume and incubated overnight at 16°C.

4.16. Use of Bacterial Cultures to amplify DNA

Bacterial strains used in this study are listed in Table 12. DNA was amplified by bacterial transformation and culture. For purified plasmids, 100ng of DNA was transformed into 10µl DH5α (Life Technologies). For ligations, 4µl of ligation mixture was transformed into 20µl DH5α. For PCR mutagenesis, 4µl digested DNA was transformed into 25µl XL-1 blue bacteria (Agilent). Bacteria were heat-shocked at 42°C for 2 min, left to recover on ice for 5 min and incubated for 1h at 200rpm in 0.5ml LB (1% (w/v) NaCl, 1% (w/v) Tryptone (DIFCO), 0.5% (w/v) Yeast extract (DIFCO); ligations and purified plasmids) or 0.5ml NZY^+ (1% (w/v) NZ amine, 0.5% (w/v) Yeast extract, 0.5% (w/v) NaCl, 12.5mM $MgCl_2$, 12.5mM $MgSO_4$, 0.4% (w/v) Glucose; PCR mutagenesis). The bacterial culture was then spread onto LB-agar plates (1.5% (w/v) bacto-agar (DIFCO) in LB) containing 100µg/ml Ampicillin (Sigma) using a disposable hockey spreader and cultured overnight at 37°C.

Individual colonies were picked using a bacterial loop and grown in 5ml LB supplemented with 100µg/ml Ampicillin overnight at 37°C, 200rpm. DNA was extracted using GenElute plasmid miniprep kit (Sigma) as per manufacturer's instructions with final elution by 50µl nuclease-free H_2O. Briefly, bacteria were pelleted by centrifugation and resuspended in 200µl cold Resuspension Buffer. Then, bacteria were lysed by the addition of 200µl Lysis Buffer and inverted to mix. Lysis was then inhibited by addition of 350µl Neutralisation/Binding Solution, and mixed by inversion. The lysate was centrifuged at 16,200g for 10 min to pellet cell debris. The GenElute Miniprep Binding Column was washed with 0.5ml Column Preparation Solution and centrifuged at 16,200g, 1 min. The cleared lysate was then spun through the column at 16,200g for 1 min, and washed by centrifugation with 0.75ml Wash Solution (+EtOH) at 16,200g for 1 min. The column was spun again to dry, and then

transferred into a clean tube. 50µl nuclease-free H_2O was added and incubated at room temperature for 1 min, then eluted by centrifugation at 16,200g for 1 min.

If a large yield of DNA was required, bacterial colonies were grown in 5ml LB/ampicillin for 8h at 37°C, 200rpm, which was then added to 250ml LB/ampicillin and cultured overnight at 37°C, 200rpm. DNA was then harvested using a GenElute HP Maxiprep Kit (Sigma). Bacterial cultures were pelleted by centrifugation at 5,000g for 10 min. Bacteria were resuspended in 12ml cold Resuspension/RNase A Solution, to which 12ml Lysis Solution was added and mixed by inversion. 12ml Neutralisation Solution was added to inhibit lysis, and was mixed by inversion. 9ml Binding Solution was added, mixed and added to a filter syringe and incubated for 5 min. 12ml Column Preparation Solution was centrifuged through a GenElute HP Maxiprep Binding Column at 3,000g for 2 min. The lysate was then filtered through the syringe onto the column, which was centrifuged at 3,000g for 2 min. 12ml Wash Solution 1 was centrifuged through the column at 3000g for 2 min, followed by 12ml Wash Solution 2 (+EtOH) at 3,000g for 5 min. DNA was eluted by the addition of 3ml Elution Solution and centrifugation at 3,000g for 5 min. The DNA was then precipitated by the addition of 0.1x volume of 3M Na-acetate (Sigma) and 0.7x volume isopropanol. The tube was mixed by inversion and centrifuged at 15,000g for 30 min to pellet DNA. The pellet was washed by 1.5ml 70% (v/v) EtOH and spun at 15,000g for 10 min. The pellet was air-dried and resuspended in approximately 200µl nuclease-free H_2O, dependent upon size.

Bacterial Strain	Initial broth	Cultured broth	Manufacturer
BL21-RIPL	LB	LB	Agilent
DH5α	LB	LB	Life Technologies
XL1-blue	NZY^+	LB	Agilent

Table 12 – list of bacterial strains used in this study

Plasmid	Origin	Bacterial Antibiotic Resistance	Inserts	Uses
Adenovirus vector	Joe Teodoro	-	(LacZ, HA-Apoptin)	Adenoviral infection
pcDNA3	Jonathon Pines	Ampicillin	(Cyclin A, Cyclin B1)	IVT, Subcloning
pcDNA3	Andy Turnell	Ampicillin	(APC3, CBP)	IVT, Subcloning
pcDNA5-FRT	Jakob Nilsson	Ampicillin	HA-APC3 K336 wt/Q/R	Incorporation into HeLa-FRT cells
3xFlag-APC8-siRNA resis-pcDNA5-FRT	Jakob Nilsson	Ampicillin	APC8 K359/K396 wt/Q/R	Incorporation into HeLa-FRT cells
pGEX-4T1	GE Healthcare	Ampicillin	APC3, APC5 and fragments	GST-proteins
CBP-pGEX-4T1	Andy Turnell	Ampicillin	(CBP)	GST-proteins
CBP-fragments-pGEX-4T1	Andy Turnell	Ampicillin	(CBP fragments)	GST-proteins
Ad5-E1A-pGEX-4T1	Andy Turnell	Ampicillin	(Ad5 12S-E1A)	GST-proteins
pSuperior.Retro.Puro	Oligoengine	Ampicillin	APC3 shRNA1 and shRNA2	Creation of dox-inducible shRNA U2OS-TetR cells
pOG44	Jakob Nilsson	Ampicillin	-	Incorporation into HeLa-FRT cells
P300 baculovirus	Lee Kraus	-	(p300)	Infection into insect cells for His-purification
POLR1A-pCR4-TOPO	IMAGE 8992019	Ampicillin	(POLR1A (RPA194))	IVT
POLR1B-pCMV-SPORT6	IMAGE 6053210	Ampicillin	(POLR1B (RPA135))	IVT

Table 13 – list of plasmids and viruses used in this study

(Inserts already provided within plasmids/viruses are enclosed by brackets)

4.17. Measuring nucleic acid concentration

DNA and RNA concentrations were measured by a NanoDrop ND-1000 Spectrophotometer and ND-1000 Spectrophotometer v3.2 software (Thermo Fisher Scientific). The absorbance at 230, 260 and 280nm wavelengths were measured and compared to H_2O control, and the ratios calculated to give DNA and RNA concentrations.

4.18. Sequencing of DNA

4µl of DNA from a miniprep or 100ng of purified DNA were used in a sequencing PCR consisting of 10ng sequencing primer (Table 11ii), 4µl 5x sequencing buffer and 1µl Big Dye Terminator (Applied

Biosystems), made up to 20µl with nuclease-free H_2O. The sequencing PCR was performed with 25 cycles of: 96°C for 10s, 55°C for 5s, 60°C for 4 min. The PCR product was precipitated by the addition of 62.5µl 100% (v/v) EtOH, 3µl 3M Na-Acetate, 14.5µl H_2O and incubation at room temperature for 30 min followed by centrifugation at 16,200g rpm for 20 min. The pellet was washed with 100µl 70% (v/v) EtOH and spun at 16,200g for 15 min. The pellet was air-dried, resuspended in 11µl HiDi formamide and heated at 100°C for 5 min. The DNA was then sequenced using a 3500xl Genetic Analyzer (Applied Biosystems) and compared to a consensus sequence by BLAST (NCBI, NIH).

4.19. *In vitro* transcription/translation

In vitro transcription/translation (IVT) was carried out using TNT-coupled rabbit reticulocyte lysate system (Promega). Reaction mixtures included: 25µl TNT rabbit reticulocyte lysate, 2µl TNT reaction buffer, 1µl TNT T7 RNA Polymerase, 1µl methionine-free amino acid mixture, 40U RNasin Ribonuclease Inhibitor (All Promega), 2µl 10mCi/ml L-α-[^{35}S]-methionine (Amersham), and 1µg DNA (Table 13) made up to a total volume of 50µl with nuclease-free H_2O. Reactions were performed at 30°C for 90 min.

4.20. *In vitro* APC/C E3 ubiquitin ligase assay

In vitro ubiquitylation assays were adapted from published protocols (Gieffers, Dube et al. 2001, Kraft, Gmachl et al. 2006). 1x10cm dish of asynchronous HeLa cells was lysed in buffer (20mM Tris-HCl pH 7.5, 100mM NaCl, 20mM β-glycerophosphate, 5mM $MgCl_2$, 0.2% (v/v) NP-40, 10% (v/v) glycerol, 1mM NaF, 0.5mM DTT), and the APC/C holoenzyme was purified by IP with 20µg APC3 AF3.1 antibodies (CRUK) or normal IgG overnight and 10µl packed Protein G-Agarose beads (KPL) for 3h, at 15rpm and 4°C. IPs were washed four times in Buffer BL (20mM Tris-HCl pH 7.5, 150mM NaCl, 0.02% (v/v) Tween-20) and twice in Buffer BH (20mM Tris–HCl pH 7.5, 450mM NaCl, 0.02% (v/v) Tween-20). To obtain APC/C activated by Cdc20, HeLa cells were arrested in prometaphase by treatment with 400ng/ml nocodazole and released for 1h into fresh growth medium prior to

harvesting. To each IP, 20µl of a reaction buffer containing 50mM Tris-HCl pH 7.5, 5mM $MgCl_2$, 25µg/ml His-E1 (Boston Biochem), 40µg/ml GST-UbcH4, GST-UbcH5 and GST-UbcH10 (Hiro Yamano, University College London), 1.25mg/ml Ubiquitin (Boston Biochem), 20µg/ml Ubiquitin aldehyde (Boston Biochem) and an ATP regeneration system (350U/ml creatine phosphokinase, 10mM creatine phosphate, 5mM ATP). 1µl [^{35}S]-substrate was then added and incubated at 37°C for 1h. The reaction mixture was separated by SDS-PAGE, sensitised with Amersham Amplify Fluorographic Reagent (GE Healthcare) for 30 min, dried under a vacuum and polyubiquitylation of substrates detected by autoradiography with X-ray film (Wolf Laboratories).

4.21. Bacterial expression of GST-fusion proteins

Full length and fragments of cDNA were cloned into pGEX 4T-1 (GE Healthcare) containing an N-terminal fusion gene for Glutathione-S-Transferase (GST), expressed in BL21 Competent Cells (Agilent) and grown overnight in 20ml LB at 37°C, 200rpm. This culture was expanded in 500ml LB for 3h at 37°C, 200rpm, then dropped to 30°C for 1h. GST-protein expression was induced by the addition of 0.5mM IPTG (Isopropyl-β-D-thio-galactoside; Sigma) and the culture was incubated at 30°C, 200rpm for 3h. Bacteria were pelleted at 5,000g, 4°C for 10 min, then lysed in 14ml GST lysis buffer (1% (v/v) Triton X-100, 1mM EDTA pH 8 in PBS). Lysates were sonicated 3x1 min on ice with 20% output and 1 min rest in between pulses. Debris was pelleted by centrifugation at 20,000g, 4°C for 2x15 min, with the supernatant collected each time. The supernatant was incubated with 1ml glutathione-agarose beads (Sigma) resuspended in GST lysis buffer overnight at 4°C, 15rpm. Beads were centrifuged at 3,000g for 2 min and washed thrice in GST lysis buffer and once in 1mM EDTA pH 8 in PBS. Protein was eluted from the beads by addition of 2ml buffer (20mM Glutathione (Sigma) in 50mM Tris pH 8). Pure GST-proteins were obtained by dialysing overnight at 4°C with 25mM Tris pH 8, 1mM Dithiothreitol (DTT; Sigma), 100mM NaCl and 10% (v/v) glycerol.

4.22. Purification of His_6-p300 expressed in insect cells

Sf9 cells were infected at a multiplicity of infection of 10 particles/cell with a baculovirus expressing His_6-p300 (Kraus and Kadonaga 1998). His_6-p300 was purified 60h post-infection, from cellular extracts (20mM Tris-HCl pH 7.5, 250mM NaCl, 10mM Imidazole (Sigma) 1% (v/v) Triton X-100) using nickel-agarose beads (Qiagen), 15rpm at 4°C for 2h. Beads were washed 5x (20mM Tris-HCl pH 7.5, 150mM NaCl, 10mM Imidazole) followed by incubation with elution buffer (20mM Tris-HCl pH 7.5, 100mM NaCl, 250mM Imidazole) twice. Eluate was dialysed in 50mM Tris-HCl pH 8, 1mM DTT, 150mM NaCl and 10% (v/v) glycerol overnight at 4°C.

4.23. GST-protein interaction with *IVT*-[^{35}S]-proteins

10µg GST-proteins were incubated with 10µl *IVT*-[^{35}S]-proteins on ice for 1h. 20µl glutathione-agarose beads were added, and incubated for 1h at 4°C, 15rpm. The beads were then washed in 50mM Tris-HCl pH 7.5, 150mM NaCl and 1% (v/v) NP-40, and the GST-fusion proteins plus interactors were eluted by addition of 20mM glutathione and 50mM Tris-HCl pH 8. The proteins were then boiled in sample buffer and separated by SDS-PAGE. The gel was sensitised in Amersham Amplify (GE Healthcare) for 30 min, dried under a vacuum and visualised by autoradiography with X-ray film (Wolf Laboratories).

4.24. *In vitro* acetyltransferase assays

The APC/C holoenzyme was purified by IP with α-APC3 AF3.1 antibodies, washed and eluted with AF3.1 peptide. Either 200ng His_6-p300 or immunoprecipitated CBP or p300 from asynchronous A549 lysates were incubated with 0.5µCi [^{3}H]-Ac-CoA (Amersham) and either 10µg of the appropriate GST-protein or 200ng immunopurified APC/C holoenzyme in a reaction buffer containing 50mM Tris pH 8, 10mM sodium butyrate, 1mM DTT and 10% (v/v) glycerol for 90 min at 37°C. The reaction mixture was separated by SDS-PAGE, sensitised with Amersham Amplify (GE Healthcare) for 30 min, dried

under a vacuum and acetylated proteins detected by autoradiography with X-ray film (Wolf Laboratories).

4.25. Mass Spectrometry

4.25.1. In-gel tryptic digestion of IPs

IPs separated by SDS-PAGE were stained overnight in colloidal Coomassie solution (0.08% (v/v) Coomassie Brilliant Blue G250 (CBB 250), 1.6% (v/v) Orthophosphoric Acid, 8% (w/v) Ammonium Sulphate, 20% (v/v) MeOH) then destained with 1% (v/v) glacial acetic acid. The bands were excised with a clean scalpel and washed twice in 50% (v/v) Acetonitrile (AcN; Millipore) and 50mM Ammonium Bicarbonate (ABC; Sigma) for 1h at 37°C with agitation. The bands were then reduced by 50mM DTT in 10% (v/v) AcN/50mM ABC for 1h at 55°C, carboxymethylated by 100mM iodoacetamide (Sigma) in 10% (v/v) AcN/50mM ABC for 30 min in the dark and washed thrice in 10% (v/v) AcN/40mM ABC for 15 min with agitation. The gel bands were then dried in a vacuum centrifuge and rehydrated with Sequence-Grade Modified Trypsin (Promega), resuspended in 10% (v/v) AcN/40mM ABC, at 37°C overnight. The bands were then washed with 3% (v/v) Formic Acid (FA; Sigma), and the supernatants containing tryptic peptides were dried until analysed. All solutions were made up in HPLC (High-Performance Liquid Chromatography)-grade H_2O (Chromanorm, VWR).

4.25.2. FASP tryptic digestion of nucleolar lysates

Pure nucleoli of nucleolar lysates from cells incubated with non-silencing, APC3 or APC5 siRNA were prepared for tryptic digest by the FASP (Filter-Aided Sample Preparation) method. Pelleted nucleoli were solubilised in 9M Urea and 100mM TEAB (Tetraethylammonium bromide; Sigma) and normalised by protein concentration. The samples were then reduced with 50mM DTT/10% (v/v) AcN/100mM TEAB for 1h at 55°C and carboxymethylated by 100mM iodoacetamide/10% (v/v) AcN/100mM TEAB for 30 min in the dark. The denatured lysate was filtered through a 0.5ml Amicon Ultra 30 kDa centrifugal filter (Millipore), washed four times with 100mM TEAB and digested with

Sequence-Grade Modified Trypsin (Promega) in 100mM TEAB at 37°C for 16h. The peptides were then centrifuged and the filtrate collected. The filter was then washed twice with 100mM TEAB to obtain tryptic peptides.

4.25.3. Dimethyl-labelling of tryptic peptides from nucleolar lysates of knockdown cells

The tryptic peptides from the normalised nucleolar lysates of APC3- or APC5-knockdown cells were incubated with 1/10x volume 10.73% (w/v) heavy formaldehyde ($[^2H]$-CH_2O); Isotec) and those from non-silencing cells were incubated with 1/10x volume 10.73% (w/v) light formaldehyde (CH_2O; Sigma), both for 1 min with constant mixing. The sample was pulse-centrifuged, and 1/10x volume 1.5M sodium cyanoborohydride added for 30s with constant mixing, followed by pulse-centrifugation and incubation for 1h on a shaker at 600rpm. To quench, 1/10x volume 10.73% (w/v) NaOH and 1/10x volume FA were added and mixed thoroughly. Equimolar heavy and light peptides were mixed and purified through a C18 reverse-phased column (Sigma), then separated by a Mixed-Mode WAX-1 LC column (Dionex) into 20 fractions, which were dried by vacuum centrifugation until required.

4.25.4. Mass spectrometric analysis of tryptic peptides

Dried tryptic peptides were resuspended in 20µl 1% (v/v) AcN/1% (v/v) FA, of which 10µl was analysed by LC-MS/MS. Each sample was loaded into an Ultimate 3000 HPLC column (Dionex) and introduced into a maXis Impact Time-of-flight (TOF) or amaZon ion-trap mass spectrometer (both Bruker Daltonics). Alternatively, samples were loaded into a Tempo nano-LC and Q-TRAP 4000 mass spectrometer (both AB SCIEX). For the Impact and amaZon, ms/ms spectra were analysed using ProteinScape (Bruker Daltonics) through comparison to a Mascot database (Matrix Science). For the Q-TRAP 4000, fragmented peptides were analysed by Analyst 1.4.2 and Bioanalyst (both AB SCIEX) and compared to a Mascot database. In both Bruker and AB SCIEX systems, acetylation and

phosphorylation modifications were included in the searches. Further acetylation residues were identified using precursor ion analysis and the MIDAS workflow (AB SCIEX). The list of identified proteins was subjected to a 1% False Discovery Rate (FDR) to reduce false positives.

To remove background proteins in the IP studies, the list of interacting proteins were compared to a normal IgG control and duplicate proteins removed. Obvious contaminants, such as keratins, were also removed. The presence of TEK boxes was determined by manual screening of protein sequences within the Uniprot database (UniProt-Consortium 2014), and D-boxes and KEN-boxes were scored by GPS-ARM (Liu, Yuan et al. 2012). Degron conservation was established by comparison of homologous protein sequences from human, rat, mouse, frog, worm, fly and budding and fission yeast by Clustal omega (Goujon, McWilliam et al. 2010, Sievers, Wilm et al. 2011, Sievers and Higgins 2014).

Quantitation of LC-MS data from identified peptides was performed using WARP-LC (Bruker) and ProteinScape, whereupon the ratios of Heavy:Light peptides were calculated to give a quantitative ratio of nucleolar proteins from non-silencing and APC3/APC5 siRNA cells.

4.26. Immunofluorescence (IF)

A confluent 10cm dish of HeLa cells was split 1 in 4 and seeded onto 12-well slides within 10cm dishes. The following day, cells were washed twice in PBS, dried and fixed in 4% (w/v) PFA in PBS for 8 min. Cells were then permeabilised in ice-cold acetone for 10 min at -20°C. Slides were air-dried, and then blocked in HINGS (Heat-Inactivated Normal Goat Serum; 20% (v/v) HINGS, 0.2% (w/v) BSA in PBS) for 45 min at room temperature. Slides were then washed twice for 10 min in PBS and incubated with primary antibodies diluted in HINGS to the appropriate concentration (Table 10) for 2h at 37°C in a humidified box. The slides were then washed twice in PBS for 10 min, followed by incubation with secondary antibody conjugated to a fluorophore (Table 10) for 2h at 37°C in a humidified box. Slides were then washed thrice for 15 min in PBS, air-dried and then mounted in Vectashield containing DAPI (4',6-diamidino-2-phenylindole; Vector Laboratories). The slides were

visualised using an LSM510 META confocal laser scanning microscope (Zeiss) and a 63x oil objective lens (Zeiss), utilising lasers with wavelengths of 364nm, 488nm and 543nm. Images were analysed and nucleoli were profiled using Zeiss LSM Image Browser (Zeiss).

4.27. Semi-quantitative measurement of *de novo* rRNA synthesis

Gene expression was ablated in HeLa cells by transfection with non-silencing, APC3, APC5 or Cdc20 siRNA. 48h later, cells were seeded onto 12-well slides. The following day, cells were incubated in 2mM 5'-Fluorouridine (5-FUrd; Sigma) for 10 min, washed thrice with ice-cold PBS, fixed for 8 min in 4% PFA and permeabilised for 10 min in 1% Triton X-100. Slides were then blocked and probed with α-BrdU and α-Fibrillarin antibodies and mounted as per standard IF procedure (Above; Table 10).

The slides were visualised using an Eclipse E600 microscope (Nikon) and a 63x oil objective lens, with the following filters: G-1a (Ex 546/10, DM 575, BA580), UV-2A (Ex 330-380, DM 400, BA420) and FITC (Ex 465-495, DM 505, BA 515-555). Images were taken with a Hamamatsu c4742-95 digital camera and imported into Volocity (Perkin Elmer). The images were then analysed using Image J (NIH). Fibrillarin staining was used to denote nucleoli, around which regions of interest were drawn. The area, mean signal and total signal from the BrdU staining were measured for each nucleolus as well as three background readings per image. The mean background signal was calculated and subtracted from nucleolar values. The mean nucleolar and total nucleolar incorporation of 5-FUrd were then calculated per nucleolus, and the total nucleolar incorporation of 5-FUrd was calculated per cell. These were then calculated relative to non-silencing controls. Significant changes in 5-FUrd incorporation were determined by a two-tailed Student's t-test ($p<0.05$).

4.28. RNA extraction

Gene expression was ablated in HeLa cells by transfection with non-silencing, APC3, APC5 or Cdc20 siRNA. RNA was harvested from cells using the RNeasy mini kit (Qiagen). Briefly, a confluent 6cm dish of cells was washed twice in PBS and lysed in 0.35ml Buffer RLT. Lysates were homogenised by

centrifugation through a QIAshredder column (Qiagen) at 16,200g for 2 min. 0.35ml 70% (v/v) EtOH was added to homogenised lysates, which were then centrifuged through an RNeasy spin column at 10,000g for 15s. Lyophilised DNase I (1500 Kunitz Units; Qiagen) was resuspended in 550µl RNase-free H_2O. 10µl of resuspended DNase I was mixed with 70µl Buffer RDD and added to the column and incubated for 15 min at room temperature. 350µl Buffer RW1 was added, and spun at 10,000g for 15s. The column was then washed twice with 500µl Buffer RPE (+EtOH) and spun at 10,000g, the first wash for 15s and the second for 2 min. The column was placed into a fresh tube and spun at 16,200g for 1 min to dry. The column was placed into a fresh collection tube, and RNA was eluted twice in 50µl nuclease-free H_2O and spun at 1,000g for 1 min to give a final volume of 100µl.

4.29. qRT-PCR

RNA was reverse-transcribed using the AMV Reverse Transcription System (Promega). 500ng RNA was made to a volume of 4.9µl in nuclease-free H_2O and heated at 70°C for 10 min. To this volume, 2µl 25mM $MgCl_2$, 1µl 10x buffer, 1µl dNTPs (10mM), 0.25µl RNasin, 0.3125µl AMV Reverse Transcriptase and 0.5µl random primers were added. An enzyme-free control (-RT) substituted H_2O for AMV Reverse Transcriptase. The reaction was incubated at room temperature for 10 min, 42°C for 1h, 95°C for 5 min and 4°C for 5 min. 40µl of nuclease-free H_2O was added to give a final cDNA concentration of 10ng/µl.

20ng cDNA was then used as a template in qPCR reactions, in which 5 replicates were performed in duplicate. TaqMan qPCR reaction mixtures contained 2µl cDNA or H_2O control, 1µl TaqMan Gene Expression assay primer/probe sets (Table 11iii), 10µl 10x Master Mix (Applied Biosystems) and 7µl nuclease-free H_2O. TaqMan qPCR reactions were analysed using a 7500 Real-time PCR system (Applied Biosystems) and were run on the following programme: 50°C for 2 min, 95°C for 10 min, then 44 cycles of 95°C for 15s and 60°C for 1 min. SYBR green qPCR reaction mixtures contained 2µl cDNA/H_2O, 100nM forward and reverse primers (Table 11iii), 2x SensiMIX SYBR No-ROX kit (Bioline)

and made up to 20µl with nuclease-free H_2O. The qPCR was performed as follows: 95°C for 10 min; 40 cycles of 95°C for 30s, 55°C for 1 min, 72°C for 1 min; followed by 95°C for 1 min, 55°C for 30s, then a slow increase to 95°C for 30s to provide a dissociation curve to prove specificity. SYBR green assays were performed upon a Stratagene Mx3005p PCR machine using MxPro software (both Agilent).

Relative gene expression was calculated using the ddCt method. Ct values were calculated as a mean of duplicated samples. The dCt was calculated by subtracting the mean control Ct from the mean test Ct for each duplicate. The mean dCt for all non-silencing siRNA samples was then calculated, and subtracted from each dCt value to give the ddCt. The percentage change in gene expression was then calculated from the ddCt value. The dCt and percentage change were then compared between APC3, APC5 or Cdc20 siRNA samples and non-silencing control, and significance calculated by a two-tailed Student's t-test ($p<0.05$).

5. CHAPTER 1: NUCLEOLAR FUNCTIONS OF APC5 AND THE ANAPHASE PROMOTING COMPLEX/ CYCLOSOME

The Anaphase Promoting Complex/Cyclosome (APC/C) is an E3 ubiquitin ligase most commonly cited for its activity during mitotic cell division, during which it targets substrates for degradation by the 26S proteasome. It is integral to numerous checkpoints within the cell cycle, such as its ubiquitylation of Securin to permit the onset of anaphase, Cyclin B1 and Aurora kinases to promote mitotic exit, and Cyclin A and Geminin to prevent early S phase entry (Peters 2006, Pines 2011).

Previous work within our laboratory has determined that the APC/C cooperates with the transcriptional activators CBP and p300 to promote transcriptional activation, cell cycle progression and cellular transformation (Turnell, Stewart et al. 2005). The interaction between CBP/p300 was shown to be specific to the APC/C subunits APC5 and APC7 through domains evolutionarily conserved in adenovirus E1A. Both APC5 and APC7 were shown to stimulate CBP and p300 acetyltransferase activity *in vitro*, and potentiate CBP/p300-dependent transcription *in vivo*. Furthermore, CBP and p300 were identified as potential APC/C substrates. This work was important in establishing a role for APC/C subunits in CBP and p300 transcription programmes, and more broadly, as a regulator of RNA polymerase II-dependent transcription (Turnell, Stewart et al. 2005).

APC5 has also been shown to be important in chromatin assembly in budding yeast, where it regulates histone acetylation by various HATs, HDACs and assembly factors (Harkness, Davies et al. 2002, Arnason, Pisclevich et al. 2005, Harkness, Arnason et al. 2005, Turner, Malo et al. 2010, Islam, Turner et al. 2011).

The APC/C subunit, APC5 is also of particular interest, as it has functions that are not dependent upon being a component of the APC/C holoenzyme, and that are independent of APC/C ubiquitin ligase activity. Indeed, there is evidence to suggest that APC5 may be found within the ribosomal fractions, where it has the potential to regulate protein translation through the binding of Poly(A) Binding Protein (PABP) and the IRES of mRNA (Koloteva-Levine, Pinchasi et al. 2004).

Given all of these attributes of APC5, the aim of this chapter was to investigate its molecular function in more detail. To achieve this, a series of experiments were undertaken to identify novel APC5-binding proteins and subsequently clarify their functional relationship with APC5 and the APC/C. This chapter details and characterises the functional relationship between APC5 and RNA Polymerase I (Pol I) during the cell cycle, and following various forms of nucleolar stress.

5.1. Identification of Novel Binding Proteins of APC5 by Mass Spectrometry

Given the aforementioned APC/C-independent function of APC5, a mass spectrometric approach was adopted to identify any potential novel APC5-binding proteins. APC5 immunoprecipitates (IPs) from asynchronous HeLa cells were compared to IgG controls, followed by a cut-off of 1% False Discovery Rate (FDR) and the removal of obvious contaminants (Figure 1.1; Appendix Figure S1.1A). Multiple subunits of the APC/C were identified, however many previously unidentified APC5-binding proteins were also recovered, including three subunits of RNA Polymerase I (Pol I): RPA194, RPA135 and RPA40 (Appendix Figures S1.1B-D). It is interesting to note that these Pol I proteins were not detected within immunoprecipitates from other APC/C subunits such as APC3 and APC7 (Chapter 2; Appendix Figure S1.4), the reasons for which will be considered in the discussion at the end of this chapter.

RNA Polymerase I (Pol I) is a macromolecular complex consisting of multiple subunits. It transcribes nucleolar ribosomal DNA (rDNA) regions to produce a 45S pre-rRNA, which is then processed into the 28S, 18S and 5.8S rRNAs required for ribosomal assembly and function (Goodfellow and Zomerdijk 2012). Since multiple subunits of Pol I were found within APC5 IPs, further experiments were commenced to determine the relationship between APC5 and Pol I.

APC/C subunits

Protein	Full Name	MW [kDa]	Score	# Peptides	S.C. [%]
APC1	Anaphase-promoting complex subunit 1	216.4	1158.0	25	13.5
APC5	Anaphase-promoting complex subunit 5	85.0	1028.4	18	22.6
APC8	Cell division cycle protein 23 homolog	68.8	1004.8	19	28.3
APC3	Cell division cycle protein 27 homolog	91.8	668.2	12	14.6
APC7	Anaphase-promoting complex subunit 7	63.1	631.8	12	23.0
APC4	Anaphase-promoting complex subunit 4	92.1	503.7	10	13.1
APC6	Cell division cycle protein 16 homolog	71.6	213.2	5	7.1

RNA Polymerase I subunits

Protein	Full Name	MW [kDa]	Score	# Peptides	S.C. [%]
RPA194	DNA-directed RNA polymerase I subunit RPA1	194.7	929.6	18	11.5
RPA40	DNA-directed RNA polymerases I and III subunit RPAC1	39.2	115.9	3	9.2
RPA135	DNA-directed RNA polymerase I subunit RPA2	128.1	112.6	3	3.3

Figure 1.1 – Selected APC5-interacting proteins identified by mass spectrometric analysis of APC5 immunoprecipitates.

Asynchronous HeLa cell lysates were incubated with 20µg APC5 antibody overnight at 4°C followed by the addition of 20µl of packed Protein G-Agarose beads for 2h. An equal amount of lysate was incubated with normal IgG and Protein G-Agarose to act as a negative control. The IPs were washed, boiled and separated by SDS-PAGE. The gel was then stained by colloidal Coomassie solution, and each lane excised with a clean scalpel. Each gel slice was reduced and alkylated, dried and incubated with trypsin overnight at 37°C. Tryptic peptides were eluted by washing twice in 3% FA and the eluate dried and resuspended in 40µl 1% AcN/FA in H_2O. 20µl was analysed by LC-MS/MS using a Bruker AmaZon ion trap mass spectrometer. Peptides were identified by ProteinScape (Bruker) through comparison to a Mascot database (Matrix Science). Both obvious contaminants and proteins identified within the IgG control were removed from the list, onto which a 1% False Discovery Rate and a cut-off Score of 30 were applied. The upper table shows APC/C subunits, the lower shows subunits of RNA Polymerase I. MW stands for molecular weight, and S.C. for sequence coverage.

5.2. Validation of the interaction between APC5 and RNA Polymerase I

In order to validate the interactions identified by the mass spectrometry screen, reciprocal IPs using HeLa cell lysates were performed between the APC/C subunits APC3, APC5 and APC7 and the Pol I subunits RPA194, RPA135 and RPA40. These were subsequently analysed by SDS-PAGE and Western blotting (Figure 1.2). All three Pol I subunits identified in the screen (RPA194, RPA135 and RPA40) were able to co-IP APC5 (Figure 1.2A), whilst APC5 pulled-down RPA194 (Figure 1.2B). Consistent with the mass spectrometry results however, neither APC3 nor APC7 were able to co-IP RPA194 (Figure 1.2B). This could be due to a number of reasons, for example if APC5 primarily interacts with RPA194 independently of the APC/C complex. It is also possible that only a small fraction of APC5 interacting with RPA194 is pulled-down by APC3 and APC7 antisera, which is below the threshold for detection by Western blotting.

The diminished ability of RPA135 to co-IP APC5 compared to RPA194 and RPA40 does not necessarily reflect a poorer binding affinity *in vivo*, as RPA135 IPs also contained much less RPA194 than RPA40 IPs (Top panel), and therefore is more likely to be due to the relatively poor capacity of the antibody for IP experiments.

Taken together, these data establish a novel interaction between Pol I and APC5 *in vivo*. This interaction was determined to be specific to APC5 rather than other APC/C subunits, and could suggest that APC5 recruits Pol I to the APC/C holoenzyme, or might indicate another APC/C-independent function for APC5. Further experiments were therefore designed to elucidate the functional relationship between APC5 and Pol I, *i.e.* to investigate whether APC5 or the APC/C can modulate the transcriptional capacity of Pol I through its E3 ubiquitin ligase activity.

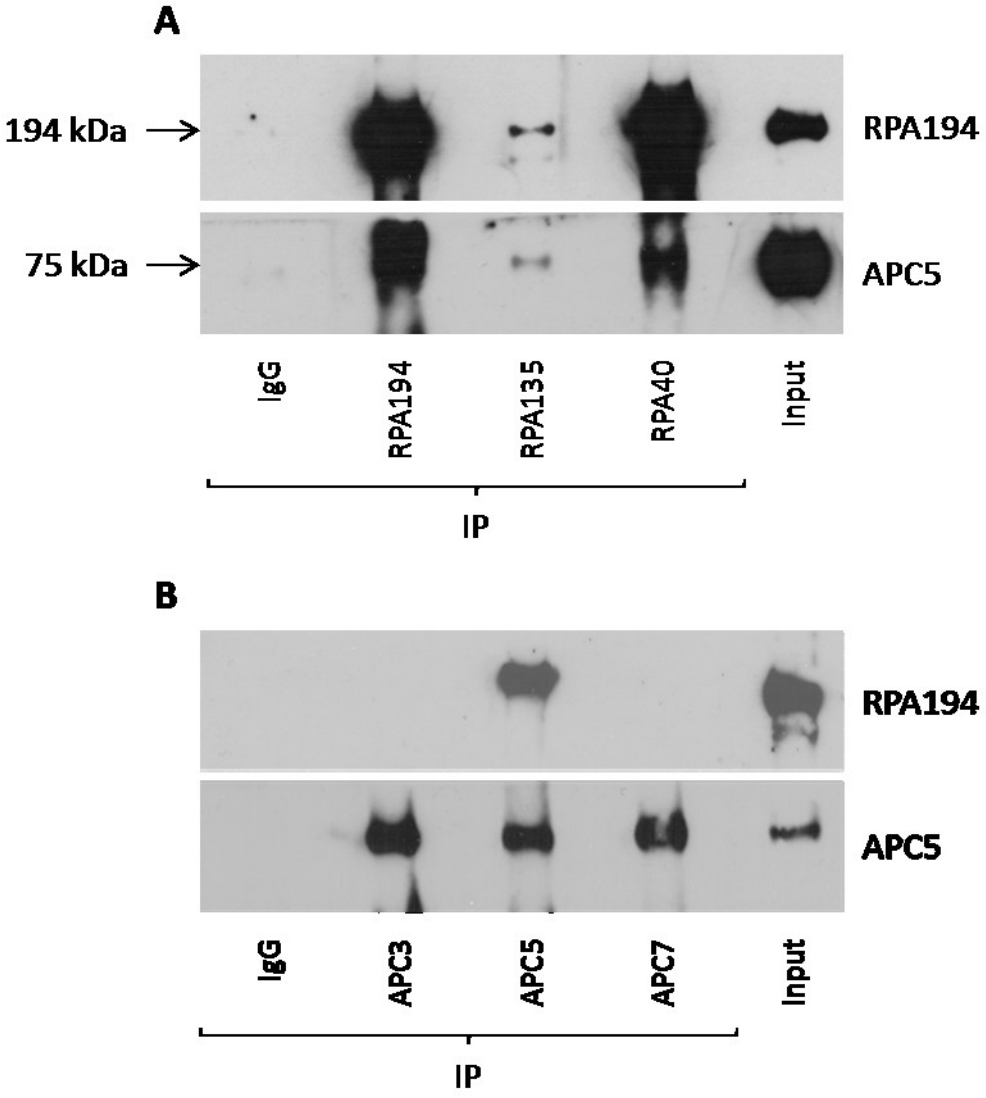

Figure 1.2 - Validation of Mass Spectrometric screen by co-IP and Western blotting: APC5 and Pol I interact *in vivo*.

HeLa cell lysates were immunoprecipitated using 5µg antibodies raised against Pol I (RPA194, RPA135 or RPA40; **A**) or APC/C (APC3, APC5, APC7; **B**) overnight at 4°C, followed by the addition 10µl of Protein G-agarose beads for 2h. IPs were washed, boiled and separated by SDS-PAGE. Proteins were detected by transfer to nitrocellulose membrane and Western blotting,

APC5 can be detected within Pol I IPs, whilst RPA194 can be pulled-down by APC5 IP, but not by APC3 or APC7.

5.3. GST-APC5 binds directly to *In Vitro* Transcribed/Translated RPA194 and RPA135

In order to determine whether the interaction between APC5 and Pol I was due to direct binding between the different proteins, an *in vitro* approach was taken. N-terminal GST tags were utilised to express APC5, or fragments thereof, in bacteria (Figure 1.3A). These were then incubated with *IVT* RPA194 or RPA135 radiolabelled by the incorporation of L-α-[^{35}S]-Methionine. GST pull-downs were collected by the addition of glutathione-agarose and separated by SDS-PAGE; specific APC5-Pol I binding was detected by autoradiography (Figure 1.3B). Whilst GST-APC5 was able to bind both RPA194 and RPA135, analysis of the four fragments of GST-APC5 suggested that the major binding site for RPA194 and RPA135 resided within the fourth fragment (567-755aa), although Fragment 2 (189-377aa) also bound strongly to RPA135 (Figure 1.3B). Interestingly, there appeared to be a low level of interaction within all fragments analysed (Figure 1.3B). Although APC5 contains multiple TPR domains, these are only located within the second, third and fourth fragments, and thus could not account for the interaction seen within the first fragment. These data indicated that APC5 can associate with both RPA194 and RPA135 directly *in vitro*, and support the *in vivo* data previously described.

Given that multiple fragments of APC5 are capable of binding RPA194 and RPA135 *in vitro*, this could suggest multiplicity in binding sites for RPA194 and RPA135 within the APC5 sequence. However, it is unknown whether this denotes a multipartite interaction between single APC5 and RPA194 or RPA135 proteins, or whether there is due to multiple APC5 and RPA194 or RPA135 proteins binding upon different locations.

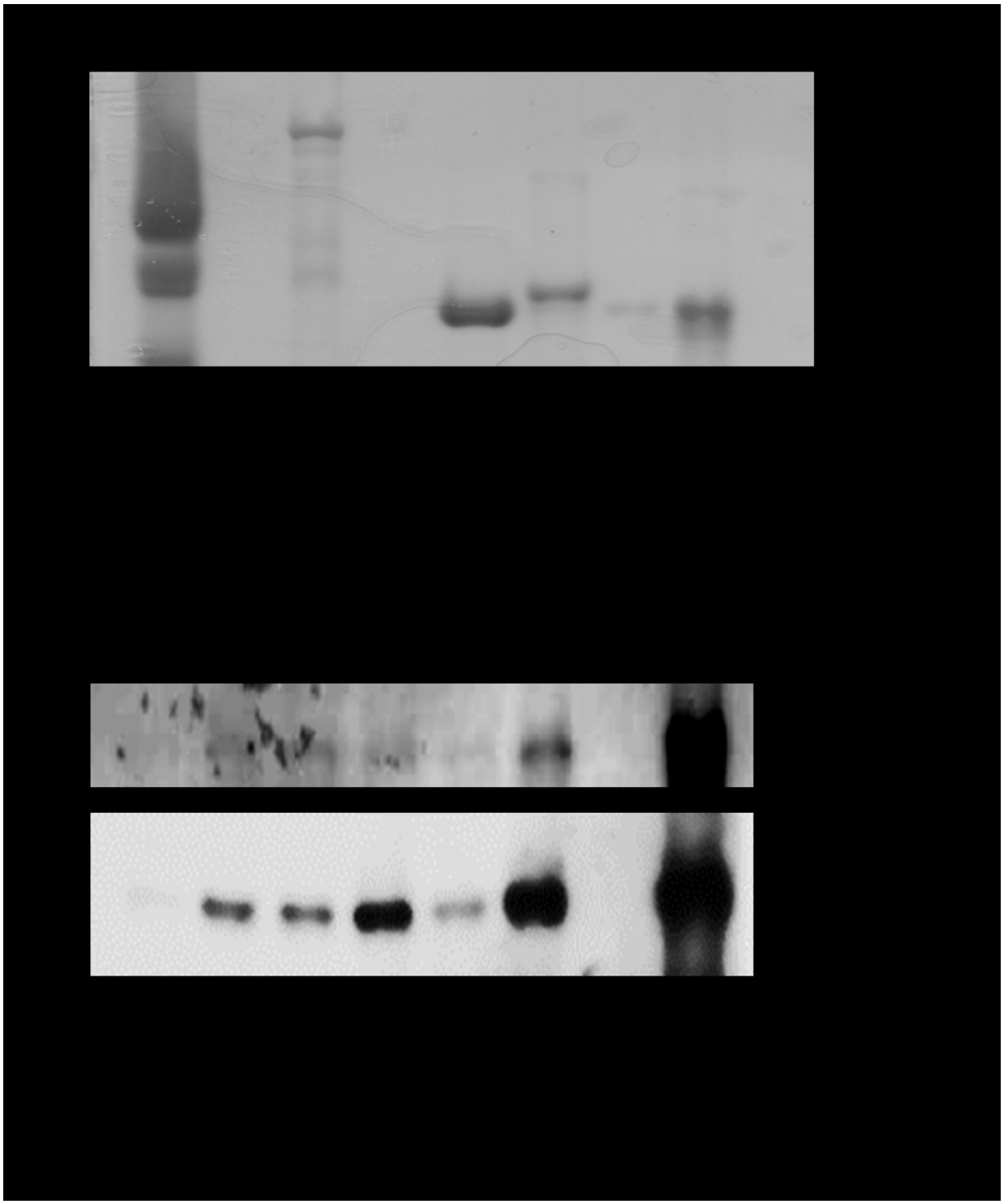

Figure 1.3 - GST-APC5 interacts with IVT RPA194 and RPA135

Full length GST-APC5 (FL) and GST-APC5 amino acid fragments 1-188, 189-377, 378-566, 567-755 were expressed in bacteria, separated by SDS-PAGE and protein levels visualised by incubation with Coomassie Solution (**A**). 10µg of each GST-protein was incubated with 10µl of either [^{35}S]-RPA194 or [^{35}S]-RPA135 on ice prior to the addition of glutathione-agarose beads. These were then washed and separated by SDS-PAGE. The gels were dried and proteins detected by autoradiography (**B**).

5.4. The interaction between APC5 and Pol I is restricted to the nucleolus

Having established a link between APC5 and Pol I, we next wished to determine the cellular localisation of this interaction. Since Pol I activity is inherent to the nucleolus, we wished to determine whether the interaction between APC5 and Pol I was also restricted to the nucleolus. To investigate this possibility, we adopted a nucleolar fractionation technique developed by Professor Angus Lamond's group (Andersen, Lyon et al. 2002). Firstly, pure nuclei were isolated from HeLa cells by Dounce homogenisation in a hypotonic lysis buffer and centrifugation through a sucrose density gradient. These nuclei were then lysed by sonication, leaving nucleoli intact, followed by further centrifugation through a higher sucrose density gradient yielding nucleoplasmic and nucleolar fractions (Figure 1.4A). Analysis of the fractionated lysates revealed that Pol I subunits were present in both nucleolar and nucleoplasmic fractions, as were many APC/C subunits (Figure 1.4B). However, of the two APC/C co-activators, Cdc20 was detected within both fractions, whilst Cdh1 was only detected within the nucleoplasmic fraction. Similarly, the nucleolar marker protein B23/Nucleophosmin was shown to be entirely nucleolar in localisation, demonstrating the validity of the protocol. The presence of multiple APC/C subunits and the ability of APC3 and APC7 to co-IP APC5 from within the nucleolus suggest a nucleolar role for the APC/C holoenzyme, and not just for APC5.

Having demonstrated the efficacy of the nucleolar isolation procedure, we were then in a position to perform APC/C and Pol I co-IPs from nucleolar and nucleoplasmic fractions. Figure 1.5 shows these results, indicating that APC5 interacts with RPA194 and RPA135 only within nucleoli and not within the nucleoplasm, despite the expression of each of these proteins within both fractions. Consistent with previous results, APC3 and APC7 antisera were unable to co-IP RPA194 and RPA135 (Figures 1.2 and 1.5). These data indicate that APC5-Pol I interaction is restricted to the nucleolus.

A

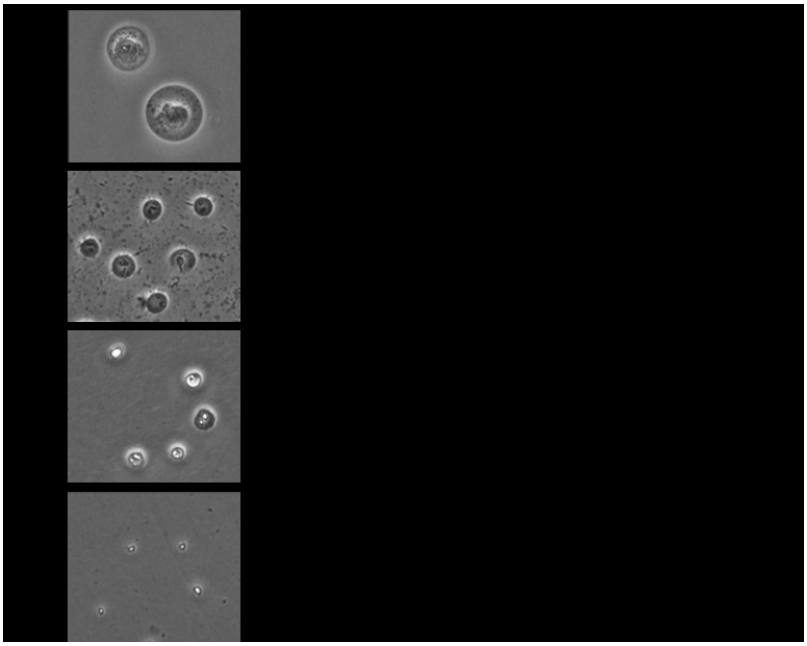

B

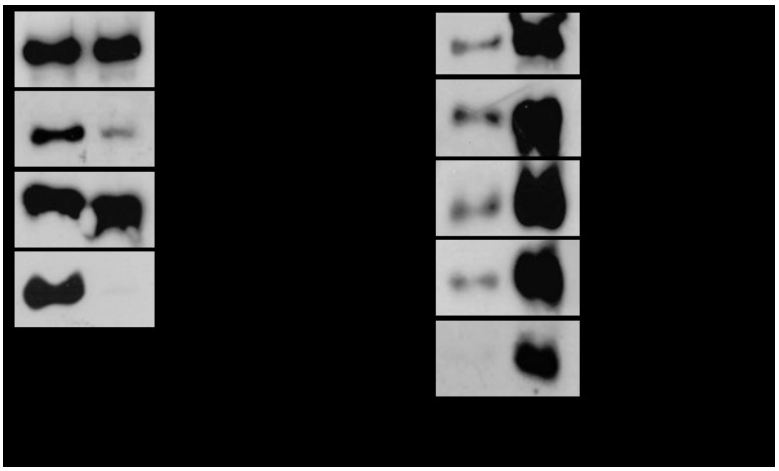

Figure 1.4 - Nucleolar Fractionation into Nucleolar and Nucleoplasmic compartments

A: Phase contrast microscopic images depicting the isolation of nucleoli by sucrose density centrifugation. i) HeLa cells were isolated by trypsination and incubated with ice-cold Buffer A (10mM HEPES pH 7.9, 10mM KCl, 1.5mM $MgCl_2$, 0.5mM DTT) for 5 min. ii) The cellular membrane was lysed by Dounce homogenisation with a tight pestle for 20 strokes, left for 10 min to rest followed by a further 20 strokes. iii) pure nuclei were pelleted by centrifugation and resuspended in Buffer S1 (0.25M Sucrose, 10mM $MgCl_2$), layered over 3ml Buffer S2 (0.35M Sucrose, 0.5mM $MgCl_2$) and centrifuged at 1,430g for 5 min. iv) The pure nuclear pellet was lysed by 8x10s pulses with a sonicator at 35% amplitude. The sonicated lysate was layered over 3ml Buffer S3 (0.88M Sucrose, 0.5mM $MgCl_2$) and centrifuged at 3,000g for 10 min to obtain a soluble nucleoplasmic fraction and pelleted nucleoli.
B: Nucleolar (NL) and Nucleoplasmic (NP) fractions were analysed by Western blotting for APC/C subunits (Right Panel) and for Pol I subunits and the nucleolar marker B23 (Left Panel)

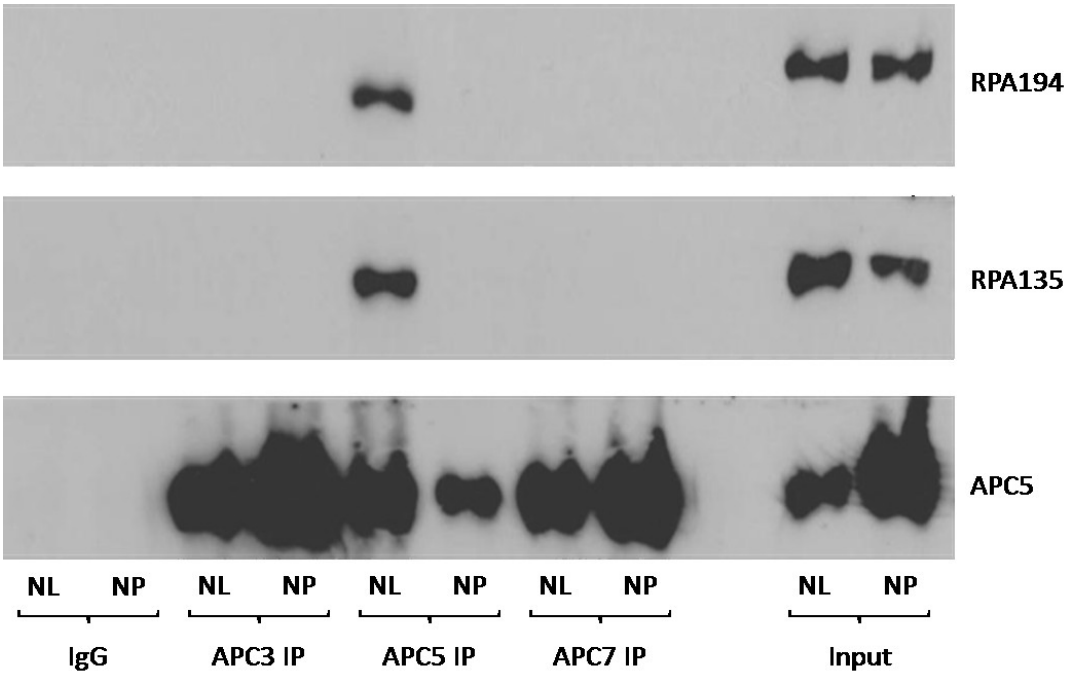

Figure 1.5 - RPA194 and RPA135 interact with APC5 within the nucleolus, but not the nucleoplasm.

Cells were separated into nucleolar (NL) and nucleoplasmic (NP) fractions. Antibodies against APC3, APC5 or APC7 were then used to co-IP any interacting proteins. These were separated by SDS-PAGE and the presence of Pol I subunits RPA194 and RPA135 as well as APC5 were detected by Western blotting.

5.5. The APC/C and Pol I co-elute following FPLC fractionation

The APC/C and Pol I both exist as macromolecular complexes of different sizes. Whilst the APC/C exists at a size of 1.2MDa *in vivo* (Chang, Zhang et al. 2014), it commonly elutes around 700-800 kDa upon FPLC fractionation. Interestingly, APC5 has previously been described as associating with heavier protein complexes which do not contain other APC/C subunits such as APC3, a vital component for APC/C activity (Koloteva-Levine, Pinchasi et al. 2004). We therefore wished to establish whether APC5, and indeed other APC/C subunits, co-eluted with Pol I subunits.

Nucleolar lysates from HeLa cells were fractionated by FPLC using a Superose-6 column. The protein was precipitated using ethanol, and resolubilised in UTB lysis buffer, followed by separation by SDS-PAGE and immunoblotting. Although APC3 could not be detected by Western blotting, another APC/C subunit, APC7, was shown to have identical co-elution patterns to APC5 (Figure 1.6). The inability to detect APC3 is unlikely to be due to its absence, moreover its protein level is likely to be below a detectable threshold, or the antibody might not bind with sufficient avidity upon the membrane since APC3 has already been shown to be part of a nucleolar APC/C complex containing APC5 (Figure 1.5).

Interestingly, the Pol I subunits RPA194, RPA135 and RPA40 were also found in the same fractions as APC5 and APC7 (Figure 1.6). This indicates that APC5 and Pol I exist in macromolecular complexes of comparable size in the nucleolus and suggests either that APC5 and Pol I are present in the same macromolecular complex, a result consistent with the interaction data, or that APC5 and Pol I exist separately in complexes of similar size and the FPLC protocol utilised did not provide the necessary resolution to distinguish between them. These observations are further complicated by the fact that subunits may not be bound to the complex at all times, for example if complex assembly occurs sequentially, hence the broad spectrum of fractions in which Pol I and APC/C are found.

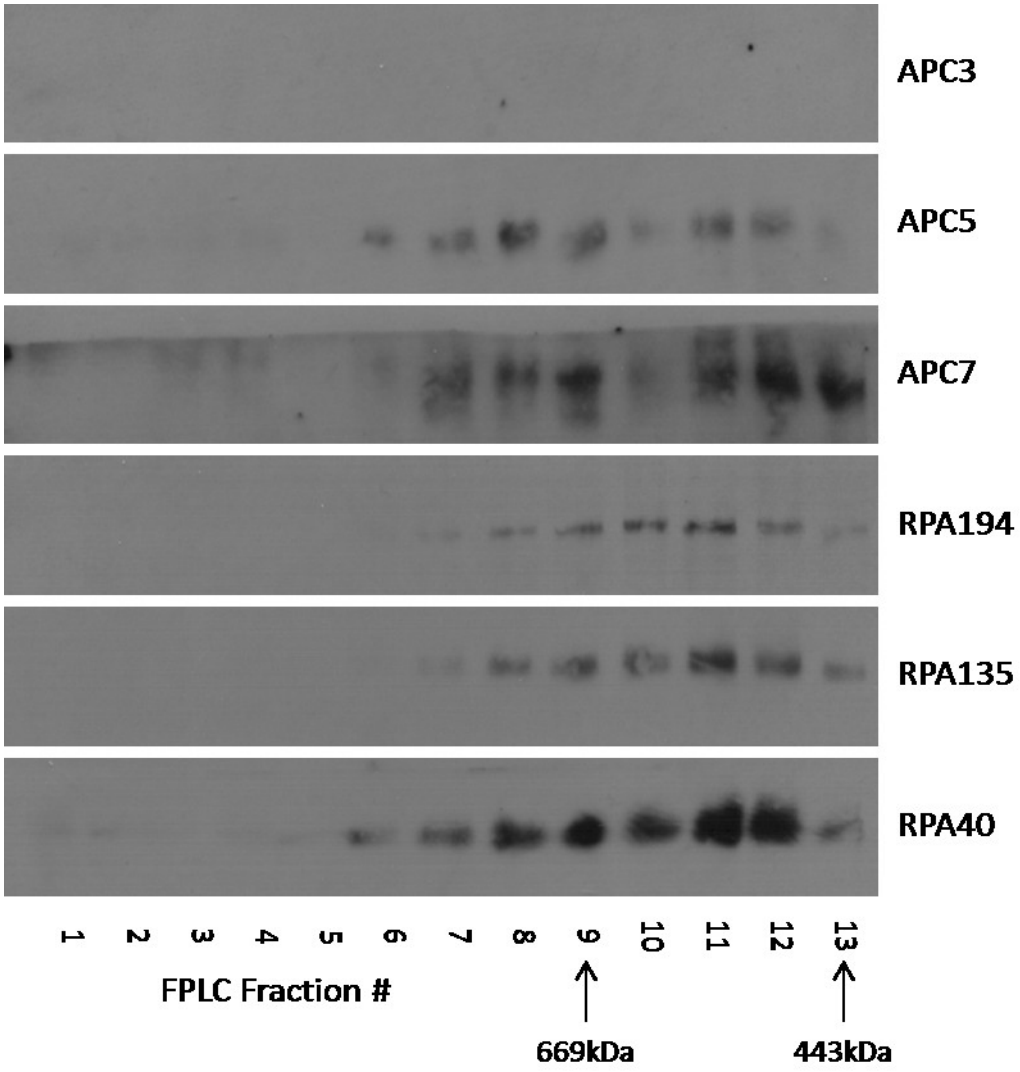

Figure 1.6 - FPLC fractionation shows similar co-elution patterns for Pol I and the APC/C.

2.5mg of nucleolar lysate from HeLa cells was loaded onto a pre-equilibrated Superose-6 column. The pressure limit was set to 1.5MPa and the flow rate to 0.5ml/min. 0.5ml fractions were collected, precipitated using 2x volume 100% ethanol and re-solubilised in UTB lysis buffer. 25% of each fraction was analysed by Western blotting for the presence of Pol I and APC/C subunits. The approximate fractions in which the markers for 669kDa and 443kDa elute are shown with arrows.

5.6. Confocal microscopy establishes co-localisation of APC/C and Pol I within the nucleolus

To provide further evidence for a physical interaction between APC5 and Pol I we used a dual staining immunofluorescence (co-IF) protocol coupled with confocal microscopy to establish their respective cellular localisation. To do this, asynchronous HeLa cells were seeded onto 12-well slides, fixed and permeabilised in 4% (w/v) PFA then ice-cold acetone, and subsequently probed with antibodies raised against APC/C subunits, RPA194 or the nucleolar marker, Fibrillarin.

Although APC5 exhibited cytoplasmic fluorescence, and to a lesser extent nucleoplasmic, there was a relatively strong signal within the nucleolus (Figure 1.7 Ai, iv). Indeed, upon comparison to the localisation of RPA194, it was evident that both APC5 and RPA194 exhibited similar nucleolar fluorescence (Figure 1.7 Ai, merge). Indeed, intensity profiles for APC5 and RPA194 were indicative of regions of substantial co-localisation (Figure 1.7 Bi).

However, due to species restriction imposed by the primary antibodies, a different nucleolar marker was required to ascertain the nucleolar localisation of other APC/C subunits. Fibrillarin is known to be expressed within the FC and DFC compartments of the nucleolus (Ochs, Lischwe et al. 1985), and exhibits equivalent expression to RPA194 (Figure 1.7 ii), thus it was chosen as an alternative nucleolar marker. Interestingly, dual staining of Fibrillarin with APC1 (Figure 1.7 iii) and APC7 (Figure 1.7 v) indicated the presence of these APC/C subunits within the nucleolus. These data are consistent with those from nucleolar fractionation studies, where APC5 and APC7, as a minor proportion of the cellular pool of the APC/C, were shown to reside within the nucleolus (Figure 1.4; Figure 1.7 i, iv, v). Despite not being able to co-IP RPA194, it is interesting to note that APC7 and APC1, as well as APC5, are expressed within the same sub-nucleolar compartments as Pol I. Taken together, these data suggest that there might be a role for the APC/C within the nucleolar regions responsible for rDNA transcription and rRNA maturation, perhaps through an interaction with Pol I, as mediated by APC5.

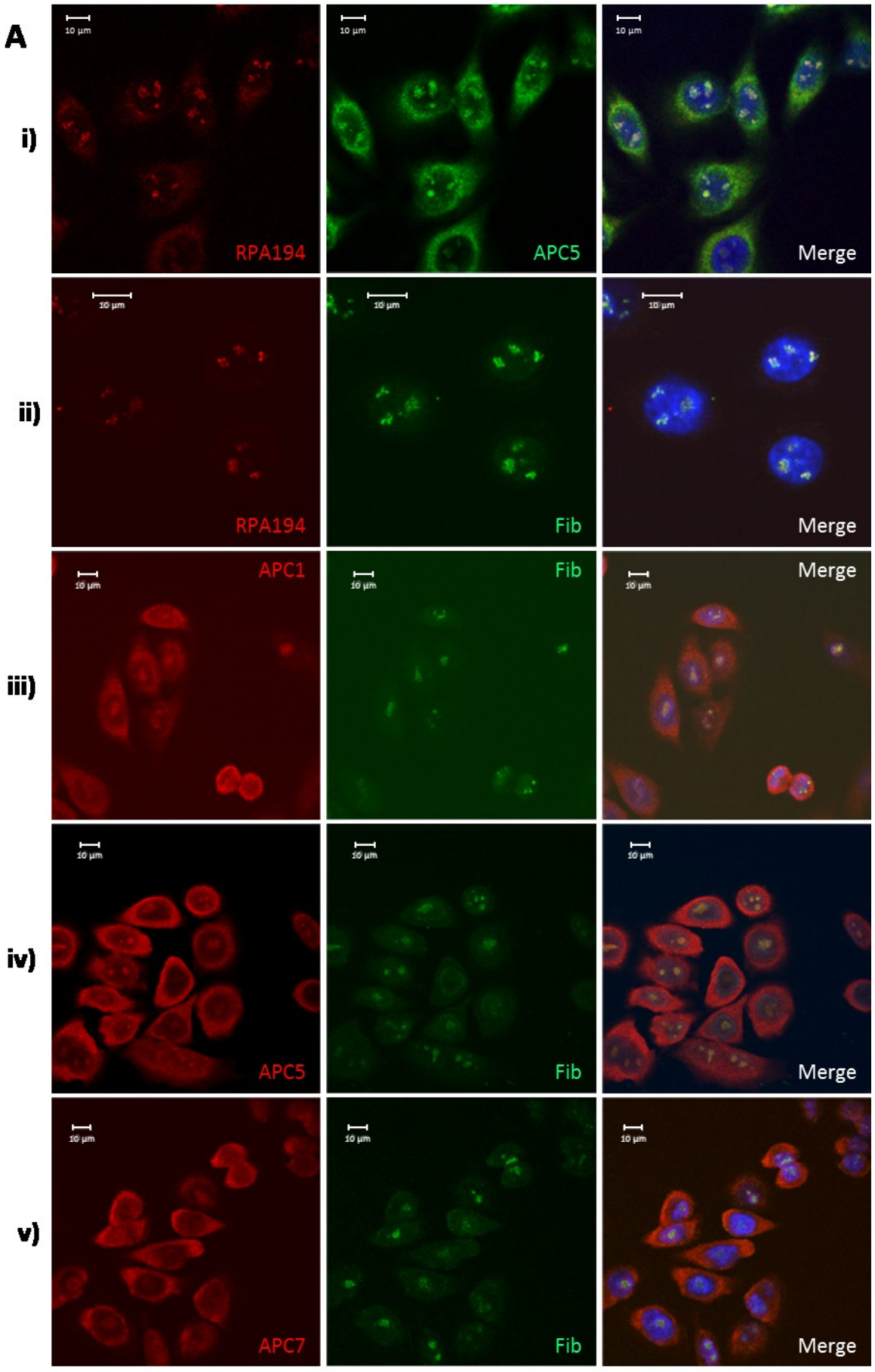
A
i)
ii)
iii)
iv)
v)
10 µm
RPA194
APC5
Merge
RPA194
Fib
Merge
APC1
Fib
Merge
APC5
Fib
Merge
APC7
Fib
Merge

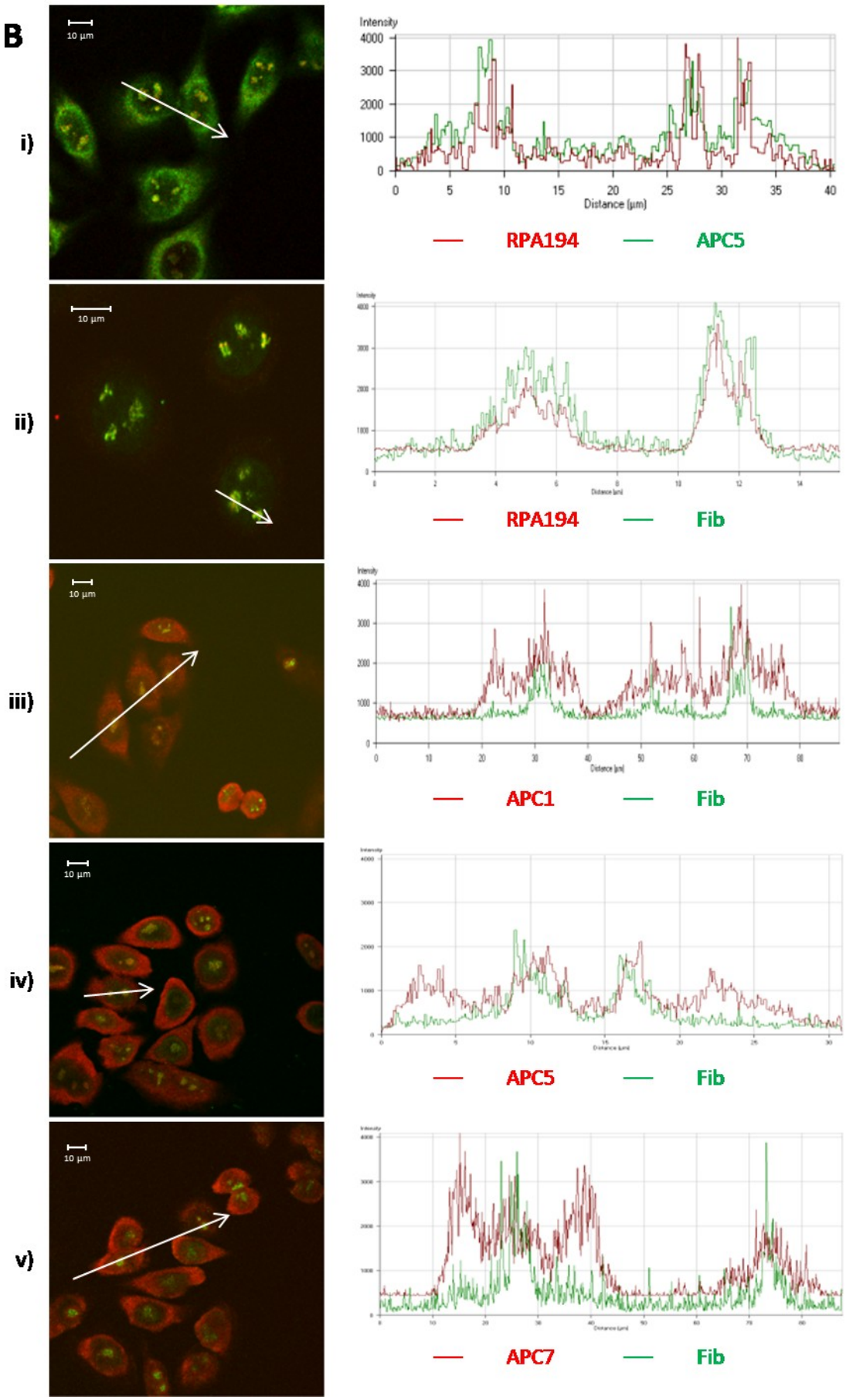
B
i)
ii)
iii)
iv)
v)
10 µm
Intensity
4000
3000
2000
1000
0
0 5 10 15 20 25 30 35 40
Distance (µm)
RPA194
APC5
RPA194
Fib
APC1
Fib
APC5
Fib
APC7
Fib

Figure 1.7 - Confocal microscopy displaying nucleolar localisation of APC/C and co-localisation of APC5 and RPA194

HeLa cells were grown upon a 12-well slide, fixed and permeabilised in 4% (w/v) PFA (8 min) then ice-cold acetone (5 min). After blocking in HINGS (45 min), the slides were incubated with the primary then secondary antibodies conjugated to a fluorophore (2h, 37°C), before being mounted in Vectashield containing DAPI to visualise DNA. The slides were imaged using an LSM510 META confocal laser scanning microscope (Zeiss) (**A**) and the nucleoli profiled using Zeiss LSM Image Browser (Zeiss) (**B**).

RPA194 was shown to co-localise with APC5 (i) and Fibrillarin (ii) within the nucleolus. Similarly various APC/C subunits were shown to be expressed within the nucleolus (iii-v). The white arrow on the image shows the direction and length of profile (B).

5.7. RPA194 and RPA135 are not substrates for APC/C E3 ubiquitin ligase activity *in vitro*.

Having previously demonstrated and subsequently validated an interaction between APC5 and Pol I both *in vivo* and *in vitro*, we next wished to determine whether the Pol I subunits, RPA194 and RPA135, were *bona fide* substrates for APC/C E3 ubiquitin ligase activity. RPA194 contains several D-boxes, whilst RPA135 contains several D-boxes and a KEN-box (Figure 1.8A). These are the canonical sequences found within APC/C substrates which are required for its ubiquitin-mediated degradation (Peters 2006, Pines 2011). Using GPS-ARM 1.0, a computerised modelling software package, it is possible to assign a score to these degron motifs, signifying their probability of being true APC/C targets (Liu, Yuan et al. 2012). RPA194 contains three D-boxes with the highest threshold of stringency and two with medium stringency, whilst RPA135 has a high-scoring KEN-box. It is therefore possible that both of these are APC/C substrates given these motifs and calculated values.

RPA194 also contains a TEK motif, which has recently been shown to provide the lysine for ubiquitylation by the APC/C within some of its substrates (Jin, Williamson et al. 2008). Other mass spectrometric studies have also shown that K1180 within the TEK motif in RPA194 is ubiquitylated *in vivo*, providing further evidence that it might be an APC/C target (Kim, Bennett et al. 2011). Interestingly, RPA194 also contains a C-terminal L-R dipeptide motif, which has recently been demonstrated to be integral to the degradation of another APC/C substrate, KIF18A (Figure 1.8A) (Sedgwick, Hayward et al. 2013).

To test the hypothesis that RPA194 and RPA135 are APC/C substrates, an *in vitro* assay was performed whereby immunopurified APC/C was incubated with *IVT* [^{35}S]-Cyclin B1, [^{35}S]-RPA194 or [^{35}S]-RPA135 in the presence of ubiquitin, E1, E2's and an ATP regeneration buffer (Figure 1.8Bi). Upon detection by autoradiography, polyubiquitin chains cause a progressive increase in size, which can be seen on Cyclin B1 as a smear within the APC3 IP lane, compared to IgG control, thereby proving it is a substrate under *in vitro* conditions. However, APC/C purified by either APC3 or APC5 IP was not able to ubiquitylate RPA194 or RPA135, suggesting that they are not substrates, at least under the *in vitro* conditions investigated here (Figure 1.8Bi). Since the majority of cells from which the APC/C is immunoprecipitated are in interphase, most APC/C in this assay is activated by Cdh1. In order to obtain a greater proportion of APC/C activated by Cdc20, the process was repeated from cells arrested in prometaphase by the mitotic spindle-inhibiting drug nocodazole and then released from the SAC for 1h (Figure 1.8Bii). This was of great importance, since Cdc20, but not Cdh1, was detected within nucleolar fractions by Western blot (Figure 1.4B). However, these were also unable to ubiquitylate RPA194 and RPA135 under these *in vitro* conditions.

A i) - RPA194

```
        10         20         30         40         50         60         70         80         90
MLISKNMPWR RLQGISFGMY SAEELKKLSV KSITNPRYLD SLGNPSANGL YDLALGPADS KEVCSTCVQD FSNCSGHLGH IELPLTVYNP
       100        110        120        130        140        150        160        170        180
LLFDKLYLLL RGSCLNCHML TCPRAVIHLL LCQLRVLEVG ALQAVYELER ILNRFLEENP DPSASEIREE LEQYTTEIVQ NNLLGSQGAH
       190        200        210        220        230        240        250        260        270
VKNVCESKSK LIALFWKAHM NAKRCPHCKT GRSVVRKEHN SKLTITFPAM VHRTAGQKDS EPLGIEEAQI GKRGYLTPTS AREHLSALWK
       280        290        300        310        320        330        340        350        360
NEGFFLNYLF SGMDDDGMES RFNPSVFFLD FLVVPPSRYR PVSRLGDQMF TNGQTVNLQA VMKDVVLIRK LLALMAQEQK LPEEVATPTT
       370        380        390        400        410        420        430        440        450
DEEKDSLIAI DRSFLSTLPG QSLIDKLYNI WIRLQSHVNI VFDSEMDKLM MDKYPGIRQI LEKKEGLFRK HMMGKRVDYA ARSVICPDMY
       460        470        480        490        500        510        520        530        540
INTNEIGIPM VFATKLTYPQ PVTPWNVQEL RQAVINGPNV HPGASMVINE DGSRTALSAV DMTQREAVAK QLLTPATGAP KPQGTKIVCR
       550        560        570        580        590        600        610        620        630
HVKNGDILLL NRQPTLHRPS IQAHRARILP EEKVLRLHYA NCKAYNADFD GDEMNAHFPQ SELGRAEAYV LACTDQQYLV PKDGQPLAGL
       640        650        660        670        680        690        700        710        720
IQDHMVSGAS MTTRGCFFTR EHYMELVYRG LTDKVGRVKL LSPSILKPFP LWTGKQVVST LLINIIPEDH IPLNLSGKAK ITGKAWVKET
       730        740        750        760        770        780        790        800        810
PRSVPGFNPD SMCESQVIIR EGELLCGVLD KAHYGSSAYG LVHCCYEIYG GETSGKVLTC LARLFTAYLQ LYRGFTLGVE DILVKPKADV
       820        830        840        850        860        870        880        890        900
KRQRIIEEST HCGPQAVRAA LNLPEAASYD EVRGKWQDAH LGKDQRDFNM IDLKFKEEVN HYSNEINKAC MPFGLHRQFP ENSLQMMVQS
       910        920        930        940        950        960        970        980        990
GAKGSTVNTM QISCLLGQIE LEGRRPPLMA SGKSLPCFEP YEFTPRAGGF VTGRFLTGIK PPEFFFHCMA GREGLVDTAV KTSRSGYLQR
      1000       1010       1020       1030       1040       1050       1060       1070       1080
CIIKHLEGLV VQYDLTVRDS DGSVVQFLYG EDGLDIPKTQ FLQPKQFPFL ASNYEVIMKS QHLHEVLSRA DPKKALHHFR AIKKWQSKHP
      1090       1100       1110       1120       1130       1140       1150       1160       1170
NTLLRRGAFL SYSQKIQEAV KALKLESENR NGRSPGTQEM LRMWYELDEE SRRKYQKKAA ACPDPSLSVW RPDIYFASVS ETFETKVDDY
      1180       1190       1200       1210       1220       1230       1240       1250       1260
SQEWAAQTEK SYEKSELSLD RLRTLLQLKW QRSLCEPGEA VGLLAAQSIG EPSTQMTLNT FHFAGRGEMN VTLGIPRLRE ILMVASANIK
      1270       1280       1290       1300       1310       1320       1330       1340       1350
TPMMSVPVLN TKKALKRVKS LKKQLTRVCL GEVLQKIDVQ ESFCMEEKQN KFQVYQLRFQ FLPHAYYQQE KCLRPEDILR FMETRFFKLL
      1360       1370       1380       1390       1400       1410       1420       1430       1440
MESIKKKNNK ASAFRNVNTR RATQRDLDNA GELGRSRGEQ EGDEEEEGHI VDAEAEEGDA DASDAKRKEK QEEEVDYESE EEEEREGEEN
      1450       1460       1470       1480       1490       1500       1510       1520       1530
DDEDMQEERN PHREGARKTQ EQDEEVGLGT EEDPSLPALL TQPRKPTHSQ EPQGPEAMER RVQAVREIHP FIDDYQYDTE ESLWCQVTVK
      1540       1550       1560       1570       1580       1590       1600       1610       1620
LPLMKINFDM SSLVVSLAHG AVIYATKGIT RCLLNETTNN KNEKELVLNT EGINLPELFK YAEVLDLRRL YSNDIHAIAN TYGIEAALRV
      1630       1640       1650       1660       1670       1680       1690       1700       1710
IEKEIKDVFA VYGIAVDPRH LSLVADYMCF EGVYKPLNRF GIRSNSSPLQ QMTFETSFQF LKQATMLGSH DELRSPSACL VVGKVVRGGT
      1720
GLFELKQPLR
```

A ii) - RPA135

```
        10         20         30         40         50         60         70         80         90
MDPGSRWRNL PSGPSLKHLT DPSYGIPREQ QKAALQELTR AHVESFNYAV HEGLGLAVQA IPPFEFAFKD ERISFTILDA VISPPTVPKG
       100        110        120        130        140        150        160        170        180
TICKEANVYP AECRGRRSTY RGKLTADINW AVNGISKGII KQFLGYVPIM VKSKLCNLRN LPPQALIEHH EEAEEMGGYF IINGIEKVIR
       190        200        210        220        230        240        250        260        270
MLIMPRRNFP IAMIRPKWKT RGPGYTQYGV SMHCVREEHS AVNMNLHYLE NGTVMLNFIY RKELFFLPLG FALKALVSFS DYQIFQELIK
       280        290        300        310        320        330        340        350        360
GKEDDSFLRN SVSQMLRIVM EEGCSTQKQV LNYLGECFRV KLNVPDWYPN EQAAEFLFNQ CICIHLKSNT EKFYMLCLMT RKLFALAKGE
       370        380        390        400        410        420        430        440        450
CMEDNPDSLV NQEVLTPGQL FLMFLKEKLE GWLVSIKIAF DKKAQKTSVS MNTDNLMRIF TMGIDLTKPF EYLFATGNLR SKTGLGLLQD
       460        470        480        490        500        510        520        530        540
SGLCVVADKL NFIRYLSHFR CVHRGADFAK MRTTTVRRLL PESWGFLCPV HTPDGEPCGL MNHLTAVCEV VTQFVYTASI PALLCNLGVT
       550        560        570        580        590        600        610        620        630
PIDGAPHRSY SECYPVLLDG VMVGWVDKDL APGIADSLRH FKVLREKRIP PWMEVVLIPM TGKPSLYPGL FLFTTPCRLV RPVQNLALGK
       640        650        660        670        680        690        700        710        720
EELIGTMEQI FMNVAIFEDE VFAGVTTHQE LFPHSLLSVI ANFIPFSDHN QSPRNMYQCQ MGKQTMGFPL LTYQDRSDNK LYRLQTPQSP
       730        740        750        760        770        780        790        800        810
LVRPSMYDYY DMDNYPIGTN AIVAVISYTG YDMEDAMIVN KASWERGFAH GSVYKSEFID LSEKIKQGDS SLVFGIKPGD PRVLQKLDDD
       820        830        840        850        860        870        880        890        900
GLPFIGAKLQ YGDPYYSYLN LNTGESFVMY YKSKENCVVD NIKVCSNDTG SGKFKCVCIT MRVPRNPTIG DKFASRHGQK GILSRLWPAE
       910        920        930        940        950        960        970        980        990
DMPFTESGMV PDILFNPHGF PSRMTIGMLI ESMAGKSAAL HGLCHDATPF IFSEENSALE YFGEMLKAAG YNFYGTERLY SGISGLELEA
      1000       1010       1020       1030       1040       1050       1060       1070       1080
DIFIGVVYYQ RLRHMVSDKF QVRTTGARDR VTNQPIGGRN VQGGIRFGEM ERDALLAHGT SFLLHDRLFN CSDRSVAHVC VKCGSLLSPL
      1090       1100       1110       1120       1130
LEKPPPSWSA MRNRKYNCTL CSRSDTIDTV SVPYVFRYFV AELAAMNIKV KLDVV
```

Figure 1.8A – D-box, KEN boxes and TEK motifs within RPA194 and RPA135

Amino acid sequences of RPA194 (**i**) and RPA135 (**ii**) were obtained from the Uniprot database and run through the GPS-ARM 1.0 software. D-boxes are highlighted in yellow, whilst KEN motifs are highlighted in blue and TEK in green. The C-terminal L-R dipeptide in RPA194 is highlighted in pink. The D-boxes that passed the high threshold are written in a red font and double underlined, whilst those of medium threshold are just written in a red font.

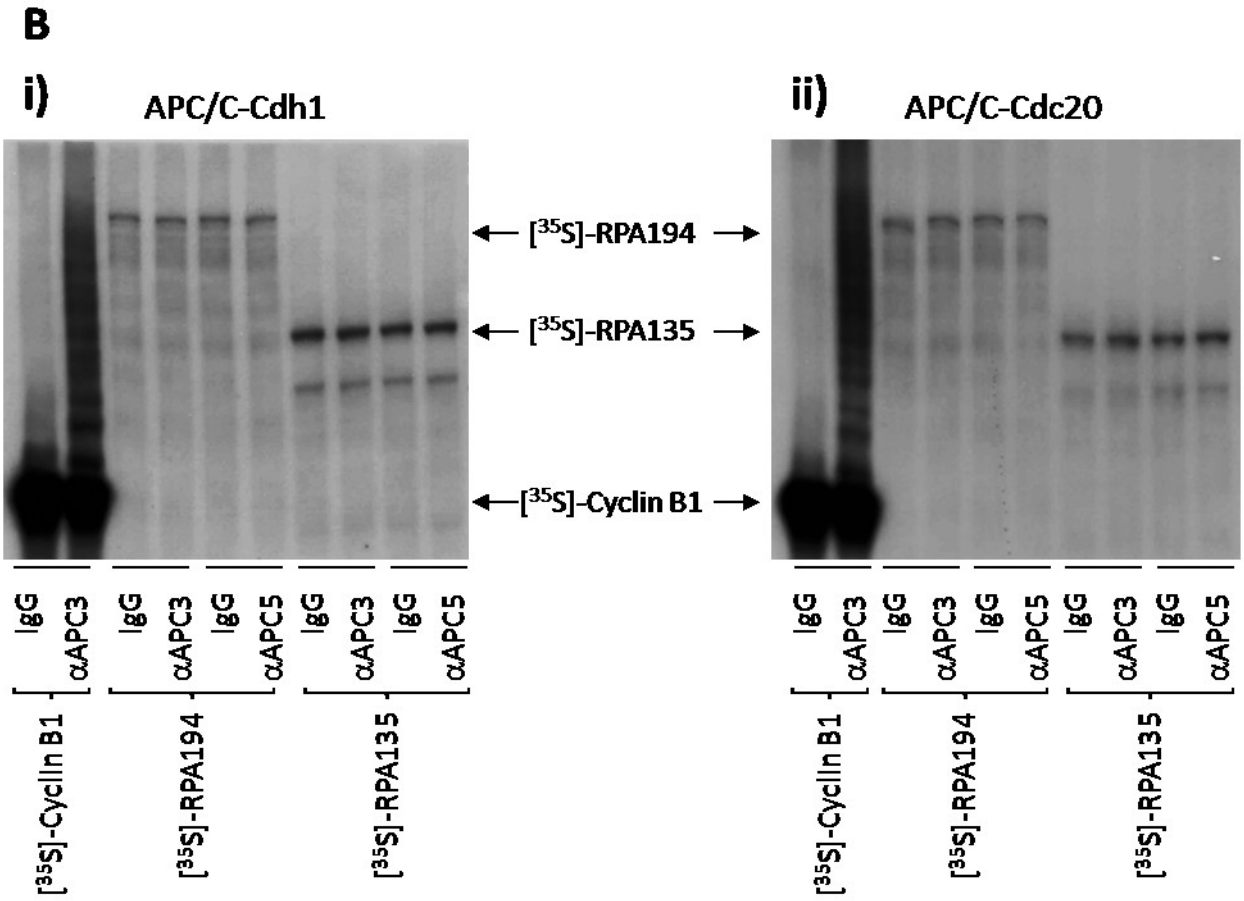

Figure 1.8B - RPA194 and RPA135 are not substrates for the APC/C *in vitro*

Either asynchronous (i) or cells arrested in prometaphase by incubation of 400ng/ml nocodazole for 20h (ii) were lysed and immunoprecipitated by the addition of 20µg of either normal IgG, APC3 or APC5 antibodies overnight followed by 10µl Protein G-agarose for 3h. The resulting IPs were washed and incubated with rabbit E1 and human E2 UbcH10 and UbcH5 together with 1µl of either [^{35}S]-Cyclin B1, [^{35}S]-RPA194 or [^{35}S]-RPA135 at 37°C for 1h prior to separation by SDS-PAGE and detection by autoradiography.

5.8. Expression of RPA194, RPA135 and RPA40 following siRNA-mediated knockdown of the APC/C

Since the *in vitro* ubiquitylation assay proved unsuccessful, we adopted alternative approaches to determine the likelihood of Pol I subunits being substrates for APC/C activity *in vivo*. Since APC/C-mediated ubiquitylation acts as a degradation signal for the 26S proteasome, ablation of APC/C activity typically results in the stabilisation of its substrates, increasing their relative abundance within the proteome, which can be detected by Western blotting. We therefore investigated the protein levels of Pol I subunits following the siRNA-mediated knockdown of APC/C subunits. Through siRNA-mediated abrogation of APC/C subunit expression, particularly following APC3 and APC5 knockdowns, it was evident that the known substrates Cyclin A, Cyclin B1 and Cdc20 were stabilised (Figure 1.9). Interestingly, RPA194 protein levels appeared to mimic these APC/C substrates following APC/C subunit knockdown, indicating that RPA194 protein levels might be regulated by APC/C activity, whether by direct or indirect means. RPA135 and RPA40, however, did not show any obvious changes in protein levels following knockdown of APC/C subunits (Figure 1.9).

5.9. Expression of RPA194, RPA135 and RPA40 through mitosis

APC/C activity is inhibited during early mitosis by the Mitotic Checkpoint Complex due to the prevention of Cdc20-mediated APC/C activation (Sudakin, Chan et al. 2001). Upon satisfaction of the SAC, the inhibition of Cdc20 is alleviated, permitting APC/C-Cdc20 to degrade its target substrates, including Securin and Cyclin B1, thereby permitting the onset of anaphase. The APC/C then exhibits a co-activator switch, becoming activated preferentially by Cdh1, thus promoting mitotic exit and re-entry into the subsequent G1 phase in cycling cells, or entry into quiescence and differentiation (Peters 2006, Musacchio and Salmon 2007, Pines 2011). As such, substrates ought to exhibit an

expression pattern inverse to that of APC/C activity, in that expression should remain high during prophase, followed by a marked decrease following anaphase progression. By synchronising cells in prometaphase with nocodazole followed by their subsequent release through mitosis, it is possible to observe protein levels throughout each mitotic phase. We therefore adopted this approach to analyse Pol I subunit expression during mitosis.

Mitotic progression can be followed by the expression of Cyclin B1, which was elevated during nocodazole arrest, and subsequently decreased as the cells entered anaphase and progressed through mitosis into G1 (Figure 1.10iv). The proportion of phosphorylated APC3, which migrated as a higher molecular weight band following SDS-PAGE, can also be used as a mitotic indicator; this is regulated by the mitotic kinases Cdk1 and Plk1 (Figure 1.10v). Similar to Cyclin B1, RPA194 protein levels were elevated during prometaphase, and started to decrease by 1h post-release, decreasing further by 2h (Figure 1.10, panel i). RPA135 was elevated slightly throughout the duration of mitosis, whilst RPA40 showed no change (Figure 1.10, ii and iii, respectively). Given these findings, it cannot be concluded definitively that RPA194 is a substrate for the APC/C; however, its stability does appear to be dependent upon APC/C activity, as RPA194 protein levels mirror those of the *bona fide* APC/C substrate Cyclin B1.

Taken together, the protein levels of RPA194 during mitosis and following siRNA-mediated knockdown of APC3 and APC5 are consistent with the notion that RPA194 could be a novel substrate for the APC/C.

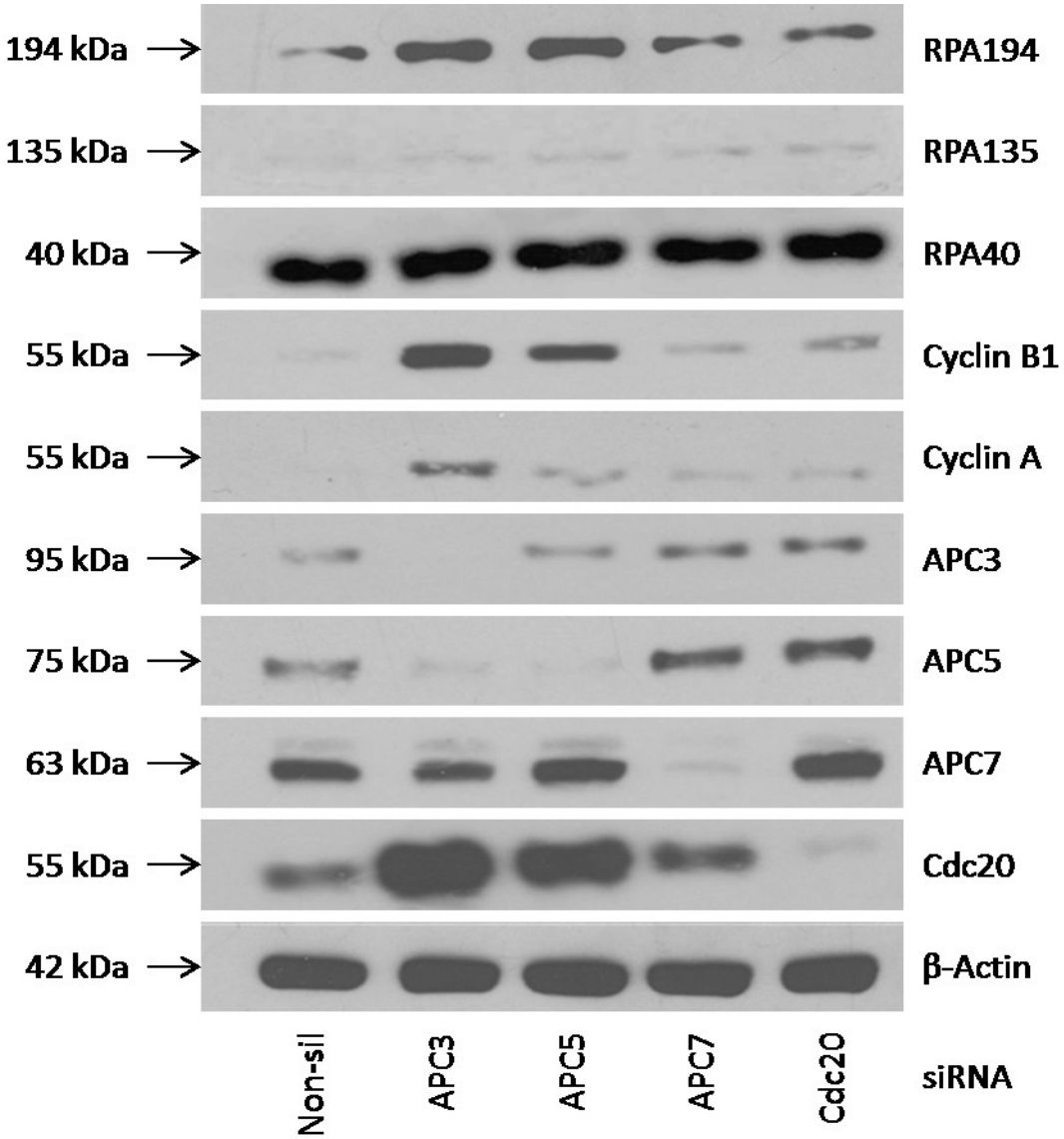

Figure 1.9 - Protein expression following siRNA-mediated knockdown of APC/C subunits

HeLa cells were harvested 72h after incubation with siRNA duplexes against either APC3, APC5, APC7 or Cdc20 mRNA or non-silencing control (non-sil). Lysates were separated by SDS-PAGE and analysed by Western blotting.

RPA194 protein levels increase following knockdown of APC3 and APC5, whilst RPA135 and RPA40 show no change in expression.

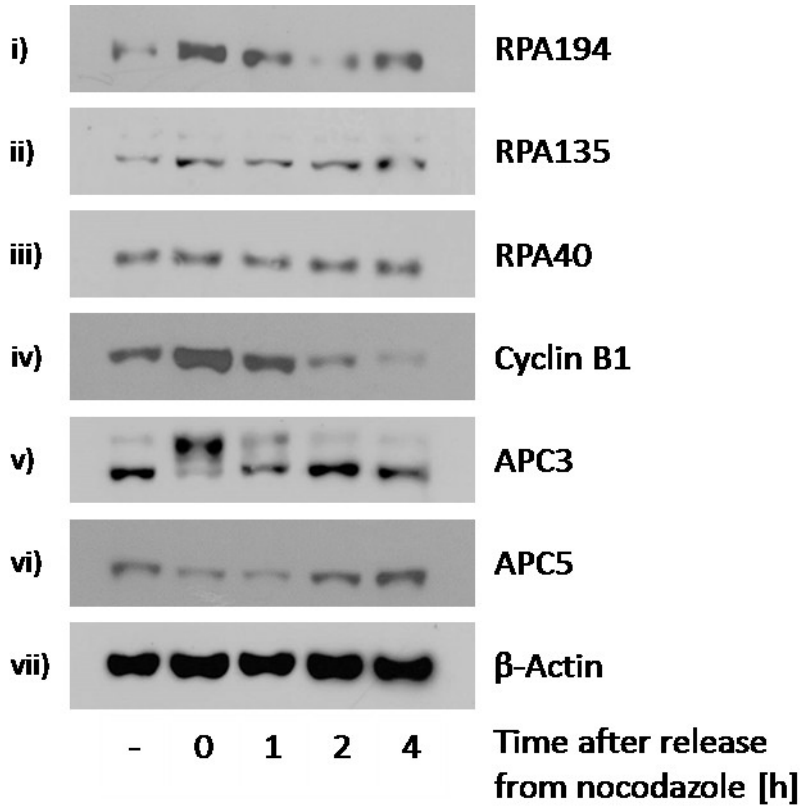

Figure 1.10 - Expression of Pol I subunits during mitotic progression

HeLa cells were treated with DMSO (-) or 400ng/ml nocodazole for 20h. Cells arrested in mitosis were obtained by mechanical shake-off and released into fresh growth medium for the time indicated (0,1,2,4h). Lysates were separated by SDS-PAGE an analysed by Western blotting with the indicated antibodies.

Cyclin B1 protein levels and the gel shift caused by APC3 phosphorylation are used as positive controls to show mitotic progression.

5.10. The APC/C regulates abundance of Pol I rRNA transcripts.

Having established a link between APC5 and Pol I and demonstrated that the APC/C might regulate RPA194 protein levels, we next investigated whether the APC/C can affect the activity of Pol I. To achieve this, we examined the relative levels of its transcriptional products upon siRNA-mediated knockdown of the APC/C.

To do this, RNA from non-silencing (LacZ), APC3, APC5 or Cdc20 knockdown HeLa cells was harvested and reverse-transcribed to form cDNA. This was then used in qPCR reactions using pre-designed TaqMan assays (Applied Biosystems) consisting of primers and probes specific to either 28S or 18S rRNA, or to the controls Hprt1 or GAPDH. Out of the two most commonly used methods of qPCR, TaqMan was chosen over SYBR green due to its increased specificity. To further decrease background signal, genomic DNA (gDNA) was digested using DNase I prior to the RT-PCR reaction. This was particularly important, because the TaqMan primers and probe for 18S and 28S rRNA do not span different exons, and therefore may amplify gDNA, and there are around 400 copies of the rDNA repeat within the human genome.

To analyse the data from the qPCR, we adopted the ddCt method. The Ct value is calculated at a fluorescence threshold during the logarithmic growth part of the curve. Duplicates are averaged, and an average of the two controls (Hprt1 and GAPDH) is calculated. The dCt is calculated by the subtraction of these averaged control Ct values from the test Ct (*i.e.* 18S or 28S) for each input sample. The mean dCt from the LacZ siRNA samples is then subtracted from each dCt value to give the ddCt, from which the percentage change in gene expression is calculated. The mean dCt and mean relative gene expression are shown (Figure 1.11A). Proof of knockdown efficiency was demonstrated by calculating the relative gene expression of APC3, APC5 and Cdc20 from each siRNA sample used (Figure 1.11B).

Following siRNA knockdown of APC3, APC5 and Cdc20, the abundance of 18S rRNA increased to a statistically significant level relative to LacZ controls (Figure 1.11A – i, right panel). It is important to note that a decrease in the value of dCt between LacZi control and the siRNA samples implies that a particular fluorescence threshold had been reached earlier, and therefore there was relatively more of the cDNA within the input, signifying an increase in RNA abundance *in vivo* (Figure 1.11A – i, left panel).

The abundance of 28S rRNA was similarly elevated following knockdown of APC3, APC5 or Cdc20 relative to LacZ controls (Figure 1.11A – ii, right panel). However, the increase in 28S rRNA was only deemed to be significant by Student's t-test ($p<0.05$) following APC5 and Cdc20 knockdown, and not APC3 (Figure 1.11A – ii) (p-value Mean dCt = 0.089, p-value Mean Relative Gene Expression = 0.11). This is likely to be due to the more variable results obtained in the APC3 siRNA samples, as shown by the wider error bars, though it does appear to follow a similar trend to the other graphs.

One flaw in the use of 28S and 18S rRNA as markers of Pol I transcription is that although indicative of Pol I activity, they have been processed from the initial 45S pre-rRNA transcript. It is therefore feasible that any differences may be attributable to an increase in pre-rRNA processing rather than heightened Pol I transcription. To address this issue it was evident that the qPCR must be repeated and the relative expression of 45S pre-rRNA must be measured. However, a pre-designed TaqMan assay was not available, and several designing software packages were unable to identify a primer and probe set with the correct biochemical properties. It was therefore necessary to utilise a SYBR green PCR instead, despite its potential drawbacks.

In a similar trend to the results seen for 18S and 28S rRNA, knockdown of APC3 and Cdc20 resulted in a significant increase in abundance of 45S pre-rRNA (Figure 1.11A – iii). However, whilst APC3 and Cdc20 knockdown caused an appreciable increase in 45S pre-rRNA, the slight increase following

knockdown of APC5 was deemed insignificant by a Student's t-test (Figure 1.11A – iii) (p-value Mean dCt = 0.85, p-value Mean Relative Gene Expression = 0.77).

Taken together, these results showed that ablation of APC/C activity through knockdown of APC/C subunits resulted in elevated levels of the 45S pre-rRNA and 28S and 18S rRNA transcripts.

Initially, the data from the APC5 knockdown qPCR seems somewhat counterintuitive. An increase in 18S and 28S rRNA was coupled with an increase in 45S pre-rRNA for both APC3 and Cdc20 knockdowns, as expected. However, for APC5 there was no change in 45S pre-rRNA transcript levels despite the relative increase for 18S and 28S rRNA. This could be attributable to two likely scenarios: firstly, any increase in Pol I transcription to produce the 45S pre-rRNA transcript was masked by a concomitant increase in the rRNA maturation pathway, resulting in a greater proportion of end-product 18S and 28S rRNA; secondly, 18S and 28S rRNA stability has increased.

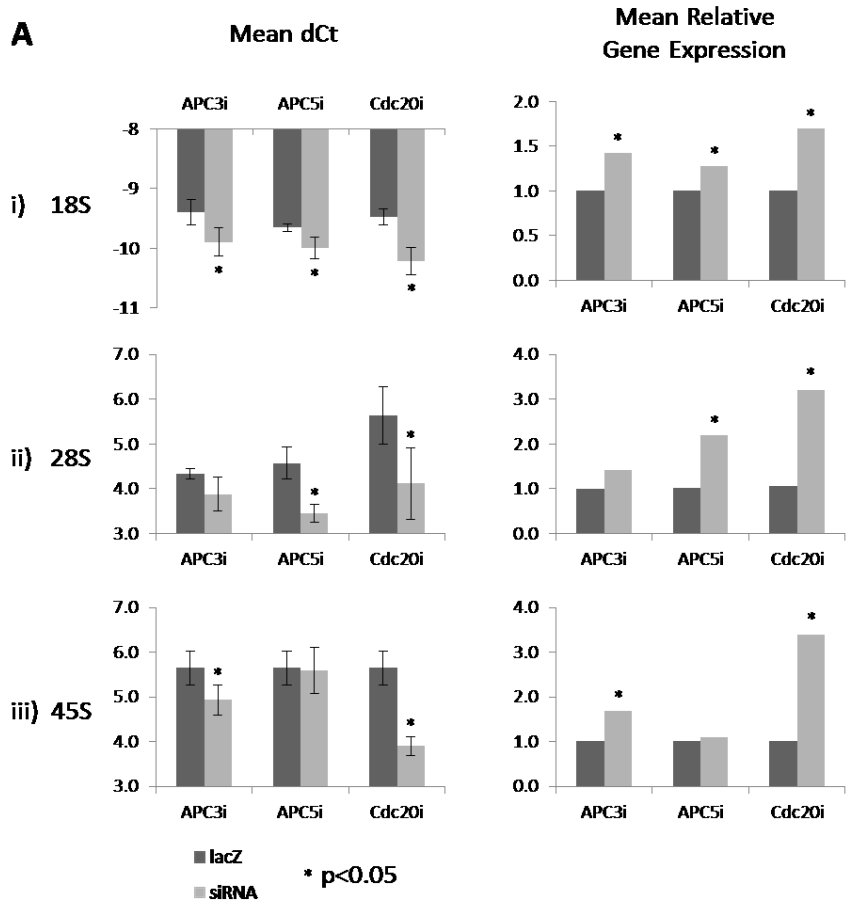

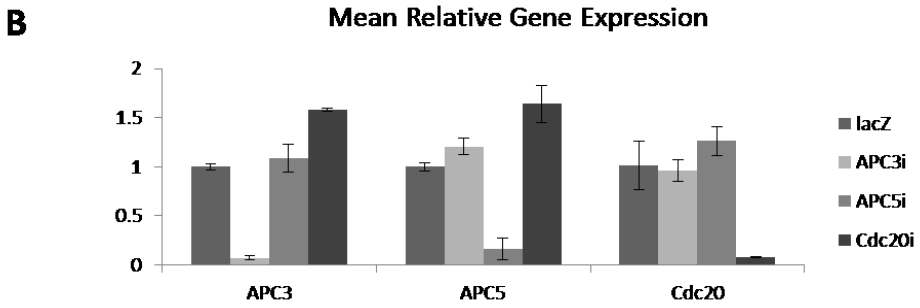

Figure 1.11 - qRT-PCR denoting relative expression of 18S and 28S rRNA, 45S pre-rRNA and APC3, APC5 and Cdc20 mRNA following knockdown of APC/C subunits.

RNA was harvested 72h after siRNA-mediated knockdown of either APC3, APC5, Cdc20 or LacZ as a non-silencing control using an RNeasy mini kit (Qiagen). QIAshredder columns were used to homogenise the lysate, and gDNA was digested with DNase I. 500ng RNA was used as input into an RT-PCR reaction to produce cDNA. 20ng of cDNA was then used as input into each qPCR reaction, with 5 biological replicates run in duplicate.

(A) Relative gene expression was calculated using the ddCt method upon Ct values obtained by TaqMan (18S, 28S rRNA) or SYBR green (45S pre-rRNA) qPCRs. The darker coloured bar depicts LacZ siRNA control, whilst the lighter bar represents the indicated APC/C siRNA. Error bars shown are standard deviation. Statistically significant changes are indicated by an asterisk as calculated by a two-tailed Student's t-test ($p<0.05$).

p-values calculated to 3 significant figures are as follows:

i) 18S – Mean dCt: APC3i (p=0.0216), APC5i (p=0.00938), Cdc20i (p=0.000593)
– Mean Relative Gene Expression: APC3i (p=0.0289), APC5i (p=0.0167), Cdc20i (p=0.00240)
ii) 28S – Mean dCt: APC3i (p=0.0884), APC5i (p=0.00641), Cdc20i (p=0.0159)
– Mean Relative Gene Expression: APC3i (p=0.106), APC5i (p=0.00143), Cdc20i (p=0.0349)
iii) 45S – Mean dCt: APC3i (p=0.0123), APC5i (p=0.850), Cdc20i (p=0.0000722)
– Mean Relative Gene Expression: APC3i (p=0.0123), APC5i (p=0.769), Cdc20i (p=0.0000332)

(B) – TaqMan qPCR of APC3, APC5 and Cdc30 cDNA highlighting efficiency of APC/C siRNA-mediated knockdown.

5.11. APC/C knockdown causes an increase in *de novo* rRNA synthesis

To assess further the effect of the ablation of APC/C activity upon Pol I activity, it was considered necessary to investigate *de novo* pre-rRNA synthesis. As such, the nucleoside analogue 5'-Fluorouridine (5-FUrd) was used as a marker for *de novo* RNA synthesis, since it incorporates into nascent RNA transcripts and can be measured semi-quantitatively by α-BrdU antibodies and IF. The use of 5-FUrd by RNA Polymerase enzymes is non-specific, such that both Pol I and Pol II will use it in the place of uridine, however it is possible to measure Pol I transcription selectively rather than Pol II by keeping incubation times and dosage low, as Pol I transcription occurs at a much higher rate than Pol II. Accordingly, HeLa cells, following siRNA-mediated knockdown of LacZ, APC3, APC5 or Cdc20 expression, were seeded onto 12-well slides and incubated with 2mM 5-FUrd for 10 minutes, followed by fixation and permeabilisation by 4% (w/v) PFA and 1% (v/v) Triton X-100. Slides were then incubated with the appropriate primary and secondary antibodies, and fluorescent images were taken and subsequently quantified using Image J.

In order to control for changes in nucleolar size and the number of active nucleoli within a cell, three different analyses were performed: the mean nucleolar BrdU fluorescence, which represents the average rate at which Pol I is transcribing each active rDNA repeat (Figure 1.12Ai); the total nucleolar BrdU fluorescence, expressed both per nucleolus (Figure 1.12Aii) and per cell (Figure 1.12Aiii), which signifies the total Pol I transcription over the 5-FUrd incubation period. For all three methods of analysis, knockdown of APC3, APC5 and Cdc20 resulted in a statistically significant increase of 5-FUrd nucleolar incorporation relative to non-silencing LacZ controls, representing an increase in *de novo* rRNA synthesis by Pol I.

Taken together, the data shown in Figures 1.11 and 1.12 highlight a novel method of regulation for Pol I transcription as orchestrated by the APC/C. Given that knockdown of APC3, APC5 and Cdc20 resulted in an increase in *de novo* pre-rRNA synthesis (Figure 1.12) and in the absolute levels of rRNA

transcripts (Figure 1.11), it can be concluded that Pol I activity is regulated, at least in part, by the APC/C holoenzyme, activated by Cdc20. This could be achieved by the targeting of RPA194 for APC/C-mediated proteolysis, under the control of APC5. However, it is also possible that APC5 has further roles in regulating mature rRNA production, given that its knockdown increased *de novo* pre-rRNA synthesis (Figure 1.12) and the levels of 18S and 28S rRNA transcripts (Figure 1.11i, ii), but not those of 45S pre-rRNA (Figure 1.11iii).

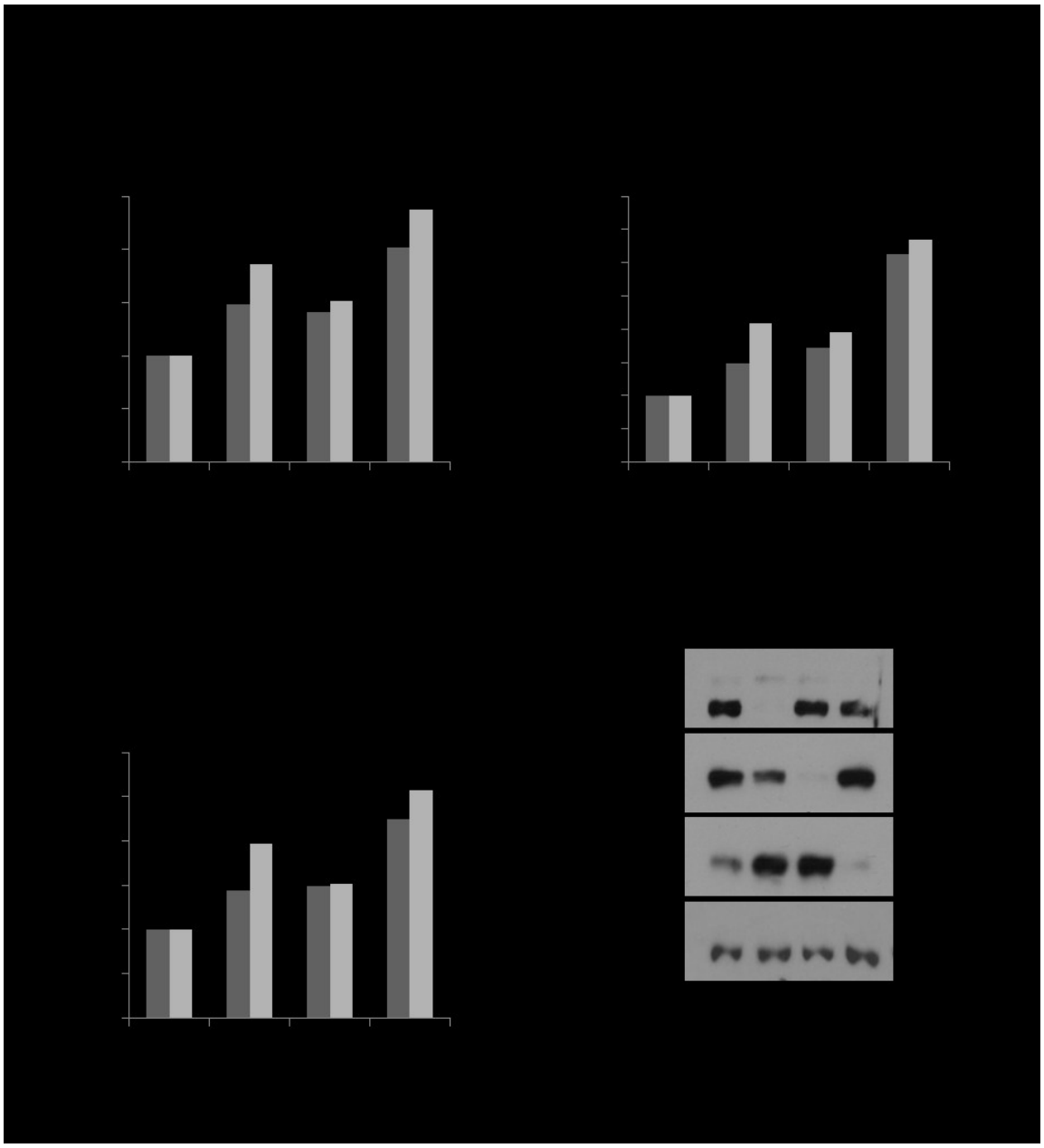

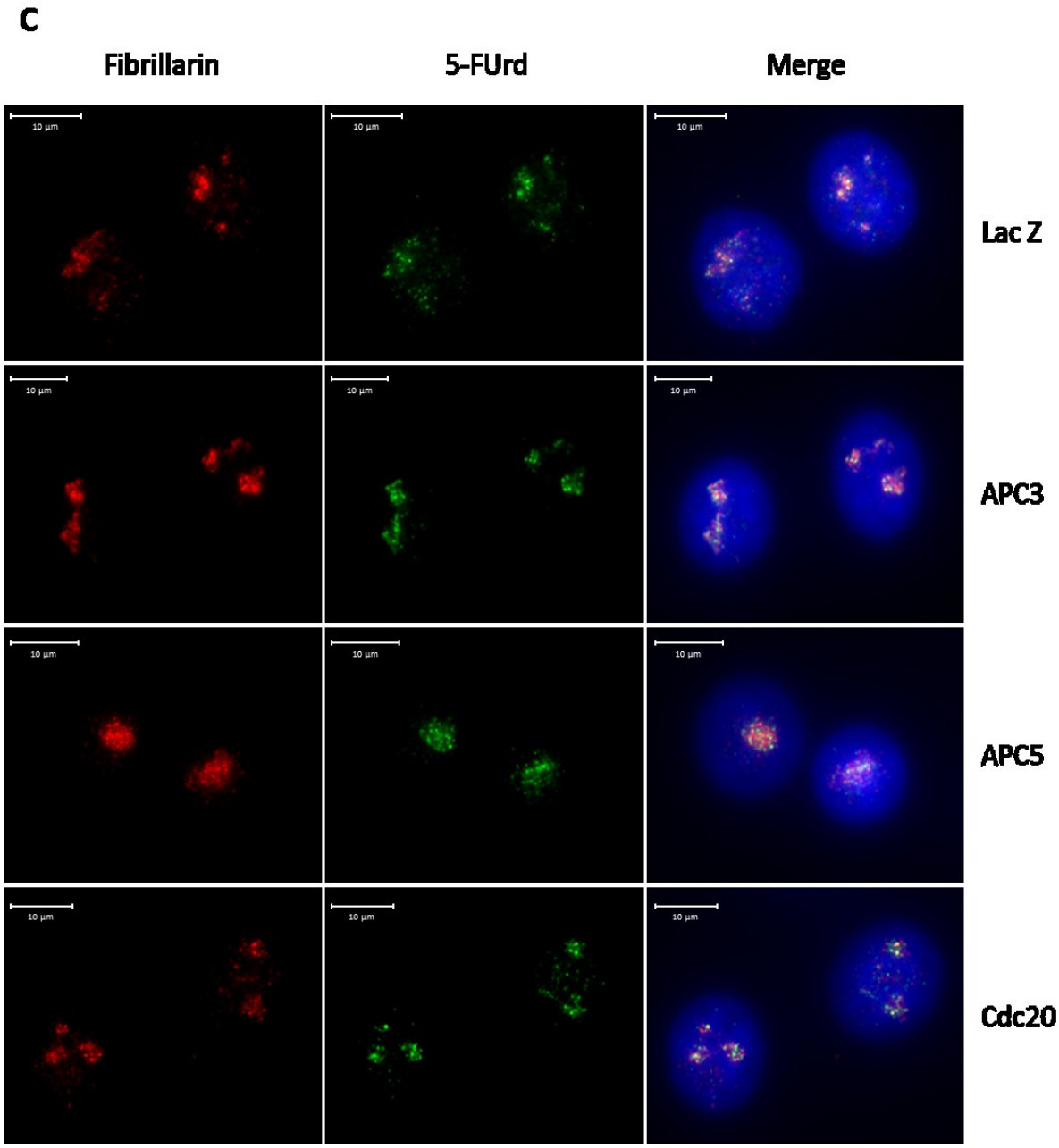

Figure 1.12 – 5'-Fluorouridine incorporation as a marker for Pol I activity following siRNA-mediated knockdown of either LacZ, APC3, APC5 or Cdc20

HeLa cells were subjected to siRNA-mediated knockdown of LacZ, APC3, APC5 or Cdc20 for 72h. Cells were then incubated with 2mM 5-FUrd for 10 minutes and processed for immunofluorescence (**A**, **C**) or Western Blotting (**B**)

(A) IF images were imported into Image J (NIH), and a region of interest drawn around each nucleolus, as denoted by Fibrillarin staining. The area, mean signal and total signal from the BrdU staining were then measured, along with 3 background readings. The average mean signal from the background values was established and use for the following calculations:

i) Mean nucleolar incorporation of 5-FUrd = Mean nucleolar signal – mean background signal

ii) Total nucleolar incorporation of 5-FUrd = Total nucleolar signal – (Area of nucleolus x mean background signal)
iii) Total nucleolar incorporation of 5-FUrd per cell = Sum of total nucleolar incorporation of 5-FUrd for all nucleoli within the same cell

The mean of these three values was calculated for each siRNA treatment and expressed relative to LacZ control. The two bars in each siRNA treatment represent two independent repeats.

All differences were calculated to be significant by a Student's t-test ($P<0.0001$).

Number of nucleoli analysed:
repeat 1 (dark bar) – LacZ (806), APC3 (685), APC5 (456), Cdc20 (495)
repeat 2 (light bar) – LacZ (641), APC3 (317), APC5 (543), Cdc20 (279)

Number of cells analysed:
repeat 1 (dark bar) – LacZ (345), APC3 (285), APC5 (212), Cdc20 (279)
repeat 2 (light bar) – LacZ (273), APC3 (144), APC5 (262), Cdc20 (155)

(**B**) Western blots verifying knockdown efficiency of APC3, APC5 and Cdc20.

(**C**) Representative IF images showing Fibrillarin staining of nucleoli (red), BrdU staining of 5-FUrd pre-rRNA incorporation (green) and merged with DNA stained with DAPI (blue).

5.12. The Chicken Anaemia Virus protein, Apoptin does not disrupt APC5 interaction with RPA194.

Having demonstrated that cellular RPA194 protein levels were at least in part dependent upon APC/C subunit expression, we wished to determine whether a functional APC/C complex was required for its interaction with APC5. In this regard, we took advantage of the ability of the Chicken Anaemia Virus (CAV) protein, Apoptin to bind APC1 and disrupt the APC/C, which has previously been shown to inhibit the E3 ligase capacity of the APC/C (Teodoro, Heilman et al. 2004).

HeLa cells were therefore infected with an Adenoviral vector expressing either LacZ or CAV Apoptin tagged with HA (HA-Apoptin). APC5 IPs were then performed to compare its ability to bind RPA194 *in vivo* in the presence or absence of HA-Apoptin (Figure 1.13). However, the expression of Apoptin did not affect the binding between APC5 and RPA194 (Figure 1.13). It can be deduced, therefore, that the interaction between APC5 and RPA194 is not dependent upon an active APC/C holoenzyme.

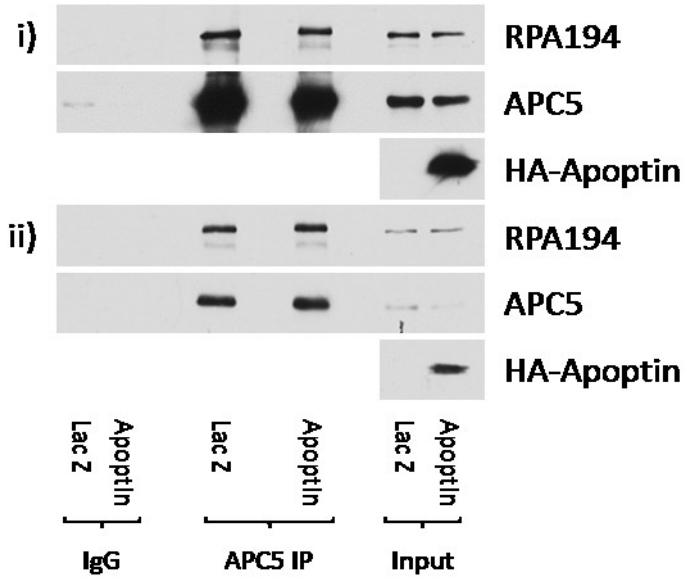

Figure 1.13 - The interaction between RPA194 and APC5 is not altered by inhibition of the APC/C by CAV Apoptin

HeLa cells were infected by 20pfu/cell adenovirus vector expressing either LacZ or HA-Apoptin cDNA for 2h. Cells were harvested 60h post-infection, either from whole cell lysates (i) or nucleolar extracts (ii), into which 5µg IgG or APC5 antibody was added overnight, followed by 10µl packed Protein G-agarose beads for 2h. These IPs were then washed, boiled, separated by SDS-PAGE and analysed by immunoblotting using the denoted antibodies. Apoptin was detected using an HA antibody.

5.13. APC5 binds Pol I both in interphase and during mitotic disassembly of the nucleolus

Transcription of rDNA has been shown to be dynamic, such that it is constantly being regulated as part of various signalling pathways. The nucleolus is integral to the cellular response to different forms of stress, and may act as a central sensory hub with an effector mechanism which results in the inhibition of rRNA synthesis and processing (Mayer and Grummt 2005, Boulon, Westman et al. 2010, Grummt 2013). As it has previously been shown that the APC/C regulates Pol I transcription (Figures 1.11 and 1.12), it was considered whether the APC/C was involved in the repression of Pol I activity as part of the stress response. To investigate this, a series of experiments were instigated to examine the interaction between APC5 and Pol I following the inhibition of rDNA transcription.

During mitosis in human cells, the nucleoli disassemble, and genomic regions of rDNA arrange into nucleolar organiser regions (NORs). Active NORs, *i.e.* those which have not become silenced by heterochromatin, retain the inhibited Pol I throughout mitosis until Cdk1 inhibition and Pol I reactivation during late mitosis, upon which pre-rRNA synthesis recommences (Hernandez-Verdun 2011). It was therefore of interest to see whether the interaction between APC5 and Pol I was altered during nocodazole-induced mitotic arrest.

HeLa cells were either grown asynchronously or arrested in prometaphase by nocodazole. The binding between APC5 and RPA194 was then analysed by Western blot analysis of APC5 IPs. The total amount of RPA194 co-immunoprecipitated by APC5 antibodies was equal between asynchronous and mitotic cells (Figure 1.14A). However, closer examination of the APC5 Western blot suggests that APC5 is depleted during mitosis, a phenomenon independently corroborated by another group (Teodoro JS, personal communication; Figures 1.10 and 1.14A). Therefore, whilst the total binding of APC5 to RPA194 remained unchanged, the binding relative to APC5 abundance was increased (Figure 1.14A). This suggests that either binding between the two proteins has increased, or that the APC5

bound to Pol I is somehow protected from its mitotic instability. As such, there is insufficient evidence provided here to establish a definitive role for APC5 in mitotic inhibition of Pol I.

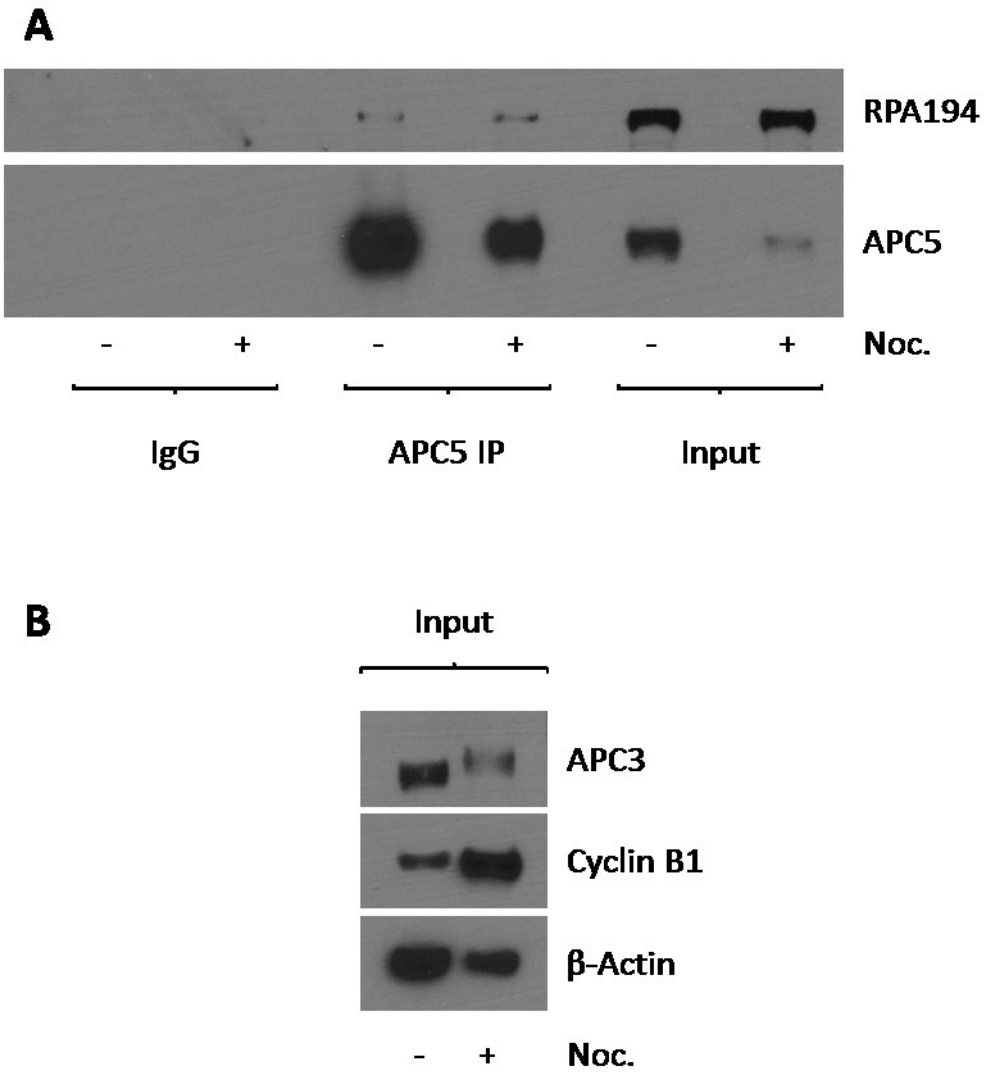

Figure 1.14 – Comparison of APC5-RPA194 interaction between asynchronous and mitotic cells.

HeLa cells were treated with DMSO (-) or 400ng/ml nocodazole (Noc.) for 20h (+). Mitotic cells in Noc-treated samples were harvested by mitotic shake-off. Lysates were normalised and APC5 IPs were performed. These were separated by SDS-PAGE and analysed by Western blotting (**A**). Further lysate controls are shown to confirm mitotic arrest (**B**).

5.14. Selective inhibition of RNA Polymerase I by Actinomycin D increases the interaction between APC5 and RPA194.

It is possible to inhibit rDNA transcription artificially using the DNA-intercalating drug Actinomycin D (Act D), which at low doses has been shown to be specific for Pol I inhibition rather than Pol II or III (Perry and Kelley 1970, Iapalucci-Espinoza and Franze-Fernández 1979). Act D treatment elicits many cellular changes, some of which are capable of altering rRNA production. One method is by inhibition of the elongation step within Pol I transcription, due to stabilisation of Topoisomerase I-cleaved DNA intermediates, causing rDNA genes to become supercoiled and increasing the proportion of Pol I holoenzymes associated with promoters (Trask and Muller 1988, Hadjiolova, Hadjiolov et al. 1995). Act D also causes nucleolar structure to become disrupted, such that the subnucleolar compartments dissociate, and proteins important for Pol I transcription, such as UBF, as well as nucleoplasmic proteins sequester into nucleolar caps around the cellular compartments in which nucleoli were originally located (Andersen, Lam et al. 2005, Shav-Tal, Blechman et al. 2005).

We therefore investigated the interaction between APC5 and Pol I during rDNA inhibition by Actinomycin D. HeLa cells were incubated with Act D, either at 0, 0.1, 0.5, 1 or 5µg/ml for 2h (Figure 1.15A – "dose response"), or at 0.1µg/ml for 0, ½, 1, 2, 4, 8 or 24h (Figure 1.15B – "time course"). The ability of Act D to inhibit RNA Pol I activity at all doses and time points used was verified by assessing the nucleolar incorporation of 5-FUrd by IF (data not shown). Subsequently, the amount of RPA194 immunoprecipitated by anti-APC5 antibodies was then analysed.

Comparing the ability of APC5 to co-IP RPA194 following the increase in Act D dosage, it was evident that a low dosage specific to Pol I inhibition (0.1µg/ml) resulted in an increased association between Pol I and APC5 (Figure 1.15A). At higher doses, where RNA Polymerase II and III enzymes are also inhibited, the interaction between APC5 and RPA194 was reduced appreciably (Figure 1.15A). Further study revealed that specific inhibition of Pol I activity by a low dose of Act D resulted in an

initial time-dependent increase in APC5-RPA194 binding, which was then followed by a clear reduction in binding, which presumably reflected increased cellular stress and the decrease in APC5 protein levels (Figure 1.15B). It can thus be concluded that specific inhibition of Pol I transcription by Act D initially stabilises the interaction between APC5 and Pol I. Whether this is a direct response to transcription inhibition or merely an indirect consequence of nucleolar dysfunction and increased Pol I bound to rDNA remains to be elucidated.

It is interesting to note that the decrease in RPA194-APC5 binding observed during increased stress mimics the decrease in APC5 protein levels, and thus could merely reflect the decreased availability of APC5 rather than a stress effector mechanism. This is in direct contrast to the mitotic decrease of APC5, during which APC5 interaction with Pol I did not decrease (Figure 1.14). APC3 protein levels also decreased during increased and prolonged transcriptional inhibitory stress, albeit at a greater rate than APC5, suggesting this could be a response affecting entire APC/C function rather than APC5-specific. However, it should also be noted that RPA194 protein levels are also reduced at both high doses of Act D (Figure 1.15A), and during prolonged Pol I inhibition (Figure 1.15B).

A

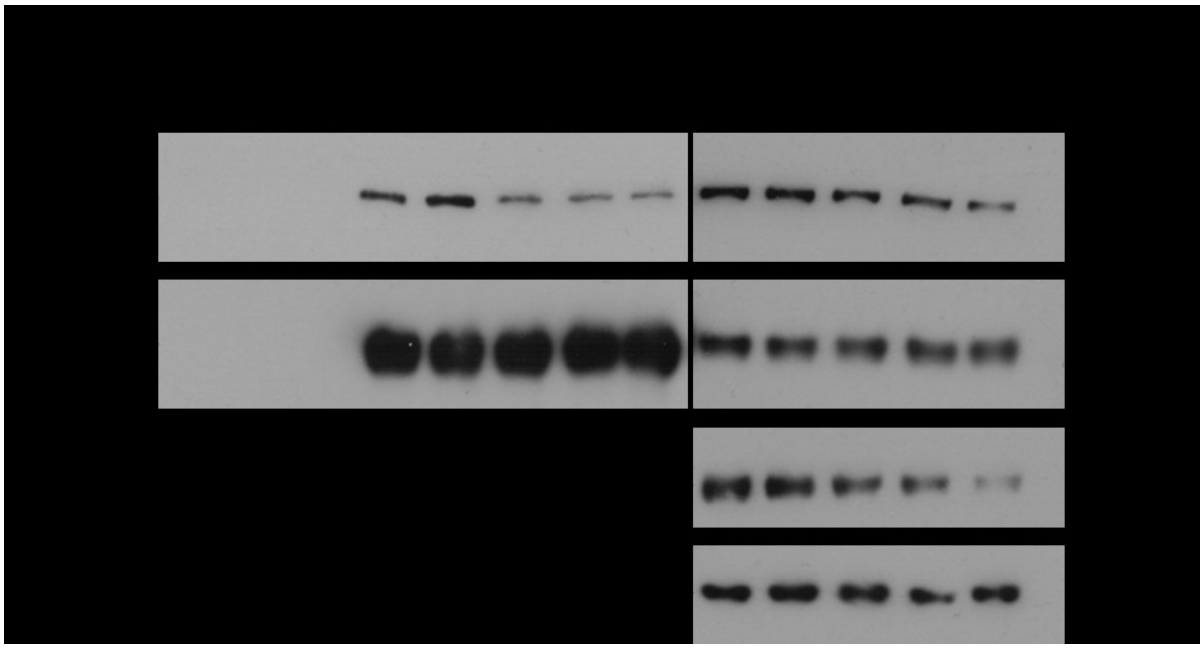

B

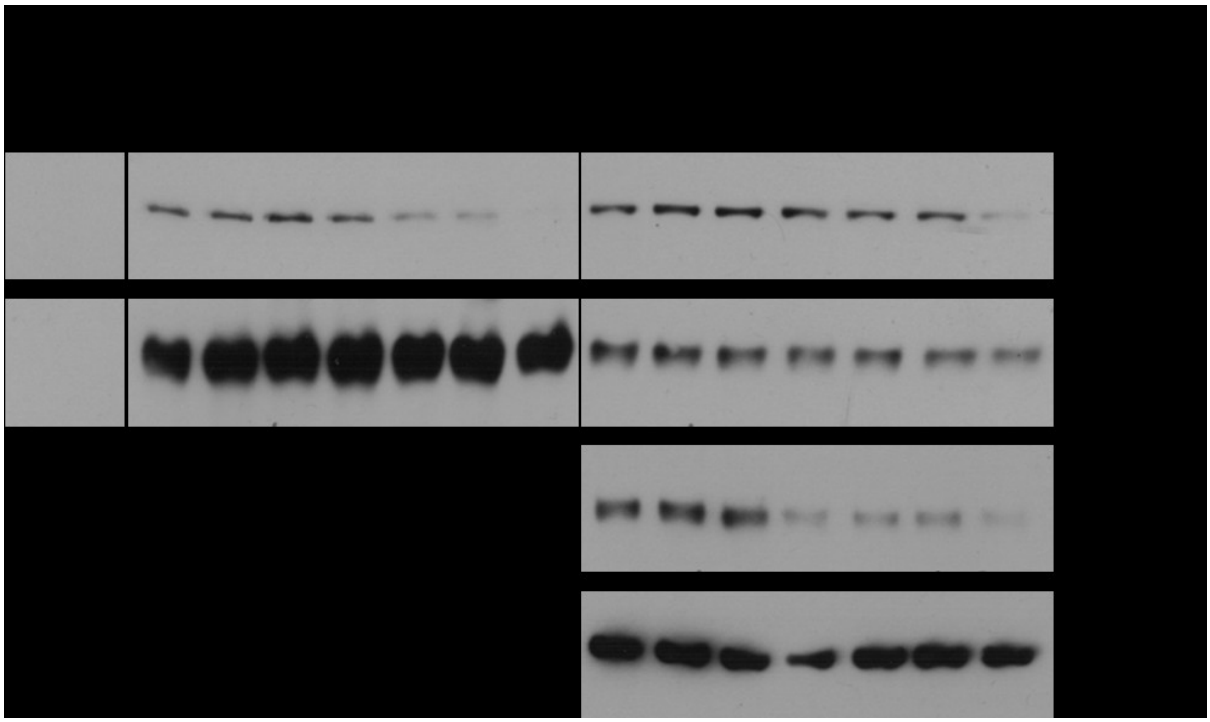

Figure 1.15 – Inhibition of rDNA transcription by Actinomycin D affects APC5 binding to Pol I

HeLa cells were incubated with Actinomycin D (Act D) for 2h at the designated doses (A), or at 0.1µg/ml for the designated time (B). Cells were harvested, incubated with APC5 antibodies overnight and Protein G-agarose for 2h. IPs were washed, separated by SDS-PAGE and analysed by Western blotting.

5.15. Glucose and Serum deprivation-induced quiescence disrupts APC5-RPA194 binding

The next form of nucleolar stress which was investigated was metabolic stress, mediated by the deprivation of glucose. This has previously been shown to decrease Pol I transcription through several different mechanisms, including the phosphorylation and inactivation of RRN3/TIF-1A by AMP-Activated Protein Kinase (AMPK) and rDNA epigenetic silencing by eNoSC (Energy-Dependent Nucleolar Silencing Complex) (Murayama, Ohmori et al. 2008, Hoppe, Bierhoff et al. 2009). In order to deplete cells of glucose, a formulation of DMEM was created which was deprived of glucose. However, the FCS used to supplement the DMEM would contain some glucose, and so this experiment was performed alongside serum starvation, which depletes cells of important proliferation growth factors and hormones required for cellular signalling to pass the restriction point in G1 and enter S phase. Therefore, HeLa cells were incubated in glucose-free, serum-free or glucose-and-serum-free growth media, or incubated in full growth media, for 20h. It is important to note that serum starvation has also been described as inducing a reduction in Pol I activity by heterochromatin remodelling of rDNA and UBF modulation (Glibetic, Taylor et al. 1995, Zillner, Filarsky et al. 2013).

Withdrawal of both glucose and FCS caused cells to enter quiescence, as shown by the decreased expression of Cyclins A, B1 and D1, Cdc20 and UbcH10, whilst removal of either glucose or FCS caused some cell cycle arrest, with glucose withdrawal proving more effective than serum starvation (Figure 1.16B). It is interesting to see, however, that the ability of APC5 to co-IP RPA194 was diminished considerably upon removal of both glucose and FCS, however removal of only either one of these supplements had no appreciable effect on Pol I binding (1.16A). This implies that rDNA inhibition following withdrawal of growth factors is not mediated by APC5; however, it may play a role following glucose starvation. As with Actinomycin D-mediated inhibition of Pol I, there was a decrease in APC5 protein levels following serum and glucose withdrawal, which is likely to be the

cause of reduced RPA194 binding to APC5. This change likely reflects induction of quiescence or pro-apoptotic pathways, but this awaits further investigation. The lack of effect upon APC5 binding to RPA194 following the removal of only glucose might be due to the presence of glucose within the FCS used to supplement the media. To test this more accurately, it would be prudent to dialyse the FCS prior to use to remove any potential respiratory substrates, yet retain its protein content.

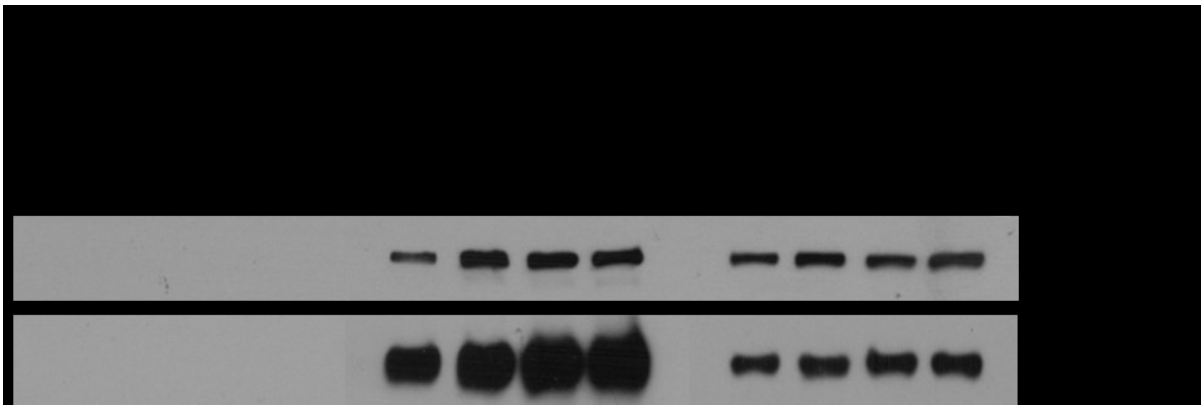

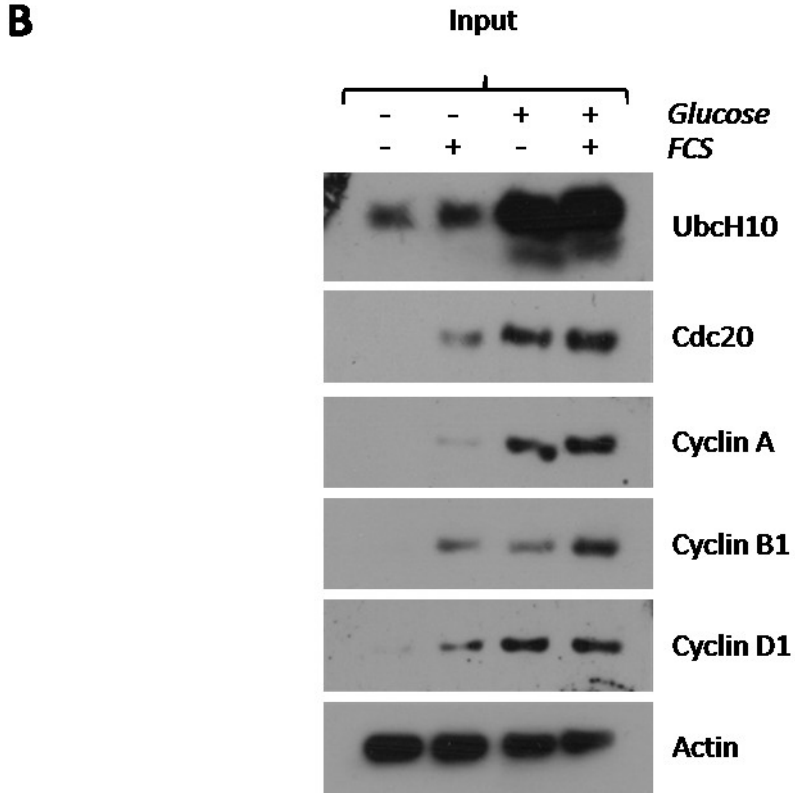

Figure 1.16 – The effect of Glucose and/or FCS deprivation on APC5-RPA194 binding

HeLa cells were washed into DMEM containing 2mM L-Glutamine and 0.375% (w/v) Sodium Bicarbonate (reduced DMEM), or reduced DMEM supplemented with either 4.5g/l glucose or 10% FCS, or both, and were cultured for 20h. Lysates were harvested and immunoprecipitated with 5µg APC5 antibody and 10µl packed Protein G-agarose beads. IPs were washed and separated by SDS-PAGE and immunoblotted with the designated antibodies.

A) APC5 IPs showing co-IP of RPA194
B) input lysates

5.16. Ionising Radiation has no effect on the interaction between APC5 and RPA194

The interaction between APC5 and Pol I was next investigated following DNA damage by UV and IR, which predominantly cause single- and double-stranded breaks, respectively. These evoke an anti-proliferative response such that the cell cycle arrests and DNA repair machinery can resolve these breakages. Should the DNA be rendered irreparable, cells undergo apoptosis via the intrinsic pathway. Errors in these processes result in cellular division in the presence of incorrectly repaired DNA, resulting in genetic instability and increased oncogenic potential (Ciccia and Elledge 2010, Iyama and Wilson 2013). The nucleolus has been implicated as playing a key role within the DNA damage response, in a p53-dependent manner. P53 is stabilised within the nucleolus (Rubbi and Milner 2003, Wsierska-Gadek and Horky 2003) and Nucleophosmin/B23 is released from the nucleolus and inhibits the p53-directed E3 ubiquitin ligase, HDM2/Mdm2 (Kurki, Peltonen et al. 2004). A p53-independent response has also been described following UV-irradiation, causing the relocalisation of Ki-67 from the nucleolus to the nucleoplasm in the absence of p53 (Al-Baker, Boyle et al. 2004). The transcription of rDNA has been shown to be inhibited by a variety of mechanisms following DNA damage, including the inactivation of necessary transcription initiation factors, such as JNK2-mediated inactivation of RRN3/TIF-1A, and the inhibition of UBF by p53 and $p14^{ARF}$ (Zhai and Comai 2000, Mayer, Bierhoff et al. 2005, Ayrault, Andrique et al. 2006). There is also evidence for ATM-dependent regulation and remodelling of the nucleolus (Kruhlak, Crouch et al. 2007). Given the known effects of DNA damage upon Pol I activity, we therefore analysed the ability of APC5 to co-IP RPA194 upon DNA damage to determine whether this poses an alternative mechanism for DNA damage-mediated Pol I inhibition.

Firstly, HeLa cells were treated with IR in order to assess the response of APC5 and its interaction with Pol I following double-stranded DNA breaks. It is evident, however, that the interaction between

APC5 and RPA194 is not affected by IR treatment (Figure 1.17), neither as a result of the activation of DNA damage signalling pathways (1h) or upon resolution of DNA breaks and Pol I reactivation (8h), implying modulation of the APC5-RPA194 interaction is not important in this signalling pathway.

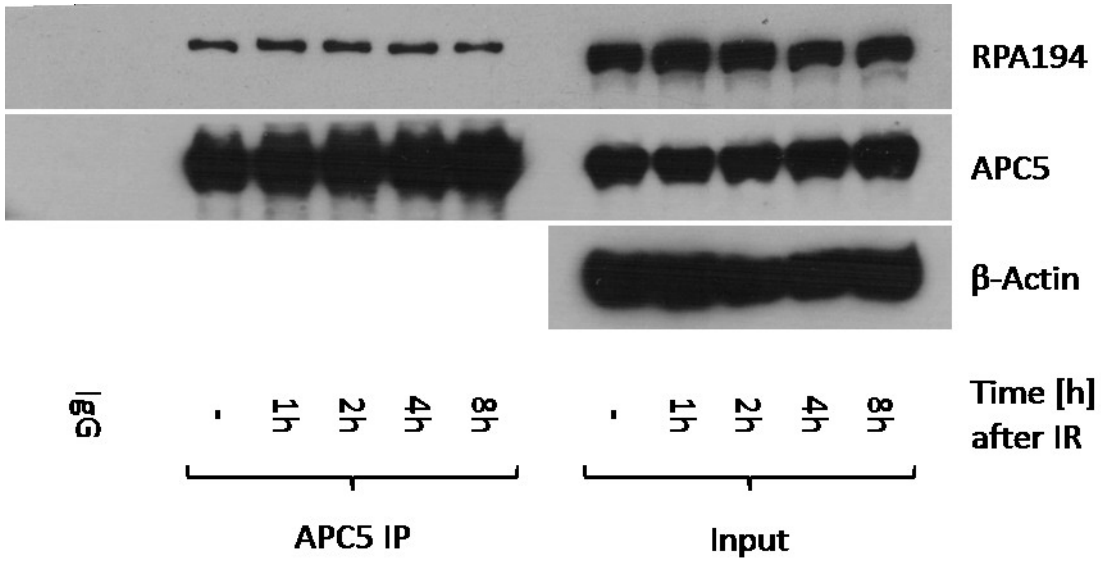

Figure 1.17 – Time course showing co-IP/Western blots of APC5 pull-down of RPA194 following IR.

Double-stranded DNA breaks were induced by 5Gy of ionising radiation. Cells were left to recover for the time indicated prior to harvesting and IP by APC5 antibodies and Protein G-agarose. IPs were washed, separated by SDS-PAGE and precipitated proteins determined by Western blotting.

5.17. Apoptosis induced by UV-irradiation causes degradation of APC5, thereby eliminating its binding to Pol I.

Having shown that double-stranded DNA break-repair pathways had no effect on the interaction between APC5 and Pol I, it was next necessary to investigate the interaction following the induction of single-stranded breaks. HeLa cells were thus treated with 25J/m^2 of UV-irradiation, and allowed to recover over a time course up to 8h to permit analysis of the initial damage-sensing response, during which time Pol I is inhibited, followed by its reactivation following DNA repair. As before, the interaction between APC5 and RPA194 was investigated by analysing the ability of APC5 to co-IP RPA194.

Results obtained from this experiment demonstrated that less RPA194 was co-precipitated by APC5 antisera both 4 and 8 hours after irradiation relative to untreated cells (Figure 1.18). However, the amount of APC5, both in the input lysate and in the IPs, decreased over the same time frame (Figure 1.18). The reduction in RPA194 co-IP could therefore be due to the reduced availability of APC5 rather than the specific modulation of APC5 binding to RPA194.

Before reaching any conclusions regarding the role of APC5 and Pol I in the DNA damage response, an important observation must be documented. Prior to harvesting, the cells did not appear to be healthy in the 4h and 8h time points, and indeed appeared to be in the initial stages of apoptosis. Subsequent immunoblotting for PARP showed that there was a lower degradation product for these samples, which is produced following cleavage by caspases, signifying some cells were starting to die by apoptosis (Figure 1.18). Therefore, it is unclear whether the different binding patterns of APC5 and RPA194 between our –UV control and 4 and 8 hours after UV treatment is a consequence of a traditional DNA repair mechanism or the stimulation of pro-apoptotic pathways.

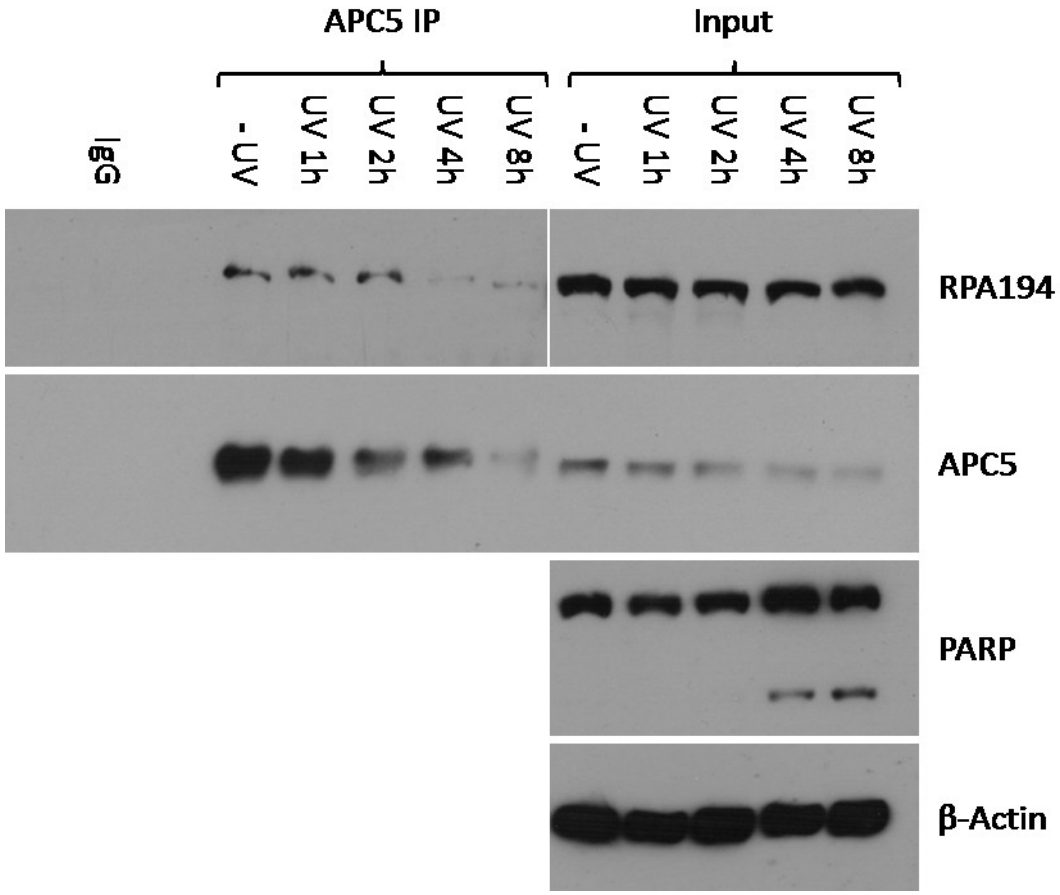

Figure 1.18 – UV-induced Apoptosis results in a decrease in binding between APC5 and RPA194

HeLa cells were irradiated with 25J/m^2 UV and cultured for the time indicated. Cells were harvested and APC5 IPs performed, which were separated by SDS-PAGE and detected by Western blotting with the designated antibodies.

5.18. Cisplatin treatment causes a decrease in APC5-Pol I interaction by degradation of APC5.

In order to determine whether APC5 degradation following UV-irradiation was part of a normal DNA damage response or as a result of the activation of pro-apoptotic signalling pathways, HeLa cells were incubated with the anti-cancer drug Cisplatin to induce an experimentally-controlled cell death. Cells were either incubated with an increasing dose (0, 10, 20, 30, 40 or 50μg/ml) of Cisplatin for 16h (Figure 1.19), or treated with 20μg/ml Cisplatin over a 48h time course (Figure 1.20). APC5 IPs were then performed, and the ability of APC5 to co-precipitate RPA194 was determined by Western blotting.

Progressively increasing the dose of Cisplatin was shown to result in considerably reduced levels of both APC3 and APC5 proteins in the cellular lysate (Figure 1.19). Moreover, Cisplatin treatment also promoted a reduction in APC5-RPA194 binding (Figure 1.19). As per previous experiments, however, it is likely that the reduction in binding could reflect the reduction in absolute levels of APC5 following Cisplatin treatment.

In order to investigate the dynamics of APC3 and APC5 instability during apoptosis, a time course was adopted following treatment with 20μg/ml Cisplatin. This concentration was chosen as it ablated p53 expression as well as showed cleavage of PARP after 16h (Figure 1.19), and therefore elicited an apoptotic response in a time scale which was easy to produce experimentally. This experiment revealed that APC3 and APC5 protein levels decreased as the cells progressed through the cellular apoptotic programme, and that APC3 levels were reduced at a faster rate than APC5 (Figure 1.20). Again, the levels of RPA194 that co-precipitated with APC5 antisera appears to follow the same pattern as APC5 degradation. These data imply that Pol I inhibition during apoptosis is regulated by means other than its interaction with APC5.

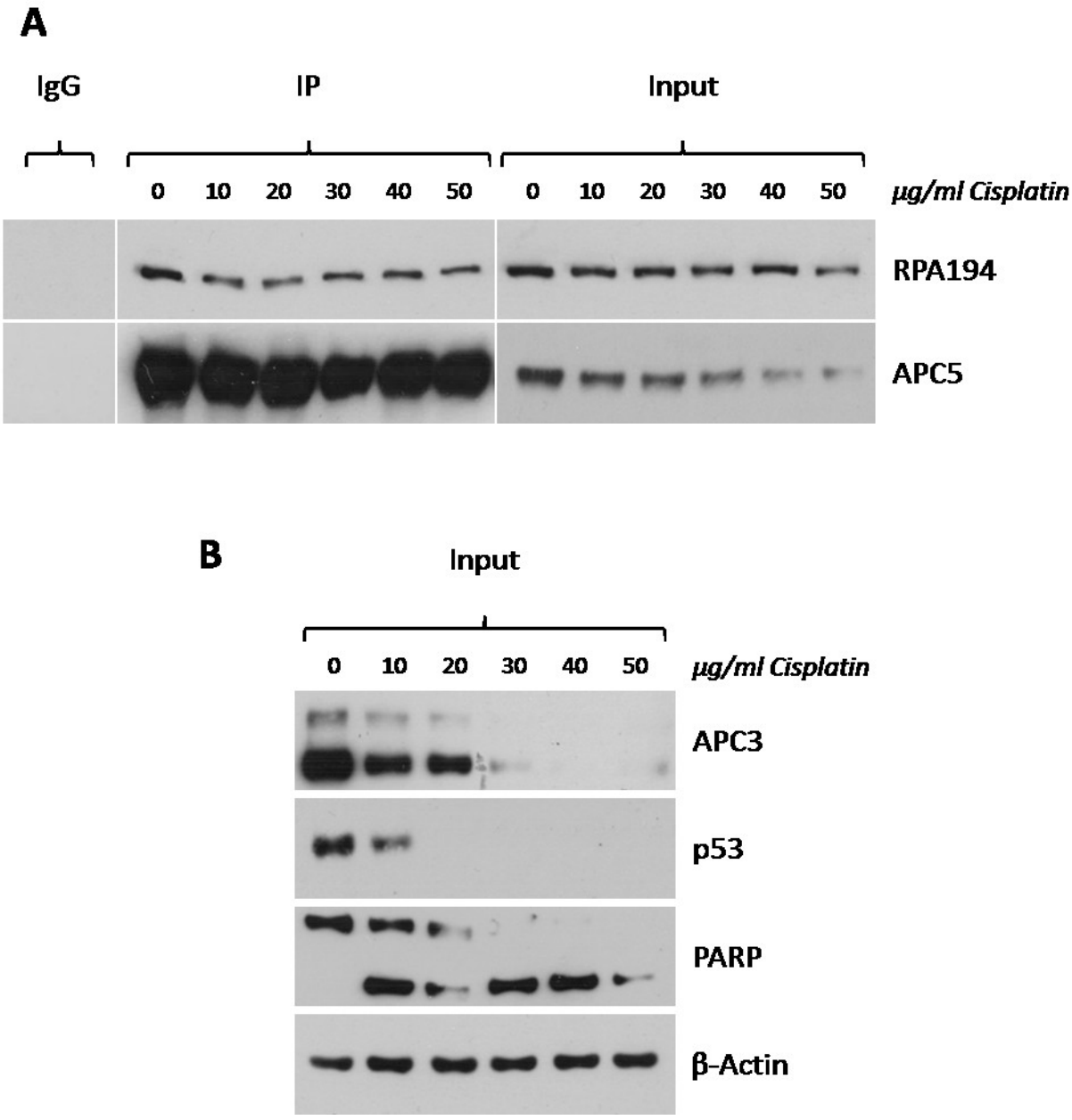

Figure 1.19 – Increased dosage of Cisplatin results in a decrease in APC5 abundance and a reduction in its binding to RPA194

HeLa cells were incubated in Cisplatin at the described dosage for 16h. Cell lysates were harvested, and subjected to APC5 IP. These were then washed, separated by SDS-PAGE and analysed by immunoblotting. **A** shows APC5 IPs, whilst further lysate blots are shown in **B**.

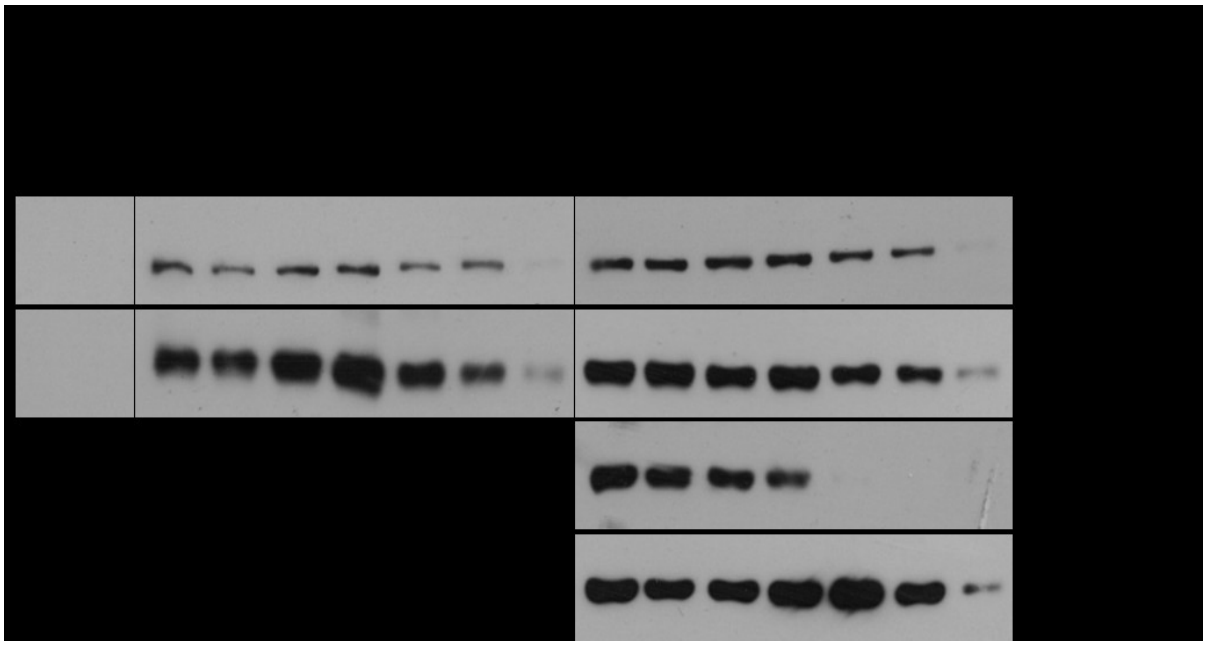

Figure 1.20 – Cisplatin time course showing progressive decrease in APC3 and APC5 abundance

HeLa cells were incubated in 20µg/ml for the designated incubation time before lysates were harvested and APC5 antibodies used to co-IP RPA194, as detected by SDS-PAGE and Western blot.

5.19. Discussion

5.19.1. APC5 interacts with RNA Polymerase I within the nucleolus

In this chapter a novel interaction between APC5 and Pol I has been identified by mass spectrometry and subsequently validated both *in vivo* by co-IP/Western blots and *in vitro* by GST pull-down assays (Figures 1.1, 1.2 and 1.3). This interaction was shown to be specific to APC5, as other APC/C subunits such as APC3 and APC7 were not able to co-IP Pol I (Figures 1.2 and 1.5) and disruption of the APC/C by CAV Apoptin did not affect the binding (Figure 1.13). The interaction between APC5 and Pol I was shown to be restricted to the nucleolus (Figure 1.5), and the APC/C subunits APC5 and APC7 co-eluted with Pol I following FPLC fractionation of nucleolar lysates (Figure 1.6). The reasons why this interaction between APC5 and Pol I is only nucleolar are not yet understood, although it is possible that post-translational modifications or further nucleolar binding factors are required to facilitate the interaction. It is also possible that APC5 associates with Pol I directly upon rDNA to regulate Pol I transcription. Although GST-APC5 was shown to bind RPA194 and RPA135 directly (Figure 1.3), it is possible that other bridging factors may have been present at low levels within the rabbit reticulocyte lysate used to transcribe and translate the Pol I subunits *in vitro*, and therefore the possibility of ancillary proteins for the APC5-Pol I interaction cannot be disregarded. However, the requirement of PTMs for the binding between APC5 and Pol I is unnecessary in this case, as proteins expressed *in vitro* do not display the same modifications as seen *in vivo*, yet binding is still observed (Figure 1.3).

In order to elucidate the mechanism of binding, GST-APC5 fragments were incubated with IVT RPA194 and RPA135 to identify putative binding domains (Figure 1.3). Binding to RPA194 and RPA135 was predominantly mediated by APC5 Fragment 4, consisting of amino acids 567-755, although Fragment 2 (amino acids 189-377) also bound strongly to RPA135; however, all four fragments of APC5 were capable of binding both RPA194 and RPA135. Although APC5 contains TPR

repeats, these are only located within the second, third and fourth fragments; this suggests that APC5 interacts with Pol I through multiple contact points. As such, it would be interesting to refine interactions to the amino acid level, and see where the key interaction sites lie within the 3D structure of the APC5 protein.

5.19.2. The APC/C exists as a holoenzyme within the nucleolus.

Mass spectrometric screens have been utilised to form a periodically-updated database containing all known nucleolar proteins (Ahmad, Boisvert et al. 2009). Within these lists, the only subunit of the APC/C which has been identified to date is APC7. Using the same nucleolar fractionation protocol deployed to create this database, experimental evidence presented within this chapter clearly shows the presence of several subunits of the APC/C within the nucleolus; APC3, APC5, APC7 and Cdc20, but not Cdh1, were identified within the nucleolar lysate by Western blotting (Figure 1.4), and APC1, APC5 and APC7 were shown to be present in the nucleolus by IF (Figure 1.7). Similarly, APC5 and APC7 co-eluted within large nucleolar complexes of the same size upon FPLC fractionation (Figure 1.6), and APC3 and APC7 co-immunoprecipitated APC5 from nucleolar lysates (Figure 1.5). Together, these data suggest the APC/C is present as a holoenzyme within the nucleolus.

Given that the APC/C exists as a nucleolar holoenzyme, it is necessary to re-examine the interaction previously described between APC5 and Pol I. Although APC3 and APC7 were unable to co-IP RPA194 (Figure 1.2), this does not necessarily mean the APC5-Pol I interaction is independent of the APC/C. Indeed, the IF staining exhibited by APC1, APC5 and APC7 all showed a degree of overlap with the nucleolus, as defined by Fibrillarin staining (Figure 1.7B). Whilst this experiment does not prove an interaction between the APC/C complex and Pol I *per se*, it suggests that the APC/C is present within the Fibrillar and Dense Fibrillar Compartments, in which Pol I transcription occurs (Goodfellow and Zomerdijk 2012). Together with the nucleolar FPLC co-elution pattern of APC5 and APC7 (Figure 1.6)

and the APC5 results discussed earlier, it is possible that APC5 might present RPA194 as a substrate for APC/C-mediated degradation. Given this notion, it would not be surprising that Pol I was not found associated with the APC/C holoenzyme. Indeed, it has been suggested to be difficult to isolate APC/C substrates through co-immunoprecipitation with APC/C subunits due to low affinity interactions (Ayad, Rankin et al. 2005).

5.19.3. RPA194 as a putative substrate for APC/C-mediated ubiquitylation

There are numerous ways to test if a protein is a substrate for APC/C-mediated ubiquitylation. Perhaps the most common approach is to IP the APC/C holoenzyme from cellular lysates and perform an *in vitro* ubiquitylation assay using [^{35}S]-labelled substrates. Indeed, we adopted this protocol to investigate whether APC/C-Cdc20 or APC/C-Cdh1 immunocomplexes would support the ubiquitylation of Pol I subunits (Figure 1.8B). Unfortunately, however, immunopurified APC/C was unable to support the ubiquitylation of *IVT*-RPA194 or -RPA135 *in vitro*. As mentioned previously, *IVT* proteins might not be appropriately post-translationally modified. Although *IVT*-RPA194 and -RPA135 can associate with GST-APC5 *in vitro* to varying degrees (Figure 1.3), it is possible that post-translational modification of APC5, RPA194 and/or RPA135 might increase binding capacity between the APC/C holoenzyme and Pol I and support APC/C-directed ubiquitylation of Pol I subunits.

Indeed, a role for PTMs as a requirement for APC/C-dependent ubiquitylation has already been suggested for the fission yeast substrate, Est1p; immunopurified APC/C complexes were unable to ubiquitylate *in vitro*-expressed Est1p, but directed its ubiquitin-mediated degradation *in vivo* (Ferguson, Chao et al. 2013). It has also been shown that other APC/C substrates require specific PTMs for ubiquitylation to occur, including the acetylation of Cyclin A (Mateo, Vidal-Laliena et al. 2009), an acetylation-sumoylation switch in BubR1 (Choi, Choe et al. 2009, Yang, Huang et al. 2012) and the phosphorylation of Mcl-1 (Harley, Allan et al. 2010) and RASSF1A (Chow, Wong et al. 2012).

Moreover, Nek2A and Aurora A have been shown to have serine residues directly preceding the KEN box (SKEN) that when phosphorylated promote APC/C-directed polyubiquitylation (Min, Mayor et al. 2013). Whilst RPA194 does not contain any KEN-boxes, it does contain a TEK motif, another proposed acceptor site for APC/C-mediated ubiquitylation (Figure 1.8A) (Jin, Williamson et al. 2008), which has been shown to be ubiquitylated *in vivo* (Kim, Bennett et al. 2011). Indeed, there are several S and Q moieties both upstream and downstream of this TEK motif, which could potentially alter its substrate potential, and RPA194 has been shown to be phosphorylated *in vivo* (Dephoure, Zhou et al. 2008, Ruse, McClatchy et al. 2008, Olsen, Vermeulen et al. 2010).

Given the inability of the APC/C to ubiquitylate RPA194 *in vitro*, it was clear that different techniques would have to be employed to determine whether RPA194 is a *bona fide* novel substrate for the APC/C. In this regard, RPA194 protein levels were analysed following inhibition of APC/C activity by subunit knockdown (Figure 1.9) and measured during a time course through mitosis (Figure 1.10), during which APC/C activity progressively increases. In both cases, RPA194 protein levels were shown to mimic those of known APC/C substrates, such as Cyclin B1.

These data suggest that the APC/C, at least in part, regulates the protein levels of RPA194. However, further study is required to be certain this is a direct consequence of APC/C-mediated ubiquitylation. Mutational analyses of the D-boxes within RPA194, as well as its TEK motif and C-terminal L-R dipeptide, would provide greater evidence that RPA194 protein levels are regulated by APC/C activity. In this regard, it would be interesting to look at the type of ubiquitin chain formed upon RPA194, particularly upon the K1180 residue within the TEK motif. This is because the APC/C predominantly forms K11 polyubiquitin chains in humans, under the influence of the chain elongation E2, UBE2S, and it is the only E3 ubiquitin ligase discovered thus far which uses K11 linkages (Jin, Williamson et al. 2008, Garnett, Mansfeld et al. 2009, Wu, Merbl et al. 2010). Should

K11 polyubiquitin chains be identified upon RPA194, it would provide further evidence that it is a substrate for APC/C-mediated ubiquitylation.

It is possible that APC5 mediates the recognition of RPA194 by the APC/C, and presents RPA194 as a substrate for ubiqutylation rather than the typical co-activators and substrate recognition proteins Cdc20 and Cdh1, which were unable to co-IP RPA194. This has previously been proposed in the case of the transcription factor E2F1, which is targeted for proteolysis by the APC/C during prometaphase (Budhavarapu, White et al. 2012). Here, it was postulated that E2F1 degradation required direct binding to APC5, whereupon E2F1 was polyubiquitylated by the APC/C (Budhavarapu, White et al. 2012). Furthermore, the *D. melanogaster* APC5 homologue, IDA, was suggested to regulate the degradation of certain substrates, as its downregulation affected Cyclin B levels but not Securin (Bentley, Williams et al. 2002).

5.19.4. The APC/C represses Pol I transcription

Next, the functional relationship between the APC/C and Pol I was investigated, specifically examining whether the APC/C affects Pol I transcription of rDNA genes. It was determined that downregulation of APC/C activity by siRNA-mediated knockdown of APC/C subunits resulted in an increase in Pol I transcription. Specifically, knockdown of APC/C subunits APC3, APC5 and the APC/C co-activator Cdc20 caused an increase in abundance in 28S and 18S rRNA (Figure 1.11A – i, ii) as well as 45S pre-rRNA (1.11A – iii) relative to non-silencing controls. Knockdown of APC3, APC5 and Cdc20 also increased the rate of *de novo* rDNA transcription, as measured by the incorporation of 5-FUrd and quantitation of nucleolar fluorescence by IF (Figure 1.12). We can therefore postulate that APC/C inhibits Pol I activity, perhaps through the targeting of RPA194 for degradation by the 26S proteasome.

Given that APC/C subunit knockdown augments Pol I transcription, one would expect the opposite effect upon Pol I transcription in the presence of increased APC/C activity, which can be introduced by overexpression of APC/C components. Should domains be discovered within RPA194 which are necessary for APC/C-mediated ubiquitylation, it would be interesting to see whether reintroduction of these non-degradable mutants would rescue the proposed Pol I downregulation upon APC/C overexpression. This would then provide more evidence that the effect of the APC/C upon Pol I activity is indeed due to regulation of RPA194 protein levels.

Although knockdown of APC5 increased the abundance of 18S and 28S rRNA transcripts, the increase in 45S pre-rRNA was deemed statistically insignificant (Figure 1.11), despite increasing *de novo* rRNA synthesis (Figure 1.12). This could be attributable to two possible scenarios: firstly, any increase in Pol I transcription to produce the 45S pre-rRNA transcript is masked by a concomitant increase in the rRNA maturation pathway, resulting in a greater proportion of end-product 18S and 28S rRNA; secondly, 18S and 28S rRNA stability has increased. Effects upon the pre-rRNA processing could be analysed by Northern blotting, with each intermediate rRNA transcript resolving quantified following their resolution by electrophoresis.

5.19.5. The interaction between APC5 and Pol I is altered during nucleolar stress

Pol I transcription is inhibited following nucleolar stresses or disruption. In order to establish whether APC5 had a role in this process, it was investigated whether the interaction between RPA194 and APC5 was similarly altered in these circumstances. It was evident that there was a decrease in this interaction between APC5 and RPA194 during extended Pol I inhibition by Act D (Figure 1.15), apoptotic induction by UV (Figure 1.18) and Cisplatin treatment (Figure 1.19) and following metabolic stress initiated by the withdrawal of glucose or serum (Figure 1.16). However, the reduction in APC5-

RPA194 binding was paralleled by a similar decline in the cellular levels of APC5 and APC3 proteins, and therefore was more likely to be caused by an inhibitory mechanism for APC/C activity as the cell switches from pro-survival signalling pathways to pro-apoptotic signalling pathways rather than a specific cellular inhibition of APC5-Pol I interaction. The mechanism by which the APC/C is inhibited during apoptosis has yet to be investigated but it is likely, given the data presented in this chapter, that APC/C subunits are targeted directly during the apoptotic programme. In this regard it would be interesting to see whether prolonged inhibition of APC/C activity promotes apoptosis, whether the reduction in APC3 and APC5 levels observed during cell death are caspase-dependent, and whether other APC/C subunits are similarly targeted.

It should be noted that RPA194 levels also decreased following these particular forms of stress. Without further analysis into the dynamics and biochemistry of the APC5-RPA194 interaction in these cases, it is impossible to draw a firm conclusion as to whether the interaction between APC5 and RPA194 has actually decreased proportionally and also whether this was as a result of RPA194 downregulation, perhaps by the APC/C.

Although high dosage and prolonged transcriptional inhibition by Act D resulted in a decrease in APC5-RPA194 binding, short-term treatment with a low dosage specific to the inhibition of Pol I transcription augmented the ability of APC5 antisera to co-precipitate RPA194 (Figure 1.15). It is therefore possible that APC5 is important in the repression of Pol I transcript elongation following treatment with Act D. However, one known consequence of Act D treatment is the stabilisation of Pol I holoenzymes upon rDNA promoters caused by an increase in transcription initiation (Hadjiolova, Hadjiolov et al. 1995). Conversely, this could indicate that APC5 might be important for transcription initiation, which could also account for the increased interaction between APC5 and RPA194 following treatment with a low dosage of Act D (Figure 1.15). Although it has been shown that APC5 and Pol I associated within the nucleolus (Figures 1.5 and 1.7), it is not known whether this

interaction occurs upon rDNA. Should this be the case, the increase in Pol I associated with rDNA could enhance the ability of APC5 to co-precipitate RPA194 following Act D treatment, regardless of any involvement of APC5 in the Act D-induced stress response. The ability of APC5 to associate with Pol I could be investigated by the use of Chomatin Immunoprecipitation (ChIP), in which IPs are performed upon cellular lysates, and the ability to pull-down DNA sequences is examined. In this regard, it would be possible to determine whether APC5 is associated with rDNA promoters or genetic elements, and thus could suggest whether APC5 is involved in Pol I transcription or elongation, respectively.

Not all forms of nucleolar stress result in RPA194 degradation or altered binding to APC5, however. Double-stranded breaks elicited by IR caused no appreciable change in the interaction between APC5 and Pol I, nor did the protein levels of APC5 and RPA194 differ compared to controls (Figure 1.17). As the cellular response and effector mechanisms of single- and double-stranded breaks differ, this result compared to that observed from UV-irradiation (Figure 1.18) is not unexpected.

5.19.6. The interaction between APC5 and RPA194 persists in mitosis

During mammalian mitosis, nucleoli disassemble following nuclear envelope breakdown and chromosome condensation, resulting in the inhibition of Pol I transcription (Hernandez-Verdun 2011). The rDNA regions form NORs, and inhibited Pol I can be found at active NORs during mitosis (Hernandez-Verdun 2011). It was therefore examined whether the interaction between APC5 and RPA194 was modulated as part of this mitotic response; however, this interaction was shown to be unaltered between asynchronous and mitotic cells (Figure 1.14).

One important observation to make is that although much of the cellular pool of APC5 is degraded during mitosis, no change in its binding capacity to RPA194 was observed (Figure 1.14). It can be hypothesised, therefore, that the APC5-RPA194 interaction is protected from the mitotic instability

of APC5. Current investigations within our laboratory aim to elucidate the mechanism and consequence of this degradation, which may in part explain why this nucleolar population of APC5 was still capable of binding, whereas APC5 depleted following quiescence or induction of apoptosis lost this capability.

5.20. Concluding remarks

In conclusion, considerable data is presented in this chapter to indicate that APC5 associates specifically with Pol I in the nucleolus, and that the Cdc20 form of the APC/C holoenzyme is also present in the nucleolus. Data is also presented to suggest that the APC/C might target RPA194 for ubiquitin-mediated proteolysis during mitosis and that APC/C-Cdc20 represses Pol I transcriptional activity. I propose a model whereby APC5 serves to recruit RPA194 to the APC/C holoenzyme whereupon RPA194 is ubiquitylated and degraded (Figure 1.21). As such, the APC/C-targeted destruction of RPA194 would serve to augment the inhibition of Pol I activity during mitosis. Given that APC5 interacted with a number of Pol I subunits, it is also possible that APC5 associates with the Pol I holoenzyme, and has additional functions in the regulation of Pol I activity, which are independent to its role as an APC/C subunit.

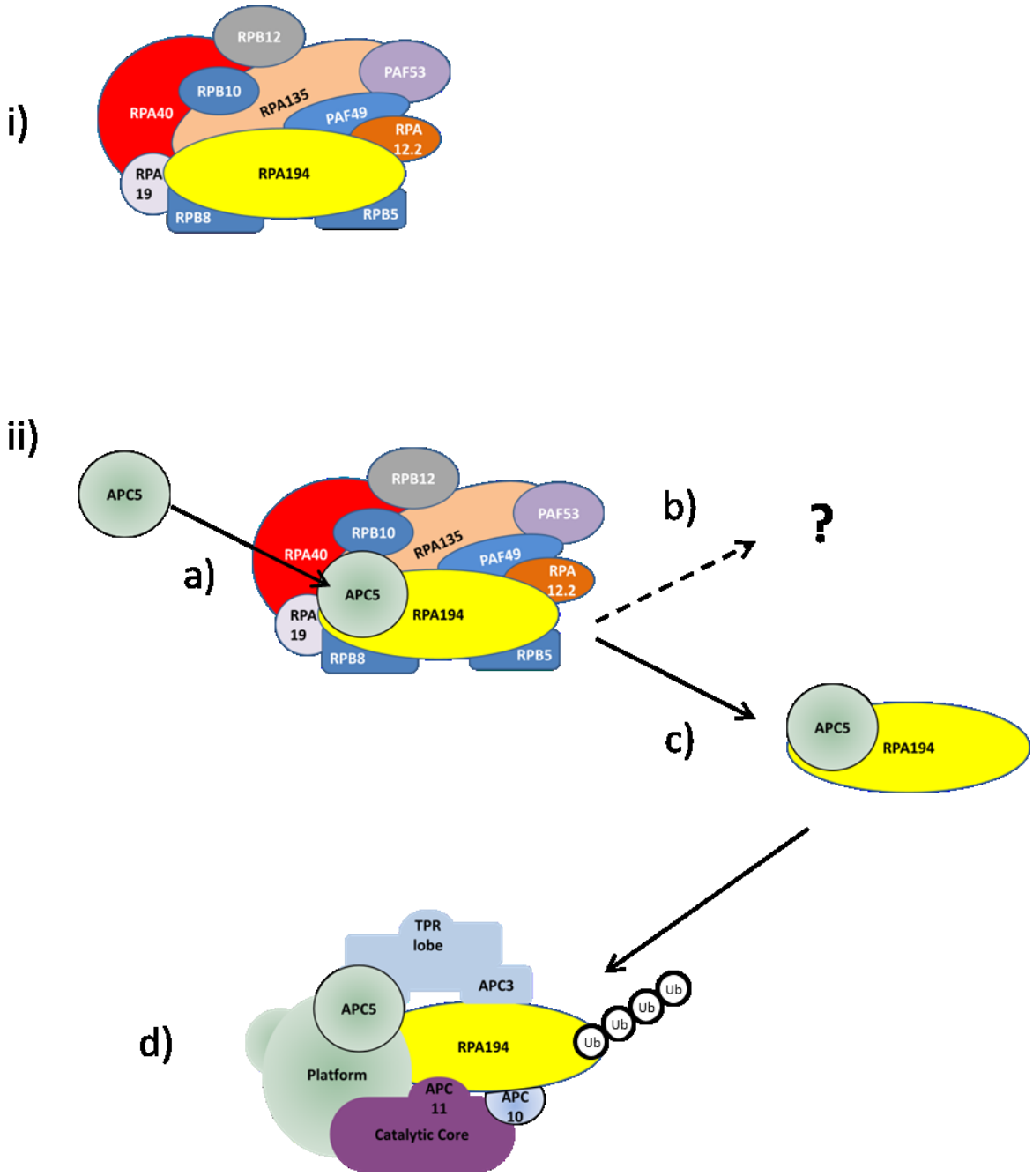

Figure 1.21 – Proposed model for the role of APC5 and the APC/C in the regulation of Pol I activity

i) Diagram of side view of RNA Polymerase I, adapted from X-ray crystallography images by (Engel, Sainsbury et al. 2013). Not shown (behind RPA194) are PAF43 and RPB6.

ii) Proposed mechanism for the targeting of RPA194 for APC/C-mediated ubiquitylation by APC5

a) APC5 associates with Pol I complex
b) Additional functions for APC5 in regulating Pol I activity?
c) APC5 recruits RPA194
d) APC5-RPA194 then associates with the APC/C holoenzyme, whereupon RPA194 is ubiquitylated and targeted for degradation by the 26S proteasome

6. CHAPTER 2: MASS SPECTROMETRY AS A TOOL TO INVESTIGATE THE ANAPHASE PROMOTING COMPLEX/CYCLOSOME

Mass spectrometry is a powerful tool that can be used to investigate protein function *in vivo*. When used as tandem mass spectrometry (MS/MS) in order to fragment tryptic peptides, it can be utilised to identify binding proteins, quantify the amount of a protein within each sample or even to identify PTMs, depending upon the controls and sample preparation techniques adopted.

In Chapter 1, LC-MS/MS was used to identify 3 subunits of RNA Polymerase I as novel binding proteins of the APC/C subunit, APC5 (Figures 1.1-1.3). The APC/C was also shown to exist as a holoenzyme within the nucleolus (Figures 1.4-1.7). As no nucleolar functions for the APC/C have been described previously, studies were commenced into the role of the APC/C within the nucleolus with the aim to identify novel substrates and binding proteins.

Rather than the more traditional mutational studies upon individual proteins, many new screening techniques have been adopted in an attempt to identify a wider range of putative novel substrates for the APC/C, including searching for APC/C degron motifs (Davey, Haslam et al. 2011, Liu, Yuan et al. 2012, Dinkel, Van Roey et al. 2014), *in vitro* expression cloning (Ayad, Rankin et al. 2005) and protein microarrays (Merbl and Kirschner 2009). Mass spectrometry has already been used to identify the di-Gly epitope left upon ubiquitylated peptides following tryptic digestion (Merbl and Kirschner 2009), and also to look at protein abundance throughout mitosis compared to those of known substrates (Singh, Winter et al. 2014).

Cdc20 and Cdh1 are the co-activators which form part of the substrate recognition particle together with APC10 (Pines 2011, Primorac and Musacchio 2013). APC5 has also been suggested to play a role

in the recognition of certain substrates (Budhavarapu, White et al. 2012), whilst APC3 has been shown to interact with proteins independently of co-activators (Pines 2011, Primorac and Musacchio 2013).

In order to identify novel interactors which might potentially regulate the APC/C and discover putative APC/C substrates, a mass spectrometric approach was adopted. The APC/C was immunoprecipitated from whole cell extracts and nucleolar fractions using antibodies raised against a number of APC/C subunits. The nucleolar abundance of proteins was also calculated following inhibition of the APC/C. Identified proteins were then searched for canonical APC/C degrons, namely D-boxes, KEN-boxes and TEK motifs. A large number of APC/C-interacting-proteins were identified as co-immunoprecipitating with the APC/C and whose nucleolar abundance increased following knockdown of APC3 and/or APC5 expression. Many of these contained typical degrons, providing an extensive list of putative APC/C substrates, as well as some known substrates. These newly identified proteins represent a wide range of cellular functions, including ribosomal biogenesis, cell cycle, ubiquitin-proteasome pathway, DNA repair, transcriptional regulation, mRNA processing, differentiation, apoptosis and metabolism.

6.1. Nucleolar binding proteins of the APC/C

In Chapter 1, evidence was presented suggesting that there is a population of the APC/C that resides within the nucleolus (Figure 1.4-1.7) and that ablation of APC/C function enhances Pol I activity (Figures 1.11-1.12). Whilst we have postulated that RPA194 could be a novel substrate, it is important to consider that there might be substrates for the APC/C in other nucleolar roles. Returning once more to mass spectrometry, IPs were performed from asynchronous HeLa cell nucleolar lysates to determine a nucleolar interactome for APC/C subunits (Figure 2.1; Appendix Figure S1.2). IPs were run in duplicate, with proteins found within the IgG control removed from the list, whilst those found in both replicates are shown in Figure 2.1. Whilst it is not the general consensus to accept proteins with a single peptide, these were included in these lists if found in both repeats.

Whilst the efficacy of APC/C IPs from nucleolar lysates was lower than that from whole cell extracts, it was clear to see that an IP from either APC3, APC5 or APC7 was able to pull down multiple APC/C subunits, suggesting that the APC/C is precipitating as a complex (Figure 2.1). Together with the data from Chapter 1, in which APC/C subunits reciprocally co-IP each other from nucleolar fractions (Figure 1.5), APC/C subunits co-elute using FPLC from nucleolar fractions (Figure 1.6) and co-localise in the nucleolus by IF (Figure 1.7), this provides further evidence that the APC/C exists as a holoenzyme within the nucleolus, despite previous evidence suggesting that the only subunit present is APC7 (Ahmad, Boisvert et al. 2009). Cdc20 and Cdh1 nucleolar IPs were also performed, however these proved to be inefficient in these conditions (data not shown).

Upon screening these co-immunoprecipitating proteins for D- and KEN-boxes, it was surprising that almost all the proteins contained one or more of these motifs (Figure 2.1; Appendix Figure S1.2). Although D-boxes are statistically more likely to appear at random, there are several more stringent D-boxes present within these proteins, *i.e.* those that contain a downstream amino acid sequence

more in comparison with those from known APC/C substrates, such as RxxLxxI/VxN, RxxLxxxxN or RxxLxxL/I/V/M, plus an extended KEN-box: KENxxxN/D (Glotzer, Murray et al. 1991, Pfleger and Kirschner 2000, Peters 2006, Barford 2011, Dinkel, Van Roey et al. 2014). Some of these proteins also contained a TEK-box, which has been proposed to contain the target lysine for ubiquitylation in some APC/C substrates (Jin, Williamson et al. 2008).

It is interesting to consider the processes in which the co-immunoprecipitating proteins have been implicated, as many of the proteins have been shown to be important in 60S and 40S ribosomal assembly, both in terms of rRNA processing and ribosomal maturation. These lists included sno-RNP components, as well as DNA repair proteins, RNA helicases and ubiquitin-proteasomal proteins. Intriguingly, all three APC/C IPs co-IP'd a number of histones, which are important in epigenetic regulation of DNA, and indeed plays a role in rDNA silencing (Figure 2.1; Appendix Figure S1.2).

ISG20L2 is of particular interest, as it contains an extended D-box sequence and was found within both APC3 (Figure 2.1A) and APC7 IPs (Figure 2.1C) as well as the RPA194 IP (Appendix Figure S1.2D), and has been shown to be important in ribosomal biogenesis though 5.8S rRNA maturation (Couté, Kindbeiter et al. 2008). Another protein important in the processing of 5.8S rRNA, SPS2L, was also shown to interact with APC7 within the nucleolus (Figure 2.1C)(Zhu, Kim et al. 2008). KRR1 was also found within the APC7 IP (Figure 2.1C), which is required for the assembly of the 40S ribosome through its activity as part of the Ribosomal Small Subunit Processome and production of mature 18S rRNA (Sasaki, Toh-E et al. 2000, Bernstein, Gallagher et al. 2004). Furthermore, the APC7 IP also contained CN021/NOP9, whilst the APC5 IP contained NOL11, which are also important in 18S rRNA production (Thomson, Rappsilber et al. 2007, Freed, Prieto et al. 2012). NOP9 contains D-boxes, whilst NOL11 contains both a D-box and a TEK motif, and therefore is a strong candidate for a novel APC/C substrate (Figure 2.1B and C).

Proteins important in ribosomal biogenesis which contain D-boxes have also been identified within the APC5 IP (Figure 2.1B), including BOP1, WDR74/NSA1, NIP7, RL5 and NOG1, which are important in rRNA processing and 60S ribosomal assembly, as well as NOG2 and RRP12, which promote the nuclear export of mature 60S ribosomes (Gautier, Bergès et al. 1997, Wu, Brockenbrough et al. 1998, Strezoska, Pestov et al. 2000, Kallstrom, Hedges et al. 2003, Saveanu, Namane et al. 2003, Oeffinger, Dlakic et al. 2004, Kressler, Roser et al. 2008, Donati, Peddigari et al. 2013). RRP12 is of interest, as it contains a highly stringent D-box as well as a TEK motif, whilst WDR74 also contains a KEN-box (Figure 2.1B). The APC5 IP also contained Cirhin, HEAT1, WDR36 and RRMJ3 which are involved in the processing of pre-rRNA intermediates into mature 18S rRNA, an important step in 40S ribosomal assembly, and BMS1 which in yeast has a role in 40S ribosomal activation (Wegierski, Billy et al. 2001, Azuma, Toyama et al. 2006, Freed and Baserga 2010, Gallenberger, Meinel et al. 2011, Morello, Coltri et al. 2011). Cirhin, WD36 and BMS1 all contain RxxL motifs, with RRMJ3 containing an extended D-box, whilst HEAT1 also contains a KEN-box (Figure 2.1B).

Furthermore the nucleolar IPs contained components of the Small Subunit Processome and U3 sno-RNPs. NOP58, IMP4, UTP6, UTP11 and UTP18, and the UTP-B proteins PWP2 and TBL3 were all identified within the APC5 IP (Figure 2.1B), whilst RRP7A and RRP7B were pulled-down by APC5 and APC7, respectively (Figure 2.1B and C). These sno-RNPs are involved in many of the rRNA processing steps (Figure 2.1B) (Dragon, Gallagher et al. 2002, Tafforeau, Zorbas et al. 2013). NOP58 and RRP7A are of particular interest, since they also contains TEK motifs, whilst TBL3 and IMP4 contain extended D-boxes (Figure 2.1B). One function of sno-RNPs is to methylate pre-rRNA transcripts as part of their maturation. Whilst this is predominantly done by Fibrillarin/Nop1, NOP2 has been suggested to act as a methyltransferase within pre-rRNA processing in yeast, and was identified as an APC5-interactor within the nucleolus (Figure 2.1B) (Sharma, Yang et al. 2013).

Other ribosomal biogenesis proteins identified within the APC5 IP include NOL6/NRAP, the rRNA processing proteins Pescadillo/Nop7, RRP5 and RBM28/Nop4, the demethylase NO66, as well as WDR46, which retains DDX21 and nucleolin within the GC to promote 18S rRNA processing (Venema and Tollervey 1996, Adams, Jakovljevic et al. 2002, Lerch-Gaggl, Haque et al. 2002, Oeffinger, Leung et al. 2002, Utama, Kennedy et al. 2002, Eilbracht, Reichenzeller et al. 2004, Hirai, Louvet et al. 2013, Lebaron, Segerstolpe et al. 2013). Of these, Pescadillo and RBM28 contain TEK motifs, whilst RRP5 contains both a high consensus D-box and TEK motif (Figure 2.1B).

APC5 also interacted with B23/Nucleophosmin, which contains an extended D-box (Figure 2.1B). B23 is important for a number of cellular processes, in particular functioning within the nucleolus, controlling transcription elongation by Pol I and pre-rRNA processing within the GC, as well as acting as part of a nucleolar stress response to ensure repression of ribosomal assembly and p53 activation (Colombo, Palacios-Callender et al. 2011, Goodfellow and Zomerdijk 2012, Grummt 2013). Should this be a novel substrate for the APC/C, it would hold significant implications for the role of the APC/C within the nucleolus.

The APC7 IP also contained two other proteins important for nucleolar function: UBP36 and CHD1 (Figure 2.1C). UBP36/USP36 is a DUB, which in yeast promotes the deubiquitylation of RPA194, thus promoting its stability (Richardson, Reed et al. 2012). Should it be a novel substrate for the APC/C, it could highlight an extra level of regulation for RPA194 ubiquitylation mediated by the APC/C.

The identification of CHD1 within the APC7 IP also provided an intriguing possibility (Figure 2.1C). CHD1 is a chromatin remodelling factor and is important in the termination of transcription for Pol I (Jones, Kawauchi et al. 2007). CHD1 also contains both a KEN box and multiple D-boxes which have been scored relatively highly by GPS-ARM software, and thus could potentially be an APC/C substrate. Another protein with epigenetic implications is the CBP/p300-inhibitor NOC2L, which was

identified within the APC5 and also contains a highly stringent D-box (Figure 2.1B). These could therefore provide a mechanism for another role for the APC/C in the regulation of Pol I transcription.

There were also a number of potential DEAD- and DEAH-domain-containing RNA helicases which contain a number of D- and KEN-boxes, particularly within the APC5 IP (Figure 2.1A-C). These are important during pre-rRNA processing, and therefore potential APC/C modulation of their stability could alter rRNA maturation and, consequently, ribosomal assembly (Lüking, Stahl et al. 1998).

The identification of SMC3, a subunit of Cohesin, also provided some interesting possibilities (Figure 2.1C). Traditionally, Cohesin is released from DNA following APC/C-mediated degradation of Securin, thereby releasing Separase to cleave Cohesin (Nasmyth 2011). However, SMC3 itself contains several extended D-boxes and was identified as an APC7-interactor, and therefore its stability and Cohesin disassembly may be regulated both directly and indirectly by the APC/C (Figure 2.1C).

Members of different DNA repair pathway have also been identified within this screen. The NHEJ protein Ku86 and SSB-ligating protein XRCC1 were identified within both APC3 and APC7 IPs and NONO was found the APC5 IP (Figure 2.1). Whilst DNA repair proteins have been implicated as residing within the nucleolus, their description as potential APC/C substrates does pose an interesting question regarding the regulation of the DNA repair pathway, since they contain D-boxes.

APC5 IPs appeared to co-IP more proteins than those by APC3 or APC7, although the Pol I subunits identified within whole cell extracts were not found within the nucleolar IPs, despite prior evidence suggesting this is the area in which they interact (Figures 1.5 and 1.7). This could be due to a difference in mass spectrometer upon which the samples were analysed. Initial identification of RPA194, RPA135 and RPA40 within APC5 IPs used an amaZon ion-trap mass spectrometer, whilst the experiments described within Chapter 2 utilised an Impact time-of-flight (TOF). The absence of Pol I proteins within the nucleolar IPs could therefore be due to the lower resolution of an ESI-TRAP, which was set to a +/- 0.05Da MS/MS threshold, as opposed to the ESI-TOF, onto which a more

stringent +/- 0.02 Da threshold was placed. However, many other nucleolar proteins were identified within APC5 IPs, implying that APC5 poses an integral role within normal nucleolar functioning, whether that be as part of a functional APC/C or acting independently.

Taken together, the data presented in Figure 2.1 suggests that the APC/C interacts with a number of nucleolar pathways, including those important in ribosomal biogenesis, pre-rRNA synthesis and processing, DNA damage reponse and mitotic progression. Further investigations into these interactions will provide evidence for supplementary roles for the APC/C within the nucleolus beyond the hypothesised ubiquitylation of RPA194.

A) – APC3 IP

APC/C subunits

Protein	Full Name	MW [kDa]	# Peptides
APC1	Anaphase-promoting complex subunit 1	216.4	8
APC3	Cell division cycle protein 27 homolog	91.8	11
APC4	Anaphase-promoting complex subunit 4	92.1	6
APC5	Anaphase-promoting complex subunit 5	85	3
APC6	Cell division cycle protein 16 homolog	71.6	3
APC8	Cell division cycle protein 23 homolog	68.8	4
APC10	Anaphase-promoting complex subunit 10	21.2	1

Nucleolar Proteins

Protein	Full Name	MW [kDa]	# Peptides	#D-box	#KEN	TEK	GPS-ARM
DDX5	Probable ATP-dependent RNA helicase DDX5	69.1	2	1	1	-	
GPTC4	G patch domain-containing protein 4	50.4	3	9.4	1	1	-
H2A1C	Histone H2A type 1-C	14.1	7	1	-	-	
H2AJ	Histone H2A.J	14	8	1	-	-	
H2AZ	Histone H2A.Z	13.5	4	1	-	-	
H2B1H	Histone H2B type 1-H	13.9	12	1	-	-	
H31	Histone H3.1	15.4	11	1	-	-	
I20L2	Interferon-stimulated 20 kDa exonuclease-like 2	39.1	4	2	-	-	***
KU86	ATP-dependent DNA helicase 2 subunit 2	82.7	3	1	-	-	***
PP1B	Serine/threonine-protein phosphatase PP1-beta catalytic subunit	37.2	5	1	-	-	
RL26L	60S ribosomal protein L26-like 1	17.2	10	1	-	-	
XRCC1	DNA repair protein XRCC1	69.5	1	5	-	-	

B) – APC5 IP

APC/C subunits

Protein	Full Name	MW [kDa]	# Peptides
APC1	Anaphase-promoting complex subunit 1	216.4	5
APC3	Cell division cycle protein 27 homolog	91.8	3
APC4	Anaphase-promoting complex subunit 4	92.1	3
APC5	Anaphase-promoting complex subunit 5	85	5
APC6	Cell division cycle protein 16 homolog	71.6	3
APC7	Anaphase-promoting complex subunit 7	63.1	1
APC8	Cell division cycle protein 23 homolog	68.8	5

Nucleolar Proteins

Protein	Full Name	MW [kDa]	# Peptides	#D-box	#KEN	TEK	GPS-ARM
BMS1	Ribosome biogenesis protein BMS1 homolog	145.7	3	9	-	-	*
BOP1	Ribosome biogenesis protein BOP1	83.6	6	4	-	-	*
CIR1A	Cirhin	76.8	3	3	-	-	
DDX17	Probable ATP-dependent RNA helicase DDX17	72.3	2	2	1	-	
DDX18	ATP-dependent RNA helicase DDX18	75.4	10	4	-	-	
DDX21	Nucleolar RNA helicase 2	87.3	14	1	-	-	***
DDX27	Probable ATP-dependent RNA helicase DDX27	89.8	8	3	-	+	***
DDX54	ATP-dependent RNA helicase DDX54	98.5	1	6	-	-	***
DDX56	Probable ATP-dependent RNA helicase DDX56	61.6	2	7	-	-	***
DHX15	Putative pre-mRNA-splicing factor ATP-dependent RNA helicase DHX15	90.9	2	9	-	+	**
DHX9	ATP-dependent RNA helicase A	140.9	8	5	-	-	**
H2B3B	Histone H2B type 3-B	13.9	4	1	-	-	
H3L	Histone H3-like	15.2	1	1	-	-	*
HDAC1	Histone deacetylase 1	55.1	1	-	-	-	
HEAT1	HEAT repeat-containing protein 1	242.2	1	9	1	-	***
IMP4[%]	U3 small nucleolar ribonucleoprotein protein IMP4	33.7	1	5	-	-	**
NIP7	60S ribosome subunit biogenesis protein NIP7 homolog	20.4	1	-	-	-	
NO66	Lysine-specific demethylase NO66	71	1	4	-	-	*
NOC2L	Nucleolar complex protein 2 homolog	84.9	1	3	-	-	***
NOG1	Nucleolar GTP-binding protein 1	73.9	10	6	-	-	*
NOG2	Nucleolar GTP-binding protein 2	83.6	5	3	-	-	

NOL11	Nucleolar protein 11	81.1	1	4	-	+	*
NOL6	Nucleolar protein 6	127.5	6	12	-	-	*
NONO	Non-POU domain-containing octamer-binding protein	54.2	7	5	-	-	*
NOP2	Putative ribosomal RNA methyltransferase NOP2	89.2	5	2	-	-	
NOP58	Nucleolar protein 58	59.5	11	3	-	+	
NPM	Nucleophosmin	32.6	1	1	-	-	***
NUMA1	Nuclear mitotic apparatus protein 1	238.1	2	19	1	+	***/ +++
PESC	Pescadillo homolog	68	2	5	-	+	*
PP1B	Serine/threonine-protein phosphatase PP1-beta catalytic subunit	37.2	2	1	-	-	
PRKDC	DNA-dependent protein kinase catalytic subunit	468.8	34	25	-	-	***
PWP2	Periodic tryptophan protein 2 homolog	102.4	2	6	-	-	
RBM28	RNA-binding protein 28	85.7	4	8	-	+	*
RL1D1	Ribosomal L1 domain-containing protein 1	54.9	12	7	-	+	**
RL3	60S ribosomal protein L3	46.1	1	3	-	-	***
RL5	60S ribosomal protein L5	34.3	4	2	-	-	
RLA0[&%]	60S acidic ribosomal protein P0	34.3	1	3	-	-	
RRMJ3	Putative rRNA methyltransferase 3	96.5	5	9	-	-	***
RRP12	RRP12-like protein	143.6	6	13	-	+	***
RRP5	Protein RRP5 homolog	208.6	1	9	-	+	***
RRP7A	Ribosomal RNA-processing protein 7 homolog A	32.3	3	3	-	+	
RRS1	Ribosome biogenesis regulatory protein homolog	41.2	2	-	-	-	
RS28	40S ribosomal protein S28	7.8	1	-	-	-	
TBL3	Transducin beta-like protein 3	89	3	6	-	-	***
UTP11	Probable U3 small nucleolar RNA-associated protein 11	30.4	1	3	-	-	*
UTP18	U3 small nucleolar RNA-associated protein 18 homolog	62	3	5	-	-	
UTP6	U3 small nucleolar RNA-associated protein 6 homolog	70.1	2	5	-	-	
WDR36	WD repeat-containing protein 36	105.3	2	2	-	-	*
WDR46	WD repeat-containing protein 46	68	2	4	-	-	**
WDR74	WD repeat-containing protein 74	42.4	2	1	1	-	

C) – APC7 IP

APC/C subunits

Protein	Full Name	MW [kDa]	# Peptides
APC1	Anaphase-promoting complex subunit 1	216.4	7
APC6	Cell division cycle protein 16 homolog	71.6	4
APC7	Anaphase-promoting complex subunit 7	63.1	20

Nucleolar Proteins

Protein	Full Name	MW [kDa]	# Peptides	#D-box	#KEN	TEK	GPS-ARM
CHD1[&]	Chromodomain-helicase-DNA-binding protein 1	196.6	1	6	1	-	**/++
CN021	Pumilio domain-containing protein C14orf21	69.4	1	5	-	-	***
DDX5	Probable ATP-dependent RNA helicase DDX5	69.1	3	1	1	-	
DDX51	ATP-dependent RNA helicase DDX51	72.4	2	6	-	-	**
DHX37	Probable ATP-dependent RNA helicase DHX37	129.5	4	5	-	-	***
H2A1C	Histone H2A type 1-C	14.1	7	1	-	-	
H2A1J	Histone H2A type 1-J	13.9	8	1	-	-	
H2B1O	Histone H2B type 1-O	13.9	14	1	-	-	
H2B2F	Histone H2B type 2-F	13.9	15	1	-	-	
I20L2	Interferon-stimulated 20 kDa exonuclease-like 2	39.1	5	2	-	-	***
KRR1	KRR1 small subunit processome component homolog	43.6	2	2	-	-	**
KU86	ATP-dependent DNA helicase 2 subunit 2	82.7	1	1	-	-	***
RRP7B	Putative ribosomal RNA-processing protein 7 homolog B	12.6	3	2	-	-	
RS27A[%]	40S ribosomal protein S27a	9.4	1	-	-	-	
SMC3	Structural maintenance of chromosomes protein 3	141.5	3	17	-	-	***
SPS2L	SPATS2-like protein	61.7	1	-	-	-	
UBP36	Ubiquitin carboxyl-terminal hydrolase 36	122.6	2	3	-	-	
XRCC1	DNA repair protein XRCC1	69.5	1	5	-	-	

Figure 2.1 – Selected nucleolar APC/C-interacting proteins identified by mass spectrometry

Nucleoli were obtained from HeLa cells, lysed and IPs using APC3 (**A**), APC5 (**B**), APC7 (**C**) and RPA194 (Appendix Figure S1.2D) antisera were performed. The IPs were washed, separated by SDS-PAGE and subjected to in-gel tryptic digestion. Peptides were eluted and analysed by LC-MS/MS using a maXis Impact (Bruker). Ionisation spectra were compared to a Mascot database (Matrix Science) and

searched using ProteinScape (Bruker). Interacting protein lists from two independent experiments were compiled and compared to a nucleolar protein database, NoPDb3, published by Prof. Lamond (Ahmad, Boisvert et al. 2009) and searched for function and protein sequence using Uniprot (UniProt-Consortium 2014). The protein sequence was then searched manually for TEK motifs and for extended D-boxes and KEN-boxes using GPS-ARM 1.0 (Liu, Yuan et al. 2012).

MW represents Molecular Weight. D-boxes and KEN boxes were analysed using GPS-ARM, with the highest threshold of motif denoted by * for D-boxes and + for KEN boxes. */+ represents a low threshold peptide, **/++ medium and ***/+++ high.

Proteins in a red font were identified in other nucleolar APC/C IPs.

[&] denotes proteins which were elevated in the nucleolus following siRNA-mediated knockdown of APC3 (Section 6.2 and Figure 2.2).

[%] denotes proteins which were elevated in the nucleolus following siRNA-mediated knockdown of APC5 (Section 6.2 and Figure 2.2).

6.2. Quantitation of nucleolar proteins following siRNA-mediated knockdown of APC3 or APC5

Another method by which it is possible to ascertain putative nucleolar APC/C substrates is to quantify the relative nucleolar abundance of proteins following ablation of expression of APC/C subunits relative to non-silencing controls. Previously, Western blots have been used to identify the stability of proteins following negation of APC/C activity, however mass spectrometry provides a more open-ended approach, since it does not require knowledge of the protein in question prior to experimental analysis as per Western blots, for which a specific primary antibody is required. Instead, lysates from knockdown cells or non-silencing controls can be labelled with "heavy" or "light" formaldehyde following tryptic digestion such that all peptides have an N-terminal dimethyl adduct containing ^{2}H or ^{1}H, respectively. This produces a mass difference between identical peptide sequences from the two siRNA treatments which can be detected using a mass spectrometer of high enough resolution. These can then be compared to produce a heavy:light peptide ratio, signifying relative abundance. Whilst this technique may produce issues, such as analytical errors, incomplete dimethylation or differing flow rates during the HPLC separation, it is considerably cheaper than other similar methods such as metabolic labelling by SILAC. Quantitation also requires both the heavy and the light forms of the peptide to be found in order to provide a ratio, and therefore not every nucleolar protein identified will produce a quantitative ratio, particularly those with low nucleolar abundance.

To investigate the effect of the APC/C activity upon the nucleolar abundance of proteins, HeLa cells were subjected to siRNA-mediated knockdown of either APC3 or APC5, or a non-silencing control (LacZ). These siRNA targets were chosen due to the fact that substrate elevation is most noticeable following the ablation of either APC3 or APC5 than other APC/C subunits such as APC7 or Cdc20 (Figure 1.9). Nucleoli were then isolated from these cells and denatured in urea prior to reduction and alkylation, followed by tryptic digest. Peptides from APC3 or APC5 knockdown cells were then

labelled with [^{2}H]-dimethyl adducts, whilst non-silencing controls were [^{1}H]-dimethyl-labelled. Equal amounts of non-silencing light-labelled peptides and either APC3i or APC5i heavy-labelled peptides were mixed, followed by fragmentation by a maXis Impact mass spectrometer and quantitative analysis using ProteinScape and WARP-LC (Bruker).

Upon comparison of APC3i or APC5i samples to non-silencing controls, several hundred proteins have increased by over 25% in abundance (Figure 2.2; Appendix Figure S1.3). This arbitrary amount was chosen in order to minimise false-positive errors. Many of these proteins also contain the consensus APC/C recognition sequences RxxL and KEN, of which several also contain the TEK motif which in some substrates provides the lysine required for APC/C-mediated ubiquitylation (Figure 2.2; Appendix Figure S1.3)(Peters 2006, Jin, Williamson et al. 2008, Pines 2011).

Proteins whose abundance increased following either APC3 or APC5 knockdown function in a number of biological processes, including DNA repair, cell cycle, rRNA and mRNA processing, nuclear membrane function, transcriptional control, apoptosis, translation, and protein folding and transport (Figure 2.2; Appendix Figure S1.3). These protein lists were scrutinised for proteins which are important in nucleolar function, Pol I transcription and rRNA processing by searching the Uniprot database in order to suggest a mechanistic outline for the earlier-described increase in Pol I transcription following APC/C inhibition (Figures 1.11 and 1.12) (UniProt-Consortium 2014).

Several proteins have been identified which are directly implicated in the regulation of Pol I transcription, including CHD1 and PTRF. These proteins are important for Pol I transcription termination and reinitiation, and contain both D- and KEN-boxes (Jansa, Burek et al. 2001, Jones, Kawauchi et al. 2007). An increased rate of transcription termination permits earlier reinitiation of transcription, thereby increasing the total rate of pre-rRNA production. If these proteins are true substrates for the APC/C, their increased stability upon downregulation of the APC/C could theoretically result in increased *de novo* pre-rRNA synthesis; APC/C knockdown was shown to

increase *de novo* pre-rRNA synthesis (Figure 1.12). CHD1 was also identified within nucleolar APC7 IPs (Figure 2.1), and so it would be highly interesting to investigate its relationship to the APC/C further.

Another method by which Pol I transcription is regulated is by epigenetic modification of rDNA genomic regions. Indeed, several different nucleolar chromatin remodelling complexes have been described, such as eNoSC and NoRC, which are able to silence rDNA repeats in response to cellular stimuli (Murayama, Ohmori et al. 2008, Guetg and Santoro 2012). Several different proteins associated with chromatin remodelling were found to have increased within the nucleolus following APC/C knockdown, some of which have previously been identified as having nucleolar localisation, including Acl6a/BAF53, CHD1, SMRD2/BAF60B and a component of eNoSC, SUV91/SUV39H1 (Wang, Côté et al. 1996, Jones, Kawauchi et al. 2007, Murayama, Ohmori et al. 2008). It is therefore feasible that knockdown of the APC/C might also produce a different epigenetic pattern upon histones, thus altering the ability of Pol I to initiate transcription.

One important function of the nucleolus is the assembly of ribosomes in order to control translation and protein synthesis. As well as the transcription of rDNA genes, this also requires the processing of the pre-rRNA into mature rRNAs and their assembly into ribosomes. Several proteins important in rRNA processing were identified as potential APC/C subunits in this screen, including IMP4 and WDR55 (Figure 2.2B and C) (Granneman, Gallagher et al. 2003, Iwanami, Higuchi et al. 2008). It is also interesting to note the increase in proteins of both the 60S and 40S ribosomes, implying that either ribosomal production itself might have increased, or nuclear export has decreased (Figure 2.2 A-C).

Given the role of the APC/C in coordinating timely anaphase progression and mitotic exit, it is unsurprising to see the abundance increase for several proteins which are involved in the cell cycle and mitosis. Nipped-B-like-protein, NIPBL, contains high-threshold KEN- and D-boxes and a TEK motif, and increased in nucleolar abundance following knockdown of both APC3 and APC5 (Figure 2.2A).

NIPBL itself is important for sister chromatid cohesion via its activity as a cohesin accessory factor, and so its targeting by the APC/C could prevent further Cohesin complex reformation during late mitosis (Bermudez, Farina et al. 2012).

Another potential substrate important in mitotic cohesion is SMC5, which also contains highly-scored D- and KEN-boxes and a TEK box and was elevated following APC3 knockdown (Figure 2.2B; Appendix Figure S1.3A). SMC5 forms a complex with SMC6 and aids chromosomal cohesion during interphase (Tapia-Alveal, Lin et al. 2014). Although SMC5 has been shown to be ubiquitylated *in vivo*, it is not known whether these are the K11 chains formed by the mammalian APC/C (Taylor, Copsey et al. 2008). SMC5 could therefore be a substrate for the APC/C given its degron motifs and mitotic functions.

The increase in abundance of WAPL, also containing D-, KEN-, and TEK-boxes, following APC5 knockdown provided evidence for a further role for the APC/C in the mitotic regulation of cohesion (Figure 2.2C; Appendix Figure S1.3B). WAPL allows decatenation and resolution of sister chromatids by the removal of Cohesin from the chromosomal arms, leaving a subpopulation of Cohesin upon the centromeres to provide sufficient cohesion to prevent early anaphase (Gandhi, Gillespie et al. 2006, Kueng, Hegemann et al. 2006). As such, it is feasible that the APC/C could target WAPL for degradation upon its reactivation following SAC satisfaction.

Other mitotic proteins which became stabilised within the nucleolus following APC/C knockdown included the previously-described substrates TOP2A and the kinesins KIF2C and KIFC1, which are important in chromosomal alignment and sister chromatid segregation as well as spindle assembly, and Plk1, an important kinase for G2/M transition (Lindon and Pines 2004, Eguren, Álvarez-Fernández et al. 2014, Singh, Winter et al. 2014). The appearance of these proteins signified that knockdown of the APC/C did indeed increase nucleolar localisation of substrates, providing support for this experimental approach.

Cytokinesis is another process in which the role of the APC/C has been extensively examined. Various proteins involved in this process have increased abundance in the nucleolar lysates following APC3 or APC5 knockdown, including the previously identified substrates Aurora Kinase B, Anillin and ECT2 (Stewart and Fang 2005, Zhao and Fang 2005, Liot, Seguin et al. 2011). Also found were two further kinesins, KIF20A and KIF23, as well as Rac GTPase activating protein 1 (RGAP1) and several cytoskeletal components such as Myosins and Nestin. It is possible that these represent novel targets for the APC/C in order to regulate mitotic exit and subsequent G1 re-entry.

In our screen, the nucleolar localisation of several important proteins from DNA repair pathways including NHEJ, HR, Base Excision Repair (BER) and Mismatched Repair (MMR) appeared to increase upon APC/C inhibition. These included 53bp1, Aprataxin, WRN, BLM helicase, DDB1, MLH1, FANCI, SMC5, TOP2A and TOP2B, MDC1, TRIPC/TRIP12 and MSH6. The APC/C has been implicated as holding a role within the response to both UV and IR, whereby its reactivation during late G1, S or G2 phases promotes degradation of pro-mitotic substrates, such as Cyclins A and B1 and Plk1, thereby promoting cell cycle arrest (Coster, Hayouka et al. 2007, Bassermann, Frescas et al. 2008, Townsend, Mason et al. 2009, Zhang, Nirantar et al. 2009). There is also a theory that it may be involved with the removal of repair proteins following the successful repair of DNA (Turnell AS and Teodoro JS, personal communication). As such, it is theoretically possible that this subgroup of nucleolar proteins might be substrates for the APC/C given the presence of motifs typical of designated targets, particularly WRN, Aprataxin, SMC5, 53bp1 and FANCI. Of these proteins, TOP2A has already been suggested as being a substrate, and MDC1 has been shown to interact with APC3 *in vivo* and potentiate its activity, although it is not a target for ubiquitylation (Coster, Hayouka et al. 2007, Townsend, Mason et al. 2009, Eguren, Álvarez-Fernández et al. 2014).

Also found within these lists were several constituent proteins of the Nuclear Pore Complex (NPC), including Nup85, Nup98, Nup107, Nup133, Nup160, Nup188, Nup205, Nup214, ELYS, Nesprin-2,

gp210, Nucleoprotein TPR and structural proteins involved in Nuclear Envelope Breakdown (NEBD) such as Lamins A/C and B1 (Güttinger, Laurell et al. 2009). Nucleoprotein TPR is of particular interest, as it also is implicated within the SAC, as well as containing extended consensus sequences for both KEN- and D-boxes as well as a TEK box, therefore is a likely candidate for a novel substrate (Schweizer, Ferrás et al. 2013). Nup205, Nesprin-2 and ELYS all contain both a TEK box and extended D-boxes, whilst Nup205 and Nesprin-2 also have high-threshold KEN-boxes.

On a cautionary note, the data demonstrated here only represents the nucleolar subpopulation of the proteins described. The identification of putative substrates is pure conjecture, as without the representative data for cytoplasmic and nucleoplasmic compartments, any increase in nucleolar abundance may simply be due to relocalisation. Similarly, it cannot be determined that any increase is due to alleviation of APC/C-mediated instability, as there are many other cellular E3 ligases responsible for proteasomal degradation, although the likelihood of these was diminished by the evaluation of APC/C degron motifs.

Although a great number of potential nucleolar APC/C substrates have been described within Figures 2.1 and 2.2, there is very little overlap between the two experiments. Only the APC5-interacting IMP4 and RLA0, and the APC7-interacting CHD1 and RS27A were both identified within APC/C nucleolar IPs and shown to increase in nucleolar abundance upon APC/C inhibition (Figures 2.1 and 2.2). In fact, a great number of APC/C-interacting proteins (Figure 2.1) were not elevated within the nucleolus following ablation of APC3 or APC5 expression (Figure 2.2). In several cases, this was because the APC/C-interacting protein from Figure 2.1 was not identified within both the heavy- and light-labelled nucleolar lysates from Figure 2.2, and therefore a relative ratio between the two could not be produced. Also, certain proteins exhibited a slight decrease in nucleolar abundance following siRNA-mediated knockdown of either APC3 or APC5, which would suggest that these are not *bona fide* substrates. Furthermore, although other proteins identified within Figure 2.1 as interacting with

the APC/C within the nucleolus, their increase within APC3- and APC5-knockdown nucleolar lysates was less than the 25% used as a cutoff for this experiment (Figure 2.2).

Conversely, a large number of proteins portrayed as putative APC/C substrates within Figure 2.2 were not identified as APC/C-interacting proteins in Figure 2.1. This is perhaps unsurprising, given that the affinity of the APC/C for substrates has been hypothesised as being low, and without inhibition of the proteasome in order to prolong APC/C-substrate interactions, some substrates might not be co-precipitated with the APC/C (Ayad, Rankin et al. 2005).

A)

Protein	Full Name	MW [kDa]	NL	APC3i increase	APC5i increase	#D-box	#KEN	TEK	GPS-ARM
APTX	Aprataxin	40.7	Y	**2.09**	**2.47**	3	-	-	
BLM	Bloom syndrome protein	158.9	Y	**1.50**	**1.31**	8	-	+	*
KI20A	Kinesin-like protein KIF20A	100.2	x	**1.60**	**1.36**	7	-	-	
KIF2C	Kinesin-like protein KIF2C	81.3	Y	**1.28**	**2.04**	1	-	-	
MYH9	Myosin-9	226.4	Y	**1.48**	**1.77**	16	1	+	**/ +++
NEST	Nestin	177.3	x	**1.48**	**1.38**	11	5	+	***/ +++
NIPBL	Nipped-B-like protein	315.9	Y	**1.79**	**1.29**	8	1	+	***/ +++
NU107	Nuclear pore complex protein Nup107	106.3	x	**2.23**	**1.39**	11	-	+	*
NU205	Nuclear pore complex protein Nup205	227.8	Y	**1.48**	**1.33**	17	1	+	***/ +++
NUP98	Nuclear pore complex protein Nup98-Nup96	187.7	x	**1.97**	**1.34**	9	-	-	***
RLA0[%]	60S acidic ribosomal protein P0	34.3	Y	**1.28**	**1.51**	3	-	-	
RSSA	40S ribosomal protein SA	32.8	Y	**1.45**	**1.47**	2	-	-	
TOP2A	DNA topoisomerase 2-alpha	174.3	Y	**1.66**	**1.68**	4	1	+	
TOP2B	DNA topoisomerase 2-beta	183.2	Y	**1.28**	**1.36**	4	1	-	*
TPR	Nucleoprotein TPR	267.1	Y	**1.70**	**1.83**	11	1	+	***/ +++

B)

Protein	Full Name	MW [kDa]	NL	APC3i increase	#D-box	#KEN	TEK	GPS-ARM
ACL6A	Actin-like protein 6A	47.4	Y	**1.47**	3	-	-	**
ANLN	Actin-binding protein anillin	124.1	Y	**1.50**	14	-	+	***
CHD1[&]	Chromodomain-helicase-DNA-binding protein 1	196.6	Y	**1.34**	6	1	-	**/ ++
DDB1	DNA damage-binding protein 1	126.9	Y	**1.35**	5	-	+	*
ELYS	Protein ELYS	252.3	Y	**1.25**	8	-	+	***
KIF23	Kinesin-like protein KIF23	110.0	Y	**1.35**	1	1	+	**/ +++
LMNA	Lamin-A/C	74.1	Y	**1.27**	9	-	-	***
LMNB1	Lamin-B1	66.4	Y	**1.52**	8	-	-	***
MLH1	DNA mismatch repair protein Mlh1	84.5	Y	**1.33**	2	-	-	***
NU133	Nuclear pore complex protein Nup133	128.9	x	**1.52**	10	1	-	***
PLK1	Serine/threonine-protein kinase PLK1	68.2	Y	**1.92**	7	-	-	***
RS10	40S ribosomal protein S10	18.9	Y	**2.30**	1	-	-	
RS26	40S ribosomal protein S26	13.0	Y	**1.60**	-	-	-	
RS3	40S ribosomal protein S3	26.7	Y	**1.94**	2	-	-	
SMC5	Structural maintenance of chromosomes protein 5	128.7	Y	**1.60**	4	1	+	***/ ++
SMRD2	SWI/SNF-related matrix-associated actin-dependent regulator of chromatin subfamily D member 2	52.3	Y	**1.27**	4	-	-	*
TP53B	Tumor suppressor p53-binding protein 1	213.4	x	**1.47**	5	3	-	+++
WDR55	WD repeat-containing protein 55	42.1	Y	**1.37**	3	-	-	**
WRN	Werner syndrome ATP-dependent helicase	162.4	Y	**1.57**	10	1	+	***/ +++

C)

Protein	Full Name	MW [kDa]	NL	APC5i increase	#D-box	#KEN	TEK	GPS-ARM
AURKB	Serine/threonine-protein kinase 12	39.3	Y	**1.51**	4	1	-	***/ +++
ECT2	Protein ECT2	100.0	x	**2.30**	5	2	-	**/ +++
FANCI	Fanconi anemia group I protein	149.2	Y	**1.71**	6	2	-	**/ +++
IMP4[%]	U3 small nucleolar ribonucleoprotein protein IMP4	33.7	Y	**1.49**	5	-	-	**
KIFC1	Kinesin-like protein KIFC1	73.7	Y	**1.49**	9	-	-	***
MDC1	Mediator of DNA damage checkpoint protein 1	226.5	Y	**1.63**	11	-	+	**
MSH6	DNA mismatch repair protein Msh6	152.7	Y	**1.26**	5	-	-	***
MYH14	Myosin-14	227.9	Y	**3.66**	33	-	+	**
MYO1C	Myosin-Ic	121.6	Y	**2.65**	12	-	-	
NU160	Nuclear pore complex protein Nup160	162.0	x	**1.29**	14	-	-	***
NU188	Nucleoporin NUP188 homolog	195.9	x	**1.56**	11	-	-	***
NU214	Nuclear pore complex protein Nup214	213.5	x	**1.61**	7	-	-	***
NUP85	Nuclear pore complex protein Nup85	75.0	x	**1.29**	5	-	-	**
PO210	Nuclear pore membrane glycoprotein 210	205.0	Y	**2.30**	8	-	-	***
PTRF	Polymerase I and transcript release factor	43.4	Y	**1.80**	6	1	-	***/ +++
RGAP1	Rac GTPase-activating protein 1	71.0	x	**3.12**	5	-	-	***
RL11	60S ribosomal protein L11	20.2	Y	**1.86**	0	1	-	
RLA2	60S acidic ribosomal protein P2	11.7	Y	**2.12**	0	0	-	
RRBP1	Ribosome-binding protein 1	152.4	Y	**1.49**	7	0	-	***
RS16	40S ribosomal protein S16	16.4	Y	**1.28**	1	0	-	
RS2	40S ribosomal protein S2	31.3	Y	**1.34**	1	0	-	
RS27A[&]	40S ribosomal protein S27a	9.4	Y	**1.34**	0	0	-	
RS30	40S ribosomal protein S30	6.6	Y	**2.52**	0	0	-	
SUV91	Histone-lysine N-methyltransferase SUV39H1	47.9	x	**1.43**	7	-	-	***
SYNE2	Nesprin-2	795.9	x	**106.00**	27	3	+	***/ +++
TRIPC	Probable E3 ubiquitin-protein ligase TRIP12	220.3	Y	**1.49**	11	-	-	**
WAPL	Wings apart-like protein homolog	132.9	Y	**3.21**	7	1	+	*/ +++

Figure 2.2 – Quantitation of selected nucleolar proteins by isotopic labelling and LC-MS/MS following APC3 or APC5 siRNA-knockdown

HeLa cells were subjected to knockdown by either non-silencing, APC3 or APC5 siRNA for 72h. Nucleolar lysates were solubilised in 9M urea/100mM TEAB and normalised by protein concentration, as calculated by Bradford assay, and centrifuged through an Amicon Ultra 30kDa filter (Millipore). The denatured proteins were then reduced by 50mM DTT for 1h at 56°C and reduced by iodoacetamide in the dark at room temperature for 30 min, and then washed 4 times with 100mM TEAB before overnight digestion at 37°C with sequence grade modified Trypsin (Promega) resuspended in 100mM TEAB. Tryptic peptides were eluted by centrifugation and dimethylated by incubation with 1/10x volume 10.73% Heavy (APC3/5i) or Light (non-sil.) formaldehyde for 1 min with constant mixing. Samples were centrifuged briefly and 1/10x volume 1.5M sodium cyanoborohydride added for 30s with constant mixing, briefly centrifuged then incubated at 600rpm for 1h. 1/10x volume of 10.73% sodium hydroxide was added, followed by 1/10x volume formic acid. Heavy- and Light-dimethyl-labelled peptides were then mixed together and purified through a C18 column, before analysis by LC-MS/MS using a maXis impact (Bruker). The Heavy/Light ratio for each peptide was produced by WarpLC and ProteinScape (Bruker), and used to calculate the Heavy/Light ratio for each protein. This was divided by the median Heavy/Light ratio to normalise input, and was averaged over two repeats, thus providing the percentage change in nucleolar abundance.

Selected proteins for which abundance increased by >25% were filtered by GPS-ARM score of D- and KEN-boxes, the presence of a TEK box, localisation and function. **A)** shows selected proteins for which an increase was seen in both APC3i and APC5i. Selected proteins for which an increase was only observed in APC3i are listed in **B)**, and an increase in APC5i are shown in **C)**. Complete lists of proteins whose nucleolar abundance increased by >25% are listed in Appendix Figure S1.3.

MW represents Molecular Weight, nucleolar proteins are denoted by a Y (yes), whilst non-nucleolar are denoted by an x in the NL (Nucleolar) column. D-boxes and KEN boxes were analysed using GPS-ARM, with the highest threshold of motif denoted by * for D-boxes and + for KEN boxes. * represents a low threshold peptide, ** medium and *** high.

Proteins also identified within nucleolar APC5 and APC7 IPs (Figure 2.1) are denoted by $^{\%}$ and $^{\&}$ respectively.

6.3. Mass spectrometric analysis of APC/C-interacting proteins

Earlier, evidence was provided that suggested a nucleolar role for the APC/C. However, the APC/C is expressed ubiquitously, with a high proportion evident within the cytoplasm as well as the nucleplasm (Figures 1.4 and 1.7). We therefore adopted a proteomic approach to identify binding proteins in whole cell extracts with an aim to discover novel putative substrates for ubiquitylation by the APC/C.

Asynchronous HeLa cells were lysed and IPs against APC3, Cdc20 and Cdh1 were performed. These particular IPs were chosen, as Cdc20 and Cdh1 are the co-activators which form part of the substrate recognition particle, and therefore any interacting proteins are likely to be APC/C substrates, activators or inhibitors (Pines 2011, Primorac and Musacchio 2013). Similarly, APC3 has been shown to be important in the recognition of substrates in the absence of co-activators, such as during the SAC (Pines 2011, Primorac and Musacchio 2013). The IPs were separated by SDS-PAGE and processed for LC-MS/MS by in-gel tryptic digestion, with the entire length of the gel being excised into 16 slices. Peptides were identified, filtered by a 1% False Discovery Rate and compared to an IgG control. Proteins unique to the IPs and identified in two independent experiments were then searched in the Uniprot database to determine protein sequence and the biological processes in which they are involved. The proteins were then analysed using GPS-ARM to determine D- and KEN-boxes in order to establish the likelihood of it being a novel substrate. Identified proteins are detailed in full in Appendix Figure S1.4, with selected proteins grouped by cellular function in Figure 2.3.

The processes which have been identified within this dataset are extensive, with particular coverage to proteins involved in the cell cycle and the ubiquitin-proteasome pathway. Also well-represented are proteins important in: the regulation of mRNA and its processing and splicing such as RNA helicases; rRNA processing and ribosomal proteins; transcriptional regulation and chromatin;

differentiation; DNA repair and oxidative stress; apoptosis; metabolism; intracellular transport, particular between the ER and Golgi and the cytoskeleton (Figure 2.3; Appendix Figure S1.4).

As a positive control, it was important to detect known interactors of APC3, Cdc20 and Cdh1 within their corresponding IPs. Fortunately, this was the case, as numerous APC/C subunits and members of the MCC, including BUB1, BUB1B/BUBR1, BUB3 and Mad2A/MD2L1, were pulled-down in each IP. The substrates PAF, KIF4A, KIF22, Fbx5/Emi, NEK2 and RIR2 were also identified within the APC3 IP, with RIR2 also discovered binding to Cdh1 (Figure 2.3B).

Further to these known interactors, many more proteins implicated in the cell cycle have been identified within these IPs. Interacting with APC3 were Cdk2, FAM96B, RHOC, ARL2 and MEK2/MP2K2 (Figure 2.3C). MEK2/MP2K2 was also identified within the Cdc20 IP, as were AKAP8, NSUN2 and S10AB (Figure 2.3C). Cdh1 also pulled-down different cell cycle proteins, namely KLHL9, Nestin and SMC4 (Figure 2.3C). Upon analysis by GPS-ARM, MEK2 has been shown to have an extended D-box, whilst Nestin contains numerous D- and KEN-boxes plus a TEK motif (Figure 2.3C). RHOC also contains a medium-threshold D-box. SMC4 is particularly interesting, as it contains fairly highly scoring D- and KEN-boxes, as well as 3 TEK motifs (Figure 2.3C).

Many proteins involved in the ubiquitin-proteasome pathway were also identified by this screen, many of which are also integral to the cell cycle. The E3 ubiquitin ligase RO52 was found to interact with both Cdc20 and Cdh1, and also contained a highly-stringent D-box sequence (Figure 2.3C). Similarly, the DUB enzyme USP9X, the RING finger protein RNF4 and the SCF E3 ubiquitin ligase component CUL1 were all identified within the APC3 IP, whilst CUL5 and SKP1 interacted with Cdc20 (Figure 2.3C). Of these, CUL5 appears to be an attractive target for APC/C-mediated ubiquitylation, as it also contains the TEK motif for the inititiation of ubiquitylation, whilst SKP1 also contains an extended KEN-box (Figure 2.3C).

Cdc20 also bound proteins implicated in differentiation and apoptosis. The proteins DMBT1, DOCK7 and Drebrin are implicated in the regulation of neurogenic differentiation (Figure 2.3H), whilst 14-3-3S, GGCT, Serpins B3 and B4 and TRAF2 all function in apoptotic pathways; GGCT and Serpins B3 and B4 contain KEN-boxes, whilst Serpin B4 also contains a TEK motif (Figure 2.3 I). The identification of these proteins is particularly interesting, as traditionally it is the co-activator Cdh1 rather than Cdc20 which is associated with quiescence and differentiation.

Another family of proteins well-represented by these data are the MCM proteins which mediate DNA replication by controlling replication licencing (Maine, Sinha et al. 1984, Costa, Hood et al. 2013, Yardimci and Walter 2014). Out of the MCM2-7 complex, MCM3, MCM4, MCM5 and MCM7 have all been identified within our dataset (Figure 2.3Di). MCM3 was found to bind both APC3 and Cdc20, whilst MCM7 was found in all three IPs. All the MCM proteins identified contain conserved D-boxes (Figure 2.3Dii), with MCM5 and MCM7 containing extended D-box sequences, whilst MCM4 contains a high-threshold D-box and a KEN box (Figure 2.3Di). These data suggest that the MCM complex could be a target for the E3 ubiquitin ligase activity of APC/C, and warrants further investigation.

Several DNA repair mechanisms exist within eukaryotic cells in order to restore defective DNA following various forms of damage. Both Msh2 and Msh6, members of the MMR pathway, were found in both APC3 and Cdh1 IPs, whilst Msh2 also bound Cdc20 (Figure 2.3E). Msh2 contains a KEN motif, whilst Msh6 contains an extended D-box commensurate with those from known APC/C substrates (Figure 2.3E). Similarly, the NER protein MMS19 was pulled down by APC3, as were TRIP13 and UBR5, which are important in the response to DSBs (Figure 2.3E). APC3 was also shown to interact with two components of the Replication Factor C complex, RFC3 and RFC5, which promote correct DNA replication both during normal S-phase and upon DNA damage (Figure 2.3E). Of these proteins, UBR5 contains multiple D-boxes, and RFC5 contains a highly-scored D-box as calculated by GPS-ARM (Figure 2.3E). Another DSB repair protein, TERA, was pulled down by both Cdc20 and Cdh1

IPs, which also contained an extended D-box motif (Figure 2.3E). Cdc20 was also able to co-IP MAPKAP2/MK2, which appears to alter mRNA stability following various forms of DNA damage (Figure 2.3E). Given the number of proteins within these data which contain degron motifs, it appears likely that the APC/C could be involved in several different DNA damage response (DDR) pathways.

Given the data presented in Figures 2.1 and 2.2, in which the APC/C was shown to bind and affect the nucleolar localisation of many proteins important in ribosomal biogenesis and translation, it is unsurprising that further proteins were also identified following immunoprecipitation from whole cell extracts. As well as many 60S and 40S ribosomal proteins, both Nucleolin and the nucleolar RNA helicase DDX21, which contains an extended D-box sequence, were also pulled down by APC3, Cdc20 and Cdh1 (Figure 2.3F). Similarly the ribosomal biogenesis protein BRX1 and the translational regulators LAR4B, TNR6B and elongation factors EF1G and EF2 were identified within these IPs (Figure 2.3F).

The APC/C has been described as holding a role in the regulation of metabolism, particularly with regard to glycolysis (Colombo, Palacios-Callender et al. 2010, Colombo, Palacios-Callender et al. 2011, Estévez-García, Cordoba-Gonzalez et al. 2014). As such, it is perhaps unsurprising that proteins from several different metabolic pathways have been represented within this dataset, which all contain D-boxes. These include C1TC, important in amino-acid biosynthesis and 1-Carbon metabolism and found in all three IPs, and K6PL and K6PP, which function in glycolysis (Figure 2.3J). Also found were CCHL, which is implicated in mitochondrial oxidative ATP synthesis, and the fatty acid metabolic proteins ACACA and APOA1 (Figure 2.3J). The Cdh1-interacting proteins ACACA, APOA1 and CCHL all contain KEN boxes, whilst C1TC, K6PL and K6PP contain TEK motifs (Figure 2.3J).

The APC/C has already been implicated in the regulation of transcription at numerous levels. It has been shown to degrade transcription factors (Park, Costa et al. 2008, Ostapenko and Solomon 2011,

Ostapenko, Burton et al. 2012), and in yeast, Apc5 mutations affect the chromatin state of active genes (Gunjan and Verreault 2003, Turner, Malo et al. 2010). Similarly in humans, APC5 and APC7 have been shown to potentiate the transcriptional capabilities of the HATs CBP and p300, and are associated with CBP/p300-regulated promoters (Turnell, Stewart et al. 2005). In our screen, and in agreement with previous mass spectrometry searches (Figures 2.1 and 2.2), multiple histones have been found (Figure 2.3G). A number of other proteins have also been identified, including two with TEK boxes – FLII (Flightless-1-homologue) and STAT3, which also contains a KEN box (Figure 2.3G). Furthermore, the histone methyltransferase DOT1L, and the transcriptional activators HELLS helicase and PURA also contain extended KEN motifs (Figure 2.3G). PURA, as well as the E3 ubiquitin ligase TRIM29 which contains several D-boxes, were found in both the Cdc20 and Cdh1 IPs, and therefore are good candidates for novel substrates (Figure 2.3G). Complementing the nucleolar APC/C IPs (Figure 2.1), several RNA helicases and mRNA processing and splicing enzymes were also found within IPs from whole cell lysates (Appendix Figure S1.4A). These are important in the processing of mRNA from nascent transcripts to those which are capable of being translated, thus play an important role in the regulation of protein synthesis.

Multiple members of the heat-shock-protein family and T-complex were also found to interact with APC3, Cdc20 or Cdh1 (Appendix Figure S1.4A). These act as molecular chaperones, ensuring the correct folding of nascent polypeptides within the Endoplasmic Reticulum, and form part of the Unfolded Protein Response. Although numerous members of each family were found, particular attention shall be drawn to TCPG, as it contains two TEK motifs and extended D-box sequences, and HS105, HS74L, HS90A, HS90B and HSP72, which all contain KEN-boxes. As yet, no link between the APC/C and protein folding has been described, therefore this could provide an interesting line of novel research in this area.

These data demonstrate the association of APC3, Cdc20 and Cdh1 with many biological processes within the cell (Figure 2.3; Appendix Figure S1.4A). Investigation into degron motifs within these interacting proteins has suggested a number of putative substrates for APC/C-mediated ubiquitylation, for which further research is required. These include proteins important in the cell cycle, such as SMC4, SKP1, RO52, RHOC and the Cullins, CUL1 and CUL5, as well as several members of the MCM2-7 complex. Also found were several members of different DNA repair pathways, including MMS19, Msh2 and Msh6, 2 subunits of Replication Factor C and the E3 ubiquitin ligase TERA. Proteins were also found to be involved in metabolism, transcriptional regulation and mRNA processing, protein folding, the ubiquitin-proteasome pathway, apoptosis and nucleolar function, namely ribosomal proteins, Nucleolin and a nucleolar rRNA helicase, DDX21.

A) <u>APC/C subunits</u>

Protein	Full Name	MW [kDa]	# Peptides		
			APC3 IP	Cdc20 IP	Cdh1 IP
APC1	Anaphase-promoting complex subunit 1	216.4	99	22	10
APC2	Anaphase-promoting complex subunit 2	93.8	40	4	-
APC3	Cell division cycle protein 27 homolog	91.8	63	17	4
APC4	Anaphase-promoting complex subunit 4	92.1	49	13	-
APC5	Anaphase-promoting complex subunit 5	85	64	2	-
APC6	Cell division cycle protein 16 homolog	71.6	41	12	2
APC7	Anaphase-promoting complex subunit 7	63.1	48	6	-
APC8	Cell division cycle protein 23 homolog	68.8	61	18	4
APC10	Anaphase-promoting complex subunit 10	21.2	15	-	-
APC12	Anaphase-promoting complex subunit CDC26	9.8	7	3	-
APC16	UPF0448 protein C10orf104	11.7	4	-	-
Cdc20	Cell division cycle protein 20 homolog	54.7	4	19	-
Cdh1	Fizzy-related protein homolog	55.1	16	-	12

B) Known Interactors and Substrates

Protein	Full Name	MW [kDa]	# Peptides			# D-box	# KEN	TEK	GPS-ARM
			APC3 IP	Cdc20 IP	Cdh1 IP				
BUB1[1]	Mitotic checkpoint serine/threonine-protein kinase BUB1	122.3	-	15	-	3	2	-	+++
BUB1B[1]	Mitotic checkpoint serine/threonine-protein kinase BUB1 beta	119.5	31	64	-	8	2	-	***/ +++
BUB3[1]	Mitotic checkpoint protein BUB3	37.1	9	17	1	1	1	-	
FBX5[2]	F-box only protein 5	50.1	13	-	-	4	1	-	***/ +++
KIF4A[3]	Chromosome-associated kinesin KIF4A	139.8	1	-	-	7	1	1	***/ +++
KIF22[4]	Kinesin-like protein KIF22	73.2	1			6	1	-	**/ +++
MD2L1[1]	Mitotic spindle assembly checkpoint protein MAD2A	23.5	6	8		-	-	-	
NEK2[5]	Serine/threonine-protein kinase Nek2	51.7	3			5	1	-	***/ +++
PAF[6]	PCNA-associated factor	12	2			1	1	-	***/ +++
RIR2[7]	Ribonucleoside-diphosphate reductase subunit M2	44.8	13		8	3	1	-	***/ +++

C) Cell Cycle and Ubiquitin-Proteasomal Pathway

Protein	Full Name	MW [kDa]	# Peptides			# D-box	# KEN	TEK	GPS-ARM
			APC3 IP	Cdc20 IP	Cdh1 IP				
AKAP8	A-kinase anchor protein 8	76.1		1		3	-	-	*
ARL2	ADP-ribosylation factor-like protein 2	20.9	2			1	-	-	
CDK2	Cell division protein kinase 2	33.9	3			3	-	-	
CUL1	Cullin-1	89.6	15			4	-	-	
CUL5	Cullin-5	90.9		9		4	-	1	
FA96B	Protein FAM96B	17.7	3			-	-	-	
KLHL9	Kelch-like protein 9	69.4			2	2	-	-	
MP2K2	Dual specificity mitogen-activated protein kinase kinase 2	44.4	2	1		1	-	-	***
NEST	Nestin	177.3			1	11	5	1	***/ +++
NSUN2	tRNA (cytosine-5-)-methyltransferase NSUN2	86.4		2		5	1	-	
PRS7	26S protease regulatory subunit 7	48.6	1			2	-	1	**
PSDE	26S proteasome non-ATPase regulatory subunit 14	34.6	1	1		-	-	-	
PSMD2	26S proteasome non-ATPase regulatory subunit 2	100.1		2		7	-	-	**

RHOC	Rho-related GTP-binding protein RhoC	22	2			3	-	-	**
RNF4	RING finger protein 4	21.3	3			1	-	-	
RO52	52 kDa Ro protein	54.1		10	7	3	-	-	***
S10AB	Protein S100-A11	11.7		2		-	-	-	
SKP1	S-phase kinase-associated protein 1	18.6	4			-	1	-	+++
SMC4	Structural maintenance of chromosomes protein 4	147.1			3	4	1	3	**/ ++
TRP13	Thyroid receptor-interacting protein 13	48.5	9			4	-	1	
USP9X	Probable ubiquitin carboxyl-terminal hydrolase FAF-X	289.4	4			13	-	-	**

D) i) MCM proteins

Protein	Full Name	MW [kDa]	# Peptides			# D-box	# KEN	TEK	GPS-ARM
			APC3 IP	Cdc20 IP	Cdh1 IP				
MCM3	DNA replication licensing factor MCM3	90.9	4	1		4	-	-	
MCM4	DNA replication licensing factor MCM4	96.5	13			5	1	-	***
MCM5	DNA replication licensing factor MCM5	82.2	2			5	-	-	*
MCM7	DNA replication licensing factor MCM7	81.3	36	2	1	6	-	-	*

ii) a) MCM3

```
sp|P25205|MCM3_HUMAN      VAKSQLLRYVLCTAPRAIPTTGRGSSGVGLTAAVTTDQETGER-RLEAGAMVLADRGVVC      407
sp|P25206|MCM3_MOUSE      VAKSQLLRYVLCTAPRAIPTTGRGSSGVGLTAAVTTDQETGER-RLEAGAMVLADRGVVC      407
tr|D3ZFP4|D3ZFP4_RAT      VAKSQLLRYVLCTAPRAIPTTGRGSSGVGLTAAVTTDQETGKGVGLPVRGLVLADRGVVC      408
sp|P49739|MCM3M_XENLA     VAKSQLLRYVLHTAPRAIPTTGRGSSGVGLTAAVTTDQETGER-RLEAGAMVLADRGVVC      407
tr|F7CH15|F7CH15_XENTR    VAKSQLLRYVLYTAPRAIPTTGRGSSGVGLTAAVTTDQETGER-RLEAGAMVLADRGVVC      407
sp|Q9XYU1|MCM3_DROME      VAKSQLLRYVLNTAPRAIPTTGRGSSGVGLTAAVTTDQETGER-RLEAGAMVLADRGVVC      402
tr|Q9XVR7|Q9XVR7_CAEEL    VAKSQLLRYVLRMAPRAITTTGRGSSGVGLTAAVTTDPDSGER-RLEAGAMVLADRGVVC      410
sp|P24279|MCM3_YEAST      TAKSQLLRFVLNTASLAIATTGRGSSGVGLTAAVTTDRETGER-RLEAGAMVLADRGVVC      471
sp|P30666|MCM3_SCHPO      TAKSQLLRFVLNTAPLAIATTGRGSSGVGLTAAVTTDKETGER-RLEAGAMVLADRGVVC      418

sp|P25205|MCM3_HUMAN      NIGLQDSLLSRFDLLFIMLDQMDPEQDREISDHVLRMHRYRAPGEQDGDAMPLGSA--VD      525
sp|P25206|MCM3_MOUSE      NIGLQDSLLSRFDLLFIMLDQMDPEQDREISDHVLRMHQYRAPGEQDGDALPLGSS--VD      525
tr|D3ZFP4|D3ZFP4_RAT      NIGLQDSLLSRFDLLFIMLDQMDPEQDREISDHVLRMHQYRAPGEQDGDALPLGSS--VD      526
sp|P49739|MCM3M_XENLA     NIGLQDSLLSRFDLLFIVLDKMDADNDQEIADHVLRMHRYRTPGEQDGYALPLGCS--VE      525
tr|F7CH15|F7CH15_XENTR    NIGLQDSLLSRFDLLFIVLDKMDADNDREIADHVLRMHRYRTPGEQDGYALPLGCS--VE      525
sp|Q9XYU1|MCM3_DROME      NIGLQDSLLSRFDLLFVMLDVIDSDVDQMISDHVVRMHRYRNPKEADGEPLSMGSS--YA      520
tr|Q9XVR7|Q9XVR7_CAEEL    NIGMQDSLLSRFDLIFVLLDEHDADKDANVAEHVLKLHTYRTQGEADGTVLPMGGG--VE      528
sp|P24279|MCM3_YEAST      NIALPDSLLSRFDLLFVVTDDINEIRDRSISEHVLRTHRYLPPGYLEGEPVRERLNLSLA      591
sp|P30666|MCM3_SCHPO      NIALPDSMLSRFDLLFIVTDDIDDKKDRALSEHVLRMHRYLPPGVEPGTPVRDSLNSVLN      538
```

b) MCM4

```
sp|P33991|MCM4_HUMAN        DGAA---------------AEDIVASEQSLGQKLVIWGTDVNVAACKENFQRFLQRFIDP        176
sp|P49717|MCM4_MOUSE        DGAA---------------AEDIVPSEQSLGQKLVIWGTDVNVATCKENFQRFLQCFTDP        175
tr|G3V681|G3V681_RAT        DGAA---------------AEDTVASEQSLGQKLVIWGTDVNVATCKEHFQRFLQCFTDP        175
sp|Q5XK83|MCM4A_XENLA       DQPA---------------AEELVTSEQSLGQKLVIWGTDVNVAICKEKFQRFVQRFIDP        171
sp|Q6GL41|MCM4_XENTR        DQPA---------------AEELVTSEQSLGQKLVIWGTDVNVATCKEKFQRFVQRFIDP        176
sp|Q26454|MCM4_DROME        GSGLEPI--PEKGS-----ETTDPVSESSQAPQLVVWGTNVVVSQCKSKFKSFIMRFIDP        178
tr|Q95XQ8|Q95XQ8_CAEEL      ----------IRGM-------EDEMAGDDGQPRLYVWGTRICVADVQRSFRDFLTTFKIS        131
sp|P30665|MCM4_YEAST        ---------TRSGVNTLDTSSSSAPPSEASEPLRIIWGTNVSIQECTTNFRNFLMSFKYK        204
sp|P29458|MCM4_SCHPO        PGVSTPSSLLFSGSDALTFSQAHPSSEVADDTVRVIWGTNVSIQESIASFRGFLRGFKKK        183

sp|P33991|MCM4_HUMAN        GALVLSDNGICCIDEFDKMNESTRSVLHEVMEQQTLSIAKAGIICQLNARTSVLAAANPI        620
sp|P49717|MCM4_MOUSE        GALVLSDNGICCIDEFDKMNESTRSVLHEVMEQQTLSIAKAGIICQLNARTSVLAAANPI        619
tr|G3V681|G3V681_RAT        GALVLSDNGICCIDEFDKMNESTRSVLHEVMEQQTLSIAKAGIICQLNARTSVLAAANPI        619
sp|Q5XK83|MCM4A_XENLA       GALVLSDNGICCIDEFDKMNESTRSVLHEVMEQQTLSIAKAGIICQLNARTSVLAAANPV        615
sp|Q6GL41|MCM4_XENTR        GALVLSDNGICCIDEFDKMNESTRSVLHEVMEQQTLSIAKAGIICQLNARTSVLAAANPV        620
sp|Q26454|MCM4_DROME        GALVLADNGVCCIDEFDKMNDSTRSVLHEVMEQQTLSIAKAGIICQLNARTSILAAANPA        622
tr|Q95XQ8|Q95XQ8_CAEEL      GALVLADNGVCCIDEFDKMNESARSVLHEVMEQQTLSIAKAGIICQLNARASVLAAANPV        579
sp|P30665|MCM4_YEAST        GALVLSDGGVCCIDEFDKMSDSTRSVLHEVMEQQTISIAKAGIITTLNARSSILASANPI        678
sp|P29458|MCM4_SCHPO        GALVLSDGGICCIDEFDKMSDATRSILHEVMEQQTVTVAKAGIITTLNARTSILASANPI        655

sp|P33991|MCM4_HUMAN        ESQWNPKKTTIENIQLPHTLLSRFDLIFLLLDPQDEAYDRRLAHHLVALYYQSEE--QAE        678
sp|P49717|MCM4_MOUSE        ESQWNPKKTTIENIQLPHTLLSRFDLIFLMLDPQDEAYDRRLAHHLVSLYYQSEE--QVE        677
tr|G3V681|G3V681_RAT        ESQWNPKKTTIENIQLPHTLLSRFDLIFLMLDPQDEAYDRRLAHHLVSLYYQSEE--QVE        677
sp|Q5XK83|MCM4A_XENLA       ESQWNPKKTTIENIQLPHTLLSRFDLIFLMLDPQDETYDRRLAHHLVALYYQSEE--QLK        673
sp|Q6GL41|MCM4_XENTR        ESQWNPKKTTIENIQLPHTLLSRFDLIFLMLDPQDETYDRRLAHHLVALYYQSEE--QMK        678
sp|Q26454|MCM4_DROME        ESQWNKRKNIIDNVQLPHTLLSRFDLIFLVLDPQDEIFDKRLASHLVSLYYVTRH--EEE        680
tr|Q95XQ8|Q95XQ8_CAEEL      DSKWNRNKTIVENITLPHTLLSRFDLIFLIVDAQDEMQDRRLGNHLVSLYFENDGN-QEK        638
sp|P30665|MCM4_YEAST        GSRYNPNLPVTENIDLPPPLLSRFDLVYLVLDKVDEKNDRELAKHLTNLYLEDKPEHISQ        738
sp|P29458|MCM4_SCHPO        GSKYNPDLPVTKNIDLPPTLLSRFDLVYLILDRVDETLDRKLANHIVSMYMEDTPEHATD        715
```

c) MCM5

```
sp|P33992|MCM5_HUMAN        KYRDELKRHYNLGEYWIEVEMEDLASFDEDLADYLYKQPAEHLQLLEEAAKEVADEVTRP        113
sp|P49718|MCM5_MOUSE        KYRDELKRHYNLGEYWIEVEMEDLASFDEELADHLHKQPAEHLQLLEEAAKEVADEVTRP        113
tr|B2GUX3|B2GUX3_RAT        KYRDELKRHYNLGEYWIEVEMEDLASFDEELADYLYKQPAEHLQLLEEAAKEVADEVTRP        113
sp|P55862|MCM5A_XENLA       KYRDELKRHYNLGEYWIEVEMEDLASFDEDLADYLYKQPTEHLQLLEEAAQEVADEVTRP        114
sp|Q561P5|MCM5_XENTR        KYRDELKRHYNLGEYWIEVEMEDLASFDEDLADYLYKQPTEHLQLLEEAAQEVADEVTRP        114
sp|Q9VGW6|MCM5_DROME        KYRDTLKRNYLNGRYFLEIEMEDLVGFDETLADKLNKQPTEHLEIFEEAARREVADEITAP        108
sp|Q21902|MCM5_CAEEL        IYRDQLKRNYFSHEYRLEINLNHLKNFDEDIEMKLRKFPGKVLPALEEAAKIVADEITTP        113
sp|P29496|MCM5_YEAST        IYRDQLRNNILVKNYSLTVNMEHLIGYNEDIYKKLSDEPSDIIPLFETAITQVAKRISIL        104
sp|P41389|MCM5_SCHPO        IYRTQLRDNLVVKQYMLNIDLRHLISYNEDLAHLLLSQPTDILPLFESAVTTVAKRLLYR        107
```

d) MCM7

```
sp|P33993|MCM7_HUMAN         ADYITAAYVEMRREAWASKDA----TYTSARTLLAILRLSTALARLRMVDVVEKEDVNEA        633
sp|Q61881|MCM7_MOUSE         ADYITAAYVEMRREARASKDA----TYTSARTLLAILRLSTALARLRMVDIVEKEDVNEA        633
tr|Q1PS21|Q1PS21_RAT         ADYITAAYVEMRREARASKDA----TYTSARTLLAILRLSTALARLRMVDIVEKEDVNEA        633
sp|Q91876|MCM7A_XENLA        ADYLTAAYVEMRKEARTNKDM----TFTSARTLLSVLRLSTALARLRLEDVVEKEDVNEA        632
sp|Q6NX31|MCM7_XENTR         ADYLTAAYVEMRKEARTNKDM----TFTSARTLLSILRLSTALARLRLEDVVEKEDVNEA        632
sp|Q9XYU0|MCM7_DROME         TDYIVGAYVELRREARNQKDM----TFTSARNLLGILRLSTALARLRLSDSVEKDDVAEA        633
tr|O16297|O16297_CAEEL       RERIVEAYVEMRRDARYSSDP----TFVSPRMILGIVRMATARAKLRLSTIVDESDVEEA        643
sp|P38132|MCM7_YEAST         NDYVVQAYIRLRQDSKREMDSKFSFGQATPRTLLGIIRLSQALAKLRLADMVDIDDVEEA        716
sp|O75001|MCM7_SCHPO         CDYVTGAYVQLRQNQKRDEANERQFAHTTPRTLLAILRMGQALARLRFSNRVEIGDVDEA        659
```

E) DNA Repair

Protein	Full Name	MW [kDa]	# Peptides			# D-box	# KEN	TEK	GPS-ARM
			APC3 IP	Cdc20 IP	Cdh1 IP				
MAPK2	MAP kinase-activated protein kinase 2	45.5		1		2	-	-	
MMS19	MMS19 nucleotide excision repair protein homolog	113.2	2			8	-	-	
MSH2	DNA mismatch repair protein Msh2	104.7	8	2	1	3	1	-	++
MSH6	DNA mismatch repair protein Msh6	152.7	7		4	5	-	-	***
RFC3	Replication factor C subunit 3	40.5	1			4	-	-	
RFC5	Replication factor C subunit 5	38.5	2			3	-	-	***
TERA	Transitional endoplasmic reticulum ATPase	89.3		1	2	5	-	-	***
UBR5	E3 ubiquitin-protein ligase UBR5	309.2	1			21	-		***

F) Ribosomal Biogenesis

Protein	Full Name	MW [kDa]	# Peptides			# D-box	# KEN	TEK	GPS-ARM
			APC3 IP	Cdc20 IP	Cdh1 IP				
BRX1	Ribosome biogenesis protein BRX1 homolog	41.4		1	1	2	-	-	
DDX17	Probable ATP-dependent RNA helicase DDX17	72.3	2	3		1	1	-	
DDX21	Nucleolar RNA helicase 2	87.3	4	21	14	1	-	-	***
DHX15	Putative pre-mRNA-splicing factor ATP-dependent RNA helicase DHX15	90.9		7	1	9	-	1	**
EF1G	Elongation factor 1-gamma	50.1		1		5	-	-	**
EF2	Elongation factor 2	95.3		15		7	-	-	
LAR4B	La-related protein 4B	80.5		5		2	-	-	
NOP2	Putative ribosomal RNA methyltransferase NOP2	89.2		1	6	2	-	-	
NUCL	Nucleolin	76.6	18	19	20	2	-	-	
R13AX	Putative 60S ribosomal protein L13a-like MGC87657	12.1	1			-	-	-	
RL27	60S ribosomal protein L27	15.8	5			-	-	-	
RL36A	60S ribosomal protein L36a	12.4	1			-	-	-	
RL36L	60S ribosomal protein L36a-like	12.5			2	-	-	-	
RS10	40S ribosomal protein S10	18.9	3	1	1	1	-	-	
RS15	40S ribosomal protein S15	17		3		1	-	-	
RS26L	Putative 40S ribosomal protein S26-like 1	13	2	1		-	-	-	
RS27	40S ribosomal protein S27	9.5	3			-	-	-	
RS27A	40S ribosomal protein S27a	9.4			1	-	-	-	
RS7	40S ribosomal protein S7	22.1	2			2	-	-	
TNR6B	Trinucleotide repeat-containing gene 6B protein	193.9			2	1	-	-	
XRN2	5'-3' exoribonuclease 2	108.5	3			5	-	-	*

G) Transcription

Protein	Full Name	MW [kDa]	# Peptides			# D-box	# KEN	TEK	GPS-ARM
			APC3 IP	Cdc20 IP	Cdh1 IP				
DOT1L	Histone-lysine N-methyltransferase, H3 lysine-79 specific	184.7	1			11	1	-	***/ +++
FLII	Protein flightless-1 homolog	144.7		1		6	-	1	**
H14	Histone H1.4	21.9			4	1	-	-	
H2AV	Histone H2A.V	13.5	2	2		1	-	-	
H3L	Histone H3-like	15.2			2	1	-	-	
HELLS	Lymphoid-specific helicase	97		42		4	1	-	**/ +++
PURA	Transcriptional activator protein Pur-alpha	34.9		1	1	5	1	-	+++
STAT3	Signal transducer and activator of transcription 3	88	1	1		3	1	1	++
TRI29	Tripartite motif-containing protein 29	65.8		1	1	3	-	-	***

H) Differentiation

Protein	Full Name	MW [kDa]	# Peptides			# D-box	# KEN	TEK	GPS-ARM
			APC3 IP	Cdc20 IP	Cdh1 IP				
DMBT1	Deleted in malignant brain tumors 1 protein	260.6		1		3	-	-	
DOCK7	Dedicator of cytokinesis protein 7	242.4		32		10	-	1	**
DREB	Drebrin	71.4		3		2	-	-	

I) Apoptosis

Protein	Full Name	MW [kDa]	# Peptides			# D-box	# KEN	TEK	GPS-ARM
			APC3 IP	Cdc20 IP	Cdh1 IP				
1433S	14-3-3 protein sigma	27.8		6		4	-	-	
GGCT	Gamma-glutamylcyclotransferase	21		1		2	1	-	*/+++
SPB3	Serpin B3	44.5		8		1	1	-	+++
SPB4	Serpin B4	44.8		7		-	2	1	+++
TRAF2	TNF receptor-associated factor 2	55.8		3		4	-	-	

J) Metabolism

Protein	Full Name	MW [kDa]	# Peptides			# D-box	# KEN	TEK	GPS-ARM
			APC3 IP	Cdc20 IP	Cdh1 IP				
ACACA	Acetyl-CoA carboxylase 1	265.4			3	13	1	-	+++
APOA1	Apolipoprotein A-I	30.8			1	6	1	-	***
C1TC	C-1-tetrahydrofolate synthase, cytoplasmic	101.5	20	12	6	4	-	1	***
CCHL	Cytochrome c-type heme lyase	30.6			2	1	1	-	***
K6PL	6-phosphofructokinase, liver type	85		1		1	-	1	
K6PP	6-phosphofructokinase type C	85.5	7	4		2	-	1	

Figure 2.3 – Mass Spectrometric identification of APC3, Cdc20 and Cdh1 IPs from whole cell extracts

Asynchronous HeLa cell lysates were incubated with 20µg normal IgG, APC3, Cdc20 or Cdh1 antisera overnight, followed by 2h with Protein G-agarose beads. The IP was then washed, boiled, separated by SDS-PAGE and stained with colloidal Coomassie solution. Gel slices were then excised, washed, reduced, alkylated then digested overnight at 37°C with trypsin. Peptides were eluted with 3%FA, dried and resuspended in 20µl 1%AcN/FA in H_2O. 10µl was loaded onto a maXis Impact (Bruker) and analysed by LC-MS/MS. Data was searched using Proteinscape (Bruker) against a Mascot database (Matrix Science). Identified peptides were filtered by a 1% False Discovery Rate and compared to a normal IgG control. Obvious contaminants were removed, and the proteins identified in two independent runs determined. The resulting interacting protein list was searched on Uniprot for protein sequence and function (UniProt-Consortium 2014). The protein sequences were then searched manually for TEK motifs and the presence of D-boxes and KEN-boxes ascertained and scored by GPS-ARM 1.0 (Liu, Yuan et al. 2012).

Conservation of degrons for the MCM proteins are shown in D ii). Only D-boxes which are conserved from yeast to human are shown, and the KEN box in MCM4. Organisms chosen include *Homo sapiens* (HUMAN), *Mus musculus* (MOUSE), *Rattus norvegicus* (RAT), *Xenopus laevis* (XENLA), *Xenopus tropicalis* (XENTR), *Drosophila melanogaster* (DROME), *Caenorhabditis elegans* (CAEEL), *Saccharomyces cerevisiae* (YEAST) and *Schizosaccharomyces pombe* (SCHPO). Alignments were performed using Clustal Omega (Goujon, McWilliam et al. 2010, Sievers, Wilm et al. 2011, Sievers and Higgins 2014)

Proteins are grouped by cellular function, with selected proteins shown in Figure 2.3. For full list of proteins in each group see Appendix Figure S1.4A. For all proteins identified within each IP see Appendix Figure S1.4B (APC3 IP), S1.4C (Cdc20 IP) and Figure S1.4C (Cdh1 IP).

References for known interactors and substrates:
1: BUB1, BUB1B, BUB3 - (Sudakin, Chan et al. 2001)
2: FBX5/Emi1 - (Hsu, Reimann et al. 2002)
3: KIF4A - (Singh, Winter et al. 2014)
4: KIF22 - (Feine, Zur et al. 2007)
5: NEK2A - (Hames, Wattam et al. 2001)
6: PAF - (Emanuele, Ciccia et al. 2011, Williamson, Banerjee et al. 2011)
7: RIR2 (murine) - (Chabes, Pfleger et al. 2003)

6.4. Discussion

In Chapter 1, a distinct nucleolar population of the APC/C was identified which might regulate Pol I activity through the targeting of RPA194 for degradation by the 26S proteasome. To investigate novel nucleolar functions for the APC/C a mass spectrometric approach was adopted. As such, IPs of APC/C subunits and co-activators were performed from nucleolar fractions (Figure 2.1), whilst the abundance of nucleolar proteins was determined following knockdown of either APC3 or APC5 (Figure 2.2). Similarly, to investigate novel functions of the APC/C in the context of the entire cell, mass spectrometric analysis of APC3 and co-activator IPs from whole cell extracts was performed (Figure 2.3).

These data contain a large number of putative substrates and interactors for the APC/C, and are detailed in full within the appendix. These proteins represent a wide range of biological processes, including: the cell cycle; Pol I transcription and ribosomal biogenesis; DNA replication and repair; metabolism; Pol II transcription; metabolism; differentiation and apoptosis.

In order to focus my attention upon certain proteins, those identified within the mass spectrometric screens were analysed for function, in particular with regard to nucleolar processes, and searched for canonical APC/C degrons, namely D-boxes, KEN-boxes and TEK motifs. Due to space and word limit considerations, the most likely substrates are described herein and the context of their potential as APC/C substrates outlined.

6.4.1. The APC/C interacts with proteins important in nucleolar function

A number of proteins identified within the IPs and whose nucleolar abundance increased following APC/C inhibition hold nucleolar functions. These include proteins which are important in the regulation of Pol I transcription, pre-rRNA processing and ribosomal assembly.

One such protein identified within the nucleolar APC7 IP is CHD1 (Figure 2.1C), which is required for elongation and termination termination of Pol I transcription in yeast and is a chromatin remodelling protein (Jones, Kawauchi et al. 2007). CHD1 contains a KEN-box, as well as a number of highly-scored D-boxes. Interestingly, CHD1 also increased in nucleolar abundance following siRNA-mediated knockdown of APC3 (Figure 2.2B). Another protein required for transcription termination and reinitiation, PTRF, was similarly elevated upon knockdown of APC5 and contains several extended D-boxes and a KEN box (Figure 2.2C) (Jansa, Burek et al. 2001). Given that transcription termination is necessary for the subsequent reinitiation of rDNA transcription by Pol I, any modulation of this process will alter the rate of Pol I transcription. Therefore, should either CHD1 or PTRF be novel substrates, it could provide extra levels of regulation for Pol I transcription mediated by the APC/C.

Pol I transcription is also regulated by epigenetic modifications of the chromatin state of rDNA. Accordingly, SUV91, a subunit of eNoSC also known as SUV39H1, was shown to increase in nucleolar abundance following knockdown of APC5 and contains extended D-boxes (Figure 2.2C). Other proteins important for chromatin remodelling were also found to increase following knockdown of either APC3 or APC5, including the aforementioned CHD1, as well as Acl6a/BAF53 and SMRD2/BAF60B, part of SWI-SNF complexes (Wang, Côté et al. 1996). Similarly, APC5 was shown to interact with NOC2L within the nucleolus (Figure 2.1B). NOC2L inhibits acetylation by CBP/p300, which has implications for Pol I transcription, as CBP-mediated acetylation of the Pol I subunit, PAF53, has been shown to repress transcription (Chen, Seiler et al. 2013).

The presence of the DUB UBP36, also known as USP36, within the APC7 IP does provide an intriguing possibility (Figure 2.1C). The *S. cerevisiae* orthologue, Ubp10, has been shown to be important in Pol I stability and rRNA production through its deubiquitylation of the yeast form of RPA194 (Richardson, Reed et al. 2012). Given our earlier evidence that RPA194 stability might be regulated, in part, by the

APC/C (Chapter 1), the targeting of UBP36 could provide an alternative regulatory mechanism for Pol I activity.

Numerous proteins important in pre-rRNA processing and maturation have also been identified within our mass spectrometric screens. These included a number of constituents of pre-ribosomes and sno-RNPs, such as RNA helicases, nucleases, methyltransferases and ribosomal proteins which are important in the folding, cleavage and maturation of pre-rRNA, as well as their transport and assembly into active ribosomes (Dragon, Gallagher et al. 2002, Mullineux and Lafontaine 2012, Tafforeau, Zorbas et al. 2013). One such protein, identified in both APC3 and APC7 nucleolar IPs, was the exoribonuclease ISG20L2, which regulates the maturation of the 5.8S rRNA required for the assembly of the 60S ribosome (Figure 2.1A, C)(Couté, Kindbeiter et al. 2008). ISG20L2 also contains a D-box sequence similar to that of known APC/C substrates (Figure 2.1A, C). It is therefore a likely candidate for a novel nucleolar substrate for the APC/C, and further work should be carried out to establish whether this is indeed the case.

Other nucleolar proteins including KRR1 and CN021/NOP9 were found to interact with APC7 (Figure 2.1C). These are important in the assembly of 40S ribosomes through the production and processing of 18S rRNA (Sasaki, Toh-E et al. 2000, Bernstein, Gallagher et al. 2004, Thomson, Rappsilber et al. 2007). Whilst KRR1 does contain D-boxes, it is the highly-scored D-box within CN021/NOP9 to which particular attention should be focussed (Figure 2.1C).

Of the multitude of proteins which were identified within the nucleolar APC5 IP, greater attention ought to be given to the D-box-containing proteins RRP12, NOP58 and WDR74, which also contain an extended D-box, a TEK motif and a KEN-box, respectively (Figure 2.1B). NOP58 is an essential component of U3 sno-RNPs, whilst RRP12 and WDR74 are important in the export of pre-ribosomes as part of their maturation (Gautier, Bergès et al. 1997, Oeffinger, Dlakic et al. 2004, Kressler, Roser et al. 2008). Similarly, BRX1 was identified within Cdc20 and Cdh1 IPs from whole cell extracts (Figure

2.3F), which in *Xenopus* and yeast has been shown to be important for 60S ribosome assembly and rRNA processing (Kaser, Bogengruber et al. 2001).

Other Small Subunit Processome and snoRNP components have also been identified within these mass spectrometry screens. These include IMP4, and the extended D-box-containing NOP2 and TBL3, which all interacted with nucleolar APC5 (Figure 2.1B), with IMP4 also increasing in nucleolar abundance following APC5 knockdown (Figure 2.2C). The methyltransferase NOP2 was also precipitated by Cdc20 and Cdh1 IPs, and therefore is also a strong contender to be an APC/C substrate (Figure 2.3F). An exonuclease, XRN2, was also identified with APC3 IPs from whole cell extracts, which is integral to early processing of pre-rRNAs together with snoRNPs (Figure 2.3F) (Miki and Großhans 2013).

APC5 also interacted with a number of proteins important in the processing of pre-rRNA to produce 18S rRNA and the production of mature 40S ribosomes, including HEAT1 and RRMJ3 (Figure 2.1B). RRMJ3 contains an extended D-box, whilst HEAT1 contains numerous extended D-boxes plus a KEN box, and therefore hold good potential in being novel APC/C substrates (Figure 2.1B). APC5 also interacted with a number of TEK-box-containing proteins important in rRNA processing, namely RRP7A, RBM28, NOL11, Pescadillo and RRP5, which also contained an extended D-box (Figure 2.1B). Similarly, WDR55, another rRNA processor, contains several D-boxes and was elevated in the nucleolus following knockdown of APC3 (Figure 2.2B).

Cleavage of pre-rRNA requires the activity of RNA helicases. These promote ATP-dependent rearrangement of the secondary structure of RNA, thereby facilitating RNA processing and splicing (Jarmoskaite and Russell 2014). Whilst RNA helicases commonly function within nuclear spliceosomes to process mRNA, a number of DEAD/H-box RNA helicases have also been identified within our mass spectrometry screens which have been implicated in rRNA processing and maturation and contain APC/C degrons. Interestingly, DDX5, containing a KEN-box and found within

nucleolar APC3 and APC7 IPs (Figure 2.1A, C), its heterodimeric partner DDX17, identified within nucleolar APC5 IPs and APC3, Cdc20 and Cdh1 IPs from whole cell extracts (Figure 2.3F), and DHX36, containing an extended D-box and stabilised in the nucleolus following APC3 knockdown (Figure 2.1B), have all been shown to colocalise *in vivo* (Ogilvie, Wilson et al. 2003, Iwamoto, Stadler et al. 2008). Nucleolar APC5 also interacted with two other RNA helicases implicated in ribosomal biogenesis, DDX27 and DH15, which both also contain highly-stringent D-box and TEK sequences (Figure 2.1B), with DHX15 also interacting with Cdc20 and Cdh1 (Figure 2.3F) (Ripmaster, Vaughn et al. 1992, Fouraux, Kolkman et al. 2002).

Special attention also ought to be drawn to DDX21, which co-immunoprecipitated with APC5 from nucleolar fractions (Figure 2.1B) and APC3, Cdc20 and Cdh1 from whole cell extracts (Figure 2.3F). DDX21 is important for both the processing of the 20S pre-rRNA into the 18S rRNA and also for 28S rRNA production (Henning, So et al. 2003, Yang, Henning et al. 2005). Given the fact that it contains a D-box highly scored by GPS-ARM and its ability to be co-precipitated with multiple APC/C subunits, it warrants further research and is a good candidate for an APC/C substrate.

Should any of these proteins be verified as APC/C substrates, such as by *in vitro* APC/C ubiquitylation assays or by it would demonstrate further mechanisms whereby the APC/C controls ribosomal production, from regulating Pol I transcription to pre-rRNA processing and ribosomal maturation.

6.4.2. The identification of mitotic cell cycle proteins as putative APC/C substrates

Given the role of the APC/C in the regulation of the cell cycle, it was unsurprising to see an abundance of proteins important in cell cycle progression interacting with, and whose nucleolar abundance was potentially regulated by, the APC/C. Many of these are important in mitosis, such as establishing and maintaining sister chromatid cohesion, chromosome condensation and cytokinesis.

6.4.2.1. Mitotic Kinases

A key mitotic kinase, Plk1, was shown to increase nucleolar abundance following knockdown of APC3 (Figure 2.2B). Plk1 is a pro-mitotic kinase that phosphorylates a plethora of proteins, including the APC/C, in order to regulate early mitosis (Kraft, Herzog et al. 2003, Petronczki, Lénárt et al. 2008, Liu, Ren et al. 2013). The APC/C subsequently targets Plk1 for degradation in order to promote mitotic exit (Lindon and Pines 2004). Similarly, nucleolar protein levels of Aurora Kinase B increased following ablation of APC5 expression (Figure 2.2C). Aurora Kinase B regulates various mitotic events prior to its ubiquitylation by the APC/C during late mitosis (Stewart and Fang 2005). These increases in substrate expression therefore acted as a proof-of-principle for this technique.

Another mitotic kinase, MP2K2, also known as MEK2, was identified within both APC3 and Cdc20 IPs and contains an extended D-box sequence (Figure 2.3C). Although this has not been identified as an APC/C substrate, it has been described as holding important roles within the cell cycle through its phosphorylation of ERK as part of the MAP kinase signalling pathway, which regulates cell cycle progression according to external stimuli through transcriptional control of Cyclin D1, and inhibition of $p27^{KIP1}$ (Rivard, Boucher et al. 1999). MEK2 has also been purported to hold another function in the activation of the G2/M checkpoint following Ionising Radiation (Abbott and Holt 1999).

6.4.2.2. Sister Chromatid Cohesion

Of these proteins, several are part of the Structural Maintenance of Chromosomes (SMC) family, which includes proteins important for chromosomal condensation and sister chromatid cohesion (Aragon, Martinez-Perez et al. 2013). One such example of a SMC family protein identified within our screen is SMC3, part of the Cohesin complex which keeps sister chromatids together until the onset of anaphase, whereupon it is cleaved under control of the APC/C (Peters 2006, Musacchio and Salmon 2007, Nasmyth 2011). Although this represents one method by which the APC/C regulates Cohesin, the identification of SMC3 within the APC7 IP and the presence of several D-boxes within its

sequence suggests that it might also be an APC/C substrate itself (Figure 2.1C). It is possible that direct cleavage of Cohesin by the APC/C could facilitate sister chromatid separation, particularly with regard to faster resolution of rDNA catenation within nucleolar regions, permitting mitotic progression with fewer delays, and therefore less susceptibility to chromosomal instability.

6.4.2.3. Chromosome Condensation

Another SMC family member, SMC4, was shown to interact with Cdh1 within whole cell extracts *in vivo* and contains D-, KEN- and TEK motifs (Figure 2.3C). SMC4 is a subunit of Condensin, which mediates the condensation of chromosomes during early mitosis (Hirano 2012, Thadani, Uhlmann et al. 2012, Piazza, Haering et al. 2013). Metazoan Condensin exists as two complexes with distinct functions; Condensin I binds to chromosomes in prometaphase following NEBD until the onset of anaphase and is involved in further condensation of chromosomes whilst Condensin II binds chromosomes throughout mitosis from prophase and is important for axial chromosomal shortening (Thadani, Uhlmann et al. 2012, Piazza, Haering et al. 2013). Condensin also appears to be important for the organisation of kinetochores, and therefore plays an important role in mitotic progression beyond that of the initial chromosomal compaction during prophase and prometaphase (Hirano 2012).

6.4.2.4. Anaphase

FAM96B, also referred to as MIP18, and MMS19 were shown to interact with APC3 (Figure 2.3C, E). Together, FAM96B and MMS19 have been suggested to play a role in chromosome segregation, since their siRNA-mediated knockdown resulted in abnormalities consistent with a function in anaphase (Ito, Tan et al. 2010). TRIP13 was also discovered within APC3 IPs (Figure 2.3C), which has recently

been shown to have a role in the silencing of the SAC through disassembly of the MCC, thereby alleviating MCC-dependent inhibition of the APC/C (Eytan, Wang et al. 2014, Wang, Sturt-Gillespie et al. 2014). TRIP13 contains both D-boxes and a TEK motif (Figure 2.3C), and therefore has potential for being an APC/C substrate. As such, it is feasible that it could be targeted itself for degradation upon completion of mitosis, since its MCC-inhibitory mechanism would no longer be required.

6.4.2.5. *Cytokinesis*

Several proteins important in cytokinesis were also identified within APC/C IPs, including Nestin, RhoC, ARL2 and KLHL9 (Figure 2.3C). Nestin was identified within the Cdh1 IP and contains extended D- and KEN-boxes as well as a TEK motif, and therefore is a strong contender for an APC/C substrate (Figure 2.3C). Interestingly, the nucleolar abundance of Nestin also increased following knockdown of either APC3 or APC5 (Figure 2.2A). Nestin has been shown to regulate the mitotic cytoskeleton by ensuring the correct disassembly and segregation of Intermediate Filaments between the two resulting daughter cells (Michalczyk and Ziman 2005). It could therefore be degraded within daughter cells under the control of APC/C-Cdh1, akin to other APC/C substrates.

6.4.3. Ubiquitin-Proteasomal Pathway proteins

Several other proteins were identified within APC/C IPs from whole cell extracts which function in the ubiquitin-proteasomal degradation pathway during the cell cycle. These included the SCF E3 ubiquitin ligase components RO52, SKP1 and CUL1, as well as CUL5, RNF4 and the DUB USP9X (Figure 2.3C). An SCF E3 ubiquitin ligase contains SKP1 and CUL1, together with an F-box protein, and ubiquitylates a wide range of substrates, with its substrate specificity conferred by the particular F-box protein contained within the complex (Skaar and Pagano 2009). One such SCF E3 ligase

containing RO52 has been shown to regulate p27 stability, as well as NFκB signalling (Sabile, Meyer et al. 2006, Wada, Niida et al. 2009). The identification of CUL1 is particularly interesting, as it is an essential part of the SCF E3 ubiquitin ligase(Yu, Gervais et al. 1998). Many SCF E3 ubiquitin ligases are important in the cell cycle, through the degradation of important cell cycle regulators. One example is SCF^{Fbxw7}, which ubiquitylates Cyclin E, c-Myc and c-Jun, whilst another SCF ligase, SCF^{Skp2}, promotes cell cycle progression through the degradation of p21 and p27 (Yu, Gervais et al. 1998, Carrano, Eytan et al. 1999, Tsvetkov, Yeh et al. 1999). Another SCF complex, $SCF^{\beta\text{-}TrCP}$, regulates the APC/C through ubiquitylation of its inhibitor Emi1; $SCF^{\beta\text{-}TrCP}$ also modulates Cdk1 activity through Wee1 and Cdc25A degradation (Frescas and Pagano 2008, Skaar and Pagano 2009). Should CUL1 be established as a novel binding protein or a substrate for the APC/C, it could permit the APC/C to modulate multiple signalling pathways through the regulation of a single protein.

Cullin 5 (CUL5) is a component of a different form of Cullin-Ring-Ligases (CRLs) termed ECS (Elongin-Cullin 2/5-SOCS-box protein). CUL5 functions in a number of antiproliferative cellular processes, such as Src-mediated transformation and ErbB2 degradation as well as downregulating MAP kinase and cAMP signalling pathways (Ehrlich, Wang et al. 2009, Bradley, Johnson et al. 2010, Teckchandani, Laszlo et al. 2014). CUL5 also contains a TEK motif, a known initiation site for APC/C-mediated ubiquitylation, and therefore is a strong candidate for an APC/C substrate. In a similar vein to CUL1, should CUL5 be designated a novel substrate for APC/C E3 ubiquitylation activity, it represents a hub protein through which the APC/C can modulate a number of processes, thereby disseminating a broad cell cycle effect through the regulation of a single protein.

These data suggest the APC/C has further roles in the regulation of mitosis beyond what has previously been published. Given the extensive list of known APC/C substrates in mitosis, these would be likely candidates for novel targets for the APC/C, and as such should be investigated further.

6.4.4. MCM and DNA replication

The Mini Chromosome Maintenance (MCM) family of proteins are integral to replication licencing and DNA synthesis, ensuring that DNA is only replicated once per cell cycle. Six of these, MCM2-7, exist as a dimeric hexamer which is recruited to origins of replication during G1 by ORC together with Cdc6 and Cdt1 to form the pre-RC, thus licensing the DNA ready for origin firing (Boos, Frigola et al. 2012, Sacco, Hasan et al. 2012). Given that the APC/C plays an important role in replication licencing, it is interesting that multiple members of the MCM family were identified within APC/C IPs, namely MCM3, MCM4, MCM5 and MCM7 (Figure 2.3D). Given that the MCM2-7 helicase appears to have evolved from a single monohexameric helicase, the presence of D-boxes within each subunit might suggest each subunit of the MCM2-7 helicase interacts with the APC/C, and indeed could be novel substrates. It is also worth noting that the D-boxes within MCM4, 5 and 7 are all extended, with downstream amino acids from the RxxL motif exhibiting homology to known substrates, whilst MCM4 also contains a KEN box (Figure 2.3D). Further research is therefore required upon these data to verify these interactions, and ascertain whether MCM proteins are indeed novel substrates for the APC/C.

6.4.5. DNA damage proteins as Potential APC/C Substrates

The nucleolus is integral to the response to DNA damage and might provide a sensory mechanism to determine the correct intracellular response (Mayer and Grummt 2005, Boulon, Westman et al. 2010, Grummt 2013). As such, it is perhaps unsurprising that many proteins involved in the repair of damaged or abnormal DNA were identified as interacting with the APC/C within whole cell and nucleolar extracts, and whose nucleolar abundance is dependent upon APC/C expression, particularly given that the APC/C is thought to re-activate upon DNA damage in order to halt cell cycle progression through ubiquitylation of Plk1, Cdc20 and Cyclin A (Sudo, Ota et al. 2001, Coster, Hayouka et al. 2007, Bassermann, Frescas et al. 2008, Townsend, Mason et al. 2009, Zhang, Nirantar

et al. 2009, Mosbech, Gibbs-Seymour et al. 2012). Identified proteins function in a range of different DNA repair pathways, including NHEJ, HR, SSB repair (including NER and BER) and MMR.

The DSB-detection protein Ku86/Ku80 was identified within the nucleolar APC7 IP and contains a high-threshold D-box (Figure 2.1C), whilst the D-box-containing NONO interacted with nucleolar APC5 (Figure 2.1B). Ku80 forms a heterodimer with Ku70, which signals DSBs, which are then ligated, assisted by NONO (Taccioli, Gottlieb et al. 1994, Bladen, Udayakumar et al. 2005, Krietsch, Caron et al. 2012). TRIP13, which co-immunoprecipitated with APC3 from whole cell extracts and whose role in mitosis has been described earlier, also promotes NHEJ (Banerjee, Russo et al. 2014). Other NHEJ proteins were stabilised within the nucleolus following inhibition of the APC/C, including 53bp1 and MDC1 (Figure 2.2B, C). MDC1 has previously been shown to interact with, and modulate the activity of, the APC/C, and has been shown to promote NHEJ at telomeres (Dimitrova and de Lange 2006, Coster, Hayouka et al. 2007, Townsend, Mason et al. 2009). 53bp1 contains both D- and KEN-boxes (Figure 2.2), whilst TRIP13 contains both D-boxes and TEK motifs (Figure 2.3C). 53bp1 has been well-characterised in its role in promoting NHEJ by the recruitment of DNA repair proteins and inhibition of HR (Ciccia and Elledge 2010, Kakarougkas and Jeggo 2014, Panier and Boulton 2014), and has also been shown to co-IP reciprocally with APC3 through its BRCT domain (Akhter, Richie et al. 2004, Woods, Mesquita et al. 2012).

The other major form of DNA repair for DSBs is HR. Proteins important in this pathway and identified by our nucleolar mass spectrometry screens include MDC1, which can also function in NHEJ. In HR, MDC1 is recruited to DSBs by γH2AX whereupon it binds and localises Rad51, NBS1 and ATM in order to promote DNA repair and HR (Zhang, Ma et al. 2005, Ciccia and Elledge 2010, Coster and Goldberg 2010). The RecQ DNA helicases, BLM and WRN, were also identified as increasing in nucleolar abundance following APC/C inhibition (Figure 2.2A, B). These are both potential substrates for the APC/C, as BLM contains several D-boxes and WRN contains both D- and KEN-boxes showing good

homology to those of known substrates as well as a TEK motif (Figure 2.2A, B). BLM helicase is important in the initial resection around the DNA breaks, whilst both WRN and BLM are important in the actual recombination event (Constantinou, Tarsounas et al. 2000, Ciccia and Elledge 2010, Iyama and Wilson 2013). Other HR proteins were identified within APC/C IPs, including TRIP12/TRIPC, which was found within APC3 IPs and contain multiple high-scoring D-boxes (Figure 2.3E), and TERA/segregase p97, which was pulled down by both Cdc20 and Cdh1 antisera and contains an extended D-box (Figure 2.3E). TRIP12 represses RNF168 ubiquitylation, thus represses and controls the K63-linked ubiquitin cascade (Gudjonsson, Altmeyer et al. 2012), whilst TERA is important in promoting DSB repair (Acs, Luijsterburg et al. 2011, Meerang, Ritz et al. 2011, Davis, Lachaud et al. 2012).

A number of proteins involved in SSB repair were identified within the mass spectrometry screens detailed within this Chapter. For example, two constituents of the Replication Factor Complex, RFC3 and RFC5, interacted with APC3 in whole cell extracts, with RFC5 containing a highly-scoring D-box (Figure 2.3E). These are important in resynthesising DNA over longer SSBs . Similarly, XRCC1 was present in nucleolar APC3 and APC7 IPs, and also contains several D-boxes (Figure 2.1A, C). XRCC1 acts in concert with LIG1 to ligate the two ends of the SSB (Thompson, Brookman et al. 1990, Iyama and Wilson 2013). An interactor of XRCC1, Aprataxin, was elevated within nucleoli following knockdown of either APC3 or APC5 and also contains a number of D-boxes (Figure 2.2A). Aprataxin has been described as a proof-reader by deadenylating SSB ends, such as those exhibited upon aborted ligations, thereby permitting religation attempts (Clements, Breslin et al. 2004, Gueven, Becherel et al. 2004, Sano, Date et al. 2004, Rass, Ahel et al. 2007).

Two components of the MMR pathway, Msh2 and Msh6, were identified within APC/C IPs from whole cell extracts, and contain degrons typical of APC/C substrates (Figure 2.3E). Similarly, Mlh1 was shown to be elevated within nucleoli following knockdown of APC3 and contains extended D-boxes

(Figure 2.2B). Msh2/Msh6 heterodimers recognise mismatched bases, whilst a heterodimer containing Mlh1 coordinates the repair response (Edelbrock, Kaliyaperumal et al. 2013, Iyama and Wilson 2013).

6.5. Concluding remarks

Mass spectrometry is a valid tool to investigate functions of the APC/C, particularly in regard to the discovery of novel substrates. As such, many proteins either interacting with, or whose nucleolar abundance is regulated by, the APC/C have been discovered. Many of these identified proteins could be novel substrates, but further validation is required. These can be tested by performing *in vitro* APC/C ubiquitylation assays, by examining protein levels following APC/C inhibition and by searching upon the putative substrate for K11-ubiquitin chains, the archetypal chain-type formed by APC/C-mediated E3 ubiquitin ligase activity.

Many of the potential substrates described within this chapter are important in the cell cycle, which is particularly interesting given the extensive list of known cell cycle substrates for the APC/C. Other proteins described here have also been implicated in the DNA damage response, replication licencing, apoptosis, glycolysis, Pol II transcription and differentiation. A great deal of nucleolar proteins have also been identified which play a role in nucleolar function, such as Pol I transcription, pre-rRNA processing and ribosomal assembly. This suggests that the APC/C could regulate rRNA production at multiple levels.

The APC/C already has an extensive list of known substrates, which grows longer as further substrates are found. Many of these substrates, and the putative substrates described within this chapter, function within the same pathway. This could provide a mechanism whereby the APC/C is able to modulate a particular pathway at multiple points, in order to elicit a faster and more

complete downstream response. Similarly, many APC/C substrates are also degraded at the same time within the cell cycle. It is feasible that the cell utilises the APC/C to target a number of substrates for degradation in order to avoid having separate E3 ubiquitin ligases for each protein, which would require a greater energy demand to maintain. Utilising one ligase also facilitates both spatial and temporal control mechanisms, which is particularly important during the cell cycle, in which a timely coordinated response is often required. Also, preferentially relying upon APC/C-mediated ubiquitylation permits a divergent response, in which multiple pathways can be targeted at once. As such, the APC/C could be described as the master regulator of mitotic and G1 phases of the cell cycle.

However, despite the ability of the APC/C to target a vast number of proteins for proteolysis, *in vivo* only a proportion of these substrates are degraded at one particular time. This suggests a level of control over which substrates are able to be recognised and ubiquitylated by the APC/C at a given time. These mechanisms are outlined within section 1.4.1, in which regulatory mechanisms for APC/C subunits and co-activators are detailed, and section 1.4.2, in which modulations upon substrates are described. Briefly, these mechanisms include pseudosubstrate blockage of substrate recognition, as exhibited by Emi1 and the MCC, spatial separation of APC/C and substrates, the presence of ancillary bridging proteins and PTMs. These PTMs can be exhibited upon APC/C subunits, such as Cdk1- and Plk1-mediated phosphorylation which activates the APC/C during mitosis, upon co-activators, such as inhibitory phosphorylation and acetylation in order to prevent their activation of the APC/C during S and G2, or upon substrates, with the precise PTM pattern determining their recognition by the APC/C. An important consideration in this regard is how these additional binding proteins and PTMs modify the structure of the APC/C, which could potentially occlude certain binding sites whilst making others accessible, thus changing substrate specificity. As such, this has a profound impact upon future research into the APC/C and the discovery of novel substrates.

7. CHAPTER 3: ACETYLATION AS A REGULATOR OF APC/C ACTIVITY

The ubiquitin ligase activity of the APC/C is tightly regulated such that it ubiquitylates its target substrates in a temporally and spatially organised manner. One method by which the APC/C is regulated is through post-translational modification (PTM). Indeed, the general consensus is that the APC/C is phosphorylated in early mitosis, particularly upon the TPR lobe, by mitotic kinases such as Cdk1 and Plk1 to prime its activation by Cdc20, and then dephosphorylated by phosphatases during late mitosis to promote a switch to Cdh1-mediated activation; conversely, phosphorylation of Cdc20 and Cdh1 prevents their activation of the APC/C during S and G2 phases (Zachariae, Schwab et al. 1998, Jaspersen, Charles et al. 1999, Kramer, Scheuringer et al. 2000, Rudner and Murray 2000, Kraft, Herzog et al. 2003, Steen, Steen et al. 2008, Labit, Fujimitsu et al. 2012, Primorac and Musacchio 2013).

However, another PTM, acetylation, has been described as potentially being as important as phosphorylation in regulating protein function *in vivo* (Kouzarides 2000, Norvell and McMahon 2010). The form of acetylation described herein is lysine acetylation, although acetylation can also be performed upon free N-terminal α-NH_2 groups. In lysine acetylation, an acetyl group (CH_3CO) is conjugated from acetyl-CoA to the ε-amine group upon lysines by a HAT, whilst deacetylation is performed by an HDAC, although there is an argument to change this terminology to a KAT (Lysine Acetyltransferase) and KDAC (Lysine Deacetylase) to reflect the lysine specificity and the identification of non-histone protein targets (Allis, Berger et al. 2007).

Previous work within our group has demonstrated a link between the HATs CBP and p300 and the APC/C, such that the APC/C and CBP/p300 reciprocally regulate each other's enzymatic activity (Turnell, Stewart et al. 2005). APC5 and APC7 can bind directly and independently to CBP and p300,

thereby stimulating their acetyltransferase activity and potentiating CBP/p300-dependent transcription (Turnell, Stewart et al. 2005). Moreover, immunopurified CBP and p300 can support the polyubiquitylation of Cyclin B1 *in vitro*, whilst CBP knockdown suppresses APC/C activity *in vivo* and delays progression through mitosis (Turnell, Stewart et al. 2005).

Furthermore, using tandem mass spectrometry (MS/MS), the fission yeast APC8 homologue, Cut23, has been shown to be acetylated *in vivo* (Kimata, Matsuyama et al. 2008). Also, SIRT2-mediated deacetylation of Cdc20 and Cdh1 is required for their activation of the APC/C; ablation of SIRT2 expression increases the protein levels of known APC/C substrates Aurora A and B (Kim, Vassilopoulos et al. 2011).

Given these findings, we postulated that the acetylation of APC/C subunits and co-activators might be integral to the regulation of APC/C function and that this could be mediated by CBP and/or p300. Data presented within this chapter describe the mass spectrometric identification of novel acetylation sites upon APC/C subunits, and the development of cell lines to analyse the biological consequences of site-specific acetylation upon APC3 and APC8. The interaction between CBP/p300 and the APC/C is characterised further: CBP and p300 interact with APC3 and promote APC3 acetylation *in vitro*, whilst CBP coordinates APC3 acetylation *in vivo*.

7.1. APC3 is acetylated by p300 *in vitro*

Previous work from our laboratory has established that there is an intimate functional relationship between CBP/p300 and the APC/C; the APC/C subunits, APC5 and APC7, potentiate CBP/p300-dependent transcription, whilst CBP/p300 regulates APC/C E3 ubiquitin ligase activity (Turnell, Stewart et al. 2005). We therefore initiated experiments to determine whether CBP/p300 could acetylate the APC/C *in vitro*.

Accordingly, recombinant His_6-tagged p300 (His_6-p300) was incubated with radiolabelled acetyl-Coenzyme A ([^{3}H]-Ac-CoA) in the absence or presence of APC/C holoenzyme, purified by immunoprecipitation from A549 cell lysate with APC3 AF3.1 antibodies and elution with AF3.1 peptide. Upon separating the reaction mixtures by SDS-PAGE and detection by autoradiography, multiple bands were seen (Figure 3.1). The majority of these bands were present in the absence of APC/C (Figure 3.1, lane 1), and reflect autoacetylation of p300. However, a single band was prominent upon the addition of the APC/C holoenzyme (lane 2). The most logical explanation for this result is that p300 has directed the acetylation of a specific APC/C subunit, or an APC/C-interacting protein. It is also possible that an APC/C-interacting protein present in the immunopurified APC/C preparation could also have mediated this acetylation in response to p300.

To determine whether the acetylated protein identified within Figure 3.1 was an APC/C subunit, an alternative approach was taken. Immunoprecipitated p300 was incubated with individual GST-APC/C subunits and [^{3}H]-Ac-CoA, separated by SDS-PAGE and detected by autoradiography (Figure 3.2). As before, autoacetylated p300 was visible in all samples, indicating that the immunoprecipitated p300 was active. Adenovirus E1A, a known substrate for p300-mediated acetylation, was also acetylated in the presence of p300 (Figure 3.2). Out of the APC/C subunits investigated, GST-APC3 was similarly acetylated under these *in vitro* conditions (Figure 3.2). Interestingly, the putative acetylated APC/C

protein visualised within Figure 3.1 migrated at approximately 100kDa, which correlates directly with the molecular weight of APC3. Taken together, these data suggest that p300 acetylates APC3 *in vitro*.

Although it would have been possible to acetylate individual GST-APC/C subunits *in vitro* using His_6-p300, for this experiment p300 was purified by IP. This enabled a direct comparison in later experiments with the related acetyltransferase, CBP, for which a His_6-tagged construct was not available (Figure 3.4)

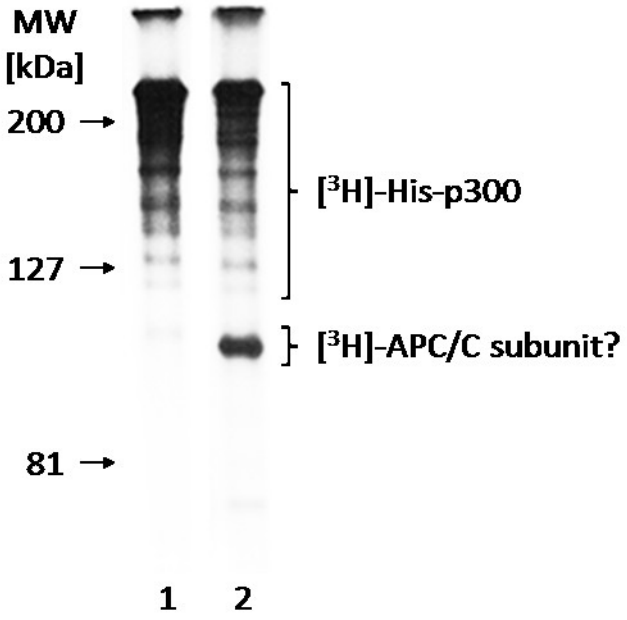

Figure 3.1 – Purified p300 acetylates a component of APC3 IPs *in vitro*

His_6-tagged p300 was expressed in Sf9 insect cells using a baculoviral vector and purified using a Nickel-affinity column. The APC/C holoenzyme was IP'd using α-APC3 AF3.1 antibodies and eluted using the AF3.1 peptide. 200ng of His_6-p300 was incubated with 0.5µCi [^{3}H]-Ac-CoA (Amersham) (lane 1) or with 0.5µCi [^{3}H]-Ac-CoA and 200ng APC/C holoenzyme (lane 2) for 90 minutes at 37°C. The resulting mixture was separated by SDS-PAGE, sensitised for 30 min with Amersham Amplify (GE Healthcare), dried and detected for autoradiography with X-ray film.

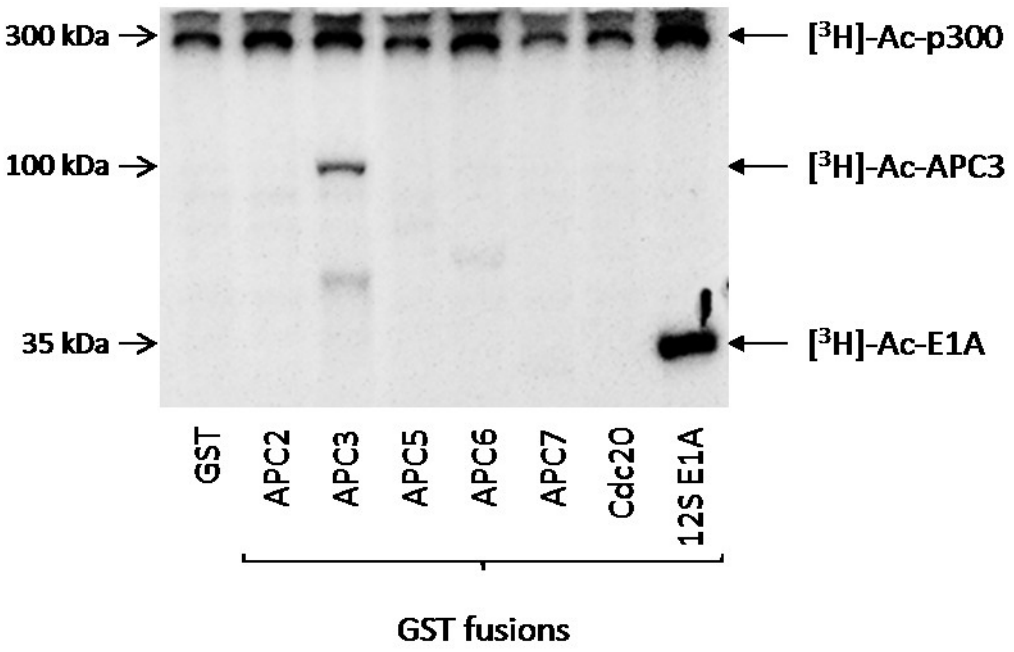

Figure 3.2 – Immunopurified p300 acetylates GST-APC3 *in vitro*

P300 was IP'd from asynchronous A549 lysates. GST and GST-fusion proteins were expressed in bacteria and purified using glutathione-agarose. P300 IPs were incubated with 10µg of the denoted GST-fusion and 0.5µCi [^{3}H]-Ac-CoA (Amersham) for 90 minutes at 37°C. The reaction mixture was separated by SDS-PAGE and detected by autoradiography.

7.2. Mass spectrometric identification of APC3 acetylation sites *in vivo*

Thus far, it has been determined that p300 acetylates APC3 *in vitro* (Figures 3.1, 3.2). Next, it was important to ascertain whether specific acetyl-lysine residues within APC3 could be determined *in vivo*. As such, APC3 IPs were performed from asynchronous A549 cells, and separated by SDS-PAGE. Gel slices were excised, and those corresponding to APC3 were processed and sent for mass spectrometric analysis in collaboration with Applied Biosystems.

Using an Information Dependent Acquisition (IDA) workflow, a number of acetylation sites were identified upon APC3: K99, K336, K396 and K700, of which acetylated K336 appeared to be the most abundant acetylated species (Figure 3.3Ai). These were assigned with high confidence, and therefore are likely to correspond to lysines acetylated *in vivo*.

However, further validation of acetyl-lysines can also be gained by analysing specific m/z peaks formed by precursor ions within the extracted ion chromatograms. Fragmentation of lysine moieties produces an immonium ion with an m/z peak of 84, whilst the immonium ion formed upon fragmentation of acetylated lysines has a higher m/z of 143.1, which can be reduced to 126.1 upon the loss of NH_3 (Kim, Kim et al. 2002, Zhang, Yau et al. 2004). By scanning the chromatograms for these immonium precursors, further Ac-K residues upon APC3 were identified (Figure 3.3Aii). Further to those described in Figure 3.3Ai, K400, K401, K421 and K724 were also shown to be acetylated (Figure 3.3Aii).

The precise LC-MS/MS system utilised for this experiment also provided a more targeted approach in the determination of acetylation residues. Using MIDAS (Multiple reaction monitoring-Initiated Detection And Sequencing; AB SCIEX) and focussing specifically upon the APC3 protein sequence, a further four acetyl-lysines were identified: K77, K418, K693 and K782 (Figure 3.3Aiii), as well as those previously described (Figure 3.3i, ii).

A

APC3 Ac-K	i) IDA	ii) Precursor Ion Analysis	iii) MIDAS
K77	-	-	18
K99	93	39	32
K336	89	85	92
K396	67	101	107
K396, K400	-	91	108
K396, K400, K401	-	63	-
K418, K421	-	-	62
K421	-	37	-
K693	-	-	31 and 75
K700	28	51	75
K724	-	41	53
K782	-	-	28

B

APC3 Ac-K336: Peptide GQTGTK*SVFSQSGNSR

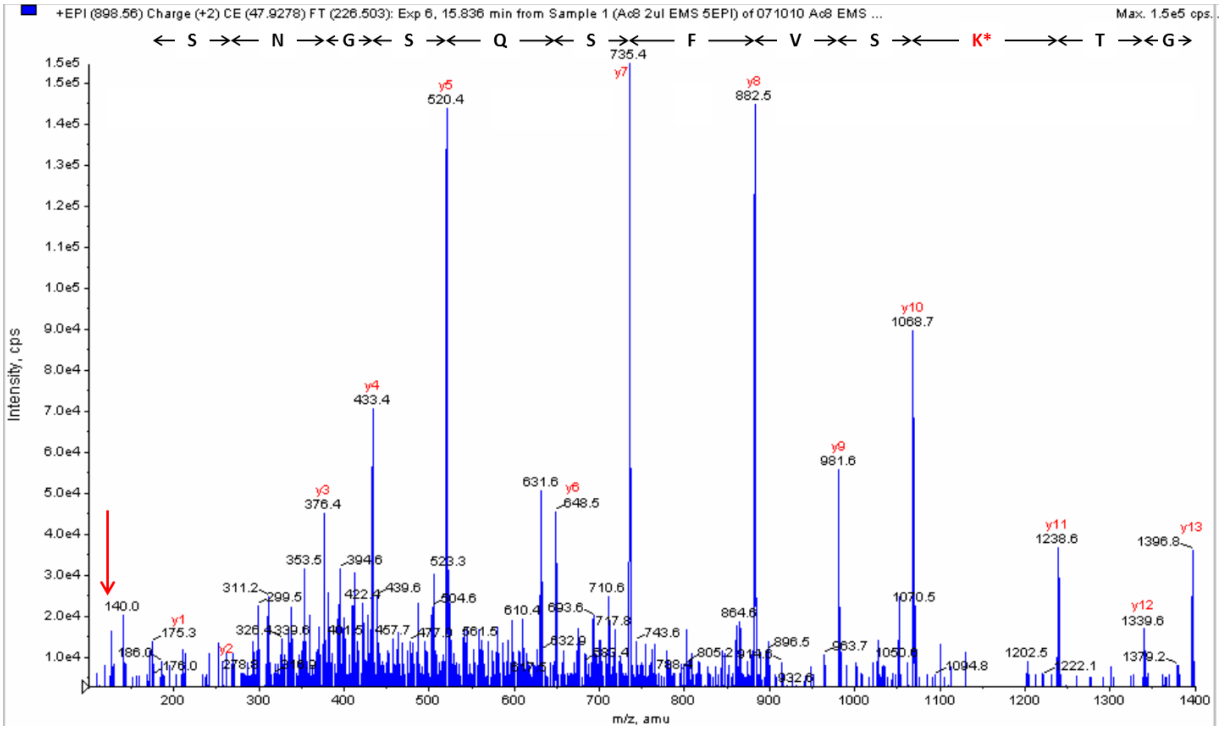

Figure 3.3 – Mass spectrometric identification of Ac-K sites within APC3 *in vivo*

APC3 was obtained by IP from asynchronous A549 cells, followed by SDS-PAGE. The gel was stained with colloidal Coomassie and the bands corresponding to APC3 were excised and fragmented by LC-MS/MS with a Tempo nano-LC and Q-TRAP System Mass Spectrometer and analysed by Analyst 1.4.2, Bioanalyst 1.4 (all AB SCIEX) and Mascot (Matrix Science). Ac-K residues were validated by i) Information Dependent Acquisition (IDA), ii) Precursor Ion Analysis and iii) MIDAS (Multiple reaction monitoring-Initiated Detection And Sequencing)

A) Mascot scores of Ac-K residues upon APC3 by i) IDA, ii) precursor ion analysis and iii) MIDAS. Should an acetyl-lysine residue not be identified by a particular analytical method, this is denoted by "-".

B) MS/MS spectrum showing identification of APC3 Ac-K336. The acetylated lysine is shown in red font, and the Immonium (-NH3) ion with m/z peak 126.1 is shown by a red arrow.

7.3. Mutation of K336 reduces the acetylation of APC3 *in vitro* by CBP and p300

Following the identification of Ac-K336 within APC3 *in vivo* (Figure 3.3) it was deemed important to establish whether this specific lysine residue was a target for p300-mediated acetylation. Given that another HAT, CBP, is known to function cooperatively with p300, it was important to ascertain whether CBP could also acetylate APC3 K336 (Kalkhoven 2004, Wang, Marshall et al. 2013). Accordingly, K336 was mutated to an arginine residue (K336R) in order to ablate acetylation, and expressed as a GST-fusion protein (Figure 3.4Aii). A GST-APC3 fragment containing this K336 residue, Fr2 (APC3 residues 206-411), was also created. *In vitro* acetyltransferase assays using immunopurified CBP and p300 were duly performed upon both full-length (FL) and Fragment 2 (Fr2) GST-APC3 K336wt and K336R.

Both full-length and fragment 2 of GST-APC3 K336wt were acetylated *in vitro* by p300 (Figure 3.4B) and CBP (Figure 3.4C). Intriguingly, mutation of K336 to K336R reduced the level of APC3 acetylation mediated by both p300 and CBP appreciably, relative to K336wt (Figure 3.4B, C). These data indicate that K336 in APC3 is a major site for both CBP- and p300- directed acetylation *in vitro*. However, as mutation of K336 to an arginine did not ablate acetylation completely, other acetylation sites are likely to exist within GST-APC3, particularly within Fragment 2. Consistent with these data K396, K400 and K411 within APC3 were all shown to be acetylated *in vivo* (Figure 3.3A).

Together, these data demonstrate that APC3 is acetylated *in vivo*, and that APC3 is an *in vitro* substrate for both CBP- and p300-directed acetylation. These suggest that CBP/p300 could play a role in the post-translational regulation of APC3, and therefore the APC/C, *in vivo*.

A

```
i)                F  R  V  L  Q  S  V  A  R  I  G  Q  T  G  T  K  S  V  F  S
K336wt   961   tttcgtgttttacagtctgttgccagaatcggccaaactggaacaaagtctgtcttctca  1020
               ||||||||||||||||||||||||||||||||||||||||||||| ||||||||||||||
K336Q    961   tttcgtgttttacagtctgttgccagaatcggccaaactggaacacagtctgtcttctca  1020
                F  R  V  L  Q  S  V  A  R  I  G  Q  T  G  T  Q  S  V  F  S

ii)               F  R  V  L  Q  S  V  A  R  I  G  Q  T  G  T  K  S  V  F  S
K336wt   961   tttcgtgttttacagtctgttgccagaatcggccaaactggaacaaagtctgtcttctca  1020
               ||||||||||||||||||||||||||||||||||||||||||||  ||||||||||||||
K336R    961   tttcgtgttttacagtctgttgccagaatcggccaaactggaacacggtctgtcttctca  1020
                F  R  V  L  Q  S  V  A  R  I  G  Q  T  G  T  R  S  V  F  S
```

B

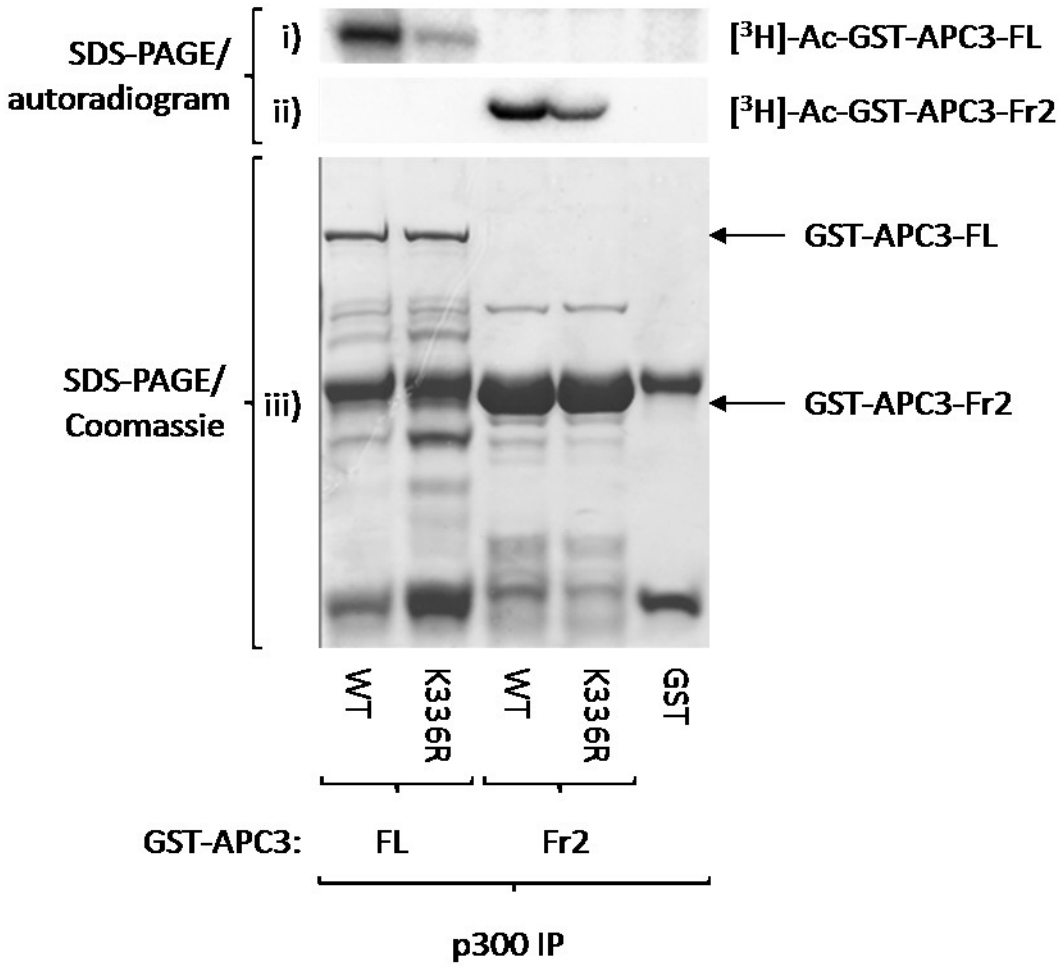

C

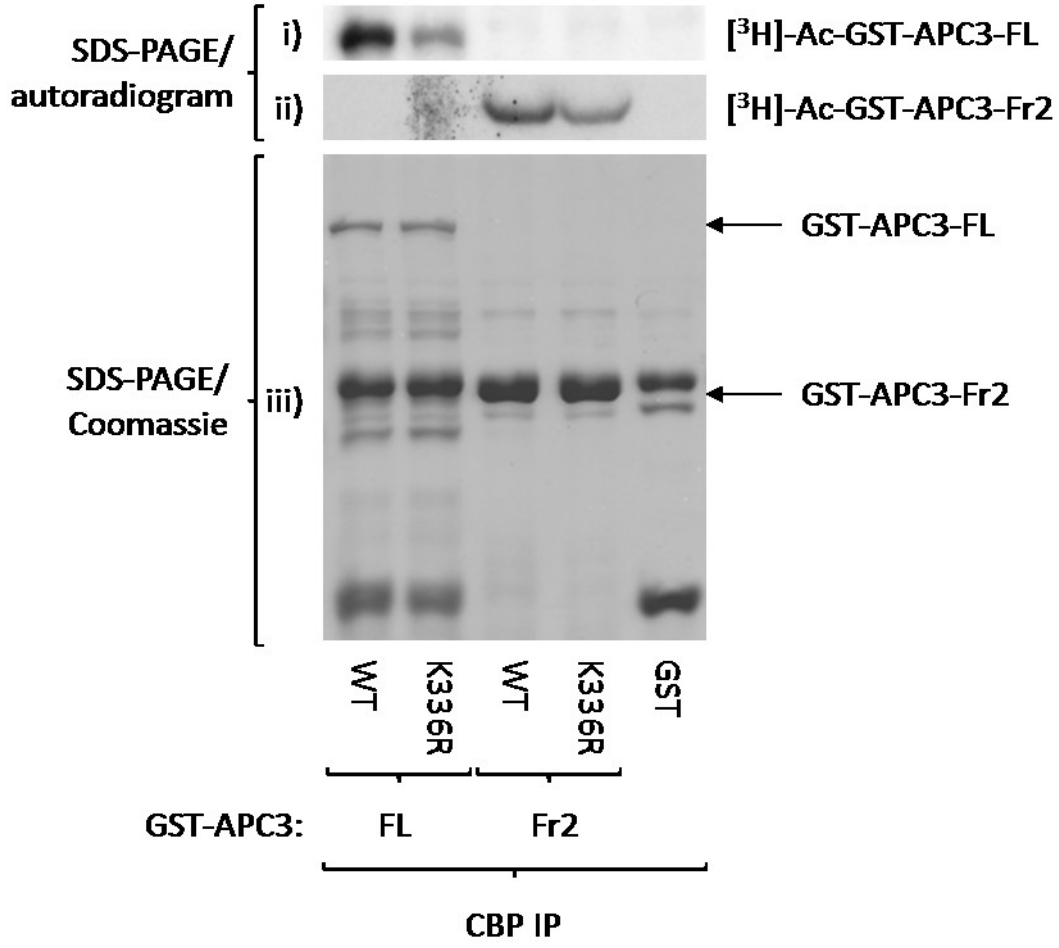

Figure 3.4 – APC3 K336R mutants exhibit decreased acetylation by CBP and p300 *in vitro*

APC3 K336 was mutated to a Q (i) or R (ii) by Quikchange Site-Directed Mutagenesis Kit (Agilent) (**A**). Both Full-length (FL) APC3 K336wt and K336R and a fragment of APC3 containing K336 (Fr2; Amino acids 206-411) were expressed in bacteria and 10µg used as a substrate for *in vitro* acetyltransferase assays by immunopurified p300 (**B**) or CBP (**C**) together with 0.5µCi [^{3}H]-Ac-CoA (Amersham). Autoradiography exposures for full-length GST-APC3 are shown in (i), and for Fragment 2 in (ii). The GST-fusion peptides are displayed as a Coomassie-stained SDS-PAGE gel in (iii).

7.4. APC3 interacts with CBP directly through the HAT domain of CBP

As CBP has been shown to acetylate APC3 *in vitro* (Figure 3.4C), we next wished to determine whether these two proteins can interact directly. As such GST-APC3 was tested for its ability to bind *IVT*-[^{35}S]-CBP by GST pull-down (Figure 3.5A). Both GST-APC3 and the positive control, adenovirus E1A, were shown to bind [^{35}S]-CBP (Figure 3.5A). These data indicate that APC3 and CBP interact directly.

In order to map the sites of interaction upon CBP, a series of GST-CBP fragments were synthesised and incubated with *IVT*-[^{35}S]-APC3 (Figure 3.5B). The only fragment in which autoradiography was detected upon incubation with [^{35}S]-APC3 was Fragment 5 (1460-1891aa) (Figure 3.5Bi), which corresponds to the HAT domain and the cysteine/histidine-rich zinc finger domains C/H2 and C/H3 (Figure 3.5Biii). Interestingly, APC5 and APC7 were also shown to interact with CBP through these domains (Turnell, Stewart et al. 2005). However, APC5 and APC7 also bound to the N-terminal region of CBP, containing the E4 and C/H1 domains, whereas APC3 did not (Figure 3.5Bi, iii) (Turnell, Stewart et al. 2005). It is therefore possible that the function of the CBP-APC3 interaction differs from that of the CBP-APC5/APC7 interaction.

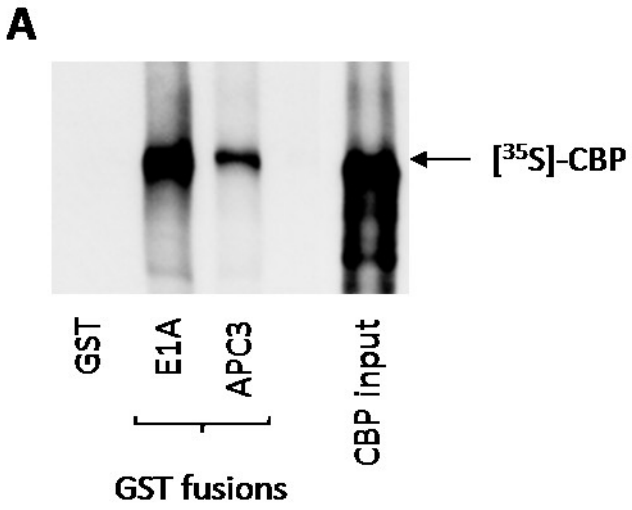

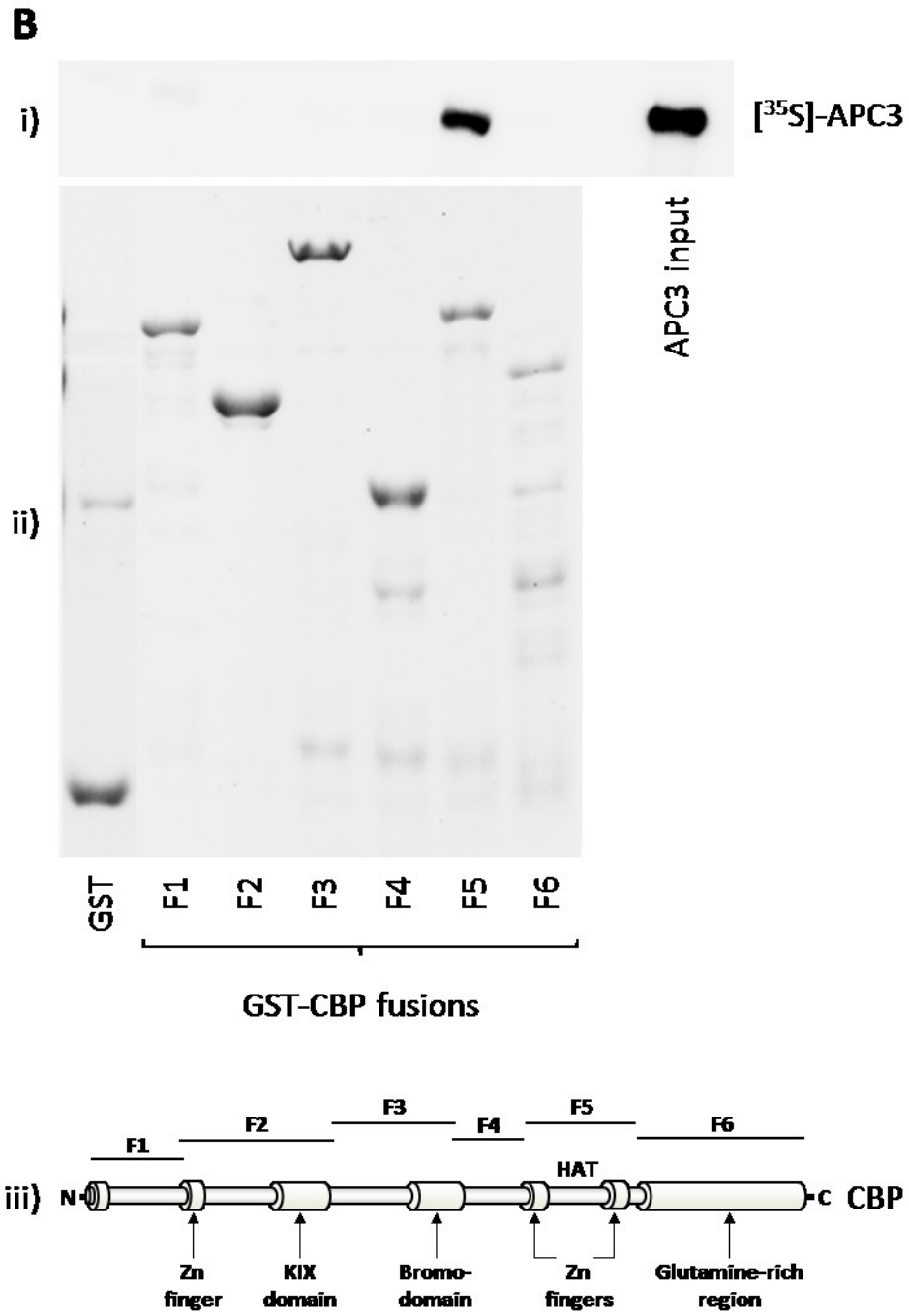

Figure 3.5 – APC3 binds to CBP *in vitro* through its HAT activity domain

10µg of bacterially-expressed GST-fusion proteins were incubated with 10µl *IVT*-[^{35}S]-APC3 or -[^{35}S]-CBP on ice, followed by the addition of glutathione-agarose beads. These were washed, separated by SDS-PAGE, dried and detected by autoradiography. **A)** Interaction of GST-E1A and GST-APC3 with [^{35}S]-CBP. **Bi)** Interaction of [^{35}S]-APC3 with GST-CBP fragments. **Bii)** Coomassie-stained SDS-PAGE gel showing GST-CBP fragments, with the domains contained in each fragment shown in **Biii)**. The amino acids corresponding to the CBP fragments are F1 (1-451), F2 (451-720), F3 (721-1100), F4 (1099-1460), F5 (1460-1891) and F6 (1892-2441).

7.5. Depletion of CBP impairs the ability of APC3 and Acetyl-Lysine to co-IP each other reciprocally

Given that APC3 can be acetylated *in vitro* by CBP and p300 (Figures 3.1, 3.2, 3.4), it was next investigated whether this correlated to acetylation of APC3 *in vivo*. As such, A549 cells were depleted of p300 or CBP by RNA interference and the ability for Ac-K and APC3 to co-IP each other reciprocally was tested (Figure 3.6).

The ability of Ac-K antibodies to IP APC3 was unchanged following knockdown of p300 compared to the non-silencing control (Figure 3.6i). However, upon ablation of CBP expression, the ability of Ac-K to co-IP APC3 was severely compromised (Figure 3.6i). This was also reflected in the diminished Ac-K band within the APC3 IP from CBP-knockdown cells, denoted by an arrow, which due to its size and the result in Figure 3.6i, is believed to be APC3 (Figure 3.6ii). Although one possible conclusion is that the ability of Ac-K to co-IP APC3 is imparted by its physical interaction with CBP, the presence of other bands within the APC3 IP and Ac-K blot suggests this particular inference would be incorrect, as it implies other proteins co-IP'ing with APC3, such as other APC/C subunits, were also acetylated.

Interestingly, this result correlates positively with previous results, in which knockdown of CBP, but not p300, reduced APC/C E3 ubiquitin ligase activity *in vitro* and stabilised known substrates (Turnell, Stewart et al. 2005). These data suggest that the ability of CBP to modulate APC/C activity is mediated by its acetylation of APC3.

Although the knockdown of p300 did not prevent the reciprocal IP of Ac-K and APC3, this does not necessarily mean that p300 cannot acetylate APC3 *in vivo*. The decrease in APC3 acetylation exhibited following knockdown of CBP might suggest that most acetylation upon APC3 is mediated by CBP, though it is still possible that other HATs, such as p300, could also acetylate APC3.

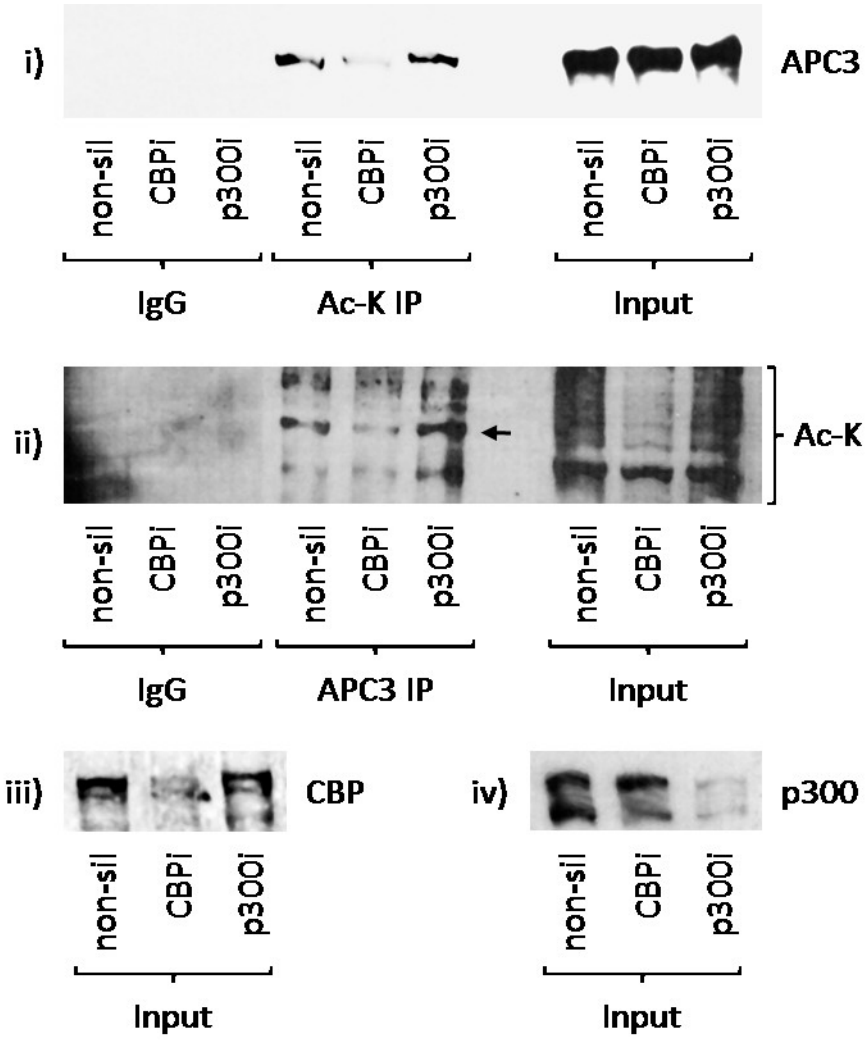

Figure 3.6 – siRNA-mediated knockdown of CBP, but not p300, reduces APC3/Ac-K reciprocal co-IPs

A549 cells were subjected to siRNA-mediated knockdown of either CBP or p300, or a non-silencing control (non-sil) for 72h before harvesting. Ac-K IPs and Western blots for APC3 (i) or APC3 IPs and Western blots for Ac-K (ii) were performed. Validation of CBP and p300 knockdown is shown in (iii) and (iv), respectively. The arrow in the Ac-K blot represents a distinct band of around 95kDa which is depleted following CBP knockdown and APC3 IP.

7.6. Investigating the biological consequences of APC3 Ac-K336

In order to determine the biological consequences of APC3 acetylation *in vivo*, cell lines were created whereby an shRNA complementary to APC3 was cloned into U2OS cells under the control of a Tet-responsive promoter. As such, treatment of these APC3 shRNA-expressing cells with doxycycline (Dox) permitted the expression of APC3 shRNA and the consequent reduction in APC3 expression (Figure 3.7A). In order to study the role of site-specific APC3 acetylation, it was anticipated that these APC3 shRNA-expressing cells would be transfected transiently with an shRNA-resistant APC3 plasmid containing the K336 mutations (Figure 3.7C). Knockdown and repletion of shRNA-resistant APC3 was considered the appropriate approach to investigate site-specific functions of APC3, as APC3 is incorporated into the APC/C as a homodimer (Zhang, Chang et al. 2013). As such, transient transfection of a mutant without knockdown of endogenous APC3 would not necessarily result in the exclusive incorporation of a mutant APC3 into the APC/C holoenzyme, and therefore any phenotype might be masked, unless the mutant is dominant-negative.

To generate the inducible APC3 shRNA U2OS cells, two different shRNAs complementary to the mRNA sequence of APC3 were therefore incorporated into a viral vector and transfected into U2OS cells expressing the Tet Repressor protein (U2OS-TetR). As cells expressing shRNA1 exhibited better knockdown than shRNA2 and display slight elevation in Cyclin B1 levels (Figure 3.7A), these were selected to produce monoclonal populations.

Although selected clones showed efficient knockdown (Figure 3.7B), this did not correlate with the typical APC/C inhibitory phenotype expected. As such, there was no increase in the protein levels of known substrates such as Cyclin B1 (Figure 3.7B) and there was no effect on cell cycle distribution (data not shown). Indeed, despite numerous repeats at varying dosage and incubation time of Dox and the testing of a large number of clones, a suitable cell line could not be established.

An alternative approach was therefore adopted; HeLa cells containing FRT recombination sites were acquired (HeLa-FRT), into which an siRNA-resistant APC3 was inserted under the control of a co-transfected cDNA, from which exogenous Flp recombinase was expressed. These cells were made resistant to APC3 siRNA by changing the nucleotide sequence complementary to the siRNA without changing the amino acid sequence (Figure 3.7C). Endogenous APC3 was then knocked-down by siRNA, thereby ensuring expression of the siRNA-resistant form only. Accordingly, siRNA-resistant forms of APC3 were created (Figure 3.7C), expressing either K336wt, the acetylation-mimetic K336Q (Figure 3.4i) or the acetylation-null K336R (Figure 3.4Aii). These siRNA-resistant APC3 plasmids were then attempted to be incorporated into HeLa-FRT cells; however, this proved to be exceedingly toxic to the cells and resulted in considerable cell death, and those that survived soon died after antibiotic selection. This process was also attempted by others, both based within our group and those of collaborating groups, with identical results.

Unfortunately therefore, despite considerable effort, we were not able to address the biological role of site-specific APC3 acetylation directly. Although not ideal, future studies will focus on investigating the effects of transient APC3 K336wt, K336Q and K336R transfection, using siRNA-resistant APC3 coupled with siRNA-mediated knockdown of endogenous APC3. Although this technique would inevitably be more variable between experiments and be clouded by incomplete knockdown, as well as theoretically being more toxic, than either of the techniques described above, it appears to be the most logical approach remaining.

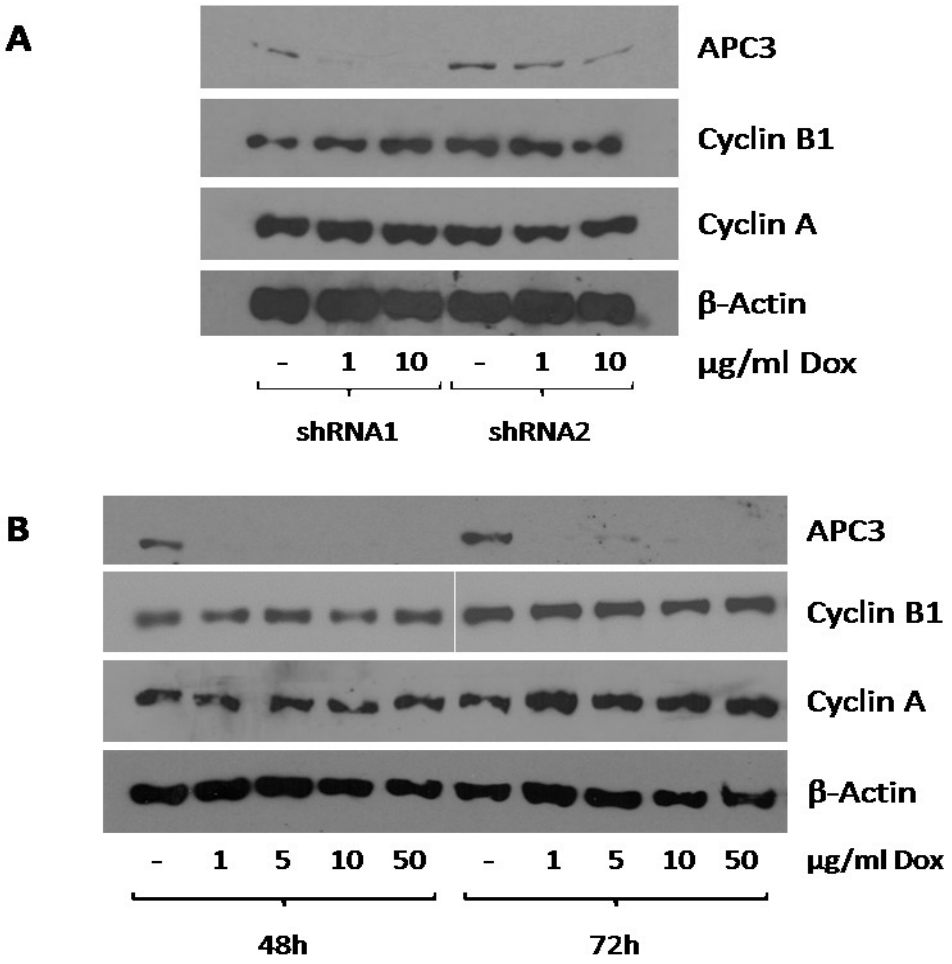

C

```
                  Q  S  G  N  S  R  E  V  T  P  I  L  A  Q  T  Q  S  S  G
APC3 wt           cagagtggaaatagccgagaggtaactccaattcttgcacaaacacaaagttctggt  1077
                  ||||||||||| | | ||||||||||||||||||||||||||||||||||||||
APC3 siRNA resis  cagagtggaaactccagggaggtaactccaattcttgcacaaacacaaagttctggt  1077
                  Q  S  G  N  S  R  E  V  T  P  I  L  A  Q  T  Q  S  S  G
```

Figure 3.7 – Generation of Dox-inducible APC3 shRNA cell lines and siRNA-resistant APC3 cDNA

Two oligo shRNA sequences complementary to APC3 (shRNA1 and shRNA2) were annealed and cloned into pSUPERIOR.retro.puro (Oligoengine), which was transfected into 293FT viral packaging cells. The viral progeny were harvested from the medium after 48h, filtered, and used to infect U2OS-TetR cells overnight. Stable transfections were selected with puromycin and established as polyclonal population, from which monoclonal cell lines were picked.

A) Polyclonal APC3 shRNA1 and shRNA2 were treated with the denoted dosage of Dox for 48h prior to harvesting. Protein expression was detected by Western blotting with the antibodies described.

B) Example of a monoclonal population established from U20S-TetR-APC3 shRNA1 cells. Cells were treated with Dox at the described dosages for either 48h or 72h. Protein expression was detected by Western blotting with the denoted primary antibodies.

C) Sequence of siRNA-resistant APC3 cDNA, with mutations conferring resistance highlighted in red

7.7. The APC/C holoenzyme is pulled-down with Acetyl-Lysine IPs.

Evidence presented within this chapter has established that APC3 is acetylated *in vivo* (Figures 3.3, 3.6), and that it can be acetylated by CBP and p300 *in vitro* (Figure 3.1, 3.2, 3.4, 3.6). However, it is unknown whether this acetylated form of APC3, or indeed other APC/C subunits, are incorporated in the APC/C holoenyzme.

To investigate this, the ability of antisera against an acetyl-lysine (Ac-K) epitope to co-IP APC/C subunits was examined. As such, Ac-K IPs from asynchronous A549 lysates were screened for APC/C subunits by SDS-PAGE and Western blotting (Figure 3.8).

Interestingly, multiple APC/C subunits were detected within Ac-K IPs, including APC3, APC5, Cdc20 and Cdh1 (Figure 3.8A). The ability of the Ac-K IPs to support the ubiquitylation of Cyclin B1 *in vitro* was also tested (Figure 3.8B). Although Ac-K IPs precipitate a number of APC/C subunits, and therefore potentially the APC/C holoenzyme (Figure 3.8A), they were unable to support the *in vitro* ubiquitylation of [^{35}S]-Cyclin A and [^{35}S]-Cyclin B1 when incubated with E1, E2s, ubiquitin and an ATP regeneration system (Figure 3.8B).

The simplest interpretation of these data is that one or more APC/C subunits within the APC/C holoenzyme are modified by directly by acetylation. Alternatively, it could be that multiple APC/C subunits are acetylated regardless of their association with the APC/C, or the APC/C holoenzyme interacts with an acetylated binding protein.

A

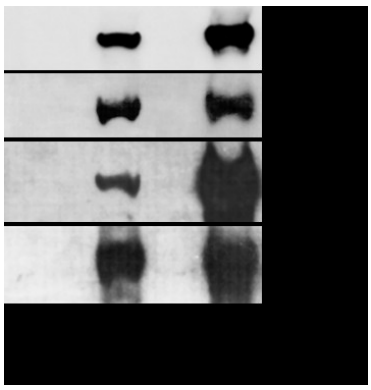

B

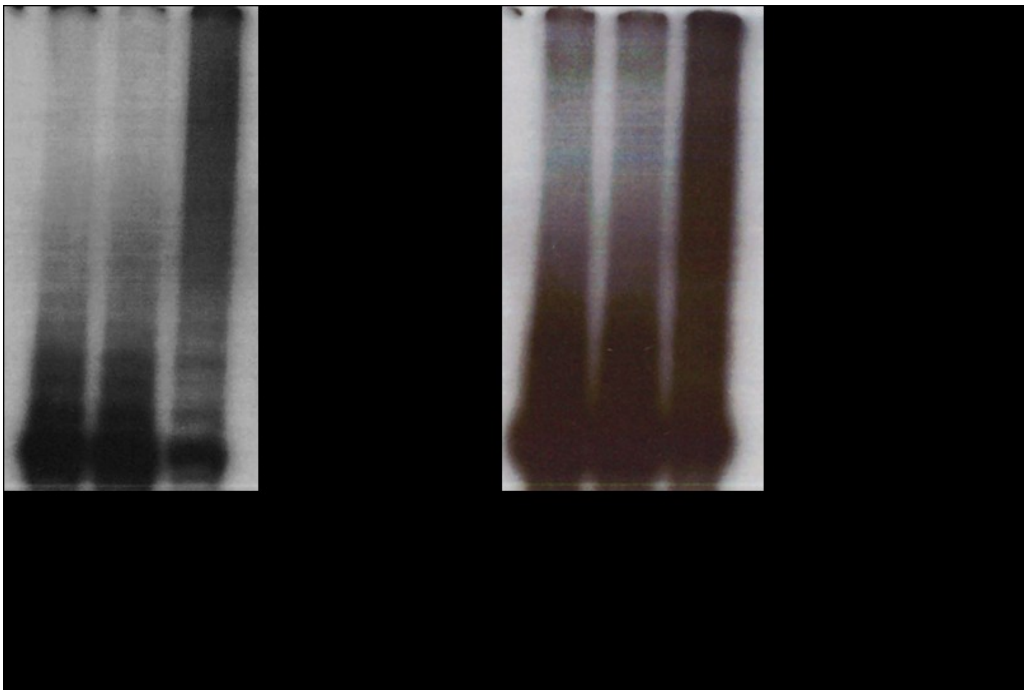

Figure 3.8 – Acetyl-lysine IPs precipitate the APC/C holoenzyme, but cannot support *in vitro* APC/C E3 ubiquitin ligase activity

A) Asynchronous A549 cells were lysed in NETN and incubated with 5µg Acetyl-lysine (Ac-K) or normal IgG control antibodies overnight followed by the addition of 10µl packed Protein G-agarose beads for 3h. The IPs were washed, boiled, separated by SDS-PAGE and interacting proteins detecting by Western blotting with the designated antibodies.

B) IPs were performed using Ac-K, APC3 or normal IgG antibodies upon asynchronous A549 cells. The IP was then incubated in the presence of rabbit E1, human UbcH4, UbcH5 and UbcH10, an ATP regeneration buffer, and 1µl *IVT* [^{35}S]-Cyclin A or [^{35}S]-Cyclin B1 for 1h at 37°C. The mixture was then separated by SDS-PAGE and polyubiquitylation detected by autoradiography as a progressive increase in size, visualised as a smear.

7.8. The APC/C is preferentially acetylated in interphase

In Figure 3.8, it was determined that Ac-K IPs could pull-down the APC/C holoenzyme from asynchronous A549s. Given that phosphorylation of the APC/C is under cell cycle control, such that mitotic kinases phosphorylate the APC/C during G2/M, and mitotic phosphatases dephosphorylate the APC/C during late mitosis, it was next investigated whether acetylation of the APC/C is similarly regulated in a temporally-coordinated manner.

Therefore, the ability of α-Ac-K antibodies to co-IP the APC/C holoenzyme was compared between asynchronous cells and cells arrested in prometaphase by overnight treatment with nocodazole. Interestingly, the αAc-K antibodies were able to co-IP APC3, APC5 and APC7 from both asynchronous and mitotic cells, however the co-IPs were more efficient from asynchronous cells than mitotic cells (Figure 3.9). These data suggest that the APC/C is either more acetylated during interphase than in mitosis, or associates with more acetylated proteins in interphase. Interestingly, the APC3 recognised by α-Ac-K antibodies during mitosis appears to be the non-phosphorylated form, as it did not exhibit the characteristic gel shift akin to mitotically phosphorylated APC3.

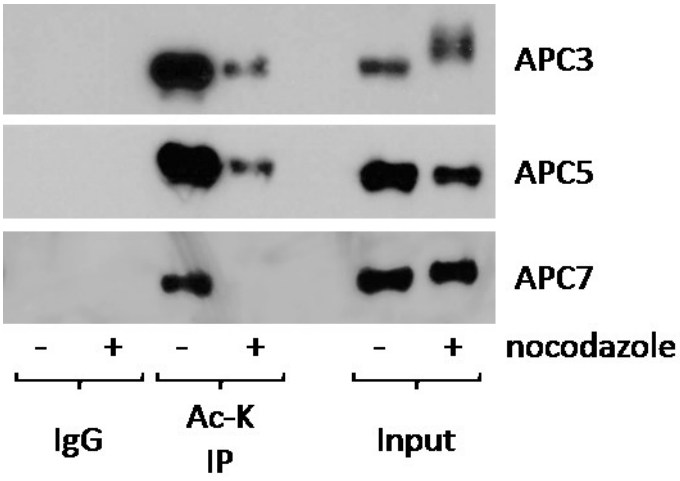

Figure 3.9 – Ac-K co-IPs more APC3, APC5 and APC7 from asynchronous lysates than mitotic lysates.

A549 cells were either grown asynchronously, or arrested in prometaphase with 400ng/ml nocodazole for 20h. Proteins concentrations were normalised prior to IP overnight with antisera against Ac-K or a normal IgG control. Protein G-agarose was added for 2h, and the IPs washed, boiled and separated by SDS-PAGE. The amount of co-IP'ing protein was determined by Western blotting with the designated antibodies.

7.9. The acetylation pattern upon APC/C subunits varies during mitotic progression

During nocodazole-induced mitotic arrest, the SAC is active, and as such represses APC/C activity through the sequestration and degradation of Cdc20 (Pan and Chen 2004, Nilsson, Yekezare et al. 2008, Ge, Skaar et al. 2009, Kulukian, Han et al. 2009, Primorac and Musacchio 2013). The APC/C is then activated upon SAC satisfaction, whereupon it degrades its target substrates in order to promote sister chromatid separation and mitotic exit (Peters 2006, Pines 2011, Primorac and Musacchio 2013). As the data presented in Figure 3.9 suggested that the APC/C is more acetylated in interphase than in mitosis, it was hypothesised that site-specific acetylation/deacetylation cycles

upon specific APC/C subunits, akin to phosphorylation/dephosphorylation, could regulate APC/C activity during SAC activation and upon SAC satisfaction.

As such, the APC/C acetylome was investigated throughout mitosis and into the next cell cycle phase. Although previous mass spectrometric analyses utilised A549 cells, for this experiment HeLa cells were used. This was because the biological function of specific identified acetyl-lysine residues were to be investigated by mutation and incorporation into FRT cells (documented above); however, A549-FRT cells were not available, whereas HeLa-FRTs were. Accordingly, HeLa cells were either grown asynchronously, or arrested in prometaphase by nocodazole, then incubated in fresh medium, in the absence of nocodazole, and allowed to pass through mitosis and re-enter G1. APC3 IPs were then performed at appropriate time points post-release to pull-down the APC/C holoenzyme, which was then analysed for acetylation by LC-MS/MS (Figure 3.10). Rather than published mass spectrometric studies, which utilised Ac-K IPs to determine a cellular acetylome (Choudhary, Kumar et al. 2009, Chuang, Lin et al. 2010, Zhao, Xu et al. 2010), the decision was made to focus upon the APC/C. By IP'ing the APC/C the samples were considerably simplified, thereby greatly increasing the likelihood of identifying PTMs and low abundance peptides.

Interestingly, this experiment determined that multiple APC/C subunits were acetylated *in vivo*, and that this acetylation pattern was dynamic, such that certain Ac-K residues were only seen at specific times within the cell cycle (Figure 3.10). Although the diminished ability of Ac-K IPs to co-IP APC/C subunits in mitosis suggests that the APC/C is more acetylated in interphase than nocodazole-arrested cells (Figure 3.9), this might not necessarily be the case; the mass spectrometric analysis provided many putative acetylation sites which were detected in mitotic extracts only (Figure 1.10). However, it is important to note that synchronising cells would enrich for any PTMs present during that particular time. As such, the likelihood of identifying mitotic-specific acetylation is greater in synchronised cells than asynchronous, despite a small proportion of asynchronous cells being in

mitosis. Therefore, the absence of positive identification of Ac-K residues does not necessarily mean that these residues are not acetylated at some point *in vivo*. It is more likely that acetylation was below the level of detection required for this experiment.

Moreover, the difference between Figures 3.9 and 3.10 might also be explained by the availability of Ac-K residues to be identified. In Figure 3.9, Ac-K IPs relied upon the Ac-K residue residing upon an external surface of the APC/C holoenzyme and being accessible to the antibody. Conversely, mass spectrometers fragment individual tryptic peptides, and, as such, have access to the entire length of each subunit. However, MS/MS requires a tryptic peptide to exist at a suitable size and m/z ratio for analysis, and therefore one does not get full sequence coverage over the APC/C subunits, which could result in Ac-K residues being present in peptides which are not fragmented by the mass spectrometer.

One interesting observation following the *in vivo* mass spectrometry data is that many of the Ac-K residues reside upon TPR subunits of the APC/C: APC3, APC5, APC6, APC7 and APC8. This correlates with the *in vivo* phosphorylation data described by several independent studies (Kraft, Herzog et al. 2003, Dephoure, Zhou et al. 2008, Steen, Steen et al. 2008, Malik, Lenobel et al. 2009, Olsen, Vermeulen et al. 2010, Hegemann, Hutchins et al. 2011, Kettenbach, Schweppe et al. 2011, Shiromizu, Adachi et al. 2013, Zhou, Di Palma et al. 2013). Interestingly, the APC8 Ac-K454 residue is homologous to the K481 residue upon Cut23 in *S. pombe*, which has previously shown to be acetylated *in vivo* (Kimata, Matsuyama et al. 2008).

Although this particular experiment identified a number of acetylation sites upon a number of APC/C subunits, including APC3, it is intriguing that the APC3 acetylation sites identified in earlier experiments which used a different LC-MS/MS protocol and machine (Figure 3.3) were not identified within this screen (Figure 3.6A, 3.10). It could be that this was a cell-specific phenomenon, or as a result of the lower tolerance permitted by greater mass accuracy and resolution of the ESI-TOF over

the Q-TRAP. It is important to note, however, that the presence of immonium ions with m/z ratio of 126.1 could not be detected by the ESI-TOF, as this value was below the lower limit for which the ESI-TOF was calibrated, and therefore precursor ion analysis could not be performed.

A

	Ac-K	AS	0h	1h	2h	4h	8h
APC1	K429	-	-	-	-	-	27.8
	K463	-	-	-	37.6	24.2	-
	K640	-	-	24.1	24.2	25.0	-
	K1709	55.3	-	-	-	-	-
APC3	K56	-	-	-	-	-	22.5
	K62	43.0	24.2	36.2	21.4	-	21.5
	K133	-	-	-	25.3	-	-
	K415	-	-	-	-	20.4	-
	K564	52.1	59.1	34.6	26.3	34.8	-
	K647	28.6	-	-	-	-	-
	K660	37.8	38.6	33.9	24.4	38.8	42.8
APC5	K167/K168^	50.7	34.5	47.8	37.9	-	-
	K289	38.4	31.6	32.9	31.3	31.9	36.7
	K562	20.4	-	27.4	-	25.5	-
	K669	-	21.7	-	-	-	-
APC6	K101	-	-	35.8*	-	-	27.0
	K129	-	-	30.9	-	-	25.6
	K138	55.5	20.2	28.0	25.5	21.5	35.6
	K154	26.1	25.9	28.9	-	-	28.4
	K325	29.6	-	-	-	-	-
APC7	K230	-	-	-	54.0	-	-
	K259	29.0	-	-	-	28.5	-
APC8	K97	-	-	-	28.3	-	-
	K113	-	28.4	35.9**	22.7	-	-
	K359	-	25.7	-	-	35.3	25.0
	K396	-	29.1	26.7	36.5	32.4	-
	K454	-	-	-	-	-	50.4
	K475	-	-	-	-	23.3	-
APC10	K6	20.3	-	20.7	20.4	-	20.2

B

i) APC8 Ac-K359 Peptide Sequence: ALK*LNPR

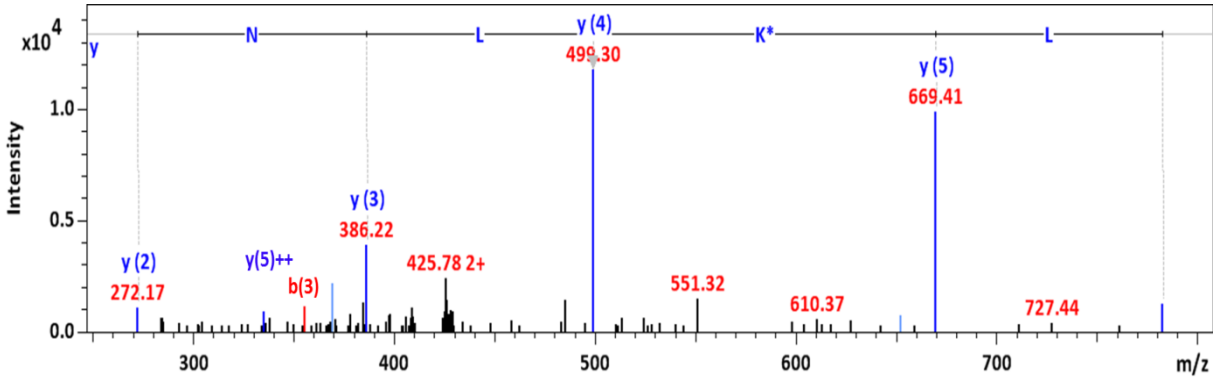

ii) APC8 Ac-K396 Peptide Sequence : HAIEVNK*R

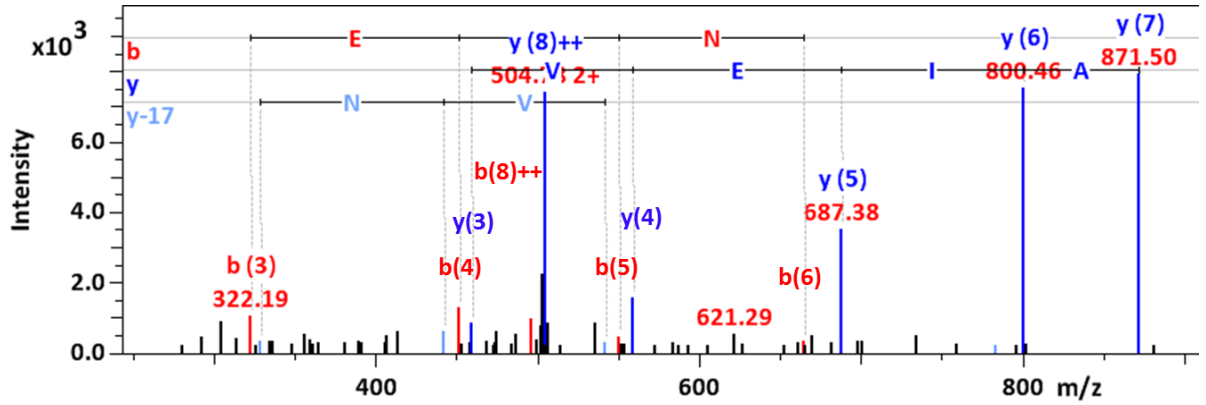

Figure 3.10 – Mass spectrometric identification of Ac-K residues within APC/C subunits during mitosis

HeLa cells were either grown asynchronously (AS) or arrested in 400ng/ml nocodazole for 20h. Cells arrested in mitosis were harvested by mechanical shake-off and released into fresh growth medium for the time indicated (0, 1, 2, 4, 8h) prior to harvesting and IP with α-APC3 antibodies. IPs were washed and separated by SDS-PAGE. The gel was stained with colloidal Coomassie, and subjected to in-gel tryptic digestion. Briefly, bands were washed, reduced, alkylated and dried prior to incubation with sequence-grade modified trypsin in 10% (v/v) AcN/40mM ABC for 16h at 37°C. Tryptic peptides were eluted in 3% FA and dried. Tryptic peptides were then resuspended in 1% (v/v) AcN/1% (v/v) FA and analysed by LC-MS/MS upon an Impact ESI-TOF mass spectrometer (Bruker) and searched using ProteinScape (Bruker) against a Mascot database (Matrix Science). Acetyl-lysine residues were identified and, where necessarily, validated manually.

A) Mascot scores of all Ac-K residues identified within APC/C subunits. AS=asynchronous. 0-8h denotes the time following release from nocodazole-mediated arrest. (^ The Ac-K in APC5 K167/K168 is present upon one of these two lysines, however it was impossible to differentiate between the two. * Another peptide containing Ac-K101 in APC6 was identified within the 1h sample with Mascot

score 21.8. ** Another peptide containing Ac-K113 in APC8 was identified within the 1h sample with Mascot score 28.7). Ac-K not identified within a specific time point are denoted by "-".

B) Extracted Ion Chromatograms for APC8 K359 (i) and K396 (ii). K* denotes the acetylated lysine.

7.10. Mutational analysis of APC8 K359 and K396

Two APC8 Ac-K residues which were assigned with particularly high confidence, K359 and K396, were found in mitotic, but not asynchronous cells (Figure 3.10B). As APC8 functional studies have been performed successfully previously using an siRNA-resistant APC8 species (Izawa and Pines 2011, Sedgwick, Hayward et al. 2013), we resolved to investigate the function of APC8 acetylation. As such, an siRNA-resistant 3xFlag-APC8 cDNA cloned into the Flp-in vector, pcDNA5-FRT, had its K359 or K396 residue mutated to a Q or R to mimic or ablate acetylation, accordingly (Figure 3.11). We have recently generated polyclonal cell lines that possess these specific APC8 mutations. Unfortunately however, time restraints meant that we were unable to investigate the biological consequences of APC8 acetylation during this study. However, we have generated an important resource that shall be used in the future to determine whether APC8 acetylation modulates APC/C ubiquitin ligase activity against known substrates, affects APC/C interaction with activators or MCC components, or affects cell cycle progression.

A

```
                          S  S  Y  I  V  S  Q  I  A  V  A  Y  H  N  I  R  D  I
APC8 wt              784 agctcgtatattgtttcccaaattgcagttgcctatcacaatatcagagatatt  837
                         |||||||||||||||||||||||||||||||| || || ||||||||||||||
APC8 siRNA resis2    784 agctcgtatattgtttcccaaattgcagttgcttaccataatatcagagatatt  837
                          S  S  Y  I  V  S  Q  I  A  V  A  Y  H  N  I  R  D  I

                           E  K  A  A  L  Y  F  Q  R  A  L  K  L  N  P  R  Y
APC8 wt              1042 gagaaagcagccttatatttccagagagccctgaaattaaatcctcggtat  1092
                          |||||||||||||||||||||||||||||||| | || || ||||||
APC8 siRNA resis1    1042 gagaaagcagccttatatttccagagagccctgaaactgaaccccggtat  1092
                           E  K  A  A  L  Y  F  Q  R  A  L  K  L  N  P  R  Y
```

B

```
                Y  S  L  R  S  Q  H  E  K  A  A  L  Y  F  Q  R  A  L  K  L
K359wt   1021 tacagtttacgttctcagcatgagaaagcagccttatatttccagagagccctgaaactg  1080
              ||||||||||||||||||||||||||||||||||||||||||||||||||||||| |||||
K359Q    1021 tacagtttacgttctcagcatgagaaagcagccttatatttccagagagccctgcaactg  1080
                Y  S  L  R  S  Q  H  E  K  A  A  L  Y  F  Q  R  A  L  Q  L

                Y  S  L  R  S  Q  H  E  K  A  A  L  Y  F  Q  R  A  L  K  L
K359wt   1021 tacagtttacgttctcagcatgagaaagcagccttatatttccagagagccctgaaactg  1080
              |||||||||||||||||||||||||||||||||||||||||||||||||||||||| ||||
K359R    1021 tacagtttacgttctcagcatgagaaagcagccttatatttccagagagccctgagactg  1080
                Y  S  L  R  S  Q  H  E  K  A  A  L  Y  F  Q  R  A  L  R  L

                T  S  A  A  I  Q  A  Y  R  H  A  I  E  V  N  K  R  D  Y R
K396wt   1141 acgtctgctgctatccaggcttatagacatgccattgaggtcaacaaacgggactacaga  1200
              |||||||||||||||||||||||||||||||||||||||||||||||| ||||||||||||||
K396Q    1141 acgtctgctgctatccaggcttatagacatgccattgaggtcaaccaacgggactacaga  1200
                T  S  A  A  I  Q  A  Y  R  H  A  I  E  V  N  Q  R  D Y  R

                T  S  A  A  I  Q  A  Y  R  H  A  I  E  V  N  K  R  D Y  R
K396wt   1141 acgtctgctgctatccaggcttatagacatgccattgaggtcaacaaacgggactacaga  1200
              |||||||||||||||||||||||||||||||||||||||||||||||| ||||||||||||||
K396R    1141 acgtctgctgctatccaggcttatagacatgccattgaggtcaacagacgggactacaga  1200
                T  S  A  A  I  Q  A  Y  R  H  A  I  E  V  N  R  R  D Y  R
```

Figure 3.11 – Mutation of siRNA-resistant APC8 K359 and K396 to Q or R

The siRNA-resistant 3xFlag-APC8-pcDNA5-FRT plasmid was provided by Jakob Nilsson, and the siRNA-resistant sequences are shown in **(A)**. The K359 and K396 residues within siRNA-resistant 3xFlag-APC8-pcDNA5-FRT were both mutated to a Q or R using PCR site-directed mutagenesis using the QuikChange kit (Agilent) according to manufacturer's recommendations **(B)**. 4.5µg of the Flp recombinase plasmid pOG44 was co-transfected with 0.5µg of siRNA-resistant 3xFlag-APC8-pcDNA5-FRT containing either K359/K396wt, K359Q, K359R, K396Q or K396R into HeLa-FRTs. DNA was mixed with OptiMEM (Life Technologies) to a total volume of 200µl and 10µl Lipofectamine 2000 (Life Technologies) mixed with 190µl OptiMEM for 5 min, then incubated together for 15 min before being added to cells incubated in 1.6ml OptiMEM. 48h later, cells were selected for positive clones with 1.5µg/ml Blasticidin (Source Bioscience) and 200µg/ml Hygromycin B (Life Technologies).

7.11. Discussion

Previous work has suggested that the APC/C subunit, APC8, might be acetylated in *S. pombe* (Kimata, Matsuyama et al. 2008). In this chapter, substantial evidence is presented to indicate that the human APC/C is acetylated *in vivo*. Mass spectrometric analyses of APC3 IPs revealed that numerous APC/C subunits were acetylated *in vivo*, and that these modifications were predominantly upon APC/C subunits that contain TPR motifs (Figure 3.3A, 3.10). This acetylation of the APC/C was dynamic, such that the precise pattern of acetylation varied between cell cycle phases. As such, α-Ac-K antibodies were able to co-IP the APC/C holoenzyme (Figure 3.8), and this phenomenon was more pronounced in asynchronous cells than in mitotic cells (Figure 3.9). Mass spectrometric analysis of APC3 IPs following a nocodazole-release time course demonstrated that different APC/C subunit lysine residues were acetylated at different times during mitosis (Figure 3.10).

Given that the APC/C has previously been identified to interact with CBP and p300 co-activators (Turnell, Stewart et al. 2005), it was postulated that these HATs could be responsible for the acetylation of the APC/C. To investigate this possibility, CBP and p300 *in vitro* acetyltransferase assays were performed in the presence of either the APC/C holoenzyme or GST-fusions of individual APC/C subunits (Figure 3.1, 3.2). These studies determined that APC3 was the most prominent target within the APC/C for CBP- and p300-mediated acetylation (Figure 3.2). However, the APC/C acetylation sites exhibited throughout mitosis were upon all TPR subunits and not just APC3, suggesting that further HATs act upon the APC/C *in vivo*, or that *in vitro* conditions are sub-optimal for acetyltransferase assays (Figure 3.10).

We also determined that, akin to APC5 and APC7, APC3 could also interact with CBP *in vitro* (Figure 3.5). Furthermore, CBP was shown to bind APC3 directly through its HAT domain (Figure 3.5). Interestingly, knockdown of CBP but not p300 repressed the ability of Ac-K to co-IP APC3 (Figure 3.6), suggesting that CBP is the main executor of APC3 acetylation *in vivo*.

The roles of site-specific APC/C lysine acetylations are currently being investigated. Initial attempts are focussing on APC3 K336, and APC8 K359 and K396, but over time it is anticipated that the role of other modifications will be investigated. Results presented herein have determined that CBP and p300 are less able to acetylate a GST-APC3 fusion protein where K336 has been mutated to R (Figure 3.4B, C). Cell lines are currently being established which express a dox-inducible siRNA-resistant version of Flag-APC3 containing either K, Q or R residues at amino acid-336, or Flag-APC8 containing either wt, Q or R at positions 359 or 396. Once monoclonal populations have been selected, these cells shall be tested for the incorporation of the Flag-tagged subunit into APC/C holoenzymes and for cell cycle effects. Then, endogenous APC3 or APC8, accordingly, shall be depleted by siRNA, and the siRNA-resistant form expressed by treatment with dox. The establishment of these cell lines will allow the effect of APC/C acetylation upon APC/C activity to be explored in detail. As such it will be important to investigate the ability of mutant APC/C to ubiquitylate known substrates and effect cell cycle progression, particularly the timing of passage through mitosis from NEBD through anaphase to cytokinesis and mitotic exit.

As discussed previously, PTMs such as phosphorylation can alter the tertiary structure of the APC/C, thereby altering its affinity for binding proteins, E2 enzymes and substrates. It is therefore possible that acetylation of the APC/C, mediated by CBP/p300, could impart similar structural changes within the APC/C and alter its affinity for interacting proteins or substrates; APC/C acetylation could therefore modulate APC/C function. Given that lysine residues are positively-charged, and that acetylation negates this charge, this could also assist in the promotion of the negative charge which facilitates E2 binding to the catalytic core of the APC/C. It would therefore be interesting to investigate the tertiary structure of the APC/C holoenzyme by X-ray crystallography and cryo-EM, as established by the Barford group (Chang, Zhang et al. 2014), following targeted acetylation and determine whether acetylation affects substrate, co-activator or E2 binding. In this regard it would

also be valuable to investigate the consequences of KQ and KR mutations upon APC/C structure, and how this also corresponds to substrate, co-activator and E2 binding.

Currently, the biological function of the acetylation of core APC/C subunits is unknown. Whilst acetylation of the co-activators, Cdc20 and Cdh1, has been shown to repress their association with the APC/C (Kim, Vassilopoulos et al. 2011), it is unknown whether acetylation of APC/C subunits results in its activation or inhibition, or as might be expected, be dependent upon the precise acetylation pattern upon the whole APC/C holoenzyme. It is interesting to note that phosphorylation of the APC/C is important in its Cdc20-mediated activation, whilst phosphorylation of Cdc20 or Cdh1 themselves is inhibitory (Zachariae, Schwab et al. 1998, Jaspersen, Charles et al. 1999, Kramer, Scheuringer et al. 2000, Rudner and Murray 2000, Kraft, Herzog et al. 2003, Steen, Steen et al. 2008, Labit, Fujimitsu et al. 2012, Primorac and Musacchio 2013). It is therefore attractive to draw a direct comparison between phosphorylation and acetylation, suggesting that the acetylation of APC/C subunits is an important event in its activation. Further evidence for this is the ability of Ac-K IPs to pull-down the APC/C holoenzyme, and that this is more prominent during interphase, in which more APC/C is active, than in prometaphase (Figure 3.8A).

Conversely, Ac-K IPs cannot support ubiquitylation of APC/C substrates *in vitro* (Figure 3.8B), despite pulling-down the APC/C holoenzyme (Figure 3.8A), suggesting that acetylated APC/C is inactive. However, given that the precise pattern of acetylation appears to change during mitotic progression, as the APC/C goes from being inhibited to becoming activated first by Cdc20 then by Cdh1, it is therefore feasible that acetylation could both activate and inhibit the APC/C, dependent upon the Ac-K residue targeted. Indeed, the ability of a single form of PTM to both activate and repress protein function is relatively commonplace, particularly with regard to regulating transcription; methylation of Histone H3K4 promotes gene transcription, whilst di- and tri-methylation upon H3K9 is associated with heterochromatin formation and gene silencing (Bártová, Krejcí et al. 2008). It is

therefore imperative that we perform siRNA/siRNA-resistant rescue experiments for individual APC/C acetylation sites in order to determine the biological consequences of site-specific APC/C subunit acetylation.

Given that a common set of APC/C subunits are subjected to both acetylation and phosphorylation it will be important to establish the precise functional relationship between these two modifications. In particular it will be important to determine the pattern of APC/C subunit PTMs during mitosis and other cell cycle phases, as it might be anticipated, that as for p53 (Gu and Zhu 2012, Taira and Yoshida 2012, Marouco, Garabadgiu et al. 2013), the PTM fingerprint of the APC/C will determine its biological function.

Lysine residues can also be subjected to PTM by methyl groups, ubiquitin and ubiquitin-like proteins. In this regard it will also be important to establish whether those APC/C lysine residues that can be modified by acetylation can also be modified by other functional groups. As such, specific PTMs upon APC/C lysine residues might regulate the biological activity of the APC/C.

7.12. Concluding Remarks

In this chapter evidence is presented to indicate that the human APC/C holoenzyme is subject to acetylation *in vivo*. In this regard, the TPR-containing APC/C subunits are a major target for acetylation. The pattern of APC/C acetylation has been shown to be dynamic in mitosis, suggesting that acetylation might affect APC/C binding to E2s, substrates and/or co-activators. The HATs CBP and p300 have been identified as key regulators of APC3 acetylation, though their role in the modification of other APC/C subunits, awaits clarification. Given that CBP/p300 have previously been determined to regulate the biological activity of the APC/C through an unknown mechanism (Turnell, Stewart et al. 2005), the data presented in this chapter suggests that CBP/p300-targeted acetylation of the APC/C regulates APC/C function.

8. DISCUSSION

The APC/C is currently believed to exist as a 1.2MDa complex containing 20 subunits (Chang, Zhang et al. 2014). However, whilst roles for many of the subunits have been described as part of the APC/C, only APC5 has been proposed to hold an APC/C-independent function, where it has been suggested to regulate IRES-dependent translation of mRNA (Koloteva-Levine, Pinchasi et al. 2004, Pines 2011, Primorac and Musacchio 2013, Chang, Zhang et al. 2014).

In order to identify novel APC5-interacting proteins, a mass spectrometric screen was performed upon APC5 IPs (Figure 1.1). This resulted in the identification of several novel binding proteins for APC5, including three subunits of Pol I: RPA194, RPA135 and RPA40 (Figure 1.1). These interactions were subsequently verified by reciprocal co-IPs and Western blotting (Figure 1.2) and GST pull-downs (Figure 1.3), which confirmed that APC5 interacted specifically with RPA194, and that APC3 and APC7 IPs were unable to co-precipitate RPA194 (Figure 1.2). Furthermore, the interaction between APC5 and Pol I was shown to be specific to the nucleolus (Figure 1.5), where the APC/C and Pol I were shown to co-localise by co-IF staining (Figure 1.7) and co-elute within fractions of the same size by FPLC (Figure 1.6).

In order to determine a functional relationship between the APC/C and Pol I, it was investigated whether the Pol I subunits identified within the mass spectrometric screen in Figure 1.1 were substrates for the APC/C. Interestingly, RPA194 and RPA135 both contain multiple canonical APC/C degrons akin to those of known APC/C substrates (Figure 1.8A) (Peters 2006, Pines 2011). RPA194 also contains a TEK motif, which has been proposed to be the site for APC/C-directed ubiquitylation in some substrates (Figure 1.8A) (Jin, Williamson et al. 2008). Furthermore, the lysine within the TEK motif in RPA194 has also been shown to be ubiquitylated *in vivo* (Kim, Bennett et al. 2011). RPA194

also contains a C-terminal L-R dipeptide identical to the APC/C substrate, KIF18A, which was required for the interaction of KIF18A with the APC/C (Sedgwick, Hayward et al. 2013).

Given these characteristics, the ability of the APC/C to regulate the abundance of Pol I subunits was investigated. Whilst ablation of APC/C activity resulted in the relative increase in RPA194 protein levels, there was very little change in the levels of RPA135 and RPA40 (Figures 1.9 and 1.10). However, immunopurified APC/C was unable to direct the polyubiquitylation of purified RPA194 protein *in vitro* (Figure 1.8B). Without proof that APC/C directly ubiquitylates RPA194, there remains doubt over whether the protein stability of RPA194 is regulated by the APC/C via direct or indirect means. Further research is currently being performed to consolidate these data. Specifically, given that the human APC/C forms K11 ubiquitin chain linkages (Jin, Williamson et al. 2008, Garnett, Mansfeld et al. 2009, Wu, Merbl et al. 2010), it is currently being determined whether K11 ubiquitin chain linkages can be detected upon RPA194 *in vivo*, which would provide further evidence that RPA194 is a *bona fide* APC/C substrate.

Following the suggestion that RPA194 is a novel substrate for APC/C-mediated proteolysis, it was examined whether APC/C activity could impact upon Pol I transcription. Accordingly, the abundance of Pol I rRNA transcripts and rate of nascent pre-rRNA synthesis were quantified following ablation of APC/C subunit expression relative to non-silencing controls (Figures 1.11 and 1.12). Inhibition of the APC/C increased the relative abundance of rRNA transcripts, as calculated by qRT-PCR (Figure 1.11), and also increased the relative incorporation of 5'-FUrd into nascent pre-rRNA, as calculated semi-quantitatively by indirect immunofluorescence, thereby signifying an increased rate of Pol I transcription (Figure 1.12). From these data, the conclusion was drawn that the APC/C negatively regulates Pol I transcription, and that this is likely to be mediated by the directed proteolysis of RPA194.

Given that over 100 substrates have already been discovered for the APC/C (Table 2) (Meyer and Rape 2011, Liu, Yuan et al. 2012, Min, Mayor et al. 2013), it is unlikely that the nucleolar APC/C holoenzyme only targets RPA194. In order to identify additional putative nucleolar substrates, two independent experiments were performed. Firstly, proteins co-precipitating with APC3, APC5 and APC7 from nucleolar lysates were identified by mass spectrometry (Figure 2.1). Secondly, the relative abundance of proteins within the nucleolar proteome was quantified following siRNA-mediated knockdown of APC3 and APC5 expression relative to non-silencing controls (Figure 2.2). Although there was not extensive overlap between these experiments, IMP4 was identified in APC5 IPs and increased in nucleolar abundance following knockdown of APC3 (Figures 2.1B and 2.2B), whilst the ribosomal protein RLA0 was also identified in APC5 IPs, yet was elevated following knockdown APC3 and APC5 (Figures 2.1B and 2.2A). Similarly, APC7 was shown to interact with CHD1 and RS27 within the nucleolus (Figure 2.1C), both of which were also elevated in the nucleolus following ablation of APC3 expression (Figure 2.2B). As such, these are the most likely alternative nucleolar substrates for the APC/C.

Further validation of each of the proteins within Figures 2.1 and 2.2 ought to be carried out, starting with the aforementioned proteins identified in both experiments. Indeed, it could be that the APC/C-directed proteolysis of these proteins could also affect the rate of Pol I transcription and the production of mature rRNAs. Should this be the case, it would be important to verify that the relative increase in Pol I transcription exhibited following inhibition of APC/C in Figures 1.11 and 1.12 is due to the alleviation of RPA194 proteolysis rather than that of any of the other proteins identified within the mass spectrometric screens (Figures 2.1 and 2.2).

Although the mass spectrometry experiments in Figures 2.1 and 2.2 focus upon nucleolar roles for the APC/C, it was also important to identify novel APC/C substrates from within other subcellular compartments. As such, IPs were performed using antisera raised against the co-activators Cdc20

and Cdh1, or APC3 (Figure 2.3). Proteins involved in a wide range of biological processes were identified, including the cell cycle, DNA repair, ribosomal biogenesis, transcription, differentiation, apoptosis and metabolism (Figure 2.3). Further validation is currently underway to determine which of these proteins are novel APC/C substrates, with particular attention being drawn to the MCM proteins (Figure 2.3D) and those involved in the cell cycle (Figure 2.3C) and DNA repair (Figure 2.3E).

Although the APC/C is known to have over 100 substrates, these are not all degraded at the same point within the cell cycle (Table 2) (Meyer and Rape 2011, Liu, Yuan et al. 2012, Min, Mayor et al. 2013). Whilst this is in part due to the sequential binding of the co-activators Cdc20 and Cdh1 in mitosis, further mechanisms in the regulation of APC/C activity exist (Pines 2011, Primorac and Musacchio 2013). One key method by which APC/C activity is regulated is through PTMs such as phosphorylation. Indeed, several groups have identified numerous phosphorylated residues in a number of APC/C subunits, particularly during mitotic progression (Zachariae, Schwab et al. 1998, Jaspersen, Charles et al. 1999, Kramer, Scheuringer et al. 2000, Rudner and Murray 2000, Kraft, Herzog et al. 2003, Steen, Steen et al. 2008, Labit, Fujimitsu et al. 2012, Primorac and Musacchio 2013). Data presented within Chapter 3 demonstrated that the human APC/C is modified by another type of PTM: acetylation.

Prior work within our laboratory has demonstrated a functional link between the HATs, CBP and p300, and the APC/C; the APC/C potentiates transcriptional transactivation by CBP/p300 whilst CBP/p300 promotes APC/C-mediated ubiquitylation (Turnell, Stewart et al. 2005). Given that CBP and p300 are acetyltransferases, it was investigated whether CBP/p300 were capable of acetylating the APC/C complex. In this regard, CBP and p300 were shown to acetylate APC3 *in vitro* (Figures 3.1, 3.2 and 3.4), whilst siRNA-mediated depletion of CBP decreased APC3 acetylation *in vivo* (Figure 3.6). Furthermore, both CBP and p300 were shown to acetylate the K336 residue within APC3 (Figure 3.4).

Although CBP and p300 were shown to acetylate APC3, mass spectrometric analysis of the APC/C holoenzyme identified a number of acetyl-lysine residues from many APC/C subunits, particularly those of the TPR subcomplex (Figures 3.3 and 3.10). Furthermore, the acetylation fingerprint was shown to be dynamic, such that various Ac-K residues were shown to be acetylated only during particular stages of the mitotic cell cycle (Figure 3.10). Given these data, it was proposed that the APC/C is regulated by acetylation *in vivo*, and that this is mediated by the HATs CBP and p300, although other HATs could also target the APC/C.

In the discussion following Chapter 3, it was further postulated that acetylation of the APC/C could alter its affinity for binding proteins, such as E2s and substrates, and therefore could regulate the efficiency of APC/C-directed ubiquitylation. As such, it is important to consider that the putative substrates identified within Chapter 2 could be dependent upon PTMs upon the APC/C, including phosphorylation and acetylation. This theory is also applicable for the APC/C-dependent ubiquitylation of RPA194. Indeed, this could explain the inability for immunopurified APC/C to ubiquitylate RPA194 *in vitro* (Figure 1.8B), as this used APC/C purified from whole cell lysates rather than from nucleolar fractions. Although PTMs are not necessarily required for the interaction between RPA194 and APC5 (Figure 1.3), it could be that nucleolar-specific PTMs upon the APC/C are required for the ubiquitylation of RPA194. This will therefore be considered in future experiments regarding the relationship between the APC/C and RNA Polymerase I.

The work presented within this thesis offers new insights into APC/C function, particularly with regard to novel roles within the nucleolus and in the regulation of transcription. Furthermore, a number of putative novel substrates for APC/C-mediated ubiquitylation have been identified and additional modes of APC/C regulation by acetylation have been described. In this regard it will be interesting to verify novel *bona fide* APC/C substrates and establish the functional consequences of APC/C acetylation.

APPENDIX – SUPPLEMENTARY MASS SPECTOMETRY DATA

FIGURE S1.1 – SUPPLEMENTARY WHOLE CELL EXTRACT APC5 IP DATA

A

Protein	Full Name	MW [kDa]	Mascot Score	# Peptides	SC [%]
AMPD2	AMP deaminase 2	100.6	1382.2	30	29.4
HOOK2	Protein Hook homolog 2	83.1	361.5	8	12.2
ROA1	Heterogeneous nuclear ribonucleoprotein A1	38.7	308.2	7	21.2
RO52	52 kDa Ro protein	54.1	249.6	5	9.7
MTNA	Methylthioribose-1-phosphate isomerase	39.1	202.4	4	9.2
PCBP1	Poly(rC)-binding protein 1	37.5	177.9	4	13.8
ROA3	Heterogeneous nuclear ribonucleoprotein A3	39.6	164.4	4	10.6
ATD3B	ATPase family AAA domain-containing protein 3B	72.5	139.1	3	4.3
AMPD3	AMP deaminase 3	88.8	126.9	3	4.2
H2B1K	Histone H2B type 1-K	13.9	126.6	3	19.0
EEA1	Early endosome antigen 1	162.4	118.4	1	1.6
KU86	ATP-dependent DNA helicase 2 subunit 2	82.7	109.3	2	3.0
IF2A	Eukaryotic translation initiation factor 2 subunit 1	36.1	107.0	1	6.3
SYTC	Threonyl-tRNA synthetase, cytoplasmic	83.4	98.5	2	3.0
MIF	Macrophage migration inhibitory factor	12.5	86.9	2	17.4
COPG2	Coatomer subunit gamma-2	97.6	81.0	1	1.4
PRDX6	Peroxiredoxin-6	25.0	80.9	2	11.6
TPM3	Tropomyosin alpha-3 chain	32.8	80.1	2	8.5
DIAP1	Protein diaphanous homolog 1	141.3	79.7	2	1.9
LEG3	Galectin-3	26.1	78.2	2	8.8

Figure S1.1A – Additional APC5-interacting proteins identified by Mass Spectrometry

B

i) RPA194: ^{115}AVIHLLLC*QLR^{125}

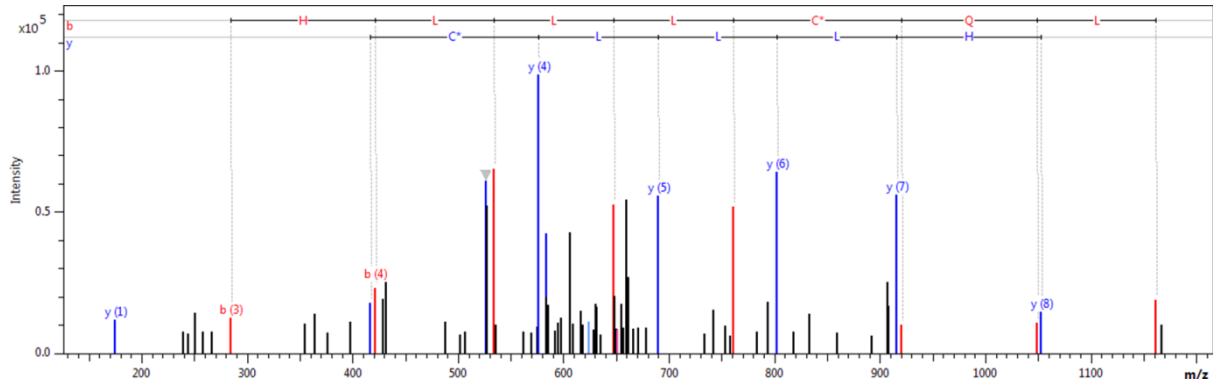

ii) RPA194: ^{373}SFLSTLPGQSLIDK^{386}

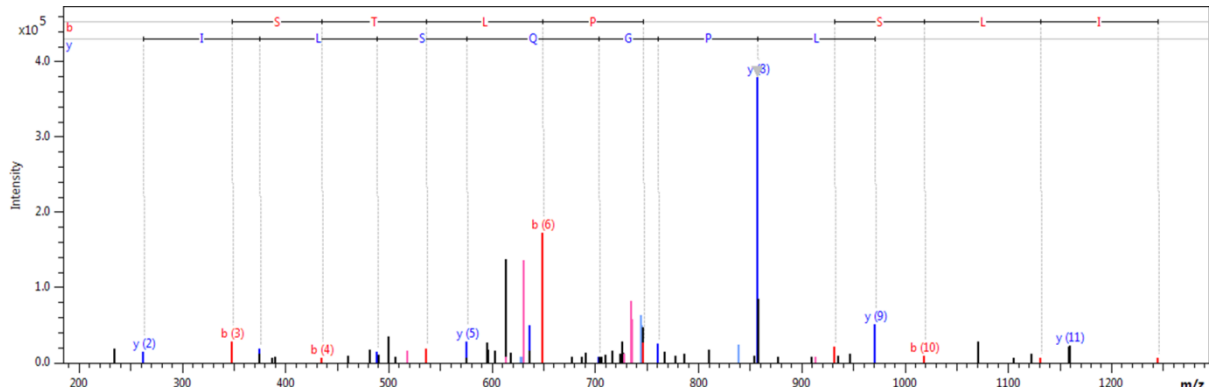

iii) RPA194: ^{1288}VCLGEVLQK^{1296}

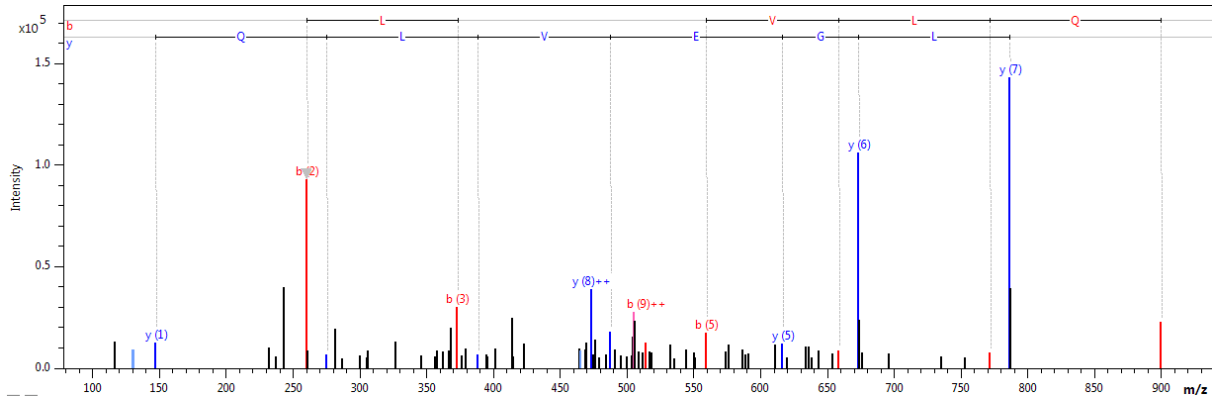

C

RPA135: ^{299}QVLNYLGEC*FR^{309}

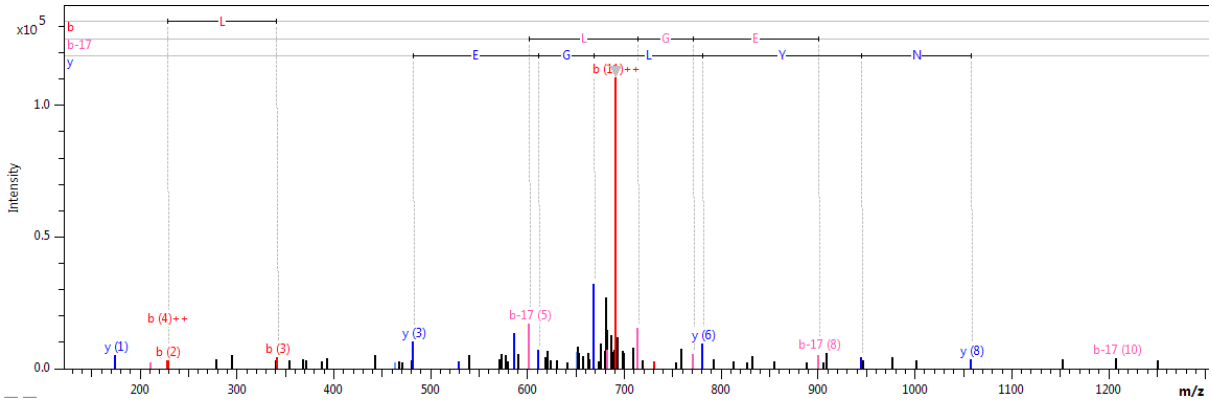

D

RPA40: ^{225}FSPVATASYR^{234}

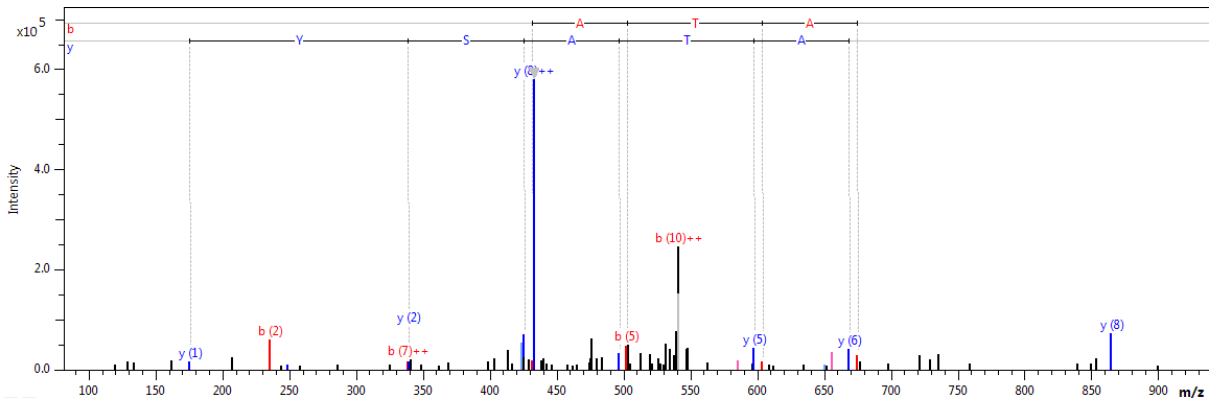

Figure S1.1B-D – Representative Extracted Ion Chromatograms for RPA194 (**B**), RPA135 (**C**) and RPA40 (**D**).

APC5 and normal IgG IPs were separated by SDS-PAGE and digested by trypsin. Peptides were reduced, carboxymethylated and analysed by LC-MS/MS using a Bruker AmaZon ion trap mass spectrometer. Peptides were identified by ProteinScape (Bruker) through comparison to a Mascot database (Matrix Science). Both obvious contaminants and proteins identified within the IgG control were removed from the list, onto which a 1% False Discovery Rate and a cut-off Score of 30 were applied. MW stands for molecular weight, and S.C. for sequence coverage.

Extracted Ion Chromatograms are shown for RPA194 (B), RPA135 (C) and RPA40 (D).

FIGURE S1.2 – SUPPLEMENTARY NUCLEOLAR IP DATA

A) Nucleolar APC3 IP

APC/C subunits

Protein	Full Name	MW [kDa]	Mascot Score	# Peptides	SC [%]
APC1	Anaphase-promoting complex subunit 1	216.4	403.8	8	4.1
APC3	Cell division cycle protein 27 homolog	91.8	624.2	11	16
APC4	Anaphase-promoting complex subunit 4	92.1	305.4	6	8.7
APC5	Anaphase-promoting complex subunit 5	85	130	3	4.9
APC6	Cell division cycle protein 16 homolog	71.6	182.7	3	5.5
APC8	Cell division cycle protein 23 homolog	68.8	147.4	4	7.7
APC10	Anaphase-promoting complex subunit 10	21.2	98.6	1	6.5

Nucleolar Proteins

Protein	Full Name	MW [kDa]	Mascot Score	# Peptides	SC [%]	# D-box	# KEN	# TEK	GPS-ARM
ACTG	Actin, cytoplasmic 2	41.8	403.1	8	23.7	3	-	-	
DDX5	Probable ATP-dependent RNA helicase DDX5	69.1	94.6	2	4.1	1	1	-	
ERH	Enhancer of rudimentary homolog	12.3	219.7	4	36.5	-	-	-	
GPTC4	G patch domain-containing protein 4	50.4	177.9	3	9.4	1	1	-	++
H2A1C	Histone H2A type 1-C	14.1	317.9	7	40.8	1	-	-	
H2AJ	Histone H2A.J	14	363.6	8	41.1	1	-	-	
H2AZ	Histone H2A.Z	13.5	216	4	31.2	1	-	-	
H2B1H	Histone H2B type 1-H	13.9	671.8	12	61.1	1	-	-	
H31	Histone H3.1	15.4	520.2	11	42.6	1	-	-	
I20L2	Interferon-stimulated 20 kDa exonuclease-like 2	39.1	256.4	4	13.9	2	-	-	***
KU86	ATP-dependent DNA helicase 2 subunit 2	82.7	125	3	4.9	1	-	-	***
MYH11	Myosin-11	227.2	59.9	2	1	17	2	-	***/ +++
PP1B	Serine/threonine-protein phosphatase PP1-beta catalytic subunit	37.2	231	5	15.6	1	-	-	
PRDX1	Peroxiredoxin-1	22.1	90.3	2	10.1	-	-	-	-
RL26L	60S ribosomal protein L26-like 1	17.2	380.7	10	49.7	1	-	-	
XRCC1	DNA repair protein XRCC1	69.5	62.8	1	1.6	5	-	-	

B) Nucleolar APC5 IP

APC/C subunits

Protein	Full Name	MW [kDa]	Mascot Score	# Peptides	SC [%]
APC1	Anaphase-promoting complex subunit 1	216.4	244.6	5	2.9
APC3	Cell division cycle protein 27 homolog	91.8	150.8	3	5.9
APC4	Anaphase-promoting complex subunit 4	92.1	151.9	3	4.5
APC5	Anaphase-promoting complex subunit 5	85	231.6	5	7.5
APC6	Cell division cycle protein 16 homolog	71.6	120.6	3	5.6
APC7	Anaphase-promoting complex subunit 7	63.1	53.5	1	2.1
APC8	Cell division cycle protein 23 homolog	68.8	193.5	5	10.6

Nucleolar Proteins

Protein	Full Name	MW [kDa]	Mascot Score	# Peptides	SC [%]	# D-box	# KEN	# TEK	GPS-ARM
ACTG	Actin, cytoplasmic 2	41.8	134.4	3	12	3	-	-	
ADT3	ADP/ATP translocase 3	32.8	75.5	2	7.4	3	-	-	
BMS1	Ribosome biogenesis protein BMS1 homolog	145.7	91.1	3	2.7	9	-	-	*
BOP1	Ribosome biogenesis protein BOP1	83.6	270.3	6	11.5	4	-	-	*
CEBPZ	CCAAT/enhancer-binding protein zeta	120.9	45.8	1	1.1	5	2	-	+++
CIR1A	Cirhin	76.8	174.1	3	6.4	3	-	-	
DDX17	Probable ATP-dependent RNA helicase DDX17	72.3	90.7	2	3.5	2	1	-	
DDX18	ATP-dependent RNA helicase DDX18	75.4	457.5	10	19.4	4	-	-	
DDX21	Nucleolar RNA helicase 2	87.3	576.5	14	18.6	1	-	-	***
DDX27	Probable ATP-dependent RNA helicase DDX27	89.8	324.4	8	12.2	3	-	+	***
DDX54	ATP-dependent RNA helicase DDX54	98.5	33.3	1	1.2	6	-	-	***
DDX56	Probable ATP-dependent RNA helicase DDX56	61.6	76.1	2	4.2	7	-	-	***
DHX15	Putative pre-mRNA-splicing factor ATP-dependent RNA helicase DHX15	90.9	115.6	2	3.3	9	-	+	**
DHX9	ATP-dependent RNA helicase A	140.9	350.6	8	7.4	5	-	-	**
GNL3	Guanine nucleotide-binding protein-like 3	62	262.2	5	14.2	3	1	-	***
H2B3B	Histone H2B type 3-B	13.9	216.6	4	27.8	1	-	-	
H3L	Histone H3-like	15.2	25.2	1	6.7	1	-	-	*
HBB	Hemoglobin subunit beta	16	67.7	1	6.8	-	-	-	
HDAC1	Histone deacetylase 1	55.1	25.6	1	2.5	-	-	-	
HEAT1	HEAT repeat-containing protein 1	242.2	63	1	0.7	9	1	-	***
HNRPG	Heterogeneous nuclear ribonucleoprotein G	42.3	112.6	2	6.6	3	-	-	*
HNRPL	Heterogeneous nuclear ribonucleoprotein L	64.1	75.4	2	3.2	3	-	-	**

HNRPU	Heterogeneous nuclear ribonucleoprotein U	90.5	58.1	2	2.4	1	-	+	*
HSPB1	Heat shock protein beta-1	22.8	28.6	1	4.4	2	-	-	
IF4A1	Eukaryotic initiation factor 4A-I	46.1	56.8	1	3.9	2	-	+	
IF6	Eukaryotic translation initiation factor 6	26.6	41.4	1	5.7	3	-	-	
IMA7	Importin subunit alpha-7	60	111.1	2	4.7	1	-	-	
IMP4	U3 small nucleolar ribonucleoprotein protein IMP4	33.7	34.1	1	3.4	5	-	-	**
KHDR1	KH domain-containing, RNA-binding, signal transduction-associated protein 1	48.2	33.9	1	3.2	3	-	-	
KI67	Antigen KI-67	358.5	258.2	5	2	5	3	+	*/ +++
MK67I	MKI67 FHA domain-interacting nucleolar phosphoprotein	34.2	232.6	4	21.5	2	-	-	*
NGDN	Neuroguidin	35.9	26	1	4.4	2	-	+	*
NIP7	60S ribosome subunit biogenesis protein NIP7 homolog	20.4	26.7	1	5.6	-	-	-	
NKRF	NF-kappa-B-repressing factor	77.6	125.9	3	5.2	2	-	-	
NO66	Lysine-specific demethylase NO66	71	28.3	1	2.2	4	-	-	*
NOC2L	Nucleolar complex protein 2 homolog	84.9	26.4	1	1.3	3	-	-	***
NOG1	Nucleolar GTP-binding protein 1	73.9	498.3	10	20.3	6	-	-	*
NOG2	Nucleolar GTP-binding protein 2	83.6	243.9	5	8.6	3	-	-	
NOL11	Nucleolar protein 11	81.1	31.2	1	1.9	4	-	+	*
NOL6	Nucleolar protein 6	127.5	323.6	6	7.4	12	-	-	*
NONO	Non-POU domain-containing octamer-binding protein	54.2	262.7	7	19.3	5	-	-	*
NOP2	Putative ribosomal RNA methyltransferase NOP2	89.2	266.8	5	8.6	2	-	-	
NOP58	Nucleolar protein 58	59.5	504.6	11	29.5	3	-	+	
NPM	Nucleophosmin	32.6	74.5	1	4.4	1	-	-	***
NUMA1	Nuclear mitotic apparatus protein 1	238.1	77.4	2	1.2	19	1	+	***/ +++
PESC	Pescadillo homolog	68	106.1	2	3.4	5	-	+	*
PLEC1	Plectin-1	531.5	1357.7	31	8.8	57	1	-	***
PP1B	Serine/threonine-protein phosphatase PP1-beta catalytic subunit	37.2	99.5	2	7.3	1	-	-	
PRKDC	DNA-dependent protein kinase catalytic subunit	468.8	1560.5	34	10.9	25	-	-	***
PWP2	Periodic tryptophan protein 2 homolog	102.4	83	2	2.6	6	-	-	
RBM28	RNA-binding protein 28	85.7	169.4	4	5.9	8	-	+	*
RL1D1	Ribosomal L1 domain-containing protein 1	54.9	542.4	12	24.9	7	-	+	**
RL3	60S ribosomal protein L3	46.1	41.3	1	3	3	-	-	***
RL5	60S ribosomal protein L5	34.3	171.7	4	16.2	2	-	-	
RLA0	60S acidic ribosomal protein P0	34.3	25.3	1	3.5	3	-	-	
RRMJ3	Putative rRNA methyltransferase 3	96.5	253.5	5	8	9	-	-	***
RRP12	RRP12-like protein	143.6	216.7	6	6.7	13	-	+	***
RRP5	Protein RRP5 homolog	208.6	38	1	1	9	-	+	***

RRP7A	Ribosomal RNA-processing protein 7 homolog A	32.3	90.7	3	11.1	3	-	+	
RRS1	Ribosome biogenesis regulatory protein homolog	41.2	75.4	2	5.8	-	-	-	
RS28	40S ribosomal protein S28	7.8	46.6	1	17.4	-	-	-	
SFPQ	Splicing factor, proline- and glutamine-rich	76.1	103.9	2	3.7	3	-	-	
SFRS1	Splicing factor, arginine/serine-rich 1	27.7	76.2	2	7.7	-	-	-	
SLTM	SAFB-like transcription modulator	117.1	55.5	1	1	11	1	-	**/ +++
TBL3	Transducin beta-like protein 3	89	132.2	3	5.3	6	-	-	***
TRAP1	Heat shock protein 75 kDa, mitochondrial	80.1	38.5	1	2	11	-	-	*
UTP11	Probable U3 small nucleolar RNA-associated protein 11	30.4	40.4	1	4.7	3	-	-	*
UTP18	U3 small nucleolar RNA-associated protein 18 homolog	62	104.2	3	7.4	5	-	-	
UTP6	U3 small nucleolar RNA-associated protein 6 homolog	70.1	87.1	2	3.7	5	-	-	
VTNC	Vitronectin	54.3	27.6	1	3.1	3	-	-	*
WDR36	WD repeat-containing protein 36	105.3	95.7	2	2.4	2	-	-	*
WDR46	WD repeat-containing protein 46	68	77.1	2	4.1	4	-	-	**
WDR74	WD repeat-containing protein 74	42.4	78.7	2	6.5	1	1	-	

Non-Nucleolar Proteins

Protein	Full Name	MW [kDa]	Mascot Score	# Peptides	SC [%]	# D-box	# KEN	# TEK	GPS-ARM
EMD	Emerin	29	26.4	1	3.9	2	-	-	***
H1FOO	Histone H1oo	35.8	27.7	1	1.4	3	-	+	
K0020	Pumilio domain-containing protein KIAA0020	73.5	669.9	15	25.3	7	1	-	***/ +++
SPT6H	Transcription elongation factor SPT6	198.9	28.4	1	0.6	10	2	-	***/ +++
TBA4B	Putative tubulin-like protein alpha-4B	27.5	78.4	1	5.8	-	-	-	
UBIQ	Ubiquitin	8.6	57.2	1	11.8	-	-	-	
ZN669	Zinc finger protein 669	52.6	31.1	1	2.2	4	-	-	***

C) Nucleolar APC7 IP

APC/C subunits

Protein	Full Name	MW [kDa]	Mascot Score	# Peptides	SC [%]
APC1	Anaphase-promoting complex subunit 1	216.4	263.8	7	3.9
APC6	Cell division cycle protein 16 homolog	71.6	228.6	4	7.1
APC7	Anaphase-promoting complex subunit 7	63.1	1144.1	20	30.8

Nucleolar Proteins

Protein	Full Name	MW [kDa]	Mascot Score	# Peptides	SC [%]	# D-box	# KEN	# TEK	GPS-ARM
ADT3	ADP/ATP translocase 3	32.8	48.6	1	3.4	3	-	-	
CHD1	Chromodomain-helicase-DNA-binding protein 1	196.6	60.6	1	0.8	6	1	-	**/ ++
CI093	Uncharacterized protein C9orf93	152.7	57.6	0	0	8	-	+	***
CN021	Pumilio domain-containing protein C14orf21	69.4	51.1	1	2	5	-	-	***
CP088	Protein C16orf88	51.6	264.9	6	17.2	1	-	+	
DDX5	Probable ATP-dependent RNA helicase DDX5	69.1	137.8	3	5.5	1	1	-	
DDX51	ATP-dependent RNA helicase DDX51	72.4	107.6	2	3.8	6	-	-	**
DHX37	Probable ATP-dependent RNA helicase DHX37	129.5	178.9	4	3.6	5	-	-	***
GPTC4	G patch domain-containing protein 4	50.4	368.8	8	21.3	1	1	-	++
H2A1C	Histone H2A type 1-C	14.1	419.4	7	40.8	1	-	-	
H2A1J	Histone H2A type 1-J	13.9	479.8	8	41.4	1	-	-	
H2B1O	Histone H2B type 1-O	13.9	717.8	14	73	1	-	-	
H2B2F	Histone H2B type 2-F	13.9	780.8	15	73	1	-	-	
HNRPD	Heterogeneous nuclear ribonucleoprotein D0	38.4	120.2	2	6.8	-	-	-	
HNRPF	Heterogeneous nuclear ribonucleoprotein F	45.6	73.8	1	4.6	-	-	-	
HNRPK	Heterogeneous nuclear ribonucleoprotein K	50.9	56.9	1	3.7	2	-	-	
I20L2	Interferon-stimulated 20 kDa exonuclease-like 2	39.1	280.4	5	19.3	2	-	-	***
KRR1	KRR1 small subunit processome component homolog	43.6	108.6	2	5.8	2	-	-	**
KU86	ATP-dependent DNA helicase 2 subunit 2	82.7	72.6	1	2	1	-	-	***
LARP7	La-related protein 7	66.9	97.8	2	4	1	1	+	***/ +++
LMNB1	Lamin-B1	66.4	197.7	4	7.5	8	-	-	***
MATR3	Matrin-3	94.6	233.9	6	7.2	5	-	-	***
MGN	Protein mago nashi homolog	17.2	37.5	1	7.5	1	-	-	
MYH10	Myosin-10	228.9	171.8	4	2.1	17	-	+	**
MYH9	Myosin-9	226.4	208.7	5	3.1	16	1	+	**/ +++
PTBP1	Polypyrimidine tract-binding protein 1	57.2	106.6	2	3.8	2	1	-	+++
RBP56	TATA-binding protein-associated factor 2N	61.8	217.1	4	10.1	-	-	-	
RS27A	40S ribosomal protein S27a	9.4	31.6	1	23.8	-	-	-	
SF3B2	Splicing factor 3B subunit 2	97.6	77.9	2	2.5	8	-	-	***
SFRS2	Splicing factor, arginine/serine-rich 2	25.5	45.1	1	3.6	-	-	-	
SFRS4	Splicing factor, arginine/serine-rich 4	56.6	192.7	4	7.9	-	-	-	
SMC3	Structural maintenance of chromosomes protein 3	141.5	174.7	3	2.5	17	-	-	***
SNW1	SNW domain-containing protein 1	61.5	42.5	1	2.4	2	-	+	*

TITIN	Titin	3813.8	41.7	0	0	70	8	+	***/+++
U5S1	116 kDa U5 small nuclear ribonucleoprotein component#	109.4	61.1	1	1.2	4	-	-	
UBP36	Ubiquitin carboxyl-terminal hydrolase 36	122.6	90	2	2.1	3	-	-	
XRCC1	DNA repair protein XRCC1	69.5	36.4	1	2.1	5	-	-	
YBOX1	Nuclease-sensitive element-binding protein 1	35.9	37.9	1	5.9	1	1	-	***/+++
ZCHC7	Zinc finger CCHC domain-containing protein 7	63	90.1	2	4.2	3	-	-	

Non-Nucleolar Proteins

Protein	**Full Name**	**MW [kDa]**	**Mascot Score**	**# Peptides**	**SC [%]**	**# D-box**	**# KEN**	**# TEK**	**GPS-ARM**
CF150	Uncharacterized protein C6orf150	58.8	36.9	1	1.9	4	1	+	***/+++
CH033	UPF0488 protein C8orf33	25	34.6	1	2.6	2	-	-	**
FKTN	Fukutin	53.7	33.8	1	1.5	1	-	-	
GRP78	78 kDa glucose-regulated protein	72.3	79.6	2	3.1	1	-	-	
LRC15	Leucine-rich repeat-containing protein 15	64.4	64.3	2	3.6	3	-	-	
LY9	T-lymphocyte surface antigen Ly-9	72.1	39.2	1	0.9	3	1	+	+++
NFM	Neurofilament medium polypeptide	102.4	114.7	3	3.4	5	-	-	***
PABP3	Polyadenylate-binding protein 3	70	36.5	1	2.2	-	-	-	
PININ	Pinin	81.6	57.2	1	1.5	3	1	-	++
RRP7B	Putative ribosomal RNA-processing protein 7 homolog B	12.6	160.5	3	22.3	2	-	-	
SF3B1	Splicing factor 3B subunit 1	145.7	51.1	2	1.5	4	-	-	**
SON	Protein SON	263.7	54.3	1	0.6	4	-	+	
SPS2L	SPATS2-like protein	61.7	31.9	1	2.2	-	-	-	
SRRM2	Serine/arginine repetitive matrix protein 2	299.4	142.8	3	1.5	12	-	-	***
UACA	Uveal autoantigen with coiled-coil domains and ankyrin repeats	162.4	49.6	1	0.4	12	-	+	***

D) RPA194 IP

Pol I subunits

Protein	Full Name	MW [kDa]	Mascot Score	#Peptides	SC [%]
RPA194	DNA-directed RNA polymerase I subunit RPA1	194.7	2994.2	61	29.5
RPA135	DNA-directed RNA polymerase I subunit RPA2	128.1	1348	28	19.1
RPA34	DNA-directed RNA polymerase I subunit RPA34	55	289.1	5	15.3
RPA49	DNA-directed RNA polymerase I subunit RPA49	53.9	90.4	2	4.6
RPA40	DNA-directed RNA polymerases I and III subunit RPAC1	39.2	395.9	7	20.5

RPAB1	DNA-directed RNA polymerases I, II, and III subunit RPABC1	24.5	366.3	6	23.3
RPAB3	DNA-directed RNA polymerases I, II, and III subunit RPABC3	17.1	207.8	3	26.7
RPAC2	DNA-directed RNA polymerases I and III subunit RPAC2	15.2	316.6	5	32.3
RPA12	DNA-directed RNA polymerase I subunit RPA12	13.9	141.7	2	19
RPAB5	DNA-directed RNA polymerases I, II, and III subunit RPABC5	7.6	37.8	1	16.4

Nucleolar Proteins

Protein	Full Name	MW [kDa]	Mscot Score	#Peptides	SC [%]
H2B1J	Histone H2B type 1-J	13.9	670.8	12	61.1
H2A1J	Histone H2A type 1-J	13.9	516.4	9	41.4
H2A1C	Histone H2A type 1-C	14.1	491.8	8	40.8
MATR3	Matrin-3	94.6	373.4	7	8.7
H33	Histone H3.3	15.3	370.9	8	33.1
MYH9	Myosin-9	226.4	253.6	6	3.3
ACTG	Actin, cytoplasmic 2	41.8	239	5	14.9
MYH10	Myosin-10	228.9	215	5	2.6
SFRS4	Splicing factor, arginine/serine-rich 4	56.6	207	4	7.5
HNRPR	Heterogeneous nuclear ribonucleoprotein R	70.9	205.5	4	7.1
I20L2	Interferon-stimulated 20 kDa exonuclease-like 2	39.1	202.9	4	13
PP1B	Serine/threonine-protein phosphatase PP1-beta catalytic subunit	37.2	202.7	5	15.6
DDX51	ATP-dependent RNA helicase DDX51	72.4	187.7	3	5.3
DDX5	Probable ATP-dependent RNA helicase DDX5	69.1	178.5	4	7
CP088	Protein C16orf88	51.6	161.5	4	11.6
EF1A3	Putative elongation factor 1-alpha-like 3	50.2	153.5	3	6.7
RBP56	TATA-binding protein-associated factor 2N	61.8	145.9	3	6.8
SF3B2	Splicing factor 3B subunit 2	97.6	137.7	3	3.7
RBM39	RNA-binding protein 39	59.3	114.8	3	6.6
DHX37	Probable ATP-dependent RNA helicase DHX37	129.5	112.3	2	2
U5S1	116 kDa U5 small nuclear ribonucleoprotein component	109.4	111.4	2	2.6
GPTC4	G patch domain-containing protein 4	50.4	108.1	2	5.2
DHX30	Putative ATP-dependent RNA helicase DHX30	133.9	97.6	2	1.6
DHX33	Putative ATP-dependent RNA helicase DHX33	78.7	83.9	2	3.3
FLNA	Filamin-A	280.6	72.6	2	0.9
ADT3	ADP/ATP translocase 3	32.8	68.1	2	6
CN021	Pumilio domain-containing protein C14orf21	69.4	60.4	1	2
PTBP1	Polypyrimidine tract-binding protein 1	57.2	53.7	2	4.1
SENP3	Sentrin-specific protease 3	65	48.1	1	3.1
TITIN	Titin	3813.8	45.6	0	0
CHD1	Chromodomain-helicase-DNA-binding protein 1	196.6	44.5	1	0.8
SMD1	Small nuclear ribonucleoprotein Sm D1	13.3	44.5	1	10.9
LMNB1	Lamin-B1	66.4	44.3	1	1.4

APOA1	Apolipoprotein A-I	30.8	43.1	1	4.1
NIPS1	Protein NipSnap homolog 1	33.3	42.1	1	3.2
PHB2	Prohibitin-2	33.3	41.9	1	3.3
HSPB1	Heat shock protein beta-1	22.8	39.2	1	4.9
ERH	Enhancer of rudimentary homolog	12.3	36.8	1	14.4
HNRPK	Heterogeneous nuclear ribonucleoprotein K	50.9	36	1	2.2
RS29	40S ribosomal protein S29	6.7	33.2	1	19.6
KRR1	KRR1 small subunit processome component homolog	43.6	33	1	2.4
RS27A	40S ribosomal protein S27a	9.4	31.7	1	23.8
RAN	GTP-binding nuclear protein Ran	24.4	29.9	1	5.1
HNRPL	Heterogeneous nuclear ribonucleoprotein L	64.1	28.7	1	1.7

Figure S1.2 – All interacting proteins from APC3 (A), APC5 (B), APC7 (C) and RPA194 (D) IPs from nucleolar lysates.

IPs from nucleolar lysates: APC3 (A), APC5 (B), APC7 (C) and RPA194 (D). The IPs were separated by SDS-PAGE and digested with trypsin. Peptides were eluted and analysed by LC-MS/MS using a maXis Impact (Bruker). Samples were compared to a Mascot database (Matrix Science) and searched using ProteinScape (Bruker). Interacting protein lists were compiled and compared to a nucleolar protein database, NoPDb3, published by Prof. Lamond (Ahmad, Boisvert et al. 2009) and searched for function and protein sequence using Uniprot (UniProt-Consortium 2014). The protein sequence was then searched manually for TEK motifs and for extended D-boxes and KEN-boxes using GPS-ARM 1.0 (Liu, Yuan et al. 2012).

MW represents Molecular Weight. D-boxes and KEN boxes were analysed using GPS-ARM, with the highest threshold of motif denoted by * for D-boxes and + for KEN boxes. */+ represents a low threshold peptide, **/++ medium and ***/+++ high.

FIGURE S1.3 – SUPPLEMENTARY NUCLEOLAR QUANTITATION DATA FOLLOWING APC3 AND APC5 KNOCKDOWN

A) APC3i

Protein	Full Name	MW [kDa]	Mascot Score	SC [%]	**% change**
AL4A1	Delta-1-pyrroline-5-carboxylate dehydrogenase, mitochondrial	61.7	48.3	1.1	**138.00**
TIAR	Nucleolysin TIAR	41.6	50.3	6.1	**138.00**
IMB1	Importin subunit beta-1	97.1	52.7	1.7	**9.86**
GLYR1	Putative oxidoreductase GLYR1	60.5	110	2.4	**7.67**
UBC9	SUMO-conjugating enzyme UBC9	18.0	48.1	6.3	**4.93**

PPWD1	Peptidylprolyl isomerase domain and WD repeat-containing protein 1	73.5	48.4	1.9	**4.76**
PPIL2	Peptidyl-prolyl cis-trans isomerase-like 2	58.8	48.7	2.7	**4.45**
ERO1A	ERO1-like protein alpha	54.4	49.4	3.0	**3.63**
MFAP1	Microfibrillar-associated protein 1	51.9	97.3	3.2	**3.63**
RIR1	Ribonucleoside-diphosphate reductase large subunit	90.0	53	2.3	**3.54**
SNRPA	U1 small nuclear ribonucleoprotein A	31.3	125.8	9.2	**3.37**
HBB	Hemoglobin subunit beta	16.0	67.8	6.8	**3.14**
COPB	Coatomer subunit beta	107.1	100.2	4.9	**3.07**
SERPH	Serpin H1	46.4	60	5.7	**2.94**
K2C75	Keratin, type II cytoskeletal 75	59.5	424.6	8.3	**2.76**
PCNA	Proliferating cell nuclear antigen	28.8	88.2	14.9	**2.76**
GLU2B	Glucosidase 2 subunit beta	59.4	57.2	1.9	**2.71**
CDYL1	Chromodomain Y-like protein	66.4	76.4	6.7	**2.65**
CBX8	Chromobox protein homolog 8	43.4	76.9	8.2	**2.60**
CCD55	Coiled-coil domain-containing protein 55	66.4	49.1	2.7	**2.56**
DHCR7	7-dehydrocholesterol reductase	54.5	60.6	2.7	**2.30**
RS10	40S ribosomal protein S10	18.9	61.1	9.7	**2.30**
RBM9	RNA-binding protein 9	41.3	59	3.8	**2.26**
VAT1	Synaptic vesicle membrane protein VAT-1 homolog	41.9	76.3	8.4	**2.26**
YETS4	YEATS domain-containing protein 4	26.5	43.3	4.8	**2.26**
ACON	Aconitate hydratase, mitochondrial	85.4	86.4	3.6	**2.23**
LDHA	L-lactate dehydrogenase A chain	36.7	118	4.5	**2.23**
NU107	Nuclear pore complex protein Nup107	106.3	128	4.1	**2.23**
CCAR1	Cell division cycle and apoptosis regulator protein 1	132.7	465.5	7.1	**2.16**
CLH1	Clathrin heavy chain 1	191.5	78.6	2.3	**2.12**
RU2B	U2 small nuclear ribonucleoprotein B''	25.5	152.8	16.4	**2.12**
APTX	Aprataxin	40.7	111.3	7.3	**2.09**
TITIN	Titin	3813.8	122.5	0.1	**2.09**
TRA2A	Transformer-2 protein homolog alpha	32.7	92.6	5.0	**2.09**
MED4	Mediator of RNA polymerase II transcription subunit 4	29.7	76.2	4.8	**2.06**
RAB5C	Ras-related protein Rab-5C	23.5	193.2	16.7	**2.06**
XPO1	Exportin-1	123.3	188.6	3.5	**2.06**
CSTF3	Cleavage stimulation factor subunit 3	82.9	72.2	3.2	**2.03**
PDIA4	Protein disulfide-isomerase A4	72.9	76.5	4.7	**2.03**
SPF45	Splicing factor 45	44.9	68	3.0	**2.03**
GLYC	Serine hydroxymethyltransferase, cytosolic	53.0	155.3	8.5	**2.00**
RPRD2	Regulation of nuclear pre-mRNA domain-containing protein 2	155.9	98.4	2.0	**2.00**
DHX36	Probable ATP-dependent RNA helicase DHX36	114.7	259	4.7	**1.97**
NUP98	Nuclear pore complex protein Nup98-Nup96	187.7	228.4	3.0	**1.97**
PR40A	Pre-mRNA-processing factor 40 homolog A	108.7	100.6	3.8	**1.97**
SYF1	Pre-mRNA-splicing factor SYF1	99.9	129	4.2	**1.97**
HCFC1	Host cell factor 1	208.6	164.1	1.7	**1.94**

RBBP7	Histone-binding protein RBBP7	47.8	70.5	6.6	**1.94**
RS3	40S ribosomal protein S3	26.7	359.1	19.3	**1.94**
PLK1	Serine/threonine-protein kinase PLK1	68.2	148.7	4.5	**1.92**
AT1A3	Sodium/potassium-transporting ATPase subunit alpha-3	111.7	150	4.6	**1.89**
ECHA	Trifunctional enzyme subunit alpha, mitochondrial	82.9	403.8	12.8	**1.89**
KIN17	DNA/RNA-binding protein KIN17	45.3	57.4	4.6	**1.89**
RBM5	RNA-binding protein 5	92.1	90.3	1.8	**1.89**
SF04	Splicing factor 4	72.4	70.9	2.3	**1.89**
GNA1	Glucosamine 6-phosphate N-acetyltransferase	20.7	133.1	12.0	**1.86**
NEUA	N-acylneuraminate cytidylyltransferase	48.3	100	12.2	**1.86**
P66A	Transcriptional repressor p66-alpha	68.0	354.7	8.4	**1.84**
DYL2	Dynein light chain 2, cytoplasmic	10.3	68.7	24.7	**1.82**
MBNL1	Muscleblind-like protein 1	41.8	56.1	7.0	**1.82**
PININ	Pinin	81.6	59.7	2.8	**1.82**
ENPL	Endoplasmin	92.4	487.8	9.0	**1.79**
FUBP2	Far upstream element-binding protein 2	73.1	149	7.9	**1.79**
NIPBL	Nipped-B-like protein	315.9	293.8	1.9	**1.79**
PSME3	Proteasome activator complex subunit 3	29.5	62	5.9	**1.79**
RAGP1	Ran GTPase-activating protein 1	63.5	237.2	6.5	**1.79**
TF2H1	General transcription factor IIH subunit 1	62.0	74.1	4.6	**1.79**
ARP2	Actin-related protein 2	44.7	94.7	5.8	**1.77**
CALR	Calreticulin	48.1	76.6	2.9	**1.77**
CH10	10 kDa heat shock protein, mitochondrial	10.9	97.5	25.5	**1.77**
CSTF1	Cleavage stimulation factor subunit 1	48.3	135.8	3.7	**1.77**
FIP1	Pre-mRNA 3'-end-processing factor FIP1	66.5	84.9	3.2	**1.77**
SF3A1	Splicing factor 3A subunit 1	88.8	44.2	2.6	**1.77**
TADBP	TAR DNA-binding protein 43	44.7	228.2	12.3	**1.77**
BRE1A	E3 ubiquitin-protein ligase BRE1A	113.6	359.1	3.6	**1.75**
EFGM	Elongation factor G, mitochondrial	83.4	62.6	2.0	**1.75**
GPTC8	G patch domain-containing protein 8	164.1	46	2.3	**1.75**
GRSF1	G-rich sequence factor 1	53.1	78.3	5.6	**1.75**
HNRPD	Heterogeneous nuclear ribonucleoprotein D0	38.4	445.9	14.6	**1.75**
P66B	Transcriptional repressor p66-beta	65.2	172.2	9.6	**1.75**
RSMB	Small nuclear ribonucleoprotein-associated proteins B and B'	24.6	316.7	21.2	**1.75**
JUND	Transcription factor jun-D	35.2	94.9	4.3	**1.73**
NUP93	Nuclear pore complex protein Nup93	93.4	193.1	3.3	**1.73**
RPAB5	DNA-directed RNA polymerases I, II, and III subunit RPABC5	7.6	110	13.4	**1.73**
LMAN1	Protein ERGIC-53	57.5	64.5	4.7	**1.70**
NU155	Nuclear pore complex protein Nup155	155.1	388.6	6.5	**1.70**
RBM25	RNA-binding protein 25	100.1	76.1	3.4	**1.70**
RBP2	E3 SUMO-protein ligase RanBP2	358.0	245.9	2.1	**1.70**
TOIP1	Torsin-1A-interacting protein 1	66.2	67.2	2.1	**1.70**
TPR	Nucleoprotein TPR	267.1	187.1	2.3	**1.70**

AIFM1	Apoptosis-inducing factor 1, mitochondrial	66.9	169.6	6.7	**1.68**
PDIA1	Protein disulfide-isomerase	57.1	109	3.1	**1.68**
SHCBP	SHC SH2 domain-binding protein 1	75.6	48	5.2	**1.68**
U2AF1	Splicing factor U2AF 35 kDa subunit	27.9	371.6	23.3	**1.68**
HNRDL	Heterogeneous nuclear ribonucleoprotein D-like	46.4	551.4	14.5	**1.66**
MATR3	Matrin-3	94.6	700.3	18.5	**1.66**
PNPT1	Polyribonucleotide nucleotidyltransferase 1, mitochondrial	85.9	68.9	1.7	**1.66**
THOC5	THO complex subunit 5 homolog	78.5	95.9	2.9	**1.66**
TOP2A	DNA topoisomerase 2-alpha	174.3	998	16.3	**1.66**
BCLF1	Bcl-2-associated transcription factor 1	106.1	147.5	3.9	**1.64**
LRC59	Leucine-rich repeat-containing protein 59	34.9	55.8	3.9	**1.64**
TRAP1	Heat shock protein 75 kDa, mitochondrial	80.1	157.8	5.4	**1.64**
ATPA	ATP synthase subunit alpha, mitochondrial	59.7	1124	28.8	**1.62**
DDX23	Probable ATP-dependent RNA helicase DDX23	95.5	343.9	7.3	**1.62**
LSM2	U6 snRNA-associated Sm-like protein LSm2	10.8	65.8	20.0	**1.62**
SRRM2	Serine/arginine repetitive matrix protein 2	299.4	344.9	3.6	**1.62**
KI20A	Kinesin-like protein KIF20A	100.2	157.6	5.2	**1.60**
RAB14	Ras-related protein Rab-14	23.9	77.3	6.5	**1.60**
RS26	40S ribosomal protein S26	13.0	113	13.0	**1.60**
SMC5	Structural maintenance of chromosomes protein 5	128.7	120.5	3.9	**1.60**
EIF1	Eukaryotic translation initiation factor 1	12.7	342.5	47.8	**1.59**
GDAP1	Ganglioside-induced differentiation-associated protein 1	41.3	77.4	4.2	**1.59**
NU153	Nuclear pore complex protein Nup153	153.8	41	1.1	**1.59**
RPB2	DNA-directed RNA polymerase II subunit RPB2	133.8	134.2	2.8	**1.59**
SMRD3	SWI/SNF-related matrix-associated actin-dependent regulator of chromatin subfamily D member 3	55.0	42.8	2.7	**1.59**
DESP	Desmoplakin	331.6	232.2	1.9	**1.57**
DHB4	Peroxisomal multifunctional enzyme type 2	79.6	457.5	15.6	**1.57**
FUBP1	Far upstream element-binding protein 1	67.5	279.7	9.8	**1.57**
HBS1L	HBS1-like protein	75.4	61.7	1.9	**1.57**
SF3B1	Splicing factor 3B subunit 1	145.7	480.7	8.1	**1.57**
VIME	Vimentin	53.6	1610.9	53.4	**1.57**
WRN	Werner syndrome ATP-dependent helicase	162.4	100	1.7	**1.57**
ADAS	Alkyldihydroxyacetonephosphate synthase, peroxisomal	72.9	57.7	2.0	**1.55**
API5	Apoptosis inhibitor 5	57.5	177.5	5.3	**1.55**
BAG2	BAG family molecular chaperone regulator 2	23.8	87.4	5.2	**1.55**
CHCH3	Coiled-coil-helix-coiled-coil-helix domain-containing protein 3, mitochondrial	26.1	79.8	11.5	**1.55**
ECH1	Delta(3,5)-Delta(2,4)-dienoyl-CoA isomerase, mitochondrial	35.8	118.7	4.9	**1.55**
PM14	Pre-mRNA branch site protein p14	14.6	123.5	22.4	**1.55**
SFRS5	Splicing factor, arginine/serine-rich 5	31.2	174.4	12.9	**1.55**
TRXR2	Thioredoxin reductase 2, mitochondrial	56.5	101.5	4.8	**1.55**
NDUBA	NADH dehydrogenase [ubiquinone] 1 beta subcomplex subunit 10	20.8	87.4	7.0	**1.53**
PRDX5	Peroxiredoxin-5, mitochondrial	22.0	68.8	8.4	**1.53**

ROA3	Heterogeneous nuclear ribonucleoprotein A3	39.6	962.8	31.5	**1.53**
SF3B2	Splicing factor 3B subunit 2	97.6	477	10.8	**1.53**
ACLY	ATP-citrate synthase	120.8	54.4	1.4	**1.52**
ERH	Enhancer of rudimentary homolog	12.3	202.4	23.1	**1.52**
LMNB1	Lamin-B1	66.4	1252.2	32.8	**1.52**
NU133	Nuclear pore complex protein Nup133	128.9	201.8	3.2	**1.52**
P5CR1	Pyrroline-5-carboxylate reductase 1, mitochondrial	33.3	122.8	4.1	**1.52**
RM47	39S ribosomal protein L47, mitochondrial	29.4	48.5	4.0	**1.52**
SCMC1	Calcium-binding mitochondrial carrier protein SCaMC-1	53.3	59	2.7	**1.52**
SF01	Splicing factor 1	68.3	106.7	4.5	**1.52**
SNF5	SWI/SNF-related matrix-associated actin-dependent regulator of chromatin subfamily B member 1	44.1	86.2	3.4	**1.52**
THOC6	THO complex subunit 6 homolog	37.5	77.8	3.2	**1.52**
TR150	Thyroid hormone receptor-associated protein 3	108.6	299.5	7.4	**1.52**
ZC11A	Zinc finger CCCH domain-containing protein 11A	89.1	155.1	3.3	**1.52**
2AAA	Serine/threonine-protein phosphatase 2A 65 kDa regulatory subunit A alpha isoform	65.3	125.4	4.8	**1.50**
ANLN	Actin-binding protein anillin	124.1	61	1.3	**1.50**
BLM	Bloom syndrome protein	158.9	117.7	1.8	**1.50**
CA077	Uncharacterized protein C1orf77	26.4	61.9	5.2	**1.50**
FUBP3	Far upstream element-binding protein 3	61.6	81.2	3.8	**1.50**
K2C5	Keratin, type II cytoskeletal 5	62.3	401.1	11.4	**1.50**
PRP4	U4/U6 small nuclear ribonucleoprotein Prp4	58.4	487.6	19.3	**1.50**
SF3A2	Splicing factor 3A subunit 2	49.2	48	6.2	**1.50**
SFRS1	Splicing factor, arginine/serine-rich 1	27.7	715.4	32.7	**1.50**
SMRD1	SWI/SNF-related matrix-associated actin-dependent regulator of chromatin subfamily D member 1	58.2	93.5	2.5	**1.50**
U5S1	116 kDa U5 small nuclear ribonucleoprotein component	109.4	649.1	13.0	**1.50**
ELAV1	ELAV-like protein 1	36.1	187.2	13.2	**1.48**
LETM1	LETM1 and EF-hand domain-containing protein 1, mitochondrial	83.3	43.4	1.6	**1.48**
MTCH2	Mitochondrial carrier homolog 2	33.3	81.4	3.0	**1.48**
MYH9	Myosin-9	226.4	75.4	0.7	**1.48**
NEST	Nestin	177.3	284.1	5.4	**1.48**
NU205	Nuclear pore complex protein Nup205	227.8	70.8	0.9	**1.48**
SF3B3	Splicing factor 3B subunit 3	135.5	722.8	13.3	**1.48**
TRI41	E3 ubiquitin-protein ligase TRIM41	71.6	48	3.2	**1.48**
ACL6A	Actin-like protein 6A	47.4	72.6	6.3	**1.47**
C1TC	C-1-tetrahydrofolate synthase, cytoplasmic	101.5	148.9	3.9	**1.47**
HNRPC	Heterogeneous nuclear ribonucleoproteins C1/C2	33.6	420.5	15.7	**1.47**
HTSF1	HIV Tat-specific factor 1	85.8	231.3	4.8	**1.47**
MBD3	Methyl-CpG-binding domain protein 3	32.8	94.5	8.6	**1.47**
PLEC1	Plectin-1	531.5	554.8	2.9	**1.47**
SEH1	Nucleoporin SEH1	39.6	100.1	8.1	**1.47**
SON	Protein SON	263.7	65.4	0.6	**1.47**

TERA	Transitional endoplasmic reticulum ATPase	89.3	347.2	10.4	**1.47**
TP53B	Tumor suppressor p53-binding protein 1	213.4	178.6	2.1	**1.47**
ESYT2	Extended synaptotagmin-2	102.3	124.5	1.1	**1.45**
GTF2I	General transcription factor II-I	112.3	562.8	13.3	**1.45**
HCD2	3-hydroxyacyl-CoA dehydrogenase type-2	26.9	428.6	41.4	**1.45**
K2C8	Keratin, type II cytoskeletal 8	53.7	2885.4	58.6	**1.45**
ODO2	Dihydrolipoyllysine-residue succinyltransferase component of 2-oxoglutarate dehydrogenase complex, mitochondrial	48.7	193.5	7.3	**1.45**
RS21	40S ribosomal protein S21	9.1	65.8	12.0	**1.45**
RSSA	40S ribosomal protein SA	32.8	96.2	8.8	**1.45**
SF3A3	Splicing factor 3A subunit 3	58.8	197.1	6.0	**1.45**
SMD3	Small nuclear ribonucleoprotein Sm D3	13.9	141.7	15.1	**1.45**
ALDOA	Fructose-bisphosphate aldolase A	39.4	949	42.6	**1.44**
ODPAT	Pyruvate dehydrogenase E1 component subunit alpha, testis-specific form, mitochondrial	42.9	79	2.8	**1.44**
RUEL1	Putative small nuclear ribonucleoprotein polypeptide E-like protein 1	10.7	54.1	12.0	**1.44**
RUVB2	RuvB-like 2	51.1	521	12.3	**1.44**
SFRS2	Splicing factor, arginine/serine-rich 2	25.5	59.4	3.6	**1.44**
SPF27	Pre-mRNA-splicing factor SPF27	26.1	66.7	5.3	**1.44**
SYMPK	Symplekin	141.1	87.8	1.8	**1.44**
TRA2B	Transformer-2 protein homolog beta	33.6	148.2	10.4	**1.44**
DECR	2,4-dienoyl-CoA reductase, mitochondrial	36.0	57.5	9.3	**1.42**
DNJA3	DnaJ homolog subfamily A member 3, mitochondrial	52.5	113.5	4.8	**1.42**
MOES	Moesin	67.8	42.7	1.6	**1.42**
PGK1	Phosphoglycerate kinase 1	44.6	83.4	4.3	**1.42**
TIM44	Mitochondrial import inner membrane translocase subunit TIM44	51.3	128	7.7	**1.42**
ACSL4	Long-chain-fatty-acid--CoA ligase 4	79.1	79.3	2.5	**1.41**
BRE1B	E3 ubiquitin-protein ligase BRE1B	113.6	81.2	2.1	**1.41**
EZRI	Ezrin	69.4	124.1	3.6	**1.41**
HNRH2	Heterogeneous nuclear ribonucleoprotein H2	49.2	654	25.8	**1.41**
IF2M	Translation initiation factor IF-2, mitochondrial	81.3	61.1	3.0	**1.41**
RS24	40S ribosomal protein S24	15.4	155.7	23.3	**1.41**
RS27	40S ribosomal protein S27	9.5	102.2	25.0	**1.41**
RUVB1	RuvB-like 1 GN=RUVBL1 PE=1 SV=1	50.2	135.5	10.7	**1.41**
TFCP2	Alpha-globin transcription factor CP2	57.2	73.4	2.8	**1.41**
ACADV	Very long-chain specific acyl-CoA dehydrogenase, mitochondrial	70.3	236.9	12.8	**1.39**
GBLP	Guanine nucleotide-binding protein subunit beta-2-like 1	35.1	308.4	10.7	**1.39**
HNRH1	Heterogeneous nuclear ribonucleoprotein H	49.2	974.7	32.7	**1.39**
INCE	Inner centromere protein	105.4	60.6	1.9	**1.39**
ROA2	Heterogeneous nuclear ribonucleoproteins A2/B1	37.4	1691	58.1	**1.39**
SC23A	Protein transport protein Sec23A	86.1	177.1	4.7	**1.39**
IMA2	Importin subunit alpha-2	57.8	445.7	15.9	**1.38**
LMNB2	Lamin-B2	67.6	469.4	9.2	**1.38**

RPB1	DNA-directed RNA polymerase II subunit RPB1	217.0	149.1	1.6	**1.38**
RU17	U1 small nuclear ribonucleoprotein 70 kDa	51.5	182.3	8.9	**1.38**
CE033	UPF0465 protein C5orf33	49.4	138.5	6.1	**1.37**
CH60	60 kDa heat shock protein, mitochondrial	61.0	1494.5	36.6	**1.37**
DHX16	Putative pre-mRNA-splicing factor ATP-dependent RNA helicase DHX16	119.2	153.6	4.3	**1.37**
HNRPL	Heterogeneous nuclear ribonucleoprotein L	64.1	611.9	25.8	**1.37**
RM39	39S ribosomal protein L39, mitochondrial	38.7	43.2	3.6	**1.37**
WDR33	WD repeat-containing protein 33	145.8	41.7	0.9	**1.37**
WDR55	WD repeat-containing protein 55	42.1	97.6	10.2	**1.37**
CPSM	Carbamoyl-phosphate synthase [ammonia], mitochondrial	164.8	1965.3	23.9	**1.35**
CUL4A	Cullin-4A	87.6	45.6	1.6	**1.35**
DDB1	DNA damage-binding protein 1	126.9	475.3	8.6	**1.35**
GRP78	78 kDa glucose-regulated protein	72.3	647	22.3	**1.35**
HSP7C	Heat shock cognate 71 kDa protein	70.9	1266.2	28.3	**1.35**
KIF23	Kinesin-like protein KIF23	110.0	184.4	3.0	**1.35**
NNTM	NAD(P) transhydrogenase, mitochondrial	113.8	107.5	3.2	**1.35**
ROA0	Heterogeneous nuclear ribonucleoprotein A0	30.8	604.4	30.2	**1.35**
SAFB2	Scaffold attachment factor B2	107.4	157	3.1	**1.35**
SF13A	Splicing factor, arginine/serine-rich 13A	31.3	222.6	13.0	**1.35**
SFRS6	Splicing factor, arginine/serine-rich 6	39.6	245.5	11.9	**1.35**
TF3C2	General transcription factor 3C polypeptide 2	100.6	69.2	1.2	**1.35**
WDR82	WD repeat-containing protein 82	35.1	159.6	10.5	**1.35**
ZN326	Zinc finger protein 326	65.6	234	4.8	**1.35**
ZN828	Zinc finger protein 828	89.0	115.6	3.9	**1.35**
C1TM	Monofunctional C1-tetrahydrofolate synthase, mitochondrial	105.7	55.3	2.6	**1.34**
CHD1	Chromodomain-helicase-DNA-binding protein 1	196.6	106.4	2.0	**1.34**
HBA	Hemoglobin subunit alpha	15.2	260.2	26.1	**1.34**
HSP71	Heat shock 70 kDa protein 1A/1B	70.0	387	7.6	**1.34**
IMMT	Mitochondrial inner membrane protein	83.6	160.7	3.2	**1.34**
SEC13	Protein SEC13 homolog	35.5	60.9	4.7	**1.34**
SMD1	Small nuclear ribonucleoprotein Sm D1	13.3	112	10.9	**1.34**
SYF2	Pre-mRNA-splicing factor SYF2	28.7	101.8	4.5	**1.34**
THOC2	THO complex subunit 2	182.7	340.2	3.6	**1.34**
ACINU	Apoptotic chromatin condensation inducer in the nucleus	151.8	249	5.1	**1.33**
ACOD	Acyl-CoA desaturase	41.5	86.8	3.6	**1.33**
AT2A2	Sarcoplasmic/endoplasmic reticulum calcium ATPase 2	114.7	151.8	4.2	**1.33**
EF1G	Elongation factor 1-gamma	50.1	207	9.2	**1.33**
FKBP8	Peptidyl-prolyl cis-trans isomerase FKBP8	44.5	61.7	3.9	**1.33**
HNRH3	Heterogeneous nuclear ribonucleoprotein H3	36.9	386.2	14.5	**1.33**
MLH1	DNA mismatch repair protein Mlh1	84.5	110	1.3	**1.33**
PR38B	Pre-mRNA-splicing factor 38B	64.4	82.8	2.6	**1.33**
SFRS9	Splicing factor, arginine/serine-rich 9	25.5	200.7	20.8	**1.33**

USMG5	Up-regulated during skeletal muscle growth protein 5	6.5	51.8	25.9	**1.33**
AMPM2	Methionine aminopeptidase 2	52.9	90.3	3.6	**1.31**
CC063	Uncharacterized protein C3orf63	188.9	88.1	2.6	**1.31**
HNRPF	Heterogeneous nuclear ribonucleoprotein F	45.6	422.9	21.7	**1.31**
RPN1	Dolichyl-diphosphooligosaccharide--protein glycosyltransferase subunit 1	68.5	113.9	1.8	**1.31**
DHSA	Succinate dehydrogenase [ubiquinone] flavoprotein subunit, mitochondrial	72.6	371.2	13.0	**1.30**
EF1D	Elongation factor 1-delta	31.1	123.7	12.8	**1.30**
FA98B	Protein FAM98B	37.2	150.4	3.9	**1.30**
GPDM	Glycerol-3-phosphate dehydrogenase, mitochondrial	80.8	216.4	6.1	**1.30**
PRC1	Protein regulator of cytokinesis 1	71.6	145.7	6.3	**1.30**
PRDX1	Peroxiredoxin-1	22.1	296.6	20.1	**1.30**
PRDX3	Thioredoxin-dependent peroxide reductase, mitochondrial	27.7	76.6	4.3	**1.30**
U520	U5 small nuclear ribonucleoprotein 200 kDa helicase	244.4	816.2	5.9	**1.30**
1433E	14-3-3 protein epsilon	29.2	209.4	12.9	**1.29**
CDK2	Cell division protein kinase 2	33.9	59.4	4.7	**1.29**
IF2P	Eukaryotic translation initiation factor 5B	138.7	431.6	6.1	**1.29**
LYRIC	Protein LYRIC	63.8	117.4	4.5	**1.29**
MTDC	Bifunctional methylenetetrahydrofolate dehydrogenase/cyclohydrolase, mitochondrial	37.9	67.7	3.1	**1.29**
ROA1	Heterogeneous nuclear ribonucleoprotein A1	38.7	1600.4	46.8	**1.29**
ARP6	Actin-related protein 6	45.8	43.4	3.0	**1.28**
GRP75	Stress-70 protein, mitochondrial	73.6	1534.6	33.6	**1.28**
K1C18	Keratin, type I cytoskeletal 18	48.0	1567.2	39.1	**1.28**
KIF2C	Kinesin-like protein KIF2C	81.3	205.7	7.4	**1.28**
LONM	Lon protease homolog, mitochondrial	106.4	129.1	4.3	**1.28**
MED1	Mediator of RNA polymerase II transcription subunit 1	168.4	136.2	1.7	**1.28**
P3C2A	Phosphatidylinositol-4-phosphate 3-kinase C2 domain-containing subunit alpha	190.6	109.1	1.5	**1.28**
RLA0	60S acidic ribosomal protein P0	34.3	202.8	7.3	**1.28**
SC22B	Vesicle-trafficking protein SEC22b	24.7	108.2	8.8	**1.28**
TOP2B	DNA topoisomerase 2-beta	183.2	520.9	6.5	**1.28**
1433T	14-3-3 protein theta	27.7	137.7	7.3	**1.27**
ACADM	Medium-chain specific acyl-CoA dehydrogenase, mitochondrial	46.6	66.9	2.9	**1.27**
ACTC	Actin, alpha cardiac muscle 1	42.0	753.1	26.8	**1.27**
ALBU	Serum albumin	69.3	146.6	5.1	**1.27**
ATAD2	ATPase family AAA domain-containing protein 2	158.5	259.1	4.7	**1.27**
ATP5J	ATP synthase-coupling factor 6, mitochondrial	12.6	45.7	17.6	**1.27**
ATP5L	ATP synthase subunit g, mitochondrial	11.4	83.6	11.7	**1.27**
CDK7	Cell division protein kinase 7	39.0	90.5	7.8	**1.27**
CMC2	Calcium-binding mitochondrial carrier protein Aralar2	74.1	52	3.9	**1.27**
DYHC1	Cytoplasmic dynein 1 heavy chain 1	532.1	71.3	0.5	**1.27**
GLYM	Serine hydroxymethyltransferase, mitochondrial	56.0	295.7	11.1	**1.27**
LC7L3	Luc7-like protein 3	51.4	114.6	7.9	**1.27**

LMNA	Lamin-A/C	74.1	2742.5	59.0	**1.27**
LPPRC	Leucine-rich PPR motif-containing protein, mitochondrial	157.8	584.4	11.1	**1.27**
MPPA	Mitochondrial-processing peptidase subunit alpha	58.2	51.4	4.4	**1.27**
P80C	Coilin	62.6	124.4	5.2	**1.27**
RALY	RNA-binding protein Raly	32.4	111.5	6.5	**1.27**
ROAA	Heterogeneous nuclear ribonucleoprotein A/B	36.2	351.8	17.5	**1.27**
S10AD	Protein S100-A13	11.5	71	11.2	**1.27**
SMRD2	SWI/SNF-related matrix-associated actin-dependent regulator of chromatin subfamily D member 2	52.3	90.5	2.9	**1.27**
STRAP	Serine-threonine kinase receptor-associated protein	38.4	107.5	12.0	**1.27**
TRI33	E3 ubiquitin-protein ligase TRIM33	122.4	115.6	3.8	**1.27**
4F2	4F2 cell-surface antigen heavy chain	68.0	109.5	5.4	**1.25**
ATPB	ATP synthase subunit beta, mitochondrial	56.5	1661.8	43.3	**1.25**
ATPG	ATP synthase subunit gamma, mitochondrial	33.0	68	4.0	**1.25**
CALX	Calnexin	67.5	240	6.6	**1.25**
COX41	Cytochrome c oxidase subunit 4 isoform 1, mitochondrial	19.6	70.4	7.1	**1.25**
ECHB	Trifunctional enzyme subunit beta, mitochondrial	51.3	54.3	2.3	**1.25**
ELYS	Protein ELYS	252.3	91.9	1.0	**1.25**
RAN	GTP-binding nuclear protein Ran	24.4	232.3	16.2	**1.25**
RAP1B	Ras-related protein Rap-1b	20.8	121.5	5.4	**1.25**
THIL	Acetyl-CoA acetyltransferase, mitochondrial	45.2	277.6	12.9	**1.25**

B) APC5i

Protein	Full Name	MW [kDa]	Mascot Score	SC [%]	% change
PIWL1	Piwi-like protein 1	98.5	30.1	1.0	**106.00**
SYNE2	Nesprin-2	795.9	52.4	0.1	**106.00**
NACA2	Nascent polypeptide-associated complex subunit alpha-2	23.2	39.1	7.0	**13.25**
TITIN	Titin	3813.8	105.3	0.1	**7.07**
MAOM	NAD-dependent malic enzyme, mitochondrial	65.4	30	2.6	**5.89**
HCFC1	Host cell factor 1	208.6	65	1.3	**4.61**
TCPQ	T-complex protein 1 subunit theta	59.6	157.6	6.6	**4.24**
MYH14	Myosin-14	227.9	49.9	0.8	**3.66**
MUTA	Methylmalonyl-CoA mutase, mitochondrial	83.1	54.2	1.5	**3.53**
COX5B	Cytochrome c oxidase subunit 5B, mitochondrial	13.7	30.2	9.3	**3.31**
SRPRB	Signal recognition particle receptor subunit beta	29.7	40.4	7.0	**3.31**
YTDC1	YTH domain-containing protein 1	84.6	33.2	1.5	**3.31**
AN32E	Acidic leucine-rich nuclear phosphoprotein 32 family member E	30.7	40.2	4.5	**3.21**
ESYT1	Extended synaptotagmin-1	122.8	169.8	2.6	**3.21**
WAPL	Wings apart-like protein homolog	132.9	121.1	2.1	**3.21**
ENOA	Alpha-enolase	47.1	423.1	16.8	**3.12**
RGAP1	Rac GTPase-activating protein 1	71.0	53	1.7	**3.12**

PECI	Peroxisomal 3,2-trans-enoyl-CoA isomerase	43.6	50.4	4.3	**2.94**
CAND1	Cullin-associated NEDD8-dissociated protein 1	136.3	91.2	2.9	**2.72**
DHB8	Estradiol 17-beta-dehydrogenase 8	27.0	84.1	10.3	**2.72**
GSTK1	Glutathione S-transferase kappa 1	25.5	101.2	11.5	**2.72**
K1C9	Keratin, type I cytoskeletal 9	62.0	69.2	6.9	**2.72**
MYO1C	Myosin-Ic	121.6	48	1.1	**2.65**
CYB5B	Cytochrome b5 type B	16.3	68.7	8.2	**2.59**
RM22	39S ribosomal protein L22, mitochondrial	23.6	55	5.8	**2.52**
RS30	40S ribosomal protein S30	6.6	57.3	16.9	**2.52**
SERA	D-3-phosphoglycerate dehydrogenase	56.6	183.6	7.3	**2.52**
APTX	Aprataxin	40.7	215.9	14.9	**2.47**
IF4G2	Eukaryotic translation initiation factor 4 gamma 2	102.3	37.1	1.4	**2.41**
KCRB	Creatine kinase B-type	42.6	152.8	13.1	**2.41**
ODP2	Dihydrolipoyllysine-residue acetyltransferase component of pyruvate dehydrogenase complex, mitochondrial	69.0	92.5	4.5	**2.41**
ECT2	Protein ECT2	100.0	29.9	1.4	**2.30**
ERO1A	ERO1-like protein alpha	54.4	36.6	3.0	**2.30**
HS90A	Heat shock protein HSP 90-alpha	84.6	399.9	10.2	**2.30**
PO210	Nuclear pore membrane glycoprotein 210	205.0	59.3	1.5	**2.30**
CISD2	CDGSH iron sulfur domain-containing protein 2	15.3	31.6	10.4	**2.26**
RTN4	Reticulon-4	129.9	42	1.2	**2.26**
SPTC1	Serine palmitoyltransferase 1	52.7	60.9	3.0	**2.26**
HS90B	Heat shock protein HSP 90-beta	83.2	491.7	10.1	**2.21**
CA131	Uncharacterized protein C1orf131	32.7	191.9	14.3	**2.16**
FPPS	Farnesyl pyrophosphate synthase	48.2	39.5	4.3	**2.16**
TRM6	tRNA (adenine-N(1)-)-methyltransferase non-catalytic subunit TRM6	55.8	62.6	3.6	**2.16**
UBP14	Ubiquitin carboxyl-terminal hydrolase 14	56.0	120.4	2.6	**2.16**
RLA2	60S acidic ribosomal protein P2	11.7	82.6	10.4	**2.12**
TKT	Transketolase	67.8	245.2	10.8	**2.12**
ALBU	Serum albumin	69.3	67.1	2.5	**2.08**
COPA	Coatomer subunit alpha	138.3	136.6	2.9	**2.08**
EF1D	Elongation factor 1-delta	31.1	63.8	4.3	**2.04**
KIF2C	Kinesin-like protein KIF2C	81.3	257.2	7.0	**2.04**
ACTN4	Alpha-actinin-4	104.8	185.4	6.5	**2.00**
RT29	28S ribosomal protein S29, mitochondrial	45.5	126.3	6.8	**2.00**
AIFM1	Apoptosis-inducing factor 1, mitochondrial	66.9	216	10.0	**1.96**
IF2B1	Insulin-like growth factor 2 mRNA-binding protein 1	63.4	64.3	5.4	**1.96**
TAGL2	Transgelin-2	22.4	66	6.0	**1.96**
TM109	Transmembrane protein 109	26.2	30.2	4.9	**1.96**
YH007	Uncharacterized protein FLJ40521	48.3	43.3	1.5	**1.96**
3MG	DNA-3-methyladenine glycosylase	32.8	96.2	11.1	**1.93**
GANAB	Neutral alpha-glucosidase AB	106.8	129.6	1.8	**1.93**
KPYM	Pyruvate kinase isozymes M1/M2	57.9	332.4	15.3	**1.93**

1433Z	14-3-3 protein zeta/delta	27.7	197.6	17.6	**1.89**
AT1A3	Sodium/potassium-transporting ATPase subunit alpha-3	111.7	91.8	1.8	**1.89**
CPSF3	Cleavage and polyadenylation specificity factor subunit 3	77.4	58.1	4.8	**1.89**
HTAI2	Oxidoreductase HTATIP2	27.1	115.7	8.7	**1.89**
PDIA1	Protein disulfide-isomerase	57.1	188.8	7.5	**1.89**
PRP4B	Serine/threonine-protein kinase PRP4 homolog	116.9	191.4	2.8	**1.89**
REN3B	Regulator of nonsense transcripts 3B	57.7	44.8	3.1	**1.89**
SPTA2	Spectrin alpha chain, brain	284.4	45.1	0.9	**1.89**
TFR1	Transferrin receptor protein 1	84.8	109.9	7.0	**1.89**
ENPL	Endoplasmin	92.4	398.5	11.1	**1.86**
MCE1	mRNA-capping enzyme	68.5	90	3.9	**1.86**
RL11	60S ribosomal protein L11	20.2	275.4	11.8	**1.86**
SCMC1	Calcium-binding mitochondrial carrier protein SCaMC-1	53.3	35.8	2.7	**1.86**
ANXA2	Annexin A2	38.6	616	35.4	**1.83**
RM41	39S ribosomal protein L41, mitochondrial	15.4	44.8	7.3	**1.83**
TPR	Nucleoprotein TPR	267.1	509.8	6.0	**1.83**
CLPP	Putative ATP-dependent Clp protease proteolytic subunit, mitochondrial	30.2	108.8	5.4	**1.80**
CQ085	Uncharacterized protein C17orf85	70.5	85	2.1	**1.80**
CY1	Cytochrome c1, heme protein, mitochondrial	35.4	116.5	7.7	**1.80**
GBLP	Guanine nucleotide-binding protein subunit beta-2-like 1	35.1	320	20.5	**1.80**
HBB	Hemoglobin subunit beta	16.0	42.6	6.8	**1.80**
PTRF	Polymerase I and transcript release factor	43.4	36.4	4.4	**1.80**
ABCD3	ATP-binding cassette sub-family D member 3	75.4	81.6	2.1	**1.77**
CG050	Uncharacterized protein C7orf50	22.1	275.3	38.7	**1.77**
ITB1	Integrin beta-1	88.4	95.8	2.5	**1.77**
MYH9	Myosin-9	226.4	48.4	1.7	**1.77**
TCPA	T-complex protein 1 subunit alpha	60.3	203.1	11.3	**1.77**
LRC59	Leucine-rich repeat-containing protein 59	34.9	61.8	6.8	**1.74**
RPN1	Dolichyl-diphosphooligosaccharide--protein glycosyltransferase subunit 1	68.5	117.5	4.4	**1.74**
RPN2	Dolichyl-diphosphooligosaccharide--protein glycosyltransferase subunit 2	69.2	82.2	2.2	**1.74**
SFXN1	Sideroflexin-1	35.6	258.6	11.8	**1.74**
SRP54	Signal recognition particle 54 kDa protein	55.7	48.5	2.8	**1.74**
ACSL3	Long-chain-fatty-acid--CoA ligase 3	80.4	117.6	4.6	**1.71**
FANCI	Fanconi anemia group I protein	149.2	123	2.1	**1.71**
MPCP	Phosphate carrier protein, mitochondrial	40.1	343.9	13.0	**1.71**
SFR14	Putative splicing factor, arginine/serine-rich 14	120.2	91.6	3.3	**1.71**
1433E	14-3-3 protein epsilon	29.2	114.6	8.2	**1.68**
HSP71	Heat shock 70 kDa protein 1A/1B	70.0	227.4	8.4	**1.68**
MED4	Mediator of RNA polymerase II transcription subunit 4	29.7	112.1	15.2	**1.68**
NNTM	NAD(P) transhydrogenase, mitochondrial	113.8	82	2.4	**1.68**
RM27	39S ribosomal protein L27, mitochondrial	16.1	32.6	6.8	**1.68**

TOP2A	DNA topoisomerase 2-alpha	174.3	1110.9	14.1	**1.68**
ANM5	Protein arginine N-methyltransferase 5	72.6	34.9	2.0	**1.66**
DHB4	Peroxisomal multifunctional enzyme type 2	79.6	363.8	12.5	**1.66**
MED24	Mediator of RNA polymerase II transcription subunit 24	110.2	232.9	5.5	**1.66**
RT25	28S ribosomal protein S25, mitochondrial	20.1	33	7.5	**1.66**
ATD3B	ATPase family AAA domain-containing protein 3B	72.5	78.8	1.9	**1.63**
CALX	Calnexin	67.5	94.2	4.9	**1.63**
FLNA	Filamin-A	280.6	105.6	2.0	**1.63**
G3BP1	Ras GTPase-activating protein-binding protein 1	52.1	51.6	2.4	**1.63**
GLU2B	Glucosidase 2 subunit beta	59.4	74.9	2.5	**1.63**
IDHP	Isocitrate dehydrogenase [NADP], mitochondrial	50.9	41.8	2.4	**1.63**
IPO5	Importin-5	123.5	34.3	1.1	**1.63**
MDC1	Mediator of DNA damage checkpoint protein 1	226.5	71.8	1.1	**1.63**
PDIA3	Protein disulfide-isomerase A3	56.7	481.1	19.8	**1.63**
PON2	Serum paraoxonase/arylesterase 2	39.4	64.5	4.5	**1.63**
QCR2	Cytochrome b-c1 complex subunit 2, mitochondrial	48.4	142.2	7.7	**1.63**
RU2A	U2 small nuclear ribonucleoprotein A'	28.4	319.8	20.4	**1.63**
SPTB2	Spectrin beta chain, brain 1	274.4	73.3	0.8	**1.63**
TBA1C	Tubulin alpha-1C chain	49.9	436.7	28.3	**1.63**
ABCF2	ATP-binding cassette sub-family F member 2	71.2	108.3	3.9	**1.61**
APOO	Apolipoprotein O	22.3	61.4	7.6	**1.61**
CALR	Calreticulin	48.1	170.2	8.6	**1.61**
NC2A	Dr1-associated corepressor	22.3	30.2	4.9	**1.61**
NU214	Nuclear pore complex protein Nup214	213.5	86.2	2.2	**1.61**
RCOR1	REST corepressor 1	53.0	135.4	2.5	**1.61**
VRK1	Serine/threonine-protein kinase VRK1	45.4	134.6	8.1	**1.61**
GRP78	78 kDa glucose-regulated protein	72.3	865.6	23.9	**1.58**
PSD12	26S proteasome non-ATPase regulatory subunit 12	52.9	79.3	3.1	**1.58**
SRBD1	S1 RNA-binding domain-containing protein 1	111.7	144.4	2.2	**1.58**
TRAP1	Heat shock protein 75 kDa, mitochondrial	80.1	401	12.2	**1.58**
ACADM	Medium-chain specific acyl-CoA dehydrogenase, mitochondrial	46.6	138.6	8.8	**1.56**
ECHA	Trifunctional enzyme subunit alpha, mitochondrial	82.9	479.3	14.9	**1.56**
HSDL2	Hydroxysteroid dehydrogenase-like protein 2	45.4	137.8	4.3	**1.56**
IDH3B	Isocitrate dehydrogenase [NAD] subunit beta, mitochondrial	42.2	118.9	10.4	**1.56**
IQGA1	Ras GTPase-activating-like protein IQGAP1	189.1	77.4	1.3	**1.56**
MAT1	CDK-activating kinase assembly factor MAT1	35.8	283.5	16.8	**1.56**
NDUA9	NADH dehydrogenase [ubiquinone] 1 alpha subcomplex subunit 9, mitochondrial	42.5	34.3	3.2	**1.56**
NDUB1	NADH dehydrogenase [ubiquinone] 1 beta subcomplex subunit 1	7.0	63.1	19.0	**1.56**
NU188	Nucleoporin NUP188 homolog	195.9	97.4	2.1	**1.56**
PDIA4	Protein disulfide-isomerase A4	72.9	72.6	4.7	**1.56**
PDIA6	Protein disulfide-isomerase A6	48.1	152.4	8.9	**1.56**
SC22B	Vesicle-trafficking protein SEC22b	24.7	304.2	20.9	**1.56**

4F2	4F2 cell-surface antigen heavy chain	68.0	90.2	8.7	**1.54**
CLH1	Clathrin heavy chain 1	191.5	185.5	3.0	**1.54**
COPZ1	Coatomer subunit zeta-1	20.2	119.2	16.9	**1.54**
G45IP	Growth arrest and DNA damage-inducible proteins-interacting protein 1	25.4	44.9	4.5	**1.54**
H32	Histone H3.2	15.4	533.7	41.2	**1.54**
IF4A1	Eukaryotic initiation factor 4A-I	46.1	622.4	30.0	**1.54**
RADI	Radixin	68.5	113	4.1	**1.54**
RM11	39S ribosomal protein L11, mitochondrial	20.7	90.7	15.6	**1.54**
RM12	39S ribosomal protein L12, mitochondrial	21.3	54	6.1	**1.54**
SLU7	Pre-mRNA-splicing factor SLU7	68.3	46.8	2.4	**1.54**
TOIP1	Torsin-1A-interacting protein 1	66.2	232.2	4.5	**1.54**
AURKB	Serine/threonine-protein kinase 12	39.3	108.4	7.8	**1.51**
C1TM	Monofunctional C1-tetrahydrofolate synthase, mitochondrial	105.7	91.8	1.1	**1.51**
HNRCL	Heterogeneous nuclear ribonucleoprotein C-like 1	32.1	445.8	17.1	**1.51**
PRDX5	Peroxiredoxin-5, mitochondrial	22.0	81.3	15.9	**1.51**
PRP6	Pre-mRNA-processing factor 6	106.9	155.9	4.4	**1.51**
PSME3	Proteasome activator complex subunit 3	29.5	47.9	5.9	**1.51**
RLA0	60S acidic ribosomal protein P0	34.3	127.5	6.6	**1.51**
SEC63	Translocation protein SEC63 homolog	87.9	39.7	1.7	**1.51**
SYDM	Aspartyl-tRNA synthetase, mitochondrial	73.5	116	2.9	**1.51**
TBA1B	Tubulin alpha-1B chain	50.1	726.9	34.8	**1.51**
TBB5	Tubulin beta chain	49.6	640.5	27.3	**1.51**
THIL	Acetyl-CoA acetyltransferase, mitochondrial	45.2	234	14.8	**1.51**
VAPB	Vesicle-associated membrane protein-associated protein B/C	27.2	51.3	4.9	**1.51**
WAC	WW domain-containing adapter protein with coiled-coil	70.7	66.3	5.4	**1.51**
AAAS	Aladin	59.5	80.4	6.6	**1.49**
AL9A1	4-trimethylaminobutyraldehyde dehydrogenase	53.8	48.1	4.3	**1.49**
ARF4	ADP-ribosylation factor 4	20.5	44.6	5.6	**1.49**
G3P	Glyceraldehyde-3-phosphate dehydrogenase	36.0	478.8	31.6	**1.49**
IMP4	U3 small nucleolar ribonucleoprotein protein IMP4	33.7	530.3	29.2	**1.49**
KIFC1	Kinesin-like protein KIFC1	73.7	233.4	8.5	**1.49**
LAT1	Large neutral amino acids transporter small subunit 1	55.0	76.7	6.7	**1.49**
RBM10	RNA-binding protein 10	103.5	144.4	2.7	**1.49**
RRBP1	Ribosome-binding protein 1	152.4	32.8	1.2	**1.49**
S10AD	Protein S100-A13	11.5	87.7	31.6	**1.49**
SMCA4	Transcription activator BRG1	184.5	231.1	2.8	**1.49**
SPT5H	Transcription elongation factor SPT5	120.9	54	2.1	**1.49**
TRIPC	Probable E3 ubiquitin-protein ligase TRIP12	220.3	192	2.9	**1.49**
C19L1	CWF19-like protein 1	60.6	54.5	2.6	**1.47**
COPG	Coatomer subunit gamma	97.7	41.6	2.1	**1.47**
DNJA3	DnaJ homolog subfamily A member 3, mitochondrial	52.5	90.8	8.1	**1.47**
HS71L	Heat shock 70 kDa protein 1-like	70.3	289	8.7	**1.47**

HSP74	Heat shock 70 kDa protein 4	94.3	68.3	3.0	**1.47**
NDUS1	NADH-ubiquinone oxidoreductase 75 kDa subunit, mitochondrial	79.4	263.1	10.0	**1.47**
RSSA	40S ribosomal protein SA	32.8	209.6	14.6	**1.47**
XPO1	Exportin-1	123.3	225.5	6.3	**1.47**
CDC2	Cell division control protein 2 homolog	34.1	162.4	13.5	**1.45**
ECH1	Delta(3,5)-Delta(2,4)-dienoyl-CoA isomerase, mitochondrial	35.8	244	17.4	**1.45**
HXK1	Hexokinase-1	102.4	31.5	1.2	**1.45**
TCPB	T-complex protein 1 subunit beta	57.5	258.4	11.6	**1.45**
ACTB	Actin, cytoplasmic 1	41.7	1072.9	41.6	**1.43**
PLEC1	Plectin-1	531.5	1407.1	6.2	**1.43**
SF01	Splicing factor 1	68.3	40.6	2.5	**1.43**
SUV91	Histone-lysine N-methyltransferase SUV39H1	47.9	70.9	6.1	**1.43**
ZN326	Zinc finger protein 326	65.6	383.5	12.5	**1.43**
1433T	14-3-3 protein theta	27.7	240.9	17.6	**1.41**
COPB	Coatomer subunit beta	107.1	53	2.4	**1.41**
DDX6	Probable ATP-dependent RNA helicase DDX6	54.4	101.7	3.1	**1.41**
EED	Polycomb protein EED	50.2	56.9	4.3	**1.41**
MORC2	MORC family CW-type zinc finger protein 2	117.7	51.1	2.6	**1.41**
STT3A	Dolichyl-diphosphooligosaccharide--protein glycosyltransferase subunit STT3A	80.5	52.4	1.7	**1.41**
CE024	UPF0461 protein C5orf24	20.1	94	7.4	**1.39**
ETHE1	Protein ETHE1, mitochondrial	27.9	95.7	12.2	**1.39**
NU107	Nuclear pore complex protein Nup107	106.3	114.5	5.6	**1.39**
P66B	Transcriptional repressor p66-beta	65.2	114.5	5.6	**1.39**
SSBP	Single-stranded DNA-binding protein, mitochondrial	17.2	201.6	28.4	**1.39**
SYPL1	Synaptophysin-like protein 1	28.5	45.4	4.2	**1.39**
TCPD	T-complex protein 1 subunit delta	57.9	524.1	17.1	**1.39**
TMM70	Transmembrane protein 70, mitochondrial	29.0	40.5	4.6	**1.39**
U5S1	116 kDa U5 small nuclear ribonucleoprotein component	109.4	566.9	12.6	**1.39**
EHD4	EH domain-containing protein 4	61.1	60.3	2.4	**1.38**
NEST	Nestin	177.3	113.5	1.7	**1.38**
NSF	Vesicle-fusing ATPase	82.5	43.9	3.1	**1.38**
P5CR1	Pyrroline-5-carboxylate reductase 1, mitochondrial	33.3	196.7	14.1	**1.38**
PPIA	Peptidyl-prolyl cis-trans isomerase A	18.0	157.1	18.8	**1.38**
RPB2	DNA-directed RNA polymerase II subunit RPB2	133.8	47.4	1.4	**1.38**
SSRD	Translocon-associated protein subunit delta	19.0	115.5	13.9	**1.38**
STML2	Stomatin-like protein 2	38.5	238.7	22.2	**1.38**
TOM40	Mitochondrial import receptor subunit TOM40 homolog	37.9	144.6	10.2	**1.38**
CISD1	CDGSH iron sulfur domain-containing protein 1	12.2	59.6	13.9	**1.36**
DYL1	Dynein light chain 1, cytoplasmic	10.4	266.7	49.4	**1.36**
KI20A	Kinesin-like protein KIF20A	100.2	39.8	1.8	**1.36**
LTV1	Protein LTV1 homolog	54.8	97.1	2.5	**1.36**
PLOD3	Procollagen-lysine,2-oxoglutarate 5-dioxygenase 3	84.7	114.1	3.3	**1.36**

RGPD4	RanBP2-like and GRIP domain-containing protein 4	198.1	166.9	2.2	**1.36**
TOP2B	DNA topoisomerase 2-beta	183.2	872.2	9.2	**1.36**
ADT2	ADP/ATP translocase 2	32.9	643.7	30.5	**1.34**
ATD3A	ATPase family AAA domain-containing protein 3A	71.3	85.5	5.5	**1.34**
EF1G	Elongation factor 1-gamma	50.1	230.2	10.1	**1.34**
EIF2A	Eukaryotic translation initiation factor 2A	64.9	123.8	5.3	**1.34**
NSL1	Kinetochore-associated protein NSL1 homolog	32.1	32.6	6.0	**1.34**
NUP98	Nuclear pore complex protein Nup98-Nup96	187.7	284.2	4.3	**1.34**
NXF1	Nuclear RNA export factor 1	70.1	236	4.0	**1.34**
PRDX3	Thioredoxin-dependent peroxide reductase, mitochondrial	27.7	166.9	5.5	**1.34**
RAB5C	Ras-related protein Rab-5C	23.5	297.5	28.2	**1.34**
RS2	40S ribosomal protein S2	31.3	123.5	15.7	**1.34**
RS27A	40S ribosomal protein S27a	9.4	151.8	40.0	**1.34**
SMD3	Small nuclear ribonucleoprotein Sm D3	13.9	447.9	47.6	**1.34**
TCP4	Activated RNA polymerase II transcriptional coactivator p15	14.4	311.2	43.3	**1.34**
UBQL1	Ubiquilin-1	62.5	31	2.7	**1.34**
VAT1	Synaptic vesicle membrane protein VAT-1 homolog	41.9	163.1	11.5	**1.34**
ZFR	Zinc finger RNA-binding protein	116.9	251.2	11.3	**1.34**
1433G	14-3-3 protein gamma	28.3	63.2	9.3	**1.33**
ATPA	ATP synthase subunit alpha, mitochondrial	59.7	920.1	29.5	**1.33**
BUB3	Mitotic checkpoint protein BUB3	37.1	540.1	20.7	**1.33**
EAF6	Chromatin modification-related protein MEAF6	21.6	39.8	11.5	**1.33**
HNRPC	Heterogeneous nuclear ribonucleoproteins C1/C2	33.6	762.4	26.5	**1.33**
NDUA7	NADH dehydrogenase [ubiquinone] 1 alpha subcomplex subunit 7	12.5	37.8	15.9	**1.33**
NU205	Nuclear pore complex protein Nup205	227.8	231.7	2.3	**1.33**
PHB2	Prohibitin-2	33.3	459.4	32.8	**1.33**
PIAS2	E3 SUMO-protein ligase PIAS2	68.2	88.2	2.4	**1.33**
RAB1A	Ras-related protein Rab-1A	22.7	224.5	26.8	**1.33**
RB12B	RNA-binding protein 12B	118.0	250.7	3.6	**1.33**
SLN13	Schlafen family member 13	102.0	64.2	2.6	**1.33**
SND1	Staphylococcal nuclease domain-containing protein 1	101.9	509.3	11.3	**1.33**
TCPG	T-complex protein 1 subunit gamma	60.5	239.1	12.5	**1.33**
THOC4	THO complex subunit 4	26.9	80.6	11.3	**1.33**
VPS35	Vacuolar protein sorting-associated protein 35	91.6	55.1	1.9	**1.33**
WIZ	Protein Wiz	178.6	53.7	0.7	**1.33**
ZN800	Zinc finger protein 800	75.2	68.4	4.4	**1.33**
ADT3	ADP/ATP translocase 3	32.8	683.4	34.2	**1.31**
ARP5L	Actin-related protein 2/3 complex subunit 5-like protein	16.9	47.9	7.8	**1.31**
BLM	Bloom syndrome protein	158.9	251.2	3.0	**1.31**
INT8	Integrator complex subunit 8	113.0	31.8	1.3	**1.31**
NELFE	Negative elongation factor E	43.2	160.8	9.2	**1.31**
NUP93	Nuclear pore complex protein Nup93	93.4	534.2	9.9	**1.31**
PNPT1	Polyribonucleotide nucleotidyltransferase 1, mitochondrial	85.9	77.6	4.0	**1.31**

PR38A	Pre-mRNA-splicing factor 38A	37.5	96.3	3.8	**1.31**
RED	Protein Red	65.6	78.4	4.1	**1.31**
RM04	39S ribosomal protein L4, mitochondrial	34.9	41.5	6.1	**1.31**
SF3A3	Splicing factor 3A subunit 3	58.8	105.3	8.4	**1.31**
THIM	3-ketoacyl-CoA thiolase, mitochondrial	41.9	59.8	7.8	**1.31**
TIM23	Mitochondrial import inner membrane translocase subunit Tim23	21.9	79.7	8.1	**1.31**
HNRL2	Heterogeneous nuclear ribonucleoprotein U-like protein 2	85.1	42.4	1.7	**1.29**
INT1	Integrator complex subunit 1	244.1	144.2	1.1	**1.29**
MPPB	Mitochondrial-processing peptidase subunit beta	54.3	66.5	5.3	**1.29**
NELFB	Negative elongation factor B	65.7	51	1.7	**1.29**
NF1	Neurofibromin	319.2	73.2	1.1	**1.29**
NIPBL	Nipped-B-like protein	315.9	350.2	2.4	**1.29**
NU160	Nuclear pore complex protein Nup160	162.0	252	2.9	**1.29**
NUP85	Nuclear pore complex protein Nup85	75.0	161.9	5.6	**1.29**
PRPS2	Ribose-phosphate pyrophosphokinase 2	34.7	31.3	3.8	**1.29**
SYTM	Threonyl-tRNA synthetase, mitochondrial	81.0	48.1	2.5	**1.29**
TBB2C	Tubulin beta-2C chain	49.8	617.2	31.0	**1.29**
TCPH	T-complex protein 1 subunit eta	59.3	185.7	9.2	**1.29**
TCPZ	T-complex protein 1 subunit zeta	58.0	118.1	5.8	**1.29**
UNG	Uracil-DNA glycosylase	34.6	38.5	3.8	**1.29**
ZC3H8	Zinc finger CCCH domain-containing protein 8	33.6	76.8	7.6	**1.29**
ATX10	Ataxin-10	53.5	39.6	3.2	**1.28**
GUAA	GMP synthase [glutamine-hydrolyzing]	76.7	181.2	5.1	**1.28**
HNRH2	Heterogeneous nuclear ribonucleoprotein H2	49.2	652.5	25.2	**1.28**
IMB1	Importin subunit beta-1	97.1	236.6	3.4	**1.28**
ODO1	2-oxoglutarate dehydrogenase, mitochondrial	115.9	145	3.6	**1.28**
RAE1L	mRNA export factor	40.9	344.9	23.9	**1.28**
RS16	40S ribosomal protein S16	16.4	305.2	25.3	**1.28**
SNUT2	U4/U6.U5 tri-snRNP-associated protein 2	65.3	35.5	2.1	**1.28**
ATP5H	ATP synthase subunit d, mitochondrial	18.5	146.8	16.1	**1.26**
ATPO	ATP synthase subunit O, mitochondrial	23.3	262.2	25.8	**1.26**
CENPL	Centromere protein L	39.0	54.1	3.5	**1.26**
CLPB	Caseinolytic peptidase B protein homolog	78.7	67.4	1.8	**1.26**
DHE3	Glutamate dehydrogenase 1, mitochondrial	61.4	121.6	6.8	**1.26**
DJC11	DnaJ homolog subfamily C member 11	63.2	56.2	2.7	**1.26**
MSH6	DNA mismatch repair protein Msh6	152.7	704.3	9.3	**1.26**
MTA1	Metastasis-associated protein MTA1	80.7	204.3	6.0	**1.26**
NCOA5	Nuclear receptor coactivator 5	65.5	124.7	3.3	**1.26**
NDUS3	NADH dehydrogenase [ubiquinone] iron-sulfur protein 3, mitochondrial	30.2	139	17.0	**1.26**
QCR1	Cytochrome b-c1 complex subunit 1, mitochondrial	52.6	247.7	14.0	**1.26**
SC23A	Protein transport protein Sec23A	86.1	106.8	1.6	**1.26**
SCC4	Cohesin loading complex subunit SCC4 homolog	69.0	90.7	3.9	**1.26**

TBRG4	Protein TBRG4	70.7	84.6	5.1	**1.26**
AT5F1	ATP synthase subunit b, mitochondrial	28.9	212.5	18.4	**1.25**
ATPG	ATP synthase subunit gamma, mitochondrial	33.0	271.9	18.5	**1.25**
EPIPL	Epiplakin	552.8	209.4	0.6	**1.25**
GHITM	Growth hormone-inducible transmembrane protein	37.2	32.6	2.9	**1.25**
GRP75	Stress-70 protein, mitochondrial	73.6	1980.9	43.7	**1.25**
HNRPR	Heterogeneous nuclear ribonucleoprotein R	70.9	614.6	16.7	**1.25**
LAP2B	Lamina-associated polypeptide 2, isoforms beta/gamma	50.6	193.1	15.6	**1.25**
NDUB4	NADH dehydrogenase [ubiquinone] 1 beta subcomplex subunit 4	15.2	81.4	14.0	**1.25**
ORC1	Origin recognition complex subunit 1	97.3	88.4	2.0	**1.25**
PTN1	Tyrosine-protein phosphatase non-receptor type 1	49.9	36	2.3	**1.25**
PYC	Pyruvate carboxylase, mitochondrial	129.6	71.7	1.2	**1.25**
RT09	28S ribosomal protein S9, mitochondrial	45.8	80.2	4.0	**1.25**
SLIRP	SRA stem-loop-interacting RNA-binding protein, mitochondrial	12.3	249.3	43.1	**1.25**
SMRD2	SWI/SNF-related matrix-associated actin-dependent regulator of chromatin subfamily D member 2	52.3	101.4	7.2	**1.25**
TRI33	E3 ubiquitin-protein ligase TRIM33	122.4	209.9	5.3	**1.25**
USMG5	Up-regulated during skeletal muscle growth protein 5	6.5	98.2	25.9	**1.25**
VDAC3	Voltage-dependent anion-selective channel protein 3	30.6	304.1	17.0	**1.25**
WDR76	WD repeat-containing protein 76	69.7	55.3	2.2	**1.25**

Figure S1.3 – Change in nucleolar abundance of proteins following knockdown of APC3 (A) or APC5 (B) as calculated by quantitative analysis of dimethyl-labelled nucleolar lysates by mass spectrometry

HeLa cells were subjected to non-silencing, APC3 or APC5 siRNA-mediated knockdown. Nucleolar lysates were obtained and digested by trypsin using a FASP protocol. Non-silencing lysates were labelled with light dimethyl, whilst APC3i and APC5i lysates were labelled with heavy dimethyl. Heavy and light peptides were then mixed in an equimolar ratio and analysed by LC-MS/MS upon an Impact ESI-TOF Mass Spectrometer (Bruker). Proteins were searched by ProteinScape (Bruker) by comparing to a Mascot database (Matrix Science). Identified proteins were then quantified using WarpLC (Bruker) and are shown here as % change. SC = sequence coverage. MW = molecular weight.

FIGURE S1.4 – SUPPLEMENTARY DATA FROM APC3, CDC20 AND CDH1 IPS FROM WHOLE CELL EXTRACTS

A) Proteins from Whole Cell Extract IPs mentioned in Chapter 2

<u>APC/C subunits</u>

Protein	Full Name	MW [kDa]	# Peptides		
			APC3 IP	Cdc20 IP	Cdh1 IP
APC1	Anaphase-promoting complex subunit 1	216.4	99	22	10
APC2	Anaphase-promoting complex subunit 2	93.8	40	4	-
APC3	Cell division cycle protein 27 homolog	91.8	63	17	4

APC4	Anaphase-promoting complex subunit 4	92.1	49	13	-
APC5	Anaphase-promoting complex subunit 5	85	64	2	-
APC6	Cell division cycle protein 16 homolog	71.6	41	12	2
APC7	Anaphase-promoting complex subunit 7	63.1	48	6	-
APC8	Cell division cycle protein 23 homolog	68.8	61	18	4
APC10	Anaphase-promoting complex subunit 10	21.2	15	-	-
APC12	Anaphase-promoting complex subunit CDC26	9.8	7	3	-
APC16	UPF0448 protein C10orf104	11.7	4	-	-
Cdc20	Cell division cycle protein 20 homolog	54.7	4	19	-
Cdh1	Fizzy-related protein homolog	55.1	16	-	12

Known Substrates and Interactors

Protein	Full Name	MW [kDa]	# Peptides			# D-box	# KEN	TEK	GPS-ARM
			APC3 IP	Cdc20 IP	Cdh1 IP				
BUB1	Mitotic checkpoint serine/threonine-protein kinase BUB1	122.3		15		3	2	-	+++
BUB1B	Mitotic checkpoint serine/threonine-protein kinase BUB1 beta	119.5	31	64		8	2	-	***/ +++
BUB3	Mitotic checkpoint protein BUB3	37.1	9	17	1	1	1	-	
FBX5	F-box only protein 5	50.1	13			4	1	-	***/ +++
KIF4A	Chromosome-associated kinesin KIF4A	139.8	1			7	1	1	***/ +++
KIF22	Kinesin-like protein KIF22	73.2	1			6	1	-	**/ +++
MD2L1	Mitotic spindle assembly checkpoint protein MAD2A	23.5	6	8		-	-	-	
NEK2	Serine/threonine-protein kinase Nek2	51.7	3			5	1	-	***/ +++
PAF	PCNA-associated factor	12	2			1	1	-	***/ +++
RIR2	Ribonucleoside-diphosphate reductase subunit M2	44.8	13		8	3	1	-	***/ +++

Cell Cycle and Ubiquitin-Proteasomal Pathway

Protein	Full Name	MW [kDa]	# Peptides			# D-box	# KEN	TEK	GPS-ARM
			APC3 IP	Cdc20 IP	Cdh1 IP				
AKAP8	A-kinase anchor protein 8	76.1		1		3	-	-	*
ARL2	ADP-ribosylation factor-like protein 2	20.9	2			1	-	-	
CDK2	Cell division protein kinase 2	33.9	3			3	-	-	
CUL1	Cullin-1	89.6	15			4	-	-	
CUL5	Cullin-5	90.9		9		4	-	1	
FA96B	Protein FAM96B	17.7	3			-	-	-	

KLHL9	Kelch-like protein 9	69.4			2	2	-	-	
MP2K2	Dual specificity mitogen-activated protein kinase kinase 2	44.4	2	1		1	-	-	***
NEST	Nestin	177.3			1	11	5	1	***/ +++
NSUN2	tRNA (cytosine-5-)-methyltransferase NSUN2	86.4		2		5	1	-	
PRS7	26S protease regulatory subunit 7	48.6	1			2	-	1	**
PSDE	26S proteasome non-ATPase regulatory subunit 14	34.6	1	1		-	-	-	
PSMD2	26S proteasome non-ATPase regulatory subunit 2	100.1		2		7	-	-	**
RHOC	Rho-related GTP-binding protein RhoC	22	2			3	-	-	**
RNF4	RING finger protein 4	21.3	3			1	-	-	
RO52	52 kDa Ro protein	54.1		10	7	3	-	-	***
S10AB	Protein S100-A11	11.7		2		-	-	-	
SKP1	S-phase kinase-associated protein 1	18.6	4			-	1	-	+++
SMC4	Structural maintenance of chromosomes protein 4	147.1			3	4	1	3	**/++
TRP13	Thyroid receptor-interacting protein 13	48.5	9			4	-	1	
USP9X	Probable ubiquitin carboxyl-terminal hydrolase FAF-X	289.4	4			13	-	-	**

MCM proteins

Protein	Full Name	MW [kDa]	# Peptides			# D-box	# KEN	TEK	GPS-ARM
			APC3 IP	Cdc20 IP	Cdh1 IP				
MCM3	DNA replication licensing factor MCM3	90.9	4	1		4	-	-	
MCM4	DNA replication licensing factor MCM4	96.5	13			5	1	-	***
MCM5	DNA replication licensing factor MCM5	82.2	2			5	-	-	*
MCM7	DNA replication licensing factor MCM7	81.3	36	2	1	6	-	-	*

Chaperones and Protein Folding

Protein	Full Name	MW [kDa]	# Peptides			# D-box	# KEN	TEK	GPS-ARM
			APC3 IP	Cdc20 IP	Cdh1 IP				
ENPL	Endoplasmin	92.4			9	8	-	-	
HS105	Heat shock protein 105 kDa	96.8	1	5		3	1	-	
HS74L	Heat shock 70 kDa protein 4L	94.4			1	3	1	-	+++
HS90A	Heat shock protein HSP 90-alpha	84.6		8		4	2	-	**/ +++
HS90B	Heat shock protein HSP 90-beta	83.2	11	15	10	3	1	-	*
HSP72	Heat shock-related 70 kDa protein 2	70	20		17	1	1	-	++

HSP74	Heat shock 70 kDa protein 4	94.3		1	2	6	-	-	
TCPB	T-complex protein 1 subunit beta	57.5		4		4	-	-	
TCPE	T-complex protein 1 subunit epsilon	59.6		12		3	-	-	
TCPG	T-complex protein 1 subunit gamma	60.5		17	5	5	-	2	***
TCPH	T-complex protein 1 subunit eta	59.3		6	2	2	-	-	
TCPQ	T-complex protein 1 subunit theta	59.6		7		1	-	-	
TCPZ	T-complex protein 1 subunit zeta	58		2		7	-	-	***

mRNA Splicing and Processing

Protein	Full Name	MW [kDa]	# Peptides			# D-box	# KEN	TEK	GPS-ARM
			APC3 IP	Cdc20 IP	Cdh1 IP				
DDX1	ATP-dependent RNA helicase DDX1	82.4	6	2	1	3	-	1	**
DDX17	Probable ATP-dependent RNA helicase DDX17	72.3	2	3		1	1	-	
DDX3X	ATP-dependent RNA helicase DDX3X	73.2	12	6	7	2	1	-	
DHX15	Putative pre-mRNA-splicing factor ATP-dependent RNA helicase DHX15	90.9		7	1	9	-	1	**
ELAV1	ELAV-like protein 1	36.1		4		1	-	-	
F118B	Protein FAM118B	39.5		9		1	-	-	***
HNRL1	Heterogeneous nuclear ribonucleoprotein U-like protein 1	95.7	2	7	5	3	-	-	**
HNRPM	Heterogeneous nuclear ribonucleoprotein M	77.5			9	5	-	-	*
HNRPQ	Heterogeneous nuclear ribonucleoprotein Q	69.6		1		1	-	-	
HNRPU	Heterogeneous nuclear ribonucleoprotein U	90.5	9	8	8	1	-	1	*
NCBP1	Nuclear cap-binding protein subunit 1	91.8		1		3	-	-	
PABP1	Polyadenylate-binding protein 1	70.6	13		17	1	-	-	
PABP3	Polyadenylate-binding protein 3	70		3		-	-	-	
PABP4	Polyadenylate-binding protein 4	70.7	9		11	2	-	-	*
RINI	Ribonuclease inhibitor	49.9		19		1	-	-	
RSMB	Small nuclear ribonucleoprotein-associated proteins B and B'	24.6		2		2	-	-	
SF3B3	Splicing factor 3B subunit 3	135.5		1	1	8	-	1	***
SMD2	Small nuclear ribonucleoprotein Sm D2	13.5	1	3		1	-	-	
UAP56	Spliceosome RNA helicase BAT1	49			1	2	-	-	
XRN2	5'-3' exoribonuclease 2	108.5	3			5	-	-	*
YTDC2	Probable ATP-dependent RNA helicase YTHDC2	160.1			3	10	1	1	***

Transcriptional Regulation

Protein	Full Name	MW [kDa]	# Peptides			# D-box	# KEN	TEK	GPS-ARM
			APC3 IP	Cdc20 IP	Cdh1 IP				
AAPK1	5'-AMP-activated protein kinase catalytic subunit alpha-1	64	1			2	-	-	***
AGO2	Protein argonaute-2	97.1			9	5	-	-	**
CN166	UPF0568 protein C14orf166	28.1	7			2	-	-	***
DOT1L	Histone-lysine N-methyltransferase, H3 lysine-79 specific	184.7	1			11	1	-	***/ +++
EF1D	Elongation factor 1-delta	31.1	1	4		-	-	-	
ELOC	Transcription elongation factor B polypeptide 1	12.5			2	-	-	-	
EWS	RNA-binding protein EWS	68.4	2	4	3	2	-	-	
FHL2	Four and a half LIM domains protein 2	32.2		1		3	-	-	
FLII	Protein flightless-1 homolog	144.7		1		6	-	1	**
H14	Histone H1.4	21.9			4	1	-	-	
H2AV	Histone H2A.V	13.5	2	2		1	-	-	
H3L	Histone H3-like	15.2			2	1	-	-	
HELLS	Lymphoid-specific helicase	97		42		4	1	-	**/ +++
PURA	Transcriptional activator protein Pur-alpha	34.9		1	1	5	1	-	+++
RFX5	DNA-binding protein RFX5	65.3		1		5	-	-	
SLIRP	SRA stem-loop-interacting RNA-binding protein, mitochondrial	12.3	2			3	-	-	***
SMRD1	SWI/SNF-related matrix-associated actin-dependent regulator of chromatin subfamily D member 1	58.2		1		3	-	-	
STAT3	Signal transducer and activator of transcription 3	88	1	1		3	1	1	++
TCP4	Activated RNA polymerase II transcriptional coactivator p15	14.4	1			-	-	-	
TRI29	Tripartite motif-containing protein 29	65.8		1	1	3	-	-	***
ZNF24	Zinc finger protein 24	42.1		1		3	-	-	

Differentiation

Protein	Full Name	MW [kDa]	# Peptides			# D-box	# KEN	TEK	GPS-ARM
			APC3 IP	Cdc20 IP	Cdh1 IP				
DMBT1	Deleted in malignant brain tumors 1 protein	260.6		1		3	-	-	
DOCK7	Dedicator of cytokinesis protein 7	242.4		32		10	-	1	**
DREB	Drebrin	71.4		3		2	-	-	

DNA repair

Protein	Full Name	MW [kDa]	# Peptides			# D-box	# KEN	TEK	GPS-ARM
			APC3 IP	Cdc20 IP	Cdh1 IP				
MAPK2	MAP kinase-activated protein kinase 2	45.5		1		2	-	-	
MMS19	MMS19 nucleotide excision repair protein homolog	113.2	2			8	-	-	
MSH2	DNA mismatch repair protein Msh2	104.7	8	2	1	3	1	-	++
MSH6	DNA mismatch repair protein Msh6	152.7	7		4	5	-	-	***
RFC3	Replication factor C subunit 3	40.5	1			4	-	-	
RFC5	Replication factor C subunit 5	38.5	2			3	-	-	***
TERA	Transitional endoplasmic reticulum ATPase	89.3		1	2	5	-	-	***
UBR5	E3 ubiquitin-protein ligase UBR5	309.2	1			21	-		***

Translation and Ribosomal Proteins

Protein	Full Name	MW [kDa]	# Peptides			# D-box	# KEN	TEK	GPS-ARM
			APC3 IP	Cdc20 IP	Cdh1 IP				
BRX1	Ribosome biogenesis protein BRX1 homolog	41.4		1	1	2	-	-	
DDX21	Nucleolar RNA helicase 2	87.3	4	21	14	1	-	-	***
EF1G	Elongation factor 1-gamma	50.1		1		5	-	-	**
EF2	Elongation factor 2	95.3		15		7	-	-	
LAR4B	La-related protein 4B	80.5		5		2	-	-	
NOP2	Putative ribosomal RNA methyltransferase NOP2	89.2		1	6	2	-	-	
NUCL	Nucleolin	76.6	18	19	20	2	-	-	
R13AX	Putative 60S ribosomal protein L13a-like MGC87657	12.1	1			-	-	-	
RL27	60S ribosomal protein L27	15.8	5			-	-	-	
RL36A	60S ribosomal protein L36a	12.4	1			-	-	-	
RL36L	60S ribosomal protein L36a-like	12.5			2	-	-	-	
RS10	40S ribosomal protein S10	18.9	3	1	1	1	-	-	
RS15	40S ribosomal protein S15	17		3		1	-	-	
RS26L	Putative 40S ribosomal protein S26-like 1	13	2	1		-	-	-	
RS27	40S ribosomal protein S27	9.5	3			-	-	-	
RS27A	40S ribosomal protein S27a	9.4			1	-	-	-	
RS7	40S ribosomal protein S7	22.1	2			2	-	-	
TNR6B	Trinucleotide repeat-containing gene 6B protein	193.9			2	1	-	-	

Apoptosis

Protein	Full Name	MW [kDa]	# Peptides			# D-box	# KEN	TEK	GPS-ARM
			APC3 IP	Cdc20 IP	Cdh1 IP				
1433S	14-3-3 protein sigma	27.8		6		4	-	-	
GGCT	Gamma-glutamylcyclotransferase	21		1		2	1	-	*/+++
SPB3	Serpin B3	44.5		8		1	1	-	+++
SPB4	Serpin B4	44.8		7		-	2	1	+++
TRAF2	TNF receptor-associated factor 2	55.8		3		4	-	-	

Metabolism

Protein	Full Name	MW [kDa]	# Peptides			# D-box	# KEN	TEK	GPS-ARM
			APC3 IP	Cdc20 IP	Cdh1 IP				
ACACA	Acetyl-CoA carboxylase 1	265.4			3	13	1	-	+++
APOA1	Apolipoprotein A-I	30.8			1	6	1	-	***
C1TC	C-1-tetrahydrofolate synthase, cytoplasmic	101.5	20	12	6	4	-	1	***
CCHL	Cytochrome c-type heme lyase	30.6			2	1	1	-	***
K6PL	6-phosphofructokinase, liver type	85		1		1	-	1	
K6PP	6-phosphofructokinase type C	85.5	7	4		2	-	1	

Transport

Protein	Full Name	MW [kDa]	# Peptides			# D-box	# KEN	TEK	GPS-ARM
			APC3 IP	Cdc20 IP	Cdh1 IP				
ESYT2	Extended synaptotagmin-2	102.3		1		8	1	-	***/ +++
GNPTA	N-acetylglucosamine-1-phosphotransferase subunits alpha/beta	143.5	16			7	1	-	***/ +++

Nuclear Pore Complex

Protein	Full Name	MW [kDa]	# Peptides			# D-box	# KEN	TEK	GPS-ARM
			APC3 IP	Cdc20 IP	Cdh1 IP				
NU205	Nuclear pore complex protein Nup205	227.8			3	17	1	1	***/ +++
NUP93	Nuclear pore complex protein Nup93	93.4		2	1	8	-	-	***
XPO1	Exportin-1	123.3	1			8	-	1	*

Cytoskeleton

Protein	Full Name	MW [kDa]	# Peptides			# D-box	# KEN	TEK	GPS-ARM
			APC3 IP	Cdc20 IP	Cdh1 IP				
CKAP4	Cytoskeleton-associated protein 4	66	7			4	-	2	***
DOCK8	Dedicator of cytokinesis protein 8	238.4		49		7	2	-	+++

B) APC3 IP from Whole Cell Extracts

APC/C subunits

Protein	Full Name	MW [kDa]	Mascot Score	# Peptides	SC [%]
APC1	Anaphase-promoting complex subunit 1	216.4	6012.6	99	39.2
APC2	Anaphase-promoting complex subunit 2	93.8	1961.5	40	38.8
APC3	Cell division cycle protein 27 homolog	91.8	4164.3	63	57.2
APC4	Anaphase-promoting complex subunit 4	92.1	2830.5	49	43.2
APC5	Anaphase-promoting complex subunit 5	85	4122.4	64	55.9
APC6	Cell division cycle protein 16 homolog	71.6	2670.6	41	39.8
APC7	Anaphase-promoting complex subunit 7	63.1	2902.4	48	48.1
APC8	Cell division cycle protein 23 homolog	68.8	3552	61	59.3
APC10	Anaphase-promoting complex subunit 10	21.2	988.2	15	61.6
APC12	Anaphase-promoting complex subunit CDC26	9.8	455	7	67.1
APC16	UPF0448 protein C10orf104	11.7	213.2	4	18.2
Cdc20	Cell division cycle protein 20 homolog	54.7	134.1	4	10.4
Cdh1	Fizzy-related protein homolog	55.1	692.2	16	34.7

Unique Interacting Proteins

Protein	Full Name	MW [kDa]	Mascot Score	# Peptides	SC [%]
4F2	4F2 cell-surface antigen heavy chain	68	161.8	3	5.6
8ODP	7,8-dihydro-8-oxoguanine triphosphatase	22.5	58.5	2	12.7
AAAT	Neutral amino acid transporter B(0)	56.6	73.9	1	2.2
AAKG1	5'-AMP-activated protein kinase subunit gamma-1	37.6	181.9	3	10.9
AAPK1	5'-AMP-activated protein kinase catalytic subunit alpha-1	64	39.5	1	1.8
ABCF2	ATP-binding cassette sub-family F member 2	71.2	151.9	4	5.8
ADT1	ADP/ATP translocase 1	33	249.8	6	21.5
ARF3	ADP-ribosylation factor 3	20.6	547.9	10	49.2
ARL1	ADP-ribosylation factor-like protein 1	20.4	63.1	1	6.1
ARL2	ADP-ribosylation factor-like protein 2	20.9	92	2	12
AT1A1	Sodium/potassium-transporting ATPase subunit alpha-1	112.8	317	5	6.9
ATP5H	ATP synthase subunit d, mitochondrial	18.5	98.7	3	18
BA2L1	Protein BAT2-like 1	165.4	716.4	15	12

BUB1B	Mitotic checkpoint serine/threonine-protein kinase BUB1 beta	119.5	1405.2	31	32.9
BUB3	Mitotic checkpoint protein BUB3	37.1	450.7	9	29.9
C109A	Coiled-coil domain-containing protein 109A	39.8	53.3	1	2.8
C1TC	C-1-tetrahydrofolate synthase, cytoplasmic	101.5	898.2	20	21.6
CAZA1	F-actin-capping protein subunit alpha-1	32.9	87.6	2	9.1
CDK2	Cell division protein kinase 2	33.9	132.7	3	11.7
CKAP4	Cytoskeleton-associated protein 4	66	423.9	7	15.9
CN166	UPF0568 protein C14orf166	28.1	266.4	7	23.8
COPB	Coatomer subunit beta	107.1	47.6	2	1.5
COX2	Cytochrome c oxidase subunit 2	25.5	41.5	1	4.4
CTNA1	Catenin alpha-1	100	35.5	1	1.9
CUL1	Cullin-1	89.6	573.2	15	18.7
CV028	UPF0027 protein C22orf28	55.2	35.8	1	2.2
CYBP	Calcyclin-binding protein	26.2	57.4	2	14.9
DDX1	ATP-dependent RNA helicase DDX1	82.4	255.2	6	9.1
DDX17	Probable ATP-dependent RNA helicase DDX17	72.3	97.1	2	3.1
DDX21	Nucleolar RNA helicase 2	87.3	176.8	4	5.9
DDX3X	ATP-dependent RNA helicase DDX3X	73.2	681.4	12	22.4
DEF1	Neutrophil defensin 1	10.2	38.5	1	9.6
DIC	Mitochondrial dicarboxylate carrier	31.3	73.9	2	6.3
DOT1L	Histone-lysine N-methyltransferase, H3 lysine-79 specific	184.7	35.7	1	0.6
DSRAD	Double-stranded RNA-specific adenosine deaminase	135.9	120.5	3	3
EF1D	Elongation factor 1-delta	31.1	37.3	1	8.5
ENPL	Endoplasmin	92.4	130.9	3	4.6
ERD22	ER lumen protein retaining receptor 2	24.4	60.6	1	5.2
ERGI1	Endoplasmic reticulum-Golgi intermediate compartment protein 1	32.6	51.4	2	7.9
EWS	RNA-binding protein EWS	68.4	153.8	2	5.8
FA96B	Protein FAM96B	17.7	118	3	39.3
FBX5	F-box only protein 5	50.1	629.6	13	32
GBB2	Guanine nucleotide-binding protein G(I)/G(S)/G(T) subunit beta-2	37.3	91.1	2	6.2
GNPTA	N-acetylglucosamine-1-phosphotransferase subunits alpha/beta	143.5	862.9	16	13.3
GNPTG	N-acetylglucosamine-1-phosphotransferase subunit gamma	34	243.9	5	19.7
H2AV	Histone H2A.V	13.5	76.4	2	12.5
HBA	Hemoglobin subunit alpha	15.2	142.1	3	28.2
HBB	Hemoglobin subunit beta	16	298.1	7	61.2
HNRL1	Heterogeneous nuclear ribonucleoprotein U-like protein 1	95.7	121.6	2	3.3
HNRPU	Heterogeneous nuclear ribonucleoprotein U	90.5	437	9	14.1
HS105	Heat shock protein 105 kDa	96.8	73.7	1	1.7
HS90B	Heat shock protein HSP 90-beta	83.2	508.2	11	17.8
HSP72	Heat shock-related 70 kDa protein 2	70	1096.9	20	29.7
IF2A	Eukaryotic translation initiation factor 2 subunit 1	36.1	72.8	1	3.8
IMPA2	Inositol monophosphatase 2	31.3	67.2	1	4.2
K1430	UPF0501 protein KIAA1430	59.4	459.1	9	17.7

K6PP	6-phosphofructokinase type C	85.5	295.6	7	10.2
KIF22	Kinesin-like protein KIF22	73.2	64	1	1.7
KIF4A	Chromosome-associated kinesin KIF4A	139.8	56.3	1	0.7
KITM	Thymidine kinase 2, mitochondrial	31	118.3	4	12.1
KT3K	Ketosamine-3-kinase	34.4	32.8	1	1.9
LEG1	Galectin-1	14.7	159.5	4	37.8
LONM	Lon protease homolog, mitochondrial	106.4	74.1	2	2.1
LRC48	Leucine-rich repeat-containing protein 48	61	54.8	1	2.1
M2OM	Mitochondrial 2-oxoglutarate/malate carrier protein	34	33.6	1	5.1
MAGD2	Melanoma-associated antigen D2	64.9	215.2	4	13.4
MAP7	Ensconsin	84	45	1	1.7
MCM3	DNA replication licensing factor MCM3	90.9	199.3	4	7.1
MCM4	DNA replication licensing factor MCM4	96.5	527	13	16.8
MCM5	DNA replication licensing factor MCM5	82.2	70.3	2	3.8
MCM7	DNA replication licensing factor MCM7	81.3	1961.4	36	42
MD2L1	Mitotic spindle assembly checkpoint protein MAD2A	23.5	296.2	6	28.3
MMS19	MMS19 nucleotide excision repair protein homolog	113.2	94.4	2	2.6
MP2K2	Dual specificity mitogen-activated protein kinase kinase 2	44.4	90.1	2	4.5
MSH2	DNA mismatch repair protein Msh2	104.7	320	8	8.9
MSH6	DNA mismatch repair protein Msh6	152.7	308.7	7	5.7
MTDC	Bifunctional methylenetetrahydrofolate dehydrogenase/cyclohydrolase, mitochondrial	37.9	64.2	1	3.1
MYL6	Myosin light polypeptide 6	16.9	42.4	1	8.6
NDKA	Nucleoside diphosphate kinase A	17.1	85.7	3	26.3
NDUAA	NADH dehydrogenase [ubiquinone] 1 alpha subcomplex subunit 10, mitochondrial	40.7	376.1	8	20.6
NEK2	Serine/threonine-protein kinase Nek2	51.7	152.2	3	7
NRDC	Nardilysin	131.5	64.7	2	1.6
OSBP1	Oxysterol-binding protein 1	89.4	33.1	1	0.7
PAF	PCNA-associated factor	12	131.6	2	16.2
PDZ11	PDZ domain-containing protein 11	16.1	154.1	3	32.9
PKHA5	Pleckstrin homology domain-containing family A member 5	127.4	149	4	5.2
PKHA6	Pleckstrin homology domain-containing family A member 6	117.1	299.2	7	8.2
PPAC	Low molecular weight phosphotyrosine protein phosphatase	18	33.3	1	5.7
PPBI	Intestinal-type alkaline phosphatase	56.8	44.2	1	3
PPIA	Peptidyl-prolyl cis-trans isomerase A	18	66.3	2	10.9
PRDX3	Thioredoxin-dependent peroxide reductase, mitochondrial	27.7	35.6	1	4.3
PRDX4	Peroxiredoxin-4	30.5	111	3	9.6
PRPS3	Ribose-phosphate pyrophosphokinase 3	34.8	100.2	3	13.2
PRS7	26S protease regulatory subunit 7	48.6	32.4	1	1.8
PSA	Puromycin-sensitive aminopeptidase	103.2	314.6	8	9.2
PSDE	26S proteasome non-ATPase regulatory subunit 14	34.6	43.3	1	4.2
R13AX	Putative 60S ribosomal protein L13a-like MGC87657	12.1	51.6	1	10.8
RAE1L	mRNA export factor	40.9	88.6	2	4.9

RAP2B	Ras-related protein Rap-2b	20.5	55.4	1	6
RFC3	Replication factor C subunit 3	40.5	65	1	3.9
RFC5	Replication factor C subunit 5	38.5	74.3	2	7.1
RHOC	Rho-related GTP-binding protein RhoC	22	83.6	2	15
RIR2	Ribonucleoside-diphosphate reductase subunit M2	44.8	671.5	13	37
RL27	60S ribosomal protein L27	15.8	195.3	5	42.6
RL36A	60S ribosomal protein L36a	12.4	44.1	1	8.5
RNF4	RING finger protein 4	21.3	112.9	3	15.3
RPAB3	DNA-directed RNA polymerases I, II, and III subunit RPABC3	17.1	100.5	1	8.7
RS10	40S ribosomal protein S10	18.9	155.4	3	14.5
RS26L	Putative 40S ribosomal protein S26-like 1	13	88.7	2	18.3
RS27	40S ribosomal protein S27	9.5	90.3	3	38.1
RS7	40S ribosomal protein S7	22.1	75.7	2	8.2
SLIRP	SRA stem-loop-interacting RNA-binding protein, mitochondrial	12.3	77.9	2	22
SMD2	Small nuclear ribonucleoprotein Sm D2	13.5	32.5	1	8.5
SPAT7	Spermatogenesis-associated protein 7	67.7	43.1	1	1.2
SRP14	Signal recognition particle 14 kDa protein	14.6	118.9	2	30.9
STAT3	Signal transducer and activator of transcription 3	88	33.7	1	3.4
SYMC	Methionyl-tRNA synthetase, cytoplasmic	101.1	44.6	1	1.1
TBL2	Transducin beta-like protein 2	49.8	46.3	1	2.9
TCP4	Activated RNA polymerase II transcriptional coactivator p15	14.4	48.3	1	8.7
TIM23	Mitochondrial import inner membrane translocase subunit Tim23	21.9	60.6	1	8.1
TIM50	Mitochondrial import inner membrane translocase subunit TIM50	39.6	46.7	1	4.8
TRIO	Triple functional domain protein	346.7	71.3	2	0.9
TXTP	Tricarboxylate transport protein, mitochondrial	34	158.6	4	13.8
UBR5	E3 ubiquitin-protein ligase UBR5	309.2	45	1	0.6
UCK2	Uridine-cytidine kinase 2	29.3	110.8	2	8.8
USP9X	Probable ubiquitin carboxyl-terminal hydrolase FAF-X	289.4	118.2	4	1.8
VAPA	Vesicle-associated membrane protein-associated protein A	27.9	34.9	1	6.4
VDAC2	Voltage-dependent anion-selective channel protein 2	31.5	47.2	2	8.5
XP32	Skin-specific protein 32	26.2	33.4	1	3.2
XPO1	Exportin-1	123.3	42.5	1	1.1
XRN2	5'-3' exoribonuclease 2	108.5	119.5	3	3.7

Proteins with a lot more peptides/higher score than IgG Control

Protein	**Full Name**	**MW [kDa]**	**Mascot Score**	**# Peptides**	**SC [%]**
EF2	Elongation factor 2	95.3	324.2	8	9.2
NUCL	Nucleolin	76.6	823.4	18	19.7
PABP1	Polyadenylate-binding protein 1	70.6	601.6	13	22.8
PABP4	Polyadenylate-binding protein 4	70.7	352.5	9	14
SKP1	S-phase kinase-associated protein 1	18.6	229.6	4	20.9
TRP13	Thyroid receptor-interacting protein 13	48.5	395.8	9	24.3

C) Cdc20 IP from Whole Cell Extracts

APC/C subunits

Protein	Full Name	MW [kDa]	Mascot Score	# Peptides	SC [%]
APC1	Anaphase-promoting complex subunit 1	216.4	984.5	22	14.4
APC2	Anaphase-promoting complex subunit 2	93.8	205.6	4	6.2
APC3	Cell division cycle protein 27 homolog	91.8	976.6	17	26.9
APC4	Anaphase-promoting complex subunit 4	92.1	560.8	13	16.7
APC5	Anaphase-promoting complex subunit 5	85	97.7	2	2.6
APC6	Cell division cycle protein 16 homolog	71.6	526	12	20.8
APC7	Anaphase-promoting complex subunit 7	63.1	270	6	12
APC8	Cell division cycle protein 23 homolog	68.8	873.4	18	32.5
APC12	Anaphase-promoting complex subunit CDC26	9.8	233.1	3	41.2
CDC20	Cell division cycle protein 20 homolog	54.7	1259.9	19	45.7

Unique Interacting Proteins

Protein	Full Name	MW [kDa]	Mascot Score	# Peptides	SC [%]
1433B	14-3-3 protein beta/alpha	28.1	97.1	3	11
1433E	14-3-3 protein epsilon	29.2	96	2	7.8
1433S	14-3-3 protein sigma	27.8	306.4	6	22.6
4F2	4F2 cell-surface antigen heavy chain	68	512.9	10	18.9
8ODP	7,8-dihydro-8-oxoguanine triphosphatase	22.5	61.6	1	6.1
ACTS	Actin, alpha skeletal muscle	42	884.4	17	30.2
AKAP8	A-kinase anchor protein 8	76.1	61.6	1	1.7
AL3A1	Aldehyde dehydrogenase, dimeric NADP-preferring	50.3	43	1	2
ARF3	ADP-ribosylation factor 3	20.6	355.4	7	28.2
AT1A1	Sodium/potassium-transporting ATPase subunit alpha-1	112.8	622.9	12	15.1
AT2A2	Sarcoplasmic/endoplasmic reticulum calcium ATPase 2	114.7	101.6	3	3.6
ATD3B	ATPase family AAA domain-containing protein 3B	72.5	255.4	6	9.1
BPA1	Bullous pemphigoid antigen 1, isoforms 1/2/3/4/5/8 (Fragment)	372	65.5	2	0.4
BRX1	Ribosome biogenesis protein BRX1 homolog	41.4	53	1	3.4
BUB1	Mitotic checkpoint serine/threonine-protein kinase BUB1	122.3	612.1	15	18.6
BUB1B	Mitotic checkpoint serine/threonine-protein kinase BUB1 beta	119.5	3875.6	64	52.2
BUB3	Mitotic checkpoint protein BUB3	37.1	928.7	17	40.2
C1TC	C-1-tetrahydrofolate synthase, cytoplasmic	101.5	594.3	12	13.8
CALL3	Calmodulin-like protein 3	16.9	99.3	3	30.2
CALM	Calmodulin	16.8	56	1	11.4
CALU	Calumenin	37.1	87.8	2	5.7
CASPA	Caspase-10	58.9	28.9	1	1
CATD	Cathepsin D	44.5	119.9	3	6.6

CAZA1	F-actin-capping protein subunit alpha-1	32.9	173.1	4	22
CMC2	Calcium-binding mitochondrial carrier protein Aralar2	74.1	53.4	2	3
CO3A1	Collagen alpha-1(III) chain	138.5	58.1	1	0.8
CUL5	Cullin-5	90.9	331.6	9	11.8
CYTA	Cystatin-A	11	77.2	2	30.6
DC1I2	Cytoplasmic dynein 1 intermediate chain 2	71.4	167	3	6.9
DDX1	ATP-dependent RNA helicase DDX1	82.4	62.2	2	2.8
DDX17	Probable ATP-dependent RNA helicase DDX17	72.3	165.1	3	5.7
DDX21	Nucleolar RNA helicase 2	87.3	964.5	21	29.4
DDX3X	ATP-dependent RNA helicase DDX3X	73.2	261.2	6	9.7
DHX15	Putative pre-mRNA-splicing factor ATP-dependent RNA helicase DHX15	90.9	293.5	7	8.6
DMBT1	Deleted in malignant brain tumors 1 protein	260.6	57.6	1	0.6
DOCK7	Dedicator of cytokinesis protein 7	242.4	1316.6	32	16.5
DOCK8	Dedicator of cytokinesis protein 8	238.4	2280	49	24.5
DREB	Drebrin	71.4	173.8	3	7.2
DSC3	Desmocollin-3	99.9	27.8	1	0.9
ECH1	Delta(3,5)-Delta(2,4)-dienoyl-CoA isomerase, mitochondrial	35.8	647	12	33.8
EF1D	Elongation factor 1-delta	31.1	196.4	4	22.1
EF1G	Elongation factor 1-gamma	50.1	52.4	1	3
ENPL	Endoplasmin	92.4	360.1	7	10.3
EPIPL	Epiplakin	552.8	533	9	2.4
ERD22	ER lumen protein retaining receptor 2	24.4	38	1	5.2
ERGI1	Endoplasmic reticulum-Golgi intermediate compartment protein 1	32.6	64	2	6.6
ESYT2	Extended synaptotagmin-2	102.3	31.3	1	1.6
EWS	RNA-binding protein EWS	68.4	170.9	4	8.1
F118B	Protein FAM118B	39.5	461.3	9	19.9
FABP5	Fatty acid-binding protein, epidermal	15.2	251.5	5	47.4
FHL2	Four and a half LIM domains protein 2	32.2	34.4	1	3.9
FKB15	FK506-binding protein 15	133.5	209.4	3	4.1
FLII	Protein flightless-1 homolog	144.7	44.8	1	1.1
GALK1	Galactokinase	42.2	281.4	6	18.4
GGCT	Gamma-glutamylcyclotransferase	21	30.3	1	5.3
GLNA	Glutamine synthetase	42	81.3	2	9.4
GOGB1	Golgin subfamily B member 1	375.8	51.8	1	0.3
H2AV	Histone H2A.V	13.5	70	2	12.5
HELLS	Lymphoid-specific helicase	97	2031.4	42	42.4
HNRL1	Heterogeneous nuclear ribonucleoprotein U-like protein 1	95.7	319.9	7	11
HNRPQ	Heterogeneous nuclear ribonucleoprotein Q	69.6	47.6	1	1.9
HNRPU	Heterogeneous nuclear ribonucleoprotein U	90.5	466.8	8	10.2
HS105	Heat shock protein 105 kDa	96.8	257.5	5	6.6
HS90A	Heat shock protein HSP 90-alpha	84.6	407.1	8	13.9
HS90B	Heat shock protein HSP 90-beta	83.2	716.2	15	23.2

HSP74	Heat shock 70 kDa protein 4	94.3	29.4	1	1.5
IDE	Insulin-degrading enzyme	117.9	54.7	1	1.1
IL1F5	Interleukin-1 family member 5	17	43.1	1	6.5
IL1F9	Interleukin-1 family member 9	18.7	39.2	1	7.1
IMB1	Importin subunit beta-1	97.1	28	1	1.4
IMMT	Mitochondrial inner membrane protein	83.6	47.7	2	3.2
INVO	Involucrin	68.4	432.6	10	21.7
K6PL	6-phosphofructokinase, liver type	85	33.9	1	1.2
K6PP	6-phosphofructokinase type C	85.5	195.1	4	5.5
KCRU	Creatine kinase U-type, mitochondrial	47	94.9	2	3.8
LAR4B	La-related protein 4B	80.5	254.8	5	7
LMNB1	Lamin-B1	66.4	160.9	3	6.1
LRCH1	Leucine-rich repeat and calponin homology domain-containing protein 1	80.8	66.2	2	3.8
LRCH3	Leucine-rich repeat and calponin homology domain-containing protein 3	86	603.8	13	22.4
LRCH4	Leucine-rich repeat and calponin homology domain-containing protein 4	73.4	345.3	8	17.7
MAPK2	MAP kinase-activated protein kinase 2	45.5	27.7	1	2.8
MCM3	DNA replication licensing factor MCM3	90.9	45.2	1	1.1
MCM7	DNA replication licensing factor MCM7	81.3	67.2	2	3.5
MD2L1	Mitotic spindle assembly checkpoint protein MAD2A	23.5	346.7	8	41
MIF	Macrophage migration inhibitory factor	12.5	43.1	1	7.8
ML12B	Myosin regulatory light chain 12B	19.8	162.4	4	23.8
MP2K2	Dual specificity mitogen-activated protein kinase kinase 2	44.4	44.8	1	2.2
MSH2	DNA mismatch repair protein Msh2	104.7	51.8	2	1.9
MYL6	Myosin light polypeptide 6	16.9	223.9	5	29.8
MYO1F	Myosin-If	124.8	40	1	1.1
NCBP1	Nuclear cap-binding protein subunit 1	91.8	29.6	1	1.5
NOP2	Putative ribosomal RNA methyltransferase NOP2	89.2	29.9	1	1.7
NSUN2	tRNA (cytosine-5-)-methyltransferase NSUN2	86.4	84.4	2	2.7
NUP93	Nuclear pore complex protein Nup93	93.4	70.4	2	2.8
PABP3	Polyadenylate-binding protein 3	70	121.8	3	5.4
PCMD2	Protein-L-isoaspartate O-methyltransferase domain-containing protein 2	41	38.4	1	2.5
PDE5A	cGMP-specific 3',5'-cyclic phosphodiesterase	99.9	28.5	1	1.3
PKP1	Plakophilin-1	82.8	86.7	2	3.5
PROF2	Profilin-2	15	74.4	1	10
PRPS2	Ribose-phosphate pyrophosphokinase 2	34.7	66.7	1	5.3
PSA	Puromycin-sensitive aminopeptidase	103.2	601.6	13	15.7
PSDE	26S proteasome non-ATPase regulatory subunit 14	34.6	27.5	1	4.2
PSMD2	26S proteasome non-ATPase regulatory subunit 2	100.1	58.8	2	4.2
PURA	Transcriptional activator protein Pur-alpha	34.9	33.5	1	2.8
RAB1C	Putative Ras-related protein Rab-1C	22	96.2	2	10.9
RAIN	Ras-interacting protein 1	103.4	29.2	1	2.4

RFX5	DNA-binding protein RFX5	65.3	54.4	1	2.4
RINI	Ribonuclease inhibitor	49.9	1181.2	19	41
RNAS7	Ribonuclease 7	17.5	53.2	1	9
RO52	52 kDa Ro protein	54.1	404.4	10	18.1
RPN1	Dolichyl-diphosphooligosaccharide--protein glycosyltransferase subunit 1	68.5	136.3	3	6.4
RS10	40S ribosomal protein S10	18.9	85.5	1	8.5
RS15	40S ribosomal protein S15	17	105.4	3	21.4
RS26L	Putative 40S ribosomal protein S26-like 1	13	38.7	1	7.8
RSMB	Small nuclear ribonucleoprotein-associated proteins B and B'	24.6	53.8	2	6.2
S10AB	Protein S100-A11	11.7	88.5	2	17.1
SAMH1	SAM domain and HD domain-containing protein 1	72.2	54.4	1	1.9
SBSN	Suprabasin	25.3	233.7	5	25.5
SF3B3	Splicing factor 3B subunit 3	135.5	43.3	1	1.2
SH3B4	SH3 domain-binding protein 4	107.4	40.9	1	1.1
SMD2	Small nuclear ribonucleoprotein Sm D2	13.5	134.5	3	25.4
SMRD1	SWI/SNF-related matrix-associated actin-dependent regulator of chromatin subfamily D member 1	58.2	29.6	1	1.7
SPAT7	Spermatogenesis-associated protein 7	67.7	39	1	1.2
SPB12	Serpin B12	46.2	43.6	1	2.2
SPB3	Serpin B3	44.5	342.7	8	22.8
SPB4	Serpin B4	44.8	363.4	7	20.3
SPB5	Serpin B5	42.1	176.7	5	13.6
SPR1A	Cornifin-A	9.9	29.4	1	9
SSBP	Single-stranded DNA-binding protein, mitochondrial	17.2	30.6	1	10.1
STAT3	Signal transducer and activator of transcription 3	88	49.6	1	1.7
SYQ	Glutaminyl-tRNA synthetase	87.7	53.3	1	2.1
TCPB	T-complex protein 1 subunit beta	57.5	159.7	4	10.1
TCPH	T-complex protein 1 subunit eta	59.3	286.7	6	11.8
TCPZ	T-complex protein 1 subunit zeta	58	52.3	2	3.6
TERA	Transitional endoplasmic reticulum ATPase	89.3	27.9	1	1.5
TFR1	Transferrin receptor protein 1	84.8	226.9	6	8.8
TGM3	Protein-glutamine gamma-glutamyltransferase E	76.6	430.9	11	20.1
TPM3	Tropomyosin alpha-3 chain	32.8	88.1	3	11.3
TRAF2	TNF receptor-associated factor 2	55.8	144.7	3	6.4
TRI29	Tripartite motif-containing protein 29	65.8	29.5	1	1.4
UCK2	Uridine-cytidine kinase 2	29.3	33.8	1	3.8
XP32	Skin-specific protein 32	26.2	35.2	1	3.2
ZCCHV	Zinc finger CCCH-type antiviral protein 1	101.4	81	1	2
ZNF24	Zinc finger protein 24	42.1	29.3	1	2.4

Proteins with a lot more peptides/higher score than IgG Control

Protein	Full Name	MW [kDa]	Mascot Score	# Peptides	SC [%]
CH60	60 kDa heat shock protein, mitochondrial	61	1898.4	32	49.2
EF2	Elongation factor 2	95.3	618	15	18.1
ELAV1	ELAV-like protein 1	36.1	178.8	4	15
FILA	Filaggrin	434.9	528.1	11	3.9
LEG7	Galectin-7	15.1	403.9	7	66.2
MYH9	Myosin-9	226.4	1063.4	21	13.5
NUCL	Nucleolin	76.6	903.6	19	20.8
POF1B	Protein POF1B	68.7	145.8	4	7.1
PYRG1	CTP synthase 1	66.6	427.5	10	19.3
S10A8	Protein S100-A8	10.8	304	7	46.2
TCPE	T-complex protein 1 subunit epsilon	59.6	458.4	12	21.4
TCPG	T-complex protein 1 subunit gamma	60.5	846.8	17	30.1
TCPQ	T-complex protein 1 subunit theta	59.6	290.9	7	14.8

D) Cdh1 IP from Whole Cell Extracts

APC/C subunits

Protein	Full Name	MW [kDa]	Mascot Score	# Peptides	SC [%]
APC1	Anaphase-promoting complex subunit 1	216.4	364.4	10	7.2
APC3	Cell division cycle protein 27 homolog	91.8	136.6	4	5.5
APC6	Cell division cycle protein 16 homolog	71.6	71.4	2	3.1
APC8	Cell division cycle protein 23 homolog	68.8	153.7	4	6.4
Cdh1	Fizzy-related protein homolog	55.1	551.1	12	26.6

Unique Interacting Proteins

Protein	Full Name	MW [kDa]	Mascot Score	# Peptides	SC [%]
4F2	4F2 cell-surface antigen heavy chain	68	219.2	4	8.7
8ODP	7,8-dihydro-8-oxoguanine triphosphatase	22.5	42.6	1	6.1
ACACA	Acetyl-CoA carboxylase 1	265.4	90.1	3	1.7
ACTG	Actin, cytoplasmic 2	41.8	1305.9	24	60
AGO2	Protein argonaute-2	97.1	384	9	12.6
APOA1	Apolipoprotein A-I	30.8	34.1	1	4.9
APOC3	Apolipoprotein C-III	10.8	86.7	1	16.2
AT1A1	Sodium/potassium-transporting ATPase subunit alpha-1	112.8	294.1	6	7
BRX1	Ribosome biogenesis protein BRX1 homolog	41.4	42.1	1	3.4
BUB3	Mitotic checkpoint protein BUB3	37.1	34.8	1	4.3

C1TC	C-1-tetrahydrofolate synthase, cytoplasmic	101.5	267.7	6	7.7
CCHL	Cytochrome c-type heme lyase	30.6	94.6	2	8.6
DC1I2	Cytoplasmic dynein 1 intermediate chain 2	71.4	49.4	1	3.3
DDX1	ATP-dependent RNA helicase DDX1	82.4	33.9	1	1.5
DDX21	Nucleolar RNA helicase 2	87.3	539.1	14	22
DDX3X	ATP-dependent RNA helicase DDX3X	73.2	323.8	7	12.7
DHX15	Putative pre-mRNA-splicing factor ATP-dependent RNA helicase DHX15	90.9	54.6	1	1.4
ELOC	Transcription elongation factor B polypeptide 1	12.5	48.6	2	19.6
ENPL	Endoplasmin	92.4	345.1	9	15.1
EWS	RNA-binding protein EWS	68.4	193	3	8.1
FAS	Fatty acid synthase	273.3	37.6	1	0.4
GBB3	Guanine nucleotide-binding protein G(I)/G(S)/G(T) subunit beta-3	37.2	36.9	1	2.9
GOGA3	Golgin subfamily A member 3	167.3	3241.4	58	41.6
H14	Histone H1.4	21.9	227	4	15.5
H3L	Histone H3-like	15.2	48.2	2	11.1
HBA	Hemoglobin subunit alpha	15.2	226.7	5	35.9
HBB	Hemoglobin subunit beta	16	156.3	4	22.4
HNRL1	Heterogeneous nuclear ribonucleoprotein U-like protein 1	95.7	215.7	5	7.1
HNRPU	Heterogeneous nuclear ribonucleoprotein U	90.5	463.7	8	13.9
HS74L	Heat shock 70 kDa protein 4L	94.4	38.1	1	1.7
HS90B	Heat shock protein HSP 90-beta	83.2	415	10	16.6
HSP72	Heat shock-related 70 kDa protein 2	70	1022.1	17	19.2
HSP74	Heat shock 70 kDa protein 4	94.3	55.2	2	3.2
IDHC	Isocitrate dehydrogenase [NADP] cytoplasmic	46.6	36.7	1	3.1
KLHL9	Kelch-like protein 9	69.4	62.6	2	3.2
LIPA1	Liprin-alpha-1	135.7	92.4	2	2.2
MCM7	DNA replication licensing factor MCM7	81.3	39.6	1	1.8
ML12B	Myosin regulatory light chain 12B	19.8	139.9	3	17.4
MSH2	DNA mismatch repair protein Msh2	104.7	40.6	1	1
MSH6	DNA mismatch repair protein Msh6	152.7	144.7	4	3.5
MTDC	Bifunctional methylenetetrahydrofolate dehydrogenase/cyclohydrolase, mitochondrial	37.9	37	1	3.1
MYL6	Myosin light polypeptide 6	16.9	75.1	2	13.9
NEST	Nestin	177.3	87.7	1	0.7
NOP2	Putative ribosomal RNA methyltransferase NOP2	89.2	214.8	6	9.6
NU205	Nuclear pore complex protein Nup205	227.8	98.1	3	1.7
NUP93	Nuclear pore complex protein Nup93	93.4	49.4	1	1.5
PPIA	Peptidyl-prolyl cis-trans isomerase A	18	41.8	1	5.5
PSA	Puromycin-sensitive aminopeptidase	103.2	456.3	12	13.6
PURA	Transcriptional activator protein Pur-alpha	34.9	50.2	1	2.8
RAB1C	Putative Ras-related protein Rab-1C	22	65	2	10.9
RIR2	Ribonucleoside-diphosphate reductase subunit M2	44.8	361.8	8	25.7
RL36L	60S ribosomal protein L36a-like	12.5	67.7	2	17.9

RO52	52 kDa Ro protein	54.1	260.3	7	14.7
RPAB3	DNA-directed RNA polymerases I, II, and III subunit RPABC3	17.1	58.4	1	8.7
RS10	40S ribosomal protein S10	18.9	68.6	1	8.5
RS27A	40S ribosomal protein S27a	9.4	41.5	1	23.8
SEMG1	Semenogelin-1	52.1	52.8	2	5.2
SF3B3	Splicing factor 3B subunit 3	135.5	49.8	1	1.2
SMC4	Structural maintenance of chromosomes protein 4	147.1	70.8	3	2.5
SSBP	Single-stranded DNA-binding protein, mitochondrial	17.2	49	1	10.1
TBB1	Tubulin beta-1 chain	50.3	107.1	3	6
TCPH	T-complex protein 1 subunit eta	59.3	70.3	2	4.2
TERA	Transitional endoplasmic reticulum ATPase	89.3	84.3	2	3
TNR6B	Trinucleotide repeat-containing gene 6B protein	193.9	76.7	2	2
TRI29	Tripartite motif-containing protein 29	65.8	35	1	2
UAP56	Spliceosome RNA helicase BAT1	49	59.4	1	3.3
VDAC2	Voltage-dependent anion-selective channel protein 2	31.5	38.8	1	4.4
YTDC2	Probable ATP-dependent RNA helicase YTHDC2	160.1	94.4	3	2.3
ZCCHV	Zinc finger CCCH-type antiviral protein 1	101.4	121.2	2	3.7

Proteins with a lot more peptides/higher score than IgG Control

Protein	**Full Name**	**MW [kDa]**	**Mascot Score**	**# Peptides**	**SC [%]**
HNRPM	Heterogeneous nuclear ribonucleoprotein M	77.5	511.7	9	16.6
MYH10	Myosin-10	228.9	605.7	15	9.2
MYH9	Myosin-9	226.4	2201.5	45	24.4
NUCL	Nucleolin	76.6	1130.6	20	20.7
PABP1	Polyadenylate-binding protein 1	70.6	722.2	17	28.6
PABP4	Polyadenylate-binding protein 4	70.7	495.7	11	16.9
TCPG	T-complex protein 1 subunit gamma	60.5	208.6	5	9.5

Figure S1.4 – Mass Spectrometric identification of APC3-, Cdc20- and Cdh1-interacting proteins from whole cell extracts

A) All proteins mentioned in Chapter 2 text. D-boxes (*) and KEN-boxes (+) were scored by GPS-ARM. High, Medium and Low thresholded peptides are denoted by ***/+++, **/++ and */+, respectively.

B-D) List of interacting proteins for APC3 (B), Cdc20 (C) and Cdh1 (D). MW=Molecular Weight. SC = Sequence Coverage.

Asynchronous HeLa cell lysates and IP'd with normal IgG, APC3, Cdc20 or Cdh1 antisera. IPs were washed, separated by SDS-PAGE and subjected to in-gel tryptic digestion. Tryptic peptides were analysed by LC-MS/MS upon an Impact ESI-TOF (Bruker), searched by ProteinScape (Bruker) by comparison to a Mascot Database (Matrix Science). A 1% FDR was applied to the results, and obvious contaminants and proteins found in the IgG control were removed from the lists.

REFERENCES

Abbott, D. W. and J. T. Holt (1999). "Mitogen-activated protein kinase kinase 2 activation is essential for progression through the G2/M checkpoint arrest in cells exposed to ionizing radiation." J Biol Chem **274**(5): 2732-2742.

Acs, K., M. S. Luijsterburg, L. Ackermann, F. A. Salomons, T. Hoppe and N. P. Dantuma (2011). "The AAA-ATPase VCP/p97 promotes 53BP1 recruitment by removing L3MBTL1 from DNA double-strand breaks." Nat Struct Mol Biol **18**(12): 1345-1350.

Adams, C. C., J. Jakovljevic, J. Roman, P. Harnpicharnchai and J. L. Woolford (2002). "Saccharomyces cerevisiae nucleolar protein Nop7p is necessary for biogenesis of 60S ribosomal subunits." RNA **8**(2): 150-165.

Agami, R. and R. Bernards (2000). Distinct initiation and maintenance mechanisms cooperate to induce G1 cell cycle arrest in response to DNA damage. Cell. United States. **102:** 55-66.

Ahlskog, J. K., J. K. Björk, A. N. Elsing, C. Aspelin, M. Kallio, P. Roos-Mattjus and L. Sistonen (2010). "Anaphase-promoting complex/cyclosome participates in the acute response to protein-damaging stress." Mol Cell Biol **30**(24): 5608-5620.

Ahmad, Y., F. M. Boisvert, P. Gregor, A. Cobley and A. I. Lamond (2009). "NOPdb: Nucleolar Proteome Database--2008 update." Nucleic Acids Res **37**(Database issue): D181-184.

Akhter, S., C. T. Richie, J. M. Deng, E. Brey, X. Zhang, C. Patrick, R. R. Behringer and R. J. Legerski (2004). "Deficiency in SNM1 abolishes an early mitotic checkpoint induced by spindle stress." Mol Cell Biol **24**(23): 10448-10455.

Al-Baker, E. A., J. Boyle, R. Harry and I. R. Kill (2004). "A p53-independent pathway regulates nucleolar segregation and antigen translocation in response to DNA damage induced by UV irradiation." Exp Cell Res **292**(1): 179-186.

Albert, B., I. Léger-Silvestre, C. Normand, M. K. Ostermaier, J. Pérez-Fernández, K. I. Panov, J. C. Zomerdijk, P. Schultz and O. Gadal (2011). "RNA polymerase I-specific subunits promote polymerase clustering to enhance the rRNA gene transcription cycle." J Cell Biol **192**(2): 277-293.

Allis, C. D., S. L. Berger, J. Cote, S. Dent, T. Jenuwien, T. Kouzarides, L. Pillus, D. Reinberg, Y. Shi, R. Shiekhattar, A. Shilatifard, J. Workman and Y. Zhang (2007). "New nomenclature for chromatin-modifying enzymes." Cell **131**(4): 633-636.

Almeida, A., J. P. Bolanos and S. Moreno (2005). Cdh1/Hct1-APC is essential for the survival of postmitotic neurons. J Neurosci. United States. **25:** 8115-8121.

Amador, V., S. Ge, P. G. Santamaría, D. Guardavaccaro and M. Pagano (2007). "APC/C(Cdc20) controls the ubiquitin-mediated degradation of p21 in prometaphase." Mol Cell **27**(3): 462-473.

Andersen, J. S., Y. W. Lam, A. K. Leung, S. E. Ong, C. E. Lyon, A. I. Lamond and M. Mann (2005). "Nucleolar proteome dynamics." Nature **433**(7021): 77-83.

Andersen, J. S., C. E. Lyon, A. H. Fox, A. K. Leung, Y. W. Lam, H. Steen, M. Mann and A. I. Lamond (2002). "Directed proteomic analysis of the human nucleolus." Curr Biol **12**(1): 1-11.

Anderson, A. A., E. S. Child, A. Prasad, L. M. Elphick and D. J. Mann (2010). "Cyclin D1 and cyclin D3 show divergent responses to distinct mitogenic stimulation." J Cell Physiol **225**(3): 638-645.

Aragon, L., E. Martinez-Perez and M. Merkenschlager (2013). "Condensin, cohesin and the control of chromatin states." Curr Opin Genet Dev **23**(2): 204-211.

Araki, M., H. Yu and M. Asano (2005). A novel motif governs APC-dependent degradation of Drosophila ORC1 in vivo. Genes Dev. United States. **19:** 2458-2465.

Arias, E. E. and J. C. Walter (2007). Strength in numbers: preventing rereplication via multiple mechanisms in eukaryotic cells. Genes Dev. United States. **21:** 497-518.

Arnason, T. G., M. G. Pisclevich, M. D. Dash, G. F. Davies and T. A. Harkness (2005). "Novel interaction between Apc5p and Rsp5p in an intracellular signaling pathway in Saccharomyces cerevisiae." Eukaryot Cell **4**(1): 134-146.

Arquint, C. and E. A. Nigg (2014). "STIL microcephaly mutations interfere with APC/C-mediated degradation and cause centriole amplification." Curr Biol **24**(4): 351-360.

Ayad, N. G., S. Rankin, M. Murakami, J. Jebanathirajah, S. Gygi and M. W. Kirschner (2003). "Tome-1, a trigger of mitotic entry, is degraded during G1 via the APC." Cell **113**(1): 101-113.

Ayad, N. G., S. Rankin, D. Ooi, M. Rape and M. W. Kirschner (2005). "Identification of ubiquitin ligase substrates by in vitro expression cloning." Methods Enzymol **399**: 404-414.

Ayrault, O., L. Andrique, D. Fauvin, B. Eymin, S. Gazzeri and P. Séité (2006). "Human tumor suppressor p14ARF negatively regulates rRNA transcription and inhibits UBF1 transcription factor phosphorylation." Oncogene **25**(58): 7577-7586.

Azuma, M., R. Toyama, E. Laver and I. B. Dawid (2006). "Perturbation of rRNA synthesis in the bap28 mutation leads to apoptosis mediated by p53 in the zebrafish central nervous system." J Biol Chem **281**(19): 13309-13316.

Banerjee, R., N. Russo, M. Liu, V. Basrur, E. Bellile, N. Palanisamy, C. S. Scanlon, E. van Tubergen, R. C. Inglehart, T. Metwally, R. S. Mani, A. Yocum, M. K. Nyati, R. M. Castilho, S. Varambally, A. M. Chinnaiyan and N. J. D'Silva (2014). "TRIP13 promotes error-prone nonhomologous end joining and induces chemoresistance in head and neck cancer." Nat Commun **5**: 4527.

Banerjee, T., S. Nath and S. Roychoudhury (2009). "DNA damage induced p53 downregulates Cdc20 by direct binding to its promoter causing chromatin remodeling." Nucleic Acids Res **37**(8): 2688-2698.

Barford, D. (2011). Structure, function and mechanism of the anaphase promoting complex (APC/C). Q Rev Biophys. England. **44:** 153-190.

Bashir, T., N. V. Dorrello, V. Amador, D. Guardavaccaro and M. Pagano (2004). Control of the SCF(Skp2-Cks1) ubiquitin ligase by the APC/C(Cdh1) ubiquitin ligase. Nature. England. **428:** 190-193.

Bassermann, F., D. Frescas, D. Guardavaccaro, L. Busino, A. Peschiaroli and M. Pagano (2008). The Cdc14B-Cdh1-Plk1 axis controls the G2 DNA-damage-response checkpoint. Cell. United States. **134:** 256-267.

Bastos de Oliveira, F. M., M. R. Harris, P. Brazauskas, R. A. de Bruin and M. B. Smolka (2012). "Linking DNA replication checkpoint to MBF cell-cycle transcription reveals a distinct class of G1/S genes." EMBO J **31**(7): 1798-1810.

Bański, P., M. Kodiha and U. Stochaj (2010). "Chaperones and multitasking proteins in the nucleolus: networking together for survival?" Trends Biochem Sci **35**(7): 361-367.

Bedford, L., J. Lowe, L. R. Dick, R. J. Mayer and J. E. Brownell (2011). Ubiquitin-like protein conjugation and the ubiquitin-proteasome system as drug targets. Nat Rev Drug Discov. England. **10:** 29-46.

Bentley, A. M., B. C. Williams, M. L. Goldberg and A. J. Andres (2002). "Phenotypic characterization of Drosophila ida mutants: defining the role of APC5 in cell cycle progression." J Cell Sci **115**(Pt 5): 949-961.

Berlingieri, M. T., P. Pallante, M. Guida, C. Nappi, V. Masciullo, G. Scambia, A. Ferraro, V. Leone, A. Sboner, M. Barbareschi, A. Ferro, G. Troncone and A. Fusco (2007). "UbcH10 expression may be a useful tool in the prognosis of ovarian carcinomas." Oncogene **26**(14): 2136-2140.

Bermudez, V. P., A. Farina, T. L. Higashi, F. Du, I. Tappin, T. S. Takahashi and J. Hurwitz (2012). "In vitro loading of human cohesin on DNA by the human Scc2-Scc4 loader complex." Proc Natl Acad Sci U S A **109**(24): 9366-9371.

Bernis, C., S. Vigneron, A. Burgess, J. C. Labbé, D. Fesquet, A. Castro and T. Lorca (2007). "Pin1 stabilizes Emi1 during G2 phase by preventing its association with SCF(betatrcp)." EMBO Rep **8**(1): 91-98.

Bernstein, K. A., J. E. Gallagher, B. M. Mitchell, S. Granneman and S. J. Baserga (2004). "The small-subunit processome is a ribosome assembly intermediate." Eukaryot Cell **3**(6): 1619-1626.

Bierhoff, H., M. Dundr, A. A. Michels and I. Grummt (2008). "Phosphorylation by casein kinase 2 facilitates rRNA gene transcription by promoting dissociation of TIF-IA from elongating RNA polymerase I." Mol Cell Biol **28**(16): 4988-4998.

Binné, U. K., M. K. Classon, F. A. Dick, W. Wei, M. Rape, W. G. Kaelin, A. M. Näär and N. J. Dyson (2007). "Retinoblastoma protein and anaphase-promoting complex physically interact and functionally cooperate during cell-cycle exit." Nat Cell Biol **9**(2): 225-232.

Bladen, C. L., D. Udayakumar, Y. Takeda and W. S. Dynan (2005). "Identification of the polypyrimidine tract binding protein-associated splicing factor.p54(nrb) complex as a candidate DNA double-strand break rejoining factor." J Biol Chem **280**(7): 5205-5210.

Blattner, C., A. Sparks and D. Lane (1999). "Transcription factor E2F-1 is upregulated in response to DNA damage in a manner analogous to that of p53." Mol Cell Biol **19**(5): 3704-3713.

Boisvert, F. M. and A. I. Lamond (2010). "p53-Dependent subcellular proteome localization following DNA damage." Proteomics **10**(22): 4087-4097.

Boos, D., J. Frigola and J. F. Diffley (2012). "Activation of the replicative DNA helicase: breaking up is hard to do." Curr Opin Cell Biol **24**(3): 423-430.

Boulon, S., B. J. Westman, S. Hutten, F. M. Boisvert and A. I. Lamond (2010). "The nucleolus under stress." Mol Cell **40**(2): 216-227.

Bradley, S. E., A. E. Johnson, I. P. Le, E. Oosterhouse, M. P. Hledin, G. A. Marquez and M. Burnatowska-Hledin (2010). "Phosphorylation of VACM-1/Cul5 by protein kinase A regulates its neddylation and antiproliferative effect." J Biol Chem **285**(7): 4883-4895.

Braglia, P., K. Heindl, A. Schleiffer, J. Martinez and N. J. Proudfoot (2010). "Role of the RNA/DNA kinase Grc3 in transcription termination by RNA polymerase I." EMBO Rep **11**(10): 758-764.

Braglia, P., J. Kawauchi and N. J. Proudfoot (2011). "Co-transcriptional RNA cleavage provides a failsafe termination mechanism for yeast RNA polymerase I." Nucleic Acids Res **39**(4): 1439-1448.

Brehm, A., E. A. Miska, D. J. McCance, J. L. Reid, A. J. Bannister and T. Kouzarides (1998). "Retinoblastoma protein recruits histone deacetylase to repress transcription." Nature **391**(6667): 597-601.

Bremm, A., S. M. Freund and D. Komander (2010). "Lys11-linked ubiquitin chains adopt compact conformations and are preferentially hydrolyzed by the deubiquitinase Cezanne." Nat Struct Mol Biol **17**(8): 939-947.

Brown, S. E. and M. Szyf (2007). "Epigenetic programming of the rRNA promoter by MBD3." Mol Cell Biol **27**(13): 4938-4952.

Budhavarapu, V. N., E. D. White, C. S. Mahanic, L. Chen, F. T. Lin and W. C. Lin (2012). "Regulation of E2F1 by APC/C Cdh1 via K11 linkage-specific ubiquitin chain formation." Cell Cycle **11**(10): 2030-2038.

Burton, J. L. and M. J. Solomon (2001). "D box and KEN box motifs in budding yeast Hsl1p are required for APC-mediated degradation and direct binding to Cdc20p and Cdh1p." Genes Dev **15**(18): 2381-2395.

Burton, J. L. and M. J. Solomon (2007). Mad3p, a pseudosubstrate inhibitor of APCCdc20 in the spindle assembly checkpoint. Genes Dev. United States. **21:** 655-667.

Burton, J. L., V. Tsakraklides and M. J. Solomon (2005). Assembly of an APC-Cdh1-substrate complex is stimulated by engagement of a destruction box. Mol Cell. United States. **18:** 533-542.

Buschhorn, B. A., G. Petzold, M. Galova, P. Dube, C. Kraft, F. Herzog, H. Stark and J. M. Peters (2011). "Substrate binding on the APC/C occurs between the coactivator Cdh1 and the processivity factor Doc1." Nat Struct Mol Biol **18**(1): 6-13.

Bártová, E., J. Krejcí, A. Harnicarová, G. Galiová and S. Kozubek (2008). "Histone modifications and nuclear architecture: a review." J Histochem Cytochem **56**(8): 711-721.

Caldecott, K. W. (2014). "DNA single-strand break repair." Exp Cell Res.

Carrano, A. C., E. Eytan, A. Hershko and M. Pagano (1999). "SKP2 is required for ubiquitin-mediated degradation of the CDK inhibitor p27." Nat Cell Biol **1**(4): 193-199.

Carroll, C. W., M. Enquist-Newman and D. O. Morgan (2005). The APC subunit Doc1 promotes recognition of the substrate destruction box. Curr Biol. England. **15:** 11-18.

Castro, A., S. Vigneron, C. Bernis, J. C. Labbe and T. Lorca (2003). "Xkid is degraded in a D-box, KEN-box, and A-box-independent pathway." Mol Cell Biol **23**(12): 4126-4138.

Cesare, A. J. (2014). "Mitosis, double strand break repair, and telomeres: A view from the end: How telomeres and the DNA damage response cooperate during mitosis to maintain genome stability." Bioessays.

Chabes, A. L., C. M. Pfleger, M. W. Kirschner and L. Thelander (2003). "Mouse ribonucleotide reductase R2 protein: a new target for anaphase-promoting complex-Cdh1-mediated proteolysis." Proc Natl Acad Sci U S A **100**(7): 3925-3929.

Chang, D. Z., Y. Ma, B. Ji, Y. Liu, P. Hwu, J. L. Abbruzzese, C. Logsdon and H. Wang (2012). "Increased CDC20 expression is associated with pancreatic ductal adenocarcinoma differentiation and progression." J Hematol Oncol **5**: 15.

Chang, L., Z. Zhang, J. Yang, S. H. McLaughlin and D. Barford (2014). "Molecular architecture and mechanism of the anaphase-promoting complex." Nature.

Chao, W. C., K. Kulkarni, Z. Zhang, E. H. Kong and D. Barford (2012). "Structure of the mitotic checkpoint complex." Nature **484**(7393): 208-213.

Chellappan, S. P., S. Hiebert, M. Mudryj, J. M. Horowitz and J. R. Nevins (1991). "The E2F transcription factor is a cellular target for the RB protein." Cell **65**(6): 1053-1061.

Chen, D., A. S. Belmont and S. Huang (2004). "Upstream binding factor association induces large-scale chromatin decondensation." Proc Natl Acad Sci U S A **101**(42): 15106-15111.

Chen, F., Z. Zhang, J. Bower, Y. Lu, S. S. Leonard, M. Ding, V. Castranova, H. Piwnica-Worms and X. Shi (2002). "Arsenite-induced Cdc25C degradation is through the KEN-box and ubiquitin-proteasome pathway." Proc Natl Acad Sci U S A **99**(4): 1990-1995.

Chen, J. and G. Fang (2001). "MAD2B is an inhibitor of the anaphase-promoting complex." Genes Dev **15**(14): 1765-1770.

Chen, S., J. Seiler, M. Santiago-Reichelt, K. Felbel, I. Grummt and R. Voit (2013). "Repression of RNA polymerase I upon stress is caused by inhibition of RNA-dependent deacetylation of PAF53 by SIRT7." Mol Cell **52**(3): 303-313.

Chen, T. R. (1988). "Re-evaluation of HeLa, HeLa S3, and HEp-2 karyotypes." Cytogenet Cell Genet **48**(1): 19-24.

Cho, H. J., E. H. Lee, S. H. Han, H. J. Chung, J. H. Jeong, J. Kwon and H. Kim (2012). "Degradation of human RAP80 is cell cycle regulated by Cdc20 and Cdh1 ubiquitin ligases." Mol Cancer Res **10**(5): 615-625.

Choi, E., H. Choe, J. Min, J. Y. Choi, J. Kim and H. Lee (2009). BubR1 acetylation at prometaphase is required for modulating APC/C activity and timing of mitosis. EMBO J. England. **28:** 2077-2089.

Choi, J. W., Y. Kim, J. H. Lee and Y. S. Kim (2013). "High expression of spindle assembly checkpoint proteins CDC20 and MAD2 is associated with poor prognosis in urothelial bladder cancer." Virchows Arch **463**(5): 681-687.

Choudhary, C., C. Kumar, F. Gnad, M. L. Nielsen, M. Rehman, T. C. Walther, J. V. Olsen and M. Mann (2009). Lysine acetylation targets protein complexes and co-regulates major cellular functions. Science. United States. **325:** 834-840.

Chow, C., N. Wong, M. Pagano, S. W. Lun, K. I. Nakayama, K. Nakayama and K. W. Lo (2012). "Regulation of APC/CCdc20 activity by RASSF1A-APC/CCdc20 circuitry." Oncogene **31**(15): 1975-1987.

Chuang, C., S. H. Lin, F. Huang, J. Pan, D. Josic and L. Y. Yu-Lee (2010). "Acetylation of RNA processing proteins and cell cycle proteins in mitosis." J Proteome Res **9**(9): 4554-4564.

Chun, A. C., K. H. Kok and D. Y. Jin (2013). "REV7 is required for anaphase-promoting complex-dependent ubiquitination and degradation of translesion DNA polymerase REV1." Cell Cycle **12**(2): 365-378.

Ciccia, A. and S. J. Elledge (2010). "The DNA damage response: making it safe to play with knives." Mol Cell **40**(2): 179-204.

Ciechanover, A. and A. L. Schwartz (1998). "The ubiquitin-proteasome pathway: the complexity and myriad functions of proteins death." Proc Natl Acad Sci U S A **95**(6): 2727-2730.

Ciosk, R., W. Zachariae, C. Michaelis, A. Shevchenko, M. Mann and K. Nasmyth (1998). An ESP1/PDS1 complex regulates loss of sister chromatid cohesion at the metaphase to anaphase transition in yeast. Cell. United States. **93:** 1067-1076.

Clague, M. J. and S. Urbe (2010). Ubiquitin: same molecule, different degradation pathways. Cell. United States, 2010 Elsevier Inc. **143:** 682-685.

Clements, P. M., C. Breslin, E. D. Deeks, P. J. Byrd, L. Ju, P. Bieganowski, C. Brenner, M. C. Moreira, A. M. Taylor and K. W. Caldecott (2004). "The ataxia-oculomotor apraxia 1 gene product has a role distinct from ATM and interacts with the DNA strand break repair proteins XRCC1 and XRCC4." DNA Repair (Amst) **3**(11): 1493-1502.

Collin, P., O. Nashchekina, R. Walker and J. Pines (2013). "The spindle assembly checkpoint works like a rheostat rather than a toggle switch." Nat Cell Biol **15**(11): 1378-1385.

Colombo, S. L., M. Palacios-Callender, N. Frakich, S. Carcamo, I. Kovacs, S. Tudzarova and S. Moncada (2011). "Molecular basis for the differential use of glucose and glutamine in cell proliferation as revealed by synchronized HeLa cells." Proc Natl Acad Sci U S A **108**(52): 21069-21074.

Colombo, S. L., M. Palacios-Callender, N. Frakich, J. De Leon, C. A. Schmitt, L. Boorn, N. Davis and S. Moncada (2010). "Anaphase-promoting complex/cyclosome-Cdh1 coordinates glycolysis and glutaminolysis with transition to S phase in human T lymphocytes." Proc Natl Acad Sci U S A **107**(44): 18868-18873.

Connors, B., L. Rochelle, A. Roberts and G. Howard (2014). "A Synthetic Interaction between CDC20 and RAD4 in Saccharomyces cerevisiae upon UV Irradiation." Mol Biol Int **2014**: 519290.

Constantinou, A., M. Tarsounas, J. K. Karow, R. M. Brosh, V. A. Bohr, I. D. Hickson and S. C. West (2000). "Werner's syndrome protein (WRN) migrates Holliday junctions and co-localizes with RPA upon replication arrest." EMBO Rep **1**(1): 80-84.

Costa, A., I. V. Hood and J. M. Berger (2013). "Mechanisms for initiating cellular DNA replication." Annu Rev Biochem **82**: 25-54.

Coster, G. and M. Goldberg (2010). "The cellular response to DNA damage: a focus on MDC1 and its interacting proteins." Nucleus **1**(2): 166-178.

Coster, G., Z. Hayouka, L. Argaman, C. Strauss, A. Friedler, M. Brandeis and M. Goldberg (2007). The DNA damage response mediator MDC1 directly interacts with the anaphase-promoting complex/cyclosome. J Biol Chem. United States. **282:** 32053-32064.

Cotto-Rios, X. M., M. J. Jones, L. Busino, M. Pagano and T. T. Huang (2011). "APC/CCdh1-dependent proteolysis of USP1 regulates the response to UV-mediated DNA damage." J Cell Biol **194**(2): 177-186.

Couté, Y., K. Kindbeiter, S. Belin, R. Dieckmann, L. Duret, L. Bezin, J. C. Sanchez and J. J. Diaz (2008). "ISG20L2, a novel vertebrate nucleolar exoribonuclease involved in ribosome biogenesis." Mol Cell Proteomics **7**(3): 546-559.

Cui, Y., X. Cheng, C. Zhang, Y. Zhang, S. Li, C. Wang and T. M. Guadagno (2010). "Degradation of the human mitotic checkpoint kinase Mps1 is cell cycle-regulated by APC-cCdc20 and APC-cCdh1 ubiquitin ligases." J Biol Chem **285**(43): 32988-32998.

da Fonseca, P. C., E. H. Kong, Z. Zhang, A. Schreiber, M. A. Williams, E. P. Morris and D. Barford (2011). Structures of APC/C(Cdh1) with substrates identify Cdh1 and Apc10 as the D-box co-receptor. Nature. England. **470:** 274-278.

Dahiya, A., S. Wong, S. Gonzalo, M. Gavin and D. C. Dean (2001). Linking the Rb and polycomb pathways. Mol Cell. United States. **8:** 557-569.

Date, D. A., A. C. Burrows and M. K. Summers (2014). "Phosphorylation regulates the p31Comet-mitotic arrest-deficient 2 (Mad2) interaction to promote spindle assembly checkpoint (SAC) activity." J Biol Chem **289**(16): 11367-11373.

Davey, N. E., N. J. Haslam, D. C. Shields and R. J. Edwards (2011). "SLiMSearch 2.0: biological context for short linear motifs in proteins." Nucleic Acids Res **39**(Web Server issue): W56-60.

Davis, E. J., C. Lachaud, P. Appleton, T. J. Macartney, I. Näthke and J. Rouse (2012). "DVC1 (C1orf124) recruits the p97 protein segregase to sites of DNA damage." Nat Struct Mol Biol **19**(11): 1093-1100.

Davis, R. J. (2000). "Signal transduction by the JNK group of MAP kinases." Cell **103**(2): 239-252.

De Antoni, A., C. G. Pearson, D. Cimini, J. C. Canman, V. Sala, L. Nezi, M. Mapelli, L. Sironi, M. Faretta, E. D. Salmon and A. Musacchio (2005). The Mad1/Mad2 complex as a template for Mad2 activation in the spindle assembly checkpoint. Curr Biol. England. **15:** 214-225.

den Elzen, N. and J. Pines (2001). "Cyclin A is destroyed in prometaphase and can delay chromosome alignment and anaphase." J Cell Biol **153**(1): 121-136.

Denissov, S., F. Lessard, C. Mayer, V. Stefanovsky, M. van Driel, I. Grummt, T. Moss and H. G. Stunnenberg (2011). "A model for the topology of active ribosomal RNA genes." EMBO Rep **12**(3): 231-237.

Dephoure, N., C. Zhou, J. Villén, S. A. Beausoleil, C. E. Bakalarski, S. J. Elledge and S. P. Gygi (2008). "A quantitative atlas of mitotic phosphorylation." Proc Natl Acad Sci U S A **105**(31): 10762-10767.

Di Fiore, B. and J. Pines (2010). How cyclin A destruction escapes the spindle assembly checkpoint. J Cell Biol. United States. **190:** 501-509.

Dick, F. A. and S. M. Rubin (2013). "Molecular mechanisms underlying RB protein function." Nat Rev Mol Cell Biol **14**(5): 297-306.

Dimitrova, N. and T. de Lange (2006). "MDC1 accelerates nonhomologous end-joining of dysfunctional telomeres." Genes Dev **20**(23): 3238-3243.

Dimova, N. V., N. A. Hathaway, B. H. Lee, D. S. Kirkpatrick, M. L. Berkowitz, S. P. Gygi, D. Finley and R. W. King (2012). "APC/C-mediated multiple monoubiquitylation provides an alternative degradation signal for cyclin B1." Nat Cell Biol **14**(2): 168-176.

Ding, Z. Y., H. R. Wu, J. M. Zhang, G. R. Huang and D. D. Ji (2014). "Expression characteristics of CDC20 in gastric cancer and its correlation with poor prognosis." Int J Clin Exp Pathol **7**(2): 722-727.

Dinkel, H., K. Van Roey, S. Michael, N. E. Davey, R. J. Weatheritt, D. Born, T. Speck, D. Krüger, G. Grebnev, M. Kuban, M. Strumillo, B. Uyar, A. Budd, B. Altenberg, M. Seiler, L. B. Chemes, J. Glavina, I. E. Sánchez, F. Diella and T. J. Gibson (2014). "The eukaryotic linear motif resource ELM: 10 years and counting." Nucleic Acids Res **42**(Database issue): D259-266.

Donati, G., S. Peddigari, C. A. Mercer and G. Thomas (2013). "5S ribosomal RNA is an essential component of a nascent ribosomal precursor complex that regulates the Hdm2-p53 checkpoint." Cell Rep **4**(1): 87-98.

Donzelli, M., M. Squatrito, D. Ganoth, A. Hershko, M. Pagano and G. F. Draetta (2002). "Dual mode of degradation of Cdc25 A phosphatase." EMBO J **21**(18): 4875-4884.

Dowdy, S. F., P. W. Hinds, K. Louie, S. I. Reed, A. Arnold and R. A. Weinberg (1993). Physical interaction of the retinoblastoma protein with human D cyclins. Cell. United States. **73:** 499-511.

Dragon, F., J. E. Gallagher, P. A. Compagnone-Post, B. M. Mitchell, K. A. Porwancher, K. A. Wehner, S. Wormsley, R. E. Settlage, J. Shabanowitz, Y. Osheim, A. L. Beyer, D. F. Hunt and S. J. Baserga (2002). "A large nucleolar U3 ribonucleoprotein required for 18S ribosomal RNA biogenesis." Nature **417**(6892): 967-970.

Drosopoulos, K., C. Tang, W. C. Chao and S. Linardopoulos (2014). "APC/C is an essential regulator of centrosome clustering." Nat Commun **5**: 3686.

Drygin, D., W. G. Rice and I. Grummt (2010). "The RNA polymerase I transcription machinery: an emerging target for the treatment of cancer." Annu Rev Pharmacol Toxicol **50**: 131-156.

Dube, P., F. Herzog, C. Gieffers, B. Sander, D. Riedel, S. A. Muller, A. Engel, J. M. Peters and H. Stark (2005). Localization of the coactivator Cdh1 and the cullin subunit Apc2 in a cryo-electron microscopy model of vertebrate APC/C. Mol Cell. United States. **20:** 867-879.

Dulić, V., E. Lees and S. I. Reed (1992). "Association of human cyclin E with a periodic G1-S phase protein kinase." Science **257**(5078): 1958-1961.

Duronio, R. J. and P. H. O'Farrell (1995). "Developmental control of the G1 to S transition in Drosophila: cyclin Eis a limiting downstream target of E2F." Genes Dev **9**(12): 1456-1468.

Edelbrock, M. A., S. Kaliyaperumal and K. J. Williams (2013). "Structural, molecular and cellular functions of MSH2 and MSH6 during DNA mismatch repair, damage signaling and other noncanonical activities." Mutat Res **743-744**: 53-66.

Eguren, M., E. Manchado and M. Malumbres (2011). "Non-mitotic functions of the Anaphase-Promoting Complex." Semin Cell Dev Biol **22**(6): 572-578.

Eguren, M., M. Álvarez-Fernández, F. García, A. J. López-Contreras, K. Fujimitsu, H. Yaguchi, J. L. Luque-García, O. Fernández-Capetillo, J. Muñoz, H. Yamano and M. Malumbres (2014). "A synthetic lethal interaction between APC/C and topoisomerase poisons uncovered by proteomic screens." Cell Rep **6**(4): 670-683.

Ehrlich, E. S., T. Wang, K. Luo, Z. Xiao, A. M. Niewiadomska, T. Martinez, W. Xu, L. Neckers and X. F. Yu (2009). "Regulation of Hsp90 client proteins by a Cullin5-RING E3 ubiquitin ligase." Proc Natl Acad Sci U S A **106**(48): 20330-20335.

Eilbracht, J., M. Reichenzeller, M. Hergt, M. Schnölzer, H. Heid, M. Stöhr, W. W. Franke and M. S. Schmidt-Zachmann (2004). "NO66, a highly conserved dual location protein in the nucleolus and in a special type of synchronously replicating chromatin." Mol Biol Cell **15**(4): 1816-1832.

El Hage, A., S. L. French, A. L. Beyer and D. Tollervey (2010). "Loss of Topoisomerase I leads to R-loop-mediated transcriptional blocks during ribosomal RNA synthesis." Genes Dev **24**(14): 1546-1558.

Eliezer, Y., L. Argaman, M. Kornowski, M. Roniger and M. Goldberg (2014). "Interplay between the DNA damage proteins MDC1 and ATM in the regulation of the spindle assembly checkpoint." J Biol Chem **289**(12): 8182-8193.

Emanuele, M. J., A. Ciccia, A. E. Elia and S. J. Elledge (2011). "Proliferating cell nuclear antigen (PCNA)-associated KIAA0101/PAF15 protein is a cell cycle-regulated anaphase-promoting complex/cyclosome substrate." Proc Natl Acad Sci U S A **108**(24): 9845-9850.

Engel, C., S. Sainsbury, A. C. Cheung, D. Kostrewa and P. Cramer (2013). "RNA polymerase I structure and transcription regulation." Nature **502**(7473): 650-655.

Engelbert, D., D. Schnerch, A. Baumgarten and R. Wasch (2008). The ubiquitin ligase APC(Cdh1) is required to maintain genome integrity in primary human cells. Oncogene. England. **27:** 907-917.

Estévez-García, I. O., V. Cordoba-Gonzalez, E. Lara-Padilla, A. Fuentes-Toledo, R. Falfán-Valencia, R. Campos-Rodríguez and E. Abarca-Rojano (2014). "Glucose and glutamine metabolism control by APC and SCF during the G1-to-S phase transition of the cell cycle." J Physiol Biochem **70**(2): 569-581.

Eytan, E., K. Wang, S. Miniowitz-Shemtov, D. Sitry-Shevah, S. Kaisari, T. J. Yen, S. T. Liu and A. Hershko (2014). "Disassembly of mitotic checkpoint complexes by the joint action of the AAA-ATPase TRIP13 and p31comet." Proc Natl Acad Sci U S A.

Fatica, A. and D. Tollervey (2002). "Making ribosomes." Curr Opin Cell Biol **14**(3): 313-318.

Fay, D. S., S. Keenan and M. Han (2002). "fzr-1 and lin-35/Rb function redundantly to control cell proliferation in C. elegans as revealed by a nonbiased synthetic screen." Genes Dev **16**(4): 503-517.

Feine, O., A. Zur, H. Mahbubani and M. Brandeis (2007). "Human Kid is degraded by the APC/C(Cdh1) but not by the APC/C(Cdc20)." Cell Cycle **6**(20): 2516-2523.

Feng, W., M. Yonezawa, J. Ye, T. Jenuwein and I. Grummt (2010). "PHF8 activates transcription of rRNA genes through H3K4me3 binding and H3K9me1/2 demethylation." Nat Struct Mol Biol **17**(4): 445-450.

Ferguson, J. L., W. C. Chao, E. Lee and K. L. Friedman (2013). "The anaphase promoting complex contributes to the degradation of the S. cerevisiae telomerase recruitment subunit Est1p." PLoS One **8**(1): e55055.

Finley, D. (2009). "Recognition and processing of ubiquitin-protein conjugates by the proteasome." Annu Rev Biochem **78**: 477-513.

Floyd, S., J. Pines and C. Lindon (2008). "APC/C Cdh1 targets aurora kinase to control reorganization of the mitotic spindle at anaphase." Curr Biol **18**(21): 1649-1658.

Foley, E. A. and T. M. Kapoor (2013). "Microtubule attachment and spindle assembly checkpoint signalling at the kinetochore." Nat Rev Mol Cell Biol **14**(1): 25-37.

Ford, E., R. Voit, G. Liszt, C. Magin, I. Grummt and L. Guarente (2006). "Mammalian Sir2 homolog SIRT7 is an activator of RNA polymerase I transcription." Genes Dev **20**(9): 1075-1080.

Foster, S. A. and D. O. Morgan (2012). "The APC/C subunit Mnd2/Apc15 promotes Cdc20 autoubiquitination and spindle assembly checkpoint inactivation." Mol Cell **47**(6): 921-932.

Fouraux, M. A., M. J. Kolkman, A. Van der Heijden, A. S. De Jong, W. J. Van Venrooij and G. J. Pruijn (2002). "The human La (SS-B) autoantigen interacts with DDX15/hPrp43, a putative DEAH-box RNA helicase." RNA **8**(11): 1428-1443.

Freed, E. F. and S. J. Baserga (2010). "The C-terminus of Utp4, mutated in childhood cirrhosis, is essential for ribosome biogenesis." Nucleic Acids Res **38**(14): 4798-4806.

Freed, E. F., J. L. Prieto, K. L. McCann, B. McStay and S. J. Baserga (2012). "NOL11, implicated in the pathogenesis of North American Indian childhood cirrhosis, is required for pre-rRNA transcription and processing." PLoS Genet **8**(8): e1002892.

French, S. L., M. L. Sikes, R. D. Hontz, Y. N. Osheim, T. E. Lambert, A. El Hage, M. M. Smith, D. Tollervey, J. S. Smith and A. L. Beyer (2011). "Distinguishing the roles of Topoisomerases I and II in relief of transcription-induced torsional stress in yeast rRNA genes." Mol Cell Biol **31**(3): 482-494.

Frescas, D. and M. Pagano (2008). "Deregulated proteolysis by the F-box proteins SKP2 and beta-TrCP: tipping the scales of cancer." Nat Rev Cancer **8**(6): 438-449.

Fromont-Racine, M., B. Senger, C. Saveanu and F. Fasiolo (2003). "Ribosome assembly in eukaryotes." Gene **313**: 17-42.

Frye, J. J., N. G. Brown, G. Petzold, E. R. Watson, C. R. Grace, A. Nourse, M. A. Jarvis, R. W. Kriwacki, J. M. Peters, H. Stark and B. A. Schulman (2013). "Electron microscopy structure of human APC/C(CDH1)-EMI1 reveals multimodal mechanism of E3 ligase shutdown." Nat Struct Mol Biol **20**(7): 827-835.

Fu, A. K., K. W. Hung, W. Y. Fu, C. Shen, Y. Chen, J. Xia, K. O. Lai and N. Y. Ip (2011). "APC(Cdh1) mediates EphA4-dependent downregulation of AMPA receptors in homeostatic plasticity." Nat Neurosci **14**(2): 181-189.

Fu, G., S. Hua, T. Ward, X. Ding, Y. Yang, Z. Guo and X. Yao (2007). "D-box is required for the degradation of human Shugoshin and chromosome alignment." Biochem Biophys Res Commun **357**(3): 672-678.

Fujita, T., W. Liu, H. Doihara, H. Date and Y. Wan (2008). "Dissection of the APCCdh1-Skp2 cascade in breast cancer." Clin Cancer Res **14**(7): 1966-1975.

Fujita, T., W. Liu, H. Doihara and Y. Wan (2008). "Regulation of Skp2-p27 axis by the Cdh1/anaphase-promoting complex pathway in colorectal tumorigenesis." Am J Pathol **173**(1): 217-228.

Fukushima, H., K. Ogura, L. Wan, Y. Lu, V. Li, D. Gao, P. Liu, A. W. Lau, T. Wu, M. W. Kirschner, H. Inuzuka and W. Wei (2013). "SCF-mediated Cdh1 degradation defines a negative feedback system that coordinates cell-cycle progression." Cell Rep **4**(4): 803-816.

Gabellini, D., I. N. Colaluca, H. C. Vodermaier, G. Biamonti, M. Giacca, A. Falaschi, S. Riva and F. A. Peverali (2003). "Early mitotic degradation of the homeoprotein HOXC10 is potentially linked to cell cycle progression." EMBO J **22**(14): 3715-3724.

Gallenberger, M., D. M. Meinel, M. Kroeber, M. Wegner, P. Milkereit, M. R. Bösl and E. R. Tamm (2011). "Lack of WDR36 leads to preimplantation embryonic lethality in mice and delays the formation of small subunit ribosomal RNA in human cells in vitro." Hum Mol Genet **20**(3): 422-435.

Gandhi, R., P. J. Gillespie and T. Hirano (2006). "Human Wapl is a cohesin-binding protein that promotes sister-chromatid resolution in mitotic prophase." Curr Biol **16**(24): 2406-2417.

Ganner, A., S. Lienkamp, T. Schäfer, D. Romaker, T. Wegierski, T. J. Park, S. Spreitzer, M. Simons, J. Gloy, E. Kim, J. B. Wallingford and G. Walz (2009). "Regulation of ciliary polarity by the APC/C." Proc Natl Acad Sci U S A **106**(42): 17799-17804.

Gao, D., H. Inuzuka, M. Korenjak, A. Tseng, T. Wu, L. Wan, M. Kirschner, N. Dyson and W. Wei (2009). Cdh1 regulates cell cycle through modulating the claspin/Chk1 and the Rb/E2F1 pathways. Mol Biol Cell. United States. **20:** 3305-3316.

Gao, D., H. Inuzuka, A. Tseng, R. Y. Chin, A. Toker and W. Wei (2009). Phosphorylation by Akt1 promotes cytoplasmic localization of Skp2 and impairs APCCdh1-mediated Skp2 destruction. Nat Cell Biol. England. **11:** 397-408.

Gao, D., H. Inuzuka, A. Tseng and W. Wei (2009). "Akt finds its new path to regulate cell cycle through modulating Skp2 activity and its destruction by APC/Cdh1." Cell Div **4**: 11.

Gao, Y. F., T. Li, Y. Chang, Y. B. Wang, W. N. Zhang, W. H. Li, K. He, R. Mu, C. Zhen, J. H. Man, X. Pan, L. Chen, M. Yu, B. Liang, Y. Chen, Q. Xia, T. Zhou, W. L. Gong, A. L. Li, H. Y. Li and X. M. Zhang (2011). "Cdk1-phosphorylated CUEDC2 promotes spindle checkpoint inactivation and chromosomal instability." Nat Cell Biol **13**(8): 924-933.

Garcia-Higuera, I., E. Manchado, P. Dubus, M. Canamero, J. Mendez, S. Moreno and M. Malumbres (2008). Genomic stability and tumour suppression by the APC/C cofactor Cdh1. Nat Cell Biol. England. **10:** 802-811.

Garg, A. V., M. Ahmed, A. N. Vallejo, A. Ma and S. L. Gaffen (2013). "The deubiquitinase A20 mediates feedback inhibition of interleukin-17 receptor signaling." Sci Signal **6**(278): ra44.

Garnett, M. J., J. Mansfeld, C. Godwin, T. Matsusaka, J. Wu, P. Russell, J. Pines and A. R. Venkitaraman (2009). "UBE2S elongates ubiquitin chains on APC/C substrates to promote mitotic exit." Nat Cell Biol **11**(11): 1363-1369.

Gautier, T., T. Bergès, D. Tollervey and E. Hurt (1997). "Nucleolar KKE/D repeat proteins Nop56p and Nop58p interact with Nop1p and are required for ribosome biogenesis." Mol Cell Biol **17**(12): 7088-7098.

Ge, S., J. R. Skaar and M. Pagano (2009). "APC/C- and Mad2-mediated degradation of Cdc20 during spindle checkpoint activation." Cell Cycle **8**(1): 167-171.

Geley, S., E. Kramer, C. Gieffers, J. Gannon, J. M. Peters and T. Hunt (2001). "Anaphase-promoting complex/cyclosome-dependent proteolysis of human cyclin A starts at the beginning of mitosis and is not subject to the spindle assembly checkpoint." J Cell Biol **153**(1): 137-148.

Germain, D., A. Russell, A. Thompson and J. Hendley (2000). "Ubiquitination of free cyclin D1 is independent of phosphorylation on threonine 286." J Biol Chem **275**(16): 12074-12079.

Giacinti, C. and A. Giordano (2006). RB and cell cycle progression. Oncogene. England. **25:** 5220-5227.

Gieffers, C., P. Dube, J. R. Harris, H. Stark and J. M. Peters (2001). "Three-dimensional structure of the anaphase-promoting complex." Mol Cell **7**(4): 907-913.

Gieffers, C., B. H. Peters, E. R. Kramer, C. G. Dotti and J. M. Peters (1999). "Expression of the CDH1-associated form of the anaphase-promoting complex in postmitotic neurons." Proc Natl Acad Sci U S A **96**(20): 11317-11322.

Giet, R., C. Petretti and C. Prigent (2005). Aurora kinases, aneuploidy and cancer, a coincidence or a real link? Trends Cell Biol. England. **15:** 241-250.

Glibetic, M., L. Taylor, D. Larson, R. Hannan, B. Sells and L. Rothblum (1995). "The RNA polymerase I transcription factor UBF is the product of a primary response gene." J Biol Chem **270**(9): 4209-4212.

Glickman, M. H. and A. Ciechanover (2002). "The ubiquitin-proteasome proteolytic pathway: destruction for the sake of construction." Physiol Rev **82**(2): 373-428.

Glotzer, M., A. W. Murray and M. W. Kirschner (1991). "Cyclin is degraded by the ubiquitin pathway." Nature **349**(6305): 132-138.

Gmachl, M., C. Gieffers, A. V. Podtelejnikov, M. Mann and J. M. Peters (2000). The RING-H2 finger protein APC11 and the E2 enzyme UBC4 are sufficient to ubiquitinate substrates of the anaphase-promoting complex. Proc Natl Acad Sci U S A. United States. **97:** 8973-8978.

Goldstein, G., M. Scheid, U. Hammerling, D. H. Schlesinger, H. D. Niall and E. A. Boyse (1975). "Isolation of a polypeptide that has lymphocyte-differentiating properties and is probably represented universally in living cells." Proc Natl Acad Sci U S A **72**(1): 11-15.

Goodfellow, S. J. and J. C. Zomerdijk (2012). "Basic mechanisms in RNA polymerase I transcription of the ribosomal RNA genes." Subcell Biochem **61**: 211-236.

Gorr, I. H., D. Boos and O. Stemmann (2005). Mutual inhibition of separase and Cdk1 by two-step complex formation. Mol Cell. United States. **19:** 135-141.

Goujon, M., H. McWilliam, W. Li, F. Valentin, S. Squizzato, J. Paern and R. Lopez (2010). "A new bioinformatics analysis tools framework at EMBL-EBI." Nucleic Acids Res **38**(Web Server issue): W695-699.

Govoni, M., F. Farabegoli, A. Pession and F. Novello (1994). "Inhibition of topoisomerase II activity and its effect on nucleolar structure and function." Exp Cell Res **211**(1): 36-41.

Granneman, S., J. E. Gallagher, J. Vogelzangs, W. Horstman, W. J. van Venrooij, S. J. Baserga and G. J. Pruijn (2003). "The human Imp3 and Imp4 proteins form a ternary complex with hMpp10, which only interacts with the U3 snoRNA in 60-80S ribonucleoprotein complexes." Nucleic Acids Res **31**(7): 1877-1887.

Grierson, P. M., S. Acharya and J. Groden (2013). "Collaborating functions of BLM and DNA topoisomerase I in regulating human rDNA transcription." Mutat Res **743-744**: 89-96.

Grossman, S. R., M. E. Deato, C. Brignone, H. M. Chan, A. L. Kung, H. Tagami, Y. Nakatani and D. M. Livingston (2003). "Polyubiquitination of p53 by a ubiquitin ligase activity of p300." Science **300**(5617): 342-344.

Grummt, I. (2013). "The nucleolus—guardian of cellular homeostasis and genome integrity." Chromosoma **122**(6): 487-497.

Gstaiger, M., R. Jordan, M. Lim, C. Catzavelos, J. Mestan, J. Slingerland and W. Krek (2001). Skp2 is oncogenic and overexpressed in human cancers. Proc Natl Acad Sci U S A. United States. **98:** 5043-5048.

Gu, B. and W. G. Zhu (2012). "Surf the post-translational modification network of p53 regulation." Int J Biol Sci **8**(5): 672-684.

Guardavaccaro, D., Y. Kudo, J. Boulaire, M. Barchi, L. Busino, M. Donzelli, F. Margottin-Goguet, P. K. Jackson, L. Yamasaki and M. Pagano (2003). "Control of meiotic and mitotic progression by the F box protein beta-Trcp1 in vivo." Dev Cell **4**(6): 799-812.

Gudjonsson, T., M. Altmeyer, V. Savic, L. Toledo, C. Dinant, M. Grøfte, J. Bartkova, M. Poulsen, Y. Oka, S. Bekker-Jensen, N. Mailand, B. Neumann, J. K. Heriche, R. Shearer, D. Saunders, J. Bartek, J. Lukas and C. Lukas (2012). "TRIP12 and UBR5 suppress spreading of chromatin ubiquitylation at damaged chromosomes." Cell **150**(4): 697-709.

Guetg, C. and R. Santoro (2012). "Formation of nuclear heterochromatin: the nucleolar point of view." Epigenetics **7**(8): 811-814.

Gueven, N., O. J. Becherel, A. W. Kijas, P. Chen, O. Howe, J. H. Rudolph, R. Gatti, H. Date, O. Onodera, G. Taucher-Scholz and M. F. Lavin (2004). "Aprataxin, a novel protein that protects against genotoxic stress." Hum Mol Genet **13**(10): 1081-1093.

Gunjan, A. and A. Verreault (2003). A Rad53 kinase-dependent surveillance mechanism that regulates histone protein levels in S. cerevisiae. Cell. United States. **115:** 537-549.

Gurden, M. D., A. J. Holland, W. van Zon, A. Tighe, M. A. Vergnolle, D. A. Andres, H. P. Spielmann, M. Malumbres, R. M. Wolthuis, D. W. Cleveland and S. S. Taylor (2010). "Cdc20 is required for the post-anaphase, KEN-dependent degradation of centromere protein F." J Cell Sci **123**(Pt 3): 321-330.

Gutierrez, G. J., T. Tsuji, M. Chen, W. Jiang and Z. A. Ronai (2010). "Interplay between Cdh1 and JNK activity during the cell cycle." Nat Cell Biol **12**(7): 686-695.

Güttinger, S., E. Laurell and U. Kutay (2009). "Orchestrating nuclear envelope disassembly and reassembly during mitosis." Nat Rev Mol Cell Biol **10**(3): 178-191.

Habu, T., S. H. Kim, J. Weinstein and T. Matsumoto (2002). "Identification of a MAD2-binding protein, CMT2, and its role in mitosis." EMBO J **21**(23): 6419-6428.

Hadjiolova, K. V., A. A. Hadjiolov and J. P. Bachellerie (1995). "Actinomycin D stimulates the transcription of rRNA minigenes transfected into mouse cells. Implications for the in vivo hypersensitivity of rRNA gene transcription." Eur J Biochem **228**(3): 605-615.

Hagting, A., N. Den Elzen, H. C. Vodermaier, I. C. Waizenegger, J. M. Peters and J. Pines (2002). "Human securin proteolysis is controlled by the spindle checkpoint and reveals when the APC/C switches from activation by Cdc20 to Cdh1." J Cell Biol **157**(7): 1125-1137.

Hames, R. S., S. L. Wattam, H. Yamano, R. Bacchieri and A. M. Fry (2001). "APC/C-mediated destruction of the centrosomal kinase Nek2A occurs in early mitosis and depends upon a cyclin A-type D-box." EMBO J **20**(24): 7117-7127.

Harkness, T. A., T. G. Arnason, C. Legrand, M. G. Pisclevich, G. F. Davies and E. L. Turner (2005). "Contribution of CAF-I to anaphase-promoting-complex-mediated mitotic chromatin assembly in Saccharomyces cerevisiae." Eukaryot Cell **4**(4): 673-684.

Harkness, T. A., G. F. Davies, V. Ramaswamy and T. G. Arnason (2002). "The ubiquitin-dependent targeting pathway in Saccharomyces cerevisiae plays a critical role in multiple chromatin assembly regulatory steps." Genetics **162**(2): 615-632.

Harley, M. E., L. A. Allan, H. S. Sanderson and P. R. Clarke (2010). "Phosphorylation of Mcl-1 by CDK1-cyclin B1 initiates its Cdc20-dependent destruction during mitotic arrest." EMBO J **29**(14): 2407-2420.

Hau, P. M., Y. L. Yip, M. S. Huen and S. W. Tsao (2011). "Loss of ΔNp63α promotes mitotic exit in epithelial cells." FEBS Lett **585**(17): 2720-2726.

Haugwitz, U., K. Tschöp and K. Engeland (2004). "SIRF--a novel regulator element controlling transcription from the p55Cdc/Fizzy promoter during the cell cycle." Biochem Biophys Res Commun **320**(3): 951-960.

Hayes, M. J., Y. Kimata, S. L. Wattam, C. Lindon, G. Mao, H. Yamano and A. M. Fry (2006). Early mitotic degradation of Nek2A depends on Cdc20-independent interaction with the APC/C. Nat Cell Biol. England. **8:** 607-614.

He, J., W. C. Chao, Z. Zhang, J. Yang, N. Cronin and D. Barford (2013). "Insights into degron recognition by APC/C coactivators from the structure of an Acm1-Cdh1 complex." Mol Cell **50**(5): 649-660.

He, Y., L. Tollini, T. H. Kim, Y. Itahana and Y. Zhang (2014). "The anaphase-promoting complex/cyclosome is an E3 ubiquitin ligase for Mdm2." Cell Cycle **13**(13): 2101-2109.

Heaney, A. P., R. Singson, C. J. McCabe, V. Nelson, M. Nakashima and S. Melmed (2000). Expression of pituitary-tumour transforming gene in colorectal tumours. Lancet. England. **355:** 716-719.

Hegemann, B., J. R. Hutchins, O. Hudecz, M. Novatchkova, J. Rameseder, M. M. Sykora, S. Liu, M. Mazanek, P. Lénárt, J. K. Hériché, I. Poser, N. Kraut, A. A. Hyman, M. B. Yaffe, K. Mechtler and J. M. Peters (2011). "Systematic phosphorylation analysis of human mitotic protein complexes." Sci Signal **4**(198): rs12.

Heindl, K. and J. Martinez (2010). "Nol9 is a novel polynucleotide 5'-kinase involved in ribosomal RNA processing." EMBO J **29**(24): 4161-4171.

Henglein, B., X. Chenivesse, J. Wang, D. Eick and C. Bréchot (1994). "Structure and cell cycle-regulated transcription of the human cyclin A gene." Proc Natl Acad Sci U S A **91**(12): 5490-5494.

Henning, D., R. B. So, R. Jin, L. F. Lau and B. C. Valdez (2003). "Silencing of RNA helicase II/Gualpha inhibits mammalian ribosomal RNA production." J Biol Chem **278**(52): 52307-52314.

Henras, A. K., J. Soudet, M. Gérus, S. Lebaron, M. Caizergues-Ferrer, A. Mougin and Y. Henry (2008). "The post-transcriptional steps of eukaryotic ribosome biogenesis." Cell Mol Life Sci **65**(15): 2334-2359.

Hernandez-Verdun, D. (2011). "Assembly and disassembly of the nucleolus during the cell cycle." Nucleus **2**(3): 189-194.

Hernandez-Verdun, D., P. Roussel, M. Thiry, V. Sirri and D. L. Lafontaine (2010). "The nucleolus: structure/function relationship in RNA metabolism." Wiley Interdiscip Rev RNA **1**(3): 415-431.

Herrero-Mendez, A., A. Almeida, E. Fernández, C. Maestre, S. Moncada and J. P. Bolaños (2009). "The bioenergetic and antioxidant status of neurons is controlled by continuous degradation of a key glycolytic enzyme by APC/C-Cdh1." Nat Cell Biol **11**(6): 747-752.

Herzog, F., I. Primorac, P. Dube, P. Lenart, B. Sander, K. Mechtler, H. Stark and J. M. Peters (2009). "Structure of the anaphase-promoting complex/cyclosome interacting with a mitotic checkpoint complex." Science **323**(5920): 1477-1481.

Hiebert, S. W., S. P. Chellappan, J. M. Horowitz and J. R. Nevins (1992). "The interaction of RB with E2F coincides with an i... [Genes Dev. 1992] - PubMed result." Genes Dev **6**(2): 177-185.

Hilioti, Z., Y. S. Chung, Y. Mochizuki, C. F. Hardy and O. Cohen-Fix (2001). The anaphase inhibitor Pds1 binds to the APC/C-associated protein Cdc20 in a destruction box-dependent manner. Curr Biol. England. **11:** 1347-1352.

Hinds, P. W., S. Mittnacht, V. Dulic, A. Arnold, S. I. Reed and R. A. Weinberg (1992). "Regulation of retinoblastoma protein functions by ectopic expression of human cyclins." Cell **70**(6): 993-1006.

Hirai, Y., E. Louvet, T. Oda, M. Kumeta, Y. Watanabe, T. Horigome and K. Takeyasu (2013). "Nucleolar scaffold protein, WDR46, determines the granular compartmental localization of nucleolin and DDX21." Genes Cells **18**(9): 780-797.

Hirano, T. (2012). "Condensins: universal organizers of chromosomes with diverse functions." Genes Dev **26**(15): 1659-1678.

Hitomi, M. and D. W. Stacey (1999). Cyclin D1 production in cycling cells depends on ras in a cell-cycle-specific manner. Curr Biol. England. **9:** 1075-1084.

Ho, A. W., A. V. Garg, L. Monin, M. R. Simpson-Abelson, L. Kinner and S. L. Gaffen (2013). "The anaphase-promoting complex protein 5 (AnapC5) associates with A20 and inhibits IL-17-mediated signal transduction." PLoS One **8**(7): e70168.

Hochstrasser, M. (2006). Lingering mysteries of ubiquitin-chain assembly. Cell. United States. **124:** 27-34.

Honda, K., H. Mihara, Y. Kato, A. Yamaguchi, H. Tanaka, H. Yasuda, K. Furukawa and T. Urano (2000). "Degradation of human Aurora2 protein kinase by the anaphase-promoting complex-ubiquitin-proteasome pathway." Oncogene **19**(24): 2812-2819.

Hoppe, S., H. Bierhoff, I. Cado, A. Weber, M. Tiebe, I. Grummt and R. Voit (2009). "AMP-activated protein kinase adapts rRNA synthesis to cellular energy supply." Proc Natl Acad Sci U S A **106**(42): 17781-17786.

Horn, S. R., M. J. Thomenius, E. S. Johnson, C. D. Freel, J. Q. Wu, J. L. Coloff, C. S. Yang, W. Tang, J. An, O. R. Ilkayeva, J. C. Rathmell, C. B. Newgard and S. Kornbluth (2011). "Regulation of mitochondrial morphology by APC/CCdh1-mediated control of Drp1 stability." Mol Biol Cell **22**(8): 1207-1216.

Hornig, N. C., P. P. Knowles, N. Q. McDonald and F. Uhlmann (2002). The dual mechanism of separase regulation by securin. Curr Biol. England. **12:** 973-982.

Hsu, J. Y., J. D. Reimann, C. S. Sorensen, J. Lukas and P. K. Jackson (2002). E2F-dependent accumulation of hEmi1 regulates S phase entry by inhibiting APC(Cdh1). Nat Cell Biol. England. **4:** 358-366.

Hu, D., W. Liu, G. Wu and Y. Wan (2011). "Nuclear translocation of Skp2 facilitates its destruction in response to TGFβ signaling." Cell Cycle **10**(2): 285-292.

Hu, K., D. Liao, W. Wu, A. J. Han, H. J. Shi, F. Wang, X. Wang, L. Zhong, T. Duan, Y. Wu, J. Cao, J. Tang, Y. Sang, L. Wang, X. Lv, S. Xu, R. H. Zhang, W. G. Deng, S. P. Li, Y. X. Zeng and T. Kang (2014). "Targeting the anaphase-promoting complex/cyclosome (APC/C)- bromodomain containing 7 (BRD7) pathway for human osteosarcoma." Oncotarget **5**(10): 3088-3100.

Huang, N. J., L. Zhang, W. Tang, C. Chen, C. S. Yang and S. Kornbluth (2012). "The Trim39 ubiquitin ligase inhibits APC/CCdh1-mediated degradation of the Bax activator MOAP-1." J Cell Biol **197**(3): 361-367.

Huang, X., M. K. Summers, V. Pham, J. R. Lill, J. Liu, G. Lee, D. S. Kirkpatrick, P. K. Jackson, G. Fang and V. M. Dixit (2011). Deubiquitinase USP37 Is Activated by CDK2 to Antagonize APC(CDH1) and Promote S Phase Entry. Mol Cell. United States, 2011 Elsevier Inc. **42:** 511-523.

Hughes, J. M. and M. Ares (1991). "Depletion of U3 small nucleolar RNA inhibits cleavage in the 5' external transcribed spacer of yeast pre-ribosomal RNA and impairs formation of 18S ribosomal RNA." EMBO J **10**(13): 4231-4239.

Hyun, S. Y., B. Sarantuya, H. J. Lee and Y. J. Jang (2013). "APC/C(Cdh1)-dependent degradation of Cdc20 requires a phosphorylation on CRY-box by Polo-like kinase-1 during somatic cell cycle." Biochem Biophys Res Commun **436**(1): 12-18.

Iapalucci-Espinoza, S. and M. T. Franze-Fernández (1979). "Effect of protein synthesis inhibitors and low concentrations of actinomycin D on ribosomal RNA synthesis." FEBS Lett **107**(2): 281-284.

Inoue, S. and H. Sato (1967). "Cell motility by labile association of molecules. The nature of mitotic spindle fibers and their role in chromosome movement." J Gen Physiol **50**(6): Suppl:259-292.

Inuzuka, H., D. Gao, L. W. Finley, W. Yang, L. Wan, H. Fukushima, Y. R. Chin, B. Zhai, S. Shaik, A. W. Lau, Z. Wang, S. P. Gygi, K. Nakayama, J. Teruya-Feldstein, A. Toker, M. C. Haigis, P. P. Pandolfi and W. Wei (2012). "Acetylation-dependent regulation of Skp2 function." Cell **150**(1): 179-193.

Islam, A., E. L. Turner, J. Menzel, M. E. Malo and T. A. Harkness (2011). "Antagonistic Gcn5-Hda1 interactions revealed by mutations to the Anaphase Promoting Complex in yeast." Cell Div **6**(1): 13.

Ito, S., L. J. Tan, D. Andoh, T. Narita, M. Seki, Y. Hirano, K. Narita, I. Kuraoka, Y. Hiraoka and K. Tanaka (2010). "MMXD, a TFIIH-independent XPD-MMS19 protein complex involved in chromosome segregation." Mol Cell **39**(4): 632-640.

Iwamoto, F., M. Stadler, K. Chalupníková, E. Oakeley and Y. Nagamine (2008). "Transcription-dependent nucleolar cap localization and possible nuclear function of DExH RNA helicase RHAU." Exp Cell Res **314**(6): 1378-1391.

Iwanami, N., T. Higuchi, Y. Sasano, T. Fujiwara, V. Q. Hoa, M. Okada, S. R. Talukder, S. Kunimatsu, J. Li, F. Saito, C. Bhattacharya, A. Matin, T. Sasaki, N. Shimizu, H. Mitani, H. Himmelbauer, A. Momoi, H. Kondoh, M. Furutani-Seiki and Y. Takahama (2008). "WDR55 is a nucleolar modulator of ribosomal RNA synthesis, cell cycle progression, and teleost organ development." PLoS Genet **4**(8): e1000171.

Iyama, T. and D. M. Wilson (2013). "DNA repair mechanisms in dividing and non-dividing cells." DNA Repair (Amst) **12**(8): 620-636.

Izawa, D. and J. Pines (2011). "How APC/C-Cdc20 changes its substrate specificity in mitosis." Nat Cell Biol **13**(3): 223-233.

Jallepalli, P. V., I. C. Waizenegger, F. Bunz, S. Langer, M. R. Speicher, J. M. Peters, K. W. Kinzler, B. Vogelstein and C. Lengauer (2001). Securin is required for chromosomal stability in human cells. Cell. United States. **105:** 445-457.

Jansa, P., C. Burek, E. E. Sander and I. Grummt (2001). "The transcript release factor PTRF augments ribosomal gene transcription by facilitating reinitiation of RNA polymerase I." Nucleic Acids Res **29**(2): 423-429.

Jansa, P. and I. Grummt (1999). "Mechanism of transcription termination: PTRF interacts with the largest subunit of RNA polymerase I and dissociates paused transcription complexes from yeast and mouse." Mol Gen Genet **262**(3): 508-514.

Jaquenoud, M., F. van Drogen and M. Peter (2002). "Cell cycle-dependent nuclear export of Cdh1p may contribute to the inactivation of APC/C(Cdh1)." EMBO J **21**(23): 6515-6526.

Jarmoskaite, I. and R. Russell (2014). "RNA helicase proteins as chaperones and remodelers." Annu Rev Biochem **83**: 697-725.

Jaspersen, S. L., J. F. Charles and D. O. Morgan (1999). "Inhibitory phosphorylation of the APC regulator Hct1 is controlled by the kinase Cdc28 and the phosphatase Cdc14." Curr Biol **9**(5): 227-236.

Jensen, S., M. Segal, D. J. Clarke and S. I. Reed (2001). "A novel role of the budding yeast separin Esp1 in anaphase spindle elongation: evidence that proper spindle association of Esp1 is regulated by Pds1." J Cell Biol **152**(1): 27-40.

Ji, M., H. Li, H. C. Suh, K. D. Klarmann, Y. Yokota and J. R. Keller (2008). Id2 intrinsically regulates lymphoid and erythroid development via interaction with different target proteins. Blood. United States. **112:** 1068-1077.

Ji, P., H. Jiang, K. Rekhtman, J. Bloom, M. Ichetovkin, M. Pagano and L. Zhu (2004). "An Rb-Skp2-p27 pathway mediates acute cell cycle inhibition by Rb and is retained in a partial-penetrance Rb mutant." Mol Cell **16**(1): 47-58.

Jia, L., S. Kim and H. Yu (2013). "Tracking spindle checkpoint signals from kinetochores to APC/C." Trends Biochem Sci **38**(6): 302-311.

Jiang, J., A. Jedinak and D. Sliva (2011). "Ganodermanontriol (GDNT) exerts its effect on growth and invasiveness of breast cancer cells through the down-regulation of CDC20 and uPA." Biochem Biophys Res Commun **415**(2): 325-329.

Jiang, L., C. G. Huang, Y. C. Lu, C. Luo, G. H. Hu, H. M. Liu, J. X. Chen and H. X. Han (2008). "Expression of ubiquitin-conjugating enzyme E2C/UbcH10 in astrocytic tumors." Brain Res **1201**: 161-166.

Jiang, L., T. Wang, Y. Bao, J. Qian, X. J. Wu, G. H. Hu and Y. C. Lu (2012). "A study of UbcH10 expression and its association with recurrence of meningiomas." J Surg Oncol **106**(3): 327-331.

Jin, L., A. Williamson, S. Banerjee, I. Philipp and M. Rape (2008). "Mechanism of ubiquitin-chain formation by the human anaphase-promoting complex." Cell **133**(4): 653-665.

Jones, H. S., J. Kawauchi, P. Braglia, C. M. Alen, N. A. Kent and N. J. Proudfoot (2007). "RNA polymerase I in yeast transcribes dynamic nucleosomal rDNA." Nat Struct Mol Biol **14**(2): 123-130.

Kakarougkas, A. and P. A. Jeggo (2014). "DNA DSB repair pathway choice: an orchestrated handover mechanism." Br J Radiol **87**(1035): 20130685.

Kalkhoven, E. (2004). "CBP and p300: HATs for different occasions." Biochem Pharmacol **68**(6): 1145-1155.

Kallstrom, G., J. Hedges and A. Johnson (2003). "The putative GTPases Nog1p and Lsg1p are required for 60S ribosomal subunit biogenesis and are localized to the nucleus and cytoplasm, respectively." Mol Cell Biol **23**(12): 4344-4355.

Kang, J., B. Goodman, Y. Zheng and D. Tantin (2011). "Dynamic regulation of Oct1 during mitosis by phosphorylation and ubiquitination." PLoS One **6**(8): e23872.

Kannan, M., S. J. Lee, N. Schwedhelm-Domeyer and J. Stegmüller (2012). "The E3 ligase Cdh1-anaphase promoting complex operates upstream of the E3 ligase Smurf1 in the control of axon growth." Development **139**(19): 3600-3612.

Karra, H., H. Repo, I. Ahonen, E. Löyttyniemi, R. Pitkänen, M. Lintunen, T. Kuopio, M. Söderström and P. Kronqvist (2014). "Cdc20 and securin overexpression predict short-term breast cancer survival." Br J Cancer **110**(12): 2905-2913.

Kaser, A., E. Bogengruber, M. Hallegger, E. Doppler, G. Lepperdinger, M. Jantsch, M. Breitenbach and G. Kreil (2001). "Brix from xenopus laevis and brx1p from yeast define a new family of proteins involved in the biogenesis of large ribosomal subunits." Biol Chem **382**(12): 1637-1647.

Kato, T., Y. Daigo, M. Aragaki, K. Ishikawa, M. Sato and M. Kaji (2012). "Overexpression of CDC20 predicts poor prognosis in primary non-small cell lung cancer patients." J Surg Oncol **106**(4): 423-430.

Ke, P. Y. and Z. F. Chang (2004). "Mitotic degradation of human thymidine kinase 1 is dependent on the anaphase-promoting complex/cyclosome-CDH1-mediated pathway." Mol Cell Biol **24**(2): 514-526.

Kerscher, O., R. Felberbaum and M. Hochstrasser (2006). "Modification of proteins by ubiquitin and ubiquitin-like proteins." Annu Rev Cell Dev Biol **22**: 159-180.

Kettenbach, A. N., D. K. Schweppe, B. K. Faherty, D. Pechenick, A. A. Pletnev and S. A. Gerber (2011). "Quantitative phosphoproteomics identifies substrates and functional modules of Aurora and Polo-like kinase activities in mitotic cells." Sci Signal **4**(179): rs5.

Kieffer, I., C. Lorenzo, C. Dozier, E. Schmitt and B. Ducommun (2007). "Differential mitotic degradation of the CDC25B phosphatase variants." Oncogene **26**(57): 7847-7858.

Kikuchi, R., H. Ohata, N. Ohoka, A. Kawabata and M. Naito (2014). "APOLLON protein promotes early mitotic CYCLIN A degradation independent of the spindle assembly checkpoint." J Biol Chem **289**(6): 3457-3467.

Kim, A. H., S. V. Puram, P. M. Bilimoria, Y. Ikeuchi, S. Keough, M. Wong, D. Rowitch and A. Bonni (2009). A centrosomal Cdc20-APC pathway controls dendrite morphogenesis in postmitotic neurons. Cell. United States. **136:** 322-336.

Kim, H. S., A. Vassilopoulos, R. H. Wang, T. Lahusen, Z. Xiao, X. Xu, C. Li, T. D. Veenstra, B. Li, H. Yu, J. Ji, X. W. Wang, S. H. Park, Y. I. Cha, D. Gius and C. X. Deng (2011). "SIRT2 maintains genome integrity and suppresses tumorigenesis through regulating APC/C activity." Cancer Cell **20**(4): 487-499.

Kim, J. Y., K. W. Kim, H. J. Kwon, D. W. Lee and J. S. Yoo (2002). "Probing lysine acetylation with a modification-specific marker ion using high-performance liquid chromatography/electrospray-mass spectrometry with collision-induced dissociation." Anal Chem **74**(21): 5443-5449.

Kim, W., E. J. Bennett, E. L. Huttlin, A. Guo, J. Li, A. Possemato, M. E. Sowa, R. Rad, J. Rush, M. J. Comb, J. W. Harper and S. P. Gygi (2011). "Systematic and quantitative assessment of the ubiquitin-modified proteome." Mol Cell **44**(2): 325-340.

Kim, Y., J. W. Choi, J. H. Lee and Y. S. Kim (2014). "MAD2 and CDC20 are Upregulated in High-grade Squamous Intraepithelial Lesions and Squamous Cell Carcinomas of the Uterine Cervix." Int J Gynecol Pathol **33**(5): 517-523.

Kimata, Y., J. E. Baxter, A. M. Fry and H. Yamano (2008). "A role for the Fizzy/Cdc20 family of proteins in activation of the APC/C distinct from substrate recruitment." Mol Cell **32**(4): 576-583.

Kimata, Y., A. Matsuyama, K. Nagao, K. Furuya, C. Obuse, M. Yoshida and M. Yanagida (2008). "Diminishing HDACs by drugs or mutations promotes normal or abnormal sister chromatid separation by affecting APC/C and adherin." J Cell Sci **121**(Pt 7): 1107-1118.

King, E. M., S. J. van der Sar and K. G. Hardwick (2007). "Mad3 KEN boxes mediate both Cdc20 and Mad3 turnover, and are critical for the spindle checkpoint." PLoS One **2**(4): e342.

King, R. W., J. M. Peters, S. Tugendreich, M. Rolfe, P. Hieter and M. W. Kirschner (1995). "A 20S complex containing CDC27 and CDC16 catalyzes the mitosis-specific conjugation of ubiquitin to cyclin B." Cell **81**(2): 279-288.

Kirkpatrick, D. S., N. A. Hathaway, J. Hanna, S. Elsasser, J. Rush, D. Finley, R. W. King and S. P. Gygi (2006). "Quantitative analysis of in vitro ubiquitinated cyclin B1 reveals complex chain topology." Nat Cell Biol **8**(7): 700-710.

Klitzing, C., R. Huss, A. L. Illert, A. Fröschl, S. Wötzel, C. Peschel, F. Bassermann and J. Duyster (2011). "APC/C(Cdh1)-mediated degradation of the F-box protein NIPA is regulated by its association with Skp1." PLoS One **6**(12): e28998.

Koegl, M., T. Hoppe, S. Schlenker, H. D. Ulrich, T. U. Mayer and S. Jentsch (1999). A novel ubiquitination factor, E4, is involved in multiubiquitin chain assembly. Cell. United States. **96:** 635-644.

Koff, A., F. Cross, A. Fisher, J. Schumacher, K. Leguellec, M. Philippe and J. M. Roberts (1991). "Human cyclin E, a new cyclin that interacts with two members of the CDC2 gene family." Cell **66**(6): 1217-1228.

Koff, A., A. Giordano, D. Desai, K. Yamashita, J. W. Harper, S. Elledge, T. Nishimoto, D. O. Morgan, B. R. Franza and J. M. Roberts (1992). "Formation and activation of a cyclin E-cdk2 complex during the G1 phase of the human cell cycle." Science **257**(5077): 1689-1694.

Koloteva-Levine, N., D. Pinchasi, I. Pereman, A. Zur, M. Brandeis and O. Elroy-Stein (2004). "The Apc5 subunit of the anaphase-promoting complex/cyclosome interacts with poly(A) binding protein and represses internal ribosome entry site-mediated translation." Mol Cell Biol **24**(9): 3577-3587.

Konishi, Y., J. Stegmuller, T. Matsuda, S. Bonni and A. Bonni (2004). Cdh1-APC controls axonal growth and patterning in the mammalian brain. Science. United States. **303:** 1026-1030.

Kouzarides, T. (2000). "Acetylation: a regulatory modification to rival phosphorylation?" EMBO J **19**(6): 1176-1179.

Kraft, C., M. Gmachl and J. M. Peters (2006). "Methods to measure ubiquitin-dependent proteolysis mediated by the anaphase-promoting complex." Methods **38**(1): 39-51.

Kraft, C., F. Herzog, C. Gieffers, K. Mechtler, A. Hagting, J. Pines and J. M. Peters (2003). "Mitotic regulation of the human anaphase-promoting complex by phosphorylation." EMBO J **22**(24): 6598-6609.

Kraft, C., H. C. Vodermaier, S. Maurer-Stroh, F. Eisenhaber and J. M. Peters (2005). The WD40 propeller domain of Cdh1 functions as a destruction box receptor for APC/C substrates. Mol Cell. United States. **18:** 543-553.

Kramer, E. R., N. Scheuringer, A. V. Podtelejnikov, M. Mann and J. M. Peters (2000). "Mitotic regulation of the APC activator proteins CDC20 and CDH1." Mol Biol Cell **11**(5): 1555-1569.

Kraus, W. L. and J. T. Kadonaga (1998). "p300 and estrogen receptor cooperatively activate transcription via differential enhancement of initiation and reinitiation." Genes Dev **12**(3): 331-342.

Kressler, D., D. Roser, B. Pertschy and E. Hurt (2008). "The AAA ATPase Rix7 powers progression of ribosome biogenesis by stripping Nsa1 from pre-60S particles." J Cell Biol **181**(6): 935-944.

Krietsch, J., M. C. Caron, J. P. Gagné, C. Ethier, J. Vignard, M. Vincent, M. Rouleau, M. J. Hendzel, G. G. Poirier and J. Y. Masson (2012). "PARP activation regulates the RNA-binding protein NONO in the DNA damage response to DNA double-strand breaks." Nucleic Acids Res **40**(20): 10287-10301.

Kruhlak, M., E. E. Crouch, M. Orlov, C. Montaño, S. A. Gorski, A. Nussenzweig, T. Misteli, R. D. Phair and R. Casellas (2007). "The ATM repair pathway inhibits RNA polymerase I transcription in response to chromosome breaks." Nature **447**(7145): 730-734.

Kueng, S., B. Hegemann, B. H. Peters, J. J. Lipp, A. Schleiffer, K. Mechtler and J. M. Peters (2006). "Wapl controls the dynamic association of cohesin with chromatin." Cell **127**(5): 955-967.

Kuhn, A. and I. Grummt (1989). "3'-end formation of mouse pre-rRNA involves both transcription termination and a specific processing reaction." Genes Dev **3**(2): 224-231.

Kuhn, C. D., S. R. Geiger, S. Baumli, M. Gartmann, J. Gerber, S. Jennebach, T. Mielke, H. Tschochner, R. Beckmann and P. Cramer (2007). "Functional architecture of RNA polymerase I." Cell **131**(7): 1260-1272.

Kulukian, A., J. S. Han and D. W. Cleveland (2009). Unattached kinetochores catalyze production of an anaphase inhibitor that requires a Mad2 template to prime Cdc20 for BubR1 binding. Dev Cell. United States. **16:** 105-117.

Kurki, S., K. Peltonen, L. Latonen, T. M. Kiviharju, P. M. Ojala, D. Meek and M. Laiho (2004). "Nucleolar protein NPM interacts with HDM2 and protects tumor suppressor protein p53 from HDM2-mediated degradation." Cancer Cell **5**(5): 465-475.

Labit, H., K. Fujimitsu, N. S. Bayin, T. Takaki, J. Gannon and H. Yamano (2012). "Dephosphorylation of Cdc20 is required for its C-box-dependent activation of the APC/C." EMBO J **31**(15): 3351-3362.

Lad, L., S. Lichtsteiner, J. J. Hartman, K. W. Wood and R. Sakowicz (2009). "Kinetic analysis of Mad2-Cdc20 formation: conformational changes in Mad2 are catalyzed by a C-Mad2-ligand complex." Biochemistry **48**(40): 9503-9515.

Lai, A., J. M. Lee, W. M. Yang, J. A. DeCaprio, W. G. Kaelin, Jr., E. Seto and P. E. Branton (1999). "RBP1 recruits both histone deacetylase-dependent and -independent repression activities to retinoblastoma family proteins." Mol Cell Biol **19**(10): 6632-6641.

Lai, F., K. Hu, Y. Wu, J. Tang, Y. Sang, J. Cao and T. Kang (2012). "Human KIAA1018/FAN1 nuclease is a new mitotic substrate of APC/C(Cdh1)." Chin J Cancer **31**(9): 440-448.

Lam, Y. A., W. Xu, G. N. DeMartino and R. E. Cohen (1997). "Editing of ubiquitin conjugates by an isopeptidase in the 26S proteasome." Nature **385**(6618): 737-740.

Lanning, C. C., J. L. Daddona, R. Ruiz-Velasco, S. H. Shafer and C. L. Williams (2004). "The Rac1 C-terminal polybasic region regulates the nuclear localization and protein degradation of Rac1." J Biol Chem **279**(42): 44197-44210.

Lara-Gonzalez, P., M. I. Scott, M. Diez, O. Sen and S. S. Taylor (2011). "BubR1 blocks substrate recruitment to the APC/C in a KEN-box-dependent manner." J Cell Sci.

Lasorella, A., J. Stegmuller, D. Guardavaccaro, G. Liu, M. S. Carro, G. Rothschild, L. de la Torre-Ubieta, M. Pagano, A. Bonni and A. Iavarone (2006). Degradation of Id2 by the anaphase-promoting complex couples cell cycle exit and axonal growth. Nature. England. **442:** 471-474.

Lebaron, S., A. Segerstolpe, S. L. French, T. Dudnakova, F. de Lima Alves, S. Granneman, J. Rappsilber, A. L. Beyer, L. Wieslander and D. Tollervey (2013). "Rrp5 binding at multiple sites coordinates pre-rRNA processing and assembly." Mol Cell **52**(5): 707-719.

Lee, M. J., B. H. Lee, J. Hanna, R. W. King and D. Finley (2011). Trimming of Ubiquitin Chains by Proteasome-associated Deubiquitinating Enzymes. Mol Cell Proteomics. United States. **10:** R110 003871.

Lehman, N. L., R. Tibshirani, J. Y. Hsu, Y. Natkunam, B. T. Harris, R. B. West, M. A. Masek, K. Montgomery, M. van de Rijn and P. K. Jackson (2007). "Oncogenic regulators and substrates of the anaphase promoting complex/cyclosome are frequently overexpressed in malignant tumors." Am J Pathol **170**(5): 1793-1805.

Lerch-Gaggl, A., J. Haque, J. Li, G. Ning, P. Traktman and S. A. Duncan (2002). "Pescadillo is essential for nucleolar assembly, ribosome biogenesis, and mammalian cell proliferation." J Biol Chem **277**(47): 45347-45355.

Lessard, F., F. Morin, S. Ivanchuk, F. Langlois, V. Stefanovsky, J. Rutka and T. Moss (2010). "The ARF tumor suppressor controls ribosome biogenesis by regulating the RNA polymerase I transcription factor TTF-I." Mol Cell **38**(4): 539-550.

Lessard, F., V. Stefanovsky, M. G. Tremblay and T. Moss (2012). "The cellular abundance of the essential transcription termination factor TTF-I regulates ribosome biogenesis and is determined by MDM2 ubiquitinylation." Nucleic Acids Res **40**(12): 5357-5367.

Leverson, J. D., C. A. Joazeiro, A. M. Page, H. Huang, P. Hieter and T. Hunter (2000). "The APC11 RING-H2 finger mediates E2-dependent ubiquitination." Mol Biol Cell **11**(7): 2315-2325.

Li, J., J. Z. Gao, J. L. Du, Z. X. Huang and L. X. Wei (2014). "Increased CDC20 expression is associated with development and progression of hepatocellular carcinoma." Int J Oncol.

Li, L., Y. Zhou, L. Sun, G. Xing, C. Tian, J. Sun, L. Zhang and F. He (2007). "NuSAP is degraded by APC/C-Cdh1 and its overexpression results in mitotic arrest dependent of its microtubules' affinity." Cell Signal **19**(10): 2046-2055.

Li, L., Y. Zhou, G. F. Wang, S. C. Liao, Y. B. Ke, W. Wu, X. H. Li, R. L. Zhang and Y. C. Fu (2011). "Anaphase-promoting complex/cyclosome controls HEC1 stability." Cell Prolif **44**(1): 1-9.

Li, M., Y. H. Shin, L. Hou, X. Huang, Z. Wei, E. Klann and P. Zhang (2008). "The adaptor protein of the anaphase promoting complex Cdh1 is essential in maintaining replicative lifespan and in learning and memory." Nat Cell Biol **10**(9): 1083-1089.

Li, R., B. Wan, J. Zhou, Y. Wang, T. Luo, X. Gu, F. Chen and L. Yu (2012). "APC/C(Cdh1) targets brain-specific kinase 2 (BRSK2) for degradation via the ubiquitin-proteasome pathway." PLoS One **7**(9): e45932.

Li, W., G. Wu and Y. Wan (2007). The dual effects of Cdh1/APC in myogenesis. FASEB J. United States. **21:** 3606-3617.

Lin, W. C., F. T. Lin and J. R. Nevins (2001). "Selective induction of E2F1 in response to DNA damage, mediated by ATM-dependent phosphorylation." Genes Dev **15**(14): 1833-1844.

Lindon, C., O. Albagli, P. Domeyne, D. Montarras and C. Pinset (2000). "Constitutive instability of muscle regulatory factor Myf5 is distinct from its mitosis-specific disappearance, which requires a D-box-like motif overlapping the basic domain." Mol Cell Biol **20**(23): 8923-8932.

Lindon, C. and J. Pines (2004). "Ordered proteolysis in anaphase inactivates Plk1 to contribute to proper mitotic exit in human cells." J Cell Biol **164**(2): 233-241.

Liot, C., L. Seguin, A. Siret, C. Crouin, S. Schmidt and J. Bertoglio (2011). "APC(cdh1) mediates degradation of the oncogenic Rho-GEF Ect2 after mitosis." PLoS One **6**(8): e23676.

Listovsky, T., Y. S. Oren, Y. Yudkovsky, H. M. Mahbubani, A. M. Weiss, M. Lebendiker and M. Brandeis (2004). Mammalian Cdh1/Fzr mediates its own degradation. EMBO J. England. **23:** 1619-1626.

Listovsky, T. and J. E. Sale (2013). "Sequestration of CDH1 by MAD2L2 prevents premature APC/C activation prior to anaphase onset." J Cell Biol **203**(1): 87-100.

Littlepage, L. E. and J. V. Ruderman (2002). "Identification of a new APC/C recognition domain, the A box, which is required for the Cdh1-dependent destruction of the kinase Aurora-A during mitotic exit." Genes Dev **16**(17): 2274-2285.

Liu, W., G. Wu, W. Li, D. Lobur and Y. Wan (2007). Cdh1-anaphase-promoting complex targets Skp2 for destruction in transforming growth factor beta-induced growth inhibition. Mol Cell Biol. United States. **27:** 2967-2979.

Liu, W., H. Xin, D. T. Eckert, J. A. Brown and J. R. Gnarra (2011). "Hypoxia and cell cycle regulation of the von Hippel-Lindau tumor suppressor." Oncogene **30**(1): 21-31.

Liu, Z., J. Ren, J. Cao, J. He, X. Yao, C. Jin and Y. Xue (2013). "Systematic analysis of the Plk-mediated phosphoregulation in eukaryotes." Brief Bioinform **14**(3): 344-360.

Liu, Z., F. Yuan, J. Ren, J. Cao, Y. Zhou, Q. Yang and Y. Xue (2012). "GPS-ARM: computational analysis of the APC/C recognition motif by predicting D-boxes and KEN-boxes." PLoS One **7**(3): e34370.

Lu, L., S. Hu, R. Wei, X. Qiu, K. Lu, Y. Fu, H. Li, G. Xing, D. Li, R. Peng, F. He and L. Zhang (2013). "The HECT type ubiquitin ligase NEDL2 is degraded by anaphase-promoting complex/cyclosome (APC/C)-Cdh1, and its tight regulation maintains the metaphase to anaphase transition." J Biol Chem **288**(50): 35637-35650.

Lukas, C., C. S. Sorensen, E. Kramer, E. Santoni-Rugiu, C. Lindeneg, J. M. Peters, J. Bartek and J. Lukas (1999). "Accumulation of cyclin B1 requires E2F and cyclin-A-dependent rearrangement of the anaphase-promoting complex." Nature **401**(6755): 815-818.

Lukasiewicz, K. B., T. M. Greenwood, V. C. Negron, A. K. Bruzek, J. L. Salisbury and W. L. Lingle (2011). "Control of centrin stability by Aurora A." PLoS One **6**(6): e21291.

Lundberg, A. S. and R. A. Weinberg (1998). "Functional inactivation of the retinoblastoma protein requires sequential modification by at least two distinct cyclin-cdk complexes." Mol Cell Biol **18**(2): 753-761.

Luo, R. X., A. A. Postigo and D. C. Dean (1998). Rb interacts with histone deacetylase to repress transcription. Cell. United States. **92:** 463-473.

Luo, X., Z. Tang, J. Rizo and H. Yu (2002). The Mad2 spindle checkpoint protein undergoes similar major conformational changes upon binding to either Mad1 or Cdc20. Mol Cell. United States. **9:** 59-71.

Längst, G., T. A. Blank, P. B. Becker and I. Grummt (1997). "RNA polymerase I transcription on nucleosomal templates: the transcription termination factor TTF-I induces chromatin remodeling and relieves transcriptional repression." EMBO J **16**(4): 760-768.

Lüking, A., U. Stahl and U. Schmidt (1998). "The protein family of RNA helicases." Crit Rev Biochem Mol Biol **33**(4): 259-296.

Macville, M., E. Schröck, H. Padilla-Nash, C. Keck, B. M. Ghadimi, D. Zimonjic, N. Popescu and T. Ried (1999). "Comprehensive and definitive molecular cytogenetic characterization of HeLa cells by spectral karyotyping." Cancer Res **59**(1): 141-150.

Magnaghi-Jaulin, L., R. Groisman, I. Naguibneva, P. Robin, S. Lorain, J. P. Le Villain, F. Troalen, D. Trouche and A. Harel-Bellan (1998). "Retinoblastoma protein represses transcription by recruiting a histone deacetylase." Nature **391**(6667): 601-605.

Mailand, N. and J. F. Diffley (2005). "CDKs promote DNA replication origin licensing in human cells by protecting Cdc6 from APC/C-dependent proteolysis." Cell **122**(6): 915-926.

Maine, G. T., P. Sinha and B. K. Tye (1984). "Mutants of S. cerevisiae defective in the maintenance of minichromosomes." Genetics **106**(3): 365-385.

Malik, R., R. Lenobel, A. Santamaria, A. Ries, E. A. Nigg and R. Körner (2009). "Quantitative analysis of the human spindle phosphoproteome at distinct mitotic stages." J Proteome Res **8**(10): 4553-4563.

Manchado, E., M. Eguren and M. Malumbres (2010). The anaphase-promoting complex/cyclosome (APC/C): cell-cycle-dependent and -independent functions. Biochem Soc Trans. England. **38:** 65-71.

Mansfeld, J., P. Collin, M. O. Collins, J. S. Choudhary and J. Pines (2011). "APC15 drives the turnover of MCC-CDC20 to make the spindle assembly checkpoint responsive to kinetochore attachment." Nat Cell Biol **13**(10): 1234-1243.

Margottin-Goguet, F., J. Y. Hsu, A. Loktev, H. M. Hsieh, J. D. Reimann and P. K. Jackson (2003). "Prophase destruction of Emi1 by the SCF(betaTrCP/Slimb) ubiquitin ligase activates the anaphase promoting complex to allow progression beyond prometaphase." Dev Cell **4**(6): 813-826.

Marouco, D., A. V. Garabadgiu, G. Melino and N. A. Barlev (2013). "Lysine-specific modifications of p53: a matter of life and death?" Oncotarget **4**(10): 1556-1571.

Marucci, G., L. Morandi, E. Magrini, A. Farnedi, E. Franceschi, R. Miglio, D. Calò, A. Pession, M. P. Foschini and V. Eusebi (2008). "Gene expression profiling in glioblastoma and immunohistochemical evaluation of IGFBP-2 and CDC20." Virchows Arch **453**(6): 599-609.

Mateo, F., M. Vidal-Laliena, N. Canela, L. Busino, M. A. Martinez-Balbas, M. Pagano, N. Agell and O. Bachs (2009). "Degradation of cyclin A is regulated by acetylation." Oncogene **28**(29): 2654-2666.

Mateo, F., M. Vidal-Laliena, M. J. Pujol and O. Bachs (2010). Acetylation of cyclin A: a new cell cycle regulatory mechanism. Biochem Soc Trans. England. **38:** 83-86.

Mateyak, M. K. and V. A. Zakian (2006). "Human PIF helicase is cell cycle regulated and associates with telomerase." Cell Cycle **5**(23): 2796-2804.

Matsumoto, A., Y. Ishibashi, M. Urashima, N. Omura, K. Nakada, K. Nishikawa, A. Shida, K. Takada, H. Kashiwagi and K. Yanaga (2014). "High UBCH10 protein expression as a marker of poor prognosis in esophageal squamous cell carcinoma." Anticancer Res **34**(2): 955-961.

May, E., J. R. Jenkins and P. May (1991). "Endogenous HeLa p53 proteins are easily detected in HeLa cells transfected with mouse deletion mutant p53 gene." Oncogene **6**(8): 1363-1365.

Mayer, C., H. Bierhoff and I. Grummt (2005). "The nucleolus as a stress sensor: JNK2 inactivates the transcription factor TIF-IA and down-regulates rRNA synthesis." Genes Dev **19**(8): 933-941.

Mayer, C. and I. Grummt (2005). "Cellular stress and nucleolar function." Cell Cycle **4**(8): 1036-1038.

Mayer, C., M. Neubert and I. Grummt (2008). "The structure of NoRC-associated RNA is crucial for targeting the chromatin remodelling complex NoRC to the nucleolus." EMBO Rep **9**(8): 774-780.

Mayer, C., K. M. Schmitz, J. Li, I. Grummt and R. Santoro (2006). "Intergenic transcripts regulate the epigenetic state of rRNA genes." Mol Cell **22**(3): 351-361.

Mayer, C., J. Zhao, X. Yuan and I. Grummt (2004). "mTOR-dependent activation of the transcription factor TIF-IA links rRNA synthesis to nutrient availability." Genes Dev **18**(4): 423-434.

McGarry, T. J. and M. W. Kirschner (1998). Geminin, an inhibitor of DNA replication, is degraded during mitosis. Cell. United States. **93:** 1043-1053.

Meerang, M., D. Ritz, S. Paliwal, Z. Garajova, M. Bosshard, N. Mailand, P. Janscak, U. Hübscher, H. Meyer and K. Ramadan (2011). "The ubiquitin-selective segregase VCP/p97 orchestrates the response to DNA double-strand breaks." Nat Cell Biol **13**(11): 1376-1382.

Mei, J., X. Huang and P. Zhang (2001). Securin is not required for cellular viability, but is required for normal growth of mouse embryonic fibroblasts. Curr Biol. England. **11:** 1197-1201.

Meloni, A. R., E. J. Smith and J. R. Nevins (1999). "A mechanism for Rb/p130-mediated transcription repression involving recruitment of the CtBP corepressor." Proc Natl Acad Sci U S A **96**(17): 9574-9579.

Merbl, Y. and M. W. Kirschner (2009). "Large-scale detection of ubiquitination substrates using cell extracts and protein microarrays." Proc Natl Acad Sci U S A **106**(8): 2543-2548.

Meyer, H. J. and M. Rape (2011). "Processive ubiquitin chain formation by the anaphase-promoting complex." Semin Cell Dev Biol **22**(6): 544-550.

Meyer, H. J. and M. Rape (2014). "Enhanced protein degradation by branched ubiquitin chains." Cell **157**(4): 910-921.

Michalczyk, K. and M. Ziman (2005). "Nestin structure and predicted function in cellular cytoskeletal organisation." Histol Histopathol **20**(2): 665-671.

Miki, T. S. and H. Großhans (2013). "The multifunctional RNase XRN2." Biochem Soc Trans **41**(4): 825-830.

Miller, G., K. I. Panov, J. K. Friedrich, L. Trinkle-Mulcahy, A. I. Lamond and J. C. Zomerdijk (2001). "hRRN3 is essential in the SL1-mediated recruitment of RNA Polymerase I to rRNA gene promoters." EMBO J **20**(6): 1373-1382.

Miller, J. J., M. K. Summers, D. V. Hansen, M. V. Nachury, N. L. Lehman, A. Loktev and P. K. Jackson (2006). Emi1 stably binds and inhibits the anaphase-promoting complex/cyclosome as a pseudosubstrate inhibitor. Genes Dev. United States. **20:** 2410-2420.

Min, M., U. Mayor and C. Lindon (2013). "Ubiquitination site preferences in anaphase promoting complex/cyclosome (APC/C) substrates." Open Biol **3**(9): 130097.

Mondal, G., S. Sengupta, C. K. Panda, S. M. Gollin, W. S. Saunders and S. Roychoudhury (2007). Overexpression of Cdc20 leads to impairment of the spindle assembly checkpoint and aneuploidization in oral cancer. Carcinogenesis. England. **28:** 81-92.

Morello, L. G., P. P. Coltri, A. J. Quaresma, F. M. Simabuco, T. C. Silva, G. Singh, J. A. Nickerson, C. C. Oliveira, M. J. Moore and N. I. Zanchin (2011). "The human nucleolar protein FTSJ3 associates with NIP7 and functions in pre-rRNA processing." PLoS One **6**(12): e29174.

Morello, L. G., C. Hesling, P. P. Coltri, B. A. Castilho, R. Rimokh and N. I. Zanchin (2011). "The NIP7 protein is required for accurate pre-rRNA processing in human cells." Nucleic Acids Res **39**(2): 648-665.

Morikawa, T., T. Kawai, H. Abe, H. Kume, Y. Homma and M. Fukayama (2013). "UBE2C is a marker of unfavorable prognosis in bladder cancer after radical cystectomy." Int J Clin Exp Pathol **6**(7): 1367-1374.

Morris, M. C., P. Kaiser, S. Rudyak, C. Baskerville, M. H. Watson and S. I. Reed (2003). "Cks1-dependent proteasome recruitment and activation of CDC20 transcription in budding yeast." Nature **423**(6943): 1009-1013.

Mosbech, A., I. Gibbs-Seymour, K. Kagias, T. Thorslund, P. Beli, L. Povlsen, S. V. Nielsen, S. Smedegaard, G. Sedgwick, C. Lukas, R. Hartmann-Petersen, J. Lukas, C. Choudhary, R. Pocock, S. Bekker-Jensen and N. Mailand (2012). "DVC1 (C1orf124) is a DNA damage-targeting p97 adaptor that promotes ubiquitin-dependent responses to replication blocks." Nat Struct Mol Biol **19**(11): 1084-1092.

Moshe, Y., O. Bar-On, D. Ganoth and A. Hershko (2011). "Regulation of the action of early mitotic inhibitor 1 on the anaphase-promoting complex/cyclosome by cyclin-dependent kinases." J Biol Chem **286**(19): 16647-16657.

Moura, I. M., M. L. Delgado, P. M. Silva, C. A. Lopes, J. B. do Amaral, L. S. Monteiro and H. Bousbaa (2014). "High CDC20 expression is associated with poor prognosis in oral squamous cell carcinoma." J Oral Pathol Med **43**(3): 225-231.

Mullineux, S. T. and D. L. Lafontaine (2012). "Mapping the cleavage sites on mammalian pre-rRNAs: where do we stand?" Biochimie **94**(7): 1521-1532.

Murayama, A., K. Ohmori, A. Fujimura, H. Minami, K. Yasuzawa-Tanaka, T. Kuroda, S. Oie, H. Daitoku, M. Okuwaki, K. Nagata, A. Fukamizu, K. Kimura, T. Shimizu and J. Yanagisawa (2008). "Epigenetic control of rDNA loci in response to intracellular energy status." Cell **133**(4): 627-639.

Musacchio, A. and E. D. Salmon (2007). The spindle-assembly checkpoint in space and time. Nat Rev Mol Cell Biol. England. **8:** 379-393.

Muth, V., S. Nadaud, I. Grummt and R. Voit (2001). "Acetylation of TAF(I)68, a subunit of TIF-IB/SL1, activates RNA polymerase I transcription." EMBO J **20**(6): 1353-1362.

Nagai, M. and T. Ushimaru (2014). "Cdh1 is an antagonist of the spindle assembly checkpoint." Cell Signal **26**(10): 2217-2222.

Naoe, H., K. Araki, O. Nagano, Y. Kobayashi, J. Ishizawa, T. Chiyoda, T. Shimizu, K. Yamamura, Y. Sasaki, H. Saya and S. Kuninaka (2010). "The anaphase-promoting complex/cyclosome activator Cdh1 modulates Rho GTPase by targeting p190 RhoGAP for degradation." Mol Cell Biol **30**(16): 3994-4005.

Nasmyth, K. (2011). "Cohesin: a catenase with separate entry and exit gates?" Nat Cell Biol **13**(10): 1170-1177.

Nath, S., T. Banerjee, D. Sen, T. Das and S. Roychoudhury (2011). Spindle Assembly Checkpoint Protein Cdc20 Transcriptionally Activates Expression of Ubiquitin Carrier Protein UbcH10. J Biol Chem. United States. **286:** 15666-15677.

Nguyen, H. G., D. Chinnappan, T. Urano and K. Ravid (2005). "Mechanism of Aurora-B degradation and its dependency on intact KEN and A-boxes: identification of an aneuploidy-promoting property." Mol Cell Biol **25**(12): 4977-4992.

Nguyen, T. B., K. Manova, P. Capodieci, C. Lindon, S. Bottega, X. Y. Wang, J. Refik-Rogers, J. Pines, D. J. Wolgemuth and A. Koff (2002). "Characterization and expression of mammalian cyclin b3, a prepachytene meiotic cyclin." J Biol Chem **277**(44): 41960-41969.

Nielsen, S. J., R. Schneider, U. M. Bauer, A. J. Bannister, A. Morrison, D. O'Carroll, R. Firestein, M. Cleary, T. Jenuwein, R. E. Herrera and T. Kouzarides (2001). Rb targets histone H3 methylation and HP1 to promoters. Nature. England. **412:** 561-565.

Nilsson, J., M. Yekezare, J. Minshull and J. Pines (2008). The APC/C maintains the spindle assembly checkpoint by targeting Cdc20 for destruction. Nat Cell Biol. England. **10:** 1411-1420.

Norvell, A. and S. B. McMahon (2010). "Cell biology. Rise of the rival." Science **327**(5968): 964-965.

Németh, A., S. Guibert, V. K. Tiwari, R. Ohlsson and G. Längst (2008). "Epigenetic regulation of TTF-I-mediated promoter-terminator interactions of rRNA genes." EMBO J **27**(8): 1255-1265.

Németh, A., J. Perez-Fernandez, P. Merkl, S. Hamperl, J. Gerber, J. Griesenbeck and H. Tschochner (2013). "RNA polymerase I termination: Where is the end?" Biochim Biophys Acta **1829**(3-4): 306-317.

O'Donohue, M. F., V. Choesmel, M. Faubladier, G. Fichant and P. E. Gleizes (2010). "Functional dichotomy of ribosomal proteins during the synthesis of mammalian 40S ribosomal subunits." J Cell Biol **190**(5): 853-866.

O'Donovan, K. J., J. Diedler, G. C. Couture, J. J. Fak and R. B. Darnell (2010). "The onconeural antigen cdr2 is a novel APC/C target that acts in mitosis to regulate c-myc target genes in mammalian tumor cells." PLoS One **5**(4): e10045.

Ochs, R. L., M. A. Lischwe, W. H. Spohn and H. Busch (1985). "Fibrillarin: a new protein of the nucleolus identified by autoimmune sera." Biol Cell **54**(2): 123-133.

Oeffinger, M., M. Dlakic and D. Tollervey (2004). "A pre-ribosome-associated HEAT-repeat protein is required for export of both ribosomal subunits." Genes Dev **18**(2): 196-209.

Oeffinger, M., A. Leung, A. Lamond, D. Tollervey and A. Lueng (2002). "Yeast Pescadillo is required for multiple activities during 60S ribosomal subunit synthesis." RNA **8**(5): 626-636.

Ogilvie, V. C., B. J. Wilson, S. M. Nicol, N. A. Morrice, L. R. Saunders, G. N. Barber and F. V. Fuller-Pace (2003). "The highly related DEAD box RNA helicases p68 and p72 exist as heterodimers in cells." Nucleic Acids Res **31**(5): 1470-1480.

Ohi, M. D., A. Feoktistova, L. Ren, C. Yip, Y. Cheng, J. S. Chen, H. J. Yoon, J. S. Wall, Z. Huang, P. A. Penczek, K. L. Gould and T. Walz (2007). "Structural organization of the anaphase-promoting complex bound to the mitotic activator Slp1." Mol Cell **28**(5): 871-885.

Ohoka, N., S. Sakai, K. Onozaki, M. Nakanishi and H. Hayashi (2010). "Anaphase-promoting complex/cyclosome-cdh1 mediates the ubiquitination and degradation of TRB3." Biochem Biophys Res Commun **392**(3): 289-294.

Ohtani, K., J. DeGregori and J. R. Nevins (1995). "Regulation of the cyclin E gene by transcription factor E2F1." Proc Natl Acad Sci U S A **92**(26): 12146-12150.

Okamoto, Y., T. Ozaki, K. Miyazaki, M. Aoyama, M. Miyazaki and A. Nakagawara (2003). "UbcH10 is the cancer-related E2 ubiquitin-conjugating enzyme." Cancer Res **63**(14): 4167-4173.

Olsen, J. V., M. Vermeulen, A. Santamaria, C. Kumar, M. L. Miller, L. J. Jensen, F. Gnad, J. Cox, T. S. Jensen, E. A. Nigg, S. Brunak and M. Mann (2010). "Quantitative phosphoproteomics reveals widespread full phosphorylation site occupancy during mitosis." Sci Signal **3**(104): ra3.

Ostapenko, D., J. L. Burton and M. J. Solomon (2012). "Identification of anaphase promoting complex substrates in S. cerevisiae." PLoS One **7**(9): e45895.

Ostapenko, D. and M. J. Solomon (2011). Anaphase Promoting Complex-dependent Degradation of Transcriptional Repressors Nrm1 and Yhp1 in S. cerevisiae. Mol Biol Cell.

Palazzo, L., R. Della Monica, R. Visconti, V. Costanzo and D. Grieco (2014). "ATM controls proper mitotic spindle structure." Cell Cycle **13**(7): 1091-1100.

Pallante, P., M. T. Berlingieri, G. Troncone, M. Kruhoffer, T. F. Orntoft, G. Viglietto, A. Caleo, I. Migliaccio, M. Decaussin-Petrucci, M. Santoro, L. Palombini and A. Fusco (2005). "UbcH10 overexpression may represent a marker of anaplastic thyroid carcinomas." Br J Cancer **93**(4): 464-471.

Pallante, P., U. Malapelle, M. T. Berlingieri, C. Bellevicine, R. Sepe, A. Federico, D. Rocco, M. Galgani, L. Chiariotti, M. Sanchez-Cespedes, A. Fusco and G. Troncone (2013). "UbcH10 overexpression in human lung carcinomas and its correlation with EGFR and p53 mutational status." Eur J Cancer **49**(5): 1117-1126.

Pan, J. and R. H. Chen (2004). Spindle checkpoint regulates Cdc20p stability in Saccharomyces cerevisiae. Genes Dev. United States. **18:** 1439-1451.

Panier, S. and S. J. Boulton (2014). "Double-strand break repair: 53BP1 comes into focus." Nat Rev Mol Cell Biol **15**(1): 7-18.

Panov, K. I., J. K. Friedrich, J. Russell and J. C. Zomerdijk (2006). "UBF activates RNA polymerase I transcription by stimulating promoter escape." EMBO J **25**(14): 3310-3322.

Panova, T. B., K. I. Panov, J. Russell and J. C. Zomerdijk (2006). "Casein kinase 2 associates with initiation-competent RNA polymerase I and has multiple roles in ribosomal DNA transcription." Mol Cell Biol **26**(16): 5957-5968.

Park, H. J., R. H. Costa, L. F. Lau, A. L. Tyner and P. Raychaudhuri (2008). Anaphase-promoting complex/cyclosome-CDH1-mediated proteolysis of the forkhead box M1 transcription factor is critical for regulated entry into S phase. Mol Cell Biol. United States. **28:** 5162-5171.

Park, K. H., S. E. Choi, M. Eom and Y. Kang (2005). Downregulation of the anaphase-promoting complex (APC)7 in invasive ductal carcinomas of the breast and its clinicopathologic relationships. Breast Cancer Res. England. **7:** R238-247.

Passmore, L. A. and D. Barford (2005). Coactivator functions in a stoichiometric complex with anaphase-promoting complex/cyclosome to mediate substrate recognition. EMBO Rep. England. **6:** 873-878.

Passmore, L. A., E. A. McCormack, S. W. Au, A. Paul, K. R. Willison, J. W. Harper and D. Barford (2003). "Doc1 mediates the activity of the anaphase-promoting complex by contributing to substrate recognition." EMBO J **22**(4): 786-796.

Pawar, S. A., T. R. Sarkar, K. Balamurugan, S. Sharan, J. Wang, Y. Zhang, S. F. Dowdy, A. M. Huang and E. Sterneck (2010). C/EBP{delta} targets cyclin D1 for proteasome-mediated degradation via induction of CDC27/APC3 expression. Proc Natl Acad Sci U S A. United States. **107:** 9210-9215.

Peart, M. J., M. V. Poyurovsky, E. M. Kass, M. Urist, E. W. Verschuren, M. K. Summers, P. K. Jackson and C. Prives (2010). "APC/C(Cdc20) targets E2F1 for degradation in prometaphase." Cell Cycle **9**(19): 3956-3964.

Pederson, T. (2011). "The nucleolus." Cold Spring Harb Perspect Biol **3**(3).

Pediconi, N., A. Ianari, A. Costanzo, L. Belloni, R. Gallo, L. Cimino, A. Porcellini, I. Screpanti, C. Balsano, E. Alesse, A. Gulino and M. Levrero (2003). "Differential regulation of E2F1 apoptotic target genes in response to DNA damage." Nat Cell Biol **5**(6): 552-558.

Penas, C., V. Ramachandran and N. G. Ayad (2011). "The APC/C Ubiquitin Ligase: From Cell Biology to Tumorigenesis." Front Oncol **1**: 60.

Perrotta, I., L. Bruno, L. Maltese, E. Russo, A. Donato and G. Donato (2012). "Immunohistochemical analysis of the ubiquitin-conjugating enzyme UbcH10 in lung cancer: a useful tool for diagnosis and therapy." J Histochem Cytochem **60**(5): 359-365.

Perry, R. P. and D. E. Kelley (1970). "Inhibition of RNA synthesis by actinomycin D: characteristic dose-response of different RNA species." J Cell Physiol **76**(2): 127-139.

Peters, J. M. (2006). "The anaphase promoting complex/cyclosome: a machine designed to destroy." Nat Rev Mol Cell Biol **7**(9): 644-656.

Petersen, B. O., C. Wagener, F. Marinoni, E. R. Kramer, M. Melixetian, E. Lazzerini Denchi, C. Gieffers, C. Matteucci, J. M. Peters and K. Helin (2000). "Cell cycle- and cell growth-regulated proteolysis of mammalian CDC6 is dependent on APC-CDH1." Genes Dev **14**(18): 2330-2343.

Petronczki, M., P. Lénárt and J. M. Peters (2008). "Polo on the Rise-from Mitotic Entry to Cytokinesis with Plk1." Dev Cell **14**(5): 646-659.

Pfleger, C. M. and M. W. Kirschner (2000). "The KEN box: an APC recognition signal distinct from the D box targeted by Cdh1." Genes Dev **14**(6): 655-665.

Pfleger, C. M., E. Lee and M. W. Kirschner (2001). "Substrate recognition by the Cdc20 and Cdh1 components of the anaphase-promoting complex." Genes Dev **15**(18): 2396-2407.

Pfleger, C. M., A. Salic, E. Lee and M. W. Kirschner (2001). "Inhibition of Cdh1-APC by the MAD2-related protein MAD2L2: a novel mechanism for regulating Cdh1." Genes Dev **15**(14): 1759-1764.

Piazza, I., C. H. Haering and A. Rutkowska (2013). "Condensin: crafting the chromosome landscape." Chromosoma **122**(3): 175-190.

Pick, J. E., M. Malumbres and E. Klann (2013). "The E3 ligase APC/C-Cdh1 is required for associative fear memory and long-term potentiation in the amygdala of adult mice." Learn Mem **20**(1): 11-20.

Pick, J. E., L. Wang, J. E. Mayfield and E. Klann (2013). "Neuronal expression of the ubiquitin E3 ligase APC/C-Cdh1 during development is required for long-term potentiation, behavioral flexibility, and extinction." Neurobiol Learn Mem **100**: 25-31.

Pines, J. (2011). "Cubism and the cell cycle: the many faces of the APC/C." Nat Rev Mol Cell Biol **12**(7): 427-438.

Pines, J. and T. Hunter (1990). "Human cyclin A is adenovirus E1A-associated protein p60 and behaves differently from cyclin B." Nature **346**(6286): 760-763.

Ping, Z., R. Lim, T. Bashir, M. Pagano and D. Guardavaccaro (2012). "APC/C (Cdh1) controls the proteasome-mediated degradation of E2F3 during cell cycle exit." Cell Cycle **11**(10): 1999-2005.

Pop, M., K. Aktories and G. Schmidt (2004). "Isotype-specific degradation of Rac activated by the cytotoxic necrotizing factor 1." J Biol Chem **279**(34): 35840-35848.

Prescott, E. M., Y. N. Osheim, H. S. Jones, C. M. Alen, J. G. Roan, R. H. Reeder, A. L. Beyer and N. J. Proudfoot (2004). "Transcriptional termination by RNA polymerase I requires the small subunit Rpa12p." Proc Natl Acad Sci U S A **101**(16): 6068-6073.

Primorac, I. and A. Musacchio (2013). "Panta rhei: the APC/C at steady state." J Cell Biol **201**(2): 177-189.

Puklowski, A., Y. Homsi, D. Keller, M. May, S. Chauhan, U. Kossatz, V. Grünwald, S. Kubicka, A. Pich, M. P. Manns, I. Hoffmann, P. Gönczy and N. P. Malek (2011). "The SCF-FBXW5 E3-ubiquitin ligase is regulated by PLK4 and targets HsSAS-6 to control centrosome duplication." Nat Cell Biol **13**(8): 1004-1009.

Qi, W. and H. Yu (2007). "KEN-box-dependent degradation of the Bub1 spindle checkpoint kinase by the anaphase-promoting complex/cyclosome." J Biol Chem **282**(6): 3672-3679.

Qiu, J., C. Zhang, Y. Lv, Y. Zhang, C. Zhu, X. Wang and W. Yao (2013). "Cdh1 inhibits reactive astrocyte proliferation after oxygen-glucose deprivation and reperfusion." Neurochem Int **63**(2): 87-92.

Quin, J. E., J. R. Devlin, D. Cameron, K. M. Hannan, R. B. Pearson and R. D. Hannan (2014). "Targeting the nucleolus for cancer intervention." Biochim Biophys Acta **1842**(6): 802-816.

Rajkumar, T., K. Sabitha, N. Vijayalakshmi, S. Shirley, M. V. Bose, G. Gopal and G. Selvaluxmy (2011). "Identification and validation of genes involved in cervical tumourigenesis." BMC Cancer **11**: 80.

Rankin, S., N. G. Ayad and M. W. Kirschner (2005). "Sororin, a substrate of the anaphase-promoting complex, is required for sister chromatid cohesion in vertebrates." Mol Cell **18**(2): 185-200.

Rape, M. and M. W. Kirschner (2004). Autonomous regulation of the anaphase-promoting complex couples mitosis to S-phase entry. Nature. England. **432:** 588-595.

Raska, I., P. J. Shaw and D. Cmarko (2006). "Structure and function of the nucleolus in the spotlight." Curr Opin Cell Biol **18**(3): 325-334.

Rass, U., I. Ahel and S. C. West (2007). "Actions of aprataxin in multiple DNA repair pathways." J Biol Chem **282**(13): 9469-9474.

Ray, S., T. Panova, G. Miller, A. Volkov, A. C. Porter, J. Russell, K. I. Panov and J. C. Zomerdijk (2013). "Topoisomerase IIα promotes activation of RNA polymerase I transcription by facilitating pre-initiation complex formation." Nat Commun **4**: 1598.

Reddy, S. K., M. Rape, W. A. Margansky and M. W. Kirschner (2007). "Ubiquitination by the anaphase-promoting complex drives spindle checkpoint inactivation." Nature **446**(7138): 921-925.

Reimann, J. D., E. Freed, J. Y. Hsu, E. R. Kramer, J. M. Peters and P. K. Jackson (2001). "Emi1 is a mitotic regulator that interacts with Cdc20 and inhibits the anaphase promoting complex." Cell **105**(5): 645-655.

Reis, A., M. Levasseur, H. Y. Chang, D. J. Elliott and K. T. Jones (2006). The CRY box: a second APCcdh1-dependent degron in mammalian cdc20. EMBO Rep. England. **7:** 1040-1045.

Reynolds, R. C., P. O. Montgomery and B. Hughes (1964). "NUCLEOLAR "CAPS" PRODUCED BY ACTINOMYCIN D." Cancer Res **24**: 1269-1277.

Richardson, L. A., B. J. Reed, J. M. Charette, E. F. Freed, E. K. Fredrickson, M. N. Locke, S. J. Baserga and R. G. Gardner (2012). "A conserved deubiquitinating enzyme controls cell growth by regulating RNA polymerase I stability." Cell Rep **2**(2): 372-385.

Rieder, C. L., R. W. Cole, A. Khodjakov and G. Sluder (1995). "The checkpoint delaying anaphase in response to chromosome monoorientation is mediated by an inhibitory signal produced by unattached kinetochores." J Cell Biol **130**(4): 941-948.

Riley, T., E. Sontag, P. Chen and A. Levine (2008). "Transcriptional control of human p53-regulated genes." Nat Rev Mol Cell Biol **9**(5): 402-412.

Ripmaster, T. L., G. P. Vaughn and J. L. Woolford (1992). "A putative ATP-dependent RNA helicase involved in Saccharomyces cerevisiae ribosome assembly." Proc Natl Acad Sci U S A **89**(23): 11131-11135.

Rivard, N., M. J. Boucher, C. Asselin and G. L'Allemain (1999). "MAP kinase cascade is required for p27 downregulation and S phase entry in fibroblasts and epithelial cells." Am J Physiol **277**(4 Pt 1): C652-664.

Rizzardi, L. F. and J. G. Cook (2012). "Flipping the switch from g1 to s phase with e3 ubiquitin ligases." Genes Cancer **3**(11-12): 634-648.

Robbins, J. A. and F. R. Cross (2010). Regulated degradation of the APC coactivator Cdc20. Cell Div. England. **5:** 23.

Robledo, S., R. A. Idol, D. L. Crimmins, J. H. Ladenson, P. J. Mason and M. Bessler (2008). "The role of human ribosomal proteins in the maturation of rRNA and ribosome production." RNA **14**(9): 1918-1929.

Rodier, G., P. Coulombe, P. L. Tanguay, C. Boutonnet and S. Meloche (2008). "Phosphorylation of Skp2 regulated by CDK2 and Cdc14B protects it from degradation by APC(Cdh1) in G1 phase." EMBO J **27**(4): 679-691.

Rodier, G., C. Makris, P. Coulombe, A. Scime, K. Nakayama, K. I. Nakayama and S. Meloche (2005). p107 inhibits G1 to S phase progression by down-regulating expression of the F-box protein Skp2. J Cell Biol. United States. **168:** 55-66.

Rodrigo-Brenni, M. C., S. A. Foster and D. O. Morgan (2010). "Catalysis of lysine 48-specific ubiquitin chain assembly by residues in E2 and ubiquitin." Mol Cell **39**(4): 548-559.

Rodrigo-Brenni, M. C. and D. O. Morgan (2007). "Sequential E2s drive polyubiquitin chain assembly on APC targets." Cell **130**(1): 127-139.

Romero, F., A. M. Gil-Bernabe, C. Saez, M. A. Japon, J. A. Pintor-Toro and M. Tortolero (2004). "Securin is a target of the UV response pathway in mammalian cells." Mol Cell Biol **24**(7): 2720-2733.

Romero, F., M. C. Multon, F. Ramos-Morales, A. Dominguez, J. A. Bernal, J. A. Pintor-Toro and M. Tortolero (2001). "Human securin, hPTTG, is associated with Ku heterodimer, the regulatory subunit of the DNA-dependent protein kinase." Nucleic Acids Res **29**(6): 1300-1307.

Ross, K. E. and O. Cohen-Fix (2003). "The role of Cdh1p in maintaining genomic stability in budding yeast." Genetics **165**(2): 489-503.

Rouquette, J., V. Choesmel and P. E. Gleizes (2005). "Nuclear export and cytoplasmic processing of precursors to the 40S ribosomal subunits in mammalian cells." EMBO J **24**(16): 2862-2872.

Rubbi, C. P. and J. Milner (2003). "Disruption of the nucleolus mediates stabilization of p53 in response to DNA damage and other stresses." EMBO J **22**(22): 6068-6077.

Rudner, A. D. and A. W. Murray (2000). "Phosphorylation by Cdc28 activates the Cdc20-dependent activity of the anaphase-promoting complex." J Cell Biol **149**(7): 1377-1390.

Ruggiero, R., A. Kale, B. Thomas and N. E. Baker (2012). "Mitosis in neurons: Roughex and APC/C maintain cell cycle exit to prevent cytokinetic and axonal defects in Drosophila photoreceptor neurons." PLoS Genet **8**(11): e1003049.

Ruse, C. I., D. B. McClatchy, B. Lu, D. Cociorva, A. Motoyama, S. K. Park and J. R. Yates (2008). "Motif-specific sampling of phosphoproteomes." J Proteome Res **7**(5): 2140-2150.

Russell, J. and J. C. Zomerdijk (2006). "The RNA polymerase I transcription machinery." Biochem Soc Symp(73): 203-216.

Sabile, A., A. M. Meyer, C. Wirbelauer, D. Hess, U. Kogel, M. Scheffner and W. Krek (2006). "Regulation of p27 degradation and S-phase progression by Ro52 RING finger protein." Mol Cell Biol **26**(16): 5994-6004.

Sacco, E., M. M. Hasan, L. Alberghina and M. Vanoni (2012). "Comparative analysis of the molecular mechanisms controlling the initiation of chromosomal DNA replication in yeast and in mammalian cells." Biotechnol Adv **30**(1): 73-98.

Sanchez, Y., J. Bachant, H. Wang, F. Hu, D. Liu, M. Tetzlaff and S. J. Elledge (1999). Control of the DNA damage checkpoint by chk1 and rad53 protein kinases through distinct mechanisms. Science. United States. **286:** 1166-1171.

Sano, Y., H. Date, S. Igarashi, O. Onodera, M. Oyake, T. Takahashi, S. Hayashi, M. Morimatsu, H. Takahashi, T. Makifuchi, N. Fukuhara and S. Tsuji (2004). "Aprataxin, the causative protein for EAOH is a nuclear protein with a potential role as a DNA repair protein." Ann Neurol **55**(2): 241-249.

Santoro, R., J. Li and I. Grummt (2002). "The nucleolar remodeling complex NoRC mediates heterochromatin formation and silencing of ribosomal gene transcription." Nat Genet **32**(3): 393-396.

Sasaki, T., A. Toh-E and Y. Kikuchi (2000). "Yeast Krr1p physically and functionally interacts with a novel essential Kri1p, and both proteins are required for 40S ribosome biogenesis in the nucleolus." Mol Cell Biol **20**(21): 7971-7979.

Saveanu, C., A. Namane, P. E. Gleizes, A. Lebreton, J. C. Rousselle, J. Noaillac-Depeyre, N. Gas, A. Jacquier and M. Fromont-Racine (2003). "Sequential protein association with nascent 60S ribosomal particles." Mol Cell Biol **23**(13): 4449-4460.

Schaefer, J. B. and D. O. Morgan (2011). "Protein-linked ubiquitin chain structure restricts activity of deubiquitinating enzymes." J Biol Chem **286**(52): 45186-45196.

Schlesinger, S., S. Selig, Y. Bergman and H. Cedar (2009). "Allelic inactivation of rDNA loci." Genes Dev **23**(20): 2437-2447.

Schmitz, K. M., C. Mayer, A. Postepska and I. Grummt (2010). "Interaction of noncoding RNA with the rDNA promoter mediates recruitment of DNMT3b and silencing of rRNA genes." Genes Dev **24**(20): 2264-2269.

Schmitz, K. M., N. Schmitt, U. Hoffmann-Rohrer, A. Schäfer, I. Grummt and C. Mayer (2009). "TAF12 recruits Gadd45a and the nucleotide excision repair complex to the promoter of rRNA genes leading to active DNA demethylation." Mol Cell **33**(3): 344-353.

Schreiber, A., F. Stengel, Z. Zhang, R. I. Enchev, E. H. Kong, E. P. Morris, C. V. Robinson, P. C. da Fonseca and D. Barford (2011). Structural basis for the subunit assembly of the anaphase-promoting complex. Nature. England. **470:** 227-232.

Schulman, B. A. and J. W. Harper (2009). "Ubiquitin-like protein activation by E1 enzymes: the apex for downstream signalling pathways." Nat Rev Mol Cell Biol **10**(5): 319-331.

Schwab, M., A. S. Lutum and W. Seufert (1997). Yeast Hct1 is a regulator of Clb2 cyclin proteolysis. Cell. United States. **90:** 683-693.

Schwab, M., M. Neutzner, D. Mocker and W. Seufert (2001). "Yeast Hct1 recognizes the mitotic cyclin Clb2 and other substrates of the ubiquitin ligase APC." EMBO J **20**(18): 5165-5175.

Schweizer, N., C. Ferrás, D. M. Kern, E. Logarinho, I. M. Cheeseman and H. Maiato (2013). "Spindle assembly checkpoint robustness requires Tpr-mediated regulation of Mad1/Mad2 proteostasis." J Cell Biol **203**(6): 883-893.

Schwickart, M., J. Havlis, B. Habermann, A. Bogdanova, A. Camasses, T. Oelschlaegel, A. Shevchenko and W. Zachariae (2004). "Swm1/Apc13 is an evolutionarily conserved subunit of the anaphase-promoting complex stabilizing the association of Cdc16 and Cdc27." Mol Cell Biol **24**(8): 3562-3576.

Sedgwick, G. G., D. G. Hayward, B. Di Fiore, M. Pardo, L. Yu, J. Pines and J. Nilsson (2013). "Mechanisms controlling the temporal degradation of Nek2A and Kif18A by the APC/C-Cdc20 complex." EMBO J **32**(2): 303-314.

Seki, A. and G. Fang (2007). "CKAP2 is a spindle-associated protein degraded by APC/C-Cdh1 during mitotic exit." J Biol Chem **282**(20): 15103-15113.

Sharma, S., J. Yang, P. Watzinger, P. Kötter and K. D. Entian (2013). "Yeast Nop2 and Rcm1 methylate C2870 and C2278 of the 25S rRNA, respectively." Nucleic Acids Res **41**(19): 9062-9076.

Shav-Tal, Y., J. Blechman, X. Darzacq, C. Montagna, B. T. Dye, J. G. Patton, R. H. Singer and D. Zipori (2005). "Dynamic sorting of nuclear components into distinct nucleolar caps during transcriptional inhibition." Mol Biol Cell **16**(5): 2395-2413.

Sherr, C. J. (1994). G1 phase progression: cycling on cue. Cell. United States. **79:** 551-555.

Shi, D., M. S. Pop, R. Kulikov, I. M. Love, A. L. Kung, A. Kung and S. R. Grossman (2009). "CBP and p300 are cytoplasmic E4 polyubiquitin ligases for p53." Proc Natl Acad Sci U S A **106**(38): 16275-16280.

Shirayama, M., W. Zachariae, R. Ciosk and K. Nasmyth (1998). "The Polo-like kinase Cdc5p and the WD-repeat protein Cdc20p/fizzy are regulators and substrates of the anaphase promoting complex in Saccharomyces cerevisiae." EMBO J **17**(5): 1336-1349.

Shiromizu, T., J. Adachi, S. Watanabe, T. Murakami, T. Kuga, S. Muraoka and T. Tomonaga (2013). "Identification of missing proteins in the neXtProt database and unregistered phosphopeptides in the PhosphoSitePlus database as part of the Chromosome-centric Human Proteome Project." J Proteome Res **12**(6): 2414-2421.

Shiue, C. N., R. G. Berkson and A. P. Wright (2009). "c-Myc induces changes in higher order rDNA structure on stimulation of quiescent cells." Oncogene **28**(16): 1833-1842.

Shyy, T. T., J. R. Subjeck, R. Heinaman and G. Anderson (1986). "Effect of growth state and heat shock on nucleolar localization of the 110,000-Da heat shock protein in mouse embryo fibroblasts." Cancer Res **46**(9): 4738-4745.

Sievers, F. and D. G. Higgins (2014). "Clustal Omega, accurate alignment of very large numbers of sequences." Methods Mol Biol **1079**: 105-116.

Sievers, F., A. Wilm, D. Dineen, T. J. Gibson, K. Karplus, W. Li, R. Lopez, H. McWilliam, M. Remmert, J. Söding, J. D. Thompson and D. G. Higgins (2011). "Fast, scalable generation of high-quality protein multiple sequence alignments using Clustal Omega." Mol Syst Biol **7**: 539.

Signoretti, S., L. Di Marcotullio, A. Richardson, S. Ramaswamy, B. Isaac, M. Rue, F. Monti, M. Loda and M. Pagano (2002). "Oncogenic role of the ubiquitin ligase subunit Skp2 in human breast cancer." J Clin Invest **110**(5): 633-641.

Silva, B. A., J. R. Stambaugh, K. Yokomori, J. V. Shah and M. W. Berns (2014). "DNA damage to a single chromosome end delays anaphase onset." J Biol Chem **289**(33): 22771-22784.

Simard, R. and W. Bernhard (1966). "[The phenomenon of nucleolar segregation: specificity of action of certain antimetabolites]." Int J Cancer **1**(5): 463-479.

Singh, S. A., D. Winter, M. Kirchner, R. Chauhan, S. Ahmed, N. Ozlu, A. Tzur, J. A. Steen and H. Steen (2014). "Co-regulation proteomics reveals substrates and mechanisms of APC/C-dependent degradation." EMBO J **33**(4): 385-399.

Sironi, L., M. Mapelli, S. Knapp, A. De Antoni, K. T. Jeang and A. Musacchio (2002). "Crystal structure of the tetrameric Mad1-Mad2 core complex: implications of a 'safety belt' binding mechanism for the spindle checkpoint." EMBO J **21**(10): 2496-2506.

Sivakumar, S., J. R. Daum, A. R. Tipton, S. Rankin and G. J. Gorbsky (2014). "The spindle and kinetochore-associated (Ska) complex enhances binding of the anaphase-promoting complex/cyclosome (APC/C) to chromosomes and promotes mitotic exit." Mol Biol Cell **25**(5): 594-605.

Skaar, J. R. and M. Pagano (2009). "Control of cell growth by the SCF and APC/C ubiquitin ligases." Curr Opin Cell Biol **21**(6): 816-824.

Skoufias, D. A., R. L. Indorato, F. Lacroix, A. Panopoulos and R. L. Margolis (2007). Mitosis persists in the absence of Cdk1 activity when proteolysis or protein phosphatase activity is suppressed. J Cell Biol. United States. **179:** 671-685.

Sloan, K. E., S. Mattijssen, S. Lebaron, D. Tollervey, G. J. Pruijn and N. J. Watkins (2013). "Both endonucleolytic and exonucleolytic cleavage mediate ITS1 removal during human ribosomal RNA processing." J Cell Biol **200**(5): 577-588.

Smith, V. E., J. A. Franklyn and C. J. McCabe (2010). Pituitary tumor-transforming gene and its binding factor in endocrine cancer. Expert Rev Mol Med. England. **12:** e38.

Soboleva, T. A. and R. T. Baker (2004). "Deubiquitinating enzymes: their functions and substrate specificity." Curr Protein Pept Sci **5**(3): 191-200.

Song, L. and M. Rape (2010). "Regulated degradation of spindle assembly factors by the anaphase-promoting complex." Mol Cell **38**(3): 369-382.

Sorensen, C. S., C. Lukas, E. R. Kramer, J. M. Peters, J. Bartek and J. Lukas (2000). "Nonperiodic activity of the human anaphase-promoting complex-Cdh1 ubiquitin ligase results in continuous DNA synthesis uncoupled from mitosis." Mol Cell Biol **20**(20): 7613-7623.

Steen, J. A., H. Steen, A. Georgi, K. Parker, M. Springer, M. Kirchner, F. Hamprecht and M. W. Kirschner (2008). "Different phosphorylation states of the anaphase promoting complex in response to antimitotic drugs: a quantitative proteomic analysis." Proc Natl Acad Sci U S A **105**(16): 6069-6074.

Stefanovsky, V., F. Langlois, T. Gagnon-Kugler, L. I. Rothblum and T. Moss (2006). "Growth factor signaling regulates elongation of RNA polymerase I transcription in mammals via UBF phosphorylation and r-chromatin remodeling." Mol Cell **21**(5): 629-639.

Stegmeier, F., M. Rape, V. M. Draviam, G. Nalepa, M. E. Sowa, X. L. Ang, E. R. McDonald, M. Z. Li, G. J. Hannon, P. K. Sorger, M. W. Kirschner, J. W. Harper and S. J. Elledge (2007). "Anaphase initiation is regulated by antagonistic ubiquitination and deubiquitination activities." Nature **446**(7138): 876-881.

Stegmuller, J., Y. Konishi, M. A. Huynh, Z. Yuan, S. Dibacco and A. Bonni (2006). Cell-intrinsic regulation of axonal morphogenesis by the Cdh1-APC target SnoN. Neuron. United States. **50:** 389-400.

Stemmann, O., H. Zou, S. A. Gerber, S. P. Gygi and M. W. Kirschner (2001). Dual inhibition of sister chromatid separation at metaphase. Cell. United States. **107:** 715-726.

Stewart, S. and G. Fang (2005). "Anaphase-promoting complex/cyclosome controls the stability of TPX2 during mitotic exit." Mol Cell Biol **25**(23): 10516-10527.

Stewart, S. and G. Fang (2005). "Destruction box-dependent degradation of aurora B is mediated by the anaphase-promoting complex/cyclosome and Cdh1." Cancer Res **65**(19): 8730-8735.

Strezoska, Z., D. G. Pestov and L. F. Lau (2000). "Bop1 is a mouse WD40 repeat nucleolar protein involved in 28S and 5. 8S RRNA processing and 60S ribosome biogenesis." Mol Cell Biol **20**(15): 5516-5528.

Strohner, R., A. Nemeth, P. Jansa, U. Hofmann-Rohrer, R. Santoro, G. Längst and I. Grummt (2001). "NoRC--a novel member of mammalian ISWI-containing chromatin remodeling machines." EMBO J **20**(17): 4892-4900.

Stroschein, S. L., S. Bonni, J. L. Wrana and K. Luo (2001). "Smad3 recruits the anaphase-promoting complex for ubiquitination and degradation of SnoN." Genes Dev **15**(21): 2822-2836.

Strunk, K. E., C. Husted, L. C. Miraglia, M. Sandahl, W. A. Rearick, D. M. Hunter, H. S. Earp and R. S. Muraoka-Cook (2007). "HER4 D-box sequences regulate mitotic progression and degradation of the nuclear HER4 cleavage product s80HER4." Cancer Res **67**(14): 6582-6590.

Sudakin, V., G. K. Chan and T. J. Yen (2001). Checkpoint inhibition of the APC/C in HeLa cells is mediated by a complex of BUBR1, BUB3, CDC20, and MAD2. J Cell Biol. United States. **154:** 925-936.

Sudakin, V., D. Ganoth, A. Dahan, H. Heller, J. Hershko, F. C. Luca, J. V. Ruderman and A. Hershko (1995). "The cyclosome, a large complex containing cyclin-selective ubiquitin ligase activity, targets cyclins for destruction at the end of mitosis." Mol Biol Cell **6**(2): 185-197.

Sudakin, V., M. Shteinberg, D. Ganoth, J. Hershko and A. Hershko (1997). "Binding of activated cyclosome to p13(suc1). Use for affinity purification." J Biol Chem **272**(29): 18051-18059.

Sudo, T., Y. Ota, S. Kotani, M. Nakao, Y. Takami, S. Takeda and H. Saya (2001). "Activation of Cdh1-dependent APC is required for G1 cell cycle arrest and DNA damage-induced G2 checkpoint in vertebrate cells." EMBO J **20**(22): 6499-6508.

Sugimoto, N., I. Kitabayashi, S. Osano, Y. Tatsumi, T. Yugawa, M. Narisawa-Saito, A. Matsukage, T. Kiyono and M. Fujita (2008). "Identification of novel human Cdt1-binding proteins by a proteomics approach: proteolytic regulation by APC/CCdh1." Mol Biol Cell **19**(3): 1007-1021.

Sullivan, M. and D. O. Morgan (2007). A novel destruction sequence targets the meiotic regulator Spo13 for anaphase-promoting complex-dependent degradation in anaphase I. J Biol Chem. United States. **282:** 19710-19715.

Taccioli, G. E., T. M. Gottlieb, T. Blunt, A. Priestley, J. Demengeot, R. Mizuta, A. R. Lehmann, F. W. Alt, S. P. Jackson and P. A. Jeggo (1994). "Ku80: product of the XRCC5 gene and its role in DNA repair and V(D)J recombination." Science **265**(5177): 1442-1445.

Tafforeau, L., C. Zorbas, J. L. Langhendries, S. T. Mullineux, V. Stamatopoulou, R. Mullier, L. Wacheul and D. L. Lafontaine (2013). "The complexity of human ribosome biogenesis revealed by systematic nucleolar screening of Pre-rRNA processing factors." Mol Cell **51**(4): 539-551.

Taguchi, S., K. Honda, K. Sugiura, A. Yamaguchi, K. Furukawa and T. Urano (2002). "Degradation of human Aurora-A protein kinase is mediated by hCdh1." FEBS Lett **519**(1-3): 59-65.

Taira, N. and K. Yoshida (2012). "Post-translational modifications of p53 tumor suppressor: determinants of its functional targets." Histol Histopathol **27**(4): 437-443.

Takahashi, A., Y. Imai, K. Yamakoshi, S. Kuninaka, N. Ohtani, S. Yoshimoto, S. Hori, M. Tachibana, E. Anderton, T. Takeuchi, Y. Shinkai, G. Peters, H. Saya and E. Hara (2012). "DNA damage signaling triggers degradation of histone methyltransferases through APC/C(Cdh1) in senescent cells." Mol Cell **45**(1): 123-131.

Takai, N., R. Hamanaka, J. Yoshimatsu and I. Miyakawa (2005). Polo-like kinases (Plks) and cancer. Oncogene. England. **24:** 287-291.

Talvinen, K., H. Karra, R. Pitkänen, I. Ahonen, M. Nykänen, M. Lintunen, M. Söderström, T. Kuopio and P. Kronqvist (2013). "Low cdc27 and high securin expression predict short survival for breast cancer patients." APMIS **121**(10): 945-953.

Tanaka, Y., K. Okamoto, K. Teye, T. Umata, N. Yamagiwa, Y. Suto, Y. Zhang and M. Tsuneoka (2010). "JmjC enzyme KDM2A is a regulator of rRNA transcription in response to starvation." EMBO J **29**(9): 1510-1522.

Tang, Z., R. Bharadwaj, B. Li and H. Yu (2001). Mad2-Independent inhibition of APCCdc20 by the mitotic checkpoint protein BubR1. Dev Cell. United States. **1:** 227-237.

Tang, Z., B. Li, R. Bharadwaj, H. Zhu, E. Ozkan, K. Hakala, J. Deisenhofer and H. Yu (2001). "APC2 Cullin protein and APC11 RING protein comprise the minimal ubiquitin ligase module of the anaphase-promoting complex." Mol Biol Cell **12**(12): 3839-3851.

Tapia-Alveal, C., S. J. Lin and M. J. O'Connell (2014). "Functional interplay between cohesin and Smc5/6 complexes." Chromosoma.

Taylor, E. M., A. C. Copsey, J. J. Hudson, S. Vidot and A. R. Lehmann (2008). "Identification of the proteins, including MAGEG1, that make up the human SMC5-6 protein complex." Mol Cell Biol **28**(4): 1197-1206.

Teckchandani, A., G. S. Laszlo, S. Simó, K. Shah, C. Pilling, A. A. Strait and J. A. Cooper (2014). "Cullin 5 destabilizes Cas to inhibit Src-dependent cell transformation." J Cell Sci **127**(Pt 3): 509-520.

Teodoro, J. G., D. W. Heilman, A. E. Parker and M. R. Green (2004). "The viral protein Apoptin associates with the anaphase-promoting complex to induce G2/M arrest and apoptosis in the absence of p53." Genes Dev **18**(16): 1952-1957.

Thadani, R., F. Uhlmann and S. Heeger (2012). "Condensin, chromatin crossbarring and chromosome condensation." Curr Biol **22**(23): R1012-1021.

Thompson, L. H., K. W. Brookman, N. J. Jones, S. A. Allen and A. V. Carrano (1990). "Molecular cloning of the human XRCC1 gene, which corrects defective DNA strand break repair and sister chromatid exchange." Mol Cell Biol **10**(12): 6160-6171.

Thomson, E., J. Rappsilber and D. Tollervey (2007). "Nop9 is an RNA binding protein present in pre-40S ribosomes and required for 18S rRNA synthesis in yeast." RNA **13**(12): 2165-2174.

Thornton, B. R., T. M. Ng, M. E. Matyskiela, C. W. Carroll, D. O. Morgan and D. P. Toczyski (2006). "An architectural map of the anaphase-promoting complex." Genes Dev **20**(4): 449-460.

Tian, W., B. Li, R. Warrington, D. R. Tomchick, H. Yu and X. Luo (2012). "Structural analysis of human Cdc20 supports multisite degron recognition by APC/C." Proc Natl Acad Sci U S A **109**(45): 18419-18424.

Townsend, K., H. Mason, A. N. Blackford, E. S. Miller, J. R. Chapman, G. G. Sedgwick, G. Barone, A. S. Turnell and G. S. Stewart (2009). "Mediator of DNA damage checkpoint 1 (MDC1) regulates mitotic progression." J Biol Chem **284**(49): 33939-33948.

Trask, D. K. and M. T. Muller (1988). "Stabilization of type I topoisomerase-DNA covalent complexes by actinomycin D." Proc Natl Acad Sci U S A **85**(5): 1417-1421.

Truong, L. N. and X. Wu (2011). "Prevention of DNA re-replication in eukaryotic cells." J Mol Cell Biol **3**(1): 13-22.

Tsai, L. H., E. Harlow and M. Meyerson (1991). "Isolation of the human cdk2 gene that encodes the cyclin A- and adenovirus E1A-associated p33 kinase." Nature **353**(6340): 174-177.

Tsunematsu, T., Y. Takihara, N. Ishimaru, M. Pagano, T. Takata and Y. Kudo (2013). "Aurora-A controls pre-replicative complex assembly and DNA replication by stabilizing geminin in mitosis." Nat Commun **4**: 1885.

Tsvetkov, L. M., K. H. Yeh, S. J. Lee, H. Sun and H. Zhang (1999). "p27(Kip1) ubiquitination and degradation is regulated by the SCF(Skp2) complex through phosphorylated Thr187 in p27." Curr Biol **9**(12): 661-664.

Tumurbaatar, I., O. Cizmecioglu, I. Hoffmann, I. Grummt and R. Voit (2011). "Human Cdc14B promotes progression through mitosis by dephosphorylating Cdc25 and regulating Cdk1/cyclin B activity." PLoS One **6**(2): e14711.

Turnell, A. S., G. S. Stewart, R. J. Grand, S. M. Rookes, A. Martin, H. Yamano, S. J. Elledge and P. H. Gallimore (2005). "The APC/C and CBP/p300 cooperate to regulate transcription and cell-cycle progression." Nature **438**(7068): 690-695.

Turner, E. L., M. E. Malo, M. G. Pisclevich, M. D. Dash, G. F. Davies, T. G. Arnason and T. A. Harkness (2010). The Saccharomyces cerevisiae anaphase-promoting complex interacts with multiple histone-modifying enzymes to regulate cell cycle progression. Eukaryot Cell. United States. **9:** 1418-1431.

UniProt-Consortium (2014). "Activities at the Universal Protein Resource (UniProt)." Nucleic Acids Res **42**(Database issue): D191-198.

Utama, B., D. Kennedy, K. Ru and J. S. Mattick (2002). "Isolation and characterization of a new nucleolar protein, Nrap, that is conserved from yeast to humans." Genes Cells **7**(2): 115-132.

Uzunova, K., B. T. Dye, H. Schutz, R. Ladurner, G. Petzold, Y. Toyoda, M. A. Jarvis, N. G. Brown, I. Poser, M. Novatchkova, K. Mechtler, A. A. Hyman, H. Stark, B. A. Schulman and J. M. Peters (2012). "APC15 mediates CDC20 autoubiquitylation by APC/C(MCC) and disassembly of the mitotic checkpoint complex." Nat Struct Mol Biol **19**(11): 1116-1123.

van Leuken, R., L. Clijsters and R. Wolthuis (2008). "To cell cycle, swing the APC/C." Biochim Biophys Acta **1786**(1): 49-59.

van Ree, J. H., K. B. Jeganathan, L. Malureanu and J. M. van Deursen (2010). "Overexpression of the E2 ubiquitin-conjugating enzyme UbcH10 causes chromosome missegregation and tumor formation." J Cell Biol **188**(1): 83-100.

Van Voorhis, V. A. and D. O. Morgan (2014). "Activation of the APC/C ubiquitin ligase by enhanced E2 efficiency." Curr Biol **24**(13): 1556-1562.

van Zon, W., J. Ogink, B. ter Riet, R. H. Medema, H. te Riele and R. M. Wolthuis (2010). "The APC/C recruits cyclin B1-Cdk1-Cks in prometaphase before D box recognition to control mitotic exit." J Cell Biol **190**(4): 587-602.

Venema, J. and D. Tollervey (1996). "RRP5 is required for formation of both 18S and 5.8S rRNA in yeast." EMBO J **15**(20): 5701-5714.

Verma, R., S. Chen, R. Feldman, D. Schieltz, J. Yates, J. Dohmen and R. J. Deshaies (2000). "Proteasomal proteomics: identification of nucleotide-sensitive proteasome-interacting proteins by mass spectrometric analysis of affinity-purified proteasomes." Mol Biol Cell **11**(10): 3425-3439.

Vintermist, A., S. Böhm, F. Sadeghifar, E. Louvet, A. Mansén, P. Percipalle and A. K. Ostlund Farrants (2011). "The chromatin remodelling complex B-WICH changes the chromatin structure and recruits histone acetyl-transferases to active rRNA genes." PLoS One **6**(4): e19184.

Vlotides, G., T. Eigler and S. Melmed (2007). Pituitary tumor-transforming gene: physiology and implications for tumorigenesis. Endocr Rev. United States. **28:** 165-186.

Vodermaier, H. C., C. Gieffers, S. Maurer-Stroh, F. Eisenhaber and J. M. Peters (2003). "TPR subunits of the anaphase-promoting complex mediate binding to the activator protein CDH1." Curr Biol **13**(17): 1459-1468.

Voges, D., P. Zwickl and W. Baumeister (1999). "The 26S proteasome: a molecular machine designed for controlled proteolysis." Annu Rev Biochem **68**: 1015-1068.

Wada, K., M. Niida, M. Tanaka and T. Kamitani (2009). "Ro52-mediated monoubiquitination of IKK{beta} down-regulates NF-{kappa}B signalling." J Biochem **146**(6): 821-832.

Waizenegger, I., J. F. Gimenez-Abian, D. Wernic and J. M. Peters (2002). Regulation of human separase by securin binding and autocleavage. Curr Biol. England. **12:** 1368-1378.

Wan, Y., X. Liu and M. W. Kirschner (2001). The anaphase-promoting complex mediates TGF-beta signaling by targeting SnoN for destruction. Mol Cell. United States. **8:** 1027-1039.

Wang, F., C. B. Marshall and M. Ikura (2013). "Transcriptional/epigenetic regulator CBP/p300 in tumorigenesis: structural and functional versatility in target recognition." Cell Mol Life Sci **70**(21): 3989-4008.

Wang, J., B. T. Dye, K. R. Rajashankar, I. Kurinov and B. A. Schulman (2009). "Insights into anaphase promoting complex TPR subdomain assembly from a CDC26-APC6 structure." Nat Struct Mol Biol **16**(9): 987-989.

Wang, K., B. Sturt-Gillespie, J. C. Hittle, D. Macdonald, G. K. Chan, T. J. Yen and S. T. Liu (2014). "Thyroid Hormone Receptor Interacting Protein 13 (TRIP13) AAA-ATPase is a Novel Mitotic Checkpoint Silencing Protein." J Biol Chem.

Wang, Q., C. Moyret-Lalle, F. Couzon, C. Surbiguet-Clippe, J. C. Saurin, T. Lorca, C. Navarro and A. Puisieux (2003). Alterations of anaphase-promoting complex genes in human colon cancer cells. Oncogene. England. **22:** 1486-1490.

Wang, R., K. M. Li, C. H. Zhou, J. L. Xue, C. N. Ji and J. Z. Chen (2011). "Cdc20 mediates D-box-dependent degradation of Sp100." Biochem Biophys Res Commun **415**(4): 702-706.

Wang, W., J. Côté, Y. Xue, S. Zhou, P. A. Khavari, S. R. Biggar, C. Muchardt, G. V. Kalpana, S. P. Goff, M. Yaniv, J. L. Workman and G. R. Crabtree (1996). "Purification and biochemical heterogeneity of the mammalian SWI-SNF complex." EMBO J **15**(19): 5370-5382.

Wang, W. and M. W. Kirschner (2013). "Emi1 preferentially inhibits ubiquitin chain elongation by the anaphase-promoting complex." Nat Cell Biol **15**(7): 797-806.

Wang, Y. and Q. Zhan (2007). "Cell cycle-dependent expression of centrosomal ninein-like protein in human cells is regulated by the anaphase-promoting complex." J Biol Chem **282**(24): 17712-17719.

Wang, Z., L. Wan, J. Zhong, H. Inuzuka, P. Liu, F. H. Sarkar and W. Wei (2013). "Cdc20: a potential novel therapeutic target for cancer treatment." Curr Pharm Des **19**(18): 3210-3214.

Wang, Z., R. Yu and S. Melmed (2001). "Mice lacking pituitary tumor transforming gene show testicular and splenic hypoplasia, thymic hyperplasia, thrombocytopenia, aberrant cell cycle progression, and premature centromere division." Mol Endocrinol **15**(11): 1870-1879.

Wasch, R., J. A. Robbins and F. R. Cross (2010). The emerging role of APC/CCdh1 in controlling differentiation, genomic stability and tumor suppression. Oncogene. England. **29:** 1-10.

Waters, J. C., R. H. Chen, A. W. Murray and E. D. Salmon (1998). "Localization of Mad2 to kinetochores depends on microtubule attachment, not tension." J Cell Biol **141**(5): 1181-1191.

Watkins, N. J. and M. T. Bohnsack (2012). "The box C/D and H/ACA snoRNPs: key players in the modification, processing and the dynamic folding of ribosomal RNA." Wiley Interdiscip Rev RNA **3**(3): 397-414.

Wegierski, T., E. Billy, F. Nasr and W. Filipowicz (2001). "Bms1p, a G-domain-containing protein, associates with Rcl1p and is required for 18S rRNA biogenesis in yeast." RNA **7**(9): 1254-1267.

Wendt, K. S., H. C. Vodermaier, U. Jacob, C. Gieffers, M. Gmachl, J. M. Peters, R. Huber and P. Sondermann (2001). "Crystal structure of the APC10/DOC1 subunit of the human anaphase-promoting complex." Nat Struct Biol **8**(9): 784-788.

Westhorpe, F. G., A. Tighe, P. Lara-Gonzalez and S. S. Taylor (2011). "p31comet-mediated extraction of Mad2 from the MCC promotes efficient mitotic exit." J Cell Sci **124**(Pt 22): 3905-3916.

Weston, C. R. and R. J. Davis (2007). "The JNK signal transduction pathway." Curr Opin Cell Biol **19**(2): 142-149.

Wickliffe, K. E., S. Lorenz, D. E. Wemmer, J. Kuriyan and M. Rape (2011). "The mechanism of linkage-specific ubiquitin chain elongation by a single-subunit E2." Cell **144**(5): 769-781.

Wilk, S. and M. Orlowski (1983). "Evidence that pituitary cation-sensitive neutral endopeptidase is a multicatalytic protease complex." J Neurochem **40**(3): 842-849.

Williamson, A., S. Banerjee, X. Zhu, I. Philipp, A. T. Iavarone and M. Rape (2011). "Regulation of ubiquitin chain initiation to control the timing of substrate degradation." Mol Cell **42**(6): 744-757.

Williamson, A., K. E. Wickliffe, B. G. Mellone, L. Song, G. H. Karpen and M. Rape (2009). "Identification of a physiological E2 module for the human anaphase-promoting complex." Proc Natl Acad Sci U S A **106**(43): 18213-18218.

Wirth, K. G., R. Ricci, J. F. Gimenez-Abian, S. Taghybeeglu, N. R. Kudo, W. Jochum, M. Vasseur-Cognet and K. Nasmyth (2004). Loss of the anaphase-promoting complex in quiescent cells causes unscheduled hepatocyte proliferation. Genes Dev. United States. **18:** 88-98.

Wolthuis, R., L. Clay-Farrace, W. van Zon, M. Yekezare, L. Koop, J. Ogink, R. Medema and J. Pines (2008). Cdc20 and Cks direct the spindle checkpoint-independent destruction of cyclin A. Mol Cell. United States. **30:** 290-302.

Woods, N. T., R. D. Mesquita, M. Sweet, M. A. Carvalho, X. Li, Y. Liu, H. Nguyen, C. E. Thomas, E. S. Iversen, S. Marsillac, R. Karchin, J. Koomen and A. N. Monteiro (2012). "Charting the landscape of tandem BRCT domain-mediated protein interactions." Sci Signal **5**(242): rs6.

Wsierska-Gadek, J. and M. Horky (2003). "How the nucleolar sequestration of p53 protein or its interplayers contributes to its (re)-activation." Ann N Y Acad Sci **1010**: 266-272.

Wu, G., S. Glickstein, W. Liu, T. Fujita, W. Li, Q. Yang, R. Duvoisin and Y. Wan (2007). The anaphase-promoting complex coordinates initiation of lens differentiation. Mol Biol Cell. United States. **18:** 1018-1029.

Wu, P., J. S. Brockenbrough, A. C. Metcalfe, S. Chen and J. P. Aris (1998). "Nop5p is a small nucleolar ribonucleoprotein component required for pre-18 S rRNA processing in yeast." J Biol Chem **273**(26): 16453-16463.

Wu, T., Y. Merbl, Y. Huo, J. L. Gallop, A. Tzur and M. W. Kirschner (2010). "UBE2S drives elongation of K11-linked ubiquitin chains by the anaphase-promoting complex." Proc Natl Acad Sci U S A **107**(4): 1355-1360.

Wu, W. J., K. S. Hu, D. S. Wang, Z. L. Zeng, D. S. Zhang, D. L. Chen, L. Bai and R. H. Xu (2013). "CDC20 overexpression predicts a poor prognosis for patients with colorectal cancer." J Transl Med **11**: 142.

Wäsch, R. and D. Engelbert (2005). "Anaphase-promoting complex-dependent proteolysis of cell cycle regulators and genomic instability of cancer cells." Oncogene **24**(1): 1-10.

Xie, C., C. Powell, M. Yao, J. Wu and Q. Dong (2014). "Ubiquitin-conjugating enzyme E2C: a potential cancer biomarker." Int J Biochem Cell Biol **47**: 113-117.

Xie, W., T. Ling, Y. Zhou, W. Feng, Q. Zhu, H. G. Stunnenberg, I. Grummt and W. Tao (2012). "The chromatin remodeling complex NuRD establishes the poised state of rRNA genes characterized by bivalent histone modifications and altered nucleosome positions." Proc Natl Acad Sci U S A **109**(21): 8161-8166.

Xu, P., D. M. Duong, N. T. Seyfried, D. Cheng, Y. Xie, J. Robert, J. Rush, M. Hochstrasser, D. Finley and J. Peng (2009). Quantitative proteomics reveals the function of unconventional ubiquitin chains in proteasomal degradation. Cell. United States. **137:** 133-145.

Yang, C., J. Hao, D. Kong, X. Cui, W. Zhang, H. Wang, X. Guo, S. Ma, X. Liu, P. Pu and B. Xu (2014). "ATM-mediated Mad1 Serine 214 phosphorylation regulates Mad1 dimerization and the spindle assembly checkpoint." Carcinogenesis **35**(9): 2007-2013.

Yang, F., L. Hu, C. Chen, J. Yu, C. B. O'Connell, A. Khodjakov, M. Pagano and W. Dai (2012). "BubR1 is modified by sumoylation during mitotic progression." J Biol Chem **287**(7): 4875-4882.

Yang, F., Y. Huang and W. Dai (2012). "Sumoylated BubR1 plays an important role in chromosome segregation and mitotic timing." Cell Cycle **11**(4): 797-806.

Yang, H., D. Henning and B. C. Valdez (2005). "Functional interaction between RNA helicase II/Gu(alpha) and ribosomal protein L4." FEBS J **272**(15): 3788-3802.

Yang, M., B. Li, D. R. Tomchick, M. Machius, J. Rizo, H. Yu and X. Luo (2007). "p31comet blocks Mad2 activation through structural mimicry." Cell **131**(4): 744-755.

Yang, Y., A. H. Kim, T. Yamada, B. Wu, P. M. Bilimoria, Y. Ikeuchi, N. de la Iglesia, J. Shen and A. Bonni (2009). "A Cdc20-APC ubiquitin signaling pathway regulates presynaptic differentiation." Science **326**(5952): 575-578.

Yardimci, H. and J. C. Walter (2014). "Prereplication-complex formation: a molecular double take?" Nat Struct Mol Biol **21**(1): 20-25.

Yu, H., J. M. Peters, R. W. King, A. M. Page, P. Hieter and M. W. Kirschner (1998). "Identification of a cullin homology region in a subunit of the anaphase-promoting complex." Science **279**(5354): 1219-1222.

Yu, Z. K., J. L. Gervais and H. Zhang (1998). "Human CUL-1 associates with the SKP1/SKP2 complex and regulates p21(CIP1/WAF1) and cyclin D proteins." Proc Natl Acad Sci U S A **95**(19): 11324-11329.

Yuan, X., W. Feng, A. Imhof, I. Grummt and Y. Zhou (2007). "Activation of RNA polymerase I transcription by cockayne syndrome group B protein and histone methyltransferase G9a." Mol Cell **27**(4): 585-595.

Yuan, X., Y. Zhou, E. Casanova, M. Chai, E. Kiss, H. J. Gröne, G. Schütz and I. Grummt (2005). "Genetic inactivation of the transcription factor TIF-IA leads to nucleolar disruption, cell cycle arrest, and p53-mediated apoptosis." Mol Cell **19**(1): 77-87.

Zachariae, W., M. Schwab, K. Nasmyth and W. Seufert (1998). "Control of cyclin ubiquitination by CDK-regulated binding of Hct1 to the anaphase promoting complex." Science **282**(5394): 1721-1724.

Zachariae, W., A. Shevchenko, P. D. Andrews, R. Ciosk, M. Galova, M. J. Stark, M. Mann and K. Nasmyth (1998). "Mass spectrometric analysis of the anaphase-promoting complex from yeast: identification of a subunit related to cullins." Science **279**(5354): 1216-1219.

Zentner, G. E., E. A. Hurd, M. P. Schnetz, L. Handoko, C. Wang, Z. Wang, C. Wei, P. J. Tesar, M. Hatzoglou, D. M. Martin and P. C. Scacheri (2010). "CHD7 functions in the nucleolus as a positive regulator of ribosomal RNA biogenesis." Hum Mol Genet **19**(18): 3491-3501.

Zhai, W. and L. Comai (2000). "Repression of RNA polymerase I transcription by the tumor suppressor p53." Mol Cell Biol **20**(16): 5930-5938.

Zhang, D., K. Zaugg, T. W. Mak and S. J. Elledge (2006). A role for the deubiquitinating enzyme USP28 in control of the DNA-damage response. Cell. United States. **126:** 529-542.

Zhang, H. S. and D. C. Dean (2001). "Rb-mediated chromatin structure regulation and transcriptional repression." Oncogene **20**(24): 3134-3138.

Zhang, J., Z. Ma, A. Treszezamsky and S. N. Powell (2005). "MDC1 interacts with Rad51 and facilitates homologous recombination." Nat Struct Mol Biol **12**(10): 902-909.

Zhang, J., L. Wan, X. Dai, Y. Sun and W. Wei (2014). "Functional characterization of Anaphase Promoting Complex/Cyclosome (APC/C) E3 ubiquitin ligases in tumorigenesis." Biochim Biophys Acta **1845**(2): 277-293.

Zhang, K. and R. Kumar (1994). "Interferon-alpha inhibits cyclin E- and cyclin D1-dependent CDK-2 kinase activity associated with RB protein and E2F in Daudi cells." Biochem Biophys Res Commun **200**(1): 522-528.

Zhang, K., P. M. Yau, B. Chandrasekhar, R. New, R. Kondrat, B. S. Imai and M. E. Bradbury (2004). "Differentiation between peptides containing acetylated or tri-methylated lysines by mass spectrometry: an application for determining lysine 9 acetylation and methylation of histone H3." Proteomics **4**(1): 1-10.

Zhang, L., R. Rahbari, M. He and E. Kebebew (2011). "CDC23 regulates cancer cell phenotype and is overexpressed in papillary thyroid cancer." Endocr Relat Cancer **18**(6): 731-742.

Zhang, T., S. Nirantar, H. H. Lim, I. Sinha and U. Surana (2009). DNA damage checkpoint maintains CDH1 in an active state to inhibit anaphase progression. Dev Cell. United States. **17:** 541-551.

Zhang, W. N., J. Zhou, T. Zhou, A. L. Li, N. Wang, J. J. Xu, Y. Chang, J. H. Man, X. Pan, T. Li, W. H. Li, R. Mu, B. Liang, L. Chen, B. F. Jin, Q. Xia, W. L. Gong, X. M. Zhang, L. Wang and H. Y. Li (2013). "Phosphorylation-triggered CUEDC2 degradation promotes UV-induced G1 arrest through APC/C(Cdh1) regulation." Proc Natl Acad Sci U S A **110**(27): 11017-11022.

Zhang, Y., G. W. Wolf, K. Bhat, A. Jin, T. Allio, W. A. Burkhart and Y. Xiong (2003). "Ribosomal protein L11 negatively regulates oncoprotein MDM2 and mediates a p53-dependent ribosomal-stress checkpoint pathway." Mol Cell Biol **23**(23): 8902-8912.

Zhang, Z., L. Chang, J. Yang, N. Conin, K. Kulkarni and D. Barford (2013). "The four canonical tpr subunits of human APC/C form related homo-dimeric structures and stack in parallel to form a TPR suprahelix." J Mol Biol **425**(22): 4236-4248.

Zhang, Z., J. Yang, E. H. Kong, W. C. Chao, E. P. Morris, P. C. da Fonseca and D. Barford (2013). "Recombinant expression, reconstitution and structure of human anaphase-promoting complex (APC/C)." Biochem J **449**(2): 365-371.

Zhao, L., L. Jiang, L. Wang, J. He, H. Yu, G. Sun, J. Chen, Q. Xiu and B. Li (2012). "UbcH10 expression provides a useful tool for the prognosis and treatment of non-small cell lung cancer." J Cancer Res Clin Oncol **138**(11): 1951-1961.

Zhao, S., W. Xu, W. Jiang, W. Yu, Y. Lin, T. Zhang, J. Yao, L. Zhou, Y. Zeng, H. Li, Y. Li, J. Shi, W. An, S. M. Hancock, F. He, L. Qin, J. Chin, P. Yang, X. Chen, Q. Lei, Y. Xiong and K. L. Guan (2010). "Regulation of cellular metabolism by protein lysine acetylation." Science **327**(5968): 1000-1004.

Zhao, W. M., J. A. Coppinger, A. Seki, X. L. Cheng, J. R. Yates and G. Fang (2008). "RCS1, a substrate of APC/C, controls the metaphase to anaphase transition." Proc Natl Acad Sci U S A **105**(36): 13415-13420.

Zhao, W. M. and G. Fang (2005). "Anillin is a substrate of anaphase-promoting complex/cyclosome (APC/C) that controls spatial contractility of myosin during late cytokinesis." J Biol Chem **280**(39): 33516-33524.

Zhao, Z. K., W. G. Wu, L. Chen, P. Dong, J. Gu, J. S. Mu, J. H. Yang and Y. B. Liu (2013). "Expression of UbcH10 in pancreatic ductal adenocarcinoma and its correlation with prognosis." Tumour Biol **34**(3): 1473-1477.

Zhou, H., S. Di Palma, C. Preisinger, M. Peng, A. N. Polat, A. J. Heck and S. Mohammed (2013). "Toward a comprehensive characterization of a human cancer cell phosphoproteome." J Proteome Res **12**(1): 260-271.

Zhou, Y., Y. P. Ching, A. C. Chun and D. Y. Jin (2003). Nuclear localization of the cell cycle regulator CDH1 and its regulation by phosphorylation. J Biol Chem. United States. **278:** 12530-12536.

Zhou, Y., R. Santoro and I. Grummt (2002). "The chromatin remodeling complex NoRC targets HDAC1 to the ribosomal gene promoter and represses RNA polymerase I transcription." EMBO J **21**(17): 4632-4640.

Zhou, Z., C. Jing, L. Zhang, F. Takeo, H. Kim, Y. Huang, Z. Liu and Y. Wan (2013). "Regulation of Rad17 protein turnover unveils an impact of Rad17-APC cascade in breast carcinogenesis and treatment." J Biol Chem **288**(25): 18134-18145.

Zhu, C. H., J. Kim, J. W. Shay and W. E. Wright (2008). "SGNP: an essential Stress Granule/Nucleolar Protein potentially involved in 5.8s rRNA processing/transport." PLoS One **3**(11): e3716.

Zhu, Y. and W. Xiao (2004). "Pdr3 is required for DNA damage induction of MAG1 and DDI1 via a bi-directional promoter element." Nucleic Acids Res **32**(17): 5066-5075.

Zillner, K., M. Filarsky, K. Rachow, M. Weinberger, G. Längst and A. Németh (2013). "Large-scale organization of ribosomal DNA chromatin is regulated by Tip5." Nucleic Acids Res **41**(10): 5251-5262.

Zou, H., T. J. McGarry, T. Bernal and M. W. Kirschner (1999). Identification of a vertebrate sister-chromatid separation inhibitor involved in transformation and tumorigenesis. Science. United States. **285:** 418-422.

Zur, A. and M. Brandeis (2002). "Timing of APC/C substrate degradation is determined by fzy/fzr specificity of destruction boxes." EMBO J **21**(17): 4500-4510.